

**THE ELECTROMAGNETIC
ORIGIN OF
QUANTUM THEORY
AND LIGHT**

Second Edition

Dale M. Grimes & Craig A. Grimes

**THE ELECTROMAGNETIC
ORIGIN OF
QUANTUM THEORY
AND LIGHT**

Second Edition

This page intentionally left blank

THE ELECTROMAGNETIC ORIGIN OF QUANTUM THEORY AND LIGHT

Second Edition

Dale M. Grimes & Craig A. Grimes

The Pennsylvania State University, USA

 World Scientific

NEW JERSEY • LONDON • SINGAPORE • BEIJING • SHANGHAI • HONG KONG • TAIPEI • CHENNAI

Published by

World Scientific Publishing Co. Pte. Ltd.

5 Toh Tuck Link, Singapore 596224

USA office: 27 Warren Street, Suite 401-402, Hackensack, NJ 07601

UK office: 57 Shelton Street, Covent Garden, London WC2H 9HE

British Library Cataloguing-in-Publication Data

A catalogue record for this book is available from the British Library.

THE ELECTROMAGNETIC ORIGIN OF QUANTUM THEORY AND LIGHT
Second Edition

Copyright © 2005 by World Scientific Publishing Co. Pte. Ltd.

All rights reserved. This book, or parts thereof, may not be reproduced in any form or by any means, electronic or mechanical, including photocopying, recording or any information storage and retrieval system now known or to be invented, without written permission from the Publisher.

For photocopying of material in this volume, please pay a copying fee through the Copyright Clearance Center, Inc., 222 Rosewood Drive, Danvers, MA 01923, USA. In this case permission to photocopy is not required from the publisher.

ISBN 981-238-925-3

Typeset by Stallion Press

Email: enquiries@stallionpress.com

Printed in Singapore.

To Janet,

for her loyalty, patience, and support.

This page intentionally left blank

Foreword

Man will occasionally stumble over the truth, but most of the time he will pick himself up and continue on.

— Winston Churchill

Einstein, Podolsky, and Rosen suggested the possibility of nonlocality of entangled electrons in 1935; Bell proved a critical theorem in 1964 and Aspect *et al* provided experimental evidence in 1982. Feynman proved nonlocality of free electrons in 1941 by proving that an electron goes from point A to point B by all possible paths. In this book we provide circumstantial evidence for nonlocality of individual eigenstate electrons.

One of Webster's definitions of pragmatism is "a practical treatment of things." In this sense one group of the founders of quantum theory, including Bohr, Heisenberg, and Pauli, were pragmatists. To explain atomic-level events, as they became known, they discarded those classical concepts that seemed to contradict, and introduced new postulates as required. On such a base they constructed a consistent explanation of observations on an atomic level of dimensions. Now, nearly a century later, it is indisputable that the mathematics of quantum theory coupled with this historic, pragmatic interpretation adequately account for most observed atomic-scaled physical phenomena. It is also indisputable that, in contrast with other physical disciplines, their interpretation requires special, rather quixotic, quantum theory axioms. For example, under certain circumstances, results precede their cause and there is an intrinsic uncertainty of physical events: The status of observable physical phenomena at any instant does not completely specify its status an instant later. Such inherent uncertainty belies all other natural philosophy. The axioms needed also require rejection of selected portions of classical electromagnetism within atoms and retention of the rest, and they supply no information about the field structure accompanying photon exchanges by atoms. With this pragmatic explanation radiating atoms are far less understood, for example, than antennas. Nonetheless

it is accepted because, prior to this work, only this viewpoint adequately explained quantum mechanics as a consistent and logical discipline.

One of Webster's definitions of idealism is "the practice of forming ideals or living under their influence." If we interpret ideal to mean scientific logic separate from the pragmatic view of quantum theory, another group of founders, including Einstein, Schrödinger, and de Broglie, were idealists. They believed that quantum theory should be explained by the same basic scientific logic that enables the classical sciences. With due respect to the work of pragmatists, at least in principle, it is easier to explain new and unexpected phenomena by introducing new postulates than it is to derive complete idealistic results.

In our view, the early twentieth century knowledge of the classical sciences was insufficient for an understanding of the connection between the classical and quantum sciences. Critical physical effects that were discovered only after the interpretation of quantum theory was complete include (i) the standing energy that accompanies and encompasses active, electrically small volumes, (ii) the power-frequency relationships in nonlinear systems, and (iii) the possible directivity of superimposed modal fields. Neither was the model of extended eigenstate electrons seriously addressed until (iv) nonlocality was recognized in the late 20th century. How could it be that such significant and basic physical phenomena would not importantly affect the dynamic interaction between interacting charged bodies?

The present technical knowledge of electromagnetic theory and electrons include these four items. We ask if this additional knowledge affects the historical interpretation of quantum theory, and, if so, how? We find combining items (i) and (iv) yields Schrödinger's equation as an energy conservation law. However, since general laws are derivable from quite disparate physical models the derivation is a necessary but insufficient condition for any proposed model. Using (i), (iii), and (iv) the full set of electromagnetic fields within a source-free region is derivable. Quite differently from energy conservation, electromagnetic fields are a unique result of sources within a region and on its boundaries, and *vice versa*. Consider concentric spheres: the inner with a small radius that just circumscribes a radiating atom and the outer of infinite radius. Imposing the measured kinematic properties of atomic radiation as a boundary condition gives the fields on the inner sphere. Viewing the outer shell as an ideal absorber from which no fields return, the result is an expression for the full set of electromagnetic photon fields at a finite radius. Postulate (iv) is that electrons are distributed entities. An electron somehow retains its individual identity while distributing itself,

with no time delay, over the full physical extent of a trapping eigenstate. Results include that an electron traveling from point A to point B goes by all possible routes and, when combined with electrodynamic forces, provides atomic stability.

With these postulates the interpretation of quantum theory developed here preserves the full applicability of electromagnetic field theory within atoms and, in turn, permits the construction of a new understanding of quantum theory. Both the magnitude and the consequences of phase quadrature, radiation reaction forces have been ignored. Yet these forces, as we show, and (iv) are responsible both for the inherent stability of isolated atoms and for a nonlinear, regenerative drive of transitions between eigenstates, that is, quantum jumps. The nonlinearity forces the Ritz power-frequency relationship between eigenstates and (ii) bans radiation of other frequencies, including transients. The radiation reaction forces require energy reception to occur at only a single frequency.

Once absorbed, the electron spreads over all available states in what might be called a wave function expansion. Since only one frequency has an available radiation path, if the same energy is later emitted the expanded wave function must collapse to the emitting-absorbing pair of eigenstates to which the frequency applies. With this view, wave function expansion after absorption and collapse before emission obey the classical rules of statistical mechanics. The radiation field, not the electron, requires the seeming difference between quantum and classical effects, i.e. wave function collapse upon measurement.

Since we reproduce the quantum theory equations, is our argument science or philosophy? For some, a result becomes a science, only if a critical experiment is found and only if it survives the test. But by that argument astronomy is and remains a philosophy. With astronomy, however, if the philosophy consistently matches enough observations with enough variety and contradicts none of them it becomes an accepted science. In our view quantum theory is, in many ways, also an observational science. A philosophy becomes a science only after it consistently matches many observations made under a large enough variety of circumstances. Our view survives this test.

Our interpretation differs dramatically from the historical one; our postulates are fewer in number and consistent with classical physics. With our postulates events precede their causes and, if all knowledge were available, would be predictable. By our interpretation of quantum theory, however,

there is no obvious way all knowledge could become available since our ability to characterize eigenstate electrons is simply too limited.

Webster's dictionary defines the Law of Parsimony as an "economy of assumption in reasoning," which is also the connotation of "Ockham's razor." Since the number of postulates necessary with this interpretation of quantum theory are both fewer in number and more consistent with the classical sciences by the Law of Parsimony the view presented in this book should be accepted.

Dale M. Grimes
Craig A. Grimes
University Park, PA, USA

Contents

| | |
|--|-----------|
| <i>Foreword</i> | vii |
| <i>Prologue</i> | xv |
| Chapter 1 Classical Electrodynamics | 1 |
| 1.1 Introductory Comments | 1 |
| 1.2 Space and Time Dependence upon Speed | 2 |
| 1.3 Four-Dimensional Space Time | 4 |
| 1.4 Newton's Laws | 6 |
| 1.5 Electrodynamics | 7 |
| 1.6 The Field Equations | 10 |
| 1.7 Accelerating Charges | 13 |
| 1.8 The Electromagnetic Stress Tensor | 14 |
| 1.9 Kinematic Properties of Fields | 17 |
| 1.10 A Lemma for Calculation of Electromagnetic Fields | 19 |
| 1.11 The Scalar Differential Equation | 21 |
| 1.12 Radiation Fields in Spherical Coordinates | 23 |
| 1.13 Electromagnetic Fields in a Box | 26 |
| 1.14 From Energy to Electric Fields | 29 |
| References | 30 |
| Chapter 2 Selected Boundary Value Problems | 31 |
| 2.1 Traveling Waves | 32 |
| 2.2 Scattering of a Plane Wave by a Sphere | 34 |
| 2.3 Lossless Spherical Scatterers | 40 |
| 2.4 Biconical Transmitting Antennas, General Comments | 45 |
| 2.5 Fields | 47 |
| 2.6 TEM Mode | 49 |
| 2.7 Boundary Conditions | 52 |
| 2.8 The Defining Integral Equations | 56 |
| 2.9 Solution of the Biconical Antenna Problem | 58 |
| 2.10 Power | 64 |
| 2.11 Biconical Receiving Antennas | 67 |
| 2.12 Incoming TE Fields | 71 |

| | | |
|---|--|------------|
| 2.13 | Incoming TM Fields | 71 |
| 2.14 | Exterior Fields, Powers, and Forces | 75 |
| 2.15 | The Cross-Sections | 80 |
| 2.16 | General Comments | 84 |
| 2.17 | Fields of Receiving Antennas | 86 |
| 2.18 | Boundary Conditions | 88 |
| 2.19 | Zero Degree Solution | 91 |
| 2.20 | Non-Zero Degree Solutions | 92 |
| 2.21 | Surface Current Densities | 94 |
| 2.22 | Power | 95 |
| | References | 98 |
| Chapter 3 Antenna Q | | 99 |
| 3.1 | Instantaneous and Complex Power in Circuits | 100 |
| 3.2 | Instantaneous and Complex Power in Fields | 103 |
| 3.3 | Time Varying Power in Actual Radiation Fields | 105 |
| 3.4 | Comparison of Complex and Instantaneous Powers | 108 |
| 3.5 | Radiation Q | 112 |
| 3.6 | Chu's Q Analysis, TM Fields | 115 |
| 3.7 | Chu's Q Analysis, Exact for TM Fields | 120 |
| 3.8 | Chu's Q Analysis, TE Field | 122 |
| 3.9 | Chu's Q Analysis, Collocated TM and TE Modes | 123 |
| 3.10 | Q the Easy Way, Electrically Small Antennas | 124 |
| 3.11 | Q on the Basis of Time-Dependent Field Theory | 125 |
| 3.12 | Q of a Radiating Electric Dipole | 131 |
| 3.13 | Q of Radiating Magnetic Dipoles | 136 |
| 3.14 | Q of Collocated Electric and Magnetic Dipole Pair | 137 |
| 3.15 | Q of Collocated Pairs of Dipoles | 140 |
| 3.16 | Four Collocated Electric and Magnetic Multipoles | 144 |
| 3.17 | Q of Multipolar Combinations | 148 |
| 3.18 | Numerical Characterization of Antennas | 152 |
| 3.19 | Experimental Characterization of Antennas | 158 |
| 3.20 | Q of Collocated Electric and Magnetic Dipoles: Numerical and Experimental Characterizations | 162 |
| | References | 169 |
| Chapter 4 Quantum Theory | | 170 |
| 4.1 | Electrons | 172 |
| 4.2 | Dipole Radiation Reaction Force | 173 |
| 4.3 | The Time-Independent Schrödinger Equation | 180 |
| 4.4 | The Uncertainty Principle | 184 |
| 4.5 | The Time-Dependent Schrödinger Equation | 186 |

| | | |
|---|--|------------|
| 4.6 | Quantum Operator Properties | 188 |
| 4.7 | Orthogonality | 189 |
| 4.8 | Harmonic Oscillators | 191 |
| 4.9 | Electron Angular Momentum, Central Force Fields | 194 |
| 4.10 | The Coulomb Potential Source | 196 |
| 4.11 | Hydrogen Atom Eigenfunctions | 199 |
| 4.12 | Perturbation Analysis | 202 |
| 4.13 | Non-Ionizing Transitions | 203 |
| 4.14 | Absorption and Emission of Radiation | 205 |
| 4.15 | Electric Dipole Selection Rules for One Electron Atoms | 208 |
| 4.16 | Electron Spin | 210 |
| 4.17 | Many-Electron Problems | 211 |
| 4.18 | Measurement Discussion | 214 |
| | References | 214 |
| Chapter 5 Radiative Energy Exchanges | | 216 |
| 5.1 | Blackbody Radiation, Rayleigh–Jeans Formula | 216 |
| 5.2 | Planck’s Radiation Law, Energy | 218 |
| 5.3 | Planck’s Radiation Law, Momentum | 220 |
| 5.4 | The Zero Point Field | 225 |
| 5.5 | The Photoelectric Effect | 226 |
| 5.6 | Power-Frequency Relationships | 229 |
| 5.7 | Length of the Wave Train and Radiation Q | 233 |
| 5.8 | The Extended Plane Wave Radiation Field | 235 |
| 5.9 | Gain and Radiation Pattern | 239 |
| 5.10 | Kinematic Values of the Radiation | 241 |
| | References | 246 |
| Chapter 6 Photons | | 247 |
| 6.1 | Telefields and Far Fields | 248 |
| 6.2 | Evaluation of Sum S_{12} on the Axes | 253 |
| 6.3 | Evaluation of Sums S_{22} and S_{32} on the Polar Axes | 257 |
| 6.4 | Evaluation of Sum S_{32} in the Equatorial Plane | 261 |
| 6.5 | Evaluation of Sum S_{22} in the Equatorial Plane | 263 |
| 6.6 | Summary of the Axial Fields | 265 |
| 6.7 | Radiation Pattern at Infinite Radius | 267 |
| 6.8 | Multipolar Moments | 270 |
| 6.9 | Multipolar Photon-Field Stress and Shear | 275 |
| 6.10 | Self-Consistent Fields | 285 |
| 6.11 | Energy Exchanges | 288 |
| 6.12 | Self-Consistent Photon-Field Stress and Shear | 291 |
| 6.13 | Thermodynamic Equivalence | 298 |
| 6.14 | Discussion | 303 |
| | References | 305 |

| | |
|---|------------|
| Chapter 7 Epilogue | 306 |
| 7.1 Historical Background | 306 |
| 7.2 Overview | 311 |
| 7.3 The Radiation Scenario | 316 |
| References | 320 |
| Appendices | 323 |
| 1 Introduction to Tensors | 323 |
| 2 Tensor Operations | 326 |
| 3 Tensor Symmetry | 327 |
| 4 Differential Operations on Tensor Fields | 328 |
| 5 Green's Function | 330 |
| 6 The Potentials | 335 |
| 7 Equivalent Sources | 335 |
| 8 A Series Resonant Circuit | 339 |
| 9 Q of Time Varying Systems | 341 |
| 10 Bandwidth | 344 |
| 11 Instantaneous and Complex Power in Radiation Fields | 345 |
| 12 Conducting Boundary Conditions | 347 |
| 13 Uniqueness | 350 |
| 14 Spherical Shell Dipole | 351 |
| 15 Gamma Functions | 354 |
| 16 Azimuth Angle Trigonometric Functions | 356 |
| 17 Zenith Angle Legendre Functions | 359 |
| 18 Legendre Polynomials | 363 |
| 19 Associated Legendre Functions | 366 |
| 20 Orthogonality | 367 |
| 21 Recursion Relationships | 368 |
| 22 Integrals of Legendre Functions | 375 |
| 23 Integrals of Fractional Order Legendre Functions | 377 |
| 24 The First Solution Form | 382 |
| 25 The Second Solution Form | 384 |
| 26 Tables of Spherical Bessel, Neumann, and Hankel Functions | 387 |
| 27 Spherical Bessel Function Sums | 392 |
| 28 Static Scalar Potentials | 395 |
| 29 Static Vector Potentials | 400 |
| 30 Full Field Expansion | 405 |
| References | 412 |
| <i>Index</i> | 413 |

Prologue

A radiating antenna sits in a standing energy field of its own making. Even at the shortest wavelengths for which antennas have been made, if the length-to-wavelength ratio is too small the amount of standing field energy is so large it essentially shuts off energy exchange. Yet an atom in the act of exchanging such energy may be scaled as an electrically short antenna, and standing energy is ignored by conventional quantum theory seemingly without consequence. Why, in one case, is standing energy dominant and, in the other, of no consequence? The framers of the historic interpretation of quantum theory could not have accounted for standing energy since an analysis of it was first formulated some twenty years after the interpretation was accomplished. Similar statements apply to the power-frequency relationships of nonlinear systems and to the possible unidirectional radiation of superimposed electromagnetic modes. Similarly, a significant and essential feature of eigenstate electrons is a time average charge distributed throughout the state. Is the calculated charge density distribution stationary or is it the time average value of a moving “point” charge? In this book we form a simplified and deterministic interpretation of quantum theory that accounts for standing energy in the radiation field, field directivity, and the power-frequency relationships using an extended electron model. It is not necessary for us to stipulate details of an extended electron. A model that expands throughout the volume of an eigenstate, one that occupies enough of an eigenstate to be stable and traverses the rest, or a nonlocal electron model are all satisfactory. By nonlocal we imply that if one entangled, nonlocal electron adapts instantaneously to changes in the other, similar intra-electron events may also occur.

We find that all the above play integral and essential roles in atomic stability and energy exchanges. Together they form a complete electromagnetic field solution of quantum mechanical exchanges of electromagnetic energy without the separate axioms of the historic interpretation.

Stable atoms occupy space measured on the picometer scale of dimensions and exchange energy during periods measured on the picosecond scale of time. Since this dimensional combination precludes direct observation, it is necessary to infer active atomic events from observations over much larger distances and times. When detailed atomic behavior first became available theoreticians attempting to understand the results separated themselves into two seemingly disparate groups, groups we refer to as scientific pragmatists and scientific idealists. The pragmatists proposed new axioms as necessary to explain the new information. The idealists sought to integrate the new information into the existing laws of theoretical physics. Since the pragmatists could successfully explain most atomic level phenomena and idealists could not, most physicists came to accept the views of the pragmatists, in spite of conceptual difficulties. Even with rejection of the other physics, however, the pragmatists could not explain a thought experiment proposed by Einstein, Podolsky and Rosen. That experiment led to the following conclusion: The behavior of two entangled particles shows that either quantum theory is incomplete or events occurring at one particle affects the other with no time delay and independently of the physical separation between them.

Acceptance of the pragmatic viewpoint also required dramatic changes both to physical and philosophical thought. For example, they concluded that equations of classical electromagnetism partially, but not fully, apply on an atomic scale of dimensions. Yet, the theory of electromagnetism shows no inherent distance or time-scale limitations. A primary purpose of this book is to derive an expression for the full set of fields present during photon emission and absorption.

Although this book is primarily a monograph, early versions were used as a text for topical courses in electromagnetic theory in the Electrical Engineering Departments of the University of Michigan and the Pennsylvania State University. A later version served as a text for a topical course in theoretical physics in the Department of Physics and Astronomy of the University of Kentucky; it was after the latter course that we began systematic work on this book. Throughout the book the theorems used were carefully reexamined and the emphasis made that best met the needs of the book. For the same purpose we extract freely and without prejudice from accepted works of electrical engineering, on the one hand, and physics, on the other; too often there is imperfect communication between the two groups. The result is an innovative way of viewing scattering phenomena, radiation exchanges, and energy transfer by electromagnetic fields.

The equations of classical electromagnetism are derived and developed in Chapter 1. The overwhelming characteristic of classical electromagnetism, in stark contrast with the pragmatic view of quantum theory, is the simplicity of the underlying postulates from which it follows. In Chapter 2 the equations developed in Chapter 1 are applied to a series of increasingly complex boundary value problems. The choice of solved problems is based on two criteria: First, the solution form is a general one that, when the modal coefficients are properly chosen, applies to any electromagnetic problem, and hence to atomic radiation. Second, each solution is electromagnetically complete, even though it is in the form of an infinite series of constant coefficients times products of radial and harmonic functions. Completeness is required to assure that no solutions have been overlooked. To illustrate the importance of completeness, note, for example, that historically the character of receiving current modes on antennas was not correctly estimated. The inherently and magnificently structured symmetry of the current modes was not and could not have been appreciated until the complete biconical receiving antenna solution became available in 1982. That is to say, the technological culture of the mid to late twentieth century, with ubiquitous antennas, did not understand the modal structure of the simplest of receiving antennas until a complete mathematical solution became available in 1982. Similarly, we cannot be sure we fully understand a radiating atom without a complete solution.

Chapter 3 deals with local standing energy fields associated with electromagnetic energy exchanges. To analyze them, it is necessary to re-examine complex power and energy in radiation fields. The use of complex power is nearly universal in the analysis of electric fields. Although complex circuit analysis provides the correct power at any terminal pair, expressions for complex power in a radiation field suppress a radius-dependent phase factor. No equation that depends upon the phase of field power versus radius can be solved using only complex power. There are many ways to avoid the difficulty; our solution is to obtain a time domain description of the fields then use it to calculate modal field energies. From them, we calculate the ratio of source-associated field energy to the average energy per radian radiated permanently away from the antenna. We confirm earlier work showing that for most antennas the ratio increases so rapidly with decreasing electrical size that antennas are subject to severe operational limitations. Nearly all-modal combinations are subject to such limitations. We also derive the multimodal combination to which such limitations do not apply.

Chapter 4 contains a brief review of quantum theory that is conventional in most ways, but unconventional in the treatment of atomic stability. We show that the standing energy of a dipole field generated by an oscillating point electron creates an expansive radiation reaction pressure on the electron. That pressure is the same order of magnitude as the trapping Coulomb pressure and is three orders of magnitude larger than the pressure of the commonly accepted radiation reaction force. We suggest that it forces an eigenstate electron to extend into charge and current densities distributed throughout the eigenstate, analogous to an oil drop spreads across a pond of water. A nonlocal electron is a satisfactory operational model for our purposes. The extended electron is not small compared with atomic dimensions and, under the influence of radiation reaction forces, forms a non-radiating array of charge and current densities. Such arrays are inherently stable and interaction between the intrinsic and orbital magnetic moments produces a continuous torque and assures continuous motion of the parts. This model and energy conservation forms an adequate basis upon which to build Schrödinger's time-independent wave equation; his time-dependent equation follows if the system remains in near-equilibrium. In this way, Schrödinger's equations are the equivalent of ensemble energy expressions in classical thermodynamics. In both places, general results are obtained without detailed knowledge of the ensemble.

Schrödinger's time-dependent wave equation treats state transitions by describing the initial and final states. Although answers are unquestionably correct, the approach gives no information about the electromagnetic fields present during emission and absorption processes, yet electromagnetic theory shows that near fields must exist. It is abundantly clear with this analysis that the existing interpretation of quantum theory is not a sufficient foundation upon which to build the full set of photon fields; with it there is and can be no counterpart to the full equation sets of Chapter 2.

Chapter 4 contains the conclusion that molecules, described as harmonic oscillators, possess a minimum level of kinetic energy even at absolute zero temperature. Chapter 5 begins with equilibrium between electromagnetic radiation and matter, i.e. the Planck radiation field, and shows there is a minimum, zero point, intensity of radiation that permeates all space. The theory shows that a requirement of equilibrium is reciprocity between the emission and absorption processes; that is, a simple time reversal switches between energy absorption and emission. It was shown in Chapter 2 that with linear systems the exchanged energy-to-momentum ratio is greater or

equal to c for emission and less than or equal to c for absorption. Equilibrium conditions, therefore, can only be met with equalities. This requirement, in turn, requires absorption without a scattered field and emission in one direction only, i.e. the emitted field has no angular spread for at least the far field energy travels in a single direction. Next we show that the Manley Rowe equations, which are meaningful *only with nonlinear systems*, correctly describe the Ritz power-frequency relationships of photons; yet the Schrödinger and Dirac equations are linear. We then impose full directivity as a boundary condition on a general, multimodal field expansion as developed in Chapter 1. The resulting modal fields are members of the set of resonant modes discussed in Chapter 3: The set with spherical Bessel functions describes a plane wave and with spherical Hankel functions is resonant. The standing energy limitations otherwise applicable to electrically small radiators do not apply. General properties of such modes are determined and discussed.

In Chapter 6 these results are combined and used to determine all radiated fields, near and far, during the inherently nonlinear eigenstate transitions, i.e. during photon exchanges. First we use a multipolar expansion about the field source to detail as much as possible the electromagnetic characteristics of photon fields, including internal pressure and shear on sources or sinks. We next use the method of self-consistent fields to express the photon fields in an expansion from infinite radius inward. This expansion permits the evaluation of the radiation reaction force of a photon field on its generating electron as a function of radius. We find that the radiation reaction pressure on the surface of a spherical, radiating atom is at least many thousands of times larger than the Coulomb attractive pressure. The reaction pressure is properly directed and phased to drive the extended electron nonlinearly and regeneratively to a rapid buildup of exchanged power. Therefore radiation in accordance with the Manley Rowe power frequency relations occurs and continues until all available energy is exchanged. The result is a physically simple, electromagnetically complete, deterministic interpretation of quantum theory.

The material is reviewed and summarized in Chapter 7, the Epilogue.

This page intentionally left blank

CHAPTER 1

Classical Electrodynamics

There are two quite disparate approaches to electromagnetic field theory. One is a deductive approach that begins with a single relativistic source potential and deduces from it the full slate of classical equations of electromagnetism. The other is an inductive approach that begins with the experimentally determined force laws and induces from them, incorporating new facts as needed, until the Maxwell equations are obtained. Although the theory was developed using the inductive approach, it is the deductive method that shows the majestic simplicity of electromagnetism.

The inductive approach is commonly used in textbooks at all levels. Coulomb's law is the usual starting point, with other effects included as needed until the full slate of measurable quantities are obtained. From this viewpoint, the potentials are but mathematical artifices that simplify force field calculations. They simplify the calculation necessary to solve for the force fields but are without intrinsic significance. The deductive approach begins with a limited axiomatic base and develops a potential theory from which, in turn, follow the force fields. In 1959 Aharonov and Bohm, using the premise that potential has a special significance, predicted an effect that was confirmed in 1960, the Aharonov–Bohm effect: Magnetic field quantization is affected by a static magnetic potential even in a region void of force fields. We conclude that the magnetic potential has a physical significance in its own right and has meaning in a way that extends beyond the calculation of force fields. There is physical significance contained in the deductive approach that is not present in the inductive one.

1.1. Introductory Comments

To begin the deductive approach, consider that the universe is totally empty of condensed matter but does contain light. What is the speed of the light? Since there is no reference frame by which to measure it, the question is moot. Therefore, introduce an asteroid large enough to support an observer

and his equipment, which determines the speed of light passing him to be v_A . Since there is nothing else in the universe, a question about the speed of the asteroid is moot. Next, introduce a second asteroid, identical to the first but separated far enough to be independent by any means of which we are currently aware. An observer on the second asteroid determines the speed of light passing him to be v_B . Will the measured values be the same? By the cosmological principle, an experiment run in one local four-space yields the same results as an identical experiment run in a different local four-space. Therefore we expect that $v_A = v_B = c$.

Next, bring the asteroids into the same local region. Either the speeds depend upon the magnitude of the local masses or they do not, and if they do not, there is no change in speed. However, in the local region, a relative speed between identical asteroids A and B may be determined. Since there is no way one asteroid can be preferred over the other in an otherwise empty universe, the two observers continue to measure the same speed. This condition requires that the speed of light be independent of the relative speed of the system on which it is measured. Next, bring in other material, bit by bit, until the universe is in its present form, and the conclusion remains the same. The speed of light is independent of the speed of the object on which it is measured, independently of the speed of other objects.

1.2. Space and Time Dependence upon Speed

Let a pulse of light be emitted from an origin in reference frame F and observed in reference frame F'. If the speed of light is the same in all reference frames, if the two frames are in relative motion, and if the origins coincide at the time the light is emitted, the light positions as measured in the two frames are:

$$x^2 + y^2 + z^2 - c^2t^2 = x'^2 + y'^2 + z'^2 - c'^2t'^2 \quad (1.2.1)$$

If the relative speed is such that F' is moving at speed ν in the z -direction with respect to F, then at low speeds:

$$x' = x; \quad y' = y; \quad z' = (z - \nu t); \quad t' = t \quad (1.2.2)$$

Since Eq. (1.2.1) is not satisfied by Eq. (1.2.2), it follows that Eq. (1.2.2) does not extend to speeds that are a significantly large fraction of c . To obtain a transition that is linear in the independent variables, and that goes

to Eq. (1.2.2) in the low speed limit, consider the linear transformation of the form:

$$x' = x; \quad y' = y; \quad z' = \gamma(z - vt); \quad t' = At + Bz \quad (1.2.3)$$

Parameters γ , A and B are undetermined but independent of both position and time. Since Eq. (1.2.3) approaches Eq. (1.2.2) in the limit of velocity v much less than c , in that limit:

$$\gamma = 1; \quad A = 1; \quad B = 0 \quad (1.2.4)$$

Since the coordinates are independent variables, combining Eqs. (1.2.1) and (1.2.3) and solving shows that:

$$\begin{aligned} z^2(\gamma^2 - 1 - c^2B^2) &= 0; \quad t^2(c^2 + \gamma^2v^2 - c^2A^2) = 0; \\ zt(v\gamma^2 + ABc^2) &= 0 \end{aligned} \quad (1.2.5)$$

Solving Eq. (1.2.5) yields:

$$A = \gamma = (1 - v^2/c^2)^{-1/2}; \quad B = -(\gamma v/c^2) \quad (1.2.6)$$

Combining yields the Lorentz transformation equations:

$$x' = x; \quad y' = y; \quad z' = \gamma(z - vt); \quad t' = \gamma(t - (vz/c^2)) \quad (1.2.7)$$

This transformation preserves the speed of light in inertial frames.

Equation (1.2.7) forms a sufficient basis upon which to determine results if events in one frame of reference are observed in another one. Let the observer be in the unprimed frame. A stick of length L_0 as determined in the moving frame, in which it is stationary, lies along the z -axis. It moves at speed v past the observer in the z -direction. A flash of light illuminates the region, during which time the observer determines the positions of the ends of the moving stick, z_1 and z_2 . It follows from Eq. (1.2.7) that the measured positions are:

$$z'_1 = \gamma(z_1 - vt_0) \quad \text{and} \quad z'_2 = \gamma(z_2 - vt_0) \quad (1.2.8)$$

The length as measured in the stationary frame is:

$$L = (z_2 - z_1) = (z'_2 - z'_1)/\gamma = L_0/\gamma \quad (1.2.9)$$

It follows that:

$$L = L_0(1 - v^2/c^2)^{1/2} \leq L_0 \quad (1.2.10)$$

The observed length of the stick is less than that measured in the rest frame; this fractional contraction is the Lorentz contraction.

Next, pulses of light are issued at times t'_2 and t'_1 , again in the moving frame. When does a stationary observer see them, and what is the time interval between them? Using Eq. (1.2.7) gives:

$$t'_2 = \gamma(t_2 - vz_2/c^2) \quad \text{and} \quad t'_1 = \gamma(t_1 - vz_1/c^2) \quad (1.2.11)$$

From Eq. (1.2.11) the time difference in the frame at which the two sources are stationary is:

$$T_0 = t'_2 - t'_1 = \gamma[(t_2 - t_1) - v(z_2 - z_1)/c^2] = \gamma T(1 - v^2/c^2) \quad (1.2.12)$$

T is the time measured in the stationary frame. Solving for T gives:

$$T = \gamma T_0 = \frac{T_0}{(1 - v^2/c^2)^{1/2}} \geq T_0 \quad (1.2.13)$$

The observer measures the time duration between pulses to be more than that measured in the rest frame; this time expansion is time dilatation.

1.3. Four-Dimensional Space Time

The equality of the speed of light in all inertial frames is the basis for a system of 4-vectors. Let x_1, x_2, x_3 represent the three spatial axes x, y, z of three dimensions and $x_4 = ict$ where $i = \sqrt{-1}$. The four space-time dimensions are:

$$(x_1, x_2, x_3, x_4) \quad (1.3.1)$$

Since three of the axes determine lengths and one determines time, a three-dimensional rotation represents a change in spatial orientation and a four-dimensional rotation includes a change in time. Such four-dimensional rotations are Lorentz transformations. These transformations are usually simple and contain a high degree of symmetry. Such transformations are covariant with respect to changes in coordinate systems; that is, an equation that represents reality in one reference frame has the same form in all other inertial frames.

The imaginary property of the fourth dimension represents an essential difference from spatial ones: the squares of the space coefficients and time coefficients have different signs. For notational purposes we use Roman or Greek subscripts to indicate, respectively, three- or four-dimensional tensors. For example, the rotation matrix element in four dimensions is $c_{\mu\nu}$

where, for velocities v directed along the x_1 -axis:

$$c_{\mu\nu} = \begin{pmatrix} \gamma & 0 & 0 & i\gamma v/c \\ 0 & 1 & 0 & 0 \\ 0 & 0 & 1 & 0 \\ -i\gamma v/c & 0 & 0 & \gamma \end{pmatrix} \quad (1.3.2)$$

Four-dimensional and three-dimensional direction cosines follow similar laws:

$$c_{\mu\nu} = c_{\nu\mu}; \quad c_{\mu\nu}c_{\mu\rho} = \delta_{\nu\rho}; \quad \det |c_{\mu\nu}| = 1 \quad (1.3.3)$$

The Lorentz direction cosines $c_{\mu\nu}$ are:

$$x'_\mu = c_{\mu\nu}x_\nu \quad (1.3.4)$$

The proper time interval, $\Delta\tau$, between two events with space-time coordinates spaced Δx_α apart is defined to be:

$$(\Delta\tau)^2 = -\frac{1}{c^2}\Delta x_\alpha\Delta x_\alpha \quad (1.3.5)$$

Using three-dimensional notation, the proper time difference is

$$(\Delta\tau)^2 = (\Delta t)^2 - \frac{(\Delta\mathbf{r})^2}{c^2} \quad (1.3.6)$$

Since $(\Delta\tau)^2$ can be zero, positive, or negative, $\Delta\tau$ may be zero, real, or imaginary. Since the speed of light is the same in all reference frames, by Eq. (1.2.1) the proper time is also the same in all reference frames. If it is real, it is “time-like” and if imaginary, it is “space-like”. If time-like, the proper time is the time separation of the two events in the same frame. If space-like, there is a frame in which c times the proper time is the spatial separation of the two events that are simultaneous in that frame.

With τ as proper time, consider the 4-vector defined by the expression:

$$U_\mu = \frac{dx_\mu}{d\tau} \quad (1.3.7)$$

Since both x_μ and τ are independent of details of the particular inertial frame in which it is measured, so is U_μ ; U_μ is therefore a 4-vector with the four components:

$$\begin{aligned} U_1 &= \frac{dx}{d\tau} = \frac{dx}{dt} \frac{dt}{d\tau} = \gamma v_x; & U_2 &= \frac{dy}{d\tau} = \frac{dy}{dt} \frac{dt}{d\tau} = \gamma v_y \\ U_3 &= \frac{dz}{d\tau} = \frac{dz}{dt} \frac{dt}{d\tau} = \gamma v_z; & U_4 &= \frac{d(ict)}{d\tau} = \gamma ic \end{aligned} \quad (1.3.8)$$

The three-dimensional velocity components are v_i and the 4-velocity components are U_μ .

A particle of mass m_0 with 4-velocity U_μ has 4-momentum given by:

$$P_\mu = m_0 U_\mu \quad (1.3.9)$$

Combining shows the momentum components to be:

$$\mathbf{p} = \gamma m_0 \mathbf{v}; \quad p_4 = \gamma m_0 i c = iW/c; \quad W = \gamma m_0 c^2 \quad (1.3.10)$$

The quantity W , defined by Eq. (1.3.10), is the energy associated with the moving mass.

The binomial expansion is:

$$(1 \pm a)^n = 1 \pm na + \frac{n}{2!}(n-1)a^2 \pm \dots \quad (1.3.11)$$

This equation combines with the definition of γ , see Eq. (1.2.6), to show that:

$$\gamma = 1 + \frac{v^2}{2c^2} + \frac{3v^4}{8c^4} + \dots \quad (1.3.12)$$

Combining Eqs. (1.3.10) and (1.3.12) shows the total energy of the particle:

$$W = m_0 c^2 \left[1 + \frac{v^2}{2c^2} + \frac{3v^4}{8c^4} + \dots \right] \quad (1.3.13)$$

In the rest frame m_0 is the rest mass. The particle energy is:

$$W_0 = m_0 c^2 \quad (1.3.14)$$

By Eq. (1.3.14), the first term of Eq. (1.3.13) is the self-energy of the mass. The second term is the kinetic energy at low speeds and the higher order terms complete the evaluation of the kinetic energy of the mass at any speed.

1.4. Newton's Laws

The Minkowski force is defined to be:

$$F_\mu = \frac{d}{d\tau} P_\mu \quad (1.4.1)$$

This force is a 4-vector with the x -directed component:

$$F_1 = \frac{d}{d\tau} (m_0 U_1) = \gamma \frac{\partial}{\partial t} (\gamma m_0 v_x) \quad (1.4.2)$$

The corresponding three-dimensional force component is:

$$F_x = \frac{\partial}{\partial t} (\gamma m_0 v_x) \quad (1.4.3)$$

The factor γ in Eq. (1.4.3) was known before the full relativistic effect was understood. Although relativity makes it abundantly clear that the result

is a space-time effect, it was historically interpreted as an increase in mass whereby the effective mass m is a function of speed:

$$m = \gamma m_0 \quad (1.4.4)$$

Even with relativity, the nomenclature remains and by definition the effective mass of a moving particle is equal to Eq. (1.4.4). Since the 4-momentum is a 4-vector, it is conserved between Lorentz frames. That is,

$$W_0^2 = W^2 - p^2 c^2 \quad (1.4.5)$$

The energy is related to momentum, in any given frame, as:

$$W^2 = m_0^2 c^4 + p^2 c^2 \quad (1.4.6)$$

Since W is second order in v/c , three-momentum is constant in low speed inertial frames. Energy is also nearly conserved. However, in high-energy systems neither energy nor momentum is conserved, only the combination. This example illustrates a general characteristic of 4-tensors that at low speeds the real and imaginary parts are separately conserved but at high speeds only the combined magnitude is conserved.

1.5. Electrodynamics

The three scalars defined so far are speed, c , time interval between events in a rest frame, τ , and mass, m_0 . A fourth is electric charge, q ; electric charge can have either sign. Just as an intrinsic part of any mass is the associated gravitational field, G , an intrinsic part of charge is the associated 4-vector potential field A_μ . Consider that the individual charges are much smaller than other dimensions and that there are many of them. For this case choose a differential volume, with dimensions (x_1, x_2, x_3) , in which each dimension is much less than any macroscopic dimension of interest but contains large numbers of charges. If both conditions are met, the tools of calculus apply. Charge density ρ is defined to be the charge per unit volume at a point. Charge density ρ_0 is defined in a frame in which the time-average position is at rest. Observers in fixed and moving frames see the same total charge but, because of the Lorentz contraction, the moving observer determines the volume containing it to be smaller by a factor of γ . Therefore, the charge density in a moving frame is increased by the factor:

$$\rho = \gamma \rho_0 \quad (1.5.1)$$

If the charge density moves with 4-velocity U_μ in a way similar to three dimensions, the 4-current density is defined to be:

$$\mathbf{J}_\mu = \rho_0 U_\mu = \{\gamma\rho_0\mathbf{v}, \gamma ic\rho_0\} = \{\mathbf{J}, ic\rho\} \quad (1.5.2)$$

The vector terms within the curly brackets, identified by bold font, indicate the first three dimensions, and the scalar term represents the fourth dimension. The 4-divergence of the current density is:

$$\frac{\partial \mathbf{J}_\mu}{\partial X_\mu} = \nabla \cdot \mathbf{J} + \frac{\partial \rho}{\partial t} = 0 \quad (1.5.3)$$

The first equality of Eq. (1.5.3) follows from definition of terms and the second is true if and only if net charge is neither created nor destroyed. Pair production or annihilation may occur but there is no change in the total charge. The zero 4-divergence shows that the net change in the four-current is always equal to zero. Physically a net change in the total charge does not occur and charges are created and destroyed only in canceling pairs.

The 4-vector potential field $A_\mu(X_\gamma)$ is defined to be the potential that satisfies the differential equation:

$$\frac{\partial^2 A_\nu}{\partial X_\beta \partial X_\beta} = -\mu \mathbf{J}_\nu \quad (1.5.4)$$

Constant μ is defined to be the permeability of free space; it is a dimension-determining constant and defined to equal $4\pi/10^7$ Henrys/meter.

Taking the 4-divergence of Eq. (1.5.4) then combining with Eq. (1.5.3) gives:

$$\frac{\partial}{\partial X_\nu} \frac{\partial^2}{\partial X_\beta \partial X_\beta} A_\nu = \frac{\partial^2}{\partial X_\beta \partial X_\beta} \frac{\partial A_\nu}{\partial X_\nu} = -\mu \frac{\partial \mathbf{J}_\nu}{\partial X_\nu} = 0$$

Combining, it follows that:

$$\partial A_\nu / \partial X_\nu = 0 \quad (1.5.5)$$

Equation (1.5.5) shows that the divergence of A_ν is zero, from which it follows that, like charge, the total amount of 4-potential does not change. If transitions are made between different reference frames changes occur in the components of the potential but not in the sum over all four components.

The four-dimensional Laplacian of Eq. (1.5.4) may be integrated over all space to obtain an expression for the potential itself. By Eq. (A.6.2) the

potential of a moving charge is:

$$A_\alpha(X_\gamma) = \frac{\mu}{4\pi} \iiint \frac{J_\alpha(\mathbf{r}', t' - R/c)}{(R - \mathbf{R} \cdot (\mathbf{v}/c))} dV' \quad (1.5.6)$$

The integral is over all source-bearing regions, dV' is differential volume, X_γ are the 4-coordinates of the field point, X'_γ are the 4-coordinates at the source point, \mathbf{R} is the vector from the source point to the field point. At low speeds Eq. (1.5.6) simplifies to:

$$A_\alpha(X_\gamma) = \frac{\mu}{4\pi} \iiint \frac{J_\alpha(\mathbf{r}', t' - R/c)}{R(X_\gamma, X'_\gamma)} dV' \quad (1.5.7)$$

Substituting in the three-dimensional values of J_α results in the three-dimensional potentials:

$$\begin{aligned} \mathbf{A}(\mathbf{r}, t) &= \frac{\mu}{4\pi} \iiint \frac{\mathbf{J}(\mathbf{r}', t' - R/c)}{R(\mathbf{r} - \mathbf{r}', t')} dV' \\ \Phi(\mathbf{r}, t) &= -icA_4(\mathbf{r}, t) = \frac{1}{4\pi\epsilon} \iiint \frac{\rho(\mathbf{r}', t' - R/c)}{R(\mathbf{r} - \mathbf{r}', t')} dV' \end{aligned} \quad (1.5.8)$$

The constant ϵ is defined to be the permittivity of free space; it is a dimension determining constant and defined to be exactly equal to $1/(\mu c^2)$ Farads/meter.

For a point charge, instead of a charge distribution, the corresponding 4-potential is:

$$A_\alpha(X_\gamma) = \frac{\mu q}{4\pi} \frac{U_\alpha(\mathbf{r}', t' - R/c)}{(R - \mathbf{R} \cdot \mathbf{v}/c)} \quad (1.5.9)$$

The three-dimensional potentials are:

$$\begin{aligned} \mathbf{A}(\mathbf{r}, t) &= \frac{\mu}{4\pi} \frac{q\mathbf{v}(\mathbf{r}', t' - R/c)}{(R - \mathbf{R} \cdot \mathbf{v}/c)} \\ \Phi(\mathbf{r}, t) &= \frac{\mu}{4\pi} \frac{q(\mathbf{r}', t' - R/c)}{(R - \mathbf{R} \cdot \mathbf{v}/c)} \end{aligned} \quad (1.5.10)$$

If the charge moves at a speed much less than c Eq. (1.5.10) is the usual three-dimensional vector and scalar potential field of individual charges.

It is apparent from Eq. (1.5.10) that a charge moving towards or away from a field point generates potentials with magnitudes respectively larger or smaller than the low speed value.

1.6. The Field Equations

If ρ_0 is the charge density in an inertial reference frame in which the average speed of the charges is zero, then $\rho = \gamma\rho_0$ is the charge density in a moving frame. The charge density and the three-dimensional current density J_i were extended to form the 4-current density, as shown by Eq. (1.5.2), from which the Laplacian of the 4-potential was defined by Eq. (1.5.4). Other useful 4-tensors follow from four-dimensional operations on the 4-potential $A_\alpha(X_\gamma)$; some especially important ones follow.

A second rank antisymmetric tensor of interest follows from the potential by the equation:

$$f_{\alpha\beta} = \frac{\partial A_\beta}{\partial X_\alpha} - \frac{\partial A_\alpha}{\partial X_\beta} \quad (1.6.1)$$

Antisymmetric 4-tensors are spatial arrays of six numbers and, in common with all antisymmetric tensors, the trace is zero:

$$f_{\alpha\alpha} = 0 \quad (1.6.2)$$

Writing out the six values that appear in the upper right portion of the 4-tensor, and using the result to define the function Φ , gives:

$$\begin{aligned} f_{12} &= \frac{\partial A_2}{\partial X_1} - \frac{\partial A_1}{\partial X_2} = \frac{\partial A_y}{\partial x} - \frac{\partial A_x}{\partial y} = B_z \\ f_{23} &= \frac{\partial A_3}{\partial X_2} - \frac{\partial A_2}{\partial X_3} = \frac{\partial A_y}{\partial z} - \frac{\partial A_z}{\partial y} = B_x \\ f_{31} &= \frac{\partial A_1}{\partial X_3} - \frac{\partial A_3}{\partial X_1} = \frac{\partial A_x}{\partial z} - \frac{\partial A_z}{\partial x} = B_y \\ f_{14} &= \frac{\partial A_4}{\partial X_1} - \frac{\partial A_1}{\partial X_4} = \frac{i}{c} \frac{\partial \Phi}{\partial x} - \frac{\partial A_x}{ic\partial t} = -\frac{i}{c} E_x \\ f_{24} &= \frac{i}{c} \frac{\partial \Phi}{\partial y} - \frac{\partial A_y}{ic\partial t} = -\frac{i}{c} E_y \\ f_{34} &= \frac{i}{c} \frac{\partial \Phi}{\partial z} - \frac{\partial A_z}{ic\partial t} = -\frac{i}{c} E_z \end{aligned} \quad (1.6.3)$$

With the deductive approach to electromagnetism Eq. (1.6.3) are the defining terms for field vectors \mathbf{E} and \mathbf{B} . The result written in tensor form is:

$$(f) = \begin{pmatrix} 0 & B_z & -B_y & -iE_x/c \\ -B_z & 0 & B_x & -iE_y/c \\ B_y & -B_x & 0 & -iE_z/c \\ iE_x/c & iE_y/c & iE_z/c & 0 \end{pmatrix} \quad (1.6.4)$$

Differentiating $f_{\alpha\beta}$ with respect to X_β results in the equality chain:

$$\frac{\partial f_{\alpha\beta}}{\partial X_\beta} = \frac{\partial}{\partial X_\beta} \left(\frac{\partial A_\beta}{\partial X_\alpha} - \frac{\partial A_\alpha}{\partial X_\beta} \right) = \frac{\partial^2 A_\beta}{\partial X_\beta \partial X_\alpha} - \frac{\partial^2 A_\alpha}{\partial X_\beta \partial X_\beta} = \mu J_\alpha \quad (1.6.5)$$

Combining terms gives:

$$\frac{\partial f_{\alpha\beta}}{\partial X_\beta} = \mu J_\alpha \quad (1.6.6)$$

Evaluation of Eq. (1.6.6) gives:

$$\begin{aligned} \frac{\partial f_{1\beta}}{\partial X_\beta} &= \frac{\partial B_z}{\partial y} - \frac{\partial B_y}{\partial z} - \frac{1}{c^2} \frac{\partial E_x}{\partial t} = \mu J_x \\ \frac{\partial f_{2\beta}}{\partial X_\beta} &= \frac{\partial B_x}{\partial z} - \frac{\partial B_z}{\partial x} - \frac{1}{c^2} \frac{\partial E_y}{\partial t} = \mu J_y \\ \frac{\partial f_{3\beta}}{\partial X_\beta} &= \frac{\partial B_y}{\partial x} - \frac{\partial B_x}{\partial y} - \frac{1}{c^2} \frac{\partial E_z}{\partial t} = \mu J_z \\ \frac{c}{i} \frac{\partial f_{4\beta}}{\partial X_\beta} &= \frac{\partial E_x}{\partial x} + \frac{\partial E_y}{\partial y} + \frac{\partial E_z}{\partial z} = \frac{\rho}{\varepsilon} \end{aligned} \quad (1.6.7)$$

These are the nonhomogeneous Maxwell equations and relate fields to sources. In three-dimensional notation:

$$\nabla \times \mathbf{B} - \frac{1}{c^2} \frac{\partial \mathbf{E}}{\partial t} = \mu \mathbf{J}; \quad \varepsilon \nabla \cdot \mathbf{E} = \rho \quad (1.6.8)$$

The nonhomogeneous Maxwell equations relate force field intensities \mathbf{E} and \mathbf{B} to sources ρ and \mathbf{J} . The first order terms of \mathbf{E} and \mathbf{B} are, respectively, independent of and proportional to the first power of the speed of the charge.

It follows from the definition of $f_{\alpha\beta}$ that:

$$\frac{\partial f_{\nu\sigma}}{\partial X_\alpha} + \frac{\partial f_{\sigma\alpha}}{\partial X_\nu} + \frac{\partial f_{\alpha\nu}}{\partial X_\sigma} = 0 \quad (1.6.9)$$

Evaluation of Eq. (1.6.9) for each tensor component gives:

$$\begin{aligned} \frac{\partial f_{12}}{\partial X_3} + \frac{\partial f_{23}}{\partial X_1} + \frac{\partial f_{31}}{\partial X_2} &= \frac{\partial B_z}{\partial z} + \frac{\partial B_x}{\partial x} + \frac{\partial B_y}{\partial y} = 0 \\ \frac{\partial f_{24}}{\partial X_1} + \frac{\partial f_{41}}{\partial X_2} + \frac{\partial f_{12}}{\partial X_4} &= \frac{1}{ic} \left(\frac{\partial E_y}{\partial x} - \frac{\partial E_x}{\partial y} + \frac{\partial B_z}{\partial t} \right) = 0 \\ \frac{\partial f_{34}}{\partial X_2} + \frac{\partial f_{42}}{\partial X_3} + \frac{\partial f_{23}}{\partial X_4} &= \frac{1}{ic} \left(\frac{\partial E_z}{\partial y} - \frac{\partial E_y}{\partial z} + \frac{\partial B_x}{\partial t} \right) = 0 \\ \frac{\partial f_{14}}{\partial X_3} + \frac{\partial f_{43}}{\partial X_1} + \frac{\partial f_{31}}{\partial X_4} &= \frac{1}{ic} \left(\frac{\partial E_x}{\partial z} - \frac{\partial E_z}{\partial x} + \frac{\partial B_y}{\partial t} \right) = 0 \end{aligned} \quad (1.6.10)$$

These are the homogeneous Maxwell equations and relate force field vectors \mathbf{E} and \mathbf{B} . In three-dimensional notation:

$$\nabla \times \mathbf{E} - \frac{\partial \mathbf{B}}{\partial t} = 0; \quad \nabla \cdot \mathbf{B} = 0 \quad (1.6.11)$$

Another useful 4-vector is the force intensity, defined by the equation:

$$F_\alpha^\nu = f_{\alpha\beta} J_\beta \quad (1.6.12)$$

Evaluation of each component of Eq. (1.6.12) gives:

$$\begin{aligned} F_1^\nu &= F_x^\nu = J_y B_z - J_z B_y + \rho E_x \\ F_2^\nu &= F_y^\nu = J_z B_x - J_x B_z + \rho E_y \\ F_3^\nu &= F_z^\nu = J_x B_y - J_y B_x + \rho E_z \\ F_4^\nu &= \frac{i}{c} (E_x J_x + E_y J_y + E_z J_z) \end{aligned} \quad (1.6.13)$$

These equations relate force and power to the interaction of the charges and the fields. In three-dimensional notation:

$$\mathbf{F}^\nu = \rho \mathbf{E} + \mathbf{J} \times \mathbf{B}; \quad -icF_4^\nu = \mathbf{E} \cdot \mathbf{J} \quad (1.6.14)$$

To assist in the interpretation of Eq. (1.6.12), consider the 4-scalar formed by taking the scalar product:

$$F_\alpha^\nu J_\alpha = f_{\alpha\beta} J_\alpha J_\beta = 0 \quad (1.6.15)$$

The second equality of Eq. (1.6.15) follows from the antisymmetric character of $f_{\alpha\beta}$ and shows that the 4-vector F_α^ν is perpendicular to the 4-current density. Since the 4-current density is proportional to the 4-velocity, it follows that F_α^ν is also perpendicular to the 4-velocity. Consider the differential with respect to proper time of the square of the 4-velocity:

$$\frac{d}{d\tau} (U_\alpha U_\alpha) = 2U_\alpha \frac{dU_\alpha}{d\tau} = \frac{d}{d\tau} (-c^2) = 0 \quad (1.6.16)$$

Therefore both the 4-acceleration and F_α^ν are perpendicular to the 4-velocity. This is a necessary but insufficient requirement for F_α^ν to be the force density.

This approach to the Maxwell equations is based upon the original axiom relating a charge to its accompanying potential. The form of the source shows that only charges produce a 4-curvature of the 4-potential field. The technique is a neat way both to package the electromagnetic

equations and to show that they take the same form in all inertial coordinate systems. The relationship between fields \mathbf{E} and \mathbf{B} and the potentials follows from Eq. (1.6.3). By direct comparison:

$$\begin{aligned} \frac{\partial A_j}{\partial x_i} - \frac{\partial A_i}{\partial x_j} = B_k &\Rightarrow \nabla \times \mathbf{A} = \mathbf{B} \\ -\frac{\partial \Phi}{\partial x_i} - \frac{\partial A_i}{\partial t} = E_i &\Rightarrow -\left(\nabla \Phi + \frac{\partial \mathbf{A}}{\partial t}\right) = \mathbf{E} \end{aligned} \quad (1.6.17)$$

1.7. Accelerating Charges

The potentials surrounding electric charges in uniform motion are given by Eq. (1.5.10) and the force fields are related to the potential by Eq. (1.6.3). The partial derivative operations of Eq. (1.6.3) take place at the field position and time, (\mathbf{r}, t) . The position and time at the source, (\mathbf{r}', t') , do not enter into the operations. To carry out the operations it is convenient to define S by the equation:

$$S = \left(\mathbf{R} - \frac{\mathbf{R} \cdot \mathbf{v}}{c}\right) \quad (1.7.1)$$

Operating upon the potential while keeping terms involving charge accelerations gives:

$$\begin{aligned} \mathbf{E} &= \frac{q}{4\pi\epsilon} \left\{ \frac{1}{\gamma^2 S^3} \left(\mathbf{R} - \mathbf{R} \frac{\mathbf{v}}{c}\right) + \frac{1}{c^2 S^3} \mathbf{R} \times \left[\left(\mathbf{R} - \mathbf{R} \frac{\mathbf{v}}{c}\right) \times \frac{\partial}{\partial t} \mathbf{v} \right] \right\} \\ \mathbf{B} &= \frac{1}{Rc} \mathbf{R} \times \mathbf{E} \end{aligned} \quad (1.7.2)$$

Keeping only first order terms in powers of v/c leads to:

$$\begin{aligned} \mathbf{E} &= \frac{q}{4\pi\epsilon R^3} \left\{ \left(\mathbf{R} - \mathbf{R} \frac{\mathbf{v}}{c}\right) + \frac{1}{c^2} \mathbf{R} \times \left(\mathbf{R} \times \frac{\partial}{\partial t} \mathbf{v}\right) \right\} \\ \mathbf{B} &= -\frac{\mu q}{4\pi R^3} \mathbf{R} \times \left(\mathbf{v} + \frac{R}{c} \frac{\partial}{\partial t} \mathbf{v}\right) \end{aligned} \quad (1.7.3)$$

The equations show that: A stationary charge produces an electric field intensity that varies as the inverse square of the radius, but there is no magnetic field. If the charge is moving, both electric and magnetic field intensities exist that are proportional to the speed of the charge and varying as the inverse square of the radius. If the charge is accelerating, both electric and magnetic field intensities exist in proportion to the acceleration of the charge and the inverse radius. Where charge distributions are applicable Eq. (1.7.3) take the form of spatial integrals over charge bearing regions.

1.8. The Electromagnetic Stress Tensor

Another result of four-dimensional field analysis is the electromagnetic stress tensor. It is defined as the symmetric, second rank 4-tensor $T_{\alpha\beta}$:

$$\mu T_{\alpha\beta} = f_{\alpha\kappa} f_{\kappa\beta} + \frac{1}{4} \delta_{\alpha\beta} f_{\nu\sigma} f_{\nu\sigma} \quad (1.8.1)$$

A symmetric 4-tensor consists of an array of ten independent numbers. It may be shown, after some algebra, that the force density 4-vector of Eq. (1.6.12) is related to the electromagnetic stress tensor as:

$$F_{\alpha}^{\nu} = \partial T_{\alpha\beta} / \partial X_{\beta} \quad (1.8.2)$$

The independent components of $T_{\alpha\beta}$ follow from Eqs. (1.6.7) and (1.8.1). The result is:

$$\begin{aligned} T_{11} &= \frac{\varepsilon}{2} (E_x^2 - E_y^2 - E_z^2) + \frac{1}{2\mu} (B_x^2 - B_y^2 - B_z^2) \\ T_{12} &= \varepsilon E_x E_y + \frac{1}{\mu} B_x B_y \\ T_{22} &= \frac{\varepsilon}{2} (E_y^2 - E_z^2 - E_x^2) + \frac{1}{2\mu} (B_y^2 - B_z^2 - B_x^2) \\ T_{23} &= \varepsilon E_y E_z + \frac{1}{\mu} B_y B_z \\ T_{33} &= \frac{\varepsilon}{2} (E_z^2 - E_x^2 - E_y^2) + \frac{1}{2\mu} (B_z^2 - B_x^2 - B_y^2) \\ T_{31} &= \varepsilon E_z E_x + \frac{1}{\mu} B_z B_x \\ T_{44} &= \frac{\varepsilon}{2} (E_x^2 + E_y^2 + E_z^2) + \frac{1}{2\mu} (B_x^2 + B_y^2 + B_z^2) \\ T_{14} &= \frac{1}{ic\mu} (E_y B_z - E_z B_y) \\ T_{24} &= \frac{1}{ic\mu} (E_z B_x - E_x B_z) \\ T_{34} &= \frac{1}{ic\mu} (E_x B_y - E_y B_x) \end{aligned} \quad (1.8.3)$$

The tensor may be written in the form:

$$(T) = \begin{pmatrix} T_{ij} & -\frac{i}{c} \mathbf{N} \\ -\frac{i}{c} \mathbf{N} & w \end{pmatrix} \quad (1.8.4)$$

By definition $w = T_{44}$ is equal to:

$$T_{44} = \frac{\varepsilon}{2}E^2 + \frac{1}{2\mu}B^2 \quad (1.8.5)$$

T_{ij} is the three-dimensional electromagnetic stress tensor:

$$(T) = \begin{pmatrix} \frac{\varepsilon}{2}[E_x^2 - E_y^2 - E_z^2] + \frac{1}{2\mu}[B_x^2 - B_y^2 - B_z^2] & \varepsilon E_x E_y + \frac{1}{\mu} B_x B_y & \varepsilon E_x E_z + \frac{1}{\mu} B_x B_z \\ \varepsilon E_y E_x + \frac{1}{\mu} B_y B_x & \frac{\varepsilon}{2}[E_y^2 - E_z^2 - E_x^2] + \frac{1}{2\mu}[B_y^2 - B_z^2 - B_x^2] & \varepsilon E_y E_z + \frac{1}{\mu} B_y B_z \\ \varepsilon E_z E_x + \frac{1}{\mu} B_z B_x & \varepsilon E_z E_y + \frac{1}{\mu} B_z B_y & \frac{\varepsilon}{2}[E_z^2 - E_x^2 - E_y^2] + \frac{1}{2\mu}[B_z^2 - B_x^2 - B_y^2] \end{pmatrix} \quad (1.8.6)$$

\mathbf{N} is the three-dimensional Poynting vector:

$$\mathbf{N} = (\mathbf{E} \times \mathbf{B})/\mu \quad (1.8.7)$$

Symmetric tensors of rank two in three dimensions reduce from six to three components by transforming to the principal axes and aligning one axis with the source field intensity. For example, if there is no magnetic field and if the electric field intensity is directed along the x -axis the tensor reduces to:

$$(T) = \frac{\varepsilon}{2} \begin{pmatrix} E^2 & 0 & 0 \\ 0 & -E^2 & 0 \\ 0 & 0 & -E^2 \end{pmatrix} \quad (1.8.8)$$

To interpret the stress tensor, consider the four-dimensional spatial integral of Eq. (1.8.2). The equation may be written:

$$\iiint \iiint c'_{\sigma\alpha} F'^{\nu}_{\alpha} dX'_1 dX'_2 dX'_3 dX'_4 = \iiint \iiint c'_{\sigma\alpha} \frac{\partial T'_{\alpha\beta}}{\partial X'_\beta} dX'_1 dX'_2 dX'_3 dX'_4 \quad (1.8.9)$$

Working with the left side:

$$\begin{aligned} \iiint \iiint c'_{\sigma\alpha} F'^{\nu}_{\alpha} dX'_1 dX'_2 dX'_3 dX'_4 &= \iiint \iiint F'_\sigma{}^\nu dX'_1 dX'_2 dX'_3 dX'_4 \\ &= \iiint \iiint F'_\sigma{}^\nu dX_1 dX_2 dX_3 dX_4 \end{aligned}$$

Working with the right side:

$$\begin{aligned} \iiint\iiint c'_{\sigma\alpha} \frac{\partial T'_{\alpha\beta}}{\partial X'_\beta} dX'_1 dX'_2 dX'_3 dX'_4 &= \iiint\iiint \frac{\partial(c'_{\sigma\alpha} T'_{\alpha\beta})}{\partial X'_\beta} dX'_1 dX'_2 dX'_3 dX'_4 \\ &= \iiint\iiint c'_{\sigma\alpha} T'_{\alpha 4} dX'_1 dX'_2 dX'_3 \end{aligned}$$

The last equality results since the integral at the limits of the spatial integrals vanish. Working with the last integral, note that:

$$c'_{\alpha\beta} T_{\sigma\alpha} = c'_{\lambda\beta} c'_{\sigma\alpha} c'_{\lambda\gamma} T'_{\alpha\gamma} \quad (1.8.10)$$

Since $c'_{\lambda\beta} c'_{\lambda\gamma} = \delta_{\beta\gamma}$ it follows that $c'_{\alpha\beta} T_{\sigma\alpha} = c'_{\sigma\alpha} T'_{\alpha\beta}$ from which $c'_{\sigma\alpha} T'_{\alpha 4} = c'_{\alpha 4} T_{\sigma\alpha}$. This leaves the equality:

$$\iiint\iiint F'_\sigma dX'_1 dX'_2 dX'_3 dX'_4 = \iiint\iiint c'_{\alpha 4} T_{\sigma\alpha} dX'_1 dX'_2 dX'_3 \quad (1.8.11)$$

Since $c'_{\alpha 4} = U_\alpha/ic$ this may be written:

$$\iiint\iiint F'_\sigma dX'_1 dX'_2 dX'_3 dX'_4 = \frac{1}{ic} \iiint\iiint T_{\sigma\alpha} U_\alpha dX_1 dX_2 dX_3 \quad (1.8.12)$$

To change the 4-integral into a three-dimensional one, differentiate by (ict) to obtain:

$$\iiint\iiint F'_\sigma dX'_1 dX'_2 dX'_3 = F_\sigma = -\frac{1}{c^2} \frac{\partial}{\partial t} \iiint\iiint T_{\sigma\alpha} U_\alpha dX_1 dX_2 dX_3 \quad (1.8.13)$$

Since all time integrals are zero at time $t = -\infty$, time integration has a value only at present time, t .

To examine results of these equations, consider a charge moving with low speed in the z -direction. With the axis in the direction of motion, the sum $T_{\sigma\alpha} U_\alpha$ takes the form:

$$T_{3\alpha} U_\alpha = \frac{\varepsilon}{2} E^2 \mathbf{v} \quad (1.8.14)$$

Combining gives:

$$\mathbf{F} = \int \mathbf{F}^v dV = \frac{d}{dt} \left\{ \frac{\mathbf{v}}{c^2} \int \left(\frac{\varepsilon}{2} E^2 \right) dV \right\} \quad (1.8.15)$$

The sign was changed to represent reaction of the field on its source, rather than *vice versa*. For a low speed particle undergoing differential acceleration

Eq. (1.8.15) takes the form:

$$\mathbf{F} = \frac{d}{dt}(\mathbf{mv}) = \frac{d\mathbf{p}}{dt} \quad (1.8.16)$$

The mass is calculated as:

$$m = \frac{1}{c^2} \int \left(\frac{\varepsilon}{2} \mathbf{E}^2 \right) dV \quad (1.8.17)$$

The interpretation accorded these equations is that Eq. (1.8.17) is Newton's law for electromagnetic mass, confirming that \mathbf{F} is a force. The expression for the mass shows that $(\varepsilon \mathbf{E}^2/2)$ is the energy density of an electric field.

1.9. Kinematic Properties of Fields

To further analyze the kinematic properties of fields, begin with the four-dimensional force equation, Eq. (1.6.14):

$$\mathbf{F}^{\nu} = \rho \mathbf{E} + \mathbf{J} \times \mathbf{B}; \quad -icF_4^{\nu} = \mathbf{E} \cdot \mathbf{J} \quad (1.9.1)$$

To express this equality in a way that depends upon the fields only, it is necessary to substitute for ρ and \mathbf{J} from the nonhomogeneous electromagnetic equations, Eq. (1.6.8):

$$\begin{aligned} \mathbf{F}^{\nu} &= \varepsilon \mathbf{E}(\nabla \cdot \mathbf{E}) - \mathbf{B} \times \left(\frac{1}{\mu} \nabla \times \mathbf{B} - \varepsilon \frac{\partial \mathbf{E}}{\partial t} \right) \\ -icF_4^{\nu} &= \mathbf{E} \cdot \left(\frac{1}{\mu} \nabla \times \mathbf{B} - \varepsilon \frac{\partial \mathbf{E}}{\partial t} \right) \end{aligned} \quad (1.9.2)$$

It is helpful to add zero to each equation in the form of terms proportional to the homogeneous Maxwell equations, Eq. (1.6.11). The added terms are:

$$\begin{aligned} &\frac{1}{\mu} \mathbf{B}(\nabla \cdot \mathbf{B}) - \varepsilon \mathbf{E} \times \left(\nabla \times \mathbf{E} + \frac{\partial \mathbf{B}}{\partial t} \right) \quad \text{and} \\ &-\mathbf{B} \cdot \left(\nabla \times \mathbf{E} + \frac{\partial \mathbf{B}}{\partial t} \right) \end{aligned} \quad (1.9.3)$$

Combining gives:

$$\begin{aligned} \mathbf{F}^{\nu} &= \varepsilon \{ \mathbf{E}(\nabla \cdot \mathbf{E}) - \mathbf{E} \times (\nabla \times \mathbf{E}) \} \\ &\quad + \frac{1}{\mu} \{ \mathbf{B}(\nabla \cdot \mathbf{B}) - \mathbf{B} \times (\nabla \times \mathbf{B}) \} - \frac{1}{c^2} \frac{\partial \mathbf{N}}{\partial t} \\ icF_4^{\nu} &= \frac{\partial}{\partial t} \left(\frac{\varepsilon}{2} \mathbf{E}^2 + \frac{1}{2\mu} \mathbf{B}^2 \right) + \nabla \cdot \mathbf{N} \end{aligned} \quad (1.9.4)$$

Writing the first of Eq. (1.9.4) in tensor form gives:

$$F_i^v = \frac{\partial}{\partial x_j} \left\{ \varepsilon \left(E_i E_j - \frac{1}{2} \delta_{ij} E_k E_k \right) + \frac{1}{\mu} \left(B_i B_j - \frac{1}{2} \delta_{ij} B_k B_k \right) \right\} - \frac{1}{c^2} \frac{\partial}{\partial t} N_i \quad (1.9.5)$$

Integrating over a closed three-dimensional volume gives:

$$\begin{aligned} \oint \left\{ \varepsilon \left(E_i E_j - \frac{1}{2} \delta_{ij} E_k E_k \right) + \frac{1}{\mu} \left(B_i B_j - \frac{1}{2} \delta_{ij} B_k B_k \right) \right\} dS_j \\ = \int \left(\frac{1}{c^2} \frac{\partial N_i}{\partial t} + F_i^v \right) dV \end{aligned} \quad (1.9.6)$$

By Eq. (1.8.16) the last term on the right is the rate of change of momentum of all charges contained within the volume, $\mathbf{p}_{\text{charge}}$. Therefore, the first term on the right is the rate of change of field momentum, $\mathbf{p}_{\text{field}}$. It follows that the left side of the equation is equal to the force on the charges and fields within the volume of integration. The results may be written as:

$$\mathbf{p}_{\text{field}} = \frac{1}{c^2} \int \mathbf{N} dV; \quad \mathbf{F}^v = \rho \mathbf{E} + \mathbf{J} \times \mathbf{B} = \frac{d}{dt} \mathbf{p}_{\text{charge}} \quad (1.9.7)$$

Since \mathbf{F}^v is a force density, it follows from Eq. (1.9.7) that the electric field intensity is a force per unit charge. Since a wave travels at speed c , by the first of Eq. (1.9.7) the momentum passing through a planar surface is:

$$\mathbf{p}_{\text{field}} = \frac{1}{c} \int \mathbf{N} \cdot d\mathbf{S} \quad (1.9.8)$$

By definition $d\mathbf{S}$ is a differential vector area normally outward from the surface.

Integrating the second of Eqs. (1.9.1) and (1.9.4) over a three-dimensional volume gives:

$$\int (\mathbf{E} \cdot \mathbf{J}) dV = \frac{d}{dt} \int \left(\frac{\varepsilon}{2} E^2 + \frac{1}{2\mu} B^2 \right) dV + \oint \mathbf{N} \cdot d\mathbf{S} \quad (1.9.9)$$

Since the field intensity is a force per unit charge it follows that the left side of Eq. (1.9.9) is the rate at which energy enters the volume of integration. Therefore the volume integral on the right side must be the rate at which energy increases in the interior, and the surface integral must be the rate at which energy exits through the surface. It follows that the energy in the

electromagnetic fields is equal to:

$$W = \int \left(\frac{\varepsilon}{2} \mathbf{E}^2 + \frac{1}{2\mu} \mathbf{B}^2 \right) dV \quad (1.9.10)$$

It also follows that the rate at which energy exits the volume through the surface is:

$$P = \oint \mathbf{N} \cdot d\mathbf{S} \quad (1.9.11)$$

A different formulation of Eq. (1.9.10) that is sometimes useful is by rewriting it in terms of the potentials. Combining Eq. (1.9.10) with Eqs. (1.6.8) and (1.6.17) results in:

$$\begin{aligned} W = \int [\rho\Phi + \mathbf{J} \cdot \mathbf{A}] dV + \oint \left[-\varepsilon(\phi\mathbf{E}) + \frac{1}{\mu}(\mathbf{A} \times \mathbf{B}) \right] \cdot d\mathbf{S} \\ + \varepsilon \int \left[-\mathbf{E} \cdot \frac{\partial \mathbf{A}}{\partial t} + \mathbf{A} \cdot \frac{\partial \mathbf{E}}{\partial t} \right] dV \end{aligned} \quad (1.9.12)$$

For a charge moving at a constant speed, or if the charge acceleration is small enough so the energy escaping into the far field is negligible, only the first term of Eq. (1.9.12) is significant. For that case the total field energy may also be expressed as:

$$W = \int [\rho\Phi + \mathbf{J} \cdot \mathbf{A}] dV \quad (1.9.13)$$

1.10. A Lemma for Calculation of Electromagnetic Fields

A lemma is needed to assist in the unrestricted and systematic calculation of electromagnetic fields about known sources. To obtain it, begin with the general form for fields in a source-free region containing time-dependent fields:

$$\nabla \times \mathbf{B} - \varepsilon\mu \frac{\partial \mathbf{E}}{\partial t} = 0 = \nabla \times \mathbf{E} + \varepsilon\mu \frac{\partial \mathbf{B}}{\partial t} \quad (1.10.1)$$

Taking the curl of Eq. (1.10.1) and then substituting back and forth as needed gives:

$$\nabla \times (\nabla \times \mathbf{B}) + \varepsilon\mu \frac{\partial^2 \mathbf{B}}{\partial t^2} = 0 = \nabla \times (\nabla \times \mathbf{E}) + \varepsilon\mu \frac{\partial^2 \mathbf{E}}{\partial t^2} \quad (1.10.2)$$

This shows that, away from sources, \mathbf{E} and \mathbf{B} satisfy the same partial differential equation.

$$\nabla^2 \Psi - \varepsilon\mu \frac{\partial^2 \Psi}{\partial t^2} = 0 \quad (1.10.3)$$

This is useful because of an associated lemma that begins with the vector field $\mathbf{F}(\mathbf{r}, t)$, defined by

$$\mathbf{F} = \nabla \times (\mathbf{r}\Psi) \quad (1.10.4)$$

The lemma is that if Ψ satisfies Eq. (1.10.3) then \mathbf{F} satisfies the differential equation:

$$\nabla \times (\nabla \times \mathbf{F}) + \varepsilon\mu \frac{\partial^2 \mathbf{F}}{\partial t^2} = 0 \quad (1.10.5)$$

To verify that Eq. (1.10.5) is correct, multiply Eq. (1.10.3) by $(-\mathbf{r})$, then take the curl:

$$-\nabla \times (\mathbf{r}\nabla^2\Psi) + \varepsilon\mu \frac{\partial^2}{\partial t^2} [\nabla \times (\mathbf{r}\Psi)] = 0 \quad (1.10.6)$$

Comparing Eqs. (1.10.4) through (1.10.6) shows that Eq. (1.10.5) is satisfied if:

$$\nabla \times \{\nabla \times [\nabla \times (\mathbf{r}\Psi)]\} = -\nabla \times (\mathbf{r}\nabla^2\Psi) \quad (1.10.7)$$

To confirm Eq. (1.10.7), begin with the identity for the curl of a scalar-vector product:

$$\nabla \times (\mathbf{r}\Psi) \equiv \Psi(\nabla \times \mathbf{r}) - \mathbf{r} \times \nabla\Psi \quad (1.10.8)$$

Since $\nabla \times \mathbf{r} \equiv 0$, it follows that:

$$\nabla \times [\nabla \times (\mathbf{r}\Psi)] = -\nabla \times (\mathbf{r} \times \nabla\Psi) \quad (1.10.9)$$

Combining Eqs. (1.10.7) and (1.10.9) gives:

$$\nabla \times [\nabla \times (\mathbf{r} \times \nabla\Psi)] - \nabla \times (\mathbf{r}\nabla^2\Psi) = 0 \quad (1.10.10)$$

Two identities from vector analysis are:

$$\begin{aligned} \nabla(\mathbf{A} \cdot \mathbf{B}) &\equiv \mathbf{A} \times (\nabla \times \mathbf{B}) + \mathbf{B} \times (\nabla \times \mathbf{A}) + (\mathbf{B} \cdot \nabla)\mathbf{A} + (\mathbf{A} \cdot \nabla)\mathbf{B} \\ \nabla \times (\mathbf{A} \times \mathbf{B}) &\equiv \mathbf{A}(\nabla \cdot \mathbf{B}) - \mathbf{B}(\nabla \cdot \mathbf{A}) + (\mathbf{B} \cdot \nabla)\mathbf{A} - (\mathbf{A} \cdot \nabla)\mathbf{B} \end{aligned} \quad (1.10.11)$$

Putting $\mathbf{A} = \mathbf{r}$ and $\mathbf{B} = \nabla\Psi$:

$$\begin{aligned} \nabla(\mathbf{r} \cdot \nabla\Psi) &\equiv (\mathbf{r} \cdot \nabla)\nabla\Psi + (\nabla\Psi \cdot \nabla)\mathbf{r} = (\mathbf{r} \cdot \nabla)\nabla\Psi + \nabla\Psi \\ \nabla \times (\mathbf{r} \times \nabla\Psi) &\equiv \mathbf{r}\nabla^2\Psi - 2\nabla\Psi + (\mathbf{r} \cdot \nabla)\nabla\Psi \end{aligned} \quad (1.10.12)$$

Combining Eqs. (1.10.10) and (1.10.12):

$$\nabla \times (\mathbf{r} \times \nabla\Psi) - \mathbf{r}\nabla^2\Psi + \nabla\Psi + \nabla(\mathbf{r} \cdot \nabla\Psi) = 0 \quad (1.10.13)$$

Since the curl of the gradient vanishes, taking the curl of Eq. (1.10.13) yields Eq. (1.10.10) and completes the proof.

1.11. The Scalar Differential Equation

To solve Eq. (1.10.3) it is useful to remove the time-dependent portion. For that purpose use the Fourier integral expansion:

$$\Psi(\mathbf{r}, t) = \int_{-\infty}^{\infty} \psi(\mathbf{r}, \omega) e^{i\omega t} d\omega \quad (1.11.1)$$

Substituting Eq. (1.11.1) into Eq. (1.10.3) leads to:

$$\int_{-\infty}^{\infty} (\nabla^2 \psi + k^2 \psi) e^{i\omega t} d\omega = 0 \quad (1.11.2)$$

By definition $k^2 = \omega^2 \epsilon \mu$. For this equation to be zero for all values of ω , the integrand of Eq. (1.11.2) must equal zero:

$$\nabla^2 \psi + k^2 \psi = 0 \quad (1.11.3)$$

This is the Helmholtz equation, solutions of which combine with Eqs. (1.10.3) to (1.10.5) to obtain the full solution for vector fields.

Certain differential vector operations in spherical coordinates are listed in Table 1.11.1. Using spherical coordinates with θ the polar angle from the z -axis, ϕ the azimuth angle from the x -axis, and r the radial distance from

Table 1.11.1. Differential vector operations, spherical coordinates.

Orthogonal line elements: $dr, r d\theta, r \sin \theta d\phi$

Gradient $\left\{ \begin{aligned} (\nabla\psi)_r &= \frac{\partial\psi}{\partial r} & (\nabla\psi)_\theta &= \frac{1}{r} \frac{\partial\psi}{\partial\theta} & (\nabla\psi)_\phi &= \frac{1}{r \sin\theta} \frac{\partial\psi}{\partial\phi} \end{aligned} \right\}$

Divergence of vector \mathbf{A} : $\frac{1}{r^2} \frac{\partial}{\partial r}(r^2 A_r) + \frac{1}{r \sin\theta} \frac{\partial}{\partial\theta}(\sin\theta A_\theta) + \frac{1}{r \sin\theta} \frac{\partial}{\partial\phi} A_\phi$

Components of curl \mathbf{A} : $\left\{ \begin{aligned} (\nabla \times \mathbf{A})_r &= \frac{1}{r \sin\theta} \left[\frac{\partial(\sin\theta A_\phi)}{\partial\theta} - \frac{\partial A_\theta}{\partial\phi} \right] \\ (\nabla \times \mathbf{A})_\theta &= \frac{1}{r \sin\theta} \frac{\partial A_r}{\partial\phi} - \frac{1}{r} \frac{\partial(r A_\phi)}{\partial r} \\ (\nabla \times \mathbf{A})_\phi &= \frac{1}{r} \left[\frac{\partial(r A_\theta)}{\partial r} - \frac{\partial A_r}{\partial\theta} \right] \end{aligned} \right\}$

Laplacian of $\Psi = \nabla^2 \Psi$: $\left\{ \frac{1}{r} \frac{\partial}{\partial r} \left(r^2 \frac{\partial\Psi}{\partial r} \right) + \frac{1}{r^2 \sin\theta} \frac{\partial}{\partial\theta} \left(\sin\theta \frac{\partial\Psi}{\partial\theta} \right) + \frac{1}{r^2 \sin^2\theta} \frac{\partial^2\Psi}{\partial\phi^2} \right\}$

the origin, by Table 1.11.1 the Helmholtz equation is given by:

$$\frac{1}{r^2 \sin \theta} \left[\sin \theta \frac{\partial \psi}{\partial \theta} \right] + \frac{1}{r^2 \sin^2 \theta} \frac{\partial^2 \psi}{\partial \phi^2} + \frac{1}{r^2} \frac{\partial}{\partial r} \left[r^2 \frac{\partial \psi}{\partial r} \right] + k^2 \psi = 0 \quad (1.11.4)$$

Dividing the equation by k^2 shows that the radial dependence of the solution is a function only of the product $\sigma = kr$, and therefore ψ may be written as $\psi(\sigma, \theta, \phi)$. A theorem applicable to problems using spherical coordinates is that the complete solution of Eq. (1.11.4) is obtained by summing over all possible functions $\psi(\sigma, \theta, \phi)$ where:

$$\psi(r, \theta, \phi) = R(\sigma)\Theta(\theta)\Phi(\phi) \quad (1.11.5)$$

To obtain $\psi(\sigma, \theta, \phi)$, it is necessary to begin by solving for the solutions of Eq. (1.11.5) that involve only one independent variable. After obtaining the functional forms, all possible products are formed and weighted by a constant multiplying coefficient. The coefficient is determined by matching boundary conditions. Finally, all individual product functions with appropriate coefficients are summed.

Substituting Eq. (1.11.5) into Eq. (1.11.4) and multiplying by $r^2/\Psi(r, \theta, \phi)$ gives:

$$\frac{1}{\Theta \sin \theta} \frac{d}{d\theta} \left(\sin \theta \frac{d\Theta}{d\theta} \right) + \frac{1}{\Phi} \frac{d^2 \Phi}{d\phi^2} + \frac{1}{R} \frac{d}{d\sigma} \left(\sigma^2 \frac{dR}{d\sigma} \right) + \sigma^2 = 0 \quad (1.11.6)$$

The first two terms are independent of the radius and the last two terms are independent of the angles, yet the two sets equal each other's negative, requiring both sets to be constant. The constant is known as the separation constant. A convenient choice of separation constant is for the radial terms to equal $\nu(\nu + 1)$ and the angular terms $-\nu(\nu + 1)$, and results in the separated, complete differential equations:

$$\frac{1}{\sigma^2} \frac{d}{d\sigma} \left(\sigma^2 \frac{dR}{d\sigma} \right) + \left(1 - \frac{\nu(\nu + 1)}{\sigma^2} \right) R = 0 \quad (1.11.7)$$

$$\frac{\Phi}{\sin \theta} \frac{d}{d\theta} \left[\sin \theta \frac{d\Theta}{d\theta} \right] + \frac{\Theta}{\sin^2 \theta} \frac{d^2 \Phi}{d\phi^2} + \nu(\nu + 1)\Theta\Phi = 0 \quad (1.11.8)$$

The radial equation is a differential equation with one independent variable. The angular equation may be written as:

$$\frac{\sin \theta}{\Theta} \frac{d}{d\theta} \left[\sin \theta \frac{d\Theta}{d\theta} \right] + \nu(\nu + 1) \sin^2 \theta + \frac{1}{\Phi} \frac{d^2 \Phi}{d\phi^2} = 0 \quad (1.11.9)$$

The first two terms of Eq. (1.11.9) are functions of θ only and the third is a function of ϕ only, yet the terms equal each other's negative. Again, both sets are constant. Putting the first two terms equal to m^2 , where m

is the second separation constant, results in two separated equations, each involving only one independent variable:

$$\frac{1}{\sin \theta} \frac{d}{d\theta} \left(\sin \theta \frac{d\Theta}{d\theta} \right) + \left(\nu(\nu + 1) - \frac{m^2}{\sin^2 \theta} \right) \Theta = 0 \quad (1.11.10)$$

$$\frac{d^2 \Phi}{d\phi^2} + m^2 \Phi = 0 \quad (1.11.11)$$

Solutions of the separated differential equations and tabulated functions are in the Appendix.

Solutions of the radial equation are spherical Bessel, Neumann, and Hankel functions, respectively, $j_\nu(\sigma)$, $y_\nu(\sigma)$, and $h_\nu(\sigma)$. A particularly important linear combination is Hankel functions of the second kind and integer order: $h_\ell(\sigma)$ where “ ℓ ” represents any integer value of “ ν ”. Solutions of the zenith angle equation are associated Legendre functions; solutions are, in some instances, of integer order and in others of noninteger order. In all cases, the orders of the radial and zenith angle solutions are the same. Trigonometric functions form the solutions of the azimuth angle equation: $\sin \phi$, $\cos \phi$, and $\exp(\pm im\phi)$. Since all solutions to be considered extend over the full range of azimuth angle, zero through 2π , only integer values of degree m , are present. With exponential notation, the exponent may have either sign. With symbol $z_\nu(\sigma)$ representing a linear combination of possible radial solution forms, rather than writing the solution as two separate sums it is written as:

$$\psi_\nu^m(r, \theta, \phi) = z_\nu(\sigma) \Theta_\nu^m(\theta) e^{-im\phi} \quad (1.11.12)$$

With this notation, completeness requires m to include the full set of positive and negative integers, however the degree of the Legendre function is always positive.

1.12. Radiation Fields in Spherical Coordinates

Replacing \mathbf{B} by $\mu\mathbf{H}$ more closely matches common usage. For what lies ahead we are concerned only with free space and there μ is merely a unit-determining parameter that measures the magnetic field in amperes per meter instead of webers per square meter.

The field calculation procedure is due to Hansen, and begins with the vector theorem that a field with zero divergence is completely specified by its curl. It is, therefore, helpful to introduce the two independent field sets:

$$\eta \mathbf{H}_1 = \mathbf{r} \times \nabla \Psi_1 \quad \text{and} \quad \mathbf{E}_2 = \mathbf{r} \times \nabla \Psi_2 \quad (1.12.1)$$

Symbol $\eta = \sqrt{\mu/\varepsilon}$ indicates the wave impedance.

Since the free space divergences of both vectors are zero, solutions of Eq. (1.12.1) provide the complete set of possible values for vectors \mathbf{H}_1 and \mathbf{E}_2 . The remaining field solutions, \mathbf{H}_2 and \mathbf{E}_1 , may be obtained from Eq. (1.12.1) using the Maxwell curl equations. The total fields, $(\mathbf{E}_1 + \mathbf{E}_2)$ and $(\mathbf{H}_1 + \mathbf{H}_2)$, are then complete. If the boundary conditions are matched, the fields are also unique.

In what follows we use the notation that time dependence is $\exp(i\omega t)$ and azimuth angle dependence is $\exp(-jm\phi)$, where $i^2 = j^2 = -1$. The reasons for separate notation are that it permits separation of polarization and time dependencies and it permits restriction of separation constant m to the field of positive integers, without loss of generality. With Hansen's method the defining terms for phasor fields are, see Eq. (1.10.4):

$$\eta\tilde{\mathbf{H}}_1 = \mathbf{r} \times \nabla\psi_1 \quad \text{and} \quad \tilde{\mathbf{E}}_2 = \mathbf{r} \times \nabla\psi_2 \quad (1.12.2)$$

A tilde over a vector indicates that it is a phasor. It is required that the scalar functions satisfy the Helmholtz equation, Eq. (1.11.3). For integer modes, the results are solutions in the form of Eq. (1.11.12):

$$\begin{aligned} \psi_1 &= F(\ell, m)z_\ell(\sigma)\Theta_\ell^m e^{-jm\phi} \\ \psi_2 &= j G(\ell, m)z_\ell(\sigma)\Theta_\ell^m e^{-jm\phi} \end{aligned} \quad (1.12.3)$$

The order is not restricted to integer values and the radial function $z_\ell(\sigma)$ may be any linear combination of spherical Bessel and Neumann functions. The zenith angle function may be any linear combination of associated Legendre functions. Both the applicable functions and the constant multiplying coefficients $F(\ell, m)$ and $G(\ell, m)$ are determined by the boundary conditions.

Applying the operation of Eq. (1.12.2) to Eq. (1.12.3) gives the result:

$$\mathbf{r} \times \nabla\psi = -\frac{\hat{\theta}}{\sin\theta} \frac{\partial\psi}{\partial\phi} + \hat{\phi} \frac{\partial\psi}{\partial\theta} \quad (1.12.4)$$

Combining gives:

$$\begin{aligned} \eta\tilde{\mathbf{H}}_1 &= F(\ell, m)z_\ell(\sigma) \left[j\hat{\theta} \frac{m\Theta_\ell^m}{\sin\theta} + \hat{\phi} \frac{d\Theta_\ell^m}{d\theta} \right] e^{-jm\phi} \\ \tilde{\mathbf{E}}_2 &= jG(\ell, m)z_\ell(\sigma) \left[j\hat{\theta} \frac{m\Theta_\ell^m}{\sin\theta} + \hat{\phi} \frac{d\Theta_\ell^m}{d\theta} \right] e^{-jm\phi} \end{aligned} \quad (1.12.5)$$

Taking the curl of the second of Eq. (1.12.5) and then applying the Maxwell curl equation leads to:

$$\eta\tilde{\mathbf{H}}_2 = -iG(\ell, m)e^{-jm\phi} \left\{ j\ell(\ell+1)\frac{z_\ell}{\sigma}\Theta_\ell^m\hat{\mathbf{r}} + z_\ell \left(j\frac{d\Theta_\ell^m}{d\theta}\hat{\theta} + \frac{m\Theta_\ell^m}{\sin\theta}\hat{\phi} \right) \right\} \quad (1.12.6)$$

The carat indicates a unit vector and a dot superscript indicates:

$$z_\ell^\bullet(\sigma) = \frac{1}{\sigma} \frac{d}{d\sigma} [\sigma z_\ell(\sigma)] \quad (1.12.7)$$

Taking the curl of the first of Eq. (1.12.5) and then applying the Maxwell curl equation leads to:

$$\tilde{\mathbf{E}}_1 = iF(\ell, m)e^{-jm\phi} \left\{ \ell(\ell+1)\frac{z_\ell}{\sigma}\Theta_\ell^m\hat{\mathbf{r}} + z_\ell^\bullet \left(\frac{d\Theta_\ell^m}{d\theta}\hat{\theta} - j\frac{m\Theta_\ell^m}{\sin\theta}\hat{\phi} \right) \right\} \quad (1.12.8)$$

The total fields are the sum of Eqs. (1.12.5), (1.12.6) and (1.12.8). They may be written as:

$$\begin{aligned} \tilde{\mathbf{E}}_r &= i \sum_{\ell=0}^{\infty} \sum_{m=0}^{\ell} i^{-\ell} F(\ell, m) \ell(\ell+1) \frac{z_\ell(\sigma)}{\sigma} \Theta_\ell^m(\cos\theta) e^{-jm\phi} \\ \eta\tilde{\mathbf{H}}_r &= -ij \sum_{\ell=0}^{\infty} \sum_{m=0}^{\ell} i^{-\ell} G(\ell, m) \ell(\ell+1) \frac{z_\ell(\sigma)}{\sigma} \Theta_\ell^m(\cos\theta) e^{-jm\phi} \\ \tilde{\mathbf{E}}_\theta &= \sum_{\ell=0}^{\infty} \sum_{m=0}^{\ell} i^{-\ell} \left[iF(\ell, m) z_\ell^\bullet \frac{d\Theta_\ell^m}{d\theta} - G(\ell, m) z_\ell \frac{m\Theta_\ell^m}{\sin\theta} \right] e^{-jm\phi} \\ \eta\tilde{\mathbf{H}}_\phi &= \sum_{\ell=0}^{\infty} \sum_{m=0}^{\ell} i^{-\ell} \left[F(\ell, m) z_\ell \frac{d\Theta_\ell^m}{d\theta} - iG(\ell, m) z_\ell^\bullet \frac{m\Theta_\ell^m}{\sin\theta} \right] e^{-jm\phi} \\ \tilde{\mathbf{E}}_\phi &= -j \sum_{\ell=0}^{\infty} \sum_{m=0}^{\ell} i^{-\ell} \left[iF(\ell, m) z_\ell^\bullet \frac{m\Theta_\ell^m}{\sin\theta} - G(\ell, m) z_\ell \frac{d\Theta_\ell^m}{d\theta} \right] e^{-jm\phi} \\ \eta\tilde{\mathbf{H}}_\theta &= j \sum_{\ell=0}^{\infty} \sum_{m=0}^{\ell} i^{-\ell} \left[F(\ell, m) z_\ell \frac{m\Theta_\ell^m}{\sin\theta} - iG(\ell, m) z_\ell^\bullet \frac{d\Theta_\ell^m}{d\theta} \right] e^{-jm\phi} \end{aligned} \quad (1.12.9)$$

Without loss of generality, the phases of constants $F(\ell, m)$ and $G(\ell, m)$ and multiplying factor $i^{-\ell}$ have been picked for later convenience. Coefficients $F(\ell, m)$ multiply the radial component of the electric field terms and are TM (transverse magnetic) fields and modes, where ‘‘T’’ indicates transverse to the radial direction. Coefficients $G(\ell, m)$ multiply the radial component of the magnetic field and are TE (transverse electric) fields and modes. Terms with $\ell = m = 0$ have no radial fields and are the TEM (transverse

electric and magnetic) fields and mode. This result is valid for all possible electromagnetic field solutions.

Keeping only the real or only the imaginary part with respect to “ j ” provides, respectively, x or y polarization of the electric field intensity. The fields are right or left circularly polarized, respectively, with $j = i$ or $j = -i$. Since this result applies to all time-dependent outgoing waves, it follows that it also applies when the rate of change is arbitrarily small. Hence, it describes fields in the limit as the frequency goes to zero, a static charge distribution. Because of this general result, it is helpful to obtain a physical view of what constitutes field sources. The sources of coefficients $F(\ell, m)$ and $G(\ell, m)$ for static fields are discussed in the appendix, Secs. A.28 and A.29.

Consider a few special cases of Eq. (1.12.9). If the described fields are contained within a source-free region of space, and if that space is loss free, solutions have positive, integer values of orders and integer values of degrees. Spherical Bessel functions, which have no singularities, form the radial portion of the solution; spherical Neumann functions, which have singularities, are not present.

Associated Legendre functions of the first kind, and of integer order, which have no singularities, form the angular portion of the solution; fractional order associated Legendre functions and those of the second kind, which have singularities, are not present.

In the main, if the fields originate at a point and support an outward flow of energy from that point, the radial portion of the solution consists of spherical Hankel functions of the second kind. A solution within an enclosed space that excludes the z -axis, but has rotational symmetry, is described by associated Legendre functions of both the first and second kind, with noninteger, positive-real orders and integer degrees.

In all cases, if the medium in which the fields exist is “lossy”, the separation constants are complex numbers with a positive real part. Since all cases of interest in this book concern lossless media and a full 2π spatial rotation about the z -axis, both the order and degree are real and degrees have only integer values.

1.13. Electromagnetic Fields in a Box

It is helpful for the analysis of radiation problems that follow to know the possible modes in a rectangular cavity, the energy associated with the different modes, and the number of independent modes that can exist. To that

end consider all possible electric field modes that can exist inside an otherwise empty, rectangular cavity that is confined by walls of infinite conductivity. From Eqs. (1.11.2) and (1.11.3) the wave number k is, by definition:

$$k = \omega/c \quad (1.13.1)$$

Whatever time dependence a set of fields may have, it is most easily analyzed at a single frequency only. For each frequency, see Eqs. (1.6.8) and (1.6.11), the Maxwell equations in an empty hollow chamber are:

$$\begin{aligned} \eta \tilde{\mathbf{H}} &= \frac{i}{k} \nabla \times \tilde{\mathbf{E}}; & \tilde{\mathbf{E}} &= -\frac{i}{k} \nabla \times (\eta \tilde{\mathbf{H}}) \\ \nabla \cdot \tilde{\mathbf{H}} &= 0; & \nabla \cdot \tilde{\mathbf{E}} &= 0 \end{aligned} \quad (1.13.2)$$

Let the cavity be a rectangular box that extends from 0 to a along the x -axis, 0 to b along the y -axis, and 0 to d along the z -axis. Boundary conditions applied to perfectly conducting walls require all parallel electric field components to be zero at the surface. Since by Eq. (A.7.3) the fields are also spatial sinusoids the most general forms of possible electric field components are:

$$\begin{aligned} E_x &= E_1 \cos(k_x x) \sin(k_y y) \sin(k_z z) e^{i\omega t} \\ E_y &= E_2 \sin(k_x x) \cos(k_y y) \sin(k_z z) e^{i\omega t} \\ E_z &= E_3 \sin(k_x x) \sin(k_y y) \cos(k_z z) e^{i\omega t} \end{aligned} \quad (1.13.3)$$

Constants E_1, E_2 , and E_3 are specific to each particular problem. Since k satisfies Eq. (A.5.17) it is also a vector, and since by Eq. (1.13.2) the divergence is equal to zero, it follows that:

$$\mathbf{k} \cdot \tilde{\mathbf{E}} = 0 = k_x E_1 + k_y E_2 + k_z E_3 \quad (1.13.4)$$

Applying this condition shows that two of the field constants can be expressed as functions of the other. The electric field set is equal to:

$$\begin{aligned} E_x &= -\frac{k_x k_z}{k_x^2 + k_y^2} E_3 \cos(k_x x) \sin(k_y y) \sin(k_z z) \cos \omega t \\ E_y &= -\frac{k_y k_z}{k_x^2 + k_y^2} E_3 \sin(k_x x) \cos(k_y y) \sin(k_z z) \cos \omega t \\ E_z &= E_3 \sin(k_x x) \sin(k_y y) \cos(k_z z) \cos \omega t \end{aligned} \quad (1.13.5)$$

This leaves Eq. (1.13.5) with only one unknown field coefficient. Operating on Eq. (1.13.3) with the first curl equation of Eq. (1.13.2) gives the

accompanying set of magnetic field components:

$$\begin{aligned}\eta H_x &= \frac{i}{k} [k_y E_3 - k_z E_2] \sin(k_x x) \cos(k_y y) \cos(k_z z) e^{i\omega t} \\ \eta H_y &= \frac{i}{k} [k_z E_1 - k_x E_3] \cos(k_x x) \sin(k_y y) \cos(k_z z) e^{i\omega t} \\ \eta H_z &= \frac{i}{k} [k_x E_2 - k_y E_1] \cos(k_x x) \cos(k_y y) \sin(k_z z) e^{i\omega t}\end{aligned}\quad (1.13.6)$$

Substituting the field coefficients of Eq. (1.13.5) into (1.13.6) shows that $H_z = 0$ and the other field components are:

$$\begin{aligned}\eta H_x &= iE_3 \left(\frac{k_y k}{k_x^2 + k_y^2} \right) \sin(k_x x) \cos(k_y y) \cos(k_z z) e^{i\omega t} \\ \eta H_y &= iE_3 \left(\frac{k_x k}{k_x^2 + k_y^2} \right) \cos(k_x x) \sin(k_y y) \cos(k_z z) e^{i\omega t}\end{aligned}\quad (1.13.7)$$

Comparing Eqs. (1.13.5) and (1.13.7) shows that the electric and magnetic fields are out of time phase. Since the ideal cavity is lossless, the energy is constant and the total electric and magnetic energy is constant. That energy is, therefore, twice the magnetic energy. Integrating over the volume, $V = abd$, gives the total energy:

$$W = \frac{\varepsilon}{16} E_3^2 \left(1 + \frac{k_z^2}{k_x^2 + k_y^2} \right) V \quad (1.13.8)$$

With ℓ , m , n equal to integers, the conducting boundary condition is:

$$k_x = \frac{\ell\pi}{a}; \quad k_y = \frac{m\pi}{b}; \quad k_z = \frac{n\pi}{d} \quad (1.13.9)$$

Combining and introducing w as the energy per unit volume gives:

$$k_x = \frac{\ell\pi}{a}; \quad k_y = \frac{m\pi}{b}; \quad k_z = \frac{n\pi}{d} \quad (1.13.10)$$

$$w = \frac{\varepsilon}{16} E_3^2 \left(1 + \frac{(n+d)^2}{(\ell/a)^2 + (m/b)^2} \right) \quad (1.13.11)$$

The dual solution follows by starting with all possible magnetic field components then put $E_z = 0$. The two polarizations are independent and give dual results.

A related problem is to find the number of possible solutions within volume V . For this case let the cavity be cubic, from which $a = b = d$. The number of available states is equal to the number of spatial points in the positive quadrant of k -space. For integers ℓ , m , n much greater than one

the number of points is nearly equal to the volume of that quadrant and, in k -space, the unit length is π/a . The total number of points is therefore $1/4$ the volume in phase space:

$$N = \frac{1}{8} \left(\frac{a}{\pi}\right)^3 \int_0^{2\pi} d\phi \int_0^\pi \sin\theta d\theta \int_0^k k^2 dk = \frac{k^3 V}{6\pi^2} \quad (1.13.12)$$

The above argument follows from possible values of the electric field intensity inside the regions then obtaining the magnetic field and the condition $H_z = 0$ from it. The argument is equally valid starting with magnetic field intensity then obtaining the electric field, and the condition $E_z = 0$ from it, and gives an equal number of solutions. Therefore the total number of possible solutions is:

$$N = \frac{k^3 V}{3\pi^2} \quad (1.13.13)$$

The two solution types represent the two possible field polarizations.

The number of states between frequencies ω and $\omega + d\omega$ follows:

$$\frac{1}{V} dN = \frac{\omega^2}{3\pi^2 c^3} d\omega \quad (1.13.14)$$

This expression may be used to evaluate the number of energy states available in free space by imagining all space to be in an enclosed system then letting the dimensions of the system become infinite.

1.14. From Energy to Electric Fields

The energy associated with an electric field is given by integral equations Eq. (1.9.10). Using it, it is commonly considered that the local energy density at each point in the field is

$$w(\mathbf{r}, t) = \varepsilon \mathbf{E}(\mathbf{r}, t) \cdot \mathbf{E}^*(\mathbf{r}, t)/4 \quad (1.14.1)$$

It is often convenient to express this energy in terms of wave number \mathbf{k} . Since \mathbf{k} is a vector it may be used as a basis for dimensions, that is, in k -space. For this purpose it is convenient to express the field in coordinate space as an integral over all constituent parts in k -space:

$$\mathbf{E}(\mathbf{r}, t) = \frac{1}{(2\pi)^2} \int_{-\infty}^{\infty} \mathbf{E}_\omega(\mathbf{k}, \omega) e^{i(\omega t - \mathbf{k} \cdot \mathbf{r})} d\mathbf{k} d\omega \quad (1.14.2)$$

To evaluate the k -space field, $\mathbf{E}_\omega(\mathbf{k}, \omega)$, consider the integral expression drawn from Eq. (1.14.2):

$$\begin{aligned} & \int_{-\infty}^{\infty} \mathbf{E}(\mathbf{r}, t) e^{-i(\omega' t - \mathbf{k}' \cdot \mathbf{r})} d\mathbf{r} dt \\ &= \int_{-\infty}^{\infty} d\mathbf{k} d\omega \int_{-\infty}^{\infty} \mathbf{E}_\omega(\mathbf{k}, \omega) e^{i([\omega - \omega']t - [\mathbf{k} - \mathbf{k}'] \cdot \mathbf{r})} d\mathbf{r} dt \\ &= (2\pi)^2 \int_{-\infty}^{\infty} d\mathbf{k} d\omega \mathbf{E}_\omega(\mathbf{k}, \omega) \delta(\omega - \omega') \delta(\mathbf{k} - \mathbf{k}') = (2\pi)^2 \mathbf{E}_\omega(\mathbf{k}', \omega') \end{aligned}$$

It follows that:

$$\mathbf{E}_\omega(\mathbf{k}, \omega) = \frac{1}{(2\pi)^2} \int_{-\infty}^{\infty} \mathbf{E}(\mathbf{r}, t) e^{-i(\omega t - \mathbf{k} \cdot \mathbf{r})} d\mathbf{r} dt \quad (1.14.3)$$

The two forms of electric field intensity, therefore, form a Fourier integral transform pair. It follows that the electric field energy in k -space is:

$$w(\mathbf{k}, \omega) = \varepsilon \mathbf{E}(\mathbf{k}, \omega) \cdot \mathbf{E}^*(\mathbf{k}, \omega) / 4 \quad (1.14.4)$$

It follows from Eqs. (1.14.1) and (1.14.4) that in both coordinate systems the field intensities are proportional to the square root of the energy density. Since only the scalar product between the field intensities is known, three-dimensional vectors are not completely specified by this argument. It is, however, complete for one-dimensional cases such as, for example, scalar fields.

References

- R. Becker, *Electromagnetic Fields and Interactions*, Blaisdell Publishing Co. and Blackie and Son (1964), reprinted by Dover Publications (1982).
- A. Einstein, B. Podolsky, N. Rosen, "Can a Quantum-Mechanical Description of Physical Reality be Considered Complete?" *Phys. Rev.* **47** (1935) 777–780.
- W.W. Hansen, "A New Type of Expansion in Radiation Problems," *Phys. Rev.* **47** (1935) 139–143.
- J.D. Jackson, *Classical Electrodynamics*, 2nd edition, John Wiley (1975).
- L.D. Landau, E.M. Lifshitz, *The Classical Theory of Fields*, trans. by H. Hamermesh, Addison-Wesley (1951).
- W.K.H. Panofsky, M. Phillips, *Classical Electricity and Magnetism*, 2nd edition, Addison-Wesley (1961).
- A. Sommerfeld, *Electrodynamics*, Academic Press (1952).
- J.A. Stratton, *Electromagnetic Theory*, McGraw-Hill (1941).
- J.B. Westgard, *Electrodynamics: A Concise Introduction*, Springer-Verlag (1997).

CHAPTER 2

Selected Boundary Value Problems

The analyses in this chapter characterize the radiation properties of passive, linear systems and provide a benchmark for later comparison with the regenerative absorption and emission processes of Chapters 5 and 6.

Interactions between objects and electromagnetic fields can be most easily analyzed if, over the spatial dimensions of interest, the electric and magnetic field magnitudes are constant, in phase, and the direction of wave propagation is perpendicular to both fields. Necessary flux closures occur outside the region of interest. By definition, a plane wave has such characteristics over all space with flux closure occurring at infinite distances. It is, therefore, convenient to solve problems of interest by imagining plane waves, even though they do not exist. Spherical waves, after all, do exist and, if the radius of the sphere is much larger than other dimensions of interest, a plane wave analysis is justified. The criterion is simply that the radius of the sphere be much larger than any other spatial dimension of interest to the problem.

In this chapter, after obtaining appropriate mathematical expressions for plane waves, scattering of such a wave by a sphere of ideally conducting material is analyzed, followed by an analysis of a biconical transmitting antenna in otherwise free space. Appropriately capped biconical antennas are of especial importance since they are the only antenna embodiment that approximate linear dipole antennas and for which exact expressions can be obtained. For an antenna with perfectly conducting arms and caps, expressions are obtained both for the input impedance and for the full set of electric and magnetic fields everywhere in space. From that field set follows surface currents, pattern directivity, field power density, etc. Next a biconical receiving antenna in otherwise empty space is analyzed as a special scattering object. As in the transmitting case, the full set of fields throughout all space is obtained. The solution includes surface currents on the antenna and both the energy and the linear momentum transferred from the wave to the antenna as a function of antenna size and load impedance.

Although exact expressions are obtained as problem solutions, the expressions are in the form of infinite sums over products of associated Legendre functions and spherical Bessel and Neumann functions. These functions can be readily evaluated at all orders in the far field and at orders less than about thirty in the near field.

2.1. Traveling Waves

The electric and magnetic fields of a unit magnitude, x -polarized, z -directed plane wave expressed in rectangular coordinates are:

$$\tilde{\mathbf{E}} = \hat{x} e^{-ikz} \quad \text{and} \quad \eta \tilde{\mathbf{H}} = \hat{y} e^{-ikz} \quad (2.1.1)$$

The same fields expressed in spherical coordinates are:

$$\begin{aligned} \tilde{\mathbf{E}} &= e^{-i\sigma \cos \theta} \{ \sin \theta \cos \phi \hat{r} + \cos \theta \cos \phi \hat{\theta} - \sin \phi \hat{\phi} \} \\ \eta \tilde{\mathbf{H}} &= e^{-i\sigma \cos \theta} \{ \sin \theta \sin \phi \hat{r} + \sin \theta \sin \phi \hat{\theta} + \cos \phi \hat{\phi} \} \end{aligned} \quad (2.1.2)$$

The fields of Eq. (1.12.9) may, of course, be used to describe plane waves; it is only necessary to obtain appropriate values for the field coefficients $F(\ell, m)$ and $G(\ell, m)$, and to evaluate the different mathematical functions. To do so it is most convenient to work with the radial field components only. Referring back to Eq. (1.12.9) and working with the TM modes, the radial component of the electric field is:

$$\tilde{E}_r = i \sum_{\ell=0}^{\infty} \sum_{m=0}^{\ell} i^{-\ell} F(\ell, m) \ell(\ell+1) \frac{z_{\ell}(\sigma)}{\sigma} \Theta_{\ell}^m(\cos \theta) e^{-jm\phi} \quad (2.1.3)$$

Since a plane wave has no singularities neither does the radial function of Eq. (2.1.3); it follows that only spherical Bessel functions form part of the solution, with $z_{\ell}(\sigma)$ replaced by $j_{\ell}(\sigma)$. Since the wave occupies all values of azimuth angles ϕ , degree m must be an integer. Since the z -axes are included in the solution only integer order, associated Legendre functions of the first kind, $P_{\ell}^m(\cos \theta)$, are present. Applying these conditions and equating Eq. (2.1.3) with the radial component of Eq. (2.1.2) gives:

$$\begin{aligned} &\sin \theta \cos \phi e^{-i\sigma \cos \theta} \\ &= i \sum_{\ell=0}^{\infty} \sum_{m=0}^{\ell} i^{-\ell} F(\ell, m) \ell(\ell+1) \frac{j_{\ell}(\sigma)}{\sigma} P_{\ell}^m(\cos \theta) e^{-jm\phi} \end{aligned} \quad (2.1.4)$$

The azimuth dependence of Eq. (2.1.4) shows that only coefficients of degree one, $F(\ell, 1)$, are different from zero, as are all imaginary parts with respect

to “ j ”. This leaves the equality:

$$e^{-i\sigma \cos \theta} = \frac{i}{\sigma} \sum_{\ell=1}^{\infty} i^{-\ell} F(\ell, 1) \ell(\ell + 1) j_{\ell}(\sigma) \frac{P_{\ell}^1(\cos \theta)}{\sin \theta} \tag{2.1.5}$$

Another expansion for the exponential is listed in Table A.27.1.2:

$$e^{-i\sigma \cos \theta} = \frac{i}{\sigma} \sum_{\ell=1}^{\infty} i^{-\ell} (2\ell + 1) j_{\ell}(\sigma) \frac{P_{\ell}^1(\cos \theta)}{\sin \theta} \tag{2.1.6}$$

Equating the two expressions shows that the coefficient is:

$$F(\ell, 1) = \frac{(2\ell + 1)}{\ell(\ell + 1)} \tag{2.1.7}$$

Entering these results into Eq. (2.1.3) gives:

$$\tilde{E}_r = i \sum_{\ell=1}^{\infty} i^{-\ell} (2\ell + 1) \frac{j_{\ell}(\sigma)}{\sigma} P_{\ell}^1(\cos \theta) \cos \phi \tag{2.1.8}$$

Working with TE modes in a similar way results in the equalities:

$$G(\ell, 1) = -\frac{(2\ell + 1)}{\ell(\ell + 1)} \tag{2.1.9}$$

$$\eta \tilde{H}_r = i \sum_{\ell=1}^{\infty} i^{-\ell} (2\ell + 1) \frac{j_{\ell}(\sigma)}{\sigma} P_{\ell}^1(\cos \theta) \sin \phi \tag{2.1.10}$$

The angular field components follow from the radial components and the form of Eq. (1.12.9)

$$\begin{aligned} \tilde{E}_{\theta} &= \sum_{\ell=1}^{\infty} i^{-\ell} \frac{(2\ell + 1)}{\ell(\ell + 1)} \left[i j_{\ell}^{\bullet}(\sigma) \frac{dP_{\ell}^1(\cos \theta)}{d\theta} + j_{\ell}(\sigma) \frac{P_{\ell}^1(\cos \theta)}{\sin \theta} \right] \cos \phi \\ \eta \tilde{H}_{\phi} &= \sum_{\ell=1}^{\infty} i^{-\ell} \frac{(2\ell + 1)}{\ell(\ell + 1)} \left[j_{\ell}(\sigma) \frac{dP_{\ell}^1(\cos \theta)}{d\theta} + i j_{\ell}^{\bullet}(\sigma) \frac{P_{\ell}^1(\cos \theta)}{\sin \theta} \right] \cos \phi \\ \tilde{E}_{\phi} &= -\sum_{\ell=1}^{\infty} i^{-\ell} \frac{(2\ell + 1)}{\ell(\ell + 1)} \left[j_{\ell}(\sigma) \frac{dP_{\ell}^1(\cos \theta)}{d\theta} + i j_{\ell}^{\bullet}(\sigma) \frac{P_{\ell}^1(\cos \theta)}{\sin \theta} \right] \sin \phi \\ \eta \tilde{H}_{\theta} &= \sum_{\ell=1}^{\infty} i^{-\ell} \frac{(2\ell + 1)}{\ell(\ell + 1)} \left[i j_{\ell}^{\bullet}(\sigma) \frac{dP_{\ell}^1(\cos \theta)}{d\theta} + j_{\ell}(\sigma) \frac{P_{\ell}^1(\cos \theta)}{\sin \theta} \right] \sin \phi \end{aligned} \tag{2.1.11}$$

Equations (2.1.8), (2.1.10), and (2.1.11) are the electric and magnetic fields of a unit magnitude, x -polarized, z -directed plane wave expressed in spherical coordinates using spherical functions.

2.2. Scattering of a Plane Wave by a Sphere

A spherical object of radius a is immersed in the plane wave described by Eqs. (2.1.8), (2.1.10), and (2.1.11). A step-wise procedure is used to analyze the interaction between a sphere and a plane wave. In the first step energy and momentum is extracted from the wave and applied to the sphere; these are extinction values of energy and momentum. In the second step the extinction values separate into parts. The scatterer permanently retains the absorbed energy and the scattered energy goes back into space. To determine the scattered fields everywhere, note that all possible fields are expressible in the form of Eq. (1.12.9). Problem solution is simplified if three characteristics of the scattered field are noted. First, since scattered fields exist on the z -axis and since only associated Legendre polynomials of integer order converge on that axis the zenith angle dependence varies as associated Legendre polynomials of integer order. Second, the total scattered power is constant in the limit of infinite radius and constant power requires outgoing fields to vary with distance as $e^{-i\sigma}/\sigma$. Only spherical Hankel functions of the second kind have the needed limiting form and satisfy the spherical Bessel differential equation. Third, the scattered field possesses only the symmetries of the scatterer and the input field. Therefore, only fields of degree one are present.

To solve for the magnitudes and phases of the scattered modes it is convenient to multiply each set of modes by sets of complex scattering coefficients: α_ℓ for TE modes and β_ℓ for TM modes. With this definition the radial components of the scattered fields are:

$$\begin{aligned}\tilde{E}_r &= i \sum_{\ell=1}^{\infty} i^{-\ell} (2\ell + 1) \frac{\beta_\ell h_\ell(\sigma)}{\sigma} P_\ell^1(\cos \theta) \cos \phi \\ \eta \tilde{H}_r &= i \sum_{\ell=1}^{\infty} i^{-\ell} (2\ell + 1) \frac{\alpha_\ell h_\ell(\sigma)}{\sigma} P_\ell^1(\cos \theta) \sin \phi\end{aligned}\tag{2.2.1}$$

Problem solution requires evaluation of each value of α_ℓ and β_ℓ . With symbol “•” defined by Eq. (1.12.7), the sum of the incident plane wave and

the scattered fields is:

$$\begin{aligned}
 \sigma \tilde{E}_r &= i \sum_{\ell=1}^{\infty} i^{-\ell} (2\ell + 1) (j_\ell + \beta_\ell h_\ell) P_\ell^1(\cos \theta) \cos \phi \\
 \sigma \eta \tilde{H}_r &= i \sum_{\ell=1}^{\infty} i^{-\ell} (2\ell + 1) (j_\ell + \alpha_\ell h_\ell) P_\ell^1(\cos \theta) \sin \phi \\
 \tilde{E}_\theta &= \sum_{\ell=1}^{\infty} i^{-\ell} \frac{2\ell + 1}{\ell(\ell + 1)} \left[i(j_\ell^\bullet + \beta_\ell h_\ell^\bullet) \frac{dP_\ell^1}{d\theta} + (j_\ell + \alpha_\ell h_\ell) \frac{P_\ell^1}{\sin \theta} \right] \cos \phi \\
 \eta \tilde{H}_\phi &= \sum_{\ell=1}^{\infty} i^{-\ell} \frac{2\ell + 1}{\ell(\ell + 1)} \left[(j_\ell + \beta_\ell h_\ell) \frac{dP_\ell^1}{d\theta} + i(j_\ell^\bullet + \alpha_\ell h_\ell^\bullet) \frac{P_\ell^1}{\sin \theta} \right] \cos \phi \\
 \tilde{E}_\phi &= - \sum_{\ell=1}^{\infty} i^{-\ell} \frac{2\ell + 1}{\ell(\ell + 1)} \left[(j_\ell + \alpha_\ell h_\ell) \frac{dP_\ell^1}{d\theta} + i(j_\ell^\bullet + \beta_\ell h_\ell^\bullet) \frac{P_\ell^1}{\sin \theta} \right] \sin \phi \\
 \eta \tilde{H}_\theta &= \sum_{\ell=1}^{\infty} i^{-\ell} \frac{2\ell + 1}{\ell(\ell + 1)} \left[i(j_\ell^\bullet + \alpha_\ell h_\ell^\bullet) \frac{dP_\ell^1}{d\theta} + (j_\ell + \beta_\ell h_\ell) \frac{P_\ell^1}{\sin \theta} \right] \sin \phi
 \end{aligned} \tag{2.2.2}$$

By Poynting’s theorem the time-average power, P_{av} , on a spherical, virtual surface of radius σ/k circumscribing the scatterer is equal to the real part of the surface integral of the radial component of complex Poynting vector, see Eq. (A.11.6)

$$P_{av} = \frac{\sigma^2}{\eta k^2} \int_0^{2\pi} d\phi \int_0^\pi \sin \theta d\theta \operatorname{Re}(N_{cr}) \tag{2.2.3}$$

Using Eq. (2.2.2) to evaluate the radial component, and “*” indicating complex conjugate, the complex Poynting vector is:

$$\begin{aligned}
 N_{cr} &= \operatorname{Re} \frac{\sigma^2}{2\eta k^2} \sum_{\ell=1}^{\infty} \sum_{n=1}^{\infty} i^{n-\ell} \left(\frac{(2\ell + 1)}{\ell(\ell + 1)} \right) \left(\frac{(2n + 1)}{n(n + 1)} \right) \\
 &\times \left\{ i \left[(j_n + \beta_n^* h_n^*) (j_\ell^\bullet + \beta_\ell h_\ell^\bullet) \left(\frac{dP_\ell^1}{d\theta} \frac{dP_n^1}{d\theta} \cos^2 \phi + \frac{P_\ell^1 P_n^1}{\sin^2 \theta} \sin^2 \phi \right) \right. \right. \\
 &- (j_\ell + \alpha_\ell h_\ell) (j_n^\bullet + \alpha_n^* h_n^*) \left. \left(\frac{dP_\ell^1}{d\theta} \frac{dP_n^1}{d\theta} \sin^2 \phi + \frac{P_\ell^1 P_n^1}{\sin^2 \theta} \cos^2 \phi \right) \right] \\
 &+ \left[(j_\ell + \alpha_\ell h_\ell) (j_n + \beta_n^* h_n^*) \left(\frac{dP_\ell^1}{d\theta} \frac{P_n^1}{\sin \theta} \sin^2 \phi + \frac{P_\ell^1}{\sin \theta} \frac{dP_n^1}{d\theta} \cos^2 \phi \right) \right. \\
 &\left. \left. + (j_n^\bullet + \alpha_n^* h_n^*) (j_\ell^\bullet + \beta_\ell h_\ell^\bullet) \left(\frac{dP_\ell^1}{d\theta} \frac{P_n^1}{\sin \theta} \cos^2 \phi + \frac{P_\ell^1}{\sin \theta} \frac{dP_n^1}{d\theta} \sin^2 \phi \right) \right] \right\} \tag{2.2.4}
 \end{aligned}$$

Inserting Eq. (2.2.4) into the integral of Eq. (2.2.3) and integrating over the azimuth angle gives:

$$\begin{aligned}
P_{\text{av}} = & \int_0^\pi \sin \theta \, d\theta \left\{ \text{Re} \frac{\pi \sigma^2}{2\eta k^2} \sum_{\ell=1}^{\infty} \sum_{n=1}^{\infty} i^{n-\ell} \left(\frac{(2\ell+1)}{\ell(\ell+1)} \right) \left(\frac{(2n+1)}{n(n+1)} \right) \right. \\
& \times \left\{ i[(j_n + \beta_n^* h_n^*)(j_\ell + \beta_\ell h_\ell) - (j_\ell + \alpha_\ell h_\ell)(j_n + \alpha_n^* h_n^*)] \right. \\
& \times \left[\frac{dP_\ell^1}{d\theta} \frac{dP_n^1}{d\theta} + \frac{P_\ell^1 P_n^1}{\sin^2 \theta} \right] + [(j_\ell + \beta_\ell h_\ell)(j_n + \alpha_n^* h_n^*) \\
& \left. \left. + (j_\ell + \alpha_\ell h_\ell)(j_n + \beta_n^* h_n^*) \right] \left[\frac{1}{\sin \theta} \frac{d(P_n^1 P_\ell^1)}{d\theta} \right] \right\} \quad (2.2.5)
\end{aligned}$$

Using integrals in Tables A.22.1.3 and A.22.1.6 to evaluate the integrals of Eq. (2.2.5) gives:

$$\begin{aligned}
P_{\text{av}} = & \frac{\pi \sigma^2}{\eta k^2} \text{Re} \sum_{\ell=1}^{\infty} i(2\ell+1) [(j_\ell + \beta_\ell^* h_\ell^*)(j_\ell + \beta_\ell h_\ell) \\
& - (j_\ell + \alpha_\ell h_\ell)(j_\ell + \alpha_\ell^* h_\ell^*)] \quad (2.2.6)
\end{aligned}$$

In the limit as the radius becomes many times larger than either radius a or wavelength λ , Eq. (2.2.6) simplifies to:

$$P_{\text{av}} = \frac{\pi}{\eta k^2} \sum_{\ell=1}^{\infty} (2\ell+1) [\text{Re}(\alpha_\ell + \beta_\ell) + (\alpha_\ell \alpha_\ell^* + \beta_\ell \beta_\ell^*)] \quad (2.2.7)$$

Energy and momentum are carried in by the plane wave; both are transferred to the scatterer. The input power is equal to the term proportional to $\text{Re}(\alpha_\ell + \beta_\ell)$. The total power first extracted from the beam is defined as extinction power, and is always positive. Changing the sign to conform to this usage, the extinction power is:

$$P_{\text{EX}} = -\frac{\pi}{\eta k^2} \text{Re} \sum_{\ell=1}^{\infty} (2\ell+1) (\alpha_\ell + \beta_\ell) \quad (2.2.8)$$

The power scattered back into the field is equal to:

$$P_{\text{SC}} = \frac{\pi}{\eta k^2} \sum_{\ell=1}^{\infty} (2\ell+1) (\alpha_\ell \alpha_\ell^* + \beta_\ell \beta_\ell^*) \quad (2.2.9)$$

Absorbed power, the negative of Eq. (2.2.7), does not reappear in the field but may be calculated by subtracting the scattered power from the extinction power. Lossless scatterers have no absorbed power and, therefore, for them Eq. (2.2.7) is equal to zero.

The critical scattering parameters are commonly normalized to a value that is independent of the magnitude of the incoming plane wave. Define scattering cross section, C_{SC} , to equal the scattered power-to-incoming power density ratio. With a unit magnitude electric field intensity the incoming power density is $1/(2\eta)$, see Eqs. (2.1.1) and (A.11.5). Values are sometimes also normalized with respect to the geometric cross section. Cross section has the dimensions of an area, and normalization with respect to the geometric cross sectional area gives a measure of size the scatterer appears to be versus the size it would appear with zero wavelength optics. Define geometric cross section, C_{GE} , to be the area the scatterer presents to the plane wave. For example, the geometric cross sectional area of a spherical scatterer of radius a is $C_{\text{GE}} = \pi a^2$.

Combining the definition with Eqs. (2.1.11) and (2.2.9) shows the scattering-to-geometric cross section ratio to be:

$$\frac{C_{\text{SC}}}{C_{\text{GE}}} = \frac{2}{k^2 a^2} \sum_{\ell=1}^{\infty} (2\ell + 1) [\alpha_{\ell} \alpha_{\ell}^* + \beta_{\ell} \beta_{\ell}^*] \quad (2.2.10)$$

Similarly, the extinction cross section, C_{EX} , is defined to equal the extinction power-to-incoming power density ratio. Combining the definition with Eqs. (2.1.11) and (2.2.8) shows the extinction-to-geometric cross section ratio to be:

$$\frac{C_{\text{EX}}}{C_{\text{GE}}} = -\frac{2}{k^2 a^2} \sum_{\ell=1}^{\infty} (2\ell + 1) \text{Re}(\alpha_{\ell} + \beta_{\ell}) \quad (2.2.11)$$

A third cross section that is often of interest is radar cross section. Define the radar cross section, C_{RCS} , to equal the quotient of the power that would be scattered if the power density were everywhere equal to its value at $\theta = \pi$ divided by the incoming power density. It is a measure of the power returned towards a single interrogating radar antenna. By definition, the power scattered in direction $\theta = \pi$ is the back-scattered power. To determine the radar cross section, evaluate Eq. (2.2.4) at $\theta = \pi$. The angular functions at that angle are equal to:

$$\frac{dP_{\ell}^1}{d\theta} = -\frac{P_{\ell}^1}{\sin \theta} = \frac{1}{2} \ell(\ell + 1)(-1)^{\ell} \quad (2.2.12)$$

Carrying out the calculation and then normalizing by both the incoming power density and the geometric cross section results in the normalized

radar cross section:

$$\begin{aligned} \frac{C_{\text{RCS}}}{C_{\text{GE}}} &= \frac{1}{k^2 a^2} \sum_{\ell=1}^{\infty} \sum_{n=1}^{\ell} (2\ell + 1)(2n + 1) \\ &\times (-1)^{\ell+n} U(\ell - n) [(\alpha_{\ell} - \beta_{\ell})(\alpha_n^* - \beta_n^*)] \end{aligned} \quad (2.2.13)$$

Function $U(\ell - n)$ is the step function:

$$U(\ell - n) = \begin{cases} 1 & \ell > n \\ 1/2 & \ell = n \\ 0 & \ell < n \end{cases} \quad (2.2.14)$$

As shown by Eq. (1.9.8) the fields carry momentum as well as energy, and momentum transfer from the field to the scatterer constitutes an applied force. The momentum transferred to the scatterer by the extinction energy is in the direction of the incoming wave and, by Eq. (1.9.8), is equal to the energy divided by c . The scattered power transfers momentum in proportion to the cosine of the angle between the incident and scattering directions. The back-scattered and forward-scattered portions of the power produce momentum respectively into or away from the direction of the beam. The sign of the total transferred momentum depends upon which type dominates, and that depends upon details of the specific scatterer. Although the resulting force is too small to be significant in most macro-scale applications, nonetheless it exists and affects all scatterers and receiving antennas.

It is also possible to calculate the force on a scatterer because of the scattered field, F_{SC} . The physical origin of the force is that the surface currents move, at least partially in phase with the incident field, and in the x -direction. The incident magnetic field intensity is y -directed. It interacts with the x -directed current density to form a z -directed force. However, this is not the way to calculate the force. For purposes of calculation, note that the momentum density is directly proportional to the power density; they differ only by a factor of c . The force is calculated using the z -component of the scattered power. It, in turn, is equal to the integral of the product of the Poynting vector and the cosine of the scattering angle. With the help of Eq. (1.9.7) the expression for the force in the direction of the plane wave is:

$$F_{\text{SC}} = -\frac{\sigma^2}{2ck^2} \int_0^{2\pi} \int_0^{\pi} \sin \theta \cos \theta \, d\theta \, \text{Re}(N_r) \quad (2.2.15)$$

Substituting the scattered fields of Eq. (2.2.1) into Eq. (2.2.15) and integrating gives

$$\begin{aligned}
 F_{\text{SC}} = & - \int_0^\pi \sin \theta \, d\theta \left\{ \frac{\pi \varepsilon \sigma^2}{2k^2} \operatorname{Re} \sum_{\ell=1}^{\infty} \sum_{n=1}^{\infty} i^{n-\ell} \left(\frac{(2\ell+1)}{\ell(\ell+1)} \right) \left(\frac{(2n+1)}{n(n+1)} \right) \right. \\
 & \times \left\{ i[\beta_\ell \beta_n^* \mathbf{h}_n^* \mathbf{h}_\ell^* - \alpha_\ell \alpha_n^* \mathbf{h}_\ell \mathbf{h}_n^*] \left[\frac{dP_\ell^1}{d\theta} \frac{dP_n^1}{d\theta} + \frac{P_\ell^1 P_n^1}{\sin^2 \theta} \right] \cos \theta \right. \\
 & \left. \left. + [\alpha_\ell \beta_n^* \mathbf{h}_\ell \mathbf{h}_n^* + \alpha_n^* \beta_\ell \mathbf{h}_\ell^* \mathbf{h}_n^*] \left[\frac{1}{\sin \theta} \frac{d(P_n^1 P_\ell^1)}{d\theta} \right] \cos \theta \right\} \right\} \quad (2.2.16)
 \end{aligned}$$

Inserting the integrals of Tables A.22.1.4 and A.22.1.7 into Eq. (2.2.16) gives:

$$\begin{aligned}
 F_{\text{SC}} = & \left\{ \frac{\pi \varepsilon \sigma^2}{k^2} \operatorname{Re} \sum_{\ell=1}^{\infty} \left(\frac{\ell(\ell+2)}{(\ell+1)} \right) [\alpha_\ell \alpha_{\ell+1}^* \mathbf{h}_{\ell+1}^* \mathbf{h}_\ell^* - \beta_\ell \beta_{\ell+1}^* \mathbf{h}_\ell \mathbf{h}_{\ell+1}^*] \right. \\
 & - \frac{\pi \varepsilon \sigma^2}{k^2} \operatorname{Re} \sum_{\ell=1}^{\infty} \left(\frac{(\ell-1)(\ell+1)}{\ell} \right) [\beta_\ell \beta_{\ell-1}^* \mathbf{h}_{\ell-1}^* \mathbf{h}_\ell^* - \alpha_\ell \alpha_{\ell-1}^* \mathbf{h}_\ell \mathbf{h}_{\ell-1}^*] \\
 & \left. - \frac{\pi \varepsilon \sigma^2}{k^2} \operatorname{Re} \sum_{\ell=1}^{\infty} \left(\frac{(2\ell+1)}{\ell(\ell+1)} \right) [\alpha_\ell \beta_\ell^* \mathbf{h}_\ell^* \mathbf{h}_\ell^* + \alpha_\ell^* \beta_\ell \mathbf{h}_\ell \mathbf{h}_\ell^*] \right\} \quad (2.2.17)
 \end{aligned}$$

In the far field Eq. (2.2.17) goes to:

$$\begin{aligned}
 F_{\text{SC}} = & - \frac{\varepsilon \pi}{k^2} \sum_{\ell=1}^{\infty} \left\{ \frac{\ell(\ell+2)}{(\ell+1)} (\alpha_\ell \alpha_{\ell+1}^* + \alpha_\ell^* \alpha_{\ell+1} + \beta_\ell \beta_{\ell+1}^* + \beta_\ell^* \beta_{\ell+1}) \right. \\
 & \left. + \frac{(2\ell+1)}{\ell(\ell+1)} (\alpha_\ell \beta_\ell^* + \alpha_\ell^* \beta_\ell) \right\} \quad (2.2.18)
 \end{aligned}$$

Using Eq. (2.2.11), the force due to reception of the extinction power, the extinction force, F_{EX} is in the direction of the incoming field. Normalizing F_{EX} by the incoming power density determines the normalized force, f_{EX} . Normalizing it by the geometric cross section gives:

$$\frac{f_{\text{EX}}}{C_{\text{GE}}} = - \frac{2}{ck^2 a^2} \sum_{\ell=1}^{\infty} (2\ell+1) \operatorname{Re}(\alpha_\ell + \beta_\ell) \quad (2.2.19)$$

Summing up Eqs. (2.2.18) and (2.2.19) gives the normalized total force on the scatterer:

$$\begin{aligned} \frac{(f_{\text{SC}} + f_{\text{EX}})}{C_{\text{GE}}} = & -\frac{2}{ck^2a^2} \sum_{\ell=1}^{\infty} \left\{ (2\ell + 1) \text{Re}(\alpha_{\ell} + \beta_{\ell}) + \frac{\ell(\ell + 2)}{(\ell + 1)} \right. \\ & \times (\alpha_{\ell}\alpha_{\ell+1}^* + \alpha_{\ell}^*\alpha_{\ell+1} + \beta_{\ell}\beta_{\ell+1}^* + \beta_{\ell}^*\beta_{\ell+1}) \\ & \left. + \frac{(2\ell + 1)}{\ell(\ell + 1)} (\alpha_{\ell}\beta_{\ell}^* + \alpha_{\ell}^*\beta_{\ell}) \right\} \end{aligned} \quad (2.2.20)$$

Although the energy absorbed by a lossless scatterer is zero the momentum transferred is not. Even lossless scatterers are accelerated in the direction of an incoming plane wave. Although the effect is small enough so that the effect of sunlight on atmospheric molecules is less significant than normal thermal unbalance, in other cases it can be significant. For example, the impulse electromagnetic wave produced by a nuclear blast results in forces of major significance.

2.3. Lossless Spherical Scatterers

The form of electromagnetic fields produced by a spherical scatterer immersed in a plane wave and the scattering coefficients α_n and β_n depend upon its electromagnetic characteristics. The special case of a perfectly conducting sphere is important since it approximates many natural objects, it is convenient to analyze, and yet it demonstrates a full range of solution characteristics. The solution procedure is to apply the boundary condition that the tangential component of the total field intensities are equal on either side of the $r = a$ boundary, see Sec. A.12. On the exterior this is the sum of the incident plane and scattered waves; with an ideally conducting scatterer the tangential component of the interior field is zero. Therefore, the following sums are equal to zero:

$$\begin{aligned} \sum_{n=1}^{\infty} \left(\frac{E_{\theta}(a, \theta, \phi)}{\cos \phi} \frac{dP_n^1}{d\theta} - \frac{E_{\phi}(a, \theta, \phi)}{\sin \phi} \frac{P_n^1}{\sin \theta} \right) &= 0 \\ \sum_{n=1}^{\infty} \left(\frac{E_{\theta}(a, \theta, \phi)}{\cos \phi} \frac{P_n^1}{\sin \theta} - \frac{E_{\phi}(a, \theta, \phi)}{\sin \phi} \frac{dP_n^1}{d\theta} \right) &= 0 \end{aligned} \quad (2.3.1)$$

Inserting Eq. (2.2.2) into Eq. (2.3.1) gives:

$$\sum_{\ell=1}^{\infty} i^{-\ell} \frac{(2\ell+1)}{\ell(\ell+1)} \left\{ i[j_{\ell}^{\bullet}(ka) + \beta_{\ell} h_{\ell}^{\bullet}(ka)] \left[\frac{dP_{\ell}^1}{d\theta} \frac{dP_n^1}{d\theta} + \frac{P_{\ell}^1 P_n^1}{\sin^2 \theta} \right] \right. \\ \left. + [j_{\ell}(ka) + \alpha_{\ell} h_{\ell}(ka)] \left[\frac{1}{\sin \theta} \frac{d(P_{\ell}^1 P_n^1)}{d\theta} \right] \right\} = 0 \quad (2.3.2)$$

$$\sum_{\ell=1}^{\infty} i^{-\ell} \frac{(2\ell+1)}{\ell(\ell+1)} \left\{ [j_{\ell}(ka) + \alpha_{\ell} h_{\ell}(ka)] \left[\frac{dP_{\ell}^1}{d\theta} \frac{dP_n^1}{d\theta} + \frac{P_{\ell}^1 P_n^1}{\sin^2 \theta} \right] \right. \\ \left. + i[j_{\ell}^{\bullet}(ka) + \beta_{\ell} h_{\ell}^{\bullet}(ka)] \left[\frac{1}{\sin \theta} \frac{d(P_{\ell}^1 P_n^1)}{d\theta} \right] \right\} = 0 \quad (2.3.3)$$

Next, form the integrals:

$$\int_0^{\pi} \sin \theta \, d\theta \sum_{n=1}^{\infty} \left(\frac{E_{\theta}(a, \theta, \phi)}{\cos \phi} \frac{dP_n^1}{d\theta} - \frac{E_{\phi}(a, \theta, \phi)}{\sin \phi} \frac{P_n^1}{\sin \theta} \right) = 0 \quad (2.3.4)$$

$$\int_0^{\pi} \sin \theta \, d\theta \sum_{n=1}^{\infty} \left(\frac{E_{\theta}(a, \theta, \phi)}{\cos \phi} \frac{P_n^1}{\sin \theta} - \frac{E_{\phi}(a, \theta, \phi)}{\sin \phi} \frac{dP_n^1}{d\theta} \right) = 0$$

Inserting the needed integral forms from Table A.22.1 into Eq. (2.3.4) gives, after simplifying:

$$\begin{aligned} j_{\ell}^{\bullet}(ka) + \beta_{\ell} h_{\ell}^{\bullet}(ka) &= 0 \\ j_{\ell}(ka) + \alpha_{\ell} h_{\ell}(ka) &= 0 \end{aligned} \quad (2.3.5)$$

Solving for the coefficients gives:

$$\alpha_{\ell}(ka) = -\frac{j_{\ell}(ka)}{h_{\ell}(ka)} \quad \text{and} \quad \beta_{\ell}(ka) = -\frac{j_{\ell}^{\bullet}(ka)}{h_{\ell}^{\bullet}(ka)} \quad (2.3.6)$$

Dual results follow if the scatterer is an ideal insulator, with the conductivity and permittivity equal to zero. For that case no current flows in the sphere and the boundary condition is that the magnetic field intensity at the surface is zero. This boundary condition combines with Eq. (2.2.2) to obtain:

$$\sum_{n=1}^{\infty} \left(\frac{H_{\phi}(a, \theta, \phi)}{\cos \phi} \frac{dP_n^1}{d\theta} + \frac{H_{\theta}(a, \theta, \phi)}{\sin \phi} \frac{P_n^1}{\sin \theta} \right) = 0 \quad (2.3.7)$$

$$\sum_{n=1}^{\infty} \left(\frac{H_{\phi}(a, \theta, \phi)}{\cos \phi} \frac{P_n^1}{\sin \theta} + \frac{H_{\theta}(a, \theta, \phi)}{\sin \phi} \frac{dP_n^1}{d\theta} \right) = 0$$

Gathering terms gives:

$$\begin{aligned} \sum_{\ell=1}^{\infty} i^{-\ell} \frac{2\ell+1}{\ell(\ell+1)} \left\{ i(\mathbf{j}_{\ell}^{\bullet} + \alpha_{\ell} \mathbf{h}_{\ell}^{\bullet}) \left[\frac{dP_{\ell}^1}{d\theta} \frac{dP_n^1}{d\theta} + \frac{P_{\ell}^1 P_n^1}{\sin^2 \theta} \right] \right. \\ \left. + (\mathbf{j}_{\ell} + \beta_{\ell} \mathbf{h}_{\ell}) \frac{1}{\sin \theta} \frac{d}{d\theta} (P_{\ell}^1 P_n^1) \right\} = 0 \\ \sum_{\ell=1}^{\infty} i^{-\ell} \frac{2\ell+1}{\ell(\ell+1)} \left\{ (\mathbf{j}_{\ell} + \beta_{\ell} \mathbf{h}_{\ell}) \left[\frac{dP_{\ell}^1}{d\theta} \frac{dP_n^1}{d\theta} + \frac{P_{\ell}^1 P_n^1}{\sin^2 \theta} \right] \right. \\ \left. + i(\mathbf{j}_{\ell}^{\bullet} + \alpha_{\ell} \mathbf{h}_{\ell}^{\bullet}) \frac{1}{\sin \theta} \frac{d}{d\theta} (P_{\ell}^1 P_n^1) \right\} = 0 \end{aligned} \quad (2.3.8)$$

Integrating Eq. (2.3.8) over the surface of a surrounding, virtual sphere gives:

$$(\mathbf{j}_{\ell}^{\bullet} + \alpha_{\ell} \mathbf{h}_{\ell}^{\bullet}) = 0 \quad (\mathbf{j}_{\ell} + \beta_{\ell} \mathbf{h}_{\ell}) = 0 \quad (2.3.9)$$

It follows that the coefficients are:

$$\alpha_{\ell}(ka) = -\frac{\mathbf{j}_{\ell}^{\bullet}(ka)}{\mathbf{h}_{\ell}^{\bullet}(ka)} \quad \text{and} \quad \beta_{\ell}(ka) = -\frac{\mathbf{j}_{\ell}(ka)}{\mathbf{h}_{\ell}(ka)} \quad (2.3.10)$$

An important special case is a scatterer with a small radius-to-wavelength ratio; for this case incorporating the values of the spherical Bessel functions in the limit as $ka \rightarrow 0$ gives:

Limit as ka becomes vanishingly small:

Ideal Conductor

$$\alpha_1(ka) = \frac{i(ka)^3}{3} \quad \text{and} \quad \beta_1(ka) = -\frac{2i(ka)^3}{3} \quad (2.3.11)$$

Ideal Insulator

$$\alpha_1(ka) = -\frac{2i(ka)^3}{3} \quad \text{and} \quad \beta_1(ka) = \frac{i(ka)^3}{3}$$

In both cases the cross sections and normalized forces defined in Sec. 2.2 are:

$$\begin{aligned} \frac{C_{\text{EX}}}{C_{\text{GE}}} = \frac{C_{\text{SC}}}{C_{\text{GE}}} = \frac{cf_{\text{EX}}}{C_{\text{GE}}} = \frac{10(ka)^4}{3} \\ \frac{C_{\text{RCS}}}{C_{\text{GE}}} = 9(ka)^4; \quad \frac{cf_{\text{SC}}}{C_{\text{GE}}} = \frac{4(ka)^4}{3} \end{aligned} \quad (2.3.12)$$

Figure 2.3.1 shows the normalized extinction cross-section for a conducting scatterer as a function of ka , for scatterers of any physical size. Since power in a plane wave is fully directed, Fig. 2.3.1 also shows the momentum transferred to the scatterer; Eq. (2.3.8) shows that for small scatterers it varies as $(ka)^4$. The largest normalized extinction cross section occurs at $ka \cong 1.2$, and is equal to 2.28. For larger values of ka the total cross section oscillates towards a limit of twice the geometric cross section, in the limit of infinite radius.

In the lossless case the extinction and scattering cross sections are equal and the total force on the illuminated sphere is the extinction plus scattered forces, $(F_{\text{EX}} + F_{\text{SC}})$. The force on the scatterer because of the scattered field is shown in Fig. 2.3.2. Electrically small objects scatter predominantly back into the direction from which the wave came, increasing the thrust in the direction of the wave. Electrically large objects scatter predominantly in the direction of the incoming wave, decreasing the thrust on the scatterer. The sign of the scattering force changes at about $ka \cong 1.38$. The largest forward magnitude is about 0.257 and occurs at $ka \cong 1.12$.

The extinction momentum is in the direction of the incoming wave. All interacting energy forms part of the extinction momentum but, upon re-radiation, it may either add or subtract momentum from the scatterer. Since the subtracted momentum cannot exceed the extinction momentum it follows that:

$$\frac{\text{Absorbed Energy}}{\text{Absorbed Momentum}} \leq c \quad (2.3.13)$$

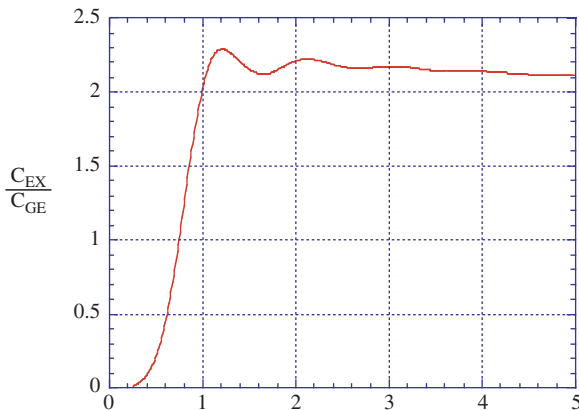


Fig. 2.3.1. Ratio of extinction-to-geometric cross-sections versus ka for a conducting sphere of radius a .

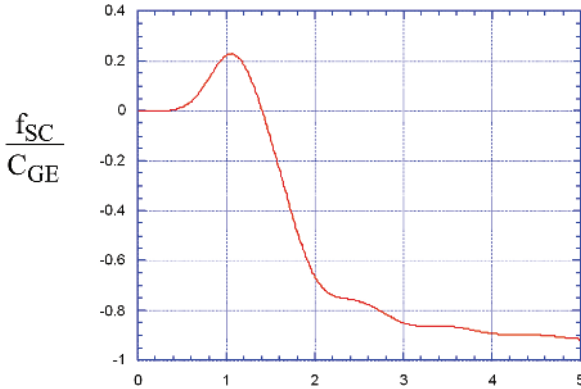


Fig. 2.3.2. Ratio of scattering force-to-geometric cross-section versus ka for a conducting sphere of radius a .

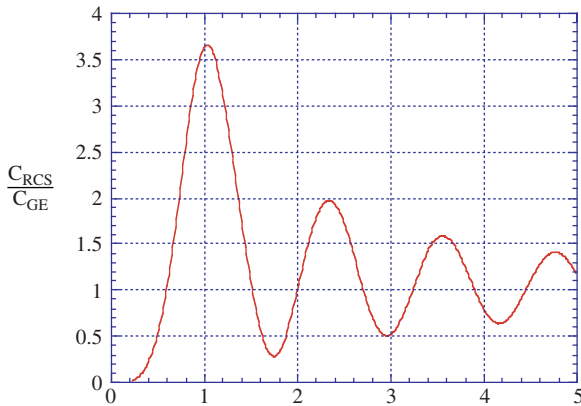


Fig. 2.3.3. Ratio of radar-to-geometric cross-sections versus ka for a conducting sphere of radius a .

Scatterers are commonly divided into groupings that depend upon the radius-to-wavelength ratio. The Rayleigh region is over frequencies for which $ka \ll 1$, the Mie region is over frequencies for which ka is on the order of one, and the optical region is over frequencies for which $ka \gg 1$.

The normalized radar cross section is shown in Fig. 2.3.3. As a point of interest, since conducting spheres that are the right size to be held in a person's hand have radar cross sections that are convenient to measure, the curve of Fig. 2.3.3 is often used as a laboratory calibration standard.

Optical scattering results determine the optical properties of the sky. A clear atmosphere of gaseous nitrogen and oxygen, without suspended particulate matter, scatters a portion of the light that passes through it. Since the molecules are much smaller than a wavelength of visible light, the scattering process selectively acts more on the shorter wavelengths than longer ones and more blue than red light is scattered. When the sun is directly overhead the sky away from the directly incoming beam is illuminated by scattered light, which is dominantly blue. Some of that dominantly blue light is scattered to the earth, giving the sky its characteristically blue color. The removal of selected wavelengths makes the sun appear yellow.

At sunrise and sunset the sun's light travels farther through the atmosphere than it does at noon and more light is scattered. The remaining direct sunlight, therefore, is dominantly red. If particulate matter, such as dust, about the size of an optical wavelength is present, scattering is insensitive to the wavelength and the sky appears to be dark.

2.4. Biconical Transmitting Antennas, General Comments

A biconical antenna is illustrated in Fig. 2.4.1. The input power is applied across a sphere of radius b , centered at the apices of the cones. The cones extend from radius b to radius a , the length of the cones, at angle ψ as

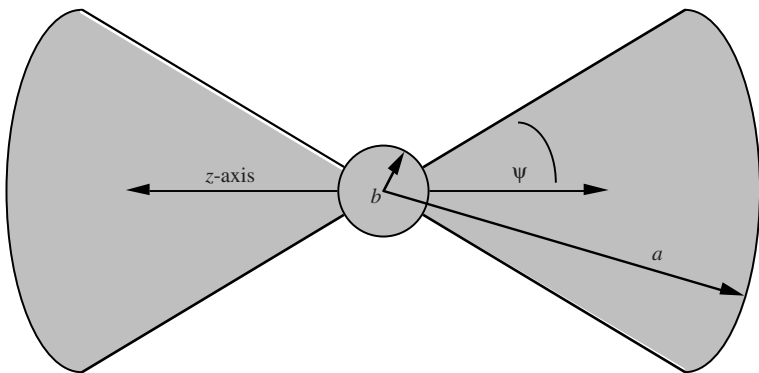


Fig. 2.4.1. Schematic illustration of a biconical antenna. The antenna arms are conical sections that extend between b and a , expansion half-angles ψ are measured from the z -axis, and the outer termination of the cone is capped by a spherical segment of radius a .

measured from the z -axis. All surfaces are ideal conductors. Source radius b is much smaller than either cone length a or wavelength λ .

Biconical antennas are unique in that they are amenable to a rigorous and complete electromagnetic analysis and are shaped similarly to many practical antennas. Any solution with fields that satisfy the Maxwell equations and for which the fields match the boundary conditions is both a unique solution, see Sec. A.13, and a complete solution. Completeness assures that all solution terms are present, in contrast with numerical solutions that begin with an assumed symmetry and obtain an iterative answer. For those cases, the output solution contains only symmetries present in the initial input and hence the solution is only as complete as the initial input.

Transmitting antennas include an energy source that applies a sinusoidal steady state voltage, or current, to source region b . The two cones, although oppositely directed, act as a transmission line and direct the energy through the inner region, radius b to radius a , as a TEM mode. The energy then passes through the open aperture at $r = a$ and enters the outer region. All radiation has rotational symmetry about the antenna axis and many wavelengths from the antenna the electric field intensity is linearly polarized in the direction of the conical axis. The impedance that the antenna presents to the source is determined by details of the antenna structure: cone angles, cone length, and the wavelength of the radiation. The outgoing waves undergo a discontinuity in the wave admittance (impedance) at the open aperture that results in infinite sets of TM modes in both the interior and exterior regions. Both inner and outer modes support standing energy and a steady state outward energy flow. Solution of the transmitting antenna problem requires solving for the input admittance, the coefficients of each of the infinite sets of interior and exterior TM modes as well as the TEM mode, and the radiation pattern.

Analysis is simplified by dividing space in the following way:

Source Region

$$r < b; \quad 0 \leq \theta \leq \pi; \quad 0 \leq \phi \leq 2\pi \quad (2.4.1)$$

Interior Region

Arms:

$$b < r < a; \quad 0 \leq \theta < \psi \quad \text{and} \quad \pi - \psi < \theta \leq \pi; \quad 0 \leq \phi \leq 2\pi \quad (2.4.2)$$

Space:

$$b < r < a; \quad \psi < \theta < \pi - \psi; \quad 0 \leq \phi \leq 2\pi \quad (2.4.3)$$

Exterior Region

Space:

$$r > a; \quad 0 \leq \theta \leq \pi; \quad 0 \leq \phi \leq 2\pi \quad (2.4.4)$$

Aperture:

$$r = a; \quad \psi \leq \theta \leq \pi - \psi; \quad 0 \leq \phi \leq 2\pi \quad (2.4.5)$$

Arms:

$$r = a; \quad 0 \leq \theta < \psi \quad \text{and} \quad \pi - \psi < \theta \leq \pi; \quad 0 \leq \phi \leq 2\pi \quad (2.4.6)$$

2.5. Fields

The first objective is to obtain an expression for all fields. The procedure begins with the general expansion, Eq. (1.12.9), and imposes boundary conditions specific to the biconical structure of Fig. 2.4.1. As was the case for the analysis of scatterers, field determination is greatly simplified by incorporating general field properties before matching the boundary conditions. General field properties are: (1) Since the antenna has rotational symmetry about the z -axis there is no dependence upon azimuth angle ϕ and only functions with degree m equal to zero form part of the solution. All coefficients $F(\nu, m)$ and $G(\nu, m)$ are equal to zero for m greater than zero. This changes the sums over orders and degrees of Eq. (1.12.9) to a sum over orders only. (2) The source drives straight currents that produce no current loops. Since TE coefficients are generated by current loops all coefficients $G(\nu, 0)$ are equal to zero. (3) A source located evenly between the two cones drives surface current density with the symmetry $I(r, \psi) = I(r, \pi - \psi)$ and surface charge density with the symmetry $\rho(r, \psi) = -\rho(r, \pi - \psi)$. By Eq. (1.12.9), and with $\nu = \ell$ an integer, E_θ is proportional to $dP_\ell(\cos \theta)/d\theta$. It is shown in Sec. A.18 that Legendre functions have either even or odd symmetry as ℓ is even or odd. Consider a Legendre function of order ℓ containing terms with the symmetry of $\cos^\ell \theta$. For that term:

$$\begin{aligned} \text{If } P_\ell(\cos \theta) \approx \cos^\ell \theta \text{ then } E_\theta &\approx \frac{dP_\ell(\cos \theta)}{d\theta} \approx \ell \cos^{\ell-1} \theta \sin \theta \\ \ell \text{ odd: } E_\theta(\sigma, \theta) = E_\theta(\sigma, \pi - \theta) \quad \text{and} \quad \ell \text{ even: } E_\theta(\sigma, \theta) &= -E_\theta(\sigma, \pi - \theta) \end{aligned} \quad (2.5.1)$$

Since the source drives only even symmetry electric fields, it follows that only odd symmetry Legendre functions appear in the field solution. Therefore, the coefficients of all even order Legendre functions are equal to zero.

The exterior region: (4) Since the z -axis is included in the field region all terms have null coefficients except Legendre functions of the first kind. (5) In the limit as the radius approaches infinity, energy conservation requires the radial dependence to be $\exp[i(\omega t - \sigma)]/\sigma$ which, in turn, requires the coefficients of all radial functions except Hankel functions of the second kind to be zero.

After incorporating the five constraints into Eq. (1.12.9) and making the notational shift, we obtain:

$$F_\ell = i^{1-\ell} F(\ell, 0)$$

The most general possible set of exterior field components is:

$$\begin{aligned} \sigma E_r &= \sum_{\ell=1;0}^{\infty} \ell(\ell+1) F_\ell h_\ell(\sigma) P_\ell(\cos \theta) \\ E_\theta &= \sum_{\ell=1;0}^{\infty} F_\ell h_\ell(\sigma) \frac{dP_\ell(\cos \theta)}{d\theta} \\ \eta H_\phi &= -i \sum_{\ell=1;0}^{\infty} F_\ell h_\ell(\sigma) \frac{dP_\ell(\cos \theta)}{d\theta} \end{aligned} \quad (2.5.2)$$

The symbol $\ell = 1;0$ indicates the sum begins with $\ell = 1$ and is over odd integers only. The constants F_ℓ form an infinite set of unknown but constant field coefficients. Complete problem solution requires obtaining a solution for each of them.

The interior region: (6) Since the cones exclude fields from the z -axis modal orders need not be integers. Since symmetry requirement (3) requires null coefficients for even functions by Eq. (A.17.26) the coefficients of the even parity portion of Legendre functions, $L_\nu(\cos \theta)$, are equal to zero. This restricts solutions to odd parity Legendre functions, $M_\nu(\cos \theta)$. It follows in the same way that the zero order Legendre function, $P_0(\cos \theta)$, has a null coefficient but, by Eqs. (A.18.14) and (A.18.15), zero order Legendre function of the second kind, $Q_0(\cos \theta)$, does not; the derivative of the zero order Legendre function of the second kind remains finite on cone surfaces.

(7) Both the source voltage and the source current are finite. The voltage and current are, respectively, proportional to σ times the electric and magnetic field intensity and the radial functions approach zero as $j_\nu(\sigma) \rightarrow \sigma^\nu$ and $y_\nu(\sigma) \rightarrow \sigma^{-(\nu+1)}$, see Eqs. (A.24.7) and (A.24.11). Therefore the input voltage and current values remain finite only if the coefficients of all spherical Neumann functions except $\nu = \ell = 0$ are equal to zero.

Incorporating these constraints into Eq. (1.12.9) and separately denoting the zero order TEM mode shows that the general forms of the interior

field components are:

$$\begin{aligned} E_r &= \sum_{\nu>0}^{\infty} \Gamma_{\nu} \nu (\nu + 1) \frac{j_{\nu}(\sigma)}{\sigma} M_{\nu}(\cos \theta) \\ E_{\theta} &= \sum_{\nu>0}^{\infty} \Gamma_{\nu} j_{\nu} \frac{dM_{\nu}}{d\theta} + i [c_0 j_0^*(\sigma) + d_0 y_0^*(\sigma)] \frac{dQ_0(\cos \theta)}{d\theta} \\ \eta H_{\phi} &= -i \sum_{\nu>0}^{\infty} \Gamma_{\nu} j_{\nu} \frac{dM_{\nu}}{d\theta} + [c_0 j_0(\sigma) + d_0 y_0(\sigma)] \frac{dQ_0(\cos \theta)}{d\theta} \end{aligned} \quad (2.5.3)$$

Coefficients of noninteger order modes, $F(\nu, 0)$ of Eq. (1.12.9), are denoted by Γ_{ν} and coefficients of zero order spherical Bessel and Neumann functions respectively by the constants c_0 and d_0 .

2.6. TEM Mode

The TEM mode may be reformulated in terms of measurable antenna parameters. Consider properties of $Q_0(\cos \theta)$, see Sec. A.18:

$$Q_0(\cos \theta) = \ln \left[\cot \left(\frac{\theta}{2} \right) \right] = \frac{1}{2} \left[\ln \left(\frac{1 + \cos \theta}{1 - \cos \theta} \right) \right] \quad (2.6.1)$$

Differentiating gives:

$$\frac{dQ_0}{d\theta} = -\frac{1}{\sin \theta} \quad (2.6.2)$$

The zero order spherical Bessel, Neumann and related functions are:

$$j_0(\sigma) = \frac{\sin \sigma}{\sigma}; \quad y_0(\sigma) = -\frac{\cos \sigma}{\sigma}; \quad j_0^*(\sigma) = \frac{\cos \sigma}{\sigma}; \quad y_0^*(\sigma) = \frac{\sin \sigma}{\sigma} \quad (2.6.3)$$

Substituting $\nu = 0$ and Eqs. (2.6.2) and (2.6.3) into Eq. (1.12.9) gives:

$$\begin{aligned} E_r &= 0 \\ \sigma E_{\theta} &= \frac{1}{i \sin \theta} (c_0 \cos \sigma + d_0 \sin \sigma) \\ \sigma \eta H_{\phi} &= \frac{1}{\sin \theta} (d_0 \cos \sigma - c_0 \sin \sigma) \end{aligned} \quad (2.6.4)$$

The voltage difference between equal radii positions on the two antenna arms is a measurable quantity. It may be calculated from knowledge of the

antenna structure and the electric field intensity using Eq. (2.6.3):

$$V(r) = \frac{\sigma}{k} \int_{\psi}^{\pi-\psi} E_{\theta} d\theta = \frac{1}{ik} (c_0 \cos \sigma + d_0 \sin \sigma) \int_{\psi}^{\pi-\psi} \frac{d\theta}{\sin \theta} \quad (2.6.5)$$

Integrating Eq. (2.6.2) shows that:

$$\int_{\psi}^{\pi-\psi} \frac{d\theta}{\sin \theta} = 2 \ln \left[\cot \left(\frac{\psi}{2} \right) \right]$$

It is useful in what lies ahead to define the line admittance of the transmission line formed by the two antenna arms to be $G(\psi)$ where:

$$G(\psi) = \frac{\pi}{\eta \ln \left[\cot \left(\frac{\psi}{2} \right) \right]} \quad (2.6.6)$$

Combining Eqs. (2.6.5) and (2.6.6) shows voltage $V(r)$ to be:

$$V(r) = \frac{2\pi}{ik\eta G(\psi)} (c_0 \cos \sigma + d_0 \sin \sigma) \quad (2.6.7)$$

Substituting Eq. (2.6.7) into the TEM component of the electric field intensity, Eq. (2.5.3), shows the zero order electric field intensity to be:

$$E_{\theta} = \frac{\eta k V(r) G(\psi)}{2\pi \sigma \sin \theta} \quad (2.6.8)$$

Since the magnetic field intensity is directed around the cone arms, the current on the antenna arms is radially directed. The use of Eq. (2.6.3) gives the relationship:

$$I(r) = \frac{\sigma}{k} \sin \theta \int_0^{2\pi} H_{\phi} d\phi = \frac{2\pi}{\eta k} (d_0 \cos \sigma - c_0 \sin \sigma) \quad (2.6.9)$$

Substituting Eq. (2.6.9) into the TEM component of the magnetic field intensity term of Eq. (2.5.3) shows the zero order magnetic field intensity to be:

$$H_{\phi} = \frac{k I(r)}{2\pi \sigma \sin \theta} \quad (2.6.10)$$

Defining position $r = a$ to be the terminus, the voltage and current there follow from Eqs. (2.6.7) and (2.6.10):

$$\begin{aligned} V(a) &= \frac{2\pi}{\eta G i k} \{c_0 \cos(ka) + d_0 \sin(ka)\} \\ I(a) &= \frac{2\pi}{\eta k} \{d_0 \cos(ka) - c_0 \sin(ka)\} \end{aligned} \quad (2.6.11)$$

Inverting Eq. (2.6.11) to obtain the field coefficients in terms of voltage and current at the antenna terminals gives:

$$\begin{aligned} c_0 &= \frac{\eta k}{2\pi} \{i G V(a) \cos(ka) - I(a) \sin(ka)\} \\ d_0 &= \frac{\eta k}{2\pi} \{I(a) \cos(ka) + i G V(a) \sin(ka)\} \end{aligned} \quad (2.6.12)$$

Next, define $Y(a)$ to be the terminator admittance:

$$Y(a) = \frac{I(a)}{V(a)}$$

Rearranging gives the voltage between, and the current on, the cone arms as a function of $Y(a)$:

$$\begin{aligned} V(r) &= \frac{V(a)}{G} \{G \cos[k(a-r)] + i Y(a) \sin[k(a-r)]\} \\ I(r) &= V(a) \{Y(a) \cos[k(a-r)] + i G \sin[k(a-r)]\} \end{aligned} \quad (2.6.13)$$

In terms of the terminator and line admittances, the admittance at each radius along the cones is:

$$Y(r) = G \frac{Y(a) \cos[k(a-r)] + i G \sin[k(a-r)]}{G \cos[k(a-r)] + i Y(a) \sin[k(a-r)]} \quad (2.6.14)$$

Use Eq. (2.6.14) to define the antenna input admittance $Y(0)$ and then put it equal to Y_0 , the admittance at $r = b$ in the limit as b approaches zero. Also, define the input voltage, $V(0)$, and current, $I(0)$, to be:

$$V(0) = \lim_{b \rightarrow 0} V(b); \quad I(0) = \lim_{b \rightarrow 0} I(b) \quad (2.6.15)$$

The input admittance is:

$$Y_0 = G \left\{ \frac{Y(a) \cos(ka) + i G \sin(ka)}{G \cos(ka) + i Y(a) \sin ka} \right\} \quad (2.6.16)$$

The radial dependence of the admittance as a function of the input and line admittances is:

$$Y(\sigma) = G \left\{ \frac{Y_0 \cos \sigma - i G \sin \sigma}{G \cos \sigma - i Y_0 \sin \sigma} \right\} \quad (2.6.17)$$

The line admittance equations have the exact form of admittance transfer along a TEM transmission line and show that the cone arms jointly act as a constant admittance line guiding the TEM mode from the source to the terminus. Quite differently from a parallel wire transmission line in which the guiding conductors remain equally spaced along the length of the line, here the guiding conductors are oppositely directed on either side of the source. Like many transmission lines the line impedance is constant, see Eq. (2.6.6). Voltage is measured between equal radius points on the cone arms and the current is measured along each arm.

2.7. Boundary Conditions

Packaging the TEM results of Sec. 2.6 into the interior field equations shows that the general form of the interior fields is:

$$\begin{aligned} E_r &= \sum_{\nu>0}^{\infty} \Gamma_{\nu} \nu (\nu + 1) \frac{j_{\nu}(\sigma)}{\sigma} M_{\nu}(\cos \theta) \\ E_{\theta} &= \sum_{\nu>0}^{\infty} \Gamma_{\nu} j_{\nu} \frac{dM_{\nu}(\cos \theta)}{d\theta} + \frac{\eta k G V(\sigma)}{2\pi \sigma \sin \theta} \\ \eta H_{\phi} &= -i \sum_{\nu>0}^{\infty} \Gamma_{\nu} j_{\nu} \frac{dM_{\nu}(\cos \theta)}{d\theta} + \frac{k I(\sigma)}{2\pi \sigma \sin \theta} \end{aligned} \quad (2.7.1)$$

The infinite set of multiplying coefficients Γ_{ν} and the input admittance $Y(0)$ are unknown and to be determined.

Since the magnetic field is entirely ϕ -directed, all currents on the cones are directed along the length of the cones. The total current consists of the sum of currents associated with the TM modes and the TEM mode. Define the TM modal current $I'(\sigma)$ to be the complementary current and the TEM modal current $I(\sigma)$ to be the principal current. The total current is the sum:

$$I_T(\sigma) = I'(\sigma) + I(\sigma) \quad (2.7.2)$$

The first term in the expression for H_ϕ shows that the complementary current, in amperes, is:

$$I'(\sigma, \psi) = \frac{2\pi\sigma}{i\eta k} \sum_{\nu>0}^{\infty} \Gamma_\nu j_\nu(\sigma) \frac{dM_\nu(\cos\theta)}{d\theta} \Big|_{\theta=\psi} \quad (2.7.3)$$

Since $j_\nu(\sigma)$ varies as σ^ν for small radii, where $\nu > 0$, it follows that the complementary current vanishes in that limit:

$$\lim_{\sigma \rightarrow 0} \Gamma(\sigma) = 0 \quad (2.7.4)$$

The principal current at the origin follows from Eqs. (2.6.9) and (2.6.12), and is:

$$\lim_{\sigma \rightarrow 0} I(\sigma) = I(a) \cos(ka) + iGV(a) \sin(ka) \quad (2.7.5)$$

Since only the principal current exists at the source, only it can support the energy flow away from the source. Since the time-average power supported by the TEM mode does not depend upon the radius, it follows that the time-average power is guided through the region by the principal current.

Application of the conducting boundary conditions to the exterior fields of Eq. (2.5.2) shows that the field intensities on the caps are related to the surface charges and currents as:

$$\begin{aligned} 0 \leq \theta < \psi \quad \text{and} \quad \pi - \psi < \theta \leq \pi; \\ \varepsilon E_r(ka, \theta, \phi) &= \frac{\varepsilon}{\sigma} \sum_{\ell=1;0}^{\infty} \ell(\ell+1) F_\ell h_\ell(ka) P_\ell(\cos\theta) = \rho(ka, \theta, \phi) \\ E_\theta(ka, \theta, \phi) &= \sum_{\ell=1;0}^{\infty} F_\ell h_\ell'(ka) \frac{dP_\ell(\cos\theta)}{d\theta} = 0 \\ H_\phi(ka, \theta, \phi) &= -\frac{i}{\eta} \sum_{\ell=1;0}^{\infty} F_\ell h_\ell(ka) \frac{dP_\ell(\cos\theta)}{d\theta} = -I_\theta(ka, \theta, \phi) \end{aligned} \quad (2.7.6)$$

Symbol $\rho(ka, \theta, \phi)$ indicates the surface charge density on the caps in coulombs per square meter and symbol $I_\theta(ka, \theta, \phi)$ indicates surface current density on the caps in amperes per meter. Application of the conducting

boundary conditions to the interior field components of Eq. (2.7.1) shows that the interior field intensities on the arms are subject to the constraints:

$$\begin{aligned}
 kb &\leq \sigma \leq ka \\
 E_r(\sigma, \psi, \phi) &= \sum_{\nu}^{\infty} \nu(\nu+1) F_{\nu} \frac{j_{\nu}(\sigma)}{\sigma} M_{\nu}(\cos \psi) = 0 \\
 \varepsilon E_{\theta}(\sigma, \psi, \phi) &= \frac{\eta k G V(\sigma)}{2\pi\sigma \sin \psi} + \varepsilon \sum_{\nu>0}^{\infty} \Gamma_{\nu} j_{\nu}^{\bullet} \frac{dM_{\nu}(\cos \theta)}{d\theta} \Big|_{\theta=\psi} \\
 &= \rho(\sigma, \psi, \phi) + \rho'(\sigma, \psi, \phi) \\
 \eta H_{\phi}(\sigma, \psi, \phi) &= -i \sum_{\nu>0}^{\infty} \Gamma_{\nu} j_{\nu} \frac{dM_{\nu}(\cos \theta)}{d\theta} \Big|_{\theta=\psi} + \frac{kI(\sigma)}{2\pi\sigma \sin \theta} \\
 &= I_r(\sigma, \psi, \phi) + I_r'(\sigma, \psi, \phi)
 \end{aligned} \tag{2.7.7}$$

Symbols with and without the primes indicate, respectively, principal and complimentary surface charge and current densities on the cone arms.

The null value of the radial field component at the conical surfaces is only satisfied by a nontrivial solution if for every value of ν :

$$M_{\nu}(\cos \psi) = 0 \tag{2.7.8}$$

Equation (2.7.8) determines an infinite and unique set of positive-real eigenvalues of ν . Plots of ν versus angle ψ for which Eq. (2.7.8) is satisfied are shown in Fig. 2.7.1 for the first through the fifth sequence of roots. Function $M_{\nu}(\cos \theta)$ is plotted versus ν in Fig. 2.7.2, showing the first 23 zeros. Plots of $M_{\nu}(\cos \theta)$ versus θ at the first two roots of $M_{\nu}[\cos(5^{\circ})]$ are illustrated by Fig. 2.7.3.

On the aperture, virtual boundary conditions apply, see Eqs. (A.12.6), and all field components are continuous through the boundary. Imposing these conditions on Eqs. (2.5.2) and (2.7.1) give the constraining equations:

$$\begin{aligned}
 \psi < \theta < \pi - \psi; \quad \sigma E_r(ka, \theta, \phi) &= \sum_{\ell=1;0}^{\infty} \ell(\ell+1) F_{\ell} h_{\ell}^{\bullet}(ka) P_{\ell}(\cos \theta) \\
 &= \sum_{\nu>0}^{\infty} \nu(\nu+1) \Gamma_{\nu} j_{\nu}^{\bullet}(ka) M_{\nu}(\cos \theta) \tag{2.7.9}
 \end{aligned}$$

$$\begin{aligned}
 \psi < \theta < \pi - \psi; \quad E_\theta(ka, \theta, \phi) &= \sum_{\ell=1;0}^{\infty} F_\ell h_\ell^*(ka) \frac{dP_\ell(\cos \theta)}{d\theta} \\
 &= \sum_{\nu}^{\infty} \Gamma_\nu j_\nu^*(ka) \frac{dM_\nu(\cos \theta)}{d\theta} + \frac{\eta kGV(a)}{2\pi\sigma \sin \theta}
 \end{aligned}
 \tag{2.7.10}$$

$$\begin{aligned}
 \psi < \theta < \pi - \psi; \quad \eta H_\phi(ka, \theta, \phi) &= -i \sum_{\ell=1;0}^{\infty} F_\ell h_\ell(ka) \frac{dP_\ell(\cos \theta)}{d\theta} \\
 &= -i \sum_{\nu}^{\infty} \Gamma_\nu j_\nu(ka) \frac{dM_\nu(\cos \theta)}{d\theta} + \frac{kV(a)}{2\pi\sigma \sin \theta}
 \end{aligned}
 \tag{2.7.11}$$

These are the field values on the interface between interior and exterior regions. This completes the discussion of the field equations at a point as boundary conditions.

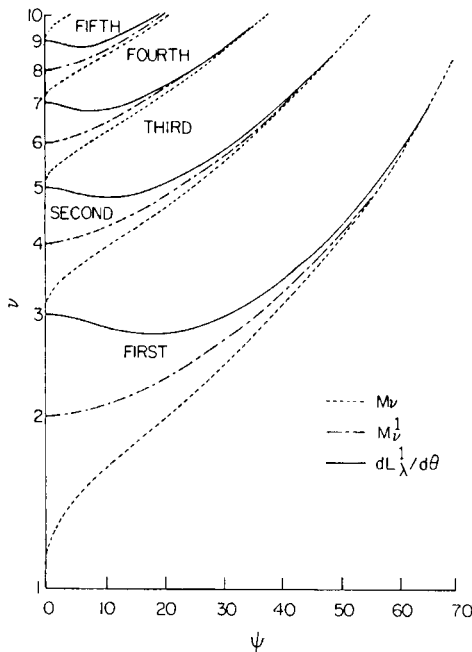


Fig. 2.7.1. Root values, noninteger Legendre functions. Plot showing values of ν for which the three functions $M_\nu(\cos \psi)$, $M_\nu^1(\cos \psi)$, and $dL_\nu^1(\cos \theta)/d\theta$ at $\theta = \psi$, are equal to zero versus cone angle ψ . Cardinal numbers indicate root order.

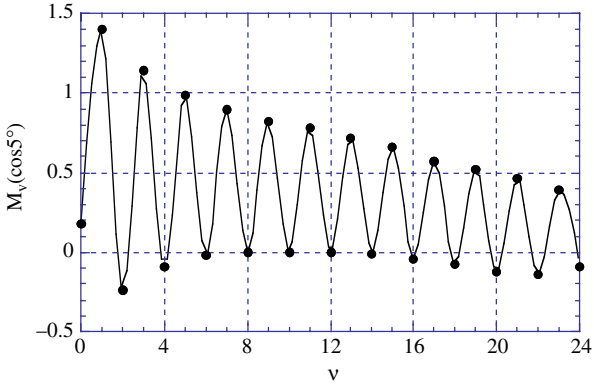


Fig. 2.7.2. The function $M_\nu[\cos(5^\circ)]$ plotted versus ν .

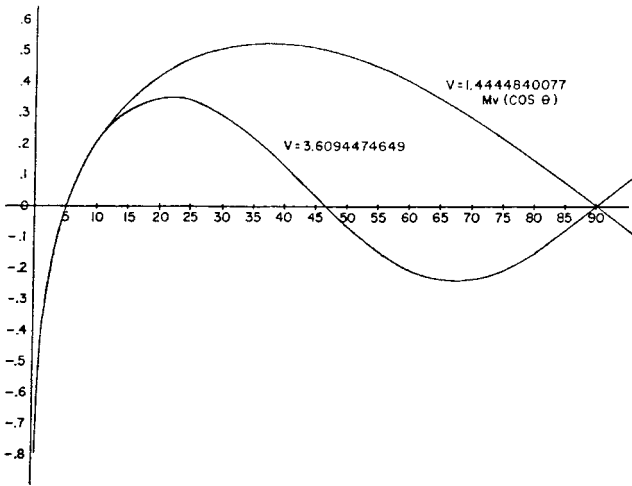


Fig. 2.7.3. Two lowest order functions $M_\nu(\cos \theta)$ versus θ ; $M_\nu[\cos(5^\circ)] = 0$.

2.8. The Defining Integral Equations

In the preceding sections, the general forms of the boundary conditions are obtained as infinite sums over radial and harmonic functions. The exact form of the functions and the relationships between them is specified. In each case what remains are sums over an infinite set of modal orders and

it remains to separate out the coefficients, one by one. In all but one case this is accomplished using the orthogonality of the Legendre functions. Sets of orthogonal integrals are formed and evaluated that change the equalities involving Legendre functions of the preceding sections into linear algebraic equations. The algebraic equations are used to solve for the coefficients.

The first algebraic equation is obtained without using orthogonality. Operating on Eq. (2.7.11) to evaluate the line integrals of the expression for H_ϕ around the periphery of the antenna arm on both sides of the $r = a$ boundary gives:

$$\begin{aligned} \int_{\psi}^{\pi-\psi} aH_\phi d\phi &= -i\frac{a}{\eta} \sum_{\ell=1}^{\infty} F_\ell h_\ell(ka) P_\ell(\cos\theta) \Big|_{\psi}^{\pi-\psi} \\ &= -i\frac{a}{\eta} \sum_{\nu}^{\infty} \Gamma_\nu j_\nu(ka) M_\nu(\cos\theta) \Big|_{\psi}^{\pi-\psi} + \frac{I(a)}{\eta G} \end{aligned} \tag{2.8.1}$$

The condition that $M_\nu(\cos\psi) = 0$ removes the sum over ν . Collecting the remaining terms and making the substitution that $I(a) = Y(a)V(a)$ gives the interior line admittance at the terminus as a function of the exterior coefficients:

$$Y(a) = \frac{2ia}{V(a)} \sum_{\ell o;1}^{\infty} F_\ell h_\ell(ka) P_\ell(\cos\psi) \tag{2.8.2}$$

Under the summation sign of Eq. (2.8.2), symbol $\ell o;1$ indicates that ℓ represents the range of odd integers with the lowest value of one. This equation, the first of the algebraic equations, equates the applied voltage and the admittance to a sum over odd order, exterior modes.

The next algebraic equation is obtained using the orthogonality of integer order Legendre functions. Multiplying Eq. (2.7.10) by $\sin\theta d\theta dP_n(\cos\theta)/d\theta$ and integrating over the aperture gives:

$$\begin{aligned} \int_0^\pi \sin\theta d\theta \frac{dP_n}{d\theta} \sum_{\ell o;1}^{\infty} F_\ell h_\ell(ka) \frac{dP_\ell}{d\theta} \\ = \int_{\psi}^{\pi-\psi} \sin\theta d\theta \frac{dP_n}{d\theta} \left\{ \sum_{\nu>0}^{\infty} \Gamma_\nu j_\nu(ka) \frac{dM_\nu}{d\theta} + \frac{\eta G V(a)}{2\pi a \sin\theta} \right\} \end{aligned} \tag{2.8.3}$$

Although with the problem as stated the limits on both integrals are from ψ to $\pi-\psi$, it follows from Eq. (2.7.6) that the sum on the left side of Eq. (2.8.3) is equal to zero over the caps. Therefore, the range of integration of the left side may be extended to the full range 0 to π without affecting the value

of the integral. Use the extended angular range and use the definitions of Tables A.22.1 and A.23.1 that:

$$I_{\ell\ell} = \frac{2}{2\ell + 1} \quad \text{and} \quad I_{\ell\nu} = \int_{\psi}^{\pi-\psi} P_{\ell}(\cos\theta)M_{\nu}(\cos\theta) \sin\theta \, d\theta \quad (2.8.4)$$

Symbol ‘I’ with two subscripts indicates an integral and with one subscript indicates current. Evaluating Eq. (2.8.3) by incorporating Eq. (2.8.4), Tables A.22.1.6, and A.23.1.1 gives:

$$\begin{aligned} \ell(\ell + 1)F_{\ell}h_{\ell}^{*}(ka)I_{\ell\ell} &= \ell(\ell + 1) \sum_{\nu>0}^{\infty} \Gamma_{\nu}j_{\nu}^{*}(ka)I_{\ell\nu} \\ &\quad - \frac{\eta\text{GV}(a)}{\pi a} P_{\ell}(\cos\psi) \end{aligned} \quad (2.8.5)$$

Equation (2.8.5) is the second algebraic expression that equates individual exterior modal coefficients to a sum over interior modal coefficients.

The third algebraic equation uses the orthogonality of fractional order Legendre functions. Begin by multiplying Eq. (2.7.11) by $\sin\theta \, d\theta \, dM_{\mu}(\cos\theta)/d\theta$ and integrating over the aperture:

$$\begin{aligned} &\int_{\psi}^{\pi-\psi} \sin\theta \, d\theta \sum_{\ell\circ;1}^{\infty} F_{\ell}h_{\ell}(ka) \frac{dP_{\ell}}{d\theta} \frac{dM_{\mu}}{d\theta} \\ &= \int_{\psi}^{\pi-\psi} \sin\theta \, d\theta \frac{dM_{\mu}}{d\theta} \left\{ \sum_{\nu}^{\infty} \Gamma_{\nu}j_{\nu}(ka) \frac{dM_{\nu}}{d\theta} + \frac{\eta\text{GV}(a)}{2\pi a \sin\theta} \right\} \end{aligned} \quad (2.8.6)$$

Evaluating the integrals of Eq. (2.8.6) using integral (A.23.1.5) with (A.23.1.1) and integral (A.23.1.7) with (A.23.1.6) gives:

$$\mu(\mu + 1)I_{\mu\mu}\Gamma_{\mu}j_{\mu}(ka) = \sum_{\ell\circ;1}^{\infty} \ell(\ell + 1)F_{\ell}h_{\ell}(ka)I_{\ell\mu} \quad (2.8.7)$$

Equation (2.8.7) is an algebraic expression that equates individual interior modal coefficients to a sum over exterior modes.

2.9. Solution of the Biconical Antenna Problem

The result of applying the orthogonality of Legendre functions to point equations is an expression for individual exterior or interior modal magnitudes as sums over interior or exterior modes, respectively.

The equations are:

$$F_\ell h_\ell^\bullet(ka) = -\frac{V(a)}{a} \frac{\eta G}{\pi} \frac{P_\ell(\cos \psi)}{\ell(\ell+1)I_{\ell\ell}} + \sum_{\nu>0}^{\infty} \Gamma_\nu j_\nu^\bullet(ka) \frac{I_{\ell\nu}}{I_{\ell\ell}} \quad (2.9.1)$$

$$\Gamma_\nu j_\nu(ka) = \frac{1}{\nu(\nu+1)} \sum_{\ell\geq 1}^{\infty} F_\ell h_\ell(ka) \ell(\ell+1) \frac{I_{\ell\nu}}{I_{\nu\nu}} \quad (2.9.2)$$

Each equation contains an infinite number of linear algebraic equations. The zero order interior mode satisfies the equation:

$$Y(a) = \frac{2ia}{V(a)} \sum_{\ell\geq 1}^{\infty} F_\ell h_\ell(ka) P_\ell(\cos \psi) \quad (2.9.3)$$

It remains to solve the three equations for the individual coefficients. After some manipulation, including multiplying through by $h_\ell(\sigma)/h_\ell^\bullet(\sigma)$, Eqs. (2.9.1) and (2.9.2) combine to form the equality:

$$\begin{aligned} F_\ell h_\ell(ka) - \sum_{n=1}^{\infty} F_n h_n(ka) \sum_{\nu>0}^{\infty} \frac{n(n+1)}{\nu(\nu+1)} \frac{I_{\ell\nu} I_{n\nu}}{I_{\ell\ell} I_{\nu\nu}} \frac{j_\nu^\bullet(ka) h_\ell(ka)}{j_\nu(ka) h_\ell^\bullet(ka)} \\ = -\frac{\eta G}{\pi} \frac{V(a)}{a} \frac{P_\ell(\cos \psi)}{\ell(\ell+1)I_{\ell\ell}} \frac{h_\ell(ka)}{h_\ell^\bullet(ka)} \end{aligned} \quad (2.9.4)$$

Equation (2.9.4) represents an infinite set of linear equations, one for each coefficient F_ℓ , and has the form:

$$x_\ell + \sum_{n=1}^{\infty} N_{\ell n} x_n = B_\ell \quad (2.9.5)$$

Because the magnitudes of coefficients F_ℓ decrease rapidly with increasing modal number, and to keep the magnitude within available computer range, it is helpful to solve the problem with the initial variable x_ℓ equal to $F_\ell h_\ell(ka)$. After solving for x_ℓ and knowing $h_\ell(ka)$, solve for F_ℓ .

Although an equation of the form of Eq. (2.9.5) may be readily solved using matrix techniques, doing so requires the series to be truncated and truncation produces errors. The solution procedure is to: (1) pick an arbitrary but specific value for the ratio $V(a)/a$, our choice was one, (2) use the matrix solution to solve for the product $F_\ell h_\ell(ka)$, (3) divide by $h_\ell(ka)$ to obtain F_ℓ . The procedure determines as many of the previously unknown exterior coefficients as needed, and is limited only by the capability of available computers. This completes the calculation of the exterior coefficients.

Knowing $F_\ell h_\ell(ka)$, Eq. (2.9.2) may be truncated and solved for F_ν , and Eq. (2.9.3) may be truncated and solved for the admittance $Y(a)$:

$$Y(a) = \frac{2iG}{V(a)/a} \sum_{\ell=1}^{\infty} F_\ell h_\ell(ka) \quad (2.9.6)$$

All quantities on the right side are known. Since for each mode $F_\ell h_\ell(ka)$ is proportional to $V(a)/a$, the magnitudes in the numerator and denominator of Eq. (2.9.6) cancel and the value of $Y(a)$ are correct for any applied voltage.

To change the field normalization to the more conveniently determined value $V(0)/a = 1$, enter the value into the first of Eq. (2.6.13) to obtain:

$$\frac{V(a)}{a} = \frac{G}{G \cos(ka) + iY(a) \sin(ka)} \quad (2.9.7)$$

Use of Eq. (2.9.7) to re-normalize F_ℓ completes the numerical analysis of biconical transmitting antennas.

Badii, Tomiyama, and Grimes used The Pennsylvania State University main frame computer, programmed for quadrupole precision, to do numerical analyses of several biconical antennas through 12-place accuracy. The analyses included series truncation with 17 external (maximum modal number of 33) and 16 internal modes. Table 2.9.1 lists, with six place accuracy, values of $F_\ell h_\ell(ka)$ and $\Gamma_\nu j_\nu(ka)$ for an antenna with $\psi = 5^\circ$ and $ka = 2$, external modes one through 17 and internal modes 1.444 through 16.391.

Table 2.9.2 lists the first six figures of F_ℓ and Γ_ν for the same antenna. The table values illustrate that the magnitudes of F_ℓ and Γ_ν respectively decrease and increase rapidly with increasing modal number. The coefficients and Eq. (2.9.7) determine the terminal admittance, $Y(a)$. $Y(a)$ and Eq. (2.6.14) determine the antenna's input impedance $Y(0)$.

Table 2.9.1. Constants for $\psi = 5^\circ$, $ka = 2$.

| ℓ | $F_\ell h_\ell(ka)$ | ν | $\Gamma_\nu j_\nu(ka)$ |
|--------|----------------------------------|-----------|-----------------------------------|
| 1 | (1.50924 - <i>i</i> 2.40989)D-01 | 0 | |
| 3 | (5.42697 - <i>i</i> 1.70419)D-02 | 1.4444840 | (4.33823 - <i>i</i> 17.5963)D-02 |
| 5 | (21.9562 - <i>i</i> 6.98844)D-03 | 3.6094475 | (3.68170 - <i>i</i> 2.37137)D-02 |
| 7 | (12.5283 - <i>i</i> 3.81076)D-03 | 5.7548721 | (2.23379 - <i>i</i> 1.17634)D-02 |
| 9 | (8.18028 - <i>i</i> 2.93358)D-03 | 7.8873272 | (2.59971 - <i>i</i> 1.27571)D-02 |
| 11 | (5.72681 - <i>i</i> 2.11622)D-03 | 10.016937 | (-10.8348 + <i>i</i> 5.10427)D-02 |
| 13 | (4.17152 - <i>i</i> 1.57614)D-03 | 12.143571 | (-8.89611 + <i>i</i> 4.07774)D-03 |
| 15 | (3.10771 - <i>i</i> 1.19513)D-03 | 14.268228 | (-3.57476 + <i>i</i> 1.60594)D-03 |
| 17 | (23.4057 - <i>i</i> 9.13644)D-04 | 16.391498 | (-19.5095 + <i>i</i> 8.62755)D-04 |

Table 2.9.2. Constants for $\psi = 5^\circ, ka = 2$.

| ℓ | F_ℓ | ν | Γ_ν |
|--------|------------------------------|----------|------------------------------|
| 1 | (-6.00998 - i 50.5094)D-02 | 0 | |
| 3 | (-9.96861 - i 36.9686)D-03 | 1.444484 | (1.32836 - i 5.387966)D-01 |
| 5 | (-3.75732 - i 11.8104)D-04 | 3.609448 | (14.3649 - i 9.25205)D-01 |
| 7 | (-6.96510 - i 20.3034)D-06 | 5.754872 | (3.36507 - i 1.77209)D+01 |
| 9 | (-7.74256 - i 21.5902)D-08 | 7.887327 | (3.04273 - i 1.49310)D+03 |
| 11 | (-5.7288 - i 15.5031)D-10 | 10.01694 | (-16.5306 + i 7.78756)D+05 |
| 13 | (-3.01440 - i 7.97810)D-12 | 12.14357 | (-2.67294 + i 1.22520)D+07 |
| 15 | (-1.18075 - i 3.07030)D-14 | 14.26823 | (-2.98297 + i 1.34009)D+09 |
| 17 | (-1.22586 - i 9.11817)D-18 | 16.39150 | (-6.07222 + i 2.68528)D+11 |

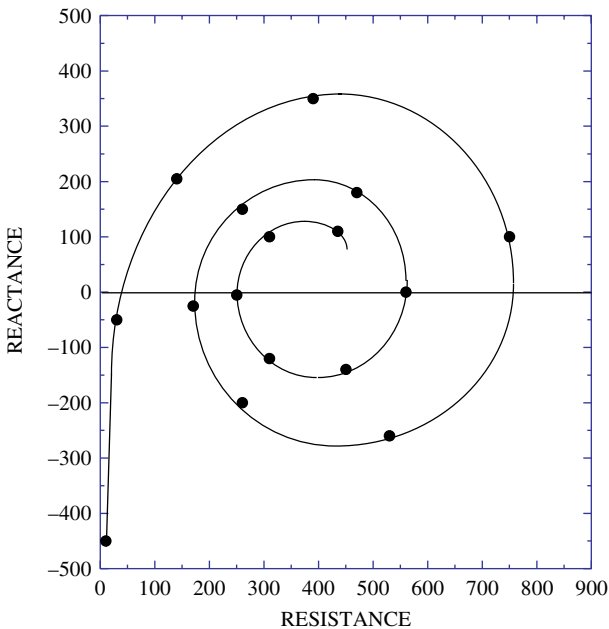


Fig. 2.9.1. Input impedance of a biconical antenna, with $\psi = 5^\circ$, as a function of arm length. Zero reactance values are at $ka = 1.11, 2.59, 4.06, 5.51, 7.14$. The first mark is at $ka = 0.5$, each succeeding mark increases ka by 0.5.

Figure 2.9.1 shows the input resistance and reactance as a function of arm length for 5° cones. The mark at about $-i450$ ohms shows the input impedance of an antenna with $ka = 0.5$; succeeding marks are spaced at intervals of cones made longer by $\Delta(ka) = 0.5$. Figure 2.9.2 shows the input

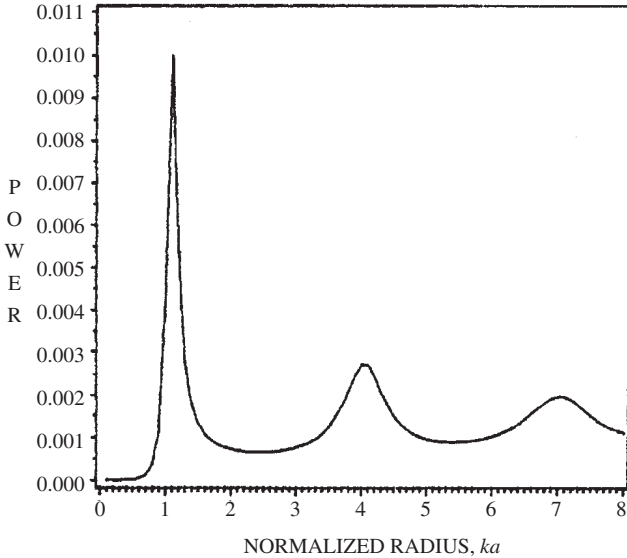


Fig. 2.9.2. Output power versus ka for a 5° , biconical, transmitting antenna. Antenna with 5° cone angles and a constant input voltage, showing radiated power peaks at $ka = 1.11, 4.06, 7.14$.

impedance of an antenna with $\psi = 5^\circ$ as a function of arm length. Note that the initial resonance is much sharper than succeeding ones; peaks are centered at about $ka \cong 1.11, 4.06, \text{ and } 7.14$.

By Eq. (2.7.6), each modal contribution to the total magnetic field intensity at the aperture is equal to $F_\ell h_\ell(ka) dP_\ell \cos(\theta)/d\theta$; the magnitude of $F_\ell h_\ell(ka)$ is listed in Table 2.9.1. From the theory of Legendre polynomials, see Table A.18.1:

$$\left. \frac{d}{d\theta} P_\ell \cos(\theta) \right|_{\pi/2} = (-1)^{(\ell-1)/2} \frac{(\ell)!!}{(\ell-1)!!} \quad (2.9.8)$$

The ratios of the modal contribution to H_ϕ to that of the exterior dipole mode at $\phi = \pi/2$ are listed in Table 2.9.3. At the aperture, the modal magnitudes decrease so slowly with increasing modal number that a reasonably accurate description of interface affects requires a large number of modes. In the far field, on the other hand, only the first few modes determine the fields.

Table 2.9.3. Magnetic field modal magnitudes.

| ℓ | Aperture Ratio | Far Field Ratio | ν | Factorial Ratio | Interior Ratio |
|--------|----------------|-----------------|-----------|-----------------|----------------|
| 1 | 1 | 1 | | | |
| 3 | 2.0005D-01 | 7.5275D-02 | 1.4444840 | 3.2498 | 2.0713 |
| 5 | 8.1033D-02 | 2.4366D-03 | 3.6094475 | 3.6529 | 5.6258D-01 |
| 7 | 4.6052D-02 | 4.2199D-05 | 5.7548721 | 3.8350 | 3.4050D-01 |
| 9 | 3.0563D-02 | 4.5092D-07 | 7.8873272 | 3.9504 | 4.0232D-01 |
| 11 | 2.1471D-02 | 3.2493D-09 | 10.016937 | 6.8083D-02 | 2.8677D-02 |
| 13 | 1.5682D-02 | 1.6767D-11 | 12.143571 | 3.8859D-01 | 1.1845D-03 |
| 15 | 1.1710D-02 | 6.4671D-14 | 14.268228 | 9.6692D-01 | 1.8995D-04 |
| 17 | 8.8363D-03 | 1.8087D-17 | 16.391498 | 1.6152 | 3.4457D-03 |

Note: All ratios are normalized by the magnitude of the exterior dipole mode. The first three columns refer to exterior fields: the first is modal number, the second the modal-to-dipole field ratio at the aperture and the third the modal-to-dipole field ratio at far field. The next three columns refer to interior fields: the first is modal number, the second the magnitude of Eq. (2.9.9), and the third modal-to-aperture field ratio.

In the interior region, modal magnitudes of $H_\phi(ka, \pi/2)$ at $\phi = \pi/2$ are equal to:

$$\Gamma_\nu j_\nu(ka) \frac{(\nu)!!}{(\nu-1)!!} \tag{2.9.9}$$

The ratio of factorials and the ratio-magnitude product for each mode are listed in Table 2.9.3. The ratio is a measure of the rate of convergence of the field expressions with increasing order. Although the external modes are monotone decreasing with increasing modal number, the internal modes are not; the interior modes decrease but not monotonically with increasing modal number. The difference is because interior-to-exterior modal coupling depends upon the numerical difference between the interior modal orders and odd integers, as well as the magnitudes of the modes.

Field values determine the charge and current densities on the antenna surfaces. Results are summarized as:

Cap: $\sigma = ka; \quad 0 \leq \theta < \psi; \quad \pi - \psi < \theta \leq \pi$

$$\rho(ka, \theta) = \varepsilon \sum_{\ell=0,1}^{\infty} \ell(\ell+1) F_\ell \frac{h_\ell(ka)}{ka} P_\ell(\cos \theta) \frac{\text{coulombs}}{\text{meter}^2} \tag{2.9.10}$$

$$I_\theta(ka, \theta) = \frac{i}{\eta} \sum_{\ell=0,1}^{\infty} F_\ell h_\ell(ka) \frac{dP_\ell(\cos \theta)}{d\theta} \frac{\text{amperes}}{\text{meter}}$$

Cones: $b < r < a$; $\theta = \psi$

$$\begin{aligned} \rho(\sigma, \psi) &= \left\{ \varepsilon \sum_{\nu>0}^{\infty} \Gamma_{\nu} j_{\nu}(\sigma) \frac{dM_{\nu}(\cos \theta)}{d\theta} \Big|_{\theta=\psi} + \frac{kGV(r)}{2\pi c\sigma \sin \psi} \right\} \frac{\text{coulombs}}{\text{meter}^2} \\ I_r(\sigma, \psi) + I_r'(r, \psi) &= \left\{ -\frac{kI(r)}{2\pi\sigma \sin \psi} + \frac{i}{\eta} \sum_{\nu>0}^{\infty} \Gamma_{\nu} j_{\nu}(\sigma) \frac{dM_{\nu}(\cos \theta)}{d\theta} \Big|_{\theta=\psi} \right\} \frac{\text{amperes}}{\text{meter}} \end{aligned} \quad (2.9.11)$$

On the cones the surface current density is radially directed and on the caps it is zenith angle directed. The two currents have quite different dependencies upon radius and zenith angle and therefore the current is not continuous through the cone-cap junction. A loop of charge accumulates at the junction with a sign and magnitude that depends upon antenna structural details and the radiated wavelength. The resulting ring charge is:

$$\begin{aligned} Q(ka, \psi) &= \frac{2\pi a}{i\omega} \left(\sum_{\ell>1}^{\infty} \beta_{\ell} h_{\ell}(ka) \frac{dP_{\ell}(\cos \psi)}{d\psi} \right. \\ &\quad \left. + \sum_{\nu>0}^{\infty} \Gamma_{\nu} j_{\nu}(ka) \frac{dM_{\nu}(\cos \psi)}{d\psi} \right) + \frac{iI(a)}{\omega \sin \psi} \end{aligned} \quad (2.9.12)$$

Similarly, charge densities on the cap and cone have quite different dependencies upon radius and zenith angle. The electric field intensity on the cone and cap are, respectively θ and r directed, and just off an ideal 90° junction the field is directed at an angle of 45° as measured from both the cone and cap.

2.10. Power

For a transmitting antenna, the time-average power in the interior and exterior regions follow by use of the fields of Eqs. (2.7.1) and (2.5.2), respectively. In the interior region, the time-average real power satisfies the transmission line rules between radii b and a . The input impedance and the radiated power are strong functions of the physical location of the standing energy wave, and it depends upon the antenna arm length.

The time-average power produced by an antenna is equal to the integral of the real part of the radial component of the complex Poynting vector at the surface of a virtual sphere, which for ease in calculation is made

concentric with the antenna. The fields of Eq. (2.5.2) show that the time-average output power is:

$$P_{av} = \frac{\sigma^2}{2\eta k^2} \operatorname{Re} \left\{ \int_0^{2\pi} d\phi \int_0^\pi \sin\theta d\theta \right. \\ \left. \times \sum_{\ell=1}^{\infty} \sum_{n=1}^{\infty} F_\ell F_n^* i h_\ell(\sigma) h_n^*(\sigma) \frac{dP_\ell}{d\theta} \frac{dP_n}{d\theta} \right\} \quad (2.10.1)$$

Replacing the Hankel functions by their far field values and evaluating the integral gives:

$$P_{av} = \frac{1}{\eta k^2} \sum_{\ell=1}^{\infty} \frac{\ell(\ell+1)}{(2\ell+1)} [F_\ell F_\ell^*] \quad (2.10.2)$$

Since all terms on the right side are known, Eq. (2.10.2) is sufficient to evaluate the output power.

The time-average power input, P_{in} , to the antenna is:

$$P_{in} = \frac{1}{2} \operatorname{Re}[V(0)I^*(0)] \quad (2.10.3)$$

By Eq. (2.6.13) the TEM voltage and current in the interior region are:

$$V(r) = \frac{V(a)}{G} \{ G \cos[k(a-r)] + iY(a) \sin[k(a-r)] \} \\ I(r) = V(a) \{ Y(a) \cos[k(a-r)] + iG \sin[k(a-r)] \} \quad (2.10.4)$$

Combining Eqs. (2.10.3) and (2.10.4) gives:

$$P_{in} = \frac{1}{2} \operatorname{Re}[V(a) V^*(a)] Y^*(a) \quad (2.10.5)$$

Since $V(a)$ and $Y(a)$ are known, Eq. (2.10.5) is sufficient to evaluate the input power.

In a lossless antenna:

$$P_{in} = P_{av} \quad (2.10.6)$$

The equality serves as a check on all procedures.

The complex power, P_c , on a concentric sphere of normalized radius σ is:

$$\begin{aligned}
 kb < \sigma < ka; \quad P_c(\sigma) &= \int_0^\pi \sin \theta \, d\theta \left\{ \frac{i\pi}{2} \sum_\nu \Gamma_\nu \Gamma_\nu^* \mathbf{j}_\nu^* \mathbf{j}_\nu \left(\frac{dM_\nu}{d\theta} \right)^2 \right. \\
 &\quad \left. + \frac{\eta k^2 G}{2\pi \sigma^2 \sin^2 \theta} V(r) I^*(r) \right\} \\
 \sigma > ka; \quad P_c(\sigma) &= \frac{i\pi \sigma^2}{\eta k^2} \int_0^\pi \left(\frac{dP_\ell}{d\theta} \right)^2 \sin \theta \, d\theta \sum_{\ell=1}^\infty F_\ell F_\ell^* h_\ell^*(\sigma) h_\ell^*(\sigma)
 \end{aligned} \tag{2.10.7}$$

With biconical antennas, the electric field intensity just off the surface of the caps has only a radial component. Therefore there is no normally directed Poynting vector and no energy is exchanged between the cap and the field. Since all aperture fields are continuous through the aperture, the total complex power is a continuous function of radius between positions $a - \delta$ and $a + \delta$, where δ is a differential radial length. Since all fields are continuous through the aperture, so is the energy density. Adjacent to the caps, the radial component of the electric field intensity and the azimuth component of the magnetic field intensity are not equal to zero. Therefore the energy per unit length as a function of radius is discontinuous between positions $a - \delta$ and $a + \delta$. The magnitude of the discontinuity increases with increasing cone angle.

Figures 2.10.1–2.10.3 describe the complex powers about three antennas with normalized arms lengths of $ka = 0.70, 1.28$, and 2.00 ; all have cone angles of one degree. The antennas are, respectively, electrically short, resonant, and electrically long. In all cases the real power, P_{real} , is constant.

The normalized complex power about an electrically short antenna, $ka = 0.7$, is shown in Fig. 2.10.1; the real power is small and the terminal impedance is capacitive. The peak reactive power is capacitive and occurs at approximately $kr = 0.1$. From there, the power decreases slowly with decreasing radius until reaching the terminals, $kr = 0$. For increasing radius it decreases more rapidly until reaching $kr = ka$, where it drops abruptly, then decreases slowly to zero with increasing radius for $kr > ka$.

The normalized complex power about a resonant antenna, $ka = 1.28$ is shown in Fig. 2.10.2; the real power is large and the terminal impedance is resistive. The capacitively phased reactive power peak of Fig. 2.10.1 has moved outward to about $kr = 0.8$. From there it decreases slowly with decreasing radius to zero at the terminals. For increasing radius it behaves very similarly to Fig. 2.10.1.

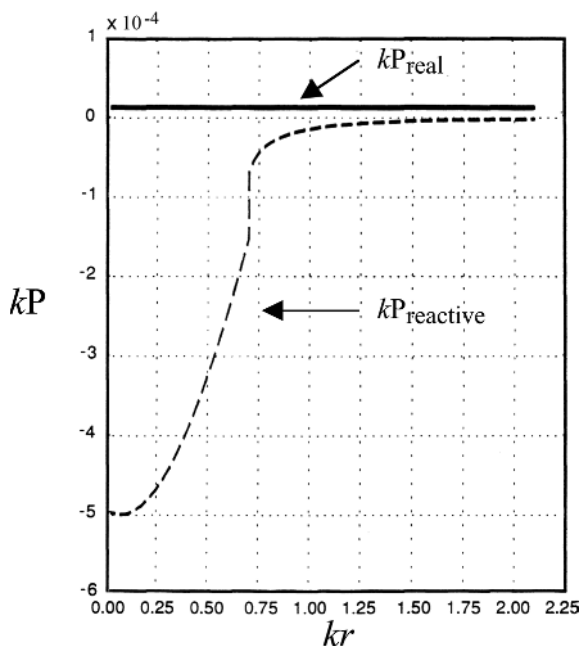


Fig. 2.10.1. Normalized real and reactive powers versus kr for a biconical transmitting antenna; applied voltage $V(0) = a$, cone angle $\psi = 1^\circ$, and $ka = 0.70$.

The normalized complex power about an electrically long antenna, $ka = 2.00$, is shown in Fig. 2.10.3; the real power is less than that of Fig. 2.10.2 and the terminal impedance is inductive. The capacitively phased reactive power peak has moved outward to about $kr = 1.6$. From there it decreases slowly with decreasing radius, passes through zero and becomes inductively phased at the terminals. For increasing radius it behaves very similarly to Figs. 2.10.1 and 2.10.2.

2.11. Biconical Receiving Antennas

For a receiving antenna to function it is necessary that a component of the electric field intensity be aligned parallel with the antenna axis; optimum operation is with full alignment. With plane waves, the directions of polarization and propagation are perpendicular and, in the analysis of scattering from a sphere, the incoming plane wave propagated in the z -direction. To analyze scattering from a receiving antenna it is convenient for the antenna axis to lie along the z -axis. It is necessary, therefore, to analyze a z -polarized plane wave and, with z -polarization, it must propagate somewhere in the

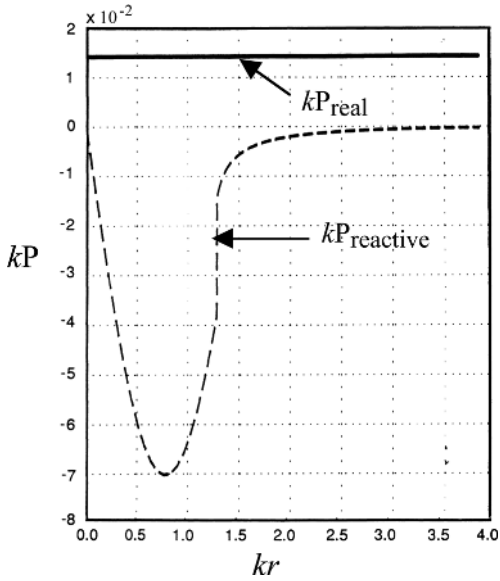


Fig. 2.10.2. Real and reactive powers versus kr for a biconical transmitting antenna; applied voltage $V(0) = a$, cone angle $\psi = 1^\circ$, and $ka = 1.28$.

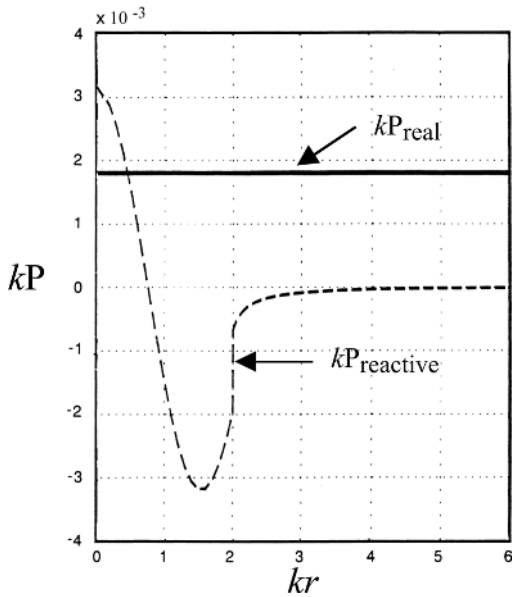


Fig. 2.10.3. Real and reactive powers versus kr for a biconical transmitting antenna; applied voltage $V(0) = a$, cone angle $\psi = 1^\circ$, and $ka = 2.00$.

xy -plane. We make the arbitrary choice that the plane wave propagates in the y -direction. It is, therefore, necessary to expand a y -directed wave in spherical coordinates. Such an expansion is done in a way similar to the way it was done for a z -directed plane wave, see Sec. 2.1. The desired exponential is:

$$e^{i(\omega t - ky)} = e^{i(\omega t - \sigma \sin \theta \sin \phi)} \quad (2.11.1)$$

Since Eq. (2.11.1) has no singularities, the spherical coordinate expansion can contain no spherical Neumann functions, no fractional order Legendre functions, and no Legendre functions of the second kind. Only spherical Bessel functions and associated Legendre polynomials remain. The most general form for the expansion is:

$$\begin{aligned} e^{-i\sigma \sin \theta \sin \phi} &= \sum_{\ell=0}^{\infty} \sum_{m=0}^{\ell} [{}^c G_{\ell}^m \cos m\phi - i {}^s G_{\ell}^m \sin m\phi] \\ &\times \frac{\ell(\ell+1)}{m} j_{\ell}(\sigma) P_{\ell}^m(\cos \theta) \end{aligned} \quad (2.11.2)$$

To complete the description it is necessary to evaluate both infinite sets of coefficients ${}^c G_{\ell}^m$ and ${}^s G_{\ell}^m$. The reverse superscripts “c” and “s” indicate coefficients of cosine and sine, respectively, and the multiplying factor $\ell(\ell+1)/m$ is chosen for later convenience. As written Eq. (2.11.2) is in the form of two sums over infinite sets of coefficients. In order to evaluate the coefficients it is necessary to reformulate the equation as a doubly infinite number of separate algebraic equations, each of which provides a definite value for one coefficient.

From the theory of spherical Bessel functions, Eq. (A.24.9):

$$j_{\ell}(\sigma) = \frac{\sigma^{\ell}}{(2\ell+1)!!} + \text{higher order terms} \quad (2.11.3)$$

Substitute Eq. (2.11.3) into the right side of Eq. (2.11.2); take ℓ differentials of both sides with respect to σ , then go to the limit as σ goes to zero. The result is the equality:

$$\begin{aligned} (-i)^{\ell} \sin^{\ell} \theta \sin^{\ell} \phi &= \sum_{\ell=0}^{\infty} \sum_{m=0}^{\ell} [{}^c G_{\ell}^m \cos m\phi - i {}^s G_{\ell}^m \sin m\phi] \\ &\times \frac{\ell(\ell+1)}{m} \frac{\ell!}{(2\ell+1)!!} P_{\ell}^m(\cos \theta) \end{aligned} \quad (2.11.4)$$

The left side of Eq. (2.11.4) involves powers of trigonometric functions. Identities that convert powers to multiples of the angles are:

n even:

$$\sin^n \phi = \frac{2}{2^n} \left\{ \sum_{k=0}^{n/2-1} (-1)^{n/2-k} \frac{(n)!}{(n-k)!k!} \cos[(n-2k)\phi] + \frac{(n)!}{(n/2)!^2} \right\} \quad (2.11.5)$$

n odd:

$$\sin^n \phi = \frac{2}{2^n} \left\{ \sum_{k=0}^{(n-1)/2} (-1)^{(n-1)/2-k} \frac{(n)!}{(n-k)!k!} \sin[(n-2k)\phi] \right\}$$

Substitute Eq. (2.11.5) into Eq. (2.11.4) and then multiply by $\cos(q\phi)$, where q is an integer, and integrate over the azimuth angle. Next, multiply by $\sin(q\phi)$ and repeat the procedure. The results, where the δ represents Kronecker delta functions and s represents an integer, are:

$$\begin{aligned} \frac{{}^c G_\ell^q}{q} \frac{\ell(\ell+1)}{(2\ell+1)!!} P_\ell^q(\cos\theta) &= \frac{(-i)^{(\ell-q)} \delta(q, 2s)}{(q/2)![(\ell-q)/2]!} \sin^\ell \theta \\ \frac{{}^s G_\ell^q}{q} \frac{\ell(\ell+1)}{(2\ell+1)!} P_\ell^q(\cos\theta) &= \frac{(-i)^{(\ell-q)} \delta(q, 2s+1)}{(q/2)![(\ell-q)/2]!} \sin^\ell \theta \end{aligned} \quad (2.11.6)$$

By Eq. (2.11.6), ${}^c G_\ell^q$ is equal to zero if q is odd and ${}^s G_\ell^q$ is equal to zero if q is even. This reduces the total number of nonzero coefficients by half.

Next, multiply the top of Eq. (2.11.6) by $P_\ell^q(\cos\theta)$ and integrate over the zenith angle. Integral forms are Eqs. (1) and (10) of Table A.22.1:

q even:

$$\frac{2^{\ell+1} \ell!(\ell+q)!}{(q/2)![(\ell-q)/2]!(2\ell+1)!} \delta(\ell+q, 2s) = \frac{{}^c G_\ell^q}{q} \frac{\ell(\ell+1)}{(2\ell+1)!!} \frac{2}{(2\ell+1)} \frac{(\ell+q)!}{(\ell-q)!} \quad (2.11.7)$$

By Eq. (2.11.7), ${}^c G_\ell^q$ is equal to zero if $\ell+q$ is odd. Since q is even, it follows that ℓ is also even. Conducting the same operation on the second of Eq. (2.11.6) shows that ${}^s G_\ell^q$ is also equal to zero if $\ell+q$ is odd. Since, for this case, q is odd, it follows that ℓ is also odd. Therefore the two groups of coefficients form non-overlapping sets and the distinction may be dropped: G_ℓ^q represents both sets of functions. This reduces the set of non-zero coefficients to one-fourth of the original number in Eq. (2.11.2).

Simplifying results gives:

$$\begin{aligned}
 G_\ell^m &= \frac{2m(2\ell + 1)(\ell - m)!\delta(\ell + m, 2q)}{2^\ell \ell(\ell + 1) \left(\frac{\ell + m}{2}\right)! \left(\frac{\ell - m}{2}\right)!} \\
 &= \frac{2m(2\ell + 1)(\ell - m)!\delta(\ell + m, 2q)}{\ell(\ell + 1)(\ell + m)!!(\ell - m)!!}
 \end{aligned}
 \tag{2.11.8}$$

This equation is correct for all modal combinations. Combining Eqs. (2.11.2) and (2.11.8) shows that the spherical coordinate expansion for a y -directed, z -polarized plane wave is:

$$\begin{aligned}
 e^{-i\sigma \sin \theta \sin \phi} &= \left\{ \sum_{\ell=0;e}^{\infty} \sum_{m\ell}^{\ell} \cos(m\phi) - i \sum_{\ell=1;o}^{\infty} \sum_{m\ell}^{\ell} \sin(m\phi) \right\} \\
 &\times \frac{\ell(\ell + 1)}{m} G_\ell^m j_\ell(\sigma) P_\ell^m(\cos \theta)
 \end{aligned}
 \tag{2.11.9}$$

2.12. Incoming TE Fields

To find the expression for the radial magnetic field component, H_r , of a y -directed plane wave with the electric field intensity z -directed, begin by noting that:

$$\begin{aligned}
 \eta H_r &= \sin \theta \cos \phi e^{-i\sigma \sin \theta \sin \phi} \\
 &= \frac{i}{\sigma} \frac{\partial}{\partial \phi} e^{-i\sigma \sin \theta \sin \phi}
 \end{aligned}
 \tag{2.12.1}$$

The first equality in Eq. (2.12.1) is by definition. Using the derivative operation of Eq. (2.12.1) on the spherical coordinate expression for the exponential form of Eq. (2.11.9) gives:

$$\eta H_r = \left[\sum_{\ell=1;o}^{\infty} \sum_{m\ell}^{\ell} \cos(m\phi) - i \sum_{\ell=2;e}^{\infty} \sum_{m\ell}^{\ell} \sin(m\phi) \right] \ell(\ell + 1) G_\ell^m \frac{j_\ell(\sigma)}{\sigma} P_\ell^m(\cos \theta)
 \tag{2.12.2}$$

Combining Eq. (2.12.2) with the same field component of Eq. (1.12.9) determines the constant field coefficients. Knowledge of the constant field coefficients and the component forms of Eq. (1.12.9) are sufficient to obtain the full set of TE modes.

2.13. Incoming TM Fields

A longer procedure is necessary to obtain the coefficients for TM modes. It is convenient to define E_r in a way analogous with Eq. (2.12.2), using

Eq. (2.13.1) to define coefficients ${}^cF_\ell^m$ and ${}^sF_\ell^m$, then solve for the constants. The general form for the field is:

$$E_r = \sum_{\ell=0}^{\infty} \sum_{m=0}^{\ell} [{}^cF_\ell^m \cos(n\phi) - i {}^sF_\ell^m \sin(n\phi)] \ell(\ell+1) \frac{j_\ell(\sigma)}{\sigma} P_\ell^m(\cos \theta) \quad (2.13.1)$$

The radial component of the y -directed plane wave is:

$$\begin{aligned} E_r &= \cos \theta e^{-i\sigma \sin \theta \sin \phi} \\ &= \frac{i}{\sigma \sin \phi} \frac{\partial}{\partial \theta} e^{-i\sigma \sin \theta \sin \phi} \end{aligned} \quad (2.13.2)$$

Using the derivative operation of Eq. (2.13.2) on the spherical coordinate expression for the exponential form of Eq. (2.11.9) gives:

$$\begin{aligned} E_r &= \frac{i}{\sin \phi} \left[\sum_{\ell e;0}^{\infty} \sum_{me}^{\ell} \cos(m\phi) - i \sum_{\ell o;1}^{\infty} \sum_{mo}^{\ell} \sin(m\phi) \right] \\ &\quad \times \frac{\ell(\ell+1)}{m} G_\ell^m \frac{j_\ell(\sigma)}{\sigma} \frac{dP_\ell^m(\cos \theta)}{d\theta} \end{aligned} \quad (2.13.3)$$

Symbols $\ell e;0$ and $\ell o;1$ indicate sums respectively over even integers starting at zero, and over odd integers starting at one. Symbols me and mo indicate sums respectively over even and odd integers. A trigonometric identity that puts Eq. (2.13.3) in a more useful form is:

$$\frac{1}{\sin \phi} \equiv 2 \sum_{s=0}^{\infty} \sin[(2s+1)\phi] \quad (2.13.4)$$

Combining Eqs. (2.13.3) and (2.13.4) results in:

$$\begin{aligned} E_r &= 2 \sum_{s=0}^{\infty} \left[i \sum_{\ell e;0}^{\infty} \sum_{me}^{\ell} \cos m\phi + \sum_{\ell o;1}^{\infty} \sum_{mo}^{\ell} \sin m\phi \right] \sin[(2s+1)\phi] \\ &\quad \times \frac{\ell(\ell+1)}{m} G_\ell^m \frac{j_\ell(\sigma)}{\sigma} \frac{dP_\ell^m(\cos \theta)}{d\theta} \end{aligned} \quad (2.13.5)$$

Other useful trigonometric identities are:

$$\begin{aligned} 2 \sin m\phi \sin(2s+1)\phi &\equiv \cos[(m-2s-1)\phi] - \cos[(m+2s+1)\phi] \\ 2 \cos m\phi \sin(2s+1)\phi &\equiv \sin[(m+2s+1)\phi] - \sin[(m-2s-1)\phi] \end{aligned} \quad (2.13.6)$$

The procedure is to substitute Eq. (2.13.6) into Eq. (2.13.5), equate Eqs. (2.13.1) and (2.13.5), differentiate both $(\ell - 1)$ times by σ , then go to the limit as σ goes to zero. The result, for ℓ odd, is:

$$\sum_{s=0}^{\infty} \left[\sum_{m=0}^{\ell} \{ \cos[(m - 2s - 1)\phi] - \cos[(m + 2s + 1)\phi] \} \right] \frac{G_{\ell}^m}{m} \frac{dP_{\ell}^m(\cos \theta)}{d\theta}$$

$$= \sum_{n=0}^{\ell} [{}^c F_{\ell}^n \cos(m\phi) - i {}^s F_{\ell}^n \sin(m\phi)] P_{\ell}^n(\cos \theta) \tag{2.13.7}$$

Next multiply Eq. (2.13.7) by $\cos(q\phi)$, where q is an integer, and integrate over the full range $\phi = 0$ to 2π . This shows that ${}^s F_{\ell}^n$ is equal to zero for odd values of ℓ ; it follows in a similar way that ${}^c F_{\ell}^n$ is equal to zero for even values of ℓ . Therefore the coefficients form non-overlapping sets and, again, the notation may be simplified by dropping the reverse superscript, with F_{ℓ}^n representing both sets of coefficients. This reduces the set of non-zero coefficients to one-fourth of the original number in Eq. (2.13.1). The resulting equality is

$$\sum_{n=0}^{\ell} \delta(q, n) F_{\ell}^n P_{\ell}^n(\cos \theta)$$

$$= \sum_{s=0}^{\infty} \sum_{m=0}^{\ell} \{ \delta(q, |m - 2s - 1|) - \delta(q, m + 2s + 1) \} \frac{G_{\ell}^m}{m} \frac{dP_{\ell}^m(\cos \theta)}{d\theta} \tag{2.13.8}$$

Evaluating the delta functions and collecting terms gives, after some algebra and with $U(q)$ representing a step function of q :

$$F_{\ell}^q P_{\ell}^q(\cos \theta) = 2U(q) \sum_{s=0}^{(\ell-q-1)/2} \frac{G_{\ell}^{q+2s+1}}{q + 2s + 1} \frac{dP_{\ell}^{q+2s+1}(\cos \theta)}{d\theta} \tag{2.13.9}$$

With the aid of Table A.21.1.1, Eq. (2.13.9) may be rewritten as:

$$F_{\ell}^q P_{\ell}^q(\cos \theta) = U(q) \sum_{s=0}^{(\ell-q-1)/2} \frac{G_{\ell}^{q+2s+1}}{q + 2s + 1}$$

$$\times [(\ell + q + 2s + 1)(\ell - q - 2s) P_{\ell}^{q+2s} - P_{\ell}^{q+2s+2}] \tag{2.13.10}$$

Multiply Eq. (2.13.10) by $P_\ell^q(\cos\theta)$ and integrate over θ using the integrals of Table A.22.1.2. After simplifying, the result is:

$$F_\ell^q = 2\ell(\ell - q)! \sum_{s=0}^{(\ell-q-1)/2} \frac{G_\ell^{q+2s+1}}{(q+2s+1)} \frac{(-1)^s U(q)}{(\ell - q - 2s - 1)!} \quad (2.13.11)$$

Combining Eqs. (2.11.9) and (2.13.11), with n equal to any of the full set of positive integers, gives:

$$F_\ell^q = \frac{4(2\ell + 1)}{(\ell + 1)} (\ell - q)! \sum_{s=0}^{(\ell-q-1)/2} \frac{(-1)^s U(q) \delta(\ell + q, 2n + 1)}{(\ell - q - 2s - 1)!! (\ell + q + 2s + 1)!!} \quad (2.13.12)$$

The sum of Eq. (2.13.12) is listed in Table A.15.1.8. Incorporating the sum, replacing q by m to give the same dummy index as Eq. (2.11.9), and letting n denote any of the full set of possible integers, the two coefficient sets F_ℓ^m and G_ℓ^m are equal to:

$$\begin{aligned} F_\ell^m &= \frac{2(2\ell + 1)}{\ell(\ell + 1)} \frac{U(m)(\ell - m)! \delta(\ell + m, 2n + 1)}{(\ell + m - 1)!! (\ell - m - 1)!!} \\ G_\ell^m &\equiv \frac{2(2\ell + 1)}{\ell(\ell + 1)} \frac{m(\ell - m)! \delta(\ell + m, 2n)}{(\ell + m)!! (\ell - m)!!} \end{aligned} \quad (2.13.13)$$

Coefficients F_ℓ^m and G_ℓ^m have opposite parity in that F_ℓ^m is other than zero only if $\ell + m$ is odd and G_ℓ^m is other than zero only if $\ell + m$ is even. At degree $m = 0$ coefficients F_ℓ^m have the maximum value and coefficients G_ℓ^m are equal to zero. Values through the first five orders are listed in Table 2.13.1.

Table 2.13.1. Values of field coefficients for a y -directed, z -polarized plane wave.

| | | | | | |
|-------------------------|--------------------------|--------------------------|---------------------------|---------------------------|----------------------------|
| $F_1^0 = \frac{3}{2}$ | $G_1^1 = \frac{3}{2}$ | | | | |
| | $F_2^1 = \frac{5}{6}$ | $G_2^2 = \frac{5}{12}$ | | | |
| $F_3^0 = \frac{7}{8}$ | $G_3^1 = \frac{7}{72}$ | $F_3^2 = \frac{7}{48}$ | $G_3^3 = \frac{7}{96}$ | | |
| | $F_4^1 = \frac{9}{160}$ | $G_4^2 = \frac{3}{160}$ | $F_4^3 = \frac{3}{160}$ | $G_4^4 = \frac{3}{320}$ | |
| $F_5^0 = \frac{11}{16}$ | $G_5^1 = \frac{11}{240}$ | $F_5^2 = \frac{11}{240}$ | $G_5^3 = \frac{11}{1920}$ | $F_5^4 = \frac{11}{5760}$ | $G_5^5 = \frac{11}{11520}$ |

2.14. Exterior Fields, Powers, and Forces

The radial field components of a y -directed, z -polarized plane wave are given by the combination of Eqs. (2.12.2), (2.13.1), and (2.13.13):

$$\begin{aligned} E_r &= \left\{ \sum_{\ell_0;1}^{\infty} \sum_{me}^{\ell-1} \cos(m\phi) - i \sum_{\ell e;2}^{\infty} \sum_{mo}^{\ell-1} \sin(m\phi) \right\} \ell(\ell+1) F_{\ell}^m \frac{j_{\ell}(\sigma)}{\sigma} P_{\ell}^m(\cos \theta) \\ \eta H_r &= \left\{ \sum_{\ell_0;1}^{\infty} \sum_{mo}^{\ell} \cos(m\phi) - i \sum_{\ell e;2}^{\infty} \sum_{me}^{\ell} \sin(m\phi) \right\} \ell(\ell+1) G_{\ell}^m \frac{j_{\ell}(\sigma)}{\sigma} P_{\ell}^m(\cos \theta) \end{aligned} \quad (2.14.1)$$

The angularly directed field components follow from Eq. (2.14.1).

One of the two differences between the field forms of the incoming plane wave and the scattered waves is that in the limit of infinite radius the scattered wave varies with distance as $\exp[i(\omega t - \sigma)]/\sigma$. This functional form requires the radial dependent functions to be spherical Hankel functions of the second kind. It is, therefore, necessary to replace the spherical Bessel functions by spherical Hankel functions. Similar to a spherical scatterer, different modes scatter with different magnitudes and different phases. To account for these changes introduce two new infinite sets of field constants, α_{ℓ}^m and β_{ℓ}^m as part of the scattered fields. Let α_{ℓ}^m be the coefficient of TE modes and β_{ℓ}^m be the coefficient of TM modes. Incorporating these results into the radial components of the scattered field gives:

$$\begin{aligned} E_r &= \left[\sum_{\ell_0;1}^{\infty} \sum_{me}^{\ell-1} \cos(m\phi) - i \sum_{\ell e;2}^{\infty} \sum_{mo}^{\ell-1} \sin(m\phi) \right] \\ &\quad \times \ell(\ell+1) \beta_{\ell}^m F_{\ell}^m \frac{h_{\ell}(\sigma)}{\sigma} P_{\ell}^m(\cos \theta) \\ \eta H_r &= \left[\sum_{\ell_0;1}^{\infty} \sum_{mo}^{\ell} \cos(m\phi) - i \sum_{\ell e;2}^{\infty} \sum_{me}^{\ell} \sin(m\phi) \right] \\ &\quad \times \ell(\ell+1) \alpha_{\ell}^m G_{\ell}^m \frac{h_{\ell}(\sigma)}{\sigma} P_{\ell}^m(\cos \theta) \end{aligned} \quad (2.14.2)$$

Problem solution requires evaluation of the full parameter sets α_{ℓ}^m and β_{ℓ}^m . As with the spherical scatterer, the total field is the sum of the incoming plane wave fields and the outwardly directed scattered fields. Summing the radial field components of Eqs. (2.14.1) and (2.14.2) gives the total radial field components. The angular field components follow directly from

the radial ones, see Eq. (1.12.9), and are:

$$\begin{aligned}
 E_\theta &= \left[\sum_{\ell_0;1}^{\infty} \sum_{me}^{\ell-1} \cos(m\phi) - i \sum_{\ell_0;2}^{\infty} \sum_{mo}^{\ell-1} \sin(m\phi) \right] F_\ell^m(\mathbf{j}_\ell^\bullet + \beta_\ell^m \mathbf{h}_\ell^\bullet) \frac{dP_\ell^m}{d\theta} \\
 &\quad - \left[\sum_{\ell_0;2}^{\infty} \sum_{me}^{\ell} \cos(m\phi) - i \sum_{\ell_0;1}^{\infty} \sum_{mo}^{\ell} \sin(m\phi) \right] G_\ell^m(j_\ell + \alpha_\ell^m h_\ell) \frac{mP_\ell^m}{\sin\theta} \\
 \eta H_\phi &= -i \left[\sum_{\ell_0;1}^{\infty} \sum_{me}^{\ell-1} \cos(m\phi) - i \sum_{\ell_0;2}^{\infty} \sum_{mo}^{\ell-1} \sin(m\phi) \right] F_\ell^m(j_\ell + \beta_\ell^m h_\ell) \frac{dP_\ell^m}{d\theta} \\
 &\quad - i \left[\sum_{\ell_0;2}^{\infty} \sum_{me}^{\ell} \cos(m\phi) - i \sum_{\ell_0;1}^{\infty} \sum_{mo}^{\ell} \sin(m\phi) \right] G_\ell^m(\mathbf{j}_\ell^\bullet + \alpha_\ell^m \mathbf{h}_\ell^\bullet) \frac{mP_\ell^m}{\sin\theta} \\
 -E_\phi &= i \left[\sum_{\ell_0;2}^{\infty} \sum_{mo}^{\ell-1} \cos(m\phi) - i \sum_{\ell_0;3}^{\infty} \sum_{me}^{\ell-1} \sin(m\phi) \right] F_\ell^m(\mathbf{j}_\ell^\bullet + \beta_\ell^m \mathbf{h}_\ell^\bullet) \frac{mP_\ell^m}{\sin\theta} \\
 &\quad - i \left[\sum_{\ell_0;1}^{\infty} \sum_{mo}^{\ell} \cos(m\phi) - i \sum_{\ell_0;2}^{\infty} \sum_{me}^{\ell} \sin(m\phi) \right] G_\ell^m(j_\ell + \alpha_\ell^m h_\ell) \frac{dP_\ell^m}{d\theta} \\
 \eta H_\theta &= \left[\sum_{\ell_0;2}^{\infty} \sum_{mo}^{\ell-1} \cos(m\phi) - i \sum_{\ell_0;3}^{\infty} \sum_{me}^{\ell-1} \sin(m\phi) \right] F_\ell^m(j_\ell + \beta_\ell^m h_\ell) \frac{mP_\ell^m}{\sin\theta} \\
 &\quad + \left[\sum_{\ell_0;1}^{\infty} \sum_{mo}^{\ell} \cos(m\phi) - i \sum_{\ell_0;2}^{\infty} \sum_{me}^{\ell} \sin(m\phi) \right] G_\ell^m(\mathbf{j}_\ell^\bullet + \alpha_\ell^m \mathbf{h}_\ell^\bullet) \frac{dP_\ell^m}{d\theta}
 \end{aligned} \tag{2.14.3}$$

Power on a circumscribing virtual sphere of radius greater than a is obtained from the radial component of the complex Poynting vector. Substituting Eq. (2.14.3) into Eq. (2.2.3) and breaking the resulting vector into four parts gives:

$$\begin{aligned}
 N_{r11} &= \frac{\text{Re}}{2\eta} \left\{ \left(\sum_{\ell_0}^{\infty} \sum_{me}^{\ell-1} \cos(m\phi) - i \sum_{\ell_0}^{\infty} \sum_{mo}^{\ell-1} \sin(m\phi) \right) \right. \\
 &\quad \times \left(\sum_{n_0}^{\infty} \sum_{pe}^{n-1} \cos(p\phi) + i \sum_{n_0}^{\infty} \sum_{po}^{n-1} \sin(p\phi) \right) \\
 &\quad \times i F_\ell^m F_n^p(\mathbf{j}_\ell^\bullet + \beta_\ell^m \mathbf{h}_\ell^\bullet)(\mathbf{j}_n + \beta_n^p \mathbf{h}_n^*) \left(\frac{dP_\ell^m}{d\theta} \frac{dP_n^p}{d\theta} \right)
 \end{aligned}$$

$$\begin{aligned}
 & \times \left(\sum_{\ell_e}^{\infty} \sum_{m_o}^{\ell-1} \cos(m\phi) - i \sum_{\ell_o}^{\infty} \sum_{m_e}^{\ell-1} \sin(m\phi) \right) \\
 & \times \left(\sum_{n_e}^{\infty} \sum_{p_o}^{n-1} \cos(p\phi) + i \sum_{n_o}^{\infty} \sum_{p_e}^{n-1} \sin(p\phi) \right) \\
 & \times i F_{\ell}^m F_n^p (\mathbf{j}_{\ell}^{\bullet} + \beta_{\ell}^m \mathbf{h}_{\ell}^{\bullet}) (\mathbf{j}_n + \beta_n^{p*} \mathbf{h}_n^*) \left(\frac{m P_{\ell}^m}{\sin \theta} \frac{p P_n^p}{\sin \theta} \right) \Big\} \tag{2.14.4}
 \end{aligned}$$

$$\begin{aligned}
 N_{r12} = & -\frac{\text{Re}}{2\eta} \left\{ \left(\sum_{\ell_o}^{\infty} \sum_{m_o}^{\ell} \cos(m\phi) - i \sum_{\ell_e}^{\infty} \sum_{m_e}^{\ell} \sin(m\phi) \right) \right. \\
 & \times \left(\sum_{n_o}^{\infty} \sum_{p_o}^n \cos(p\phi) + i \sum_{n_e}^{\infty} \sum_{p_e}^n \sin(p\phi) \right) \\
 & \times i G_{\ell}^m G_n^p (\mathbf{j}_{\ell} + \alpha_{\ell}^m \mathbf{h}_{\ell}) (\mathbf{j}_n + \alpha_n^{p*} \mathbf{h}_n^*) \left(\frac{dP_{\ell}^m}{d\theta} \frac{dP_n^p}{d\theta} \right) \\
 & \times \left(\sum_{\ell_e}^{\infty} \sum_{m_e}^{\ell} \cos(m\phi) - i \sum_{\ell_o}^{\infty} \sum_{m_o}^{\ell} \sin(m\phi) \right) \\
 & \times \left(\sum_{n_e}^{\infty} \sum_{p_e}^n \cos(p\phi) + i \sum_{n_o}^{\infty} \sum_{p_o}^n \sin(p\phi) \right) \\
 & \left. \times i G_{\ell}^m G_n^p (\mathbf{j}_{\ell} + \alpha_{\ell}^m \mathbf{h}_{\ell}) (\mathbf{j}_n + \alpha_n^{p*} \mathbf{h}_n^*) \left(\frac{m P_{\ell}^m}{\sin \theta} \frac{p P_n^p}{\sin \theta} \right) \right\} \tag{2.14.5}
 \end{aligned}$$

$$\begin{aligned}
 N_{r21} = & \frac{\text{Re}}{2\eta} \left\{ \left(\sum_{\ell_o}^{\infty} \sum_{m_e}^{\ell-1} \cos(m\phi) - i \sum_{\ell_e}^{\infty} \sum_{m_o}^{\ell-1} \sin(m\phi) \right) \right. \\
 & \times \left(\sum_{n_e}^{\infty} \sum_{p_e}^n \cos(p\phi) + i \sum_{n_o}^{\infty} \sum_{p_o}^n \sin(p\phi) \right) \\
 & \times i F_{\ell}^m G_n^p (\mathbf{j}_{\ell}^{\bullet} + \beta_{\ell}^m \mathbf{h}_{\ell}^{\bullet}) (\mathbf{j}_n + \alpha_n^{p*} \mathbf{h}_n^*) \left(\frac{p P_n^p}{\sin \theta} \frac{dP_{\ell}^m}{d\theta} \right) \\
 & \left. + \left(\sum_{\ell_e}^{\infty} \sum_{m_o}^{\ell-1} \cos(m\phi) - i \sum_{\ell_o}^{\infty} \sum_{m_e}^{\ell-1} \sin(m\phi) \right) \right\}
 \end{aligned}$$

$$\begin{aligned} & \times \left(\sum_{no}^{\infty} \sum_{po}^n \cos(p\phi) + i \sum_{ne}^{\infty} \sum_{pe}^n \sin(p\phi) \right) \\ & \times \left. i F_{\ell}^m G_n^p(j_{\ell}^{\bullet} + \beta_{\ell}^m h_{\ell}^{\bullet})(j_n^{\bullet} + \alpha_n^{p*} h_n^{\bullet*}) \left(\frac{m P_{\ell}^m}{\sin \theta} \frac{dP_n^p}{d\theta} \right) \right\} \quad (2.14.6) \end{aligned}$$

$$\begin{aligned} N_{r22} = & -\frac{\text{Re}}{2\eta} \left\{ \left(\sum_{\ell e}^{\infty} \sum_{me}^{\ell} \cos(m\phi) - i \sum_{\ell o}^{\infty} \sum_{mo}^{\ell} \sin(m\phi) \right) \right. \\ & \times \left(\sum_{no}^{\infty} \sum_{pe}^{n-1} \cos(p\phi) + i \sum_{ne}^{\infty} \sum_{po}^{n-1} \sin(p\phi) \right) \\ & \times i F_{\ell}^m G_n^p(j_{\ell} + \alpha_{\ell}^m h_{\ell})(j_n + \beta_n^{p*} h_n^*) \left(\frac{m P_{\ell}^m}{\sin \theta} \frac{dP_n^p}{d\theta} \right) \\ & + \left(\sum_{\ell o}^{\infty} \sum_{mo}^{\ell} \cos(m\phi) - i \sum_{\ell e}^{\infty} \sum_{me}^{\ell} \sin(m\phi) \right) \\ & \times \left(\sum_{ne}^{\infty} \sum_{po}^{n-1} \cos(p\phi) + i \sum_{no}^{\infty} \sum_{pe}^{n-1} \sin(p\phi) \right) \\ & \left. \times i F_{\ell}^m G_n^p(j_{\ell} + \alpha_{\ell}^m h_{\ell})(j_n + \beta_n^{p*} h_n^*) \left(\frac{p P_n^p}{\sin \theta} \frac{dP_{\ell}^m}{d\theta} \right) \right\} \quad (2.14.7) \end{aligned}$$

The total surface power is equal to the surface integral of Eqs. (2.14.4) to (2.14.7). Integrating over the azimuth angle gives a Kronecker delta function of m and p , decreasing the number of sums by one. Results are shown in Eqs. (2.14.8) and (2.14.9):

$$\begin{aligned} & \int_0^{2\pi} d\phi (N_{r11} + N_{r12}) \\ & = \text{Re} \left[\left(\sum_{\ell o} \sum_{no} \sum_{me} + \sum_{\ell e} \sum_{ne} \sum_{mo} \right) i F_{\ell}^m F_n^m(j_{\ell}^{\bullet} + \beta_{\ell}^m h_{\ell}^{\bullet})(j_n + \beta_n^{m*} h_n^*) \right. \\ & \quad \left. - \left(\sum_{\ell o} \sum_{no} \sum_{mo} + \sum_{\ell e} \sum_{ne} \sum_{me} \right) i G_{\ell}^m G_n^m(j_{\ell} + \alpha_{\ell}^m h_{\ell})(j_n^{\bullet} + \alpha_n^{m*} h_n^{\bullet*}) \right] \\ & \times \frac{\pi}{2\eta} [1 + \delta(m, 0)] \left(\frac{dP_{\ell}^m}{d\theta} \frac{dP_n^m}{d\theta} + \frac{m^2 P_{\ell}^m P_n^m}{\sin^2 \theta} \right) \quad (2.14.8) \end{aligned}$$

$$\begin{aligned}
 & \int_0^{2\pi} d\phi(N_{r21} + N_{r22}) \\
 &= \text{Re} \left\{ \left(\sum_{\ell_e} \sum_{n_o} \sum_{m_o} + \sum_{\ell_o} \sum_{n_e} \sum_{m_e} \right) iF_\ell^m G_n^m (j_\ell^\bullet + \beta_\ell^m h_\ell^\bullet) (j_n^\bullet + \alpha_n^{m^*} h_n^{*\bullet}) \right. \\
 & \quad \left. - \left(\sum_{\ell_e} \sum_{n_o} \sum_{m_e} + \sum_{\ell_o} \sum_{n_e} \sum_{m_o} \right) iF_\ell^m G_n^m (j_\ell + \alpha_\ell^m h_\ell) (j_n + \beta_n^{m^*} h_n^*) \right\} \\
 & \quad \times \frac{\pi}{\eta} \frac{m}{\sin \theta} (P_\ell^m P_n^m) \tag{2.14.9}
 \end{aligned}$$

To complete the evaluation it is necessary to integrate Eqs. (2.14.8) and (2.14.9) over the zenith angle. The integral of Eq. (2.14.9) gives a null result. Evaluating the integral of Eq. (2.14.8) and replacing the coefficients by the values of Eq. (2.13.13) gives:

$$\begin{aligned}
 P_{av} &= \frac{4\pi\sigma^2}{\eta k^2} \text{Re} \left\{ \left[\sum_{\ell_o}^{\infty} \sum_{m_e}^{\ell-1} + \sum_{\ell_e}^{\infty} \sum_{m_o}^{\ell-1} \right] \right. \\
 & \quad \left. \times \frac{U(m)(2\ell+1)(\ell-m)!(\ell+m)!!}{\ell(\ell+1)(\ell-m-1)!(\ell+m-1)!!} i(j_\ell^\bullet + \beta_\ell^m h_\ell^\bullet)(j_\ell + \beta_\ell^{m^*} h_\ell^*) \right\} \\
 & \quad - \frac{4\pi\sigma^2}{\eta k^2} \text{Re} \left\{ \left[\sum_{\ell_o}^{\infty} \sum_{m_o}^{\ell} + \sum_{\ell_e}^{\infty} \sum_{m_e}^{\ell} \right] \right. \\
 & \quad \left. \times \frac{m^2(2\ell+1)(\ell-m-1)!(\ell+m-1)!!}{\ell(\ell+1)(\ell-m)!(\ell+m)!!} i(j_\ell + \alpha_\ell^m h_\ell)(j_\ell^\bullet + \alpha_\ell^{m^*} h_\ell^{*\bullet}) \right\} \tag{2.14.10}
 \end{aligned}$$

In the limit of infinite radius, Eq. (2.14.10) goes to:

$$\begin{aligned}
 P_{av} &= \frac{4\pi}{\eta k^2} \left\{ \left[\sum_{\ell_o}^{\infty} \sum_{m_e}^{\ell-1} + \sum_{\ell_e}^{\infty} \sum_{m_o}^{\ell-1} \right] \right. \\
 & \quad \left. \times \frac{U(m)(2\ell+1)(\ell-m)!(\ell+m)!!}{\ell(\ell+1)!(\ell-m-1)!(\ell+m-1)!!} (\text{Re}\beta_\ell^m + \beta_\ell^m \beta_\ell^{m^*}) \right\} \\
 & \quad + \frac{4\pi}{\eta k^2} \left\{ \left[\sum_{\ell_o}^{\infty} \sum_{m_o}^{\ell} + \sum_{\ell_e}^{\infty} \sum_{m_e}^{\ell} \right] \right. \\
 & \quad \left. \times \frac{m^2(2\ell+1)(\ell-m-1)!(\ell+m-1)!!}{\ell(\ell+1)(\ell-m)!(\ell+m)!!} (\text{Re}\alpha_\ell^m + \alpha_\ell^m \alpha_\ell^{m^*}) \right\} \tag{2.14.11}
 \end{aligned}$$

The terms are interpreted similarly to those of Eq. (2.2.7) for scattering from a sphere: terms proportional to both $\alpha_n^m \alpha_n^{m*}$ and $\beta_n^m \beta_n^{m*}$ describe time-average power scattered away from the antenna; each term is positive. Terms proportional to $\text{Re} \alpha_n^m$ and $\text{Re} \beta_n^m$ are negative and describe inwardly directed power; the time integral of Eq. (2.14.11) is the negative of the extinction (absorbed plus scattered) energy. For an ideal antenna with shorted terminals, the two sets of terms have equal magnitude and opposite sign and sum to zero.

2.15. The Cross-Sections

The purpose of this section is to compare and contrast the scattering properties of spheres with those of a biconical receiving antenna. One view of a receiving antenna is as a “lossy” scatterer. Cross-sections were defined in Sec. 2.2. Analogously with Eq. (2.2.10), the scattering cross section C_{SC} is defined to equal the ratio of scattered power to the input power density. The geometric cross section is equal to the cross sectional area of the scatterer. Using Eq. (2.14.11) to determine the scattered power, for a spherical scatterer of radius a the scattering-to-geometric cross section ratio is:

$$\begin{aligned} \frac{C_{\text{SC}}}{C_{\text{GE}}} &= \frac{8}{k^2 a^2} \left\{ \left[\sum_{\ell_o}^{\infty} \sum_{m_e}^{\ell-1} + \sum_{\ell_e}^{\infty} \sum_{m_o}^{\ell-1} \right] \right. \\ &\quad \times \frac{U(m)(2\ell+1)(\ell-m)!!(\ell+m)!!}{\ell(\ell+1)(\ell-m-1)!!(\ell+m-1)!!} (\beta_{\ell}^m \beta_{\ell}^{m*}) \left. \right\} \\ &\quad + \frac{8}{k^2 a^2} \left\{ \left[\sum_{\ell_o}^{\infty} \sum_{m_o}^{\ell} + \sum_{\ell_e}^{\infty} \sum_{m_e}^{\ell} \right] \right. \\ &\quad \times \frac{m^2(2\ell+1)(\ell-m-1)!!(\ell+m-1)!!}{\ell(\ell+1)(\ell-m)!!(\ell+m)!!} (\alpha_{\ell}^m \alpha_{\ell}^{m*}) \left. \right\} \quad (2.15.1) \end{aligned}$$

The normalized extinction cross-section C_{EX} is equal to the ratio of the total power extracted from the incoming plane wave to the geometric cross sectional area of the scatterer. For a spherical scatterer of radius a and using Eq. (2.14.11) to determine the total power extracted from the wave,

the extinction-to-geometric cross-section ratio is:

$$\begin{aligned} \frac{C_{\text{EX}}}{C_{\text{GE}}} = & -\frac{4}{k^2 a^2} \left\{ \left[\sum_{\ell_0}^{\infty} \sum_{m_e}^{\ell-1} + \sum_{\ell_e}^{\infty} \sum_{m_o}^{\ell-1} \right] \right. \\ & \times \frac{U(m)(2\ell+1)(\ell-m)!!(\ell+m)!!}{\ell(\ell+1)(\ell-m-1)!!(\ell+m-1)!!} (\text{Re} \beta_{\ell}^m) \left. \right\} \\ & - \frac{8}{k^2 a^2} \left\{ \left[\sum_{\ell_0}^{\infty} \sum_{m_o}^{\ell} + \sum_{\ell_e}^{\infty} \sum_{m_e}^{\ell} \right] \right. \\ & \times \frac{m^2(2\ell+1)(\ell-m-1)!!(\ell+m-1)!!}{\ell(\ell+1)(\ell-m)!!(\ell+m)!!} (\text{Re} \alpha_{\ell}^m) \left. \right\} \quad (2.15.2) \end{aligned}$$

The absorption cross-section, C_{AB} , is equal to the absorbed power-to-cross sectional area of the scatterer ratio. Using Eq. (2.14.11), the value is:

$$\begin{aligned} \frac{C_{\text{AB}}}{C_{\text{GE}}} = & -\frac{4}{k^2 a^2} \left\{ \left[\sum_{\ell_0}^{\infty} \sum_{m_e}^{\ell-1} + \sum_{\ell_e}^{\infty} \sum_{m_o}^{\ell-1} \right] \right. \\ & \times \frac{(2\ell+1)(\ell-m)!!(\ell+m)!!}{\ell(\ell+1)(\ell-m-1)!!(\ell+m-1)!!} (\text{Re} \beta_{\ell}^m - \beta_{\ell}^m \beta_{\ell}^{m*}) \left. \right\} \\ & - \frac{8}{k^2 a^2} \left\{ \left[\sum_{\ell_0}^{\infty} \sum_{m_o}^{\ell} + \sum_{\ell_e}^{\infty} \sum_{m_e}^{\ell} \right] \right. \\ & \times \frac{m^2(2\ell+1)(\ell-m-1)!!(\ell+m-1)!!}{\ell(\ell+1)(\ell-m)!!(\ell+m)!!} (\text{Re} \alpha_{\ell}^m - \alpha_{\ell}^m \alpha_{\ell}^{m*}) \left. \right\} \quad (2.15.3) \end{aligned}$$

The thrust on the antenna from the total power absorbed is c times the value of extinction power, Eq. (2.15.2). The thrust on the antenna from the scattered power is equal to the component of scattered wave in the direction of the incoming field integrated over a virtual surface:

$$F_{\text{ySC}} = -\frac{\sigma^2}{2\eta k^2} \int_0^{2\pi} \sin \phi \, d\phi \int_0^{\pi} \sin^2 \theta \, d\theta \, \text{Re}(N_{\text{r}}) \quad (2.15.4)$$

Inserting the scattered field terms of Eq. (2.14.3) into Eq. (2.15.4) gives:

$$\begin{aligned}
& \int_0^{2\pi} N_r \sin \phi \, d\phi \\
&= \frac{\pi \operatorname{Re}}{4\eta} \left(\sum_{\ell o} \sum_{ne} \sum_{me} + \sum_{\ell e} \sum_{no} \sum_{mo} \right) \left\{ (F_\ell^m F_n^{m+1} \beta_\ell^m \beta_n^{m+1} \mathbf{h}_\ell \cdot \mathbf{h}_n^*) [1 + \delta(m)] \right. \\
&\quad \times \left(\frac{dP_\ell^m}{d\theta} \frac{dP_n^{m+1}}{d\theta} + \frac{m(m+1)}{\sin^2 \theta} P_\ell^m P_n^{m+1} \right) \\
&\quad - (F_\ell^m F_n^{m-1} \beta_\ell^m \beta_n^{m-1} \mathbf{h}_\ell \cdot \mathbf{h}_n^*) [1 + \delta(m-1)] \\
&\quad \times \left. \left(\frac{dP_\ell^m}{d\theta} \frac{dP_n^{m-1}}{d\theta} + \frac{m(m-1)}{\sin^2 \theta} P_\ell^m P_n^{m-1} \right) \right\} \\
&\quad - \frac{\pi \operatorname{Re}}{4\eta} \left(\sum_{\ell o} \sum_{ne} \sum_{mo} + \sum_{\ell e} \sum_{no} \sum_{me} \right) \left\{ (G_\ell^m G_n^{m+1} \alpha_\ell^m \alpha_n^{m+1} \mathbf{h}_\ell \mathbf{h}_n^*) \right. \\
&\quad \times \left(\frac{dP_\ell^m}{d\theta} \frac{dP_n^{m+1}}{d\theta} + \frac{m(m+1)}{\sin^2 \theta} P_\ell^m P_n^{m+1} \right) - (G_\ell^m G_n^{m-1} \alpha_\ell^m \alpha_n^{m-1} \mathbf{h}_\ell \mathbf{h}_n^*) \\
&\quad \times \left. \left(\frac{dP_\ell^m}{d\theta} \frac{dP_n^{m-1}}{d\theta} + \frac{m(m-1)}{\sin^2 \theta} P_\ell^m P_n^{m-1} \right) \right\} \\
&\quad + \frac{\pi \operatorname{Re}}{4\eta} \left(\sum_{\ell o} \sum_{no} \sum_{me} + \sum_{\ell e} \sum_{ne} \sum_{mo} \right) \left\{ (G_n^{m+1} F_\ell^m \alpha_n^{m+1} \beta_\ell^m \mathbf{h}_\ell \cdot \mathbf{h}_n^*) [1 + \delta(m)] \right. \\
&\quad \times \left(\frac{m P_\ell^m}{\sin \theta} \frac{dP_n^{m+1}}{d\theta} + \frac{(m+1) P_n^{m+1}}{\sin \theta} \frac{dP_\ell^m}{d\theta} \right) \\
&\quad - G_n^{m-1} F_\ell^m \alpha_n^{m-1} \beta_\ell^m \mathbf{h}_\ell \cdot \mathbf{h}_n^* \left(\frac{m P_\ell^m}{\sin \theta} \frac{dP_n^{m-1}}{d\theta} + \frac{(m-1) P_n^{m-1}}{\sin \theta} \frac{dP_\ell^m}{d\theta} \right) \left. \right\} \\
&\quad + \frac{\pi \operatorname{Re}}{4\eta} \left(\sum_{\ell o} \sum_{no} \sum_{mo} + \sum_{\ell e} \sum_{ne} \sum_{me} \right) \\
&\quad \times \left\{ (G_\ell^m F_n^{m-1} \alpha_\ell^m \beta_n^{m-1} \mathbf{h}_\ell \mathbf{h}_n^*) [1 + \delta(m-1)] \right. \\
&\quad \times \left(\frac{m P_\ell^m}{\sin \theta} \frac{dP_n^{m-1}}{d\theta} + \frac{(m-1) P_n^{m-1}}{\sin \theta} \frac{dP_\ell^m}{d\theta} \right) \\
&\quad - G_\ell^m F_n^{m+1} \alpha_\ell^m \beta_n^{m+1} \mathbf{h}_\ell \mathbf{h}_n^* \left(\frac{m P_\ell^m}{\sin \theta} \frac{dP_n^{m+1}}{d\theta} + \frac{(m+1) P_n^{m+1}}{\sin \theta} \frac{dP_\ell^m}{d\theta} \right) \left. \right\} \\
& \tag{2.15.5}
\end{aligned}$$

Next, integrate Eq. (2.15.4) to find the directed power through a virtual circumscribing sphere, with the aid of Tables A.22.1.8, 22.1.9, 22.1.11, and 22.1.12. In the limit where the scattered waves extend to infinite radius,

the normalized y -directed force due to the scattered field is:

$$\begin{aligned}
 \frac{cf_{ySC}}{C_{GE}} = & -\frac{4}{k^2 a^2} \left\{ \left(\sum_{\ell_o} \sum_{m_e} + \sum_{\ell_e} \sum_{m_o} \right) \right. \\
 & \times \left((\beta_\ell^m \beta_{\ell+1}^{m+1*} + \beta_\ell^{m*} \beta_{\ell+1}^{m+1}) \frac{U(m)(\ell-m)!(\ell+2)!!}{(\ell+1)^2(\ell-m-1)!(\ell+m-1)!!} \right. \\
 & \left. \left. + (\beta_\ell^m \beta_{\ell-1}^{m+1*} + \beta_\ell^{m*} \beta_{\ell-1}^{m+1}) \frac{U(m)(\ell-m)!(\ell+m)!!}{(\ell)^2(\ell-m-3)!(\ell+m-1)!!} \right) \right\} \\
 & + \left(\sum_{\ell_o} \sum_{m_o} + \sum_{\ell_e} \sum_{m_e} \right) \\
 & \times \left((\alpha_\ell^m \alpha_{\ell+1}^{m+1*} + \alpha_\ell^{m*} \alpha_{\ell+1}^{m+1}) \frac{m(m+1)(\ell-m-1)!(\ell+m+1)!!}{(\ell+1)^2(\ell-m)!(\ell+m)!!} \right. \\
 & \left. + (\alpha_\ell^m \alpha_{\ell-1}^{m+1*} + \alpha_\ell^{m*} \alpha_{\ell-1}^{m+1}) \frac{m(m+1)(\ell-m-1)!(\ell+m+1)!!}{(\ell)^2(\ell-m-2)!(\ell+m)!!} \right) \\
 & + \left(\sum_{\ell_o} \sum_{m_e} + \sum_{\ell_e} \sum_{m_o} \right) (\alpha_\ell^{m+1*} \beta_\ell^m + \alpha_\ell^{m+1} \beta_\ell^{m*}) \\
 & \times \left(\frac{(m+1)(2\ell+1)(\ell-m)!(\ell+m)!!}{\ell^2(\ell+1)^2(\ell-m-1)!(\ell+m-1)!!} \right) \\
 & - \left(\sum_{\ell_o} \sum_{m_o} + \sum_{\ell_e} \sum_{m_e} \right) (\alpha_\ell^m \beta_\ell^{m+1*} + \alpha_\ell^{m*} \beta_\ell^{m+1}) \\
 & \times \left(\frac{m(2\ell+1)(\ell-m-1)!(\ell+m+1)!!}{\ell^2(\ell+1)^2(\ell-m-2)!(\ell+m)!!} \right) \left. \right\} \quad (2.15.6)
 \end{aligned}$$

The normalized force due to the extinction power is:

$$\begin{aligned}
 \frac{cf_{yEX}}{C_{GE}} = & -\frac{8}{k^2 a^2} \left\{ \left[\sum_{\ell_o} \sum_{m_e}^{\ell-1} + \sum_{\ell_e} \sum_{m_o}^{\ell-1} \right] \frac{U(m)(2\ell+1)(\ell-m)!(\ell+m)!!}{\ell(\ell+1)(\ell-m-1)!(\ell+m-1)!!} \operatorname{Re} \beta_\ell^m \right. \\
 & \left. + \left[\sum_{\ell_o} \sum_{m_o}^{\ell} + \sum_{\ell_e} \sum_{m_e}^{\ell} \right] \frac{m^2(2\ell+1)(\ell-m-1)!(\ell+m-1)!!}{\ell(\ell+1)(\ell-m)!(\ell+m)!!} \operatorname{Re} \alpha_\ell^m \right\} \quad (2.15.7)
 \end{aligned}$$

To compare results obtained using y - and z -directed incoming plane waves, consider scattering by an ideally conducting sphere. For a z -directed wave, the coefficients are given by Eqs. (2.3.5) and (2.3.6) for a y -directed

wave, the boundary conditions follow from Eq. (2.15.3), and are:

$$\mathbf{j}_\ell^*(ka) + \beta_\ell^m \mathbf{h}_\ell^*(ka) = 0 \quad \mathbf{j}_\ell(ka) + \alpha_\ell^m \mathbf{h}_\ell(ka) = 0 \quad (2.15.8)$$

These lead to:

$$\beta_\ell^m(ka) = -\frac{\mathbf{j}_\ell^*(ka)}{\mathbf{h}_\ell^*(ka)} \quad \alpha_\ell^m(ka) = -\frac{\mathbf{j}_\ell(ka)}{\mathbf{h}_\ell(ka)} \quad (2.15.9)$$

These equations show that the coefficients are independent of degree. For the case where the scatterer radius is much less than a wavelength the dipole coefficients are:

$$\begin{aligned} \beta_1^0(ka) &= -\frac{2/3}{2/3 - i/(ka)^3} \cong \frac{2(ka)^3}{3i} \\ \alpha_1^1(ka) &= -\frac{(ka)/3}{(ka)/3 + i/(ka)^2} \cong \frac{i(ka)^3}{3} \end{aligned} \quad (2.15.10)$$

The cross sections and normalized forces are:

$$\frac{C_{\text{EX}}}{C_{\text{GE}}} = \frac{C_{\text{SC}}}{C_{\text{GE}}} = \frac{c f_{\text{EX}}}{C_{\text{GE}}} = \frac{10(ka)^4}{3} \quad (2.15.11)$$

These results are equal to those of Eqs. (2.3.11) and (2.3.12).

2.16. General Comments

Biconical receiving antennas are of special significance for the same reasons biconical transmitting antennas are: only biconical and ellipsoidal shapes closely represent practical antennas and only for them do mathematically complete solutions exist. The list of practical antennas that biconical shapes approach is longer than the list for ellipsoidal ones. The receiving antenna problem is a scattering problem. The antenna is immersed in an otherwise steady state plane wave. Some of the incoming energy, the extinction energy, is transferred to the scatterer and the rest continues unperturbed; part of the extinction energy is absorbed and the rest is radiated away as a scattered field. The objective is to analyze a biconical receiving antenna of arbitrary cone length and half angle and with an arbitrary value of impedance attached to the terminals. A full analysis requires knowing all fields at all points in space. This is obtained by matching the full sets of possible field forms in the external and internal regions, see Fig. 2.4.1, to conducting boundary conditions at the antenna surfaces and to virtual boundary conditions in the open aperture. The extinction energy and momentum, the scattered energy and momentum, and the surface charge and current densities may be evaluated once the fields are known. The absorbed power and the impedance at the antenna terminals follow from the surface currents and the interior fields.

For transmission, either voltage $V(0)$ from a constant voltage source or current $I(0)$ from a constant current source is applied between the terminals of the cones at $r = b$. There are no incident fields. For reception, the power sink at $r < b$ is a passive, isotropic energy absorber. Extinction power is extracted from an incident, y -directed plane wave; some is scattered and some is absorbed. It is convenient to break space into regions similar to those of transmitting antennas. The regions are:

Sink Region

$$r < b; \quad 0 \leq \theta \leq \pi; \quad 0 \leq \phi \leq 2\pi \quad (2.16.1)$$

Interior Region:

Arms:

$$b < r < a; \quad 0 \leq \theta < \psi \quad \text{and} \quad \pi - \psi < \theta \leq \pi; \quad 0 \leq \phi \leq 2\pi \quad (2.16.2)$$

Space:

$$b < r < a; \quad \psi < \theta < \pi - \psi; \quad 0 \leq \phi \leq 2\pi \quad (2.16.3)$$

Exterior Region:

Space:

$$r > a; \quad 0 \leq \theta \leq \pi; \quad 0 \leq \phi \leq 2\pi \quad (2.16.4)$$

Aperture:

$$r = a; \quad \psi \leq \theta \leq \pi - \psi; \quad 0 \leq \phi \leq 2\pi \quad (2.16.5)$$

Arms:

$$r = a; \quad 0 \leq \theta < \psi \quad \text{and} \quad \pi - \psi < \theta \leq \pi; \quad 0 \leq \phi \leq 2\pi \quad (2.16.6)$$

The spherical coordinate expansion for a y -directed plane wave, Eqs. (2.14.1)–(2.14.3) contain products of trigonometric functions, harmonic spherical functions, and spherical Bessel functions of integer order, with orders ranging from one to infinity. Although exterior and interior modal products of different degrees are orthogonal, exterior and interior modes of different orders are not. Each exterior order contributes to all interior orders of the same degree. Interior modes are associated with surface current and charge densities on the cones. All driven antenna modes absorb energy and momentum from the plane wave, some of each is absorbed and some of each is scattered away. The zero degree plane wave modes excite TM scattering modes and TM and TEM interior modes similar to the transmitter modes; modes known as transmitter modes. Higher degree exterior modes excite both TM and TE scattered and interior modes. With

these modes the extinction and scattered energies are equal and result in the absorption of momentum but not energy from the wave; these are the receiver modes.

As an example of receiver modes, at low enough frequencies a surface current flows along the illuminated face of the antenna; it is largest near the caps. (Detailed sketches are shown in Fig. 2.21.1.) Going toward the conical apices at each differential length some of the current terminates on local electric charge densities, until it disappears entirely at the terminals. At the cone-cap junction, some charge is stored and some passes through onto the cap. Since the currents into and out of the cone-cap junctions are not necessarily equal, an oscillating ring of charge resides there. A similar current distribution is repeated, but oppositely directed, on the shadowed side of the antenna. The current pattern generates a magnetic dipole moment; the cross sectional area of the dipole is the geometrical cross section of the cones perpendicular both to the incoming wave and to the antenna axis, in this case the x -direction. By Lenz's law, the phase of the generated magnetic moment is opposite that of the incoming magnetic field and results in a scattered wave.

Just as for transmission, the charge and current densities on the cones are functions of the interior fields and those on the caps are functions of the exterior fields. The signs of adjacent arm and cap surface and line charge densities may or may not be the same. The current that flows from the cone to the cone-cap junction is not necessarily equal to the current that flows from the junction to the cap and, as noted, differences result in a ring of charge at the junction.

2.17. Fields of Receiving Antennas

Combining Eqs. (2.13.13) and (2.14.3) shows the TM and TE modes respectively to be proportional $\delta(\ell + m, 2n + 1)$ and $\delta(\ell + m, 2n)$, and expresses the condition that the associated Legendre polynomials satisfy the symmetry conditions:

$$\begin{aligned} \text{TM modes} \quad P_\ell^m(\cos \theta) &= -P_\ell^m(-\cos \theta) \\ \text{TE modes} \quad P_\ell^m(\cos \theta) &= P_\ell^m(\cos \theta) \end{aligned} \quad (2.17.1)$$

The total exterior field, the modal fields of the plane and scattered waves, are equal to the sum of Eqs. (2.14.1)–(2.14.3). A complete field evaluation requires evaluation of the scattering field coefficients.

The interior modal structure of a receiving antenna depends upon the symmetries both of the driving field and the antenna. For the antenna axis parallel with the direction of polarization, the antenna implementation

retains the symmetry of the external fields in the internal region. As was the case for a transmitting antenna, finite interior fields require the multiplying coefficient of all functions $y_\nu(\sigma)$ to be equal to zero for $\nu > 0$. Coefficients of the $j_\nu(\sigma)$ functions are nonzero for both TM and TE modes. The symmetry of the interior TM and TE modes remains the same as the exterior symmetry, with undetermined coefficients respectively defined to be Γ_ν^m and Λ_ν^m . A full solution requires evaluation of the functional relationships between internal coefficients Γ_ν^m and Λ_ν^m and the scattering coefficients α_ℓ^m and β_ℓ^m .

Combining all the above for the interior fields, the zero degree terms have the same form as the transmitter terms, Eq. (2.7.1), and combine with the higher degree terms requirements to provide the expanded equation set:

$$\begin{aligned}
 E_r &= \sum_{\nu>0}^{\infty} \left[\sum_{me}^{\infty} \cos m\phi - i \sum_{mo}^{\infty} \sin m\phi \right] \nu(\nu+1) \Gamma_\nu^m \frac{j_\nu(\sigma)}{\sigma} M_\nu^m(\cos\theta) \\
 \eta H_r &= \sum_{\nu>0}^{\infty} \left[\sum_{mo}^{\infty} \cos m\phi - i \sum_{me}^{\infty} \sin m\phi \right] \nu(\nu+1) \Lambda_\nu^m \frac{j_\nu(\sigma)}{\sigma} L_\nu^m(\cos\theta) \\
 E_\theta &= \frac{\eta G V(r)}{2\pi r \sin\theta} + \sum_{\nu>0}^{\infty} \left[\sum_{me}^{\infty} \cos m\phi - i \sum_{mo}^{\infty} \sin m\phi \right] \Gamma_\nu^m j_\nu^*(\sigma) \frac{dM_\nu^m}{d\theta} \\
 &\quad - \sum_{\nu>0}^{\infty} \left[\sum_{me}^{\infty} \cos m\phi - i \sum_{mo}^{\infty} \sin m\phi \right] \Lambda_\nu^m j_\nu(\sigma) \frac{m L_\nu^m}{\sin\theta} \\
 \eta H_\phi &= \frac{\eta I(r)}{2\pi r \sin\theta} - i \sum_{\nu>0}^{\infty} \left[\sum_{me}^{\infty} \cos m\phi - i \sum_{mo}^{\infty} \sin m\phi \right] \Gamma_\nu^m j_\nu(\sigma) \frac{dM_\nu^m}{d\theta} \\
 &\quad - i \sum_{\nu>0}^{\infty} \left[\sum_{me}^{\infty} \cos m\phi - i \sum_{mo}^{\infty} \sin m\phi \right] \Lambda_\nu^m j_\nu(\sigma) \frac{m L_\nu^m}{\sin\theta} \\
 E_\phi &= -i \sum_{\nu>0}^{\infty} \left[\sum_{mo}^{\infty} \cos m\phi - i \sum_{me}^{\infty} \sin m\phi \right] \Gamma_\nu^m j_\nu^*(\sigma) \frac{m M_\nu^m}{\sin\theta} \\
 &\quad + \sum_{\nu>0}^{\infty} \left[\sum_{mo}^{\infty} \cos m\phi - i \sum_{me}^{\infty} \sin m\phi \right] \Lambda_\nu^m j_\nu(\sigma) \frac{dL_\nu^m}{d\theta} \\
 \eta H_\theta &= \sum_{\nu>0}^{\infty} \left[\sum_{mo}^{\infty} \cos m\phi - i \sum_{me}^{\infty} \sin m\phi \right] \Gamma_\nu^m j_\nu(\sigma) \frac{m M_\nu^m}{\sin\theta} \\
 &\quad + \sum_{\nu>0}^{\infty} \left[\sum_{mo}^{\infty} \cos m\phi - i \sum_{me}^{\infty} \sin m\phi \right] \Lambda_\nu^m j_\nu^*(\sigma) \frac{dL_\nu^m}{d\theta}
 \end{aligned} \tag{2.17.2}$$

As was the case for transmission, in the limit as b goes to zero the only nonzero terms just off the $r = b$ surface are the TEM components of E_θ and H_ϕ . The TEM fields guide the energy through the interior region. Repeating the procedure of Eq. (2.9.6), evaluate the integral using Eq. (2.17.2):

$$\int_{-\psi}^{\psi} d\theta H_\phi|_{m=0}$$

The result is the algebraic equation:

$$\frac{V(a)}{a} = \frac{2iG}{Y_R(a)} \sum_{\ell} D_{\ell}^0(j_{\ell} + \beta_{\ell}^0 h_{\ell}) \quad (2.17.3)$$

2.18. Boundary Conditions

Several boundary conditions have been built into field Eqs. (2.14.2) and (2.14.3): Rotational symmetry requires m to be an integer and regularity of the zenith angle functions on the exterior axes, $r > a$, requires integer order Legendre functions of the first kind. The limiting condition as the radius becomes infinite requires spherical Hankel functions of the second kind. In the interior, regularity of the functions at $r = b$ requires the coefficients of all negative order Bessel functions to be zero. The boundary conditions still to be applied are:

Interior region, $b < r < a, \theta = \psi$ and $\theta = \pi - \psi$: On the cone arms the tangential components of the electric field intensity, E_r and E_ϕ , and the normal component of the magnetic field intensity, H_θ , are zero.

Exterior region, $r = a, \theta < \psi$ and $\theta > \pi - \psi$: The tangential components of the electric field intensity, E_θ and E_ϕ , and the normal component of the magnetic field intensity, H_r , are zero.

Boundary, $r = a, \psi < \theta < \pi - \psi$: All fields are continuous through the virtual interface between internal and external regions.

To satisfy the first boundary condition, note that the tangential component of the electric field and the normal component of the magnetic field are equal to zero at the surface of the cone. From Eq. (2.17.2), the sums are equal to zero for all interior radii only if:

$$M_{\nu}^m(\cos \psi) = 0 \quad \text{and} \quad dL_{\nu}^m(\cos \theta)/d\theta|_{\theta=\psi} = 0 \quad (2.18.1)$$

For each degree, an infinite number of orders satisfy Eq. (2.18.1). Figure 2.7.1 includes plots of the first few values of ν and ψ for functions with $m = 1$ that satisfy these boundary conditions. In the limit as

ψ approaches zero the first solutions for the odd and even functions occur respectively at $\nu = 2$ and 3.

To satisfy the second boundary condition from Eq. (2.14.3) it is necessary that:

$$\begin{aligned} \theta < \psi \quad \text{and} \quad \theta > \pi - \psi \\ E_\theta(ka, \theta, \phi) = 0 \quad \text{and} \quad E_\phi(ka, \theta, \phi) = 0 \end{aligned} \quad (2.18.2)$$

To satisfy the third boundary condition, with δ a vanishingly small positive number, it is necessary that:

$$\begin{aligned} \psi < \theta < \pi - \psi \\ E(ka - \delta, \theta, \phi) = E(ka + \delta, \theta, \phi) \\ H(ka - \delta, \theta, \phi) = H(ka + \delta, \theta, \phi) \end{aligned} \quad (2.18.3)$$

The fields on the left side of Eq. (2.18.3) are those of Eq. (2.17.2). The fields on the right side of Eq. (2.18.3) are the sum of Eqs. (2.14.1)–(2.14.3). Desired algebraic equations are most easily obtained using the second and third boundary conditions to construct the four integral equalities of Eqs. (2.18.4) through (2.18.7). In addition to these four equalities, the process is to be repeated with a similar set of integral equations after replacing $\sin(m\phi)$ by $\cos(m\phi)$ and $\cos(m\phi)$ by $-\sin(m\phi)$. Although the zenith angle limits on both integrals would be ψ to $\pi - \psi$ the second boundary condition permits changing the limits to (0 to π) for the electric field components.

$$\begin{aligned} \int_{\psi}^{\pi-\psi} \sin \theta \, d\theta \int_0^{2\pi} d\phi \left\{ E_\theta \frac{dP_\ell^m}{d\theta} \cos(m\phi) - E_\phi \frac{mP_\ell^m}{\sin \theta} \sin(m\phi) \right\}_{\sigma=ka-\delta} \\ = \int_0^{\pi} \sin \theta \, d\theta \int_0^{2\pi} d\phi \left\{ E_\theta \frac{dP_\ell^m}{d\theta} \cos(m\phi) - E_\phi \frac{mP_\ell^m}{\sin \theta} \sin(m\phi) \right\}_{\sigma=ka+\delta} \end{aligned} \quad (2.18.4)$$

$$\begin{aligned} \int_{\psi}^{\pi-\psi} \sin \theta \, d\theta \int_0^{2\pi} d\phi \left\{ H_\phi \frac{dM_\nu^m}{d\theta} \cos(m\phi) + H_\theta \frac{mM_\nu^m}{\sin \theta} \sin(m\phi) \right\}_{\sigma=ka-\delta} \\ = \int_{\psi}^{\pi-\psi} \sin \theta \, d\theta \int_0^{2\pi} d\phi \left\{ H_\phi \frac{dM_\nu^m}{d\theta} \cos(m\phi) + H_\theta \frac{mM_\nu^m}{\sin \theta} \sin(m\phi) \right\}_{\sigma=ka+\delta} \end{aligned} \quad (2.18.5)$$

$$\begin{aligned}
& \int_{\psi}^{\pi-\psi} \sin \theta \, d\theta \int_0^{2\pi} d\phi \left\{ E_{\theta} \frac{mP_{\ell}^m}{\sin \theta} \cos(m\phi) - E_{\phi} \frac{dP_{\ell}^m}{d\theta} \sin m\phi \right\}_{\sigma=ka-\delta} \\
&= \int_0^{\pi} \sin \theta \, d\theta \int_0^{2\pi} d\phi \left\{ E_{\theta} \frac{mP_{\ell}^m}{\sin \theta} \cos(m\phi) - E_{\phi} \frac{dP_{\ell}^m}{d\theta} \sin m\phi \right\}_{\sigma=ka+\delta}
\end{aligned} \tag{2.18.6}$$

$$\begin{aligned}
& \int_{\psi}^{\pi-\psi} \sin \theta \, d\theta \int_0^{2\pi} d\theta \left\{ H_{\phi} \frac{mL_{\nu}^m}{\sin \theta} \cos(m\phi) + H_{\theta} \frac{dL_{\nu}^m}{d\theta} \sin(m\phi) \right\}_{\sigma=ka-\delta} \\
&= \int_{\psi}^{\pi-\psi} \sin \theta \, d\theta \int_0^{2\pi} d\theta \left\{ H_{\phi} \frac{mL_{\nu}^m}{\sin \theta} \cos(m\phi) + H_{\theta} \frac{dL_{\nu}^m}{d\theta} \sin(m\phi) \right\}_{\sigma=ka+\delta}
\end{aligned} \tag{2.18.7}$$

Carrying out the integral operations of Eqs. (2.18.4) through (2.18.7) with the similar set obtained by replacing $\sin(m\phi)$ by $\cos(m\phi)$ and $\cos(m\phi)$ by $-\sin(m\phi)$ results in the four linear equations:

$$\begin{aligned}
& \ell(\ell+1)j_{\ell}^{\bullet}F_{\ell}^mI_{\ell\ell} + \ell(\ell+1)\beta_{\ell}^m h_{\ell}^{\bullet}F_{\ell}^mI_{\ell\ell} \\
&= \ell(\ell+1) \sum_{\nu_0}^{\infty} \Gamma_{\nu}^m j_{\nu}^{\bullet} K_{\ell\nu} - \frac{\eta G V(a)}{\pi a} P_{\ell} \delta(m, 0) + 2mP_{\ell}^m \sum_{\rho}^{\infty} \Lambda_{\rho}^m j_{\rho} L_{\rho}^m
\end{aligned} \tag{2.18.8}$$

$$\nu(\nu+1)\Gamma_{\nu}^m j_{\nu}^{\bullet} K_{\nu\nu} = \sum_n^{\infty} n(n+1)F_n^m j_n K_{n\nu} + \sum_n^{\infty} n(n+1)F_n^m \beta_n^m h_n K_{n\nu} \tag{2.18.9}$$

$$\ell(\ell+1)G_{\ell}^m j_{\ell}^{\bullet} I_{\ell\ell} + \ell(\ell+1)G_{\ell}^m \alpha_{\ell}^m h_{\ell}^{\bullet} I_{\ell\ell} = \sum_{\rho}^{\infty} \rho(\rho+1)\Lambda_{\rho}^m j_{\rho} I_{\ell\rho} \tag{2.18.10}$$

$$\begin{aligned}
\rho(\rho+1)\Lambda_{\rho}^m j_{\rho}^{\bullet} I_{\rho\rho} &= \rho(\rho+1) \sum_r^{\infty} G_r^m j_r^{\bullet} I_{r\rho} + \rho(\rho+1) \sum_r^{\infty} G_r^m \alpha_r^m h_r^{\bullet} I_{r\rho} \\
&\quad - 2mL_{\rho}^m \sum_n^{\infty} F_n^m j_n P_n^m - 2mL_{\rho}^m \sum_n^{\infty} F_n^m \beta_n^m h_n P_n^m
\end{aligned} \tag{2.18.11}$$

All but five terms are known in Eqs. (2.18.8)–(2.18.11): $V(a)$, α_{ℓ}^m , β_{ℓ}^m , Λ_{ρ}^m , and Γ_{ν}^m . Problem solution requires evaluation of each of them. With transmission there were but three unknowns: $Y_T(a)$, β_{ℓ} , and Γ_{ν} .

2.19. Zero Degree Solution

Since only the zero degree modes carry absorbed power, as discussed in Sec. 2.7 it is convenient to analyze them first. Equation (2.17.3) and the $m = 0$ portion of Eqs. (2.18.8) through (2.18.11) are:

$$\begin{aligned} \frac{V(a)}{a} &= \frac{2iG}{Y_R(a)} \sum_{no}^{\infty} F_n^0(j_n + \beta_n^0 h_n) \\ \ell(\ell + 1)F_{\ell}^0 \beta_{\ell}^0 h_{\ell} \mathbf{I}_{\ell\ell} &= -\ell(\ell + 1)F_{\ell}^0 j_{\ell} \mathbf{I}_{\ell\ell} - \frac{\eta G V(a)}{\pi a} P_{\ell} + \ell(\ell + 1) \sum_{\nu}^{\infty} \Gamma_{\nu} j_{\nu} \mathbf{K}_{\ell\nu} \\ \nu(\nu + 1)\Gamma_{\nu} j_{\nu} \mathbf{K}_{\nu\nu} &= \sum_{no}^{\infty} n(n + 1)F_n^0 j_n \mathbf{K}_{n\nu} + \sum_{no}^{\infty} n(n + 1)F_n^0 \beta_n^0 h_n \mathbf{K}_{n\nu} \end{aligned} \quad (2.19.1)$$

The transmitter coefficients β_{ℓ} and the receiver products $F_{\ell}^0 \beta_{\ell}^0$ play similar roles: both sets of coefficients multiply TM fields that emanate from the antenna. Although Eq. (2.19.1) and Eqs. (2.9.1) to (2.9.3) are similar in form, a different approach to problem solution is helpful.

A case of special interest is an equated load. For this case, the receiver antenna load impedance equals the input impedance the transmitter antenna applies to incoming power. To analyze this case, adjust the driving field so that $V(0) = a$. The antenna parameters given in Eq. (2.19.1) are then the same as those of the transmitter case of Eqs. (2.9.1) to (2.9.3). Since identical equations give identical solutions:

$$\frac{\beta_{\ell} h_{\ell}}{F_{\ell}^0} = j_{\ell} + \beta_{\ell}^0 h_{\ell} \quad (2.19.2)$$

Equation (2.19.2) shows that the relative phases and magnitudes of the transmitted and scattered fields per mode, ℓ , are not the same. Several coefficient values are tabulated in Table 2.19.3. Values are calculated using the numerical results of Table 2.19.1 and Eq. (2.19.2) for the special case $Y_R(a) = Y_T(a)$, $ka = 2$, $\psi = 5^{\circ}$, and $V(0) = a$.

Comparison of the transmitting and receiving equations shows that:

$$\Gamma_{\nu}^0 = \Gamma_{\nu} \quad (2.19.3)$$

That is, the internal field coefficients for the two cases are the same. Equations (2.19.2) and (2.19.3) contrast the relationships between the transmission and reception coefficients. Comparing Eqs. (2.9.6) and (2.19.1) shows that the termination admittances $Y(a)$ for the two cases are identical. Equation (2.6.16) translates the admittance $Y(r)$ to the terminals and

Table 2.19.1. Values of β_ℓ^0 for the special case of an equated load, $ka = 2$, $\psi = 5^\circ$, and $V(0) = a$.

| ℓ | Real Part, β_ℓ^0 | Imaginary Part, β_ℓ^0 | \times Order of Magnitude |
|--------|---------------------------|--------------------------------|-----------------------------|
| 1 | -1.0073 | +0.15175 | 1 |
| 3 | -1.3064 | -0.14110 | 10^{-2} |
| 5 | -5.4652 | -1.5762 | 10^{-3} |
| 7 | -1.1887 | -3.4642 | 10^{-5} |

confirms that the terminal impedances of the antenna as a transmitter and as a receiver are identical.

$$Y_R(0) = Y_T(0) \quad (2.19.4)$$

For an arbitrary but known load impedance, the solution procedure is to use Eq. (2.6.17) to solve for $Y(a)$ and then combine with Eqs. (2.19.1) to (2.19.3) to obtain the linear equation:

$$\begin{aligned} \beta_\ell^0 h_\ell = & \frac{h_\ell}{F_\ell^0 h_\ell \cdot I_{\ell\ell}} \left\{ -F_{\ell j}^0 \cdot I_{\ell\ell} - \frac{2\eta i G^2 P_\ell}{\pi \ell(\ell+1) Y_R(a)} \sum_{n_0}^{\infty} F_{n_0}^0 j_n \right. \\ & + \sum_{\nu}^{\infty} \sum_{n_0}^{\infty} F_n^0 \frac{n(n+1) j_\nu \cdot j_n K_{\ell\nu} K_{n\nu}}{\nu(\nu+1) j_\nu K_{\nu\nu}} - \frac{2\eta i G^2 P_\ell}{\pi \ell(\ell+1) Y_R(a)} \sum_{n_0}^{\infty} F_n^0 \beta_n^0 h_n \\ & \left. + \sum_{\nu}^{\infty} \sum_{n_0}^{\infty} F_n^0 \frac{n(n+1) j_\nu \cdot K_{\ell\nu} K_{n\nu}}{\nu(\nu+1) j_\nu K_{\nu\nu}} \beta_n^0 h_n \right\} \quad (2.19.5) \end{aligned}$$

Symbols $I_{\ell\ell}$ and $K_{\ell\nu}$ and others represent integrals listed in Tables A.22.1 and A.23.1. The equation form is the same as Eq. (2.9.5), and the solution technique is the same. Since all terms in Eq. (2.19.5) are known except β_ℓ^0 it may be solved first for $\beta_\ell^0 h_\ell$ and then for β_ℓ^0 . Once the β_ℓ^0 are known, Eq. (2.19.1) may be used to solve for $V(a)$. The value of Γ_ν^0 may be obtained using Eq. (2.19.3). The zero degree solution is then complete.

2.20. Non-Zero Degree Solutions

To find the solution for $m > 0$, solve for the exterior field parameters α_ℓ^m and β_ℓ^m using Eqs. (2.18.8) through (2.18.11). Rewriting them in the forms

that most easily does this:

$$\begin{aligned}
 (\beta_\ell^m h_\ell) = & \frac{h_\ell}{\ell(\ell+1)h_\ell^\bullet F_\ell^m I_{\ell\ell}} \left\{ -\ell(\ell+1)F_\ell^m j_\bullet I_{\ell\ell} \right. \\
 & + \ell(\ell+1) \sum_\nu \sum_n^\infty F_n^m \frac{n(n+1)j_n j_\bullet K_{n\nu} K_{1\nu}}{\nu(\nu+1)j_\nu K_{\nu\nu}} \\
 & \times 2mP_\ell^m \sum_\rho \sum_r^\infty G_r^m \frac{j_\rho j_r^\bullet L_\rho^m I_{r\rho}}{j_\rho^\bullet I_{\rho\rho}} - 4m^2 P_\ell^m \sum_\rho \sum_n^\infty F_n^m \frac{j_\rho j_n (L_\rho^m)^2 P_n^m}{\rho(\rho+1)j_\rho^\bullet I_{\rho\rho}} \\
 & + 2mP_\ell^m \sum_\rho \sum_r^\infty G_r^m \frac{j_\rho h_r^\bullet L_\rho^m I_{r\rho}}{j_\rho^\bullet h_r I_{\rho\rho}} (\alpha_r^m h_r) \\
 & - 4m^2 P_\ell^m \sum_\rho \sum_n^\infty F_n^m \frac{j_\rho (L_\rho^m)^2 P_n^m}{\rho(\rho+1)j_\rho^\bullet I_{\rho\rho}} (\beta_n^m h_n) \\
 & \left. + \ell(\ell+1) \sum_\nu \sum_n^\infty F_n^m \frac{n(n+1)j_\nu^\bullet K_{n\nu} K_{\ell\nu}}{\nu(\nu+1)j_\nu K_{\nu\nu}} (\beta_n^m h_n) \right\} \tag{2.20.1}
 \end{aligned}$$

$$\begin{aligned}
 (\alpha_\ell^m h_\ell) = & \frac{1}{\ell(\ell+1)G_\ell^m I_{\ell\ell}} \left\{ -\ell(\ell+1)G_\ell^m j_\bullet I_{\ell\ell} \right. \\
 & + \sum_\rho \sum_r^\infty G_r^m \frac{\rho(\rho+1)j_\rho j_r^\bullet I_{r\rho} I_{\ell\rho}}{j_\rho^\bullet I_{\rho\rho}} - 2m \sum_\rho \sum_n^\infty F_n^m \frac{j_\rho j_n I_{\ell\rho} L_\rho^m P_n^m}{j_\rho^\bullet I_{\rho\rho}} \\
 & \times \sum_\rho \sum_r^\infty G_r^m \frac{\rho(\rho+1)j_\rho h_r^\bullet I_{r\rho} I_{\ell\rho}}{j_\rho^\bullet h_r I_{\rho\rho}} (\alpha_r^m h_r) \\
 & \left. - 2m \sum_\rho \sum_n^\infty F_n^m \frac{j_\rho I_{\ell\rho} L_\rho^m P_n^m}{j_\rho^\bullet I_{\rho\rho}} (\beta_n^m h_n) \right\} \tag{2.20.2}
 \end{aligned}$$

Equations (2.20.1) and (2.20.2) have the general algebraic form:

$$\begin{aligned}
 x_\ell + \sum_n^\infty N_{\ell n} x_n + \sum_r^\infty M_{\ell r} y_r &= B_\ell \\
 y_\ell + \sum_n^\infty S_{\ell n} x_n + \sum_r^\infty R_{\ell r} y_r &= A_\ell
 \end{aligned} \tag{2.20.3}$$

All needed integrals are listed in Tables A.22.1 and A.23.1 and all other parameters are known. The sums of Eqs. (2.20.1) and (2.20.2) may be truncated and solved concurrently for coefficients α_ℓ^m and β_ℓ^m , from which

Γ_ν^m and Λ_ν^m follow directly. Knowledge of these four parameters provides the total solution of the fields around a receiving antenna.

Although the integral of products of Legendre functions of integer and noninteger orders, $M_\nu(\cos\theta)P_\ell(\cos\theta)$ for example, are largest if ν is nearly equal to ℓ , none of them vanish. Therefore cross coupling exists between all modes of the same degree, m . Coupling between α_ℓ^m and β_ℓ^m terms shows that all modes, even and odd, of the same degree are coupled. That is, each TM mode and each TE mode interacts with all other modes, both TM and TE. Each value of β_ℓ^m and α_ℓ^m depends both upon all values of β_λ^m and α_λ^m , but are independent of β_ℓ^p and α_ℓ^p for $m \neq p$.

Since for $m = 0$ and ψ approaching zero the order approaches an integer value quite slowly, the integrals of cross modal terms remain significantly large, and therefore, coupling is significantly large even for ψ near zero.

2.21. Surface Current Densities

A conducting boundary condition is that the surface current density, $\tilde{\mathbf{I}}$, in amperes per meter is related to the magnetic field adjacent to it by the vector-phasor relationship

$$\tilde{\mathbf{I}} = n \times \tilde{\mathbf{H}} \quad (2.21.1)$$

Unit vector n is normal to and outbound from the conductor. Knowledge of the field coefficients permits the calculation of all antenna currents. Figure 2.21.1 illustrates surface current patterns for the lowest order exterior modes, $(\ell, m) = (1, 0)$ and $(1, 1)$ and the three lowest order interior ones, modes $(\nu, m) = (0, 0)$, $(1 + \delta, 0)$, and $(2 + \delta, 1)$, where δ is a vanishingly small positive number. The exact interior modal number depends upon the value of ψ : with 5° cones the modal numbers $1 + \delta$ and $2 + \delta$ are respectively 1.444 484 and 2.022 029. The figure depicts current patterns for a small antenna, $a < \pi/4$. A plane wave is incident from the left, with a z -directed electric field intensity. In the interior the TEM mode fields, see Eq. (2.7.1), are largest at $r = b$. The current of mode $(1 + \delta, 0)$ has rotational symmetry around the cones. The current of mode $(2 + \delta, 1)$ is in phase with mode $(1 + \delta, 0)$ on the front face and out of phase on the back face; it is equal to zero in between. Both are TM driven modes, both are zero at the origin, both are large near $r = a$, and both are zero at the sink. The current of mode $(1 + \delta, 0)$ produces a z -directed electric dipole moment. The current of mode $(2 + \delta, 1)$ produces a y -directed magnetic dipole mode, with a magnetic field phased according to Lenz's law. In the exterior, the currents of the two lowest modes, $(1, 0)$ and $(1, 1)$, produce respectively

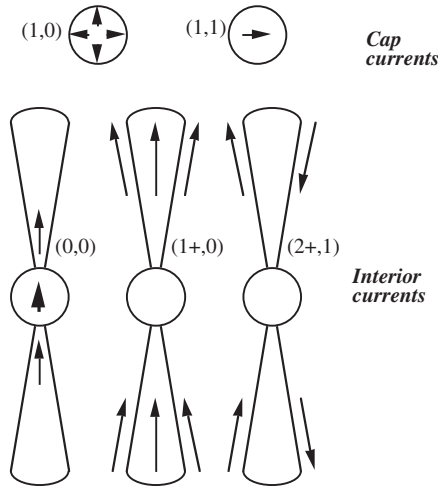


Fig. 2.21.1. Receiving modal surface currents, wave incoming from left. In the interior region the $(0,0)$ current is maximum and the $(1+,0)$ and $(2+,1)$ currents are zero at $r = 0$. The $(1+,0)$ current is unidirectional and rotationally symmetric around the arms. The $(2+,1)$ current is bi-directional, creating a magnetic moment directed in accordance with Lenz's law. In the exterior, the $(1,0)$ cap currents are θ -directed, rotationally symmetric and zero at the midpoint. The $(1,1)$ currents are x -directed with a maximum at the midpoints.

TM and TE fields. The cap current density of mode $(1,0)$ is θ -directed and zero at the center, and the current density of mode $(1,1)$ is x -directed and maximum at the center.

2.22. Power

The time-average power on the surface of a virtual surface of radius σ/k that circumscribes the antenna is

$$P = \frac{\sigma^2}{k^2} \int_0^{2\pi} d\phi \int_0^\pi \sin \theta d\theta \operatorname{Re}(N_r) \tag{2.22.1}$$

For receiving antennas, the time-average received power is equal to the negative of the real part of Eq. (2.22.1), after inserting the coefficients evaluated in Secs. 2.19 and 2.20. The power and the cross sections were calculated in Secs. 2.14 and 2.15. The normalized absorption cross section

C_{AB}/C_{GE} , see Eq. (2.15.3), is:

$$\begin{aligned} \frac{C_{AB}}{C_{GE}} = & -\frac{4}{k^2 a^2} \left\{ \left[\sum_{\ell o}^{\infty} \sum_{m e}^{\ell-1} + \sum_{\ell e}^{\infty} \sum_{m o}^{\ell-1} \right] \right. \\ & \times \frac{(2\ell+1)(\ell-m)!(\ell+m)!!}{\ell(\ell+1)(\ell-m-1)!(\ell+m-1)!!} [\text{Re}(\beta_\ell^m) + \beta_\ell^m \beta_\ell^{m*}] \left. \right\} \\ & - \frac{8}{k^2 a^2} \left\{ \left[\sum_{\ell o}^{\infty} \sum_{m o}^{\ell} + \sum_{\ell e}^{\infty} \sum_{m e}^{\ell} \right] \right. \\ & \times \frac{m^2(2\ell+1)(\ell-m-1)!(\ell+m-1)!!}{\ell(\ell+1)(\ell-m)!(\ell+m)!!} [\text{Re}(\alpha_\ell^m) + \alpha_\ell^m \alpha_\ell^{m*}] \left. \right\} \end{aligned} \quad (2.22.2)$$

As was shown for a sphere, Secs. 2.2 and 2.3, the portion of Eq. (2.22.2) proportional to the real part of the coefficients represents the extinction power extracted from the wave, and the portion proportional to sum of the square of the coefficients represents power scattered away from the antenna. The sum, expressed by Eq. (2.22.2), is the power absorbed by the antenna.

The incoming wave transfers both momentum and energy to the antenna. Since the incoming plane wave is y -directed, linear momentum is transferred to the antenna in that direction. The force on the scatterer is related to the momentum transferred as:

$$F_y = \frac{d}{dt} \text{ (linear momentum)} \quad (2.22.3)$$

The net force applied to the antenna follows from the rate of momentum absorption and scattering, and is equal to:

$$F_y = \frac{\sigma^2}{ck^2} \int_0^{2\pi} \sin \phi \, d\phi \int_0^\pi N_r \sin^2 \theta \, d\theta \quad (2.22.4)$$

By Eq. (2.15.7) the normalized force, f_y , due to the extinction power is:

$$\begin{aligned} \frac{cf_{yEX}}{C_{GE}} = & -\frac{8\epsilon}{k^2 a^2} \left\{ \left[\sum_{\ell o}^{\infty} \sum_{m e}^{\ell-1} + \sum_{\ell e}^{\infty} \sum_{m o}^{\ell-1} \right] \frac{U(m)(2\ell+1)(\ell-m)!(\ell+m)!!}{\ell(\ell+1)(\ell-m-1)!(\ell+m-1)!!} \text{Re}(\beta_\ell^m) \right. \\ & \left. + \left[\sum_{\ell o}^{\infty} \sum_{m o}^{\ell} + \sum_{\ell e}^{\infty} \sum_{m e}^{\ell} \right] \frac{m^2(2\ell+1)(\ell-m-1)!(\ell+m-1)!!}{\ell(\ell+1)(\ell-m)!(\ell+m)!!} \text{Re}(\alpha_\ell^m) \right\} \end{aligned} \quad (2.22.5)$$

By Eq. (2.15.6) the normalized scattering force is:

$$\begin{aligned}
 \frac{cf_{ySC}}{C_{GE}} = & -\frac{4}{k^2 a^2} \left\{ \left(\sum_{\ell_o} \sum_{me} + \sum_{\ell_e} \sum_{mo} \right) \right. \\
 & \times \left((\beta_{\ell}^m \beta_{\ell+1}^{m+1*} + \beta_{\ell}^{m*} \beta_{\ell+1}^{m+1}) \frac{U(m)(\ell-m)!(\ell+m+2)!!}{(\ell+1)^2(\ell-m-1)!(\ell+m-1)!!} \right. \\
 & + \left. (\beta_{\ell}^m \beta_{\ell-1}^{m+1*} + \beta_{\ell}^{m*} \beta_{\ell-1}^{m+1}) \frac{U(m)(\ell-m)!(\ell+m)!!}{\ell^2(\ell-m-3)!(\ell+m-1)!!} \right) \\
 & + \left(\sum_{\ell_o} \sum_{mo} + \sum_{\ell_e} \sum_{me} \right) \left((\alpha_{\ell}^m \alpha_{\ell+1}^{m+1*} + \alpha_{\ell}^{m*} \alpha_{\ell+1}^{m+1}) \right. \\
 & \times \frac{m(m+1)(\ell-m-1)!(\ell+m+1)!!}{(\ell+1)^2(\ell-m)!(\ell+m)!!} + (\alpha_{\ell}^m \alpha_{\ell-1}^{m+1*} + \alpha_{\ell}^{m*} \alpha_{\ell-1}^{m+1}) \\
 & \times \left. \frac{m(m+1)(\ell-m-1)!(\ell+m+1)!!}{\ell^2(\ell-m-2)!(\ell+m)!!} \right) \\
 & + \left(\sum_{\ell_o} \sum_{me} + \sum_{\ell_e} \sum_{mo} \right) (\alpha_{\ell}^{m+1*} \beta_{\ell}^m + \alpha_{\ell}^{m+1} \beta_{\ell}^{m*}) \\
 & \times \left(\frac{(m+1)(2\ell+1)(\ell-m)!(\ell+m)!!}{\ell^2(\ell+1)^2(\ell-m-1)!(\ell+m-1)!!} \right) \\
 & - \left(\sum_{\ell_o} \sum_{mo} + \sum_{\ell_e} \sum_{me} \right) (\alpha_{\ell}^m \beta_{\ell}^{m+1*} + \alpha_{\ell}^{m*} \beta_{\ell}^{m+1}) \\
 & \times \left. \left(\frac{m(2\ell+1)(\ell-m-1)!(\ell+m+1)!!}{\ell^2(\ell+1)^2(\ell-m-2)!(\ell+m)!!} \right) \right\} \tag{2.22.6}
 \end{aligned}$$

For the special case $m = 0$, the scattering cross-section and normalized force terms are:

$$\frac{C_{SC}}{C_{GE}} = \frac{4}{k^2 a^2} \sum_{\ell_o}^{\infty} \frac{(2\ell+1)\ell!^2}{\ell(\ell+1)[(\ell-1)!!]^2} \beta_{\ell}^0 \beta_{\ell}^{0*} \tag{2.22.7}$$

$$\begin{aligned}
 \frac{cf_{ySC}}{C_{GE}} = & -\frac{2}{k^2 a^2} \sum_{\ell_o} \left\{ (\beta_{\ell}^0 \beta_{\ell+1}^{1*} + \beta_{\ell}^{0*} \beta_{\ell+1}^1) \frac{\ell!(\ell+2)!!}{(\ell+1)^2[(\ell-1)!!]^2} \right. \\
 & + (\beta_{\ell}^0 \beta_{\ell-1}^{1*} + \beta_{\ell}^{0*} \beta_{\ell-1}^1) \frac{\ell!^2}{\ell^2(\ell-3)!(\ell-1)!!} \\
 & \left. + (\alpha_{\ell}^{1*} \beta_{\ell}^0 + \alpha_{\ell}^1 \beta_{\ell}^{0*}) \frac{2(2\ell+1)\ell!^2}{\ell^2(\ell+1)^2[(\ell-1)!!]^2} \right\} \tag{2.22.8}
 \end{aligned}$$

If the antenna is electrically small and only the dipole terms are significantly large, Eq. (2.22.8) shows that:

$$\frac{cf_{ySC}}{C_{GE}} = -\frac{3}{k^2 a^2} (\alpha_1^{1*} \beta_1^0 + \alpha_1^1 \beta_1^{0*}) \quad (2.22.9)$$

Although the energy density-to-linear momentum density in the incoming plane wave is c , as discussed in Sec. 2.3 the received energy-to-momentum ratio satisfies the relationship:

$$\frac{\text{Received Energy}}{\text{Received Momentum}} \leq c \quad (2.22.10)$$

This is in contrast with a transmitting antenna. When transmitting power is radiated over a spread of angles and the average value of the cosine of the angle can never be greater than one. Therefore, the transmitted energy-to-momentum ratio obeys the relationship:

$$\frac{\text{Transmitted Energy}}{\text{Transmitted Momentum}} \geq c \quad (2.22.11)$$

References

- V. Badii, "Numerical Analysis of the Transmitting Biconical Antenna," Electrical Engineering doctoral dissertation, Pennsylvania State University, 1988. Available from University Microfilm, Ann Arbor MI.
- V. Badii, K. Tomiyama, D.M. Grimes, "Biconical Transmitting Antennas, A Numerical Analysis," *Appl. Computat. Electromagn. Soc. J.* **5** (1990) 62–93.
- D.M. Grimes, "Biconical Receiving Antennas," *J. Math. Phys.* **23** (1982) 897–914.
- D.M. Grimes, C. A. Grimes, "Transmission and Reception of Power by Antennas," in T. W. Barrett, D. M. Grimes, *Advanced Electromagnetism: Foundations, Theory and Applications*, World Scientific Publishing (1995) pp. 763–791.
- H. Hertz, *Electric Waves: Researches on the Propagation of Electric Action with Finite Velocity Through Space* (1893) Translated by D.E. Jones, Dover Publications (1962).
- G. Mie, "A Contribution to Optical Extinction by Metallic Colloidal Suspensions," *Ann. Physik.* **25** (1908) 377.
- W.K.H. Panofsky, M. Phillips, *Classical Electricity and Magnetism*, 2nd edition Addison-Wesley (1962).
- S.A. Schelkunoff, *Advanced Antenna Theory*, John Wiley (1952).
- S.A. Schelkunoff, *Applied Mathematics for Engineers and Scientists*, 2nd edition Van Nostrand (1965).
- W.R. Smythe, *Static and Dynamic Electricity*, 3rd edition McGraw-Hill (1968).
- H.C. Van de Hulst, *Light Scattering by Small Particles*, John Wiley (1957).

CHAPTER 3

Antenna Q

It is commonplace to use complex notation when analyzing electromagnetic fields and their properties. The primary reason is with variables expressed in terms of exponentials of imaginary arguments the operations of differential and integral calculus become simple arithmetic ones. This changes a real vector field to a phasor vector field. Although it simplifies analytical operations it introduces complications. Phasor notation begins with a physical quantity expressed using real trigonometric functions and to that adds the imaginary term necessary to change the trigonometric function to an exponential term with an imaginary argument and the same real part. Doing a linear operation on the exponential function is in many cases much easier than operating directly on the trigonometric function, and discarding the imaginary part leaves the same real part. However a disadvantage becomes apparent during multiplication. For example, taking the product of two trigonometric functions gives the desired real value. Taking the product of two phasor exponentials returns that value and the product of imaginary parts. It is necessary to construct special rules of multiplication to obtain the correct answer.

There is also another and more subtle difficulty with complex notation. Given an electric voltage and dependent current expressed in trigonometric forms, the product of the two is a time varying power. Part is in time phase with the input voltage and part is in phase quadrature. This time varying power can, without loss of generality, be expressed using complex variables. It is not a phasor since both real and imaginary parts have physical significance. It is a complete description of physical reality and ‘ i ’ indicates a time operation. Such complex powers when referenced to the same phase add by simple addition. However, since the phasing of the power is referenced to the phase of the voltage if another voltage-current pair is brought into the system to combine the powers it is necessary to use the same phase as a reference. An important and common example is the power and energy

fields about a radiating electric dipole. For this case the reference phase at any point is a function of the radial distance from the dipole. A breakdown into in- and out-of-phase powers varies with distance. Since the phasing is generally determined at the specific radius of interest in many cases this is not a significant issue. It does imply, however, that certain theorems of complex variables do not apply to complex radiation power fields since the theorems are based upon a constant background phase.

3.1. Instantaneous and Complex Power in Circuits

To make a critical examination of power and energy in radiation fields using complex numbers, and since one-dimensional electrical circuits are simpler systems than three-dimensional electromagnetic fields, we begin with electrical circuits. Consider the time-varying power and energy of an electrical circuit that is driven by a sinusoidal, steady state source. With χ and ζ representing circuit-dependent phase constants, the input voltage and current to an electrical circuit are:

$$v(t) = V_0 \cos(\omega t - \chi) \quad \text{and} \quad i(t) = I_0 \cos(\omega t - \zeta) \quad (3.1.1)$$

With this notation, either V_0 or I_0 can be the independent variable with the other being the dependent variable. Both are real, time-independent quantities. The power at the terminals follows from the force laws, and is the simple product:

$$\begin{aligned} p(t) &= v(t)i(t) \\ &= \frac{1}{2}V_0I_0\{\cos(\zeta - \chi) + \cos(\zeta + \chi)\cos(2\omega t) \\ &\quad + \sin(\zeta + \chi)\sin(2\omega t)\} \end{aligned} \quad (3.1.2)$$

Trigonometric identities may be used to transform Eq. (3.1.2) into the more useful form:

$$\begin{aligned} p(t) &= \frac{1}{2}V_0I_0\{\cos(\zeta - \chi)[1 + \cos(2\omega t - 2\xi)] \\ &\quad + \sin(\zeta - \chi)\sin(2\omega t - 2\xi)\} \end{aligned} \quad (3.1.3)$$

Although either a plus or minus sign could be placed in front of the $\sin(\zeta - \chi)$ term, a positive sign is convenient and leads to no loss of generality.

It follows from Eq. (3.1.3) that the three numbers needed to characterize the power are the product V_0I_0 , the phase difference $(\zeta - \chi)$, and the phase angle ξ . The equation also shows that the term proportional to

$\cos(\zeta - \chi)[1 + \cos(2\omega t - 2\xi)]$ is zero twice each field cycle, it is never negative, and it describes the time-average energy flow into the circuit. The term proportional to $\sin(\zeta - \chi) \sin(2\omega t - 2\xi)$ is in time-quadrature with the first term and changes sign twice each power cycle; it describes the lossless, oscillatory energy flow between the circuit and the energy source and is not associated with a time-average energy flow. In many cases, instantaneous phase ξ is irrelevant and appears only as unwanted clutter. For such cases, the quantities $\zeta - \chi$ and $V_0 I_0$ determine the important properties of the power and no other information is either needed or desired. For such cases, phase factor ξ is suppressed and real power, $p_r(t)$, and reactive power, $p_X(t)$, are defined by the equations:

$$\begin{aligned} p_r(t) &= \frac{1}{2} V_0 I_0 \cos(\zeta - \chi) [1 + \cos(2\omega t)] \\ p_X(t) &= \frac{1}{2} V_0 I_0 \sin(\zeta - \chi) \sin(2\omega t) \end{aligned} \quad (3.1.4)$$

Since only two pieces of information are included and since complex numbers have two places available to carry information, this power may be conveniently described by complex numbers.

To restate the same physical situation using complex numbers, write the input voltage and current in phasor form:

$$V(t) = V_0 e^{i(\omega t - \chi)} \quad I(t) = I_0 e^{i(\omega t - \zeta)} \quad (3.1.5)$$

Equation (3.1.5) differs from Eq. (3.1.1) in that virtual terms, the imaginary parts of Eq. (3.1.5), have been added to the phase of each variable. The real parts of Eq. (3.1.5) are equal to the actual values of Eq. (3.1.1). Equation (3.1.5) is used to form the product:

$$P_c = \frac{1}{2} V(t) I(t)^* \quad (3.1.6)$$

The real part, P_r , and imaginary part, P_i , of Eq. (3.1.6) are:

$$\begin{aligned} P_c &= P_r + iP_i = \frac{1}{2} V_0 I_0 e^{i(\zeta - \chi)} \\ &= \frac{1}{2} V_0 I_0 [\cos(\zeta - \chi) + i \sin(\zeta - \chi)] \end{aligned} \quad (3.1.7)$$

Comparison of Eq. (3.1.3) with Eq. (3.1.7) shows that the latter contains all information except the suppressed phase factor. The real part is equal to the magnitude of the time-average input power and the imaginary part is equal to the magnitude of the oscillating power. In this case, both real and imaginary parts of the power represent actual quantities. The phase-quadrature difference between real and reactive powers is indicated by an

“ i ” in Eq. (3.1.7). Equations (3.1.4) and (3.1.7) are but different notations for the same physics. Neither contains information about phase angle ξ .

By definition the Thévenin circuit input impedance elements are

$$R = \frac{V_0}{I_0} \cos(\zeta - \chi) \quad \text{and} \quad X = \frac{V_0}{I_0} \sin(\zeta - \chi) \quad (3.1.8)$$

Combining Eqs. (3.1.7) and (3.1.8) shows that the complex power may be expressed as:

$$P_c = \frac{1}{2} I_0 I_0^* (R + iX) \quad (3.1.9)$$

With Eq. (3.1.9), I_0 has been modified to a complex number that includes factor $\exp(-i\zeta)$.

Consider next the case of two isolated electrical circuits. It is easy to show that the total power is the simple sum of the power in each circuit, as described by Eq. (3.1.2). The sum is:

$$\begin{aligned} p(t) &= \sum_{k=1}^2 v_k(t) i_k(t) \\ &= \frac{1}{2} \sum_{k=1}^2 V_k I_k \{ \cos(\zeta_k - \chi_k) + \cos(\zeta_k + \chi_k) \cos(2\omega t) \\ &\quad + \sin(\zeta_k + \chi_k) \sin(2\omega t) \} \end{aligned} \quad (3.1.10)$$

To learn how to express the information contained in Eq. (3.1.10) using complex notation begin by rewriting it in a form similar to that of Eq. (3.1.3):

$$\begin{aligned} p(t) &= \frac{1}{2} \sum_{k=1}^2 [V_k I_k \cos(\zeta_k - \chi_k)] [1 + \cos(2\omega t - \xi)] \\ &\quad + K_{12} \sin(2\omega t - \xi) \end{aligned} \quad (3.1.11)$$

Insisting that Eqs. (3.1.10) and (3.1.11) be identical and solving for K_{12} results in the equality:

$$\begin{aligned} K_{12}^2 &= V_1^2 I_1^2 \sin^2(\zeta_1 - \chi_1) + V_2^2 I_2^2 \sin^2(\zeta_2 - \chi_2) \\ &\quad + 2V_1 V_2 [-\sin(\chi_1 - \chi_2) \sin(\zeta_1 - \zeta_2) \\ &\quad + \sin(\zeta_1 - \chi_2) \sin(\zeta_2 - \chi_1)] \end{aligned} \quad (3.1.12)$$

Consider the special case where one of the two equalities apply:

$$\zeta_1 = \zeta_2 \quad \text{or} \quad \chi_1 = \chi_2 \quad (3.1.13)$$

For either case, Eq. (3.1.12) simplifies to:

$$K_{12} = V_1 I_1 \sin(\zeta_1 - \chi_1) + V_2 I_2 \sin(\zeta_2 - \chi_2) \quad (3.1.14)$$

Combining Eq. (3.1.14) with Eq. (3.1.11) shows that:

$$\begin{aligned}
 p(t) = & \frac{1}{2} \sum_{k=1}^2 V_k I_k \{ \cos(\zeta_k - \chi_k) [1 + \cos(2\omega t - \xi)] \\
 & + \sin(\zeta_k - \chi_k) \sin(2\omega t - \xi) \}
 \end{aligned} \tag{3.1.15}$$

According to Eq. (3.1.15) if either of the two conditions of Eq. (3.1.13) are met the two circuit's powers combine by simple addition. Within interconnected electric circuits, the Kirchoff circuit laws assure that one of the conditions of Eq. (3.1.13) is met, either between circuit nodes or along circuit branches. For these special cases, the complex power is the simple sum over the power of the different circuit elements:

$$P_c = \frac{1}{2} \sum_k V_k I_k e^{i(\zeta_k - \chi_k)} \tag{3.1.16}$$

As we shall see, different modes of multimodal radiation fields do not meet the conditions of Eq. (3.1.13) and therefore Eq. (3.1.16) does not apply.

3.2. Instantaneous and Complex Power in Fields

To analyze power and energy about an antenna it is enough to consider only antennas with rotational symmetry about the z -axis. With this choice the field solutions are of degree zero and there is no dependence on the azimuth angle. Since, as will be shown, the essential points of interest depend only upon the radial field functions, and since the radial field functions are independent of degree, results are general and apply to a full multipolar expansion. Written in phasor form, but keeping the retarded time phase dependence, in terms of the letter functions of Appendix A.26, the general form of the field expansion terms, Eq. (1.12.9), is:

$$\begin{aligned}
 \sigma^2 \tilde{\mathbf{E}}_r &= \sum_{\ell=1}^{\infty} F_{\ell} \ell(\ell+1) [B_{\ell}(\sigma) + i A_{\ell}(\sigma)] P_{\ell}(\cos \theta) e^{-i\sigma} \\
 \sigma^2 \eta \tilde{\mathbf{H}}_r &= - \sum_{\ell=1}^{\infty} G_{\ell} \ell(\ell+1) [B_{\ell}(\sigma) + i A_{\ell}(\sigma)] P_{\ell}(\cos \theta) e^{-i\sigma} \\
 \sigma \hat{\mathbf{E}}_{\theta} &= \sum_{\ell=1}^{\infty} F_{\ell} [D_{\ell}(\sigma) + i C_{\ell}(\sigma)] \frac{dP_{\ell}(\cos \theta)}{d\theta} e^{-i\sigma}
 \end{aligned}$$

$$\begin{aligned}
\sigma\eta\hat{H}_\phi &= \sum_{\ell=1}^{\infty} F_\ell[A_\ell(\sigma) - iB_\ell(\sigma)] \frac{dP_\ell(\cos\theta)}{d\theta} e^{-i\sigma} \\
\sigma\tilde{E}_\phi &= \sum_{\ell=1}^{\infty} G_\ell[A_\ell(\sigma) - iB_\ell(\sigma)] \frac{dP_\ell(\cos\theta)}{d\theta} e^{-i\sigma} \\
\sigma\eta\tilde{H}_\theta &= - \sum_{\ell=1}^{\infty} G_\ell[D_\ell(\sigma) + iC_\ell(\sigma)] \frac{dP_\ell(\cos\theta)}{d\theta} e^{-i\sigma} \quad (3.2.1)
\end{aligned}$$

Every radiating antenna field with rotational symmetry about the z -axis may be fully described by picking appropriate choices of multiplying coefficients F_ℓ and G_ℓ .

After making use of Eq. (3.2.1) and Table A.22.1.6, the surface integral of the complex Poynting vector evaluated on a circumscribing, spherical surface of radius σ/k is:

$$\begin{aligned}
P_c(\sigma) &= \oint N_c \cdot d\mathbf{S} \\
&= \frac{\pi}{\eta k^2} \sum_{\ell=1}^{\infty} \frac{\ell(\ell+1)}{(2\ell+1)} \{ (F_\ell F_\ell^* + G_\ell G_\ell^*) [A_\ell(\sigma)D_\ell(\sigma) - B_\ell(\sigma)C_\ell(\sigma)] \\
&\quad + i(F_\ell F_\ell^* - G_\ell G_\ell^*) [A_\ell(\sigma)C_\ell(\sigma) + B_\ell(\sigma)D_\ell(\sigma)] \} \quad (3.2.2)
\end{aligned}$$

The absence of cross product terms between TM and TE modes shows that the two modal types act independently. The sign of the imaginary term depends upon whether the field is TE or TM; if both are present and of equal magnitude the net is zero. Since each modal coefficient is multiplied by its own complex conjugate, a phase difference between sources has no affect and all modal phase factors are suppressed.

Examination of Eq. (3.2.2) shows that the two numbers needed to evaluate the modal power are weighted sums over $(A_\ell D_\ell - B_\ell C_\ell)$ and $(A_\ell C_\ell + B_\ell D_\ell)$. By Table A.26.2.8, $(A_\ell D_\ell - B_\ell C_\ell)$ is equal to one for all orders. The second term is defined to be:

$$\gamma_\ell(\sigma) = A_\ell(\sigma)C_\ell(\sigma) + B_\ell(\sigma)D_\ell(\sigma) \quad (3.2.3)$$

Values of $\gamma_\ell(\sigma)$ are listed in Table 3.2.1.

Table 3.2.1 shows that the magnitude of $\gamma_\ell(\sigma)$ increases precipitously with small and decreasing values of σ and with increasing modal number ℓ . All signs in Table 3.2.1 are the same and $\gamma_\ell(\sigma)$ is a monotone decreasing function of σ . Taking $\gamma_\ell(\sigma)$ as a measure of reactive power, the surface reactance has the same sign for all radii: capacitive for TM modes and inductive for TE modes. This is in marked contrast with the numerical analysis of

Table 3.2.1. Radial dependence of $\gamma_\ell(\sigma)$.

| |
|--|
| $\gamma_1(\sigma) = -\frac{1}{\sigma^3}$ |
| $\gamma_2(\sigma) = -\frac{18}{\sigma^5} - \frac{3}{\sigma^3}$ |
| $\gamma_3(\sigma) = -\frac{675}{\sigma^7} - \frac{90}{\sigma^5} - \frac{6}{\sigma^3}$ |
| $\gamma_4(\sigma) = -\frac{44100}{\sigma^9} - \frac{4725}{\sigma^7} - \frac{270}{\sigma^5} - \frac{10}{\sigma^3}$ |
| $\gamma_5(\sigma) = -\frac{4465125}{\sigma^{11}} - \frac{396900}{\sigma^9} - \frac{18900}{\sigma^7} - \frac{630}{\sigma^5} - \frac{15}{\sigma^3}$ |
| $\gamma_6(\sigma) = -\frac{648,336,150}{\sigma^{13}} - \frac{49,116,375}{\sigma^{11}} - \frac{1984500}{\sigma^9} - \frac{56700}{\sigma^7} - \frac{1260}{\sigma^5} - \frac{21}{\sigma^3}$ |

center-driven biconical antennas where the sign of the reactance of a TM antenna at the input terminals is primarily a function of normalized cone length. This emphasizes, see Fig. 2.9.1, that changes in the sign of the input reactance versus antenna radius for TM sources are due to the transmission line character of the antenna arms and not to intrinsic properties of the radiating surface.

3.3. Time Varying Power in Actual Radiation Fields

The actual fields, from which the phasor fields of Eq. (3.2.1) follow, are listed in Eq. (3.3.1). The driving source varies with time as $\cos(\omega t)$. If the constant coefficients of Eq. (3.2.1) are entirely real or entirely imaginary, respectively the upper or lower set of terms within the square brackets in each field component of Eq. (3.3.1) applies. Although the absolute phases of the elements are not important to our results, the phase differences between modes are. Since by proper adjustment of the time origin all phase relationships are expressible as sums over the upper and lower terms, results of analyzing this set of field equations are general.

$$\sigma^2 \mathbf{E}_r = \sum_{\ell=1}^{\infty} F_\ell \ell(\ell+1) \begin{bmatrix} B_\ell \cos(\omega t_R) - A_\ell \sin(\omega t_R) \\ A_\ell \cos(\omega t_R) + B_\ell \sin(\omega t_R) \end{bmatrix} P_\ell(\cos \theta)$$

$$\sigma^2 \eta \mathbf{H}_r = - \sum_{\ell=1}^{\infty} G_\ell \ell(\ell+1) \begin{bmatrix} B_\ell \cos(\omega t_R) - A_\ell \sin(\omega t_R) \\ A_\ell \cos(\omega t_R) + B_\ell \sin(\omega t_R) \end{bmatrix} P_\ell(\cos \theta)$$

$$\begin{aligned}
\sigma E_\theta &= \sum_{\ell=1}^{\infty} F_\ell \left[\frac{D_\ell \cos(\omega t_R) - C_\ell \sin(\omega t_R)}{C_\ell \cos(\omega t_R) + D_\ell \sin(\omega t_R)} \right] \frac{dP_\ell(\cos \theta)}{d\theta} \\
\sigma \eta H_\phi &= \sum_{\ell=1}^{\infty} F_\ell \left[\frac{A_\ell \cos(\omega t_R) + B_\ell \sin(\omega t_R)}{-B_\ell \cos(\omega t_R) + A_\ell \sin(\omega t_R)} \right] \frac{dP_\ell(\cos \theta)}{d\theta} \\
\sigma E_\phi &= \sum_{\ell=1}^{\infty} G_\ell \left[\frac{A_\ell \cos(\omega t_R) + B_\ell \sin(\omega t_R)}{-B_\ell \cos(\omega t_R) + A_\ell \sin(\omega t_R)} \right] \frac{dP_\ell(\cos \theta)}{d\theta} \\
\sigma \eta H_\theta &= \sum_{\ell=1}^{\infty} G_\ell \left[\frac{-D_\ell \cos(\omega t_R) + C_\ell \sin(\omega t_R)}{-C_\ell \cos(\omega t_R) - D_\ell \sin(\omega t_R)} \right] \frac{dP_\ell(\cos \theta)}{d\theta} \quad (3.3.1)
\end{aligned}$$

Using Eq. (3.3.1) to evaluate the radial component of the time-dependent Poynting vector then integrating over a constant radius surface centered at the origin gives the surface power:

$$\begin{aligned}
p(\sigma, t_R) &= \oint \mathbf{N} \cdot d\mathbf{S} \\
&= \frac{\pi}{\eta k^2} \sum_{\ell=1}^{\infty} \frac{\ell(\ell+1)}{(2\ell+1)} [F_\ell^2 + G_\ell^2] \{A_\ell D_\ell [1 \pm \cos(2\omega t_R)] \\
&\quad - B_\ell C_\ell [1 \mp \cos(2\omega t_R)] \mp (A_\ell C_\ell - B_\ell D_\ell) \sin(2\omega t_R)\} \quad (3.3.2)
\end{aligned}$$

The upper or lower signs respectively apply to the upper or lower terms in the square brackets of Eq. (3.3.1). The sign choice depends upon the phase of the modes but does not depend upon the TM or TE character of the modes. Hence, in contrast with results obtained using phasor fields, Eq. (3.3.2) depends upon the relative phases of the driving modes.

Examination of Eq. (3.3.2) shows that it contains three separate parameters: weighted sums over $A_\ell D_\ell$, $B_\ell C_\ell$, and $A_\ell C_\ell - B_\ell D_\ell$. For what follows it is necessary to work with functions with a zero asymptotic limit at infinity. For that purpose, define $\alpha_\ell(\sigma)$ and $\beta_\ell(\sigma)$ to be:

$$\begin{aligned}
\alpha_\ell(\sigma) &= (A_\ell D_\ell + B_\ell C_\ell) - (-1)^\ell \\
\beta_\ell(\sigma) &= (A_\ell C_\ell - B_\ell D_\ell) \quad (3.3.3)
\end{aligned}$$

Combining Eq. (3.3.2) with Eq. (3.3.3) shows that:

$$\begin{aligned}
p(\sigma, t_R) &= \frac{\pi}{\eta k^2} \sum_{\ell=1}^{\infty} \frac{\ell(\ell+1)}{(2\ell+1)} [F_\ell^2 + G_\ell^2] \{ [1 \pm (-1)^\ell \cos(2\omega t_R)] \\
&\quad \pm [\alpha_\ell(\sigma) \cos(2\omega t_R) - \beta_\ell(\sigma) \sin(2\omega t_R)] \} \quad (3.3.4)
\end{aligned}$$

Within the curly brackets of Eq. (3.3.4), the envelope of the first term is independent of distance from the antenna. Functions $\alpha_\ell(\sigma)$ and $\beta_\ell(\sigma)$

are represented by alternating series and oscillating functions of distance. Functional values of $\alpha_\ell(\sigma)$ and $\beta_\ell(\sigma)$ are listed in Tables 3.3.1 and 3.3.2 for $\ell = 1$ through 6.

The first term in Eq. (3.3.4) is the real power $p_r(\sigma, t_R)$ where:

$$p_r(\sigma, t_R) = \frac{\pi}{\eta k^2} \sum_{\ell=1}^{\infty} \frac{\ell(\ell+1)}{(2\ell+1)} [F_\ell^2 + G_\ell^2] [1 \pm (-1)^\ell \cos(2\omega t_R)] \quad (3.3.5)$$

This equation describes power that travels ever outward at speed c in the form of periodic, trigonometric pulses. There is no time-independent,

Table 3.3.1. Radial dependence of $\alpha_\ell(\sigma)$.

| |
|---|
| $\alpha_1(\sigma) = \frac{2}{\sigma^2}$ |
| $\alpha_2(\sigma) = \frac{36}{\sigma^4} - \frac{18}{\sigma^2}$ |
| $\alpha_3(\sigma) = \frac{1350}{\sigma^6} - \frac{720}{\sigma^4} + \frac{72}{\sigma^2}$ |
| $\alpha_4(\sigma) = \frac{88200}{\sigma^8} - \frac{49350}{\sigma^6} + \frac{6000}{\sigma^4} - \frac{200}{\sigma^2}$ |
| $\alpha_5(\sigma) = \frac{8,930,250}{\sigma^{10}} - \frac{5,159,700}{\sigma^8} + \frac{699300}{\sigma^6} - \frac{31500}{\sigma^4} + \frac{450}{\sigma^2}$ |
| $\alpha_6(\sigma) = \frac{1,296,672,300}{\sigma^{12}} - \frac{766,215,450}{\sigma^{10}} + \frac{111,370,140}{\sigma^8} - \frac{5,900,580}{\sigma^6} + \frac{123480}{\sigma^4} - \frac{882}{\sigma^2}$ |

Table 3.3.2. Radial dependence of $\beta_\ell(\sigma)$.

| |
|---|
| $\beta_1(\sigma) = -\frac{1}{\sigma^3} + \frac{2}{\sigma}$ |
| $\beta_2(\sigma) = -\frac{18}{\sigma^5} + \frac{33}{\sigma^3} - \frac{6}{\sigma}$ |
| $\beta_3(\sigma) = -\frac{675}{\sigma^7} \frac{1250}{\sigma^5} - \frac{276}{\sigma^3} + \frac{12}{\sigma}$ |
| $\beta_4(\sigma) = -\frac{44100}{\sigma^9} + \frac{83475}{\sigma^7} - \frac{20220}{\sigma^5} + \frac{1300}{\sigma^3} - \frac{20}{\sigma}$ |
| $\beta_5(\sigma) = -\frac{4,465,125}{\sigma^{11}} + \frac{8,533,350}{\sigma^9} - \frac{2,201,850}{\sigma^7} + \frac{169470}{\sigma^5} - \frac{4425}{\sigma^3} + \frac{30}{\sigma}$ |
| $\beta_6(\sigma) = -\frac{648,336,150}{\sigma^{13}} + \frac{1,247,555,935}{\sigma^{11}} - \frac{335,975,850}{\sigma^9} + \frac{28,797,930}{\sigma^7}$ $- \frac{961380}{\sigma^5} + \frac{12201}{\sigma^3} - \frac{42}{\sigma}$ |

radius-dependent phase term and the magnitude does not approach a limit at infinite radius.

The distance dependent power terms in Eq. (3.3.4) are given by $p_i(\sigma, t_R)$ where:

$$p_i(\sigma, t_R) = \pm \frac{\pi}{\eta k^2} \sum_{\ell=1}^{\infty} \frac{\ell(\ell+1)}{(2\ell+1)} [F_{\ell}^2 + G_{\ell}^2] \\ \times [\alpha_{\ell}(\sigma) \cos(2\omega t_R) - \beta_{\ell}(\sigma) \sin(2\omega t_R)] \quad (3.3.6)$$

As may be seen from Tables 3.3.1 and 3.3.2, the maximum of the envelope for each term occurs at the antenna surface and it goes asymptotically to zero at infinite radius.

3.4. Comparison of Complex and Instantaneous Powers

In the discussion to follow only TM modes are analyzed. The result carries over in the same form with TE modes, only the sign of the imaginary part changes. With electric circuits, the complex power form of Eq. (3.1.4) is determined by Eq. (3.1.3) and, conversely, Eq. (3.1.3) is partially determined by Eq. (3.1.4). In a similar way, the time-dependent field power of Eq. (3.3.2) leads to the complex power of Eq. (3.2.2). Equation (3.3.2) may be put in the form:

$$P_c(\sigma, t_R) = \frac{\pi}{\eta k^2} \sum_{\ell=1}^{\infty} \frac{\ell(\ell+1)}{(2\ell+1)} F_{\ell}^2 \{ [1 \pm \cos(2\omega t_R - 2\xi)] \\ + \gamma_{\ell}(\sigma) \sin(2\omega t_R - 2\xi) \} \quad (3.4.1)$$

The instantaneous power expression for the identical set of electromagnetic fields is given by Eq. (3.3.4), and repeated here for TM modes only:

$$p(\sigma, t_R) = \frac{\pi}{\eta k^2} \sum_{\ell=1}^{\infty} \frac{\ell(\ell+1)}{(2\ell+1)} F_{\ell}^2 \{ [1 \pm (-1)^{\ell} \cos(2\omega t_R)] \\ \pm [\alpha_{\ell}(\sigma) \cos(2\omega t_R) - \beta_{\ell}(\sigma) \sin(2\omega t_R)] \} \quad (3.4.2)$$

Equations (3.4.1) and (3.4.2) are descriptions of the same energy flow and the curly brackets of the equations are multiplied by identical factors but contain, respectively, two and three time-dependent terms.

The first term of Eq. (3.4.1) is the real part of the complex power. It does not go to a limit at infinite radius, it is equal to zero twice each field cycle, and it is never negative; it describes a unidirectional energy flow away from the source. The gamma power term of Eq. (3.4.1) is in phase quadrature

with the real power and, by definition, is the reactive part of the complex power. It goes to zero in the limit of infinite radius; at each point it oscillates between equal negative and positive values and hence describes radially directed, alternating power. The time-dependent terms contain identical mode- or radius-dependent, time-independent phase factors.

The first term of Eq. (3.4.2) is the real power. Like its counterpart in Eq. (3.4.1), it does not go to a limit at infinite radius, it is equal to zero twice each field cycle, and it is never negative. It, too, describes a unidirectional energy flow away from the source. The real power and $\alpha_\ell(\sigma)$ power are in time phase, and both are in time quadrature with $\beta_\ell(\sigma)$ power. Both $\alpha_\ell(\sigma)$ and $\beta_\ell(\sigma)$ powers go to zero in the limit of infinite radius; at each point both oscillate between equal negative and positive parts and hence both describe radially-directed, alternating power. There are no mode- or radius-dependent, time-independent phase factors.

The phases of the real part of the complex power and the real power differ by a radius-dependent phase factor. Since the instantaneous power represents an actual physical entity, it follows that the real part of the complex power does not. A quantitative expression for phase angle $\xi_\ell(\sigma)$ may be obtained by equating Eqs. (3.4.1) and (3.4.2). The result is:

$$\tan(2\xi_\ell) = \frac{A_\ell B_\ell}{A_\ell^2 - B_\ell^2} \quad (3.4.3)$$

It follows from Eq. (3.4.1) that the group velocity of the real part of the complex power is:

$$v_{\text{gp}} = \frac{c}{1 + d\xi_\ell/d\sigma} \quad (3.4.4)$$

It may be verified using Table A.26.2.20 that:

$$\frac{d}{d\sigma} \left(\frac{A_\ell B_\ell}{A_\ell^2 - B_\ell^2} \right) \leq 0 \quad (3.4.5)$$

Combining Eqs. (3.4.3) and (3.4.5) with functional properties of the tangent gives:

$$d\xi_\ell/d\sigma \leq 0 \quad (3.4.6)$$

Combining Eqs. (3.4.4) and (3.4.6) shows that the real part of the complex power, Eq. (3.4.1), propagates faster than the speed of light. A basic tenet of physics is that the speed of electromagnetic energy is never greater than c . This suggests that the complex power is not a physical entity and it does not describe an actual energy flow. In contrast, the first term of Eq. (3.4.2) does travel at the speed of light and does describe actual energy flow.

Table 3.4.1. Radius for which selected values of phase angle occur, three lowest modes.

| $\xi_\ell(\sigma)$ | $\ell = 1$ | $\ell = 2$ | $\ell = 3$ |
|--------------------|------------|------------|------------|
| 0 | 0 | 0 | 0 |
| $-\pi/2$ | 0.618 | 0.777 | 0.785 |
| $-\pi$ | 1 | 1.414 | 1.566 |
| $-3\pi/2$ | 1.618 | 1.882 | 2.221 |
| -2π | ∞ | 2.449 | 2.739 |
| $-5\pi/2$ | | 4.104 | 3.289 |
| -3π | | ∞ | 4.310 |
| $-7\pi/2$ | | | 7.852 |
| -4π | | | ∞ |

It follows from Eq. (3.4.1) that if the calculus operations of differentiating or integrating complex power with respect to the radius is done, the calculation must include operations on the function $\xi_\ell(\sigma)$. Yet with complex power, knowledge of $\xi_\ell(\sigma)$ is suppressed and unavailable. Therefore, it is not possible to carry out such operations from knowledge of only complex power.

If suppressed phase angle $\xi_\ell(\sigma)$ of mode ℓ is assigned a value of zero at a vanishingly small radius, the value decreases with increasing radius to equal $-(\ell + 1)\pi$ at infinite radius. Table 3.4.1 lists values of σ for which the phase angle reaches selected values as a function of radius and modal number.

Since the use of complex power is uncompromised in electric circuits, the complex power expression of Eq. (3.4.1), re-expressed as Eq. (3.4.7), applies to the driving circuitry, including the input side of the radiating surface, $\sigma = ka$:

$$\begin{aligned}
 P_c(\sigma, t_R) &= \frac{\pi}{\eta k^2} \sum_{\ell=1}^{\infty} \frac{\ell(\ell+1)}{(2\ell+1)} F_\ell^2 \{ [A_\ell D_\ell - B_\ell C_\ell] [1 \pm \cos(2\omega t_R - 2\xi_\ell)] \\
 &\quad \mp [A_\ell C_\ell + B_\ell D_\ell] \sin(2\omega t_R - 2\xi_\ell) \} \quad (3.4.7)
 \end{aligned}$$

The time-dependent power expression of Eq. (3.4.2), re-expressed as Eq. (3.4.8), applies to the external region, including the output side of the radiating surface $\sigma = ka$:

$$\begin{aligned}
 p(\sigma, t_R) &= \frac{\pi}{\eta k^2} \sum_{\ell=1}^{\infty} \frac{\ell(\ell+1)}{(2\ell+1)} F_\ell^2 \{ [A_\ell D_\ell - B_\ell C_\ell] \pm [A_\ell D_\ell + B_\ell C_\ell] \cos(2\omega t_R) \\
 &\quad \mp [A_\ell C_\ell - B_\ell D_\ell] \sin(2\omega t_R) \} \quad (3.4.8)
 \end{aligned}$$

The mean square value of the time varying portions are respectively given by:

$$\begin{aligned} & [A_\ell D_\ell - B_\ell C_\ell]^2 + [A_\ell C_\ell + B_\ell D_\ell]^2 \\ & = [A_\ell D_\ell + B_\ell C_\ell]^2 + [A_\ell C_\ell - B_\ell D_\ell]^2 \end{aligned} \quad (3.4.9)$$

It follows by inspection that Eq. (3.4.9) is an identity. Therefore, the total power is continuous through the interface. The left side terms are the magnitudes of the real plus imaginary parts of the input complex power on the source side. On the right side, the first term applies to the time variation of the real power and the in-phase oscillatory power. The second term represents the out-of-phase oscillatory power.

The first two terms inside the curly brackets of Eq. (3.4.8) may be written as:

$$\begin{aligned} & [A_\ell D_\ell - B_\ell C_\ell] \pm [A_\ell D_\ell + B_\ell C_\ell] \cos(2\omega t_R) \\ & = [A_\ell D_\ell - B_\ell C_\ell] [1 \pm (-1)^\ell \cos(2\omega t_R)] \\ & \quad \pm [A_\ell D_\ell + B_\ell C_\ell - (-1)^\ell] \cos(2\omega t_R) \end{aligned} \quad (3.4.10)$$

Comparison of Eqs. (3.4.7) and (3.4.8) as modified by Eq. (3.4.10) at $\sigma = ka$ shows that the real power undergoes a phase discontinuity of $2\xi_\ell$ as it passes through the antenna. The absolute phase is determined by the phase of the source and the antenna circuit impedances.

In summary, although the total time-dependent power is continuous through the interface between the source and field regions, the separation of that power into constituent parts is different. On the source side, the power separates into real and reactive parts the time varying portions of which are in time quadrature. Power that is in phase with the input power represents power loss from the system. On the field side, power that is in phase with the real power does not represent power loss; some oscillatory power is in phase with the real power and some is in phase quadrature.

At the surface of a radiating sphere, it is correct to write the complex power in the form of Eq. (3.2.2) as:

$$\begin{aligned} P_c(ka) & = \oint N_c \cdot d\mathbf{S} \\ & = \frac{\pi}{\eta k^2} \sum_{\ell=1}^{\infty} \frac{\ell(\ell+1)}{(2\ell+1)} \{ (F_\ell F_\ell^* + G_\ell G_\ell^*) [A_\ell(ka)D_\ell(ka) - B_\ell(ka)C_\ell(ka)] \\ & \quad + i(F_\ell F_\ell^* - G_\ell G_\ell^*) [A_\ell(ka)C_\ell(ka) + B_\ell(ka)D_\ell(ka)] \} \end{aligned} \quad (3.4.11)$$

The equation is correct only at radius a and the imaginary part equality does not extend to larger radii. The equality also shows another important

mathematical feature of electromagnetic radiation: The upper and lower terms, respectively $(A_\ell D_\ell - B_\ell C_\ell)$ and $(A_\ell C_\ell + B_\ell D_\ell)$, relate to the Bessel and Neumann functions as:

$$\begin{aligned} (A_\ell D_\ell - B_\ell C_\ell) &= (j_\ell y_\ell^\bullet - y_\ell j_\ell^\bullet) \\ (A_\ell C_\ell + B_\ell D_\ell) &= (j_\ell j_\ell^\bullet + y_\ell y_\ell^\bullet) \end{aligned} \quad (3.4.12)$$

The upper part of Eq. (3.4.12), a quantity proportional to the real output power, consists of the products of terms proportional to products of one spherical Bessel functions versus one spherical Neumann function. We conclude that electromagnetic energy can only be radiated away from a source if fields proportional to both functions are present. The lower part of Eq. (3.4.12), a quantity proportional to the imaginary part of the surface power, consists of products of terms proportional to Bessel functions plus those proportional to Neumann functions. This term, therefore, is present with all fields.

Since outward modal speeds differ, consider complex power notation for radiation emitted from radius a . At radius $b > a$ the intermodal phase differences differ from the emitted ones and wave reconstruction does not accurately reproduce the emitted one.

3.5. Radiation Q

Most expressions for Q are based upon the solution forms of Appendix 25, not Appendix 24. Although the equations of Appendix 25 are adequate so long as Eq. (A.24.6) accurately represents Eq. (A.25.1), if the modal numbers increase without limit it is necessary to use the equations of Appendix 24. Therefore, the proofs may not apply in the limit of large modal numbers.

An informative and convenient measure of anything that oscillates is its Q. In many instances Q is a measure both of how rapidly an undriven oscillator decays and of the bandwidth over which it effectively responds to a driving source. Consider as an example a series electric circuit consisting of all three passive circuit elements: inductance, capacitance, and resistance. Let the circuit be driven by time-dependent voltage $v(t)$ that produces current flow $i(t)$. The integro-differential equation the circuit satisfies is:

$$L \frac{di(t)}{dt} + Ri(t) + \frac{1}{C} \int i(t) dt = v(t) \quad (3.5.1)$$

The homogeneous equation has the form of the harmonic oscillator equation:

$$\frac{d^2 i(t)}{dt^2} + \frac{R}{L} \frac{di(t)}{dt} + \frac{1}{LC} i(t) = 0 \quad (3.5.2)$$

The current as a function of time is equal to:

$$i(t) = I_0 e^{st} \quad (3.5.3)$$

Substituting Eq. (3.5.3) into Eq. (3.5.2) shows that:

$$s = -\frac{R}{2L} \pm \sqrt{\frac{R^2}{4L^2} - \frac{1}{LC}} \quad (3.5.4)$$

Introduce the notation:

$$\alpha = \frac{R}{2L} \quad \text{and} \quad \omega_0 = \frac{1}{\sqrt{LC}} \quad (3.5.5)$$

Combining shows the homogeneous current to be:

$$i(t) = I_0 e^{-\alpha t} e^{\pm t \sqrt{\alpha^2 - \omega_0^2}} \quad (3.5.6)$$

The character of the solution depends upon the relative sizes of α and ω_0 . Consider first the special case where:

$$\omega_0 > \alpha \quad (3.5.7)$$

Combining Eqs. (3.5.7) and (3.5.6) gives:

$$i(t) = I_0 e^{-\alpha t} e^{\pm it \sqrt{\omega_0^2 - \alpha^2}} \quad (3.5.8)$$

The energy of the system is proportional to:

$$W(t) \approx i(t)i^*(t) = I_0 I_0^* e^{-2\alpha t} \quad (3.5.9)$$

The power out, that is the rate of energy decay, is:

$$P(t) \approx \frac{d}{dt} [i(t)i^*(t)] = -2\alpha I_0 I_0^* e^{-2\alpha t} \quad (3.5.10)$$

A dimensionless quantity that measures the quality of an oscillating system, see Eq. (A.9.11), is:

$$Q = \left| \frac{\omega W_{\text{pk}}(t)}{P_{\text{av}}(t)} \right| \rightarrow \frac{\omega}{2\alpha} \quad (3.5.11)$$

Q , the quality factor of the oscillating system, measures the rate of the decay of the envelope of the available energy $W(t)$, which is equal to the peak value $W_{\text{pk}}(t)$. $P(t)$ is the time-average rate of energy dissipation.

With this circuit bandwidth is inversely proportional to Q ; this may be shown by noting that the input impedance of the RLC circuit is:

$$Z(\omega) = R + i\omega L \left(1 - \frac{\omega_0^2}{\omega^2} \right) \quad (3.5.12)$$

The bandwidth of any system is defined to be the frequency difference between half-power points. In this case the lowest impedance occurs for frequency $\omega = \omega_0$, at which frequency the impedance is purely resistive and equal to R . Half-power points occur when the magnitude of the impedance is equal to the square root of two times R . This happens when the real and reactive parts are equal. If ω_1 is the frequency at a half power point, it follows that:

$$R = \omega_1 L \left(\frac{1 - \omega_0^2}{\omega_1^2} \right) \quad (3.5.13)$$

Expanding the equation shows that:

$$(\omega_1 - \omega_0)(\omega_1 + \omega_0) = \frac{\omega_1 R}{L} \quad (3.5.14)$$

Bandwidth is particularly useful if it is reasonably small, and if it is small, Eq. (3.5.14) is approximately equal to:

$$\delta\omega = \frac{R}{2L}$$

The substitution has been made that $\delta\omega = \pm(\omega_1 - \omega_0)$, the frequency difference between one of the half-power points and the resonance frequency. Using the definitions of Eqs. (3.5.5) and (3.5.11), the total bandwidth, B , normalized to the actual frequency is:

$$B = \frac{\delta\omega}{\omega_0} = \frac{1}{Q} \quad (3.5.15)$$

It follows that in a low-loss, series resonant system Q is a direct measure of and inversely proportional to the bandwidth, see also Eq. (A.10.6).

A special case is that of a lossy inductor. Although Q follows from Eq. (3.5.11), because of the importance of the case consider another viewpoint. The steady state input impedance for a lossy inductor driven at frequency ω is:

$$Z = R + i\omega L \quad (3.5.16)$$

If the current is $I_0 \cos(\omega t)$, the energy stored in the inductance and the power loss in the resistance are:

$$\begin{aligned} W(t) &= \frac{1}{4} L I_0^2 [1 + \cos(2\omega t)] \\ P(t) &= \frac{1}{2} R I_0^2 [1 + \cos(2\omega t)] \end{aligned} \quad (3.5.17)$$

Combining the definition of Eq. (3.5.11) with Eq. (3.5.17) shows that:

$$Q = \frac{\omega L}{R} = \tan \zeta \quad (3.5.18)$$

Angle ζ is the phase angle of the impedance. A similar expression holds for lossy capacitors. This is a convenient measure of Q when operating far from the resonant frequency.

Radiation Q is important with antennas since it is often necessary to radiate a certain amount of time-average power at a given frequency. It follows that the peak standing energy that must be present in the local fields about an antenna is:

$$W_{\text{pk}} = \frac{P_{\text{av}}}{\omega} Q \quad (3.5.19)$$

The larger the standing energy the larger will be the antenna surface currents, the ohmic loss, and the amount of energy that returns to the source twice each field cycle. If Q is large enough, the magnitude of standing energy required may be more than the source can supply.

Although antenna Q is important, calculation is made difficult because the energy radiated permanently away from the antenna is not absorbed. With circuits, energy once absorbed is no longer a factor. With fields, all energy remains. In the steady state the source has, ideally, been active since time $t = -\infty$ and there is an infinite amount of field energy. From the viewpoint of the antenna, energy that permanently leaves it is the equivalent to energy dissipation in a resistor. Since only energy that returns to the source affects it, the critical question in Q calculations is how to separate energy that returns to the source upon modulation changes from energy that does not.

3.6. Chu's Q Analysis, TM Fields

Although circuits are closed systems and as such amenable to a direct calculation of Q, antennas by their very nature are open systems. From the viewpoint of the antenna, energy that permanently leaves it is the equivalent to energy dissipation in a resistor. However, an energy field that

is infinite in extent surrounds every steady state oscillator that has been radiating since time $t = -\infty$, and the total amount of radiated energy is infinite. Substituting infinite energy into the numerator of Eq. (3.5.11) would show that the Q of any antenna operating in the steady state is infinite and the bandwidth is zero. However events at the antenna cannot be affected by energy that has permanently left the system. Therefore the critical question is: As modulation changes occur how much energy returns to source, thereby affecting it?

Chu was the first to quantify the relationship between Q and the electric size of certain antennas. With his method he was able to sidestep the problem of evaluating the returned energy. He considered TM modes with rotational symmetry about the z -axis that were generated by sources on the surface of a radiating shell of radius a . He then used conventional circuit techniques to find modal Q s of zero degree, phasor field equations with TM sources. The phasor field components are:

$$\begin{aligned}\sigma^2 \tilde{E}_r &= \sum_{\ell=1}^{\infty} \ell(\ell+1) F_{\ell}(B_{\ell} + i A_{\ell}) P_{\ell}(\cos \theta) e^{-i\sigma} \\ \sigma \tilde{E}_{\theta} &= \sum_{\ell=1}^{\infty} F_{\ell}(D_{\ell} + i C_{\ell}) \frac{d}{d\theta} P_{\ell}(\cos \theta) e^{-i\sigma} \\ \sigma \eta \tilde{H}_{\phi} &= \sum_{\ell=1}^{\infty} F_{\ell}(A_{\ell} - i B_{\ell}) \frac{d}{d\theta} P_{\ell}(\cos \theta) e^{-i\sigma}\end{aligned}\quad (3.6.1)$$

To separate the analysis from a specific antenna he constructed the smallest virtual sphere that just circumscribed the antenna and replaced the actual antenna with the virtual surface sources that produce identical external fields, see Sec. A.7. He analyzed only the field energy external to the sphere. Since he ignored interior energies, the calculated Q is the least possible value for any antenna that can fit inside the virtual sphere. That is, with an antenna of length $2a$ Chu's results are based upon exterior fields only. Interior field energy will add an undetermined amount to Q .

The complex power on the surface of the virtual sphere follows from the complex Poynting theorem:

$$P_c = \frac{2\pi}{\eta k^2} \sum_{\ell=1}^{\infty} F_{\ell} F_{\ell}^* \frac{\ell(\ell+1)}{(2\ell+1)} (A_{\ell} + i B_{\ell})(D_{\ell} + i C_{\ell}) \quad (3.6.2)$$

Chu next introduced voltage V_{ℓ} and current I_{ℓ} , respectively proportional to E_{θ} and H_{ϕ} , as a generalized force and flow. The complex surface power

for each mode of Eq. (3.6.2) may be written as:

$$P_{c\ell} = \frac{2\pi}{\eta k^2} F_\ell F_\ell^* \frac{\ell(\ell+1)}{(2\ell+1)} (A + iB)(D + iC) = \frac{V_\ell I_\ell^*}{2} \quad (3.6.3)$$

Since, for each mode, the angular electric-to-magnetic field ratio does not depend upon either zenith or azimuth angle, defining modal impedance $Z_\ell(\sigma)$ to equal the ratio $E_{\theta\ell}/H_{\phi\ell}$ gives the result:

$$Z_\ell(\sigma) = \frac{E_{\theta\ell}}{H_{\phi\ell}} = \frac{V_\ell}{I_\ell} = \eta \left[\frac{D_\ell(\sigma) + iC_\ell(\sigma)}{A_\ell(\sigma) - iB_\ell(\sigma)} \right] \quad (3.6.4)$$

Equations (3.6.3) and (3.6.4) are both satisfied if:

$$\begin{aligned} V_\ell &= \frac{F_\ell}{k} \sqrt{\frac{4\pi\ell(\ell+1)}{3(2\ell+1)}} (D_\ell + iC_\ell) e^{-i\sigma} \\ I_\ell &= \frac{F_\ell}{\eta k} \sqrt{\frac{4\pi\ell(\ell+1)}{3(2\ell+1)}} (A_\ell - iB_\ell) e^{-i\sigma} \end{aligned} \quad (3.6.5)$$

The modal impedance of Eq. (3.6.4) may be used to synthesize equivalent circuits that simulate the affect of the antenna upon its source. To do so break the quotient into partial fractions. For the dipole case, $\ell = 1$, the impedance has the form:

$$Z_{1E}(\sigma) = \frac{\eta/i\sigma^2 + \eta/\sigma + i\eta}{1/\sigma + i} = \eta/i\sigma + \frac{1}{1/i\eta\sigma + 1/\eta} \quad (3.6.6)$$

To evaluate the impedance at the spherical surface $r = a$, replace k by ω/c and simplify:

$$Z_{1E}(ka) = \frac{i}{\omega\epsilon a} + \frac{1}{1/\eta + i/\omega\mu a} \quad (3.6.7)$$

The circuit with the impedance characteristics of Eq. (3.6.7) consists of a capacitor of (ϵa) farads in series with a shunt configuration of an inductor of (μa) henries and a resistor of η ohms. For small values of ka , the input impedance is large and dominated by the capacitive reactance. Power to the far field is represented by power dissipated in the resistor.

The quotient of Eq. (3.6.4) using partial fractions is valid for each value of ℓ . The resulting circuit is shown in Fig. 3.6.1. The circuit is a reactive ladder network with a single terminating resistor. Each additional modal number adds an additional L-C pair to the circuit ladder. Power in the ladder network represents power flows made necessary by the changing geometry of the field as the radius increases. For electrically small antennas the input impedance is dominated by the first capacitor in series with

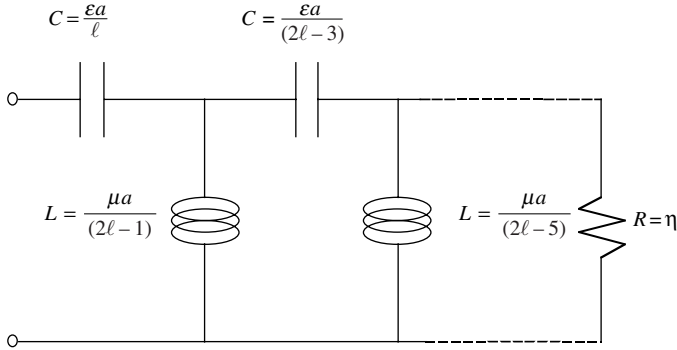


Fig. 3.6.1. TM multipolar equivalent circuit.

the first inductor. The input reactance is dominantly capacitive so long as $\ell(2\ell - 1) \gg k^2 a^2$.

Turning to field properties, the impedance of a virtual shell of arbitrary radius, $r = \sigma/k$, may be expressed as:

$$Z_{\ell E}(\sigma) = R_{\ell}(\sigma) + i X_{\ell}(\sigma) \tag{3.6.8}$$

Inserting the letter functions of the spherical Bessel and Neumann functions shows that:

$$\begin{aligned} R_{\ell}(\sigma) &= \eta \left[\frac{A_{\ell}(\sigma)D_{\ell}(\sigma) - B_{\ell}(\sigma)C_{\ell}(\sigma)}{A_{\ell}(\sigma)^2 + B_{\ell}(\sigma)^2} \right] \\ X_{\ell}(\sigma) &= \eta \left[\frac{A_{\ell}(\sigma)C_{\ell}(\sigma) + B_{\ell}(\sigma)D_{\ell}(\sigma)}{A_{\ell}(\sigma)^2 + B_{\ell}(\sigma)^2} \right] \end{aligned} \tag{3.6.9}$$

Values of both numerators and the denominator are listed in Table 3.6.1 for several modes; there are no resonances and the reactance is negative for all values of σ . No resonances are expected since, as illustrated by biconical antennas, resonance occurs when the combination of antenna arms, acting as transmission lines, and the surface impedance resonates. Resonance does not occur because of impedance changes on the spherical surface. Rather than evaluate Q separately for each modal equivalent circuit, Chu stated that the work involved would be “tedious” and sought approximate values that were easier to calculate. Since he was interested in electrically small antennas, he approximated the equivalent circuit as a series circuit then added a lossless inductor needed to make the system resonant. Therefore his resonance arises quite differently from one dependent upon antenna

Table 3.6.1. Table of functions needed for equivalent impedances.

| ℓ | $A_\ell C_\ell + B_\ell D_\ell$ | $A_\ell^2 + B_\ell^2$ |
|--------|--|---|
| 1 | $-\frac{1}{\sigma^3}$ | $1 + \frac{1}{\sigma^2}$ |
| 2 | $-\frac{3}{\sigma^3} - \frac{18}{\sigma^5}$ | $1 + \frac{3}{\sigma^2} + \frac{9}{\sigma^4}$ |
| 3 | $-\frac{6}{\sigma^3} - \frac{75}{\sigma^5} - \frac{675}{\sigma^7}$ | $1 + \frac{6}{\sigma^2} + \frac{45}{\sigma^4} + \frac{225}{\sigma^6}$ |
| 4 | $-\frac{10}{\sigma^3} - \frac{220}{\sigma^5} - \frac{4725}{\sigma^7} - \frac{44100}{\sigma^9}$ | $1 + \frac{10}{\sigma^2} + \frac{135}{\sigma^4} + \frac{1575}{\sigma^6} + \frac{11025}{\sigma^8}$ |
| 5 | $-\frac{15}{\sigma^3} - \frac{630}{\sigma^5} - \frac{18900}{\sigma^7}$ $-\frac{396900}{\sigma^9} - \frac{4465125}{\sigma^{11}}$ | $1 + \frac{15}{\sigma^2} + \frac{305}{\sigma^4} + \frac{6300}{\sigma^6}$ $+\frac{99285}{\sigma^{10}} + \frac{893025}{\sigma^{10}}$ |

arm length. This circuit has the same input impedance as a spherical shell of radius a radiating an electric multipole mode of order ℓ .

Since at resonance the time-average values of electric and magnetic energy are equal, Chu took the peak value of the stored energy to be twice the time-average stored electric energy. With a series RLC circuit, the relationships between the input reactance and reactive elements L_ℓ and C_ℓ are:

$$X_\ell = \left(\omega L_\ell - \frac{1}{\omega C_\ell} \right) \quad \text{and} \quad \frac{dX_\ell}{d\omega} = \frac{1}{\omega} \left(\omega L_\ell + \frac{1}{\omega C_\ell} \right) \quad (3.6.10)$$

Solving for the values of the elements as a function of the reactance gives:

$$C_\ell = \frac{2}{\omega^2} \left(\frac{dX_\ell}{d\omega} - \frac{X_\ell}{\omega} \right)^{-1}; \quad L_\ell = \frac{1}{2} \left(\frac{dX_\ell}{d\omega} + \frac{X_\ell}{\omega} \right) \quad (3.6.11)$$

Chu put the time-average radiated power equal to that dissipated in the resistor. Combining the above shows that:

$$P_\ell = \frac{1}{2} R_\ell I_\ell I_\ell^* = \frac{\eta}{2(A_\ell^2 + B_\ell^2)} I_\ell I_\ell^* \quad (3.6.12)$$

Using Eqs. (3.6.8) and (3.6.11), the time-average stored electric energy is:

$$W_\ell = \frac{1}{4\omega^2 C_\ell} I_\ell I_\ell^* = \frac{I_\ell I_\ell^*}{8} \left(\frac{dX_\ell}{d\omega} - \frac{X_\ell}{\omega} \right) \quad (3.6.13)$$

Using Eq. (3.6.7), the calculated modal value of Q is:

$$Q_{\ell E} = \frac{\omega}{2\eta} \left(\frac{dX_\ell}{d\omega} - \frac{X_\ell}{\omega} \right) (A_\ell^2 + B_\ell^2) \quad (3.6.14)$$

This general solution for the special case $\ell = 1$ reduces to:

$$A_1^2 + B_1^2 = \frac{1 + (ka)^2}{(ka)^2} \quad \text{and} \quad X_1 = -\frac{\eta}{(ka)[1 + (ka)^2]} \quad (3.6.15)$$

$$Q_{1E} = \frac{1}{(ka)^3} \left[\frac{1 + 2(ka)^2}{1 + (ka)^2} \right] \quad (3.6.16)$$

In the limit of electrically small antennas:

$$\lim_{ka \rightarrow 0} Q_{1E} = \frac{1}{(ka)^3} + \frac{1}{(ka)} \quad (3.6.17)$$

Chu stated that this approximate result is adequate for practical antennas.

3.7. Chu's Q Analysis, Exact for TM Fields

Although Chu's technique for approximating the value of Q for each equivalent circuit is adequate for practical purposes, a more exact analysis is needed if critical comparisons with other analytical techniques are to be made. For this purpose we make an exact analysis of the dipole circuit of Fig. 3.6.1, $\ell = 1$, and from the analysis obtain an exact value of antenna Q.

Let $i_1(t)$ and $i_2(t)$ be the currents respectively through the capacitor and the inductor of Fig. 3.6.1 for $\ell = 1$; the current through the resistor is $i_1(t) - i_2(t)$:

$$Ri_1(t) = L \frac{di_2(t)}{dt} + Ri_2(t) \quad (3.7.1)$$

The instantaneous energies stored in the capacitor and inductor are:

$$w_C(t) = \frac{q_1^2(t)}{2C} \quad \text{and} \quad w_L(t) = \frac{Li_2^2(t)}{2} \quad (3.7.2)$$

The power dissipated in the resistor is:

$$p(t) = R[i_1(t) - i_2(t)]^2 \quad (3.7.3)$$

For sinusoidal steady state operation, introduce:

$$i_2(t) = I_2 \cos(\omega t) \quad (3.7.4)$$

Combining shows the charge on the capacitor to be:

$$q_1(t) = \int i_1(t) dt = \frac{I_2}{\omega} \left[\sin(\omega t) + \frac{\omega L}{R} \cos(\omega t) \right] \quad (3.7.5)$$

Resulting energies and power are:

$$w_C(t) = \frac{I_2^2}{4\omega} \left\{ \left(\frac{1}{\omega C} + \frac{\omega L^2}{CR^2} \right) - \left(\frac{1}{\omega C} - \frac{\omega L^2}{CR^2} \right) \cos(2\omega t) + \frac{2L}{CR} \sin(2\omega t) \right\} \quad (3.7.6)$$

$$w_L(t) = \frac{I_2^2}{4\omega} \omega L [1 + \cos(2\omega t)] \quad (3.7.7)$$

$$p(t) = \frac{\omega^2 L^2}{2R} I_2^2 [1 - \cos(2\omega t)] \quad (3.7.8)$$

Use of component values from Fig. 3.6.1 in Eqs. (3.7.6)–(3.7.8) gives:

$$w_C(t) = \frac{\eta I_2^2}{4\omega} \left\{ \left(\frac{1}{(ka)} + (ka) \right) - \left(\frac{1}{(ka)} - (ka) \right) \cos(2\omega t) + 2 \sin(2\omega t) \right\} \quad (3.7.9)$$

$$w_L(t) = \eta I_2^2 \frac{(ka)}{4\omega} [1 + \cos(2\omega t)] \quad (3.7.10)$$

$$p(t) = \eta I_2^2 \frac{(ka)^2}{2} [1 - \cos(2\omega t)] \quad (3.7.11)$$

The total reactive energy is the sum of Eqs. (3.7.9) and (3.7.10):

$$w_X(t) = \frac{\eta I_2^2}{4\omega} \left\{ \left(\frac{1}{(ka)} + 2(ka) \right) - \left(\frac{1}{(ka)} - 2(ka) \right) \cos(2\omega t) + 2 \sin(2\omega t) \right\} \quad (3.7.12)$$

The cyclical peak of stored energy is:

$$W_{pk} = \frac{\eta I_2^2}{4\omega} \left\{ \left(\frac{1}{(ka)} + 2(ka) \right) + \frac{1}{(ka)} \sqrt{1 + 4(ka)^4} \right\} \quad (3.7.13)$$

The time-average output power is:

$$P_{av} = \eta I_2^2 \frac{(ka)^2}{2} \quad (3.7.14)$$

Combining gives:

$$Q = \frac{\omega W_{pk}}{P_{av}} \geq \frac{1}{2(ka)^3} \left(1 + \sqrt{1 + 4(ka)^4} \right) + \frac{1}{(ka)} \quad (3.7.15)$$

This is the exact expression for the Q of the circuit of Fig. 3.6.1 for the special case $\ell = 1$. In the limit as ka goes to zero Eq. (3.7.15) is equal to Eq. (3.6.17).

3.8. Chu's Q Analysis, TE Field

The fields about a z -directed magnetic multipole follow from Eq. (3.2.1):

$$\begin{aligned}\sigma^2 \eta H_r &= - \sum_{\ell=1}^{\infty} \ell(\ell+1) G_\ell [B_\ell(\sigma) + i A_\ell(\sigma)] P_\ell(\cos \theta) \\ \sigma \eta H_\theta &= - \sum_{\ell=1}^{\infty} G_\ell [D_\ell(\sigma) + i C_\ell(\sigma)] \frac{d}{d\theta} P_\ell(\cos \theta) \\ \sigma E_\phi &= \sum_{\ell=1}^{\infty} G_\ell [A_\ell(\sigma) - i B_\ell(\sigma)] \frac{d}{d\theta} P_\ell(\cos \theta)\end{aligned}\quad (3.8.1)$$

Following the procedure used for TM modes, for the TE modes introduce a generalized force and flow as a voltage and a current, this time proportional respectively to E_ϕ and $-H_\theta$. Each mode then satisfies the power equation:

$$P_c = \frac{2\pi}{\eta k^2} G_\ell G_\ell^* \frac{\ell(\ell+1)}{(2\ell+1)} [A_\ell(\sigma) - i B_\ell(\sigma)] [D_\ell(\sigma) - i C_\ell(\sigma)] = \frac{1}{2} V_\ell I_\ell^* \quad (3.8.2)$$

Like TM modes, for each TE mode the angular electric-to-magnetic field ratio depends upon radius, not angle. Defining modal admittance Y_ℓ to equal the ratio $H_{\theta\ell}/E_{\phi\ell}$, it follows that:

$$Y_{\ell M}(\sigma) = - \frac{H_{\theta\ell}}{E_{\phi\ell}} = \frac{I_\ell}{V_\ell} = \frac{1}{\eta} \left[\frac{D_\ell(\sigma) + i C_\ell(\sigma)}{A_\ell(\sigma) - i B_\ell(\sigma)} \right] \quad (3.8.3)$$

Both Eqs. (3.8.2) and (3.8.3) are satisfied if:

$$\begin{aligned}V_\ell &= \frac{G_\ell}{k} \sqrt{\frac{4\pi\ell(\ell+1)}{3(2\ell+1)}} [A_\ell(\sigma) - i B_\ell(\sigma)] e^{-i\sigma} \\ I_\ell &= \frac{G_\ell}{\eta k} \sqrt{\frac{4\pi\ell(\ell+1)}{3(2\ell+1)}} [D_\ell(\sigma) + i C_\ell(\sigma)] e^{-i\sigma}\end{aligned}\quad (3.8.4)$$

Comparison of Eqs. (3.6.4) and (3.8.4) shows that:

$$Y_{\ell M}(\sigma) = \frac{1}{\eta^2} Z_{\ell E}(\sigma) \quad (3.8.5)$$

Repeating the procedure used to evaluate the TM equivalent circuits gives the equivalent circuits for TE modes. The resulting circuit is shown in Fig. 3.8.1; it is the dual of Fig. 3.6.1.

Since the circuits are exact duals, each power and energy of Sec. 3.6 has an exact counterpart in Sec. 3.8, though what is capacitive becomes inductive, and *vice versa*. For example, the input impedance of electrically small electric dipoles is equal to the large input admittance of electrically small

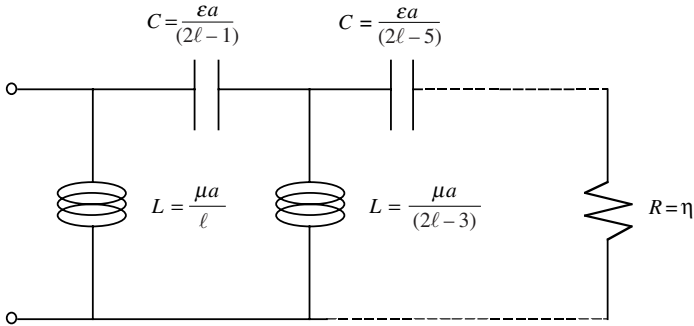


Fig. 3.8.1. TE multipolar equivalent circuit.

magnetic dipoles. If the circuit used to calculate Q is a parallel capacitor, inductor, and resistor the magnitudes of energies are unchanged, though the forms are reversed. Q therefore is the same. This circuit for the two structures has the same input impedance as a spherical shell of radius a radiating magnetic multipole mode of order ℓ .

$$Q_{1M} \geq \frac{1}{2(ka)^3} \left(1 + \sqrt{1 + 4(ka)^4} \right) + \frac{1}{ka} \tag{3.8.6}$$

In the limit of electrically small antennas:

$$\lim_{ka \rightarrow 0} Q_{1M} \geq \frac{1}{(ka)^3} + \frac{1}{(ka)} \tag{3.8.7}$$

3.9. Chu's Q Analysis, Collocated TM and TE Modes

In addition to analyzing individual moments, Chu also analyzed parallel, superimposed TE + TM modes of the same order, phased to produce circular polarization. A basic difficulty is that to add modal powers it is necessary to account for phase differences, yet phase information is not contained in the complex power expressions. There are, however, other ways to account for the phase difference; Chu did this by requiring circular polarization. With both modes present and the field circularly polarized, the standing energy oscillates between the radiation fields of the two dipoles. The average standing electric energy in the TM mode is the capacitive energy obtained using Eq. (3.6.10). Since the TE mode is its exact dual, the magnetic energy stored in the TE mode is equal to the electric energy in the TM mode.

Therefore the total standing electric energy is:

$$W_{\ell}(\sigma) = \frac{1}{4\omega^2 C_{\ell}} \mathbf{I}_{\ell} \mathbf{I}_{\ell}^* + \frac{\mathbf{L}_{\ell}}{4} \mathbf{I}_{\ell} \mathbf{I}_{\ell}^* = \frac{1}{4} \mathbf{I}_{\ell} \mathbf{I}_{\ell}^* \frac{dX_{\ell}}{d\omega} \quad (3.9.1)$$

The time-average radiated power is twice that of Eq. (3.6.12):

$$P_{\ell} = \mathbf{R}_{\ell} \mathbf{I}_{\ell} \mathbf{I}_{\ell}^* = \eta \mathbf{I}_{\ell} \mathbf{I}_{\ell}^* (ka)^2 / [1 + (ka)^2] \quad (3.9.2)$$

The reactance is given by Eq. (3.6.10). For radiating dipoles the derivative is:

$$\frac{dX_{\ell}}{d\omega} = \frac{(ka)}{\omega} \frac{dX_{\ell}}{d(ka)} = \frac{\eta}{\omega} \frac{[1 + 3(ka)^2]}{(ka)[1 + (ka)^2]^2}$$

Combining the above gives the dipole Q:

$$Q \geq \frac{1 + 3(ka)^2}{2(ka)^3 [1 + (ka)^2]} \cong \frac{1}{2(ka)^3} + \frac{1}{ka} \quad (3.9.3)$$

For electrically small antennas, this Q is approximately half that of either dipole acting alone. The interpretation is that since the standing energy simply moves back and forth between reactive elements the total value is nearly the same as for either dipole acting alone and the radiated energy is twice that of a single dipole. Therefore, Q is reduced by an approximate factor of two.

3.10. Q the Easy Way, Electrically Small Antennas

It is possible to solve for Q from the impedance most easily by use of Chu's equivalent circuits. For antennas electrically small enough so that $\ell(2\ell - 1) \gg k^2 a^2$, the input reactance is dominated by the first reactive element, a capacitor for TM modes and an inductor for TE modes, and Q is very nearly equal to:

$$Q_{\ell} = \tan[\zeta_{\ell}(\sigma)] \quad (3.10.1)$$

Combining Eq. (3.10.1), Chu's equivalent circuits, and the impedance results of Sec. 3.2 shows that the modal Qs of electrically small antennas are, very nearly:

$$Q_{\ell} \geq |\gamma_{\ell}| \quad (3.10.2)$$

Values of γ_{ℓ} are listed in Table 3.2.1. Keeping only the lead term gives:

$$Q \geq \frac{\ell[(2\ell - 1)!!]^2}{(ka)^{2\ell+1}} \quad (3.10.3)$$

3.11. Q on the Basis of Time-Dependent Field Theory

The analytical works that follow are based upon the analysis of an idealized radiating sphere. Experimental or numerical confirmation, however, requires actual or numerical embodiments and, in the main, embodiments are made of straight wires and wire loops, not spheres. The analyses to come assume no source coupling between modes and therefore the desired modes, and only those modes, exist.

With this analysis, as with Chu's, only fields at a radius greater than the radius of the virtual, source-containing sphere of radius a are considered. Ignoring fields at smaller radii has the great advantage that results are not specific to a particular antenna. However, although the interior volume for an electrically small antenna is small, for a fixed moment the field magnitude increases rapidly enough with decreasing radius so the interior energy remains a significant portion of the total standing energy. For the spherical shell dipole analyzed in Sec. A.14 the interior energy is half that of the exterior energy. For biconical transmitting antennas, see Eq. (2.7.1), the TEM mode and an infinite number of TM modes are included. For biconical receiving antennas, see Eq. (2.17.2), the TEM mode and infinite numbers both of TM and TE modes are included. Nonetheless, to keep the results general and solvable it is necessary to ignore interior fields when calculating Q.

To calculate the Q of a multiport antenna, an antenna driven by more than one terminal pair, it is necessary to account for suppressed phase angles. Since phase angles are an integral part of actual fields, we begin with a general multipolar expansion for phasor fields and then transform phasor fields into actual fields. The phasor form of the multipolar field expansion is:

$$\begin{aligned}\tilde{\mathbf{E}}_r &= i \sum_{\ell=0}^{\infty} \sum_{m=0}^{\ell} i^{-\ell} F(\ell, m) \ell(\ell+1) \frac{h_{\ell}(\sigma)}{\sigma} P_{\ell}^m(\cos \theta) e^{-jm\phi} \\ \eta \tilde{\mathbf{H}}_r &= -ij \sum_{\ell=0}^{\infty} \sum_{m=0}^{\ell} i^{-\ell} G(\ell, m) \ell(\ell+1) \frac{h_{\ell}(\sigma)}{\sigma} P_{\ell}^m(\cos \theta) e^{-jm\phi} \\ \tilde{\mathbf{E}}_{\theta} &= \sum_{\ell=0}^{\infty} \sum_{m=0}^{\ell} i^{-\ell} \left[i F(\ell, m) h_{\ell}^{\bullet}(\sigma) \frac{d}{d\theta} P_{\ell}^m(\cos \theta) \right. \\ &\quad \left. - G(\ell, m) h_{\ell}(\sigma) \frac{m}{\sin \theta} P_{\ell}^m(\cos \theta) \right] e^{-jm\phi}\end{aligned}$$

$$\begin{aligned}
\eta\tilde{H}_\phi &= \sum_{\ell=0}^{\infty} \sum_{m=0}^{\ell} i^{-\ell} \left[F(\ell, m) h_\ell(\sigma) \frac{d}{d\theta} P_\ell^m(\cos\theta) \right. \\
&\quad \left. - i G(\ell, m) h_\ell^\bullet(\sigma) \frac{m}{\sin\theta} P_\ell^m(\cos\theta) \right] e^{-jm\phi} \\
\tilde{E}_\phi &= -j \sum_{\ell=0}^{\infty} \sum_{m=0}^{\ell} i^{-\ell} \left[i F(\ell, m) h_\ell^\bullet(\sigma) \frac{m}{\sin\theta} P_\ell^m(\cos\theta) \right. \\
&\quad \left. - G(\ell, m) h_\ell(\sigma) \frac{d}{d\theta} P_\ell^m(\cos\theta) \right] e^{-jm\phi} \\
\eta\tilde{H}_\theta &= j \sum_{\ell=0}^{\infty} \sum_{m=0}^{\ell} i^{-\ell} \left[F(\ell, m) h_\ell(\sigma) \frac{m}{\sin\theta} P_\ell^m(\cos\theta) \right. \\
&\quad \left. - i G(\ell, m) h_\ell^\bullet(\sigma) \frac{d}{d\theta} P_\ell^m(\cos\theta) \right] e^{-jm\phi} \tag{3.11.1}
\end{aligned}$$

We examine the Q of different modes and modal combinations by considering a series of examples. The first example is the set of TM modes of degree zero. For this case, Chu's "omnidirectional" case, all coefficients except $F(\ell, 0)$ are equal to zero and, for simplicity in notation, is put equal to $i^{\ell-1}$. After replacing Hankel functions by equivalent letter functions, see Appendix A.26, and accounting for the suppressed dependence upon retarded time, t_R , the actual field terms are:

$$\begin{aligned}
\sigma^2 E_r &= \sum_{\ell=1}^{\infty} \ell(\ell+1) [B_\ell(\sigma) \cos(\omega t_R) - A_\ell(\sigma) \sin(\omega t_R)] P_\ell(\cos\theta) \\
\sigma E_\theta &= \sum_{\ell=1}^{\infty} [D_\ell(\sigma) \cos(\omega t_R) - C_\ell(\sigma) \sin(\omega t_R)] \frac{d}{d\theta} P_\ell(\cos\theta) \tag{3.11.2} \\
\sigma \eta H_\phi &= \sum_{\ell=1}^{\infty} [A_\ell(\sigma) \cos(\omega t_R) + B_\ell(\sigma) \sin(\omega t_R)] \frac{d}{d\theta} P_\ell(\cos\theta)
\end{aligned}$$

The total energy density, w_T , at each point in the field is:

$$w_T = \frac{\varepsilon}{2} \mathbf{E} \cdot \mathbf{E} + \frac{\mu}{2} \mathbf{H} \cdot \mathbf{H} \tag{3.11.3}$$

Substituting the field forms of Eq. (3.11.2) into the energy density expression shows that for each mode:

$$\begin{aligned}
 w_T = \frac{\varepsilon}{4} \left\{ \frac{\ell^2(\ell+1)^2}{\sigma^4} \right. \\
 \times [(A_\ell^2 + B_\ell^2) - (A_\ell^2 - B_\ell^2) \cos(2\omega t_R) - 2A_\ell B_\ell \sin(2\omega t_R)] [P_\ell(\cos \theta)]^2 \\
 + \frac{1}{\sigma^2} [(A_\ell^2 + B_\ell^2 + C_\ell^2 + D_\ell^2) + (A_\ell^2 - B_\ell^2 - C_\ell^2 + D_\ell^2) \cos(2\omega t_R) \\
 \left. + 2(A_\ell B_\ell - C_\ell D_\ell) \sin(2\omega t_R) \right] \left[\frac{dP_\ell(\cos \theta)}{d\theta} \right]^2 \Big\} \quad (3.11.4)
 \end{aligned}$$

For brevity, the dependence of the letter functions upon σ is suppressed. The right side, top row of Eq. (3.11.4) is the energy of the radial component of the electric field intensity. The remaining terms are the combined energies of the angular field components. The first and second lines have different parity with respect to the zenith angle.

The modal components of the Poynting vector are:

$$\begin{aligned}
 N_r &= \frac{1}{2\eta\sigma^2} \{ (A_\ell D_\ell - B_\ell C_\ell) + (A_\ell D_\ell + B_\ell C_\ell) \cos(2\omega t_R) \\
 &\quad - (A_\ell C_\ell - B_\ell D_\ell) \sin(2\omega t_R) \} \left(\frac{dP_\ell(\cos \theta)}{d\theta} \right)^2 \\
 N_\theta &= -\frac{\ell(\ell+1)}{2\eta\sigma^3} \{ 2A_\ell B_\ell \cos(2\omega t_R) - (A_\ell^2 - B_\ell^2) \\
 &\quad \times \sin(2\omega t_R) \} P_\ell(\cos \theta) \frac{dP_\ell(\cos \theta)}{d\theta} \\
 N_\phi &= 0
 \end{aligned} \quad (3.11.5)$$

The continuity equation describes energy conservation in the field, and is:

$$\nabla \cdot \mathbf{N} + \frac{\partial w_T}{\partial t} = 0 \quad (3.11.6)$$

The equality of Eq. (3.11.6) is readily verified by substituting Eqs. (3.11.4) and (3.11.5) into it and then taking the time integral.

We seek to separate the total energy density into a part that travels with the wave on its outbound journey and a part that separates from the wave, remaining within the local region of the antenna. Separated power may be calculated by riding with the wave and determining, at each point, the rate at which energy departs from it. For this purpose note that the divergence of the power at constant retarded time is equal to the negative

rate at which energy per unit volume separates from the wave:

$$\nabla_R \cdot \mathbf{N} = -\frac{\partial w_S}{\partial t_R} \quad (3.11.7)$$

Symbol w_S indicates the energy density at each point that separates from the outbound wave and oscillates over a distance of $\lambda/2$; we define it to be standing energy density. Symbol ∇_R operates at constant retarded time. The divergence operation of Eq. (3.11.7) is aided by values obtained by taking the derivatives of Tables A.26.2.13 and A.26.2.14. The results are:

$$\begin{aligned} \nabla_R \cdot \mathbf{N}_\theta &= \frac{k\ell(\ell+1)}{2\eta\sigma^4} [2A_\ell B_\ell \cos(2\omega t_R) - (A_\ell^2 - B_\ell^2) \sin(2\omega t_R)] \\ &\quad \times \left\{ \ell(\ell+1) [P_\ell(\cos\theta)]^2 - \left[\frac{d}{d\theta} P_\ell(\cos\theta) \right]^2 \right\} \\ \nabla_R \cdot \mathbf{N}_r &= \frac{k}{2\eta\sigma^2} \left[\frac{d}{d\theta} P_\ell(\cos\theta) \right]^2 \\ &\quad \times \left\{ \left[2 \frac{\ell(\ell+1)}{\sigma^2} A_\ell B_\ell - 2(A_\ell - D_\ell)(B_\ell + C_\ell) \right] \cos(2\omega t_R) \right. \\ &\quad \left. - \left[\frac{\ell(\ell+1)}{\sigma^2} (A_\ell^2 - B_\ell^2) - (A_\ell^2 - B_\ell^2 - C_\ell^2 - D_\ell^2) \right. \right. \\ &\quad \left. \left. + 2(A_\ell D_\ell + B_\ell C_\ell) \right] \sin(2\omega t_R) \right\} \end{aligned} \quad (3.11.8)$$

Summing the components of Eq. (3.11.8) and then taking the indefinite integral with respect to retarded time gives:

$$\begin{aligned} w_S &= \frac{\varepsilon K}{4} + \frac{\varepsilon}{4} \left\{ -\frac{\ell^2(\ell+1)^2}{\sigma^4} \{ (A_\ell^2 - B_\ell^2) \cos(2\omega t_R) \right. \\ &\quad \left. + 2A_\ell B_\ell \sin(2\omega t_R) \} [P_\ell(\cos\theta)]^2 \right. \\ &\quad \left. + \frac{1}{\sigma^2} \{ [(A_\ell - D_\ell)^2 - (B_\ell + C_\ell)^2] \cos(2\omega t_R) \right. \\ &\quad \left. + 2(A_\ell - D_\ell)(B_\ell + C_\ell) \sin(2\omega t_R) \} \left[\frac{dP_\ell(\cos\theta)}{d\theta} \right]^2 \right\} \end{aligned} \quad (3.11.9)$$

K is a constant of integration, with dimensions chosen for later convenience. There are two requirements on K : Since it is an energy density it can never be negative and it must appear in the w_T expression. This is the equivalent of requiring that both zenith angle parities in Eq. (3.11.9) be

everywhere greater than or equal to zero. Evaluating K and entering it into Eq. (3.11.9) gives:

$$\begin{aligned}
 w_S = \frac{\varepsilon}{4} \left\{ \frac{\ell^2(\ell+1)^2}{\sigma^4} \{ (A_\ell^2 + B_\ell^2) - (A_\ell^2 - B_\ell^2) \cos(2\omega t_R) - 2A_\ell B_\ell \sin(2\omega t_R) \} \right. \\
 \times [P_\ell(\cos\theta)]^2 + \frac{1}{\sigma^2} \left\{ [(A_\ell - D_\ell)^2 + (B_\ell + C_\ell)^2] \right. \\
 + [(A_\ell - D_\ell)^2 - (B_\ell + C_\ell)^2] \cos(2\omega t_R) \\
 \left. \left. + 2(A_\ell - D_\ell)(B_\ell + C_\ell) \sin(2\omega t_R) \right\} \left[\frac{dP_\ell(\cos\theta)}{d\theta} \right]^2 \right\} \quad (3.11.10)
 \end{aligned}$$

This is the source-associated energy density. It is separate from the traveling wave and oscillates about a fixed position in the field. The top row of Eq. (3.11.4) is the energy density of the radial field component and the other terms are the energy densities of the angular field components. Comparison of Eqs. (3.11.4) with (3.11.10) shows that the top lines are identical: all energy of the radial field component remains attached to the source. Some energy of the angular field components remains attached to the source and the rest does not.

Subtracting w_S from w_T gives the energy that remains part of the traveling wave: the field-associated energy density w_δ .

$$\begin{aligned}
 w_\delta = \frac{\varepsilon}{2\sigma^2} [(A_\ell D_\ell - B_\ell C_\ell) + (A_\ell D_\ell + B_\ell C_\ell) \cos(2\omega t_R) \\
 - (A_\ell C_\ell - B_\ell D_\ell) \sin(2\omega t_R)] \left[\frac{dP_\ell(\cos\theta)}{d\theta} \right]^2 \quad (3.11.11)
 \end{aligned}$$

The expressions for N_r and w_δ differ by a multiplicative factor equal to the speed of light, c . A characteristic of traveling energy is that power is equal to the product of the energy density and the speed of travel. The movement of w_δ produces the radially directed power density. Its value at the generating surface $r = a$ determines the antenna input impedance. Both w_T and w_S are positive real, physical entities, but w_δ connotes power and hence can be negative.

For single modes, an alternative and simpler derivation of the standing energy is to divide the radial component of the Poynting vector by c and subtract the result, Eq. (3.11.11), from the total energy density expression, Eq. (3.11.4). The result repeats the source associated energy density, Eq. (3.11.10). Although the technique is arguably correct for single modes, the process does not generalize to multi-modal situations.

Consider what happens if the source is suddenly disconnected. Since nothing travels outward faster than the speed of light, the originally out-bound portion of the field continues without change, and energy W_δ is transported on out into free space. Energy W_S is fixed in position. As the fields at radius less than r collapse, the energy density exterior to that radius becomes larger than those nearer, producing an inward pressure. We presume, therefore, that energy W_S returns to the source.

During steady state operation, it is helpful to determine energies at the time a given wave is emitted. In a form of the ergodic theorem this is equal to the spatial integral of the energy in its outward journey. In such terms the total standing energy is equal to the volume integral of w_S :

$$W_S = \frac{1}{k^3} \int_{ka}^{\infty} \sigma^2 d\sigma \int_0^{2\pi} d\phi \int_0^\pi \sin\theta d\theta w_S(\sigma, t_R) \quad (3.11.12)$$

Substituting Eq. (3.11.10) into Eq. (3.11.12) and integrating over the full solid angle leaves:

$$\begin{aligned} W_S = & \frac{\pi\varepsilon}{k^3} \frac{\ell(\ell+1)}{(2\ell+1)} \int_{ka}^{\infty} d\sigma \left\{ 4A_\ell(A_\ell - D_\ell) \right. \\ & + \frac{d}{d\sigma}(A_\ell C_\ell + B_\ell D_\ell + 2A_\ell B_\ell) \\ & - \frac{d}{d\sigma}(A_\ell C_\ell - B_\ell D_\ell) \cos(2\omega t_R) \\ & \left. - \frac{d}{d\sigma}(A_\ell D_\ell + B_\ell C_\ell - (-1)^\ell) \sin(2\omega t_R) \right\} \quad (3.11.13) \end{aligned}$$

The radial integrals can be done with the assistance of Tables A.26.2.11 through A.26.2.14. Doing the integrals shows the standing energy to be:

$$\begin{aligned} W_S = & \frac{\pi\varepsilon}{k^3} \frac{\ell(\ell+1)}{(2\ell+1)} \left\{ -(A_\ell C_\ell + B_\ell D_\ell + 2A_\ell B_\ell) \right. \\ & + 4 \int_{ka}^{\infty} d\sigma A_\ell(A_\ell - D_\ell) + (A_\ell C_\ell - B_\ell D_\ell) \cos(2\omega t_R) \\ & \left. + (A_\ell D_\ell + B_\ell C_\ell - (-1)^\ell) \sin(2\omega t_R) \right\} \quad (3.11.14) \end{aligned}$$

In Eq. (3.11.14), the letter functions are evaluated at $r = a$. The peak energy value is:

$$\begin{aligned} W_{\text{Spk}} = & \frac{\pi\varepsilon}{k^3} \frac{\ell(\ell+1)}{(2\ell+1)} \left\{ -(A_\ell C_\ell + B_\ell D_\ell + 2A_\ell B_\ell) + 4 \int_{ka}^{\infty} d\sigma A_\ell(A_\ell - D_\ell) \right. \\ & \left. + \sqrt{(A_\ell^2 + B_\ell^2)(C_\ell^2 + D_\ell^2) - 2(-1)^\ell(A_\ell D_\ell + B_\ell C_\ell) + 1} \right\} \quad (3.11.15) \end{aligned}$$

The total output power on the antenna surface is obtained by taking the surface integral of N_r :

$$\begin{aligned} P &= \frac{\sigma^2}{k^2} \int_0^{2\pi} d\phi \int_0^\pi \sin\theta d\theta N_r(\sigma, t_R) \\ &= \frac{\ell(\ell+1)}{\eta k^2 (2\ell+1)} \left\{ 1 + (A_\ell D_\ell + B_\ell C_\ell) \cos(2\omega t_R) \right. \\ &\quad \left. - (A_\ell C_\ell - B_\ell D_\ell) \sin(2\omega t_R) \right\} \end{aligned} \quad (3.11.16)$$

By Eq. (3.5.11), the ratio of the peak of Eq. (3.11.15) to the time-average of Eq. (3.11.16) determines Q:

$$Q \geq \frac{\omega W_S|_{\text{peak}}}{P|_{\text{average}}} \quad (3.11.17)$$

Combining Eq. (3.11.15) with the values of Eqs. (3.11.16) and (3.11.17) to give an expression for the Q of arbitrary mode ℓ of radiation:

$$\begin{aligned} Q_\ell \geq \frac{1}{2} \left\{ - (A_\ell C_\ell + B_\ell D_\ell + 2A_\ell B_\ell) + 4 \int_\infty^{ka} d\sigma A_\ell (A_\ell - D_\ell) \right. \\ \left. + \sqrt{(A_\ell^2 + B_\ell^2)(C_\ell^2 + D_\ell^2) - 2(-1)^\ell (A_\ell D_\ell + B_\ell C_\ell) + 1} \right\} \end{aligned} \quad (3.11.18)$$

3.12. Q of a Radiating Electric Dipole

The actual fields of a time-varying, z -directed electric dipole follow from Eq. (3.11.1). With coefficient $F(1,0)$ equal to one and with all others equal to zero the fields are:

$$\begin{aligned} \sigma^2 E_r &= -2 \left[\cos(\omega t_R) + \frac{1}{\sigma} \sin(\omega t_R) \right] \cos\theta \\ \sigma E_\theta &= \left[-\frac{1}{\sigma} \cos(\omega t_R) + \left(1 - \frac{1}{\sigma^2} \right) \sin(\omega t_R) \right] \sin\theta \\ \sigma \eta H_\phi &= \left[-\frac{1}{\sigma} \cos(\omega t_R) + \sin(\omega t_R) \right] \sin\theta \end{aligned} \quad (3.12.1)$$

The energy densities follow from Eqs. (3.11.4), (3.11.10) and (3.11.11):

$$w_T = \frac{\varepsilon}{4} \left\{ \left\{ \frac{4}{\sigma^4} [1 + \cos(2\omega t_R)] + \frac{8}{\sigma^5} \sin(2\omega t_R) + \frac{4}{\sigma^6} [1 - \cos(2\omega t_R)] \right\} \cos^2 \theta \right. \\ \left. + \left\{ \left(\frac{2}{\sigma^2} + \frac{1}{\sigma^6} \right) [1 - \cos(2\omega t_R)] + \frac{4}{\sigma^4} \cos(2\omega t_R) \right. \right. \\ \left. \left. - \left(\frac{4}{\sigma^3} - \frac{2}{\sigma^5} \right) \sin(2\omega t_R) \right\} \sin^2 \theta \right\} \quad (3.12.2)$$

$$w_S = \frac{\varepsilon}{4} \left\{ \left\{ \frac{4}{\sigma^4} [1 + \cos(2\omega t_R)] + \frac{8}{\sigma^5} \sin(2\omega t_R) \theta + \frac{4}{\sigma^6} [1 - \cos(2\omega t_R)] \right\} \cos^2 \theta \right. \\ \left. + \frac{1}{\sigma^6} [1 - \cos(2\omega t_R)] \sin^2 \theta \right\} \quad (3.12.3)$$

$$w_\delta(t_R) = \frac{\varepsilon}{2} \left\{ \frac{1}{\sigma^2} [1 - \cos(2\omega t_R)] + \frac{2}{\sigma^4} \cos(2\omega t_R) \theta \right. \\ \left. - \left(\frac{2}{\sigma^3} - \frac{1}{\sigma^5} \right) \sin(2\omega t_R) \right\} \sin^2 \theta \quad (3.12.4)$$

The energy density described by the first lines of Eqs. (3.12.2) and (3.12.3) is centered on the antenna axis and is the energy of the radially directed component of the electric field intensity. The predominant portion of w_S is due to the radial field component and w_δ energy is entirely due to the radial field components. The second lines are centered at $\theta = \pi/2$; in Eq. (3.12.2), it is the energy of the angularly directed field components and, in Eq. (3.12.3), it is the energy of the nearest angular field term. Plots of w_S at four different times are shown in Fig. 3.12.1 for $ka = 0.1$; note the changes of scale.

The components of the Poynting vector follow from Eq. (3.11.5):

$$N_r = \frac{1}{2\eta} \left\{ \frac{1}{\sigma^2} [1 - \cos(2\omega t_R)] + \frac{2}{\sigma^4} \cos(2\omega t_R) \right. \\ \left. - \left(\frac{2}{\sigma^3} - \frac{1}{\sigma^5} \right) \sin(2\omega t_R) \right\} \sin^2 \theta \quad (3.12.5)$$

$$N_\theta = \frac{1}{2\eta} \left\{ -\frac{4}{\sigma^4} \cos(2\omega t_R) + \left(\frac{2}{\sigma^3} - \frac{2}{\sigma^5} \right) \sin(2\omega t_R) \right\} \sin \theta \cos \theta \quad (3.12.6)$$

Substituting values of the letter functions into Eq. (3.11.14) gives:

$$W_S = \frac{2\pi\varepsilon}{3k^3} \left\{ \frac{2}{(ka)} [1 + \cos(2\omega t_R)] + \frac{2}{(ka)^2} \sin(2\omega t_R) \right. \\ \left. + \frac{1}{(ka)^3} [1 - \cos(2\omega t_R)] \right\} \quad (3.12.7)$$

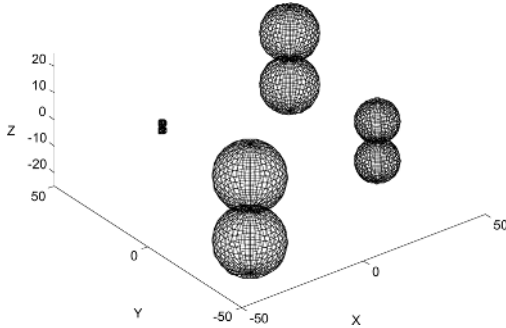


Fig. 3.12.1. Standing energy density of Eq. (3.12.7), a z -directed electric dipole. Plots are shown at the four times $2\omega t_R = 0, \pi/2, \pi$, and $3\pi/2$ at the range $ka = 0.1$. The standing energy density is centered on the z -axis.

Similarly evaluating Eq. (3.11.16) gives:

$$p = \frac{4\pi}{3\eta k^2} \left\{ [1 - \cos(2\omega t_R)] + \frac{2}{(ka)^2} \cos(2\omega t_R) - \left(\frac{2}{(ka)} - \frac{1}{(ka)^3} \right) \sin(2\omega t_R) \right\} \quad (3.12.8)$$

To relate Eq. (3.12.8) to the input impedance, rewrite it in the form of time-dependent complex power:

$$P_c = \frac{4\pi}{3\eta k^2} \left\{ [1 - \cos(2\omega t_R - 2\xi(\sigma))] + \frac{1}{(ka)^3} \sin(2\omega t_R - 2\xi(\sigma)) \right\} \quad (3.12.9)$$

Since the radius of the generating surface is fixed and there is but a single mode, the value of $\xi(\sigma)$ is unimportant. The complex power follows from Eq. (3.12.9) and is:

$$P_c(\sigma) = \frac{4\pi}{3\eta k^2} \left[1 + \frac{i}{(ka)^3} \right] \quad (3.12.10)$$

The antenna input impedance follows from Eq. (3.12.10).

Substituting values of the letter functions into Eq. (3.11.18) gives:

$$Q \geq \frac{1}{2(ka)^3} \left[1 + \sqrt{1 + 4(ka)^4} \right] + \frac{1}{(ka)} \quad (3.12.11)$$

Table 3.12.1. Radiating, z -directed electric dipole.

$$\begin{aligned}
w_T(t_R) &= \frac{\varepsilon}{4} \left\{ \left\{ \frac{4}{\sigma^6} [1 - \cos(2\omega t_R)] + \frac{8}{\sigma^5} \sin(2\omega t_R) + \frac{4}{\sigma^4} [1 + \cos(2\omega t_R)] \right\} \cos^2 \theta \right. \\
&\quad \left. + \left\{ \left(\frac{2}{\sigma^2} + \frac{1}{\sigma^6} \right) [1 - \cos(2\omega t_R)] + \frac{4}{\sigma^4} \cos(2\omega t_R) \right. \right. \\
&\quad \left. \left. - \left(\frac{4}{\sigma^3} - \frac{2}{\sigma^5} \right) \sin(2\omega t_R) \right\} \sin^2 \theta \right\} \\
w_S(t_R) &= \frac{\varepsilon}{4} \left\{ \left\{ \frac{4}{\sigma^6} [1 - \cos(2\omega t_R)] + \frac{8}{\sigma^5} \sin(2\omega t_R) + \frac{4}{\sigma^4} [1 + \cos(2\omega t_R)] \right\} \cos^2 \theta \right. \\
&\quad \left. + \left\{ \frac{1}{\sigma^6} [1 - \cos(2\omega t_R)] \right\} \sin^2 \theta \right\} \\
w_\delta(t_R) &= \frac{\varepsilon}{2} \left\{ \frac{1}{\sigma^2} [1 - \cos(2\omega t_R)] - \left(\frac{2}{\sigma^3} - \frac{1}{\sigma^5} \right) \sin(2\omega t_R) + \frac{2}{\sigma^4} \cos(2\omega t_R) \right\} \sin^2 \theta \\
N_r(t_R) &= \frac{1}{2\eta} \left\{ \frac{1}{\sigma^2} [1 - \cos(2\omega t_R)] - \left(\frac{2}{\sigma^3} - \frac{1}{\sigma^5} \right) \sin(2\omega t_R) + \frac{2}{\sigma^4} \cos(2\omega t_R) \right\} \sin^2 \theta \\
N_\theta(t_R) &= \frac{1}{2\eta} \left[-\frac{4}{\sigma^4} \cos(2\omega t_R) + \left(\frac{2}{\sigma^3} - \frac{2}{\sigma^5} \right) \sin(2\omega t_R) \right] \sin \theta \cos \theta \\
N_\phi(t_R) &= 0 \\
W_S &= \frac{2\pi\varepsilon}{3k^3} \left\{ \frac{1}{(ka)^3} [1 - \cos(2\omega t_R)] + \frac{2}{(ka)^2} \sin(2\omega t_R) + \frac{2}{(ka)} [1 + \cos(2\omega t_R)] \right\} \\
P &= \frac{4\pi}{3\eta k^2} \left\{ [1 - \cos(2\omega t_R)] - \left(\frac{2}{(ka)} - \frac{1}{(ka)^3} \right) \sin(2\omega t_R) + \frac{2}{(ka)^2} \cos(2\omega t_R) \right\} \\
Q &\geq \frac{1}{2(ka)^3} \left(1 + \sqrt{1 + 4(ka)^4} \right) + \frac{1}{(ka)} \quad \text{Gain} = \frac{3}{2}
\end{aligned}$$

This is the same value obtained using the exact analysis of Chu's equivalent circuit, Eq. (3.7.15). In the electrically small limit Q goes to:

$$Q \geq \frac{1}{(ka)^3} + \frac{1}{(ka)} \quad (3.12.12)$$

Analytical results are summarized in Table 3.12.1.

To examine the effect of coordinate rotation, rotate the dipole from the z - to the x -direction. This illustrates the role of antenna rotations that appear in the more complicated modal structures. The force fields of an x -directed electric dipole follow from Eq. (3.11.1) with $F(1, 1) = 1$, all other coefficients equal zero, and keeping only the real part with respect to j , are given by Eq. (3.12.13). Analytical results are summarized in Table 3.12.2.

Table 3.12.2. Summary of results, x -directed electric dipole.

$$\begin{aligned}
w_T(t_R) &= \frac{\varepsilon}{4} \left\{ 4 \left[\frac{1}{\sigma^6} [1 - \cos(2\omega t_R)] + \frac{2}{\sigma^5} \sin(2\omega t_R) + \frac{1}{\sigma^4} [1 + \cos(2\omega t_R)] \right] \sin^2 \theta \cos^2 \phi \right. \\
&\quad \left. + \left[\left(\frac{2}{\sigma^2} + \frac{1}{\sigma^6} \right) [1 - \cos(2\omega t_R)] + \frac{4}{\sigma^4} \cos(2\omega t_R) - \left(\frac{4}{\sigma^3} - \frac{2}{\sigma^5} \right) \sin(2\omega t_R) \right] \right. \\
&\quad \left. \times (\cos^2 \theta \cos^2 \phi + \sin^2 \phi) \right\} \\
w_S(t_R) &= \frac{\varepsilon}{4} \left\{ 4 \left[\frac{1}{\sigma^6} [1 - \cos(2\omega t_R)] + \frac{2}{\sigma^5} \sin(2\omega t_R) + \frac{1}{\sigma^4} [1 + \cos(2\omega t_R)] \right] \sin^2 \theta \cos^2 \phi \right. \\
&\quad \left. + \frac{1}{\sigma^6} [1 - \cos(2\omega t_R)] (\cos^2 \theta \cos^2 \phi + \sin^2 \phi) \right\} \\
w_\delta(t_R) &= \frac{\varepsilon}{2} \left[\frac{1}{\sigma^2} [1 - \cos(2\omega t_R)] - \left(\frac{2}{\sigma^3} - \frac{1}{\sigma^5} \right) \sin(2\omega t_R) + \frac{2}{\sigma^4} \cos(2\omega t_R) \right] \\
&\quad \times (\cos^2 \theta \cos^2 \phi + \sin^2 \theta) \\
N_r(t_R) &= \frac{1}{2\eta} \left[\frac{1}{\sigma^2} [1 - \cos(2\omega t_R)] - \left(\frac{2}{\sigma^3} - \frac{1}{\sigma^5} \right) \sin(2\omega t_R) + \frac{2}{\sigma^4} \cos(2\omega t_R) \right] \\
&\quad \times (\cos^2 \theta \cos^2 \phi + \sin^2 \theta) \\
N_\theta(t_R) &= \frac{1}{2\eta} \left\{ -\frac{4}{\sigma^4} \cos(2\omega t_R) + \left(\frac{2}{\sigma^3} - \frac{2}{\sigma^5} \right) \sin(2\omega t_R) \right\} \sin \theta \cos \theta \cos^2 \phi \\
N_\phi(t_R) &= \frac{1}{2\eta} \left\{ -\frac{4}{\sigma^4} \cos(2\omega t_R) + \left(\frac{2}{\sigma^3} - \frac{2}{\sigma^5} \right) \sin(2\omega t_R) \right\} \sin \theta \sin \phi \cos \phi \\
W_S &= \frac{2\pi\varepsilon}{3k^2} \left\{ \frac{1}{(ka)^3} [1 - \cos(2\omega t_R)] + \frac{2}{(ka)^2} \sin(2\omega t_R) + \frac{2}{(ka)} \cos(2\omega t_R) \right\} \\
p &= \frac{4\pi}{3\eta k^2} \left\{ [1 - \cos(2\omega t_R)] - \left(\frac{2}{(ka)} - \frac{1}{(ka)^3} \right) \sin(2\omega t_R) + \frac{2}{(ka)^2} \cos(2\omega t_R) \right\} \\
Q &\geq \frac{1}{2(ka)^3} \left(1 + \sqrt{1 + 4(ka)^4} \right) + \frac{1}{(ka)}
\end{aligned}$$

Power maximum occurs at $\theta = \pi/2$.

$$\begin{aligned}
\sigma^2 E_r &= 2[B \cos(\omega t_R) - A \sin(\omega t_R)] \sin \theta \cos \phi \\
\sigma E_\theta &= [D \cos(\omega t_R) - C \sin(\omega t_R)] \cos \theta \cos \phi \\
\sigma \eta H_\phi &= [A \cos(\omega t_R) + B \sin(\omega t_R)] \cos \theta \cos \phi \\
\sigma E_\phi &= -[D \cos(\omega t_R) - C \sin(\omega t_R)] \sin \phi \\
\sigma \eta H_\theta &= [A \cos(\omega t_R) + B \sin(\omega t_R)] \sin \phi
\end{aligned} \tag{3.12.13}$$

The force fields of Table 3.12.1 result if $F(1, 1) = 1$, all other coefficients are equal to zero, and only the real part with respect to j is retained.

3.13. Q of Radiating Magnetic Dipoles

Although the electric and magnetic dipole fields are simply duals, the sources are physically quite different. Sources of TM and TE fields, see Secs. A.28 and A.29, are respectively linear currents and current loops and for which intrinsic symmetry differences exist. An ideal biconical antenna, a TM field source, driven by an ideal terminal set located at the conical apices results in fields with rotational symmetry about the antenna axis. If the lengths of the cones are equal and much less than a wavelength replacing the cones by equivalent sources, see Appendix A.7, on the surface of a circumscribing sphere centered at the conical apices produces a dipolar source directed along the antenna axis. As the ratio of cone length to wavelength increases higher order modes are excited but the symmetry remains; all driven modes have degree zero. As shown in Chapter 2 resonance is a property of the antenna arms and occurs when the cone lengths are about $\lambda/4$.

Things are not so simple with TE field sources, of which magnetic dipoles are the simplest example. Consider the current loop to lie in the xy -plane at $z = 0$. Driving the loop requires it to be broken at some point and the driving terminals inserted. If the diameter of the loop is small enough the current is uniform around the loop and the displacement of the center of the loop from the terminals, equal to the loop radius, is not significant. The actual loop may be replaced by a virtual surface centered on the center of the loop and supporting a magnetic dipole. As the ratio of loop diameter to wavelength increases, see Fig. 3.13.1, the displacement of the center of the virtual sphere from the terminals increases and the current varies with position on the loop. Current at a point away from the terminals

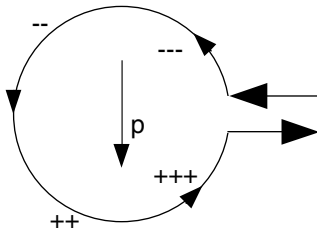


Fig. 3.13.1. Actual wire loop, current is not uniform around the loop.

may be quite different from that at the terminals: rotational symmetry is broken. This lack of rotational symmetry is an intrinsic characteristic of loop-generated magnetic moments, and is inconsistent with assumptions necessary to derive results of superimposed electric and magnetic multipolar moments. Nonetheless we examine the properties of idealized magnetic multipoles.

Consider zero degree TE modes. To obtain the fields, put all coefficients of Eq. (3.11.1) except $G(\ell, 0)$ equal to zero and, for simplicity in notation, make the arbitrary choice that $G(\ell, 0)i^{\ell-1} = -1$. After putting $j = i$, replacing Hankel functions by letter functions, and accounting for the suppressed time dependence the actual values of the remaining field terms are:

$$\begin{aligned}\sigma^2\eta H_r &= \sum_{\ell=1}^{\infty} \ell(\ell+1)[A_\ell(\sigma)\cos(\omega t_R) + B_\ell(\sigma)\sin(\omega t_R)]P_\ell(\cos\theta) \\ \sigma E_\phi &= -\sum_{\ell=1}^{\infty} [B_\ell(\sigma)\cos(\omega t_R) - A_\ell(\sigma)\sin(\omega t_R)]\frac{d}{d\theta}P_\ell(\cos\theta) \\ \sigma\eta H_\theta &= -\sum_{\ell=1}^{\infty} [C_\ell(\sigma)\cos(\omega t_R) + D_\ell(\sigma)\sin(\omega t_R)]\frac{d}{d\theta}P_\ell(\cos\theta)\end{aligned}\quad (3.13.1)$$

Results of a radiating, z -directed magnetic dipole are tabulated in Table 3.13.1; magnitudes are identical with the electric dipole case and only the phases of the time-dependent terms differ. The force fields of this table result from Eq. (3.13.1) for case $\ell = 1$.

3.14. Q of Collocated Electric and Magnetic Dipole Pair

Since the TE and TM field components of z -directed antennas do not overlap, when evaluating the energy densities it is necessary to determine the integration constants for each solution *before* summing over the vector fields. The vector field equations for $F(1, 0) = -G(1, 0) = 1$, all other coefficients are equal to zero, and $j = i$ are shown in Eq. (3.14.1).

$$\begin{aligned}\sigma^2 E_r &= -2 \left[\cos(\omega t_R) + \frac{1}{\sigma} \sin(\omega t_R) \right] \cos\theta \\ \sigma^2 \eta H_r &= 2 \left[-\frac{1}{\sigma} \cos(\omega t_R) + \sin(\omega t_R) \right] \cos\theta\end{aligned}$$

Table 3.13.1. Radiating, z-directed magnetic dipole.

$$\begin{aligned}
w_T(t_R) &= \frac{\varepsilon}{4} \left\{ \left\{ \frac{4}{\sigma^6} [1 + \cos(2\omega t_R)] - \frac{8}{\sigma^5} \sin(2\omega t_R) + \frac{4}{\sigma^4} [1 - \cos(2\omega t_R)] \right\} \cos^2 \theta \right. \\
&\quad + \left\{ \left(\frac{2}{\sigma^2} + \frac{1}{\sigma^6} \right) [1 + \cos(2\omega t_R)] - \frac{4}{\sigma^4} \cos(2\omega t_R) \right. \\
&\quad \left. \left. + \left(\frac{4}{\sigma^3} - \frac{2}{\sigma^5} \right) \sin(2\omega t_R) \right\} \sin^2 \theta \right\} \\
w_S(t_R) &= \frac{\varepsilon}{4} \left\{ \left\{ \frac{4}{\sigma^6} [1 + \cos(2\omega t_R)] - \frac{8}{\sigma^5} \sin(2\omega t_R) + \frac{4}{\sigma^4} [1 - \cos(2\omega t_R)] \right\} \cos^2 \theta \right. \\
&\quad \left. + \left\{ \frac{1}{\sigma^6} [1 + \cos(2\omega t_R)] \right\} \sin^2 \theta \right\} \\
w_\delta(t_R) &= \frac{\varepsilon}{2} \left\{ \frac{1}{\sigma^2} [1 + \cos(2\omega t_R)] + \left(\frac{2}{\sigma^3} - \frac{1}{\sigma^5} \right) \sin(2\omega t_R) - \frac{2}{\sigma^4} \cos(2\omega t_R) \right\} \sin^2 \theta \\
N_r(t_R) &= \frac{1}{2\eta} \left\{ \frac{1}{\sigma^2} [1 + \cos(2\omega t_R)] + \left(\frac{2}{\sigma^3} - \frac{1}{\sigma^5} \right) \sin(2\omega t_R) - \frac{2}{\sigma^4} \cos(2\omega t_R) \right\} \sin^2 \theta \\
N_\theta(t_R) &= \frac{1}{2\eta} \left\{ -\frac{4}{\sigma^4} \cos(2\omega t_R) + \left(\frac{2}{\sigma^3} - \frac{2}{\sigma^5} \right) \sin(2\omega t_R) \right\} \sin \theta \cos \theta \\
&\quad - \frac{1}{\eta} \left\{ \frac{1}{\sigma^6} [1 - \cos(2\omega t_R)] + \frac{2}{\sigma^4} \cos(2\omega t_R) - \left(\frac{1}{\sigma^3} - \frac{2}{\sigma^5} \right) \sin(2\omega t_R) \right\} \sin \theta \\
N_\phi(t_R) &= 0 \\
W_S &= \frac{2\pi\varepsilon}{3k^3} \left\{ \frac{1}{(ka)^3} [1 + \cos(2\omega t_R)] - \frac{2}{(ka)^2} \sin(2\omega t_R) + \frac{2}{(ka)} [1 - \cos(2\omega t_R)] \right\} \\
P &= \frac{4\pi}{3\eta k^3} \left\{ [1 + \cos(2\omega t_R)] + \left(\frac{2}{(ka)} - \frac{1}{(ka)^3} \right) \sin(2\omega t_R) - \frac{2}{(ka)^2} \cos(2\omega t_R) \right\} \\
Q &\geq \frac{1}{2(ka)^3} \left(1 + \sqrt{1 + 4(ka)^4} \right) + \frac{1}{(ka)} \quad \text{Gain} = \frac{3}{2}
\end{aligned}$$

$$\begin{aligned}
\sigma E_\theta &= \left[-\frac{1}{\sigma} \cos(\omega t_R) + \left(1 - \frac{1}{\sigma^2} \right) \sin(\omega t_R) \right] \sin \theta \\
\sigma \eta H_\phi &= \left[-\frac{1}{\sigma} \cos(\omega t_R) + \sin(\omega t_R) \right] \sin \theta \\
\sigma E_\phi &= - \left[\cos(\omega t_R) + \frac{1}{\sigma} \sin(\omega t_R) \right] \sin \theta \\
\sigma \eta H_\theta &= \left[\left(1 - \frac{1}{\sigma^2} \right) \cos(\omega t_R) + \frac{1}{\sigma} \sin(\omega t_R) \right] \sin \theta \quad (3.14.1)
\end{aligned}$$

Table 3.14.1. Collocated, radiating z -directed electric and magnetic dipoles producing circularly polarized fields.

$$w_T = \frac{\varepsilon}{2} \left\{ \left(\frac{4}{\sigma^6} + \frac{4}{\sigma^4} \right) \cos^2 \theta + \left(\frac{2}{\sigma^2} + \frac{1}{\sigma^6} \right) \sin^2 \theta \right\}$$

$$w_S = \frac{\varepsilon}{2} \left\{ \left(\frac{4}{\sigma^6} + \frac{4}{\sigma^4} \right) \cos^2 \theta + \frac{1}{\sigma^6} \sin^2 \theta \right\}; \quad w_\delta = \frac{\varepsilon}{\sigma^2} \sin^2 \theta$$

$$N_r(t_R) = \frac{1}{\eta\sigma^2} \sin^2 \theta; \quad N_\theta(t_R) = 0; \quad N_\phi(t_R) = -\frac{2}{\eta\sigma^3} \sin \theta \cos \theta$$

$$W_S = \frac{8\pi\varepsilon}{3k^3} \left[\frac{1}{2(ka)^3} + \frac{1}{(ka)} \right]; \quad P = \frac{8\pi}{3\eta k^2}$$

$$Q \geq \frac{1}{2(ka)^3} + \frac{1}{(ka)} \quad \text{Gain} = \frac{3}{2}$$

The far field is circularly polarized. A table of dynamic values similar to those of Tables 3.12.1 and 3.13.1 is given in Table 3.14.1. The three energy densities and the radial component of the Poynting vector are all time-independent. Since there are two sources, each of which produces the same average output power as listed in Tables 12.1 and 13.1, the time-average value for this case is double that of the previous cases. The zenith and azimuth components of the Poynting vector respectively are and are not equal to zero. The gain and pattern are the same as for individual dipoles. Since the total standing energy of both dipoles is nearly equal to the peak value of either, Q is about half that of an isolated dipole.

If the phase of the magnetic dipole of Table 3.14.1 is shifted by $\pi/2$ so $G(1, 0) = -i$ the TM modal terms are the same as listed in Eq. (3.12.1) and the TE modal terms are given by Eq. (3.14.2):

$$\begin{aligned} \sigma^2 \eta H_r &= 2 \left[\cos(\omega t_R) + \frac{1}{\sigma} \sin(\omega t_R) \right] \cos \theta \\ \sigma E_\phi &= - \left[\frac{1}{\sigma} \cos(\omega t_R) - \sin(\omega t_R) \right] \sin \theta \\ \sigma \eta H_\theta &= \left[\frac{1}{\sigma} \cos(\omega t_R) - \left(1 - \frac{1}{\sigma^2} \right) \sin(\omega t_R) \right] \sin \theta \end{aligned} \quad (3.14.2)$$

The powers and energies produced by the electric and magnetic moments are in phase. Time-dependent powers sum to twice the values of Table 3.12.1. Both gain and Q are equal to those of Table 3.12.1. Although

the integration constant is introduced quite differently in collocated parallel and crossed moments, the calculated Q is the same.

Next consider collocated x -directed electric dipole and y -directed magnetic dipole sources. For this configuration the fields strongly overlap and the integration constant is determined after summing over the vector fields. Fields with $F(1, 1) = 1$, $G(1, 1) = -i$, all other coefficients are equal to zero, and $j = i$ are listed in Eq. (3.14.3):

$$\begin{aligned}
 \sigma^2 E_r &= -2 \left[\cos(\omega t_R) + \frac{1}{\sigma} \sin(\omega t_R) \right] \sin \theta \cos \phi \\
 \sigma^2 \eta H_r &= -2 \left[\cos(\omega t_R) + \frac{1}{\sigma} \sin(\omega t_R) \right] \sin \theta \sin \phi \\
 \sigma E_\theta &= \left\{ \left[\frac{1}{\sigma} \cos(\omega t_R) - \sin(\omega t_R) \right] \right. \\
 &\quad \left. + \left[\frac{1}{\sigma} \cos(\omega t_R) - \left(1 - \frac{1}{\sigma^2} \right) \sin(\omega t_R) \right] \cos \theta \right\} \cos \phi \\
 \sigma E_\phi &= - \left\{ \left[\frac{1}{\sigma} \cos(\omega t_R) - \sin(\omega t_R) \right] \cos \theta \right. \\
 &\quad \left. + \left[\frac{1}{\sigma} \cos(\omega t_R) - \left(1 - \frac{1}{\sigma^2} \right) \sin(\omega t_R) \right] \right\} \sin \phi \\
 \eta H_\phi &= -E_\phi \cot \phi; \quad \eta H_\theta = E_\phi \tan \phi
 \end{aligned} \tag{3.14.3}$$

Far fields are linearly polarized. Dynamic values are listed in Table 3.14.2. As in the case of Eq. (3.14.2) the energy and power terms are in phase, the energy and power terms are doubled, and Q is equal to that of either dipole radiating in isolation. The radial and zenith portions of the Poynting vector contain factors that are proportional, respectively, to $\cos \theta$ and $\sin \theta$. The terms are suppressed in the table since they do not affect the total energies.

3.15. Q of Collocated Pairs of Dipoles

We seek to generalize Chu's field-induced limitations on mixed TE + TM radiation emitted from a confined region. Since Chu confined his TE + TM analysis to a case where the two sources had no overlapping parallel field components it was not necessary to consider mutual coupling, and since he confined his attention to near-resonance effects it was not necessary to account for the different input impedances of different modes. We seek to analyze general conditions that require accounting for both things. Doing so shows the properties of particular modal combinations to be desirable, but we do not address the design and construction of such sources. In Chapter 6

Table 3.14.2. Collocated, radiating z -directed electric and magnetic dipoles producing linearly polarized fields.

$$\begin{aligned}
w_T(t_R) &= \frac{\varepsilon}{4} \left\{ \left\{ \frac{4}{\sigma^6} [1 - \cos(2\omega t_R)] + \frac{8}{\sigma^5} \sin(2\omega t_R) + \frac{4}{\sigma^4} [1 + \cos(2\omega t_R)] \right\} \sin^2 \theta \right. \\
&\quad + \left\{ \left(\frac{2}{\sigma^2} + \frac{1}{\sigma^6} \right) [1 - \cos(2\omega t_R)] \right. \\
&\quad \left. \left. + \frac{4}{\sigma^4} \cos(2\omega t_R) - \left(\frac{4}{\sigma^3} - \frac{2}{\sigma^5} \right) \sin(2\omega t_R) \right\} (1 + \cos^2 \theta) \right\} \\
w_S(t_R) &= \frac{\varepsilon}{4} \left\{ \left\{ \frac{4}{\sigma^6} [1 - \cos(2\omega t_R)] + \frac{8}{\sigma^5} \sin(2\omega t_R) + \frac{4}{\sigma^4} [1 + \cos(2\omega t_R)] \right\} \sin^2 \theta \right. \\
&\quad \left. + \left\{ \frac{1}{\sigma^6} [1 - \cos(2\omega t_R)] \right\} (1 + \cos^2 \theta) \right\} \\
w_\delta(t_R) &= \frac{\varepsilon}{2} \left\{ \frac{1}{\sigma^2} [1 - \cos(2\omega t_R)] + \frac{2}{\sigma^4} \cos(2\omega t_R) - \left(\frac{2}{\sigma^3} - \frac{1}{\sigma^5} \right) \sin(2\omega t_R) \right\} (1 + \cos^2 \theta) \\
N_r(t_R) &= \frac{1}{2\eta} \left\{ \frac{1}{\sigma^2} [1 - \cos(2\omega t_R)] + \frac{2}{\sigma^4} \cos(2\omega t_R) - \left(\frac{2}{\sigma^3} - \frac{1}{\sigma^5} \right) \sin(2\omega t_R) \right\} (1 + \cos \theta)^2 \\
N_\theta(t_R) &= \frac{1}{\eta} \left[\frac{2}{\sigma^4} \cos(2\omega t_R) - \left(\frac{1}{\sigma^3} - \frac{1}{\sigma^5} \right) \sin(2\omega t_R) \right] \sin \theta \cos \theta; \quad N_\phi(t_R) = 0 \\
W_S(t) &= \frac{4\pi\varepsilon}{3k^3} \left\{ \frac{1}{(ka)^3} [1 - \cos(2\omega t_R)] + \frac{2}{(ka)^2} \sin(2\omega t_R) + \frac{2}{(ka)} [1 + \cos(2\omega t_R)] \right\} \\
p &= \frac{8\pi}{3\eta\kappa^3} \left\{ [1 - \cos(2\omega t_R)] - \left(\frac{2}{(ka)} - \frac{1}{(ka)^3} \right) \sin(2\omega t_R) + \frac{2}{(ka)^2} \cos(2\omega t_R) \right\} \\
Q &\geq \frac{1}{2(ka)^3} \left(1 + \sqrt{1 + 4(ka)^4} \right) + \frac{1}{(ka)} \quad \text{Gain} = 3
\end{aligned}$$

we also show that such combinations are common in nature, and govern the emission and absorption of photons.

The output powers of superimposed modes with overlapping, parallel fields are orthogonal and, for that reason, independent. Quite differently, if there are positions of overlapping, parallel modal fields the local energy at each field point depends upon details of the overlap. The position and magnitudes of the energies, in turn, determine both pattern directivity and radiation Q. An equivalent circuit that describes the properties of a multimodal ensemble must necessarily account for individual modal properties, mutual couplings, and different input impedances. At the time of writing no such equivalent circuit has been proposed and there is no suggestion that it is possible to construct one. Furthermore, see Sec. 3.4, power fields

cannot be fully described using complex numbers and circuits support complex power. Yet the conclusion of Sec. 3.5, that Qs defined by Eqs. (3.5.11) and (3.5.15) are equal, applies only to equivalent circuits. We conclude, therefore, there is no proof that in such an ensemble bandwidth can be deduced from the stored energy of the multimodal fields. If Qs are needed to determine both energy and bandwidth it is necessary to obtain them separately: field energies using Eq. (3.5.11) and bandwidth from the input impedance.

For the generalizations to follow it is necessary to make detailed definitions of resonance and bandwidth. Resonance occurs in a center-driven dipole, see Fig. 2.9.2, if there is no reactance at the input terminals, and occurs because of the phase delay in the antenna arms. A condition for resonance of a radiating surface is the absence of surface reactive power; this definition implies the radiating surface is fed by a distributed source. Surface modes have no intrinsic resonance; surfaces can be made resonant only by reactive power cancellation by equal magnitude, out of phase similar modes, TE or TM, or equal magnitude, in-phase dissimilar modes, TE and TM.

A more restrictive resonance condition, and the condition used in this book, is the absence of net reactive power at all points on the radiating surface. This condition is met only by in-phase TE and TM modes of the same order, degree, and magnitude. By this definition, the frequency of resonance depends both upon the electric size of the radiating spherical shell and upon the relative magnitudes of the drives. Changing relative source magnitudes changes the center frequency of the resonance band. Since magnitudes may be varied independently of the frequency the operational range of the radiator is limited only by limitations on possible drive magnitudes and there are no inherent, field determined limitations on the operational frequency range. In that sense the bandwidth is infinite.

To examine the affect of phasing on pairs of dipoles with overlapping, parallel fields, consider the superposition of an x -directed electric dipole and a y -directed magnetic dipole. If the relative phasing of the dipoles is $F(1, 1) = 1, G(1, 1) = -1$, all other coefficients are equal to zero, and $j = i$ the fields of Eq. (3.15.1) result:

$$\begin{aligned}\sigma^2 E_r &= 2[B \cos(\omega t_R) - A \sin(\omega t_R)] \sin \theta \cos \phi \\ \sigma^2 \eta H_r &= 2[A \cos(\omega t_R) + B \sin(\omega t_R)] \sin \theta \sin \phi \\ \sigma E_\theta &= \{[D \cos(\omega t_R) - C \sin(\omega t_R)] \cos \theta \\ &\quad - [B \cos(\omega t_R) - A \sin(\omega t_R)]\} \cos \phi\end{aligned}$$

$$\begin{aligned}
\eta\sigma\mathbf{H}_\phi &= \{[A \cos(\omega t_R) + B \sin(\omega t_R)] \cos \theta \\
&\quad + [C \cos(\omega t_R) + D \sin(\omega t_R)]\} \cos \phi \\
\sigma\mathbf{E}_\phi &= -\{[D \cos(\omega t_R) - C \sin(\omega t_R)] \\
&\quad - [B \cos(\omega t_R) - A \sin(\omega t_R)] \cos \theta\} \sin \phi \\
\eta\sigma\mathbf{H}_\theta &= \{[A \cos(\omega t_R) + B \sin(\omega t_R)] \\
&\quad + [C \cos(\omega t_R) + D \sin(\omega t_R)] \cos \theta\} \sin \phi
\end{aligned} \tag{3.15.1}$$

Output power is centered on the positive z -axis and is equal to zero on the negative z -axis. The far field is circularly polarized. Dynamic values are listed in Table 3.15.1 where again power and energy terms proportional to $\cos \theta$ are ignored. Q is reduced below that of Table 3.14.1. This is because some of the energy that is source-associated with parallel radiating elements becomes field-associated with orthogonal elements.

A second possible pairing of dipoles is two collocated, perpendicularly directed electric dipoles driven $\pi/2$ out of phase. The fields of Eq. (3.15.2) result if coefficient $F(1, 1) = 1$, all others are zero, and $j = i$. Output power is centered at $\theta = \pi/2$ and circularly polarized. As with the perpendicular electric and magnetic dipoles of Table 3.14.2, since the field components strongly overlap energy densities are combined before the integration constant is evaluated. The result is similar to in-phase electric and magnetic moments in that the standing energy of the two dipoles peak out of phase, and the peak standing energy is about equal to that of a single dipole. Since the output power is twice that of a single dipole, Q is reduced by about a factor of two. This is similar to, and for the same reason as, the reduction in Q shown in Table 3.14.1.

$$\begin{aligned}
\sigma^2\mathbf{E}_r &= 2[B_1 \cos(\omega t_R - \phi) - A_1 \sin(\omega t_R - \phi)] \sin \theta \\
\sigma\mathbf{E}_\theta &= [D_1 \cos(\omega t_R - \phi) - C_1 \sin(\omega t_R - \phi)] \cos \theta \\
\sigma\eta\mathbf{H}_\phi &= [A_1 \cos(\omega t_R - \phi) + B_1 \sin(\omega t_R - \phi)] \cos \theta \\
\sigma\mathbf{E}_\phi &= [C_1 \cos(\omega t_R - \phi) + D_1 \sin(\omega t_R - \phi)] \\
\sigma\eta\mathbf{H}_\theta &= [B_1 \cos(\omega t_R - \phi) - A_1 \sin(\omega t_R - \phi)]
\end{aligned} \tag{3.15.2}$$

The azimuth energy flow produces a z -directed angular momentum. Results are listed in Table 3.15.2. Different from the previous electric dipole cases, but like the counterpart of Table 3.15.1, a term proportional to σ^{-6} appears as part of the outgoing energy. It forms part of the standing energy in other special cases; among the results is that the w_δ/N_r ratio is no longer equal to c . The energy shifts position from standing to traveling energy and results in Q being further reduced, to the value of Table 3.15.1.

Table 3.15.1. Collocated, radiating x - and y -directed electric and magnetic dipoles, circular polarization.

$$\begin{aligned}
 w_T(t_R) &= \frac{\varepsilon}{2} \left\{ \left(\frac{2}{\sigma^4} + \frac{2}{\sigma^6} \right) \sin^2 \theta + \left[\left(\frac{2}{\sigma^4} - \frac{2}{\sigma^6} \right) \cos(2\omega t_R) + \frac{4}{\sigma^5} \sin(2\omega t_R) \right] \sin^2 \theta \cos(2\phi) \right. \\
 &\quad + \left(\frac{1}{\sigma^2} + \frac{1}{2\sigma^6} \right) (1 + \cos^2 \theta) + \left\langle \left(\frac{1}{\sigma^2} - \frac{2}{\sigma^4} + \frac{1}{2\sigma^6} \right) \cos(2\omega t_R) \right. \\
 &\quad \left. \left. + \left(\frac{2}{\sigma^3} - \frac{1}{\sigma^5} \right) \sin(2\omega t_R) \right\rangle \sin^2 \theta \cos(2\phi) \right\} \\
 w_S(t_R) &= \frac{\varepsilon}{2} \left\{ \left(\frac{2}{\sigma^4} + \frac{2}{\sigma^6} \right) \sin^2 \theta + \left\langle \left(\frac{2}{\sigma^4} - \frac{3}{2\sigma^6} \right) \cos(2\omega t_R) + \frac{4}{\sigma^5} \sin(2\omega t_R) \right\rangle \right. \\
 &\quad \left. \times \sin^2 \theta \cos(2\phi) \right\} \\
 w_\delta(t_R) &= \frac{\varepsilon}{2} \left\{ \left(\frac{1}{\sigma^2} + \frac{1}{2\sigma^6} \right) (1 + \cos^2 \theta) + \left\langle \left(\frac{1}{\sigma^2} - \frac{2}{\sigma^4} \right) \cos(2\omega t_R) \right. \right. \\
 &\quad \left. \left. + \left(\frac{2}{\sigma^3} - \frac{1}{\sigma^5} \right) \sin(2\omega t_R) \right\rangle \sin^2 \theta \cos(2\phi) \right\} \\
 N_r &= \frac{1}{2\eta} \left\{ \frac{1}{\sigma^2} (1 + \cos^2 \theta) + \left[\left(\frac{1}{\sigma^2} - \frac{2}{\sigma^4} \right) \cos(2\omega t) + \left(\frac{2}{\sigma^3} - \frac{1}{\sigma^5} \right) \sin(2\omega t) \right] \right. \\
 &\quad \left. \times \sin^2 \theta \cos(2\phi) \right\} \\
 N_\theta &= \frac{1}{\eta} \left\{ \frac{2}{\sigma^4} \cos(2\omega t_R) - \left(\frac{1}{\sigma^3} - \frac{1}{\sigma^5} \right) \sin(2\omega t_R) \right\} \sin \theta \cos \theta \cos(2\phi) \\
 N_\phi &= \frac{1}{\eta} \left\{ -\frac{1}{\sigma^3} \cos \theta + \left\langle -\frac{2}{\sigma^4} \cos(2\omega t_R) + \left(\frac{1}{\sigma^3} - \frac{1}{\sigma^5} \right) \sin(2\omega t_R) \right\rangle \right\} \sin \theta \sin(2\phi) \\
 W_S &= \frac{8\pi\varepsilon}{3k^3} \left[\frac{1}{3(ka)^3} + \frac{1}{(ka)} \right]; \quad P = \frac{8\pi}{3\eta k^2} \\
 Q &\geq \frac{1}{3(ka)^3} + \frac{1}{(ka)}
 \end{aligned}$$

3.16. Four Collocated Electric and Magnetic Multipoles

Dipoles: Table 3.16.1 tabulates results of four collocated electric and magnetic dipoles generating equal time-average output powers. The electric dipoles have the same orientation and phasing as the example of Table 3.15.2. The magnetic dipoles have the same orientation and phasing as the electric ones, and produce the dual results of Table 3.15.2. Electric and magnetic dipole pairs lie along both the x - and y -axes. Two pairs of electric and magnetic dipoles are formed into two units and driven in

Table 3.15.2. Collocated radiating x - and y -directed electric dipoles, circular polarization.

$$\begin{aligned}
w_T(t_R) &= \frac{\varepsilon}{4} \left\langle \left\{ \frac{4}{\sigma^6} [1 - \cos(2\omega t_R - 2\phi)] + \frac{8}{\sigma^5} \sin(2\omega t_R - 2\phi) \right. \right. \\
&\quad \left. \left. + \frac{4}{\sigma^4} [1 + \cos(2\omega t_R - 2\phi)] \right\} \sin^2 \theta + \left\{ \left(\frac{2}{\sigma^2} + \frac{1}{\sigma^6} \right) (1 + \cos^2 \theta) \right. \right. \\
&\quad \left. \left. + \left[\left(\frac{2}{\sigma^2} - \frac{4}{\sigma^4} + \frac{1}{\sigma^6} \right) \cos(2\omega t_R - 2\phi) \right. \right. \right. \\
&\quad \left. \left. \left. + \left(\frac{4}{\sigma^3} - \frac{2}{\sigma^5} \right) \sin(2\omega t_R - 2\phi) \right] \sin^2 \theta \right\} \right\rangle \\
w_S(t_R) &= \frac{\varepsilon}{4} \left\{ \frac{1}{\sigma^6} [4 - 3 \cos(2\omega t_R - 2\phi)] + \frac{8}{\sigma^5} \sin(2\omega t_R - 2\phi) \right. \\
&\quad \left. + \frac{4}{\sigma^4} [1 + \cos(2\omega t_R - 2\phi)] \right\} \sin^2 \theta \\
w_\delta(t_R) &= \frac{\varepsilon}{2} \left\{ \left(\frac{1}{\sigma^2} + \frac{1}{2\sigma^6} \right) (1 + \cos^2 \theta) + \left[\left(\frac{1}{\sigma^2} - \frac{2}{\sigma^4} \right) \cos(2\omega t_R - 2\phi) \right. \right. \\
&\quad \left. \left. + \left(\frac{2}{\sigma^3} - \frac{1}{\sigma^5} \right) \sin(2\omega t_R - 2\phi) \right] \sin^2 \theta \right\} \\
N_r(t_R) &= \frac{1}{2\eta} \left\{ \frac{1}{\sigma^2} (1 + \cos^2 \theta) + \left[\left(\frac{1}{\sigma^2} - \frac{2}{\sigma^4} \right) \cos(2\omega t_R - 2\phi) \right. \right. \\
&\quad \left. \left. + \left(\frac{2}{\sigma^3} - \frac{1}{\sigma^5} \right) \sin(2\omega t_R - 2\phi) \right] \sin^2 \theta \right\} \\
N_\theta(t_R) &= \frac{1}{\eta} \left\{ \frac{2}{\sigma^4} \cos(2\omega t_R - 2\phi) - \left(\frac{1}{\sigma^3} - \frac{1}{\sigma^5} \right) \sin(2\omega t_R - 2\phi) \right\} \sin \theta \cos \theta \\
N_\phi(t_R) &= \frac{1}{\eta} \left\{ \left(\frac{1}{\sigma^3} + \frac{1}{\sigma^5} \right) + \left(\frac{1}{\sigma^3} - \frac{1}{\sigma^5} \right) \cos(2\omega t_R - 2\phi) + \frac{2}{\sigma^4} \sin(2\omega t_R - 2\phi) \right\} \sin \theta \\
W_S &= \frac{8\pi\varepsilon}{3k^3} \left[\frac{1}{3(ka)^3} + \frac{1}{(ka)} \right] \quad P = \frac{8\pi}{3\eta k^2} \\
Q &\geq \left[\frac{1}{3(ka)^3} + \frac{1}{(ka)} \right] \quad \text{Gain} = \frac{3}{2}
\end{aligned}$$

phase quadrature. Since the resulting circularly polarized field components overlap, the energy densities are combined before the integration constant is evaluated. Since no net energy leaves the traveling wave in its journey from the antenna surface to infinity, there is no source associated standing

Table 3.16.1. Four superimposed x - and y -oriented electric and magnetic dipoles, circular polarization.

$$w_T = \frac{\varepsilon}{2} \left\{ \left(\frac{4}{\sigma^4} + \frac{4}{\sigma^6} \right) \sin^2 \theta + \left(\frac{2}{\sigma^2} + \frac{1}{\sigma^6} \right) (1 + \cos^2 \theta) + \frac{4}{\sigma^2} \cos \theta \right\}$$

$$w_S = 0$$

$$w_\delta = \frac{\varepsilon}{2} \left\{ \left(\frac{4}{\sigma^4} + \frac{4}{\sigma^6} \right) \sin^2 \theta + \left(\frac{2}{\sigma^2} + \frac{1}{\sigma^6} \right) (1 + \cos^2 \theta) + \frac{4}{\sigma^2} \cos \theta \right\}$$

$$N_r = \frac{1}{\eta \sigma^2} \left\{ (1 + \cos^2 \theta) + \left(2 + \frac{1}{\sigma^4} \right) \cos \theta \right\}$$

$$N_\theta = \frac{2}{\eta \sigma^6} \sin \theta$$

$$N_\phi = \frac{2}{\eta} \left[\frac{1}{\sigma^3} \cos \theta + \left(\frac{1}{\sigma^3} + \frac{1}{\sigma^5} \right) \right] \sin \theta$$

$$W_S = 0 \quad p = \frac{16\pi}{3\eta k^2}$$

$$Q \geq 0 \quad \text{Gain} = 3$$

energy. The vector fields are:

$$\begin{aligned}
 \sigma^2 E_r &= 2[B_1 \cos(\omega t_R - \phi) - A_1 \sin(\omega t_R - \phi)] \sin \theta \\
 \sigma^2 \eta H_r &= -2[A_1 \cos(\omega t_R - \phi) + B_1 \sin(\omega t_R - \phi)] \sin \theta \\
 \sigma E_\theta &= \{ [D_1 \cos(\omega t_R - \phi) - C_1 \sin(\omega t_R - \phi)] \cos \theta \\
 &\quad + [A_1 \cos(\omega t_R - \phi) + B_1 \sin(\omega t_R - \phi)] \} \\
 \sigma \eta H_\phi &= \{ [A_1 \cos(\omega t_R - \phi) + B_1 \sin(\omega t_R - \phi)] \cos \theta \\
 &\quad + [D_1 \cos(\omega t_R - \phi) - C_1 \sin(\omega t_R - \phi)] \} \\
 \sigma E_\phi &= \{ -[B_1 \cos(\omega t_R - \phi) - A_1 \sin(\omega t_R - \phi)] \cos \theta \\
 &\quad + [C_1 \cos(\omega t_R - \phi) + D_1 \sin(\omega t_R - \phi)] \} \\
 \sigma \eta H_\theta &= \{ -[C_1 \cos(\omega t_R - \phi) + D_1 \sin(\omega t_R - \phi)] \cos \theta \\
 &\quad + [B_1 \cos(\omega t_R - \phi) - A_1 \sin(\omega t_R - \phi)] \}
 \end{aligned} \tag{3.16.1}$$

Resonance requires the equality $F(1, 1) = -G(1, 1)$. If that criterion is met and $j = i$ the input equivalent circuit is a simple resistance and Q can only be said to be greater than or equal to zero.

To examine the significance of a possible zero Q, note the peak value of standing energy about any radiator is equal to:

$$W_{\text{pk}} = \frac{QP_{\text{av}}}{\omega} \quad (3.16.2)$$

This energy returns to the antenna when, for example, a shift in frequency or source shutdown occurs. No matter how large the amount of energy available and no matter how small the acceptable time-average power, there is a minimum acceptable value of Q. Applications that appear to be impractical for dipole antennas because of the magnitude of required energy include radiative decay of atomic states and very low frequency communication. Quite differently, the lower limit on Q, as tabulated in Table 3.16.1, is zero. This implies that the full amount of energy that enters the field continues on to the far field and there is no lower limit on the possible antenna diameter-to-wavelength ratio. This does not imply, during steady state operation, that the local energy is zero; it implies only that all standing energy ultimately travels outward to the far field.

Multipoles: A similar but expanded antenna is obtained by replacing the dipoles of Table 3.16.1 by omnidirectional modes of arbitrary order. The modes are located, oriented, and phased similarly to those of Table 3.16.1. With coefficients $F(\ell, 1) = 1, G(\ell, 1) = -1$, all others equal to zero, and $j = i$, the vector fields are:

$$\begin{aligned} \sigma^2 \mathbf{E}_r &= \ell(\ell + 1) [B_\ell \cos(\omega t_R - \phi) - A_\ell \sin(\omega t_R - \phi)] S_\ell \sin \theta \\ \sigma^2 \eta \mathbf{H}_r &= -\ell(\ell + 1) [A_\ell \cos(\omega t_R - \phi) + B_\ell \sin(\omega t_R - \phi)] S_\ell \sin \theta \\ \sigma \mathbf{E}_\theta &= \{ [D_\ell \cos(\omega t_R - \phi) - C_\ell \sin(\omega t_R - \phi)] T_\ell \\ &\quad + [A_\ell \cos(\omega t_R - \phi) + B_\ell \sin(\omega t_R - \phi)] S_\ell \} \\ \sigma \eta \mathbf{H}_\phi &= \{ [A_\ell \cos(\omega t_R - \phi) + B_\ell \sin(\omega t_R - \phi)] T_\ell \\ &\quad + [D_\ell \cos(\omega t_R - \phi) - C_\ell \sin(\omega t_R - \phi)] S_\ell \} \\ \sigma \mathbf{E}_\phi &= \{ -[B_\ell \cos(\omega t_R - \phi) - A_\ell \sin(\omega t_R - \phi)] T_\ell \\ &\quad + [C_\ell \cos(\omega t_R - \phi) + D_\ell \sin(\omega t_R - \phi)] S_\ell \} \\ \sigma \eta \mathbf{H}_\theta &= \{ -[C_\ell \cos(\omega t_R - \phi) + D_\ell \sin(\omega t_R - \phi)] T_\ell \\ &\quad + [B_\ell \cos(\omega t_R - \phi) - A_\ell \sin(\omega t_R - \phi)] S_\ell \} \end{aligned} \quad (3.16.3)$$

where

$$S_\ell = P_\ell^1(\cos \theta) / \sin \theta \quad \text{and} \quad T_\ell = dP_\ell^1(\cos \theta) / d\theta \quad (3.16.4)$$

Resonance is assured by the equality $F(1, 1) = -G(1, 1)$, the input impedance is purely resistive, Q is equal to or greater than zero, and gain increases as the fourth power of the modal number.

Table 3.16.2. Four superimposed x - and y -oriented electric and magnetic multipoles. The power and energy results show that the zero-Q aspect extends through all modal orders.

$$w_{\Gamma} = \frac{\varepsilon}{2} \left\{ \frac{\ell(\ell+1)}{\sigma^4} (A_{\ell}^2 + B_{\ell}^2) S_{\ell}^2 \sin^2 \theta \right. \\ \left. + \frac{1}{\sigma^2} (A_{\ell}^2 + B_{\ell}^2 + C_{\ell}^2 + D_{\ell}^2) (S_{\ell}^2 + T_{\ell}^2) + \frac{4}{\sigma^2} S_{\ell} T_{\ell} (A_{\ell} D_{\ell} - B_{\ell} C_{\ell}) \right\}$$

$$w_{\text{S}} = 0$$

$$w_{\delta} = \frac{\varepsilon}{2} \left\{ \frac{\ell(\ell+1)}{\sigma^4} (A_{\ell}^2 + B_{\ell}^2) S_{\ell}^2 \sin^2 \theta \right. \\ \left. + \frac{1}{\sigma^2} (A_{\ell}^2 + B_{\ell}^2 + C_{\ell}^2 + D_{\ell}^2) (S_{\ell}^2 + T_{\ell}^2) + \frac{4}{\sigma^2} S_{\ell} T_{\ell} (A_{\ell} D_{\ell} - B_{\ell} C_{\ell}) \right\}$$

$$N_{\text{r}} = \frac{1}{\eta \sigma^2} \{ (A_{\ell} D_{\ell} - B_{\ell} C_{\ell}) (S_{\ell}^2 + T_{\ell}^2) + (A_{\ell}^2 + B_{\ell}^2 + C_{\ell}^2 + D_{\ell}^2) S_{\ell} T_{\ell} \}$$

$$N_{\theta} = -\frac{\ell(\ell+1)}{\eta \sigma^3} (A_{\ell} C_{\ell} + B_{\ell} D_{\ell}) S_{\ell}^2 \sin \theta$$

$$N_{\phi} = \frac{\ell(\ell+1)}{\eta \sigma^3} [(A_{\ell} D_{\ell} - B_{\ell} C_{\ell}) S_{\ell} T_{\ell} + (A_{\ell}^2 + B_{\ell}^2) S_{\ell}^2] \sin \theta$$

$$W_{\text{S}} = 0 \quad \text{p} = \frac{4\pi}{\eta k^2} \frac{\ell^2(\ell+1)^2}{(2\ell+1)}$$

$$Q \geq 0$$

Table 3.16.2 confirms that the zero-Q aspect extends through all orders. Since modes of different orders operate independently, the minimum Q of any combination of such modes is zero.

3.17. Q of Multipolar Combinations

Several authors suggest proofs of the Q of multimodal fields using methods other than those discussed in Secs. 3.6–3.16. Their analyses fall into two categories: One finds the standing energy then uses Eq. (3.5.15) to determine the bandwidth; the other applies theorems of complex variables to complex power fields. We find that although these techniques are adequate for many common radiators, they are insufficient for more complex radiating systems.

Power Field Analyses: It is shown in Sec. 3.4 that three numbers are necessary at each point to fully describe a power field. Since complex variables

have but two it is not possible to describe all such fields using complex variables. In earlier published analyses we attempted to retain both phasor fields and complex power by modifying formulas as needed and, in doing so, made a significant error. Our discussions in Grimes and Grimes (1995) and (1997), therefore, are in error.

Several others have authored papers that represent complex power using complex variables then use theorems of complex variables to derive limits on Q. These cases depend upon power being fully described by a complex number field: the mathematics is correct but the physics is not. Although the papers are in error they seem not to have significantly effected professional opinions. Therefore details are left to other discussions, Grimes and Grimes (2001).

Standing Energy Analyses: A method of calculating Q that has significantly affected professional opinions began with a satisfactory analysis by Collin and Rothschild (1964). Their paper begins with the smallest possible circumscribing, virtual sphere, radius a , that circumscribes a radiator. Actual sources are replaced by virtual sources on the surface of that sphere. The procedure applies to phasor radiation fields of degree zero. The technique applied to TM multipolar phasor fields follow from Eq. (1.12.9):

$$\begin{aligned}\sigma^2 \tilde{E}_r &= \sum_{\ell=1}^{\infty} \ell(\ell+1) F_{\ell}(B_{\ell} + iA_{\ell}) P_{\ell}(\cos \theta) e^{-i\sigma} \\ \sigma \tilde{E}_{\theta} &= \sum_{\ell=1}^{\infty} F_{\ell}(D_{\ell} + iC_{\ell}) \frac{d}{d\theta} P_{\ell}(\cos \theta) e^{-i\sigma} \\ \sigma \eta \tilde{H}_{\phi} &= \sum_{\ell=1}^{\infty} F_{\ell}(A_{\ell} - iB_{\ell}) \frac{d}{d\theta} P_{\ell}(\cos \theta) e^{-i\sigma}\end{aligned}\tag{3.17.1}$$

The surface integral of the complex Poynting vector over a closed volume, see Appendix 11, satisfies the equality:

$$\oint \mathbf{N}_c \cdot d\mathbf{S} = P_{rc} + 2i\omega(W_E - W_M)\tag{3.17.2}$$

P_{rc} is the time-average output power, W_E and W_M are the time-average energies of the electric and magnetic fields.

Substituting Eq. (3.17.1) into Eq. (3.17.2) gives:

$$\begin{aligned} \oint \mathbf{N}_c \cdot d\mathbf{S} &= 2\pi \frac{F_\ell F_n^*}{2\eta k^2} \int_0^\pi [1 + i(A_n C_\ell + B_n D_\ell)] \frac{dP_n}{d\theta} \frac{dP_\ell}{d\theta} \sin\theta d\theta \\ &= \frac{2\pi F_\ell F_n^*}{\eta k^2} \frac{\ell(\ell+1)}{(2\ell+1)} [1 + i(A_\ell C_\ell + B_\ell D_\ell)] \end{aligned}$$

Combining shows that:

$$\begin{aligned} P_{rc} &= \frac{2\pi F_\ell F_n^*}{\eta k^2} \frac{\ell(\ell+1)}{(2\ell+1)} \\ (W_M - W_E) &= \frac{\pi \varepsilon F_\ell F_n^*}{k^3} \frac{\ell(\ell+1)}{(2\ell+1)} (A_\ell C_\ell + B_\ell D_\ell) \end{aligned} \quad (3.17.3)$$

Values of $(A_\ell C_\ell + B_\ell D_\ell)$ are shown in Table 3.2.1.

The total, time-average energy density at each point outside the source region follows from the field expressions:

$$\begin{aligned} w = w_E + w_M &= \frac{\varepsilon}{4} \left[\frac{1}{\sigma^4} \ell(\ell+1)n(n+1)F_\ell F_n^* (A_\ell A_n + B_\ell B_n) P_\ell P_n \right. \\ &\quad \left. + \frac{1}{\sigma^2} F_\ell F_n^* (A_\ell A_n + B_\ell B_n + C_\ell C_n + D_\ell D_n) \frac{dP_\ell}{d\theta} \frac{dP_n}{d\theta} \right] \end{aligned} \quad (3.17.4)$$

Integrating the energy density over a volume between spherical shells of radius ka and kR , where R is larger than a , gives:

$$\begin{aligned} W_E + W_M &= \frac{\pi \varepsilon}{2k^3} \frac{2\ell(\ell+1)}{(2\ell+1)} F_\ell F_n^* \\ &\quad \times \int_{ka}^{kR} \left[\frac{1}{\sigma^2} \ell(\ell+1)(A_\ell^2 + B_\ell^2) + (A_\ell^2 + B_\ell^2 + C_\ell^2 + D_\ell^2) \right] d\sigma \end{aligned} \quad (3.17.5)$$

Values of the integrand for the three lowest modes are:

$$\begin{aligned} \frac{2}{\sigma^2} (A_1^2 + B_1^2) + (A_1^2 + B_1^2 + C_1^2 + D_1^2) &= 2 + \frac{2}{\sigma^2} + \frac{3}{\sigma^4} \\ \frac{6}{\sigma^2} (A_2^2 + B_2^2) + (A_2^2 + B_2^2 + C_2^2 + D_2^2) &= 2 + \frac{6}{\sigma^2} + \frac{27}{\sigma^4} + \frac{90}{\sigma^6} \\ \frac{12}{\sigma^2} (A_3^2 + B_3^2) + (A_3^2 + B_3^2 + C_3^2 + D_3^2) &= 2 + \frac{12}{\sigma^2} + \frac{18}{\sigma^4} - \frac{180}{\sigma^6} + \frac{4725}{\sigma^8} \end{aligned} \quad (3.17.6)$$

When integrated over exterior space the additive term “2” on the right sides of Eq. (3.17.6) is singular. However, since the source is affected only

by energy that returns to it upon modulation changes, and since far field terms do not return, that energy should not be entered into the numerator of Eq. (3.11.17). The far field terms support real power, and the energy density associated with real output power is N_r/c . Collin and Rothschild, therefore, subtracted this real energy term from the total energy density. With subscript "S" indicating only the standing energy portion of the field energy they obtained the equalities:

$$W_E + W_M - \frac{P_{rc}}{c} = W_{ES} + W_{MS}$$

$$W_{ES} + W_{MS} = \frac{\pi\epsilon}{2k^3} \frac{2\ell(\ell+1)}{(2\ell+1)} F_\ell F_\ell^* \int_{ka}^{\infty} \left[\frac{1}{\sigma^2} \ell(\ell+1)(A_\ell A_n + B_\ell B_n) + (A_\ell^2 + B_\ell^2 + C_\ell^2 + D_\ell^2) - 2 \right] d\sigma \quad (3.17.7)$$

They also note that since the time-average electric and magnetic energies in a plane wave are equal:

$$W_E - W_M = W_{ES} - W_{MS} \quad (3.17.8)$$

$$(W_{MS} - W_{ES}) = \frac{\pi\epsilon F_\ell F_\ell^*}{k^3} \frac{\ell(\ell+1)}{(2\ell+1)} (A_\ell C_\ell + B_\ell D_\ell) \quad (3.17.9)$$

The dipole case, for example, is:

$$W_{ES} + W_{MS} = \frac{2\pi\epsilon}{3k^3} F_1 F_1^* \left[\frac{2}{(ka)} + \frac{1}{(ka)^3} \right] \quad (3.17.10)$$

$$W_{ES} - W_{MS} = \frac{2\pi\epsilon}{3k^3} F_1 F_1^* \frac{1}{(ka)^3}$$

Combining Eqs. (3.17.9) and (3.17.10) gives:

$$W_{ES} = \frac{2\pi\epsilon F_1 F_1^*}{3k^3} \left(\frac{1}{(ka)^3} + \frac{1}{(ka)} \right) \quad (3.17.11)$$

This leads to the expression for Q:

$$Q = \frac{2\omega W_{ES}}{P_r} \rightarrow \left(\frac{1}{(ka)^3} + \frac{1}{(ka)} \right) \quad (3.17.12)$$

This is the same as the value obtained by Chu using the approximate method he described as being adequate.

For TM or TE modes Collin puts the magnitude of the average electric and magnetic energies equal at resonance, instead of the out-of-phase energies of the Thévenin equivalent RLC circuit. That is, the problem is treated as if all reactive elements are driven in phase. A glance at the multipolar equivalent circuits of Secs. 3.6 and 3.8 shows this not to be the case. Since

the Thévenin equivalent circuits are not a simple series connection of capacitors and inductors the appropriate energies are neither all electric nor all magnetic. Although the resulting error is small for electrically small dipoles, differences between calculated and actual values increase with increasing modal number and leaves a qualitative difference between Eqs. (3.17.12) and (3.6.17) even for dipoles. Although Chu chose his less accurate answer, Eq. (3.6.17), as a mathematical convenience Eq. (3.17.12) is Collin's (1964) best answer.

Although Fante (1969) correctly questioned the ultimate applicability of Collin's technique for mixed TE and TM modes, he applied it to them. The technique is supported by Collin (1998), who cites the orthogonality of TE and TM modal energies as justification for extending the technique to mixed TE and TM modes. In our view although both the modal energy and power are orthogonal the standing and traveling parts of the energy are *not* separately orthogonal.

Numerical analyses and experimental measurements designed to test Collin's argument are presented in the following three sections. It is shown that the amount of energy returned to the source upon modulation changes depends upon the relative phasing of mixed TE and TM modes: the modes are not independent. For this reason, and since he leaves unstated and unsupported postulates that (1) all standing energy should be entered in the numerator in Eq. (3.5.11), and (2) an equality exists between the Qs of Eqs. (3.5.11) and (3.5.15), we find the technique to be unacceptable.

However, neither do we prove the calculated values of Q, as described in Secs. 3.10–3.16, are correct; it is only that Q can be no less than the calculated values. Actual values of Q require knowledge of the transient fields during modulation changes and such transient field solutions are not available. For example, using the technique of Sec. 3.11 the lowest provable limit on Q is zero in one particularly interesting case. This does not mean Q is absolutely equal to zero, only there is no proof it is not. The work appears to describe reality, however, because (1) the analysis is logically self-consistent, (2) the predictions agree with the numerical and experimental results of the next three sections, and (3) the results are consistent with results calculated in Chapter 6 for naturally occurring photon radiation.

3.18. Numerical Characterization of Antennas

In an effort to confirm the Q model presented within this chapter, the radiation properties of a radiating spherical surface have been numerically

modeled using finite difference time domain, FDTD. Accurate numerical modeling requires the properties of the radiating sphere to be retained, while eliminating properties of the driving network, a network which for the multi-dipole source includes power splitters, cables, and possibly multiple phase shifters. Source Q is based upon Eq. (3.5.11):

$$Q = \frac{\omega W_{pk}}{P} \quad (3.18.1)$$

This equation is applicable to any antenna design, independently of its complexity.

The technique makes possible determination of the energy that returns from the standing energy field back to the antenna. The measurement begins by driving the antenna to steady state. Time-average output power P is numerically obtained by integrating over a virtual sphere that circumscribes the source. After steady state operation has been reached, the voltage source is turned off, after which the local standing energy field collapses. The source-associated portion of the standing energy returns to the antenna from which, in turn, it is either reflected back into space or absorbed by the antenna. In the numerical model, the antenna is driven by a $50\ \Omega$ source that absorbs returning energy. The absorbed and reflected energies are summed to obtain W_{pk} .

The time domain technique avoids spurious errors due to unwanted power reflections within the feed network. For example, when a single generator, through a power splitter and a feed network in which one arm has a $\pi/2$ voltage phase shift, the waves reflected from the antennas back to the generator drives two antennas are π out of phase and cancel. No reflected power is measured. This null result does not mean that the Q of the antenna is zero, or that the antenna input impedance is purely real. Rather it indicates that techniques for determining Q are required that separate transmission line effects from antenna performance.

The analytical techniques used to determine the radiation Q of a source necessarily solve for the steady state fields external to a virtual sphere enclosing the radiation source. Doing so ignores standing energy at radii less than the length of the antenna arms, hence the analytic expressions for the standing energy are inherently too small. In contrast, the numerical technique accounts for all standing energy in the near field. It forms a check on analytic techniques and a guide for experimental implementation. The total energy returned to the antenna is a simple sum over the energies returned and reflected by each element.

The numerical method for determining Q begins by determining the power that passes through a large radius, circumscribing sphere. That power is put equal to P in Eq. (3.18.1). After source turn-off the voltage across the source resistor, V_{in} , is determined and used to calculate the source current, I_{in} . These values are combined and integrated over time to obtain the returned energy:

$$W_{\text{returned}} = \int I_{in}(t)V_{in}(t)dt = \int [I_{in}(t)]^2 R_S dt \quad (3.18.2)$$

R_S is the $50\ \Omega$ resistance of the source. I_{in} is the current that flows through the resistor and V_{in} is the voltage across the antenna terminals. Both voltage and current are determined using FDTD, then the time integral of Eq. (3.18.2) is evaluated and entered as the energy portion of the numerator of Eq. (3.18.1). The portion of the original (at source turn-off) standing energy that escapes outward is obtained by calculating the instantaneous power on the surface of an encompassing virtual sphere of radius R at times $t > R/c$, integrating over both the surface and time. Details of the finite difference time domain FDTD code used in this work are given in the two references by Liu *et al.*

For certain antennas the standing energy varies with time, hence use of Eq. (3.18.1) to determine Q requires repeating the calculation process over a range of turn-off phase angles to obtain the peak value W_{Spk} . However for other antennas, such as a turnstile antenna with the two dipoles driven in phase quadrature, the source-associated standing energy is time independent.

Biconical Dipole Antennas: A field-based analysis of a single electric dipole is given in Sec. 3.12; Q is listed in Table 3.12.1. A terminal-based analysis of the same antenna is shown in Sec. 3.7 and listed in Eq. (3.7.15). Results are identical and equal to:

$$Q = \frac{1}{2(ka)^3} \left[1 + \sqrt{1 + 4(ka)^4} \right] + \frac{1}{(ka)} \quad (3.18.3)$$

A 5° -arm angle, biconical antenna was the basis for a numerical analysis. The dipole was divided into 13 discrete radial segments; for $ka = 6$ each radial segment length is $0.073\ \lambda$. To ensure steady state operation the dipole was driven for eleven time-periods before the source voltage was turned-off. During steady state operation power on a spherical surface of radius R about the source was determined and entered as the denominator of Eq. (3.18.1). For the first standing energy measurement, turn-off was done at the most negative value of input power, point A of Fig. 3.18.1. At each

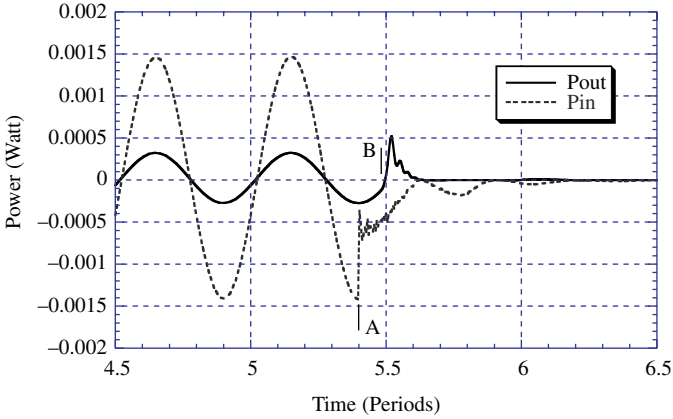


Fig. 3.18.1. Time analysis of a single biconical TM dipole.

field point for time $t > R/c$ the fields collapsed. Some of what was standing energy moves outward away from the antenna and some moves inward toward it. Some of the collapsing power is dissipated in the source resistor and some is reflected back into space. The returned energy is measured then the process is repeated with a different cyclical turn-off phase until the maximum returned energy is obtained. The maximum energy is substituted into the numerator of Eq. (3.18.1).

The instantaneous power at the antenna terminals, P_{in} , is calculated and plotted as the dashed curve of Fig. 3.18.1, where outwardly and inwardly directed power is respectively positive and negative. It has the form:

$$p(\sigma, t) = P[1 + \gamma(\sigma) \cos(2\omega t_R)] \quad (3.18.4)$$

The steady state portion of the curve is dominated by the reactive term. For the first iteration the source is turned off at time $t = A$, at which time there is a maximum rate of reactive energy return to the antenna. After turn-off the terminal power drops abruptly, then takes what appears to be an exponentially damped, oscillatory form. Oscillations occur at a wavelength less than that of the driven field.

The instantaneous power at the surface of an encompassing, virtual sphere one wavelength in radius is also calculated and plotted as the solid curve of Fig. 3.18.1. In the steady state regime since magnitude $\gamma(\sigma) = 1/\sigma^3$ is a monotone, rapidly decreasing function of radius the peak-to-peak magnitude is much less at the field point than it is at the terminals.

P_{in} is the instantaneous power at the antenna terminals and P_{out} is the power on the surface of the encompassing, virtual sphere one wavelength in diameter, shown at the same retarded time. Source turn-off occurs at the most negative value of P_{in} , time $t = A$. Some standing energy travels inward and is absorbed by the input resistor and some travels outward. At time B the field collapse reaches radius R surrounding the antenna.

After source turn-off the output power remains continuous, then becomes increasingly positive until reaching a positive value larger than the maximum steady state value, then decays to zero. The figure verifies that there is continued emission of energy after the source has been discontinued, and such energy can come only from what was once standing energy.

Since the source-associated standing energy of a single dipole is time dependent, the measured Q depends upon the phase at which the source is turned off. The numerically determined variation in source-associated standing energy of a biconical TM dipole of electrical size $ka = 0.6$ is shown in Fig. 3.18.2 with $t = 0$ defined to be when P_{in} is at its most negative point.

Comparative values of Q calculated using Eq. (3.18.1) and obtained numerically using the described technique are shown in Fig. 3.18.3. As expected, in all cases the numerically calculated values are slightly larger: the analytic expressions do not consider the standing energy contained at radii less than the antenna arm length and the numerical calculations do. Furthermore for $ka > 1.1$ octupole moment radiation becomes

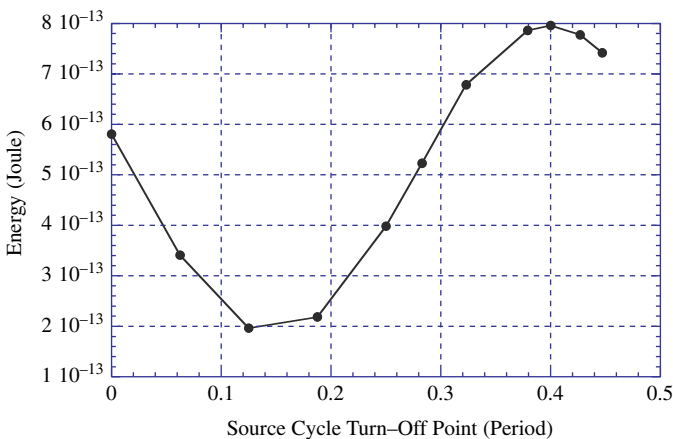


Fig. 3.18.2. Source-associated standing energy for a biconical TM dipole.

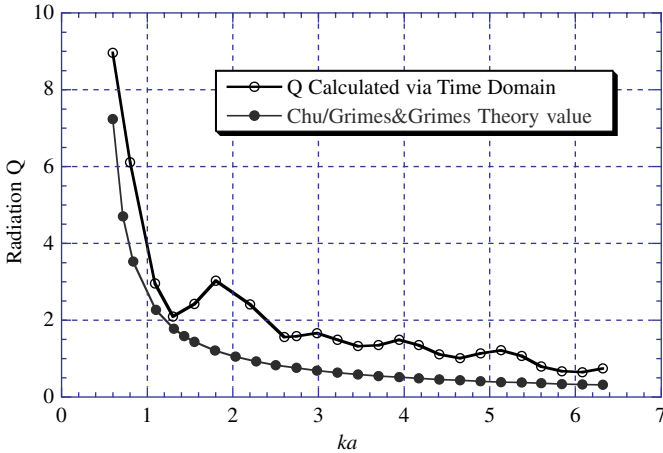


Fig. 3.18.3. Numerically (open dots) and theoretically (solid dots) determined radiation Q of a biconical antenna versus electrical length ka .

important. Such effects are accounted for in the numerical analyses but not in the analytical curves. The octupolar moment introduces oscillations in the powers and energies and result in the oscillatory Q behavior of Fig. 3.18.3.

Turnstile Antennas: A turnstile antenna consists of two collocated and spatially orthogonal electrical dipoles. A turnstile antenna is the simplest multi-element antenna for which theory shows that Q is dependent upon inter-element phasing. When the two dipoles are driven in phase the far field is linearly polarized and Q is the same as for a single electric dipole, Eq. (3.12.11). However when the dipoles are driven in phase-quadrature, see Sec. 3.15, the fields are circularly polarized and Q is given by:

$$Q = \frac{1}{3(ka)^3} + \frac{1}{(ka)} \quad (3.18.5)$$

The dipole is of electrical length $ka = 0.6$ and the plot is a function of source turn-off point. The time reference zero point is the minimum value of P_{in} .

In the electrically small limit, the relative phasing of the dipoles produces a factor of three difference in Q. The difference serves as an important test case for the different models.

To make a comparative numerical analysis each biconical electric dipole making up the turnstile antenna was divided into 13 discrete radial segments; when $ka = 6$, each radial segment is equivalent to about 0.073λ .

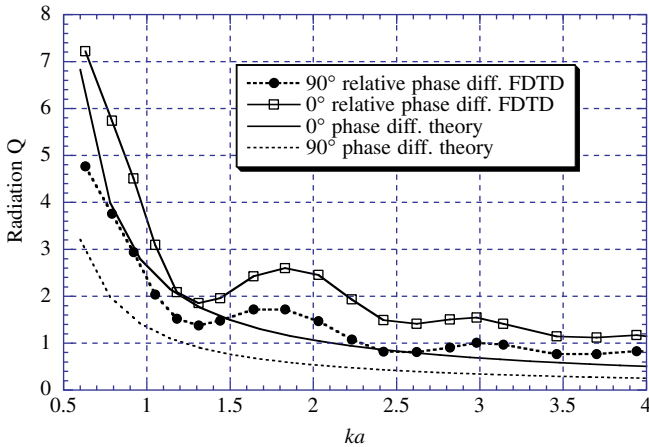


Fig. 3.18.4. Numerical and analytical values of radiation Q versus ka for a turnstile antenna, when phased to support linear polarization and when phased to support circular polarization.

Plots of numerically determined Q versus relative electrical size, ka , for a turnstile antenna when the dipoles are in phase and out of phase are shown in Fig. 3.18.4. The data show that the relative phasing between the two dipoles affects Q . Since the analytic solutions do not account for standing energy within the inner region of the antenna, calculated Q values are expected to be larger than the theoretical predictions; Fig. 3.18.4 shows that to be the case. Also as expected the largest fractional reduction in Q occurs with a phase difference of 90° . As with a single biconical antenna when the turnstile antenna supports linear polarization the standing energy is time varying. It is, therefore, necessary to determine the source turn-off point that produces the largest calculated Q . This point was determined to be the same point it was for a single biconical antenna. A plot of Q reduction in switching from in-phase to phase quadrature as a function of ka is shown in Fig. 3.18.5.

The figures show that the relative phasing between the dipoles affects the radiation Q of turnstile antennas. This change in Q is due to a change in field structure that, in turn, affects the fraction of the standing energy that returns to the radiating source.

3.19. Experimental Characterization of Antennas

Biconical Dipole Antennas: A technique similar to the numerical one may be used to experimentally determine antenna Q . The block diagram of

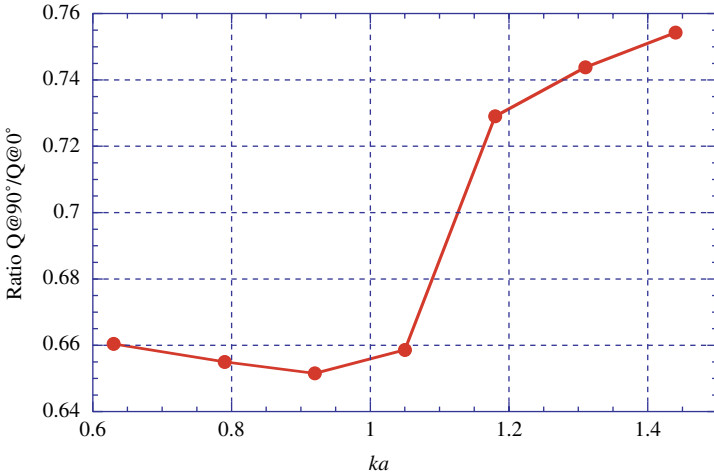


Fig. 3.18.5. Fractional reduction in Q versus ka obtained by shifting the relative phase between dipoles of turnstile antenna from 0° to 90° .

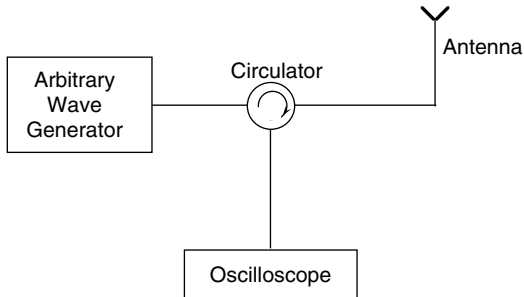


Fig. 3.19.1. Experimental set-up for determining the radiation Q of a single antenna.

the experimental system for a single port antenna is shown in Fig. 3.19.1. A wave generator drives a circulator that in turn drives the antenna. The return from the antenna passes back to the circulator and from it to an integrating oscilloscope; the portion of the power reflected from the antenna back into space is unknown. The experimental procedure is to obtain steady state operation, determine the real power P using a network analyzer, then switch off the generator. Energy returned from the antenna after source turn-off is directed by the circulator to the transient-capturing oscilloscope, put equal to the source-associated standing energy and entered in the numerator of Eq. (3.18.1). The Q measurement technique isolates

antenna performance from the feed network and enables characterization of the antenna itself.

As detailed in the C. A. Grimes *et al.* references, a Tektronix 500 MHz arbitrary waveform generator (AWG610), which is able to terminate the waveform virtually without a measurable transient, was used as the source generator. The antenna was suspended in an anechoic chamber, driven from the AWG610 through a circulator, with the reflected waveform captured with an oscilloscope through the other circulator port. A HP 54845 A oscilloscope with a sampling rate of 8 G samples/second and an advanced triggering option that capture waveforms up to 1.5 GHz was used to capture the transient signal returning from the antenna after source turn-off. All components in the experimental setup were $50\ \Omega$ devices. The generator output power in steady state was determined from the measured voltage and found to be about 7.1 mW (8.5 dBm). The circulator effectively divided the input and reflected signals so the generator always saw the network as a $50\ \Omega$ load and delivered the same power.

Using the programming capabilities of the AWG610, a waveform of frequency 450 MHz was generated and delivered to the antenna. The duration of the source signal was pre-selected, the antenna was driven until it reached the steady state, and then switched off. There was no detectable transient response. It was found that signals of 25 ns duration, about 12 periods at 450 MHz, were enough to reach steady state. After the waveform was turned off the power returned from the antenna to the oscilloscope was measured and time integrated to obtain the source-associated energy. A typical reflected power waveform for a wire dipole of length $0.2\ \lambda$ is shown in Fig. 3.19.2. All oscillations after turn-off are due to returned power.

The time-average power radiated by the antenna was measured indirectly. The scattering parameters of the three port network of Fig. 3.19.1 without the generator, oscilloscope, and antenna were measured with a HP8753D network analyzer. The antenna was then connected to the system and the network analyzer was used to determine the input impedance. This was sufficient to permit calculation of the voltage and currents at the terminals of each port when the generator produces its measured voltage, the antenna presents its measured impedance, and the oscilloscope supplies a fifty-ohm load. The calculated real power at the antenna terminals is equal to the radiated power. The power reflected and captured with the oscilloscope was also calculated. Calculated and measured values of reflected power were the same.

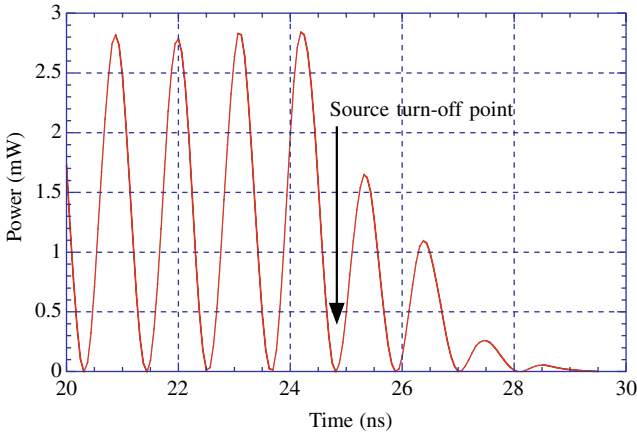


Fig. 3.19.2. Measured values of reflected power for a 0.2λ -electric dipole antenna.

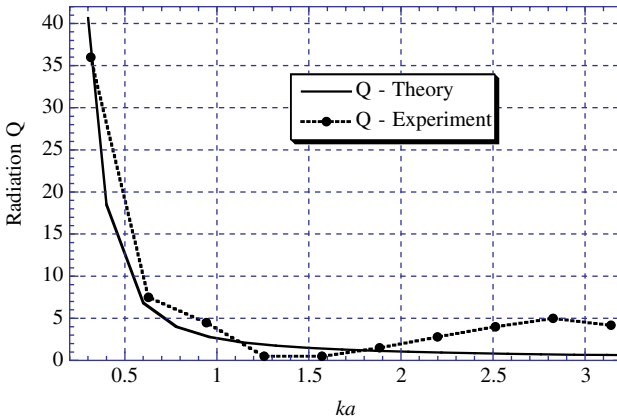


Fig. 3.19.3. Experimentally determined Q versus electrical length of thin-wire electric dipoles.

Turnstile Antennas: The radiation Q of the turnstile antenna is measured in a way that is similar to antennas with a single input port. The network needed to characterize a turnstile antenna is shown in Fig. 3.19.4. A hybrid 3dB-splitter forwards equal power to each dipole, a phase shifter adjusts the phase difference between the dipole drives, an attenuator compensates for the loss in the phase shifter, and circulators separate incoming from reflected signals. The antenna is a two-port system, the scattering

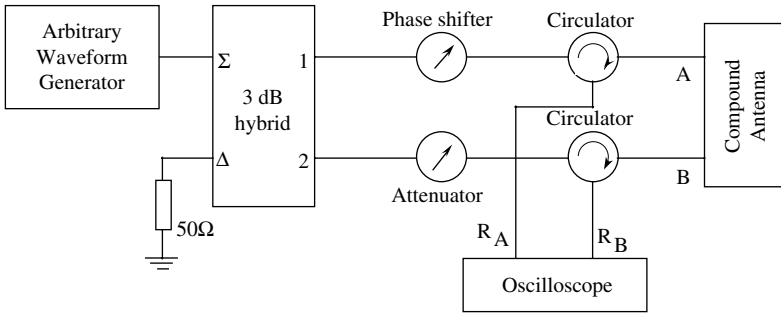


Fig. 3.19.4. Experimental set-up for measuring Q of the turnstile antenna.

parameters of which are measured by the network analyzer. The scattering parameters of a five-port network (six with the hybrid port connected to a $50\ \Omega$ resistor) were measured. Then using network theory the power radiated by the turnstile antenna was determined. This approach accounts for parasitic coupling between the two dipoles. The oscilloscope captured the reflected waveforms and the reflected powers were determined from them. The source-associated standing energy of the turnstile antenna was determined by summing the time integrals of reflected powers from the two dipoles.

A turnstile antenna was implemented using thin wire, equal length dipoles and measured using the setup described in Fig. 3.19.4. Q was determined with both the drives in phase (linear polarization) and the drives in phase quadrature (circular polarization.) Measured values of Q versus the electrical length of the lines are plotted in Fig. 3.19.5. Results confirm that the radiation Q of this antenna is a function of the difference of driving phase between the two dipoles.

3.20. Q of Collocated Electric and Magnetic Dipoles: Numerical and Experimental Characterizations

The antenna discussed in Sec. 3.16 consists of four collocated dipoles; an electric and magnetic dipole pair radiating equal powers is oriented parallel with the x -axis and an identical pair is oriented along the y -axis. The configuration is depicted in Fig. 3.20.1. The electric moments are implemented as straight wires and the magnetic moments as rectangular loops. The magnetic loops are positioned to the side of the electric dipoles in a way that produces strong coupling between the x -directed electric moment and the

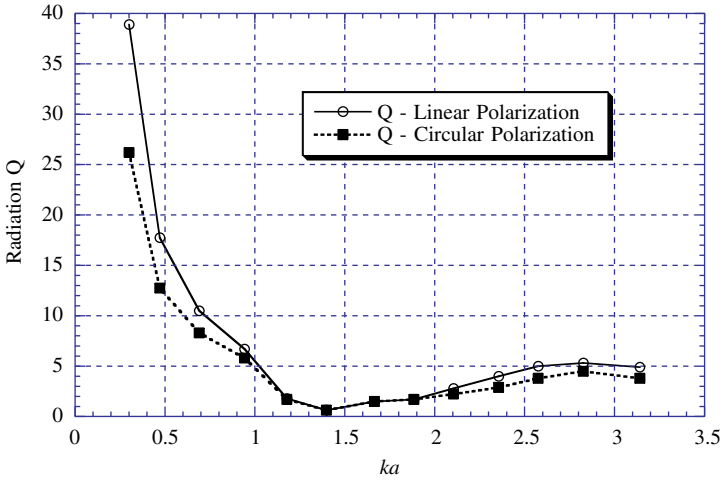


Fig. 3.19.5. Q of a thin-wire, turnstile antenna versus electrical length of the dipoles, for in-phase drives and phase quadrature drives.

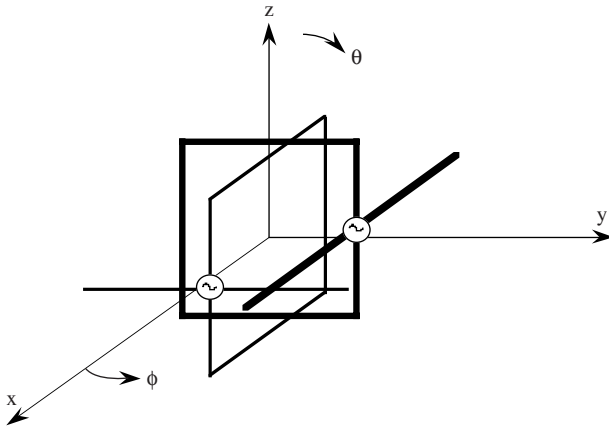


Fig. 3.20.1. Implementation sketch of antenna comprised of two dipole-pair elements, each element provides equal TE and TM power. Lines of different thickness differentiate the two sets of dipole-pair elements.

y -directed magnetic moment, and symmetrically between the other pair. By the analysis of Sec. 3.16 if driven with the proper phases the lower limit on radiation Q is equal to or greater than zero.

Early attempts to characterize this antenna design used separate feeds for each dipole and were unsuccessful due to unwanted and interfering

power transfer between dipole feeds. This implementation uses two separate dipole-pair elements, with equal power from the electric and magnetic moments. With this design rather than interfering, the coupling appears to contribute to the desired outputs. The radiation Q of the antenna system is determined using the numerical and experimental techniques detailed in Sec. 3.19. Q values were measured as functions of the phasing between the dipole pairs and the relative electrical size, ka .

Two things determine the relative phasing of the different radiators: the driving phase and local coupling. Similarly directed dipoles are driven by the same set of terminals and by the strong local field interaction between the x -directed electric moment and y -directed magnetic moment, as well as between the other two of elements. It is found that if the two driving ports are in phase the radiation is similar to that of Table 3.14.2 and Q is given by Eq. (3.18.3). With the driving ports in phase quadrature, the generated radiation is similar to that of Table 3.16.1, for which Q has no analytical lower limit.

The single dipole pair embodiment is shown in Fig. 3.20.2. A Method of Moments (MoM) analysis was done to ensure that the elements radiate equal TE and TM power. The fields on the surface of the smallest virtual sphere that circumscribes the radiating elements were computed using NEC4 MoM. Using the technique described in Sec. 3.18 the calculated fields were equated to the equivalent terms in a multipolar field expansion to

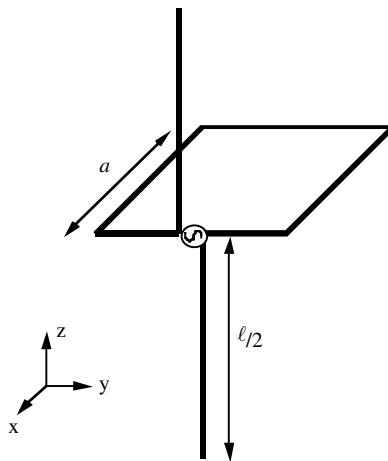


Fig. 3.20.2. A Single electric and magnetic dipole pair.

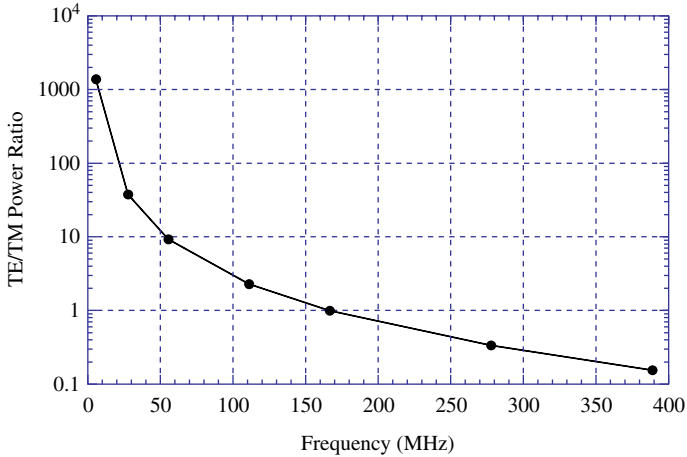


Fig. 3.20.3. The TE/TM power ratio versus frequency from the single dipole-pair element pair shown in Fig. 3.20.2, with dimensions $a = \ell/2 = 12$ cm.

determine the TM dipole field coefficient F and the TE dipole field coefficient G , see Eq. (3.11.1). Figure 3.20.3 shows the calculated TE/TM power ratio plot for the structure of Fig. 3.20.2 with loop sides $a = \ell/2 = 12$ cm. As shown in Fig. 3.20.3 for these dimensions the element radiates equal TE and TM power at 166.67 MHz. Since the dimensions scale linearly with frequency for loop side $a = \ell/2 = 4$ cm the equal power frequency is 500 MHz.

The four-dipole source was modeled numerically. Since straight-wire elements were used for the antenna implementation, FDTD computations were made using a rectangular, three-dimensional computer code based on the Yee cell. The problem space was chosen as $120 \times 120 \times 120$ cells, with cell dimension $\Delta x = \Delta y = \Delta z = 5$ mm; a perfectly matched absorbing boundary layer was used to terminate the computational space. Each radiating element consisted of a square loop and a straight-wire electric dipole. For the numerical computations, the dimensions of the antenna were held constant at loop side length 12 cm and electric dipole length 24 cm. The operational frequency was varied above and below 166.67 MHz, the frequency at which the TE and TM time-average powers were equal. For experimental characterization a thin-wire antenna of loop side $a = \ell/2 = 4$ cm was built and tested in an anechoic chamber.

The FDTD-determined radiation Q of the antenna for which $ka = 0.42$ versus the source turn-off point is shown in Fig. 3.20.4, relative to the minimum input power point. Theory indicates that the source-associated

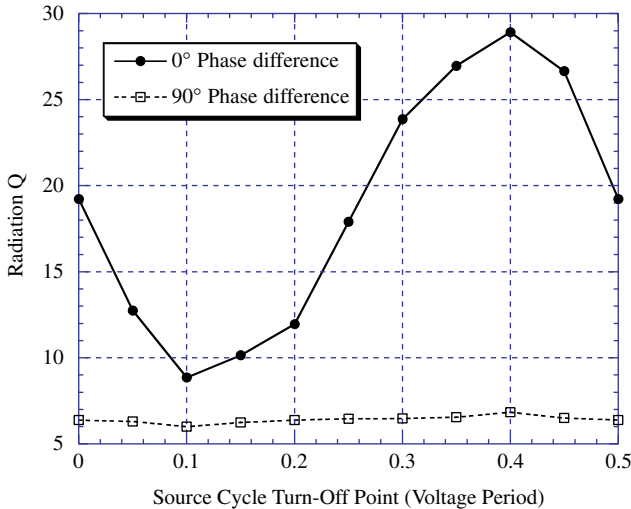


Fig. 3.20.4. Numerically determined Q as a function of source-turn off point. Referred to the input power minimum, for dipole-pair elements in phase and phased to support circular polarization; $ka = 0.42$.

standing energy is time varying for all relative phases except 90° , when the dipole pairs support circular polarization. As seen in Fig. 3.20.4, Q is independent of source turn-off point when circular polarization is maintained. However for other relative phases, Q varies with source turn-off point; the correct value of Q is the largest value that is determined when the source-associated standing energy is a maximum.

The numerically and experimentally determined radiation Q of the antenna at $ka = 0.42$ versus phase difference between elements is shown in Fig. 3.20.5. In agreement with theory, the radiation Q is dependent upon relative phasing between the antenna elements. When driven in phase Q is approximately that of an electric dipole of the same size. When driven out of phase antenna Q is reduced by an approximate factor of 4.5 from the in-phase results. For this relative electrical size, the measured Q value is approximately a factor of three below the minimum Q value determined by Chu for an antenna of the same electrical size.

The sensitivity of Q to distance along the z -axis between the elements is shown in Fig. 3.20.6. Using antennas for which $ka = 0.42$ the antennas were displaced in steps of 5 mm for the numerical model with dimensions of $a = \ell/2 = 12$ cm. Steps of 1.67 mm were taken for the experimental work with dimensions of $a = \ell/2 = 4$ cm. With 90° relative phasing between the

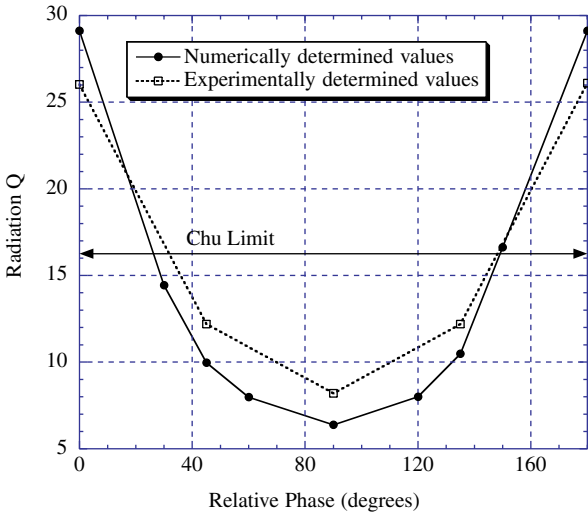


Fig. 3.20.5. Numerically and experimentally determined Q versus relative phase between dipole-pair elements; $ka = 0.42$.

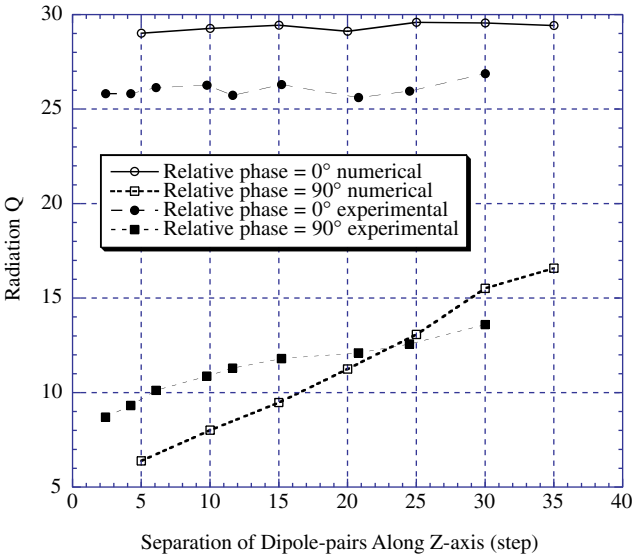


Fig. 3.20.6. Numerically and experimentally determined Q as a function of spacing between dipole-pair elements. Step size was 5 mm with the numerical model and 1.67 mm with the experimental model, $ka = 0.42$.

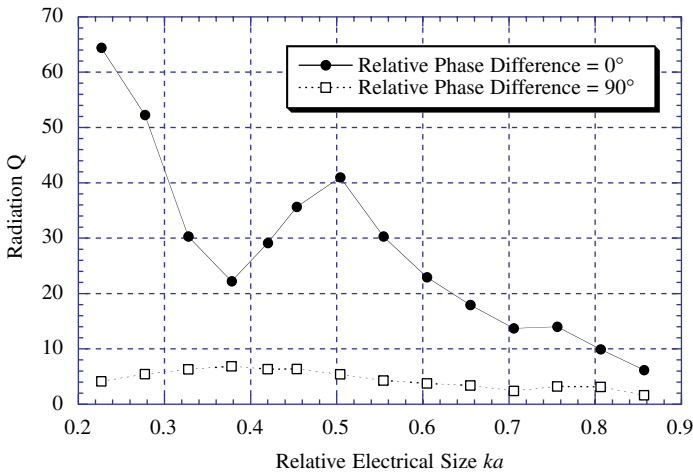


Fig. 3.20.7. Numerically determined Q of antenna. Dimensions $a = \ell/2 = 12$ cm, shows effect of relative phasing between dipole-pair elements and electrical size ka .

dipole-pair elements the radiation Q is respectively small and large when the displacement is small and large. In contrast, when the four dipoles are in phase the radiation Q is approximately that of an electric dipole of the same ka independently of the spacing. Experiments moving the dipole-pairs relative to each other in the other two dimensions showed similar results; the Q of 90° phased dipole-pair is sensitive to relative location, i.e. modal coupling, and the Q of the in-phase dipole pairs is not.

The numerically determined Q versus the relative electrical size of the antenna is shown for in-phase drives and for phase quadrature drives in Fig. 3.20.7. The trends shown by the numerical work were confirmed experimentally over the more limited range of $ka = 0.37$ to $ka = 0.42$; the circuit devices, not the antenna, determined the frequency limits. The circulators imposed the low frequency limit and the Tektronix Arbitrary Wave Generator AWG610 imposed the high frequency limit.

At $ka = 0.23$ the Q of the circularly polarized antenna is more than a factor of 20 below Chu's limit. The oscillations seen in the in-phase Q results are due to higher order modes that cause variations in the outbound real power. The in-phase results show the familiar $1/(ka)^3$ dependence of Q as the antenna becomes electrically small. In contrast, with the two dipole-pair elements phased to support circular polarization Q is relatively insensitive to frequency. The frequency response seen in Fig. 3.20.7 is indicative that

the current and charge distributions on the dipole-pair elements self-adjust to support radiation fields that minimize source-associated standing energy and hence Q.

We conclude that the numerical and experimental results support the analytical Q results within the limits imposed by our irreducible differences between analytical, numerical, and experimental embodiments.

References

- L.J. Chu, "Physical Limitations of Omni-Directional Antennas," *J. Appl. Phys.* **19** (1948) 1163–1175.
- R.E. Collin, "Minimum Q of Small Antennas," *J. Electro. Waves Appl.* **12** (1998) 1369–1393.
- R. E. Collin, S. Rothschild, "Evaluation of Antenna Q," *IEEE Trans. Antennas and Propagation* **12** (1964) 23–27.
- R.L. Fante, "Quality Factor of General Ideal Antennas," *IEEE Trans. Antennas Propagation* **AP-17** (1969) 151–155.
- C.A. Grimes, G. Liu, F. Tefiku, D.M. Grimes, "Time Domain Measurement of Antenna Q," *Microw. Opt. Technol. Lett.* **25** (2000) 95–100.
- C.A. Grimes, G. Liu, D.M. Grimes, K.G. Ong, "Characterization of a Wideband, Low-Q, Electrically Small Antenna," *Microw. Opt. Technol. Lett.* **27** (2000) 53–58.
- D.M. Grimes, C.A. Grimes, "A Classical Field Theory Explanation of Photons," in *Advanced Electromagnetism*, T.W. Barrett, D.M. Grimes, World Scientific Publishing Co. (1995), pp. 250–277.
- D.M. Grimes, C.A. Grimes, "Power in modal radiation fields: Limits of the complex Poynting theorem and the potential for electrically small antennas," *J. Electro. Waves Appl.* **11** (1997) 1721–1747.
- D.M. Grimes, C.A. Grimes, "Power in Modal Radiation Fields: Limits of the Complex Poynting Theorem and the Potential for Electrically Small Antennas," *J. Electro. Waves Appl.* **12** (1998) 1369–1393.
- D.M. Grimes, C.A. Grimes, "Radiation Q of Dipole-Generated Fields," *Radio Sci.* **34** (1999) 281–296.
- D.M. Grimes, C.A. Grimes, "Minimum Q of Electrically Small Antennas: A Critical Review," *Microw. Opt. Technol. Lett.* **28** (2001) 172–177.
- R.F. Harrington, "Effect of Antenna Size on Gain, Bandwidth, and Efficiency," *J. Res. Nat. Bureau Stand.* **64D** (1960) 1–12.
- G. Liu, C.A. Grimes, D.M. Grimes, "A Time Domain Technique For Determining Antenna Q," *Microw. Opt. Technol. Lett.* **21** (1999) 395–398.
- G. Liu, K.G. Ong, C.A. Grimes, D.M. Grimes, "Comparison of Time and Frequency Domain Numerical Modeling of Outbound And Local Power from Two Perpendicularly Oriented, Electrically Small TM Dipoles," *Int. J. Numer. Model.* **12** (1999) 229–241.

CHAPTER 4

Quantum Theory

Chapter 2 contains an analysis of scattering from idealized spheres and biconical antennas. Both structures respond linearly to imposed fields. Results show that independently of the antenna impedance a significant portion of the incoming energy is scattered. For an electrically small scatterer of decreasing size, it is shown in Chapter 3 that the amount of energy affected by the scatterer becomes ever smaller. The radiation Q of the absorbing field becomes limitlessly large, and effectively stops radiative energy exchanges by mechanically rigid, electrically small objects.

Chapter 3 also contains a discussion of real and reactive powers on the surface of a circumscribing surface, virtual or real, about a radiating source. The solution includes a set of fields for which the surface is resonant and to which the accepted proof of the large radiation Q of electrically small radiating objects does not apply. Energy is permanently radiated away from the region by this modal field set and, as we will show, carries with it the kinematic properties of photons. These field properties are dramatically different from those of low-order modal radiation fields produced by electrically small radiators of fixed dimensions.

Although the next logical step is to analyze scattering from an electrically small, active region, before doing so it is necessary to examine certain properties special to such regions. The remainder of this chapter is dedicated to such an analysis. It is, in many ways, a conventional review of the quantum theory of atoms, but is dramatically different in certain key concepts. For example, it has been known for nearly a century that electrons exhibit both particle and wave properties. Although wave-particle duality has been discussed in depth by conventional quantum theory, the affect of an extensive electron, such as a cloud of charge extended throughout an eigenstate, has not. In this work extended electrons form an integral part of the theory. We show that the full applicability of the classical electromagnetic equations within atoms is retained if eigenstate electrons are extended.

A critical factor of historic importance is that the accepted radiation reaction force on a radiating point charge arises only from energy that permanently leaves the charge. The resulting reaction force acts only to retard the motion of the charge and is several orders of magnitude smaller than the Coulomb force. It is not so commonly understood that an oscillating point charge is also enmeshed in a standing electromagnetic energy field of its own making; the reactive radiation reaction force from this local, oscillating dipolar energy field is $(1/ka)^3$ times larger. It does not brake the charge but acts to distort and expand it. Although this force has the same magnitude as the attracting Coulomb force, conventional quantum theory ignores it.

Consider the scenario as an empty eigenstate captures an electron. As a point-electron approaches a trapping potential it loses energy by bremsstrahlung until confined. Once confined it is acted on by Coulomb, centrifugal, tidal, and electrodynamic forces as well as self-binding ones. By the classical laws a point electron with an appropriate value of angular momentum will form a temporarily elliptical orbit with the nucleus at one of the foci. This produces two results on the orbit: First, the intrinsic and orbital magnetic moments interact in a way that produces a continuous torque, and thus a rotation of the orbit. Second, orbiting objects accelerate and, by the laws of classical electromagnetism, Eq. (1.7.3), accelerating charges radiate. By this effect a point charge will lose energy until it spirals into the nucleus. Eigenstate electrons, however, are intrinsically stable. Dirac emphasized there is a “remarkable stability of atoms and molecules.”

Whatever structure a confined electron might have a theorem of classical electromagnetism states that replacing its radiating structure with equivalent sources on the surface of a circumscribing sphere, virtual or real, leaves the external fields unchanged. After so doing, we note that standing electromagnetic energy produces both pressure and shears on the radiating shell. Before assessing the “remarkable stability” note that reactive energy plays a dominant role in determining the properties of electrically small antennas and although the atomic diameter-to-optical wavelength ratio is much smaller, on the order of $1/1000$, conventional quantum theory ignores it.

In another dramatic difference with antenna theory, quantum theory supplies no details about the near electromagnetic fields during energy exchanges; there is no equivalent to the full field sets of Chapter 2 developed for scatterers and for antennas: the quantum theory description of radiation exchange is incomplete. The remaining chapters of this book contain an examination of quantum radiation that includes effects of reactive energy.

On this physical basis, we describe the complete steady state radiation field of photons.

An ideal electron embodiment for our purpose is a nonlocal electron, with its nonlocality characteristic present both with and without the entanglement of other electrons, but which somehow retains its individual identity. The arguments of this book are based upon such an embodiment. The model violates neither physical laws nor experimental facts yet it permits the development of quantum physics based upon classical electrodynamics and the conservation of energy. With the model an eigenstate electron may be described as a charged cloud in a state of confined, nonradiating motion. On the basis of this model the uncertainty principle results from necessarily incomplete information about the system and the exclusion principle results since the cloud is granular on a string scale of dimensions. The units of which the electron is composed are necessarily minute compared with the total electron and remain always in dynamic equilibrium. Although the mathematical results are the same as those of historically accepted quantum theory the philosophical implications are quite different. Such differences are discussed in subsequent parts of the book.

4.1. Electrons

An isolated, static array of point electric charges cannot be held in equilibrium by electrostatic forces alone. Since opposite charges collapse upon themselves and like charges repel, a charge distribution is only stable if something other than electrostatic forces are involved. Since an electron contains at least a dominantly negative charge and since it is stable it follows that something other than electrostatic forces are involved.

An electron's physical extent has important repercussions. An early attempt to determine the size of an electron equated the electrostatic energy to its mass using Eq. (1.3.14), $W = m_0 c^2$. By classical electrostatics the energy of a virtual shell of radius R_L carrying charge e is:

$$W = \frac{e^2}{4\pi\epsilon R_L} \quad (4.1.1)$$

The energy relationship results in radius R_L :

$$R_L = \left(\frac{e^2}{m_0} \right) \times 10^{-7} \cong 2.82 \times 10^{-15} \text{ m} \quad (4.1.2)$$

This is the Lorentz radius of an electron; it is the radius an electron would have if only electrostatic energies were present.

There have been many experimental and theoretical attempts to determine electron size. One method is based upon accurately determining the ratio between intrinsic values of magnetic moment and angular momentum: g-factor data. Such measurements show that the electron diameter is not more than about 10^{-22} m. Scattering experiments show that electrons have no internal structure on the smallest scale of dimensions at which measurements are possible, about 10^{-18} m. Theoretical quantum electrodynamic arguments point to a structureless particle with a vanishingly small radius. String theory modifies the quantum electrodynamic results to show a diameter on the order of 10^{-35} m. Since atoms are typically about 10^{-10} m in diameter, apparently all would agree that electrons are much smaller than atoms.

It is indisputable that according to the classical equations accelerating point charges lose energy. It is also indisputable that atoms are stable. It is therefore widely accepted that classical electromagnetic theory is inconsistent with atomic stability. But do electrons, as described above, become extended when trapped in an eigenstate? A primary motive of the rest of this book is to show that extended eigenstate electrons are sufficient for the classical laws to predict atomic stability and to show that only radiation changes with the kinematic properties of photons can exist.

4.2. Dipole Radiation Reaction Force

This section contains the major arguments in support of our postulate that radiation-induced forces render eigenstate electrons into extended ones and extended ones into a dynamic, evolving ensemble of charge and current densities. The smallest eddy size is determined by how finely the electron charge is subdivided and internal forces require the ensemble to remain in continual motion. Several studies show that there are an infinite number of possible stable arrays, see Kim and Wolf. For purposes of analysis we break the ensemble into spherical shells, of vanishingly small thickness, centered on the nucleus. Although a shell in isolation would have the characteristics calculated in what follows they, of course, are not isolated. Available solutions are valid only in charge-free regions. We presume, however, relative magnitudes and symmetries are retained in charge-bearing regions. The analysis is qualitatively important and guides us to expected results.

Impedance: To examine the fields produced by an accelerating, point electron of charge e spiraling towards an atomic nucleus, consider the fields of Eq. (1.7.3). For simplicity let the electron velocity v remain much less than the speed of light and let it be located distance r from the origin. For that case the radiation fields are:

$$\mathbf{E} = \frac{\mu e}{4\pi r} \left[\hat{\mathbf{r}} \times \left(\hat{\mathbf{r}} \times \frac{\partial \mathbf{v}}{\partial t} \right) \right] \quad \mathbf{H} = \frac{e}{4\pi c r} \left(\frac{\partial \mathbf{v}}{\partial t} \times \hat{\mathbf{r}} \right) \quad (4.2.1)$$

To simplify the algebra, although the acceleration is radially directed consider it to be $\pm z$ -directed; a more realistic radial acceleration model complicates matters and adds nothing essential. With $\pm z$ -directed acceleration the generated force fields are:

$$\mathbf{E} = \frac{\mu e \hat{\theta}}{4\pi r} \frac{\partial v}{\partial t} \sin \theta \quad \mathbf{H} = \frac{e \hat{\phi}}{4\pi c r} \frac{\partial v}{\partial t} \sin \theta \quad (4.2.2)$$

The radial component of the Poynting vector is:

$$N_r = \frac{\mu}{c} \left[\frac{e}{4\pi R} \frac{\partial v}{\partial t} \right]^2 \sin^2 \theta \quad (4.2.3)$$

It follows that the radiated power is:

$$P = \frac{\mu e^2}{6c\pi} \left[\frac{\partial v}{\partial t} \right]^2 \quad (4.2.4)$$

Energy conservation requires the time-average radiated and generated power to be equal. This in turn requires a radiation reaction braking force, F_{RR} , acting on the electron to satisfy the condition:

$$\int_0^\tau \mathbf{F}_{RR} \cdot \mathbf{v} dt + \frac{\mu e^2}{6\pi c} \int_0^\tau \left[\frac{\partial v}{\partial t} \right]^2 dt = 0 \quad (4.2.5)$$

Time τ is the period required for an integer number of rotations of the electron about the nucleus. Doing the integral by parts leads to:

$$\int_0^\tau \left(\mathbf{F}_{RR} - \frac{\mu e^2}{6\pi c} \frac{\partial^2 \mathbf{v}}{\partial t^2} \right) \cdot \mathbf{v} dt = \frac{\mu e^2}{6\pi c} \frac{\partial \mathbf{v}}{\partial t} \cdot \mathbf{v} \quad (4.2.6)$$

With oscillatory motion, such as an electron orbiting an atomic nucleus, the right side is equal to zero, leaving the integral equal to zero. With \mathbf{p} equal to the dipole moment and the integrand is equal to zero:

$$\mathbf{F}_{RR}|_{\text{real}} = \frac{\mu e^2}{6\pi c} \frac{\partial^2 \mathbf{v}}{\partial t^2} = \frac{\mu e}{6\pi c} \frac{\partial^3 \mathbf{p}}{\partial t^3} = \frac{\mu e \omega^3}{6\pi c} \mathbf{p} \quad (4.2.7)$$

Equation (4.2.7) expresses the time-average value of the radiation reaction force on the electron due to dipole-radiated energy as it permanently leaves

the system. This radiation reaction force is a braking force that acts on the entire charge but has no effect on the shape of the electron.

Results from Chapter 3 include that a dipole radiating from within an electrically small region of radius a supports a reactive power that is larger than the real power by a factor of about $1/(ka)^3$. In the mid-optical frequency range and with an atom of radius 0.1 nm the factor is on the order of $1/(ka)^3 \cong 10^9$. It follows that the reactive radiation reaction force is 10^9 times larger than the braking force of Eq. (4.2.7). Multiplying Eq. (4.2.7) by $1/(ka)^3$ shows that the radiation reaction force due to the reactive energy is:

$$\mathbf{F}_{\text{reactive}} = \frac{e}{6\pi\epsilon_0 a^3} \mathbf{P} \quad (4.2.8)$$

Equation (4.2.8), the time-average value of the reactive radiation reaction force on the electron, is the same order of magnitude as the Coulomb attractive force. Yet this force is ignored by the historic interpretation of quantum theory.

A more formal derivation of the reactive radiation reaction force of Eq. (4.2.8) follows by viewing a radiating electron as an electric dipole and using the radiation impedance of Eq. (3.6.4). After substituting for the letter functions and doing the long division, we may write the input impedance of Eq. (3.6.4) on a virtual sphere of radius $r = \sigma/k$ as follows:

$$\begin{aligned} Z &= \eta \frac{D_1 + iC_1}{A_1 - iB_1} = \frac{\eta/\sigma^2 + i\eta/\sigma - \eta}{i/\sigma - 1} \\ &= \eta/i\sigma + i\eta\sigma + \eta\sigma^2 - i\eta\sigma^3 - \eta\sigma^4 + i\eta\sigma^5 + \dots \end{aligned} \quad (4.2.9)$$

Defining a generalized voltage and current leads directly from Eq. (4.2.9) to the voltage-current relationship:

$$V_1 = (\eta/i\sigma + i\eta\sigma + \eta\sigma^2 - i\eta\sigma^3 - \eta\sigma^4 + i\eta\sigma^5 + \dots) I_1$$

Replacing σ by (ka) gives, on the radiating surface:

$$V_1 = \mu \left(\frac{c^2}{i\omega a} + i\omega a + \omega^2 \frac{a^2}{c} - i\omega^3 \frac{a^3}{c^2} - \omega^4 \frac{a^4}{c^3} + i\omega^5 \frac{a^5}{c^4} + \dots \right) I_1 \quad (4.2.10)$$

After the second term, each succeeding term is (ka) times the previous one. Therefore the magnitude of each succeeding term is down by a factor of about 1000 in the mid-optical frequency range and the series converges rapidly. Odd and even powers of (ka) respectively describe oscillatory and outgoing energy. In this model of generalized force and flow the voltage is proportional to the driving force and the current is proportional to the

magnitude of the dipole moment. To go from generalized parameters to specific ones, introduce unknown constant K by the relationship:

$$V_1 = KF_1 \quad \text{and} \quad I_1 = i\omega p_1 \quad (4.2.11)$$

By definition, F_1 is the total, dipolar, radiation reaction force and p_1 is the electric dipole moment. Combining Eqs. (4.2.10) and (4.2.11), then switching to time notation by replacing $i\omega$ with a time derivative shows:

$$F_1(t) = \frac{\mu}{K} \left(\frac{c^2}{a} p_1(t) + a \frac{d^2}{dt^2} p_1(t) - \frac{a^2}{c} \frac{d^3}{dt^3} p_1(t) + \frac{a^3}{c^2} \frac{d^4}{dt^4} p_1(t) - \frac{a^4}{c^3} \frac{d^5}{dt^5} p_1(t) + \dots \right) \quad (4.2.12)$$

The third term within the round brackets of Eq. (4.2.12) is the first term that contributes to energy loss from the oscillator; it is equivalent to Eq. (4.2.7). Making the equality shows that:

$$K = \frac{6\pi a^2}{e}$$

Substituting K back into Eq. (4.2.12) gives:

$$F_1(t) = \frac{e p_1(t)}{6\pi \epsilon a^3} + \frac{e}{6\pi \epsilon a c^2} \frac{d^2}{dt^2} p_1(t) - \frac{e}{6\pi \epsilon c^3} \frac{d^3}{dt^3} p_1(t) + \frac{ea}{6\pi \epsilon c^4} \frac{d^4}{dt^4} p_1(t) - \dots \quad (4.2.13)$$

Equation (4.2.13) is the complete expression for the electric dipolar, radiation reaction force with steady state radiation. Terms with an even or odd number of time derivatives, respectively, represent reactive energy exchange or resistive energy loss. The first term is a restoring force due to the local standing energy field. The second term is the effective mass of the standing energy field. The third term is the first term that leads to an energy loss from the system, etc.

The lead term of Eq. (4.2.13) is not small compared with other forces. To evaluate it, note that p_1 is a product of e times a geometric factor, solvable using Eq. (A.28.7). The value is $p_1 = 2ea$ if the radiating system is a point electron oscillating between points at $z = \pm a$; it is $p_1 = 2ea/3$ if the charge is distributed proportional to $\cos\theta$ over sphere of radius a , see Eq. (A.14.2). We arbitrarily pick $p_1 = ea$. Inserting this value into Eq. (4.2.13) and taking the ratio to a similar expression for Coulomb's law

gives the dipolar-to-Coulomb's law force ratio of:

$$F_{di}/F_C \approx 2/3 \tag{4.2.14}$$

This shows the average expansive force is the same order of magnitude as the attractive force itself. It acts to extend the radiating surface to an ever-larger size and vanishes only if the charge is restructured to be nonradiating.

This leads to the following scenario: As a point charge approaches a trapping potential it loses energy by bremsstrahlung until confined. Once confined it starts to form into an elliptical orbit with the charge at one of the foci and generates electric dipole radiation. The reactive force, with primary magnitudes nearly equal the Coulomb attractive force, acts both to extend the shell and to create stable current eddies.

Electromagnetic Stress Tensor: All radiation fields carry with them the kinematic properties of energy, momentum, and angular momentum, and these kinematic properties produce both pressure and, in some cases, shears on radiating surfaces. This section contains mechanistic electromagnetic stress tensor results of dipole radiation reaction pressure and shear on a radiating shell generating an electric dipolar field. The argument can be extended to any mode and, by superposition of fields, to any combination of modes. This section uses the three spatial dimensions of Eq. (1.8.2). For a resting sphere, the equation is:

$$F_i^v = \partial T_{ij} / \partial x_j \tag{4.2.15}$$

F^v , the force per unit volume, is given by Eq. (1.6.14) and the electromagnetic stress tensor, T_{ij} , is given by Eq. (1.8.6). Changing from rectangular to spherical coordinates may be done directly or by extension and gives:

$$\begin{aligned}
 & (T_{ij}) \\
 = & \left(\begin{array}{ccc}
 \left(\frac{\epsilon}{2} [E_r^2 - E_\theta^2 - E_\phi^2] \right. & (\epsilon E_r E_\theta + \mu H_r H_\theta) & (\epsilon E_r E_\phi + \mu H_r H_\phi) \\
 \left. + \frac{\mu}{2} [H_r^2 - H_\theta^2 - H_\phi^2] \right) & & \\
 (\epsilon E_\theta E_r + \mu H_\theta H_r) & \left(\frac{\epsilon}{2} [E_\theta^2 - E_\phi^2 - E_r^2] \right. & (\epsilon E_\theta E_\phi + \mu H_\theta H_\phi) \\
 & \left. + \frac{\mu}{2} [H_\theta^2 - H_\phi^2 - H_r^2] \right) & \\
 (\epsilon E_\phi E_r + \mu H_\phi H_r) & (\epsilon E_\phi E_\theta + \mu H_\phi H_\theta) & \left(\frac{\epsilon}{2} [E_\phi^2 - E_r^2 - E_\theta^2] \right. \\
 & & \left. + \frac{\mu}{2} [H_\phi^2 - H_r^2 - H_\theta^2] \right)
 \end{array} \right)
 \end{aligned}
 \tag{4.2.16}$$

On a spherical surface centered at the origin, diagonal matrix element $T_{rr}(t_R)$ describes surface pressure and off-diagonal matrix elements $S_{r\theta}(t_R)$

and $S_{r\phi}(t_R)$ describe surface shears. The forms of the equations apply both to exterior and interior surface fields.

The generating source is a virtual sphere of radius a that supports surface charge and current densities that, in turn, generate stress tensor components:

$$\begin{aligned} T_{rr}(t_R) &= \frac{\varepsilon}{2} [E_r^2 - E_\theta^2 - E_\phi^2] + \frac{\mu}{2} [H_r^2 - H_\theta^2 - H_\phi^2] \\ S_{r\theta}(t_R) &= \varepsilon E_r E_\theta + \mu H_r H_\theta \quad S_{r\phi}(t_R) = \varepsilon E_r E_\phi + \mu H_r H_\phi \end{aligned} \quad (4.2.17)$$

The fields are evaluated just off the surface in question, interior or exterior.

Coulomb's law forms an important example. Charge q at the center of the virtual sphere produces, just off either surface of a virtual shell the field and the tensor components:

$$E_r = \frac{q}{4\pi\varepsilon a^2} \quad T_{rr} = \frac{q}{32\pi^2\varepsilon a^4} = p \quad S_{r\theta} = 0 \quad (4.2.18)$$

T_{rr} gives the net pressure, p , on the shell. At that surface the inner and outer fields have equal magnitudes and the pressures are oppositely directed.

Consider the z -directed, phasor, electric dipolar fields, both exterior and interior, produced by a spherical shell supporting the charge density of Eq. (A.14.1). The field forms are given by Eqs. (A.14.7) and (A.14.8). With subscripts "e" and "i" representing respectively exterior and interior regions and for the special case $ka \ll 1$:

$$\begin{aligned} \mathbf{E}_e &= \frac{3}{2} \left(\frac{q}{4\pi\varepsilon a^2} \right) (ka)^3 \\ &\times \left\{ 2\hat{r} \left(\frac{1}{\sigma^3} + \frac{i}{\sigma^2} \right) \cos\theta + \hat{\theta} \left(\frac{1}{\sigma^3} + \frac{i}{\sigma^2} - \frac{1}{\sigma} \right) \sin\theta \right\} e^{i\omega t_R} \end{aligned} \quad (4.2.19)$$

$$\eta \mathbf{H}_e = \frac{3}{2} \left(\frac{3q}{4\pi\varepsilon a^2} \right) (ka)^3 \hat{\phi} \left(\frac{i}{\sigma^2} - \frac{1}{\sigma} \right) \sin\theta e^{i\omega t_R}$$

$$\mathbf{E}_i = \left(\frac{q}{4\pi\varepsilon a^2} \right) \{ \hat{r} \cos\theta - \hat{\theta} \sin\theta \} e^{i\omega t} \quad (4.2.20)$$

$$\eta \mathbf{H}_i = i \left(\frac{q}{8\pi\varepsilon a^2} \right) \hat{\phi} \sigma \sin\theta e^{i\omega t}$$

Since the magnetic field has no radial component, shear arises from only the electric field. Also, since the magnetic field strength is less than the electric by a factor of (ka) we solve for the pressure due to only the electric field. Under these conditions for the unbalanced surface pressure, exterior minus interior values, normalized by the Coulomb surface pressure of

Eq. (4.2.18), is:

$$p_N = \left[2 \cos^2 \theta - \frac{5}{16} \sin^2 \theta \right] [1 + \cos(2\omega t_R)] \quad (4.2.21)$$

This equation shows the pressure to be expansive at angles less than about 68.5° and greater than 111.5° and compressive in between. Since the average magnitude ratio is about one, it follows that the dipole and monopole effects are about equal. Since the pressure is expansive on the z -axis and compressive in the xy -plane, the pressure tends to distort the original sphere into a radiating bicone with extended caps. Integrating the net pressure over the surface to obtain the ratio of radiation expansion force to the Coulomb attraction force gives:

$$\frac{\text{Expansive dipole force}}{\text{Attractive Coulomb force}} = \frac{11}{6} [1 + \cos(2\omega t_R)] \quad (4.2.22)$$

A plot of Eq. (4.2.21) is shown in Fig. 4.2.1. note the expansive pressure at the poles is four times the Coulomb compression.

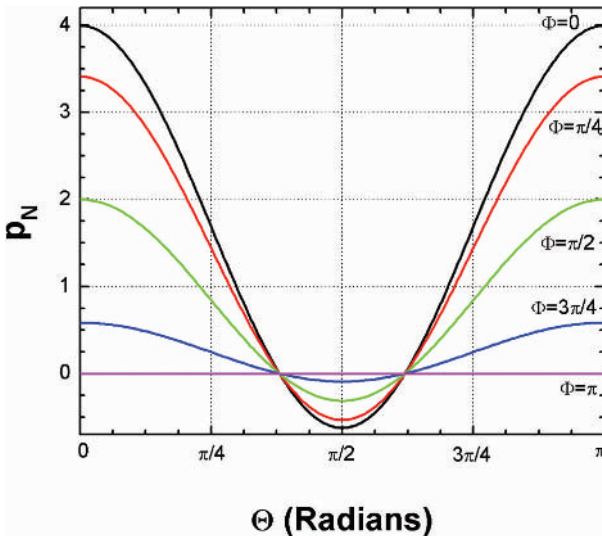


Fig. 4.2.1. Normalized surface pressure p_N on a spherical shell radiating as a z -directed electric dipole versus zenith angle θ of radius $ka = 1$ at $2\omega t_R = 0, \pi/4, \pi/2, 3\pi/4, \text{ and } \pi$.

The normalized exterior and interior surface shears calculated using Eqs. (4.2.17), (4.2.19), and (4.2.20) are:

$$\begin{aligned} S_{eN} &= \frac{9}{2} \sin \theta \cos \theta [1 + \cos(2\omega t_R)] \\ S_{iN} &= -\sin \theta \cos \theta [1 + \cos(2\omega t_R)] \end{aligned} \quad (4.2.23)$$

The shears have identical time and angular dependence but are oppositely directed; the directional opposition acts to form θ -directed eddy currents. Like pressure, the magnitudes of the eddy-producing surface shears are approximately equal to the binding Coulomb force.

4.3. The Time-Independent Schrödinger Equation

The science of statistical mechanics consists of analyzing large numbers of identical, interacting particles taken as a single ensemble. The state of the ensemble is specified by the positions and velocities of the particles, and is sufficient to determine the kinetic and potential energies of the system. With particles modeled as realistically as possible, there is little or no difficulty interpreting an experiment that measures the ensemble-average of a kinematic variable. The state of an isolated ensemble at any instant determines its future values. Since large ensembles contain too many degrees of freedom to detail, no attempt is made to obtain precise, detailed calculations. Instead, most probable values averaged over all particles are calculated and assigned as ensemble-average values.

A single electron trapped by the Coulomb force of a positive nucleus accelerates. Section 4.2 shows both pressure and shear on trapped electrons acting to transform them into ensembles of charge and current densities. Since our present knowledge does not permit solving for the exact array, in common with statistical mechanics it is necessary to consider such eigenstate electrons on a statistical basis. Physical properties are calculated by imposing conservation laws. A primary result of imposing energy conservation on such an ensemble is the Schrödinger equation. First published in 1926, it is a mathematical description of the quantum character of electrons. Schrödinger discovered the usefulness of the differential equation that bears his name:

$$-\frac{\hbar^2}{2m} \nabla^2 U(\mathbf{r}) + \Lambda(\mathbf{r})U(\mathbf{r}) = WU(\mathbf{r}) \quad (4.3.1)$$

In this equation $2\pi\hbar$ is Planck's constant, $\Lambda(\mathbf{r})$ is the electrostatic potential, and $U(\mathbf{r})$ is the wave function. The time average value of electric charge

density at each point in space is:

$$\rho(\mathbf{r}) = eU^*(\mathbf{r})U(\mathbf{r}) \quad (4.3.2)$$

Although Schrödinger discovered that solutions of his equation correctly described the actions of electrons, he was not led to the result by first principles. The equation is invaluable for describing atomic level phenomena but solutions are statistical in character and there is no way to determine a unique physical basis for the equation. For example, the equation itself is no help in determining whether $eU(r)U^*(r)$ represents an actual static charge density, the fraction of the time a point electron occupies a particular differential volume, or something in between. It is only known that solving Eq. (4.3.1) for $U(r)$ then evaluating $eU(r)U^*(r)$ gives the correct time-average spatial charge distribution for many electron systems.

Since Schrödinger first presented the equation, it has been shown that many different postulate sets yield it as a derived result. Since the interpretation depends upon the nature of the model used to derive it no single result is a sufficient basis for deciding if a particular model is correct. This section derives the Schrödinger equation using a thermodynamic approach and results are interpreted accordingly. A precise description of an extended, moving, bound charge density trapped by an electrostatic force and coupled to its own magnetic field is beyond our capability; we simply do not know enough about electrons. Therefore, in a way similar to thermodynamics we seek an energy function from which follows general ensemble properties without detailed knowledge of the ensemble. The approach is adequate to obtain time-average values of kinematic properties, i.e. expectation values.

The approach begins by noting that a dynamic charge distribution supports time-average values of charge and current densities, respectively $\rho(\mathbf{r})$ and $\rho(\mathbf{p})$, within the spatial range \mathbf{r} and $\mathbf{r} + d\mathbf{r}$ and the momentum range \mathbf{p} and $\mathbf{p} + d\mathbf{p}$. Momentum densities are directly proportional to current densities. Let an electron occupy a single eigenstate and let the charge density be everywhere the same sign. The constraint is expressed by introducing complex functions $U(\mathbf{r})$ and $\Gamma(\mathbf{p})$, defined by the relationships:

$$eU^*(\mathbf{r})U(\mathbf{r}) = \rho(\mathbf{r}) \quad \text{and} \quad e\Gamma^*(\mathbf{p})\Gamma(\mathbf{p}) = \rho(\mathbf{p}) \quad (4.3.3)$$

$U(\mathbf{r})$ and $\Gamma(\mathbf{p})$ are complex functions and, by definition, wave functions. It follows that

$$\int U^*(\mathbf{r})U(\mathbf{r})dV = 1 = \int \Gamma^*(\mathbf{p})\Gamma(\mathbf{p})dV_p \quad (4.3.4)$$

Differentials dV and dV_p represent, respectively, differential volume in space and momentum coordinates.

Since $U(\mathbf{r})$ and $\Gamma(\mathbf{p})$ describe the same dynamic charge distribution, they are relatable. Each position in coordinate space receives contributions from the full range of momenta in proportion to the value of $\Gamma(\mathbf{p})$ at each velocity, and *vice versa*. Therefore we seek a linear transformation between the two coordinate systems that satisfies the conditions:

$$U(\mathbf{r}) = L\{\Gamma(\mathbf{p})\} \quad \text{and} \quad \Gamma(\mathbf{p}) = L^{-1}\{U(\mathbf{r})\} \quad (4.3.5)$$

L is a linear operator and L^{-1} is its inverse. A general linear function that meets these requirements is the Fourier integral transform pair:

$$\begin{aligned} U(\mathbf{r}) &= \left[\frac{1}{2\pi\hbar} \right]^{3/2} \int \Gamma(\mathbf{p}) \exp\left(\frac{i\mathbf{r} \cdot \mathbf{p}}{\hbar}\right) dV_p \\ \Gamma(\mathbf{p}) &= \left[\frac{1}{2\pi\hbar} \right]^{3/2} \int U(\mathbf{r}) \exp\left(\frac{\mathbf{r} \cdot \mathbf{p}}{i\hbar}\right) dV \end{aligned} \quad (4.3.6)$$

The constant \hbar is a dimension-determining constant; its magnitude must be determined by experiment. Dropping to one dimension for simplicity, Eq. (4.3.6) takes the form:

$$\begin{aligned} U(x) &= \left[\frac{1}{2\pi\hbar} \right]^{1/2} \int \Gamma(p) \exp\left(\frac{ixp}{\hbar}\right) dp \\ \Gamma(p) &= \left[\frac{1}{2\pi\hbar} \right]^{1/2} \int U(x) \exp\left(\frac{xp}{i\hbar}\right) dx \end{aligned} \quad (4.3.7)$$

This procedure for going from charge density to wave functions and the Fourier transforms of Eq. (4.3.6) parallels the method of going from electric energy density to electric field intensity, see Sec. 1.14. The significant difference is that the electric field intensity forms a vector field and the wave functions form a scalar field.

The expectation value of momentum, $\langle p \rangle$ follows from the above, and is given by the equation:

$$\langle p \rangle = \int p \Gamma^*(p) \Gamma(p) dp \quad (4.3.8)$$

The same value may be calculated using $U(x)$. To do so, substitute $\Gamma(p)$ from the second part of Eq. (4.3.7) into Eq. (4.3.8). The result is:

$$\langle p \rangle = \left(\frac{1}{2\pi\hbar} \right)^{1/2} \int_{-\infty}^{\infty} p \Gamma^*(p) \int_{-\infty}^{\infty} U(x) \exp\left(\frac{xp}{i\hbar}\right) dx \quad (4.3.9)$$

Integrating the second integral by parts gives:

$$\langle p \rangle = \left(\frac{1}{2\pi\hbar} \right)^{1/2} \int_{-\infty}^{\infty} \Gamma^*(p) \left\{ i\hbar U(x) \Big|_{-\infty}^{\infty} - i\hbar \int_{-\infty}^{\infty} \frac{\partial U(x)}{\partial x} \exp\left(\frac{xp}{i\hbar}\right) dx \right\}$$

Since an acceptable wave function is equal to zero at infinity, the first term within the brackets vanishes. Substituting the complex conjugate of the first of Eq. (4.3.7) into the second term and reversing the order of integration gives:

$$\langle p \rangle = - \int_{-\infty}^{\infty} U^*(x) \left[\frac{\hbar}{i} \frac{\partial U(x)}{\partial x} \right] dx \quad (4.3.10)$$

Equation (4.3.10) is an example of the general case: A dynamic variable in momentum space may be replaced by an operation in dimensional space, and *vice versa*. Letting O indicate that the variable is written in operator form, in three dimensions the momentum operator is:

$$O(\mathbf{p}) = \frac{\hbar}{i} \nabla \quad (4.3.11)$$

It is understood that the operator acts on wave function $U(\mathbf{r})$. Repeating the above procedure for p^n shows, after n partial integrations, that the result generalizes to:

$$O(p^n) = \left(\frac{\hbar}{i} \right)^n \nabla^n \quad (4.3.12)$$

With this result, it is not necessary to solve for both $U(\mathbf{r})$ and $\Gamma(\mathbf{p})$ to solve a kinematic problem. It is only necessary to work with one functional type, typically $U(\mathbf{r})$, and express conjugate variables in operator form.

A conservation law of primary importance is the low speed energy of an electron with total energy W . The sum of kinetic plus potential energies is:

$$W = \frac{1}{2m} \int dV_p [p^2 \Gamma^*(\mathbf{p}) \Gamma(\mathbf{p})] + \int dV [\Lambda(\mathbf{r}) U^*(\mathbf{r}) U(\mathbf{r})] \quad (4.3.13)$$

An arbitrary constant, such as the self-energy of the electron, may be added without affecting results to follow. Applying Eq. (4.3.12) to Eq. (4.3.13) gives the result:

$$\int dV U^*(r) \left\{ -\frac{\hbar^2}{2m} \nabla^2 U(\mathbf{r}) + [\Lambda(\mathbf{r}) - W] U(\mathbf{r}) \right\} = 0 \quad (4.3.14)$$

Although it is only necessary for the integral to equal zero the more stringent condition that the integrand equal zero at all points within the region may also be applied. Doing so returns Eq. (4.3.1), the time-independent

Schrödinger wave equation. Function $U(\mathbf{r})$ is a wave function that provides the time average charge density of the electron of interest at each point.

The above development shows that the Schrödinger equation is a statement of energy conservation in which Planck's constant appears as a phase-determining normalization constant in the scalar product between velocity and position vectors, see Eq. (4.3.6). The Schrödinger equation is correct only at electron speeds much less than c and it does not account for electron spin; it is necessary to add electron spin separately to the wave equation. In contrast, Dirac's equations apply in all inertial systems and spin is an integral part of the whole. Although Dirac's work is of singular importance to quantum theory, it does not assist in resolving basic issues of photon exchanges considered here. Therefore, it is not discussed in this work.

4.4. The Uncertainty Principle

By the uncertainty principle, it is not possible to determine simultaneously the exact value of conjugate variables, for example position and momentum. The more accurately the position of a point electron is known the less accurately the momentum can be known, and *vice versa*. As a simple example, consider the case of an electron described by a Gaussian wave function. That is, $U(x)$ is proportional to $\exp(-x^2/B)$, where B is undetermined but constrained to be positive:

$$0 < B < \infty \quad (4.4.1)$$

The electron is confined to position zero only if B increases without limit and the smaller the value of B the larger the physical extent of the charge distribution. The system is normalized if the probability density at each point is:

$$U^*(x)U(x) = \sqrt{\frac{2}{\pi B}} \exp\left(-\frac{2x^2}{B}\right) \quad (4.4.2)$$

The expectation value of x^2 may be calculated using the integrals of Table 4.4.1:

$$\langle x^2 \rangle = \sqrt{\frac{2}{\pi B}} \int_{-\infty}^{\infty} \exp\left(-\frac{2x^2}{B}\right) x^2 dx = \frac{B}{4} \quad (4.4.3)$$

Substituting $U(x)$ into the second of Eq. (4.3.7) results in the momentum space form of the wave function:

$$\Gamma(p) = \left(\frac{B}{2\pi\hbar^2}\right)^{1/4} \exp\left(-\frac{B}{4\hbar^2}p^2\right) \quad (4.4.4)$$

Table 4.4.1. Short list of Gaussian integrals.

$$\int_0^{\infty} \exp(-a^2 x^2) dx = \frac{\sqrt{\pi}}{2a}$$

$$\int_0^{\infty} x^2 \exp(-x^2) dx = \frac{\sqrt{\pi}}{4}$$

$$\int_0^{\infty} \exp(-a^2 x^2) \cos(bx) dx = \frac{\sqrt{\pi}}{2a} \exp\left(-\frac{b^2}{4a^2}\right)$$

Using Eq. (4.4.4) to calculate the mean-square value of momentum gives:

$$\langle p^2 \rangle = \left(\frac{B}{2\pi\hbar^2} \right)^{1/2} \int_{-\infty}^{\infty} \exp\left(-\frac{Bp^2}{2\hbar^2}\right) p^2 dp = \frac{\hbar^2}{B} \quad (4.4.5)$$

Recalculating $\langle p^2 \rangle$ in coordinate space using operator notation gives, after some calculation:

$$\langle p^2 \rangle = -\hbar^2 \left(\frac{2}{\pi B} \right)^{1/2} \int_{-\infty}^{\infty} \exp\left(-\frac{x^2}{B}\right) \frac{d^2}{dx^2} \left[\exp\left(-\frac{x^2}{B}\right) \right] dx = \frac{\hbar^2}{B} \quad (4.4.6)$$

By inspection the r.m.s. values of position and momentum satisfy the parabolic relationship:

$$\sqrt{\langle x^2 \rangle \langle p^2 \rangle} = \frac{\hbar}{2} \quad (4.4.7)$$

By Eq. (4.4.7) it is not possible to know position and momentum more accurately than $\Delta x \Delta p \approx \hbar$, where Δx and Δp are, respectively, uncertainty in the measurement of position and momentum. This is a quantitative statement of the uncertainty principle. It results from the properties of the Fourier integral transform relationships relating the wave functions in momentum and coordinate space. The same is true for all conjugate pairs, i.e. pairs related by Fourier transforms; they satisfy the parabolic uncertainty relationship of Eq. (4.4.7). It may be shown that a Gaussian wave function provides the least possible uncertainty; all other wave functions provide a greater uncertainty than that of Eq. (4.4.7).

By the electron model of Sec. 4.2 and the development of Sec. 4.3, the uncertainty is due to incomplete information about the intra-electron ensemble. If the structure of an electron and its binding were known, in principle at least, an exact solution would permit calculation of the full physical result.

4.5. The Time-Dependent Schrödinger Equation

Solutions of the time-independent Schrödinger equation describe time-average values of the kinematic parameters and, of course, time-average values are constant. However, the time-averages are taken over time intervals that are long only when compared with changes in the electron configuration within the state. Time variations over such periods that are short compared with the time scales of macroscopic events are often of interest. In this section, we examine changes during times that are longer than needed for electron configuration changes but short compared with macroscopic times. The result determines the initial variation of expectation values away from equilibrium positions by calculating changes that occur slowly enough so ensemble averages always remain in near-equilibrium conditions. If the potential changes too rapidly, or if the potential change is too large, the near-equilibrium condition is violated and the Schrödinger equation ceases to apply. In summary, the Schrödinger time-dependent equation applies only if the ensemble remains in a near-equilibrium condition.

To find the time behavior of the expectation values, begin by defining the time dependent function:

$$\psi(\mathbf{r}, t) = U(\mathbf{r})e^{i\omega t} \quad (4.5.1)$$

Use of the exponential time function places no restrictions on well-behaved functions since the time variation can be constructed by integrating appropriately weighted exponentials. Using this notation time dependence of the charge density in coordinate space is, see Eq. (4.3.2):

$$\rho(\mathbf{r}, t) = e\psi^*(\mathbf{r}, t)\psi(\mathbf{r}, t) \quad (4.5.2)$$

The momentum density is shown in Eq. (4.3.10). If charge and mass density are evenly distributed throughout the eigenstate:

$$\mathbf{J}(\mathbf{r}, t) = \frac{e}{m}\mathbf{p}(\mathbf{r}, t) \quad (4.5.3)$$

Combining Eqs. (4.3.10) and (4.5.3) and requiring the current density to be real gives the current density expression:

$$\mathbf{J}(\mathbf{r}, t) = \frac{\hbar e}{2im} [\psi^*(\mathbf{r}, t)\nabla\psi(\mathbf{r}, t) - \psi(\mathbf{r}, t)\nabla\psi^*(\mathbf{r}, t)] \quad (4.5.4)$$

It is shown in Sec. 4.3 that the time-independent Schrödinger equation is a statement of the conservation of energy. The time-dependent Schrödinger equation follows from the time-independent one after combining it with the

conversation of charge. The continuity equation is a statement of charge conservation, and given by:

$$\nabla \cdot \mathbf{J}(\mathbf{r}, t) + \frac{\partial \rho(\mathbf{r}, t)}{\partial t} = 0 \quad (4.5.5)$$

Development of the time-dependent equation begins with these equations. The rate of change of charge density is:

$$\frac{\partial \rho(\mathbf{r}, t)}{\partial t} = e \left[\psi^*(\mathbf{r}, t) \frac{\partial}{\partial t} \psi(\mathbf{r}, t) + \psi(\mathbf{r}, t) \frac{\partial}{\partial t} \psi^*(\mathbf{r}, t) \right] \quad (4.5.6)$$

The divergence of the current density is:

$$\nabla \cdot \mathbf{J}(\mathbf{r}, t) = \frac{\hbar e}{2im} [\psi^*(\mathbf{r}, t) \nabla^2 \psi(\mathbf{r}, t) - \psi(\mathbf{r}, t) \nabla^2 \psi^*(\mathbf{r}, t)] \quad (4.5.7)$$

Substituting Eqs. (4.5.5) and (4.5.6) into Eq. (4.5.7), multiplying by (\hbar/ie) , and adding and subtracting potential $\Lambda(r)$ gives:

$$\begin{aligned} \psi^*(\mathbf{r}, t) \left[-\frac{\hbar^2}{2m} \nabla^2 \psi(\mathbf{r}, t) + \Lambda(\mathbf{r})\psi(\mathbf{r}, t) + \frac{\hbar}{i} \frac{\partial}{\partial t} \psi(\mathbf{r}, t) \right] \\ - \psi(\mathbf{r}, t) \left[-\frac{\hbar^2}{2m} \nabla^2 \psi^*(\mathbf{r}, t) + \Lambda(\mathbf{r})\psi^*(\mathbf{r}, t) - \frac{\hbar}{i} \frac{\partial}{\partial t} \psi^*(\mathbf{r}, t) \right] = 0 \end{aligned} \quad (4.5.8)$$

To connect with the time-independent equation, we seek wave function $\psi(\mathbf{r}, t)$ that, as the time dependence becomes vanishingly slow, goes to:

$$\begin{aligned} U^*(\mathbf{r}) \left[-\frac{\hbar^2}{2m} \nabla^2 U(\mathbf{r}) + \Lambda U(\mathbf{r}) - WU(\mathbf{r}) \right] \\ - U(\mathbf{r}) \left[-\frac{\hbar^2}{2m} \nabla^2 U^*(\mathbf{r}) + \Lambda U^*(\mathbf{r}) - WU^*(\mathbf{r}) \right] = 0 \end{aligned} \quad (4.5.9)$$

Since each line of Eq. (4.5.9) is equal to zero, so are the two lines of Eq. (4.5.8) in the low speed limit, and since the equation holds for all nonrelativistic speeds, the time-dependent wave equation is:

$$\int \psi^*(\mathbf{r}, t) \left[-\frac{\hbar^2}{2m} \nabla^2 \psi(\mathbf{r}, t) + \Lambda(\mathbf{r})\psi(\mathbf{r}, t) + \frac{\hbar}{i} \frac{\partial}{\partial t} \psi(\mathbf{r}, t) \right] dV = 0 \quad (4.5.10)$$

Insisting that not just the integral but also the integrand equal zero results in the Schrödinger time-dependent equation:

$$-\frac{\hbar}{i} \frac{\partial}{\partial t} \psi(\mathbf{r}, t) = H\psi(\mathbf{r}, t) = W\psi(\mathbf{r}, t) \quad (4.5.11)$$

The Hamiltonian operator, H , is defined to be the operator that acts on the wave function to produce the time dependence and state energy of Eq. (4.5.11). From the first equality:

$$H\psi(\mathbf{r}, t) = -\frac{\hbar^2}{2m}\nabla^2\psi(\mathbf{r}, t) + \Lambda(\mathbf{r})\psi(\mathbf{r}, t) \quad (4.5.12)$$

From the second equality:

$$\psi(\mathbf{r}, t) = \psi(\mathbf{r}, t_0) \exp\left(\frac{iW}{\hbar}t\right) \quad (4.5.13)$$

The initial value of the wave function is the equilibrium value:

$$\psi(\mathbf{r}, t_0) = U(\mathbf{r}) \quad (4.5.14)$$

An important result of Eq. (4.5.13) is that the frequency of an eigenstate is related to the energy as:

$$\omega = W/\hbar \quad (4.5.15)$$

This equation is the basis for the experimental determination of \hbar .

The time-independent Schrödinger equation combines conservation of energy and charge. It is thermodynamic-like in that only time-average averages over times long compared with the periods of possible intra-state movements are described. Therefore although Eq. (4.5.11) provides correct time-average values it does not imply a time-line of actual events. Also, it describes only linear phenomena and therefore applies only to incremental changes that occur at the onset of atomic instability, not to a full transition.

4.6. Quantum Operator Properties

An extension of the logic that supported the use of operators to calculate momentum generalizes to include functions of momentum. To make the generalization consider the integral:

$$I = \int_{-\infty}^{\infty} [\Gamma_R^*(\mathbf{p})\mathbf{p}\Gamma_S(\mathbf{p})]dV_p \quad (4.6.1)$$

$\Gamma_R(\mathbf{p})$ and $\Gamma_S(\mathbf{p})$ represent eigenfunction solutions of the same differential equation. For each function $\Gamma_R(\mathbf{p})$, there exists a Fourier integral transform function in coordinate space, $U_R(\mathbf{r})$. To rewrite the integral of Eq. (4.6.1) using spatial functions, repeat the procedure used going from Eq. (4.3.8) to Eq. (4.3.10). Taking the gradient in the direction of the momentum and

working with the “S” functions, the integral of Eq. (4.6.1) becomes:

$$I = \int_{-\infty}^{\infty} U_R^*(\mathbf{r}) \left[\frac{\hbar}{i} \nabla U_S(\mathbf{r}) \right] dV \quad (4.6.2)$$

Similarly, working with the “R” functions gives:

$$I = \int_{-\infty}^{\infty} U_S(\mathbf{r}) \left[\frac{\hbar}{i} \nabla U_R(\mathbf{r}) \right]^* dV \quad (4.6.3)$$

Since all physical results are real, Eq. (4.6.3) is equal to its own complex conjugate:

$$\int_{-\infty}^{\infty} U_S^*(\mathbf{r}) \left[\frac{\hbar}{i} \nabla U_R(\mathbf{r}) \right] dV = \int_{-\infty}^{\infty} U_S(\mathbf{r}) \left[-\frac{\hbar}{i} \nabla U_R^*(\mathbf{r}) \right] dV \quad (4.6.4)$$

Combining Eqs. (4.6.2) and (4.6.4) gives:

$$\int_{-\infty}^{\infty} U_R^*(\mathbf{r}) \left[\frac{\hbar}{i} \nabla U_S(\mathbf{r}) \right] dV = \int_{-\infty}^{\infty} U_S(\mathbf{r}) \left[\frac{\hbar}{i} \nabla U_R(\mathbf{r}) \right]^* dV \quad (4.6.5)$$

The result generalizes to:

$$\int_{-\infty}^{\infty} U_R^*(\mathbf{r}) O[U_S(\mathbf{r})] dV = \int_{-\infty}^{\infty} U_S(\mathbf{r}) \langle O[U_S(\mathbf{r})] \rangle^* dV \quad (4.6.6)$$

The symbol “O” indicates any quantum mechanical operator. An operator that satisfies Eq. (4.6.6) is, by definition, a Hermitian operator.

4.7. Orthogonality

To examine the orthogonality properties of wave function $\psi(r, t)$, let O be a quantum theory operator, let $\psi_R(r, t)$ and $\psi_S(r, t)$ be time-dependent eigenfunctions, and let I_R and I_S be the corresponding state values. That is:

$$O\psi_R(\mathbf{r}, t) = I_R\psi_R(\mathbf{r}, t) \quad \text{and} \quad O\psi_S(\mathbf{r}, t) = I_S\psi_S(\mathbf{r}, t) \quad (4.7.1)$$

All functions $\psi_R(r, t)$ that satisfies this equation are eigenfunctions and constants I_R are state values. Multiplying the left equation by $\psi_S^*(r, t)$, the right equation by $\psi_R^*(r, t)$, subtracting one from the other, and integrating

over the volume gives:

$$\begin{aligned} \int [\psi_R^* I_S \psi_S - \psi_S^* I_R \psi_R] dV &= \int [\psi_R^* O \psi_S - \psi_S (O \psi_R)^*] dV \\ &= (I_S - I_R) \int \psi_R^* \psi_S dV \end{aligned} \quad (4.7.2)$$

It follows from Eq. (4.6.6) that:

$$\int [\psi_R^* (O \psi_S) - \psi_S (O \psi_R)^*] dV = 0 \quad (4.7.3)$$

Combining Eqs. (4.7.2) and (4.7.3) gives:

$$(I_S - I_R) \int \psi_R^* \psi_S dV = 0 \quad (4.7.4)$$

If a system has more than one eigenfunction with the same state energy the system is degenerate; the number of solutions that produce the same state energy is the degree of degeneracy. A conclusion from Eq. (4.7.4) is that if the states are not degenerate the functions are orthogonal; if the state energies are equal the functions are degenerate and may or may not be orthogonal.

Wherever solutions of a single operator result in many eigenfunctions, $\psi_S(\mathbf{r}, t)$, the physical result is a sum, weighted by constants a_S , over all possible eigenfunctions:

$$\Psi(\mathbf{r}, t) = \sum_{S=1}^{\infty} a_S \psi_S(\mathbf{r}, t) \quad (4.7.5)$$

$\psi_S(\mathbf{r}, t)$ are normalized wave functions. Requiring that the total wave function be normalized gives:

$$\int \Psi^* \Psi dV = \sum_{R=1}^{\infty} \sum_{S=1}^{\infty} a_R a_S^* \int \psi_R \psi_S^* dV = \sum_{R=1}^{\infty} a_R a_R^* = 1 \quad (4.7.6)$$

Equation (4.7.6) shows that the sum over the magnitudes of all coefficients is one. This leads to the conclusion that:

$$\langle O \rangle = \int \psi^* O \psi dV = \sum_{R=1}^{\infty} \sum_{S=1}^{\infty} a_R a_S^* \int \psi_S^* O \psi_R dV = \sum_{R=1}^{\infty} I_R a_R a_R^* \quad (4.7.7)$$

In words, the expectation value of any dynamic function “O” is the sum over the probabilities that the electron occupies a particular state multiplied by the state value. For any particular measurement, the use of operator $\langle O \rangle$

produces only a particular value $a_R a_R^*$. With a linear system, a single electron enters into a statistically weighted fraction of all available eigenstates.

The initial rate of change of an expectation value follows. Differentiating the first equality of Eq. (4.7.7) with respect to time gives:

$$\frac{d}{dt} \langle O \rangle = \int \left(\frac{\partial \psi^*}{\partial t} O \psi + \psi^* O \frac{\partial \psi}{\partial t} \right) dV \quad (4.7.8)$$

Using Eq. (4.5.11), this may be written as:

$$\frac{d}{dt} \langle O \rangle = -\frac{i}{\hbar} \int (\psi^* O (H\psi) - (H\psi)^* (O\psi)) dV \quad (4.7.9)$$

Incorporating Eq. (4.6.6):

$$\frac{d}{dt} \langle O \rangle = -\frac{i}{\hbar} \int \psi^* (OH - HO) \psi dV \quad (4.7.10)$$

For the special case where $O = r$:

$$\langle \mathbf{p} \rangle = m \frac{d}{dt} \langle \mathbf{r} \rangle = \frac{im}{\hbar} (H\mathbf{r} - \mathbf{r}H) \quad (4.7.11)$$

The bracket on the right side of Eq. (4.7.11) is defined to be the commutator of the indicated variable. This particular bracket is the commutator of position.

4.8. Harmonic Oscillators

Harmonic oscillators appear in different forms throughout all of physics. Examples include RC circuits, the displacement of violin strings, and the oscillations of two atoms bound together as a molecule. Consider the latter case as an example of a one-dimensional problem. To make a quantum mechanical analysis of a harmonic oscillator, let the total energy H be the sum of kinetic and potential parts:

$$H = \frac{p^2}{2m} + \frac{1}{2} \alpha x^2 \quad (4.8.1)$$

In this case α is a constant specific to a particular molecule.

The applicable Schrödinger equations are:

$$\int U^*(x) \left(-\frac{\hbar^2}{2m} + \frac{1}{2}\alpha x^2 \right) U(x) dx = W \quad (4.8.2)$$

$$W\psi(x, t) = -\frac{\hbar}{i} \frac{\partial \psi(x, t)}{\partial t}$$

Since W is constant, it follows from the second part of Eq. (4.8.2) that:

$$\psi(x, t) = U(x)e^{iW/kT} \quad (4.8.3)$$

The first part of Eq. (4.8.2) is satisfied if:

$$-\frac{\hbar^2}{2m} \frac{d^2 U(x)}{dx^2} + \left(\frac{1}{2}\alpha x^2 - W \right) U(x) = 0 \quad (4.8.4)$$

The equation is most easily solved after using the substitution:

$$\rho = \xi x \quad (4.8.5)$$

Combining Eqs. (4.8.4) and (4.8.5) gives:

$$\frac{d^2 U(\rho)}{d\rho^2} + \left(\frac{2Wm}{\hbar^2 \xi^2} - \frac{\alpha m}{\hbar^2 \xi^4} \rho^2 \right) U(\rho) = 0 \quad (4.8.6)$$

It is convenient to make the substitutions:

$$\gamma^4 = \frac{m\alpha}{\hbar^2} \quad \text{and} \quad \lambda = \frac{2W}{\hbar\sqrt{\alpha/m}} \quad (4.8.7)$$

With these substitutions the differential equation is:

$$U''(\rho) + (\lambda - \rho^2)U(\rho) = 0 \quad (4.8.8)$$

Primes indicate derivatives with respect to ρ . In the limit as ρ becomes large the term $\lambda U(\rho)$ becomes negligibly small. The equation and its solution take the forms:

$$U''(\rho) - \rho^2 U(\rho) = 0 \quad (4.8.9)$$

$$U(\rho) \approx e^{\pm \rho^2/2}$$

Since the positive sign is inconsistent with a localized charge physical reality, the negative sign is used in the exponential. With $H(\rho)$ as a slowly varying

function of ρ at large radii Eq. (4.8.6) may be written:

$$U(\rho) = AH(\rho)e^{-\rho^2/2} \quad (4.8.10)$$

Substituting Eq. (4.8.10) into Eq. (4.8.8) gives:

$$H''(\rho) - 2\rho H'(\rho) + (\lambda - 1)H(\rho) = 0 \quad (4.8.11)$$

The solution is most conveniently found using a series expansion:

$$H(\rho) = \sum_{s=0}^{\infty} a_s \rho^s \quad (4.8.12)$$

Substituting Eq. (4.8.12) into Eq. (4.8.11) gives:

$$\frac{a_{s+2}}{a_s} = \frac{2s - (\lambda - 1)}{(s + 2)(s + 1)} \quad (4.8.13)$$

In the limit as "s" becomes indefinitely large, the ratio of Eq. (4.8.13) goes to:

$$\frac{a_{s+2}}{a_s} \rightarrow \frac{2}{s} \quad (4.8.14)$$

The value of Eq. (4.8.14) is also equal to the ratio of the equivalent terms in the expansion of $\exp(\rho^2)$. Combining it with Eq. (4.8.10) gives the unacceptable result that it becomes infinite with ρ . Therefore an acceptable function is obtained only if the numerator of Eq. (4.8.13) vanishes. This occurs if, with n an integer:

$$\lambda = 2n + 1 \quad (4.8.15)$$

This terminates the series and makes functions $H_n(\rho)$ polynomials of largest power λ . Although the resulting polynomials, Hermite polynomials, follow from this recursion relationship we have no need for them. Combining Eqs. (4.8.13) and (4.8.7) shows the energy to be:

$$W_n = (2n + 1)\hbar\omega_0/2 \quad \text{where } \omega_0 = \sqrt{\alpha/m} \quad (4.8.16)$$

The eigenstate energies shown by Eq. (4.8.16) are equally spaced and separated by energy $\hbar\omega_0$. Therefore energy changes occur in energy units of magnitude $\hbar\omega_0$. The equation also shows the lowest possible eigenstate energy is $\hbar\omega/2$. That is, even at an absolute temperature of zero the eigenstate electron energy density remains equal to $\hbar\omega/2$.

4.9. Electron Angular Momentum, Central Force Fields

By definition, the angular momentum, l , in kinematic and operator forms is:

$$l \equiv \mathbf{r} \times \mathbf{p} = \frac{\hbar}{i} \mathbf{r} \times \nabla \quad (4.9.1)$$

The first equality follows from classical mechanics and the second from quantum theory operator notation. By Eq. (4.9.1) the operator form of the angular momentum components about each of the three axes is:

$$\begin{aligned} l_x &= \frac{\hbar}{i} \left(y \frac{\partial}{\partial z} - z \frac{\partial}{\partial y} \right) = -\frac{\hbar}{i} \left(\sin \phi \frac{\partial}{\partial \theta} + \cot \theta \cos \phi \frac{\partial}{\partial \phi} \right) \\ l_y &= \frac{\hbar}{i} \left(z \frac{\partial}{\partial x} - x \frac{\partial}{\partial z} \right) = \frac{\hbar}{i} \left(\cos \phi \frac{\partial}{\partial \theta} - \cot \theta \sin \phi \frac{\partial}{\partial \phi} \right) \\ l_z &= \frac{\hbar}{i} \left(x \frac{\partial}{\partial y} - y \frac{\partial}{\partial x} \right) = \frac{\hbar}{i} \left(\frac{\partial}{\partial \phi} \right) \end{aligned} \quad (4.9.2)$$

The first set of equalities in Eq. (4.9.2) follows directly from Eq. (4.9.1) and the second follows after changing to spherical coordinates.

Another quantity of interest is the magnitude of the angular momentum. The operator form of the square of the angular momentum follows from Eq. (4.9.2); evaluation gives:

$$l_x^2 + l_y^2 = -\hbar^2 \left(\frac{\partial^2}{\partial \theta^2} + \cot^2 \theta \frac{\partial^2}{\partial \phi^2} + \cot \theta \frac{\partial}{\partial \theta} \right) \quad l_z^2 = -\hbar^2 \left(\frac{\partial^2}{\partial \phi^2} \right)$$

The sum is:

$$l^2 = l_x^2 + l_y^2 + l_z^2 = -\hbar^2 \left(\frac{1}{\sin \theta} \frac{\partial}{\partial \theta} \left[\sin \theta \frac{\partial}{\partial \theta} \right] + \frac{1}{\sin^2 \theta} \frac{\partial^2}{\partial \phi^2} \right) \quad (4.9.3)$$

The electrostatic force fields about atomic nuclei have spherical symmetry. With spherical symmetry the potential is a function only of the magnitude of the radius and there is no angular dependence. For this case the Schrödinger equation has the form:

$$-\frac{\hbar^2}{2m} \nabla^2 U(\mathbf{r}) + \Lambda(\mathbf{r})U(\mathbf{r}) = WU(\mathbf{r}) \quad (4.9.4)$$

Introducing the Laplacian operator in spherical coordinates and rearranging terms gives:

$$\begin{aligned} &\frac{1}{\sin \theta} \frac{\partial}{\partial \theta} \left[\sin \theta \frac{\partial U(r, \theta, \phi)}{\partial \theta} \right] + \frac{1}{\sin^2 \theta} \left[\frac{\partial^2 U(r, \theta, \phi)}{\partial \phi^2} \right] \\ &= -\frac{\partial}{\partial r} \left[r^2 \frac{\partial U(r, \theta, \phi)}{\partial r} \right] + \frac{2m}{\hbar^2} [W + \Lambda(r)] r^2 U(r, \theta, \phi) \end{aligned} \quad (4.9.5)$$

To solve the Laplacian, break function $U(r, \theta, \phi)$ into functions of a single variable; that is, put $U(r, \theta, \phi)$ equal to product function $R(r)\Theta(\theta)\Phi(\phi)$ then sum over all possible solutions:

$$U(r, \theta, \phi) = \sum R(r)\Theta(\theta)\Phi(\phi) \quad (4.9.6)$$

Substituting the single function product form into Eq. (4.9.5) then multiplying by the inverse results in the equality:

$$\begin{aligned} \frac{1}{\Theta \sin \theta} \frac{d}{d\theta} \left(\sin \theta \frac{d\Theta}{d\theta} \right) + \frac{1}{\Phi \sin^2 \theta} \left(\frac{d^2\Phi}{d\phi^2} \right) \\ = -\frac{d}{Rdr} \left(r^2 \frac{dR}{dr} \right) + \frac{2m}{\hbar^2} [W + \Lambda(r)]r^2 \end{aligned} \quad (4.9.7)$$

Since the left side of the equation is only a function of angles and the right side is only a function of radius, each side is constant. It is most convenient to put the separation constant equal to $-\ell(\ell + 1)$. In a similar way, with separation constant m , the terms on the left side of Eq. (4.9.7) break into functions of θ alone and ϕ alone. The result is two complete differential equations:

$$\begin{aligned} \frac{d^2\Phi}{d\phi^2} + m^2\Phi = 0 \\ \frac{1}{\sin \theta} \frac{d}{d\theta} \left[\sin \theta \frac{d\Theta}{d\theta} \right] + \left[\ell(\ell + 1) - \frac{m^2}{\sin^2 \theta} \right] \Theta = 0 \end{aligned} \quad (4.9.8)$$

The ϕ solutions may be written either as

$$\Phi(\phi) = A_m \cos(m\phi) + B_m \sin(m\phi) \quad \text{or} \quad C_m e^{im\phi} + D_m e^{-im\phi} \quad (4.9.9)$$

Since solutions that describe physical reality cannot be multivalued, m must be an integer. If the solution is proportional to either A_m or B_m , by the third part of Eq. (4.9.2) the z -component of angular momentum is zero; if the solution is proportional to C_m or D_m the z -component of angular momentum, l_z , is:

$$l_z = \pm m\hbar \quad (4.9.10)$$

Combining Eq. (4.9.3) with the θ -dependent part of Eq. (4.9.8) shows that the angular momentum satisfies the equation:

$$l^2 = \ell(\ell + 1)\hbar^2 \quad (4.9.11)$$

The θ -equation provides a physically real solution only if ℓ is an integer and solutions with integer values of ℓ are associated Legendre functions.

The two separation constants, ℓ and m , are both integers and in the equations of quantum theory are called quantum numbers. The ranges in which such solutions exist are:

$$0 \leq \ell < \infty \quad \text{and} \quad -\ell \leq m \leq \ell \quad (4.9.12)$$

Comparison of the above shows that under all circumstances:

$$l^2 > l_z^2 \quad (4.9.13)$$

Therefore angular momentum is never entirely about a single axis. This point supports electron configurational aspects discussed in later sections.

4.10. The Coulomb Potential Source

Let a point charge of magnitude $+Ze$ attract an electron of charge $-e$. The resulting potential energy is:

$$\Lambda(r) = -\frac{Ze^2}{4\pi\epsilon r} \quad (4.10.1)$$

Combining Eq. (4.10.1) and the radial portion of Eq. (4.9.7) results in:

$$-\frac{\hbar^2}{2m} \frac{1}{r^2} \frac{d}{dr} \left(r^2 \frac{dR}{dr} \right) - \frac{Ze^2}{4\pi\epsilon r} R + \frac{\ell(\ell+1)\hbar^2}{2mr^2} R = WR \quad (4.10.2)$$

The total energy W is less than or greater than zero respectively for bound or free electrons. This equation is most easily solved by introducing the parameter α and variable ρ where, by definition:

$$\rho = \alpha r \quad (4.10.3)$$

It is helpful to introduce the additional definitions:

$$\alpha^2 = \frac{8m|W|}{\hbar^2} \quad \text{and} \quad n = \frac{Ze^2}{4\pi\epsilon\hbar} \sqrt{\frac{m}{2|W|}} = \frac{Ze^2 m}{2\pi\epsilon\alpha\hbar^2} \quad (4.10.4)$$

If the electron energy is negative, substituting ρ back into Eq. (4.10.2) and using Eq. (4.10.4) gives:

$$\frac{1}{\rho^2} \frac{d}{d\rho} \left(\rho^2 \frac{dR}{d\rho} \right) - \frac{\ell(\ell+1)}{\rho^2} R + \frac{nR}{\rho} - \frac{R}{4} = 0 \quad (4.10.5)$$

To solve Eq. (4.10.5), begin with the asymptotic limit at infinity. As ρ increases without limit the asymptotic differential equation is:

$$\frac{d^2 R}{d\sigma^2} - \frac{R}{4} = 0 \quad (4.10.6)$$

The solution of Eq. (4.10.6) is:

$$R(\rho) = F(\rho)e^{-\rho/2} + G(\rho)e^{\rho/2} \quad (4.10.7)$$

The conditions on Eq. (4.10.6) are that, in the asymptotic limit of large radius, $F(\rho)$ and $G(\rho)$ must change much more slowly with ρ than the exponential terms and, since the total charge is finite, function $R(\rho)$ must vanish at infinity. It follows that since a non-zero value of function $G(\rho)$ does not represent physical reality it is multiplied by zero. Substituting the remaining form $F(\rho)e^{-\rho/2}$ into Eq. (4.10.5) results in the differential equation:

$$\frac{d^2F}{d\rho^2} + \left(\frac{2}{\rho} - 1\right) \frac{dF}{d\rho} + \left(\frac{n-1}{\rho} - \frac{\ell(\ell+1)}{\rho^2}\right) F = 0 \quad (4.10.8)$$

A convenient solution method for Eq. (4.10.8) is a power series expansion. The solution procedure begins by forming the summation:

$$F(\rho) = \rho^s \sum_{j=0}^{\infty} a_j \rho^j \quad (4.10.9)$$

Solution requires that $a_0 \neq 0$ and $a_j \geq 0$. Substituting Eq. (4.10.9) into Eq. (4.10.8) results in the sum:

$$\begin{aligned} & [s(s+1) - \ell(\ell+1)]\rho^{-2} + \sum_{j=0}^{\infty} \{[(s+j+1)(s+j+2) - \ell(\ell+1)]a_{j+1} \\ & - (s+j+1-n)a_j\}\rho^{j-1} = 0 \end{aligned} \quad (4.10.10)$$

Since a_0 is not equal to zero, the first term of Eq. (4.10.10) requires that either $s = \ell$ or $s = -(\ell+1)$. Since the latter is singular at the origin, it cannot represent physical reality. Substituting $s = \ell$ into Eq. (4.10.10) results in the coefficient ratio:

$$\frac{a_{j+1}}{a_j} = \frac{j+1+\ell-n}{(j+1)(j+2\ell+2)} \quad (4.10.11)$$

As index 'j' increases without limit Eq. (4.10.11) goes asymptotically to the index of the expansion for e^ρ . Combining this with Eq. (4.10.7) shows that the radial function is proportional to $e^{\rho/2}$ in the limit of very large ρ , a physically unacceptable result. Hence a nontrivial solution of $F(\rho)$ exists if and only if the series terminates, and the series terminates only if n is an

integer. For that case, Eq. (4.10.4) shows that state energy W_n is equal to:

$$W_n = -\frac{mZ^2e^4}{32\pi^2\varepsilon^2n^2\hbar^2} \quad (4.10.12)$$

This result shows that an infinite number of energy state values exist, that the energy is independent of quantum numbers ℓ and m , and that the state energy varies as the inverse square of quantum number n .

It is helpful to define radius r_0 as:

$$r_0 = \frac{2Z}{n\alpha} \quad \text{hence} \quad r_0 = \frac{4\pi\varepsilon\hbar^2}{me^2} \quad (4.10.13)$$

Evaluating Eq. (4.10.13) shows that:

$$r_0 = 5.29172 \times 10^{-11} \text{ m} \quad (4.10.14)$$

By definition, r_0 is the Bohr radius. The electrostatic energy may also be written as:

$$W_n = \frac{Ze^2}{8\pi\varepsilon} \langle 1/r \rangle \quad (4.10.15)$$

Combining Eqs. (4.10.12), (4.10.13), and (4.10.15) shows that:

$$\langle 1/r \rangle = Z/(n^2r_0) \quad (4.10.16)$$

In the limit of large values of n , the energy goes to zero and the expectation value of the radius of the electron state becomes infinite: the electron is distributed over all space.

To solve for the radial function, rewrite Eq. (4.10.11) as:

$$a_{j+1} = \frac{(j + \ell + 1 - n)}{(j + 2\ell + 2)(j + 1)} a_j \quad (4.10.17)$$

From Eq. (4.10.17), each coefficient gives:

$$a_j = (-1)^j \left(\frac{(n - \ell - 1)!(2\ell + 1)!}{(n - j - \ell - 1)!j!(2\ell + j + 1)!} \right) a_0$$

To put this notation in agreement with common usage, define a_0 to be:

$$a_0 = -\frac{(n + \ell)!^2}{(n - \ell - 1)!(2\ell + 1)!}$$

Combining gives:

$$a_j = (-1)^{j+1} \left\{ \frac{(n + \ell)!^2}{(n - j - \ell - 1)!j!(2\ell + j + 1)!} \right\} \quad (4.10.18)$$

Table 4.10.1. Values of $R_n^\ell(\sigma)$ for $n = 1-4$.

| | $n = 1$ | $n = 2$ | $n = 3$ | $n = 4$ |
|-----------------|----------------|------------------------------|-------------------------------------|--|
| $R_n^0(\sigma)$ | $-e^{-\rho/2}$ | $-(2)!(2 - \rho)e^{-\rho/2}$ | $-3(6 - 6\rho + \rho^2)e^{-\rho/2}$ | $-24(4 - 6\rho + 2\rho^2 - \rho^3)e^{-\rho/2}$ |
| $R_n^1(\sigma)$ | | $-(3)!\rho e^{-\rho/2}$ | $-(4)!(4 - \rho)\rho e^{-\rho/2}$ | $-60(20 - 10\rho + 3\rho^2)\rho e^{-\rho/2}$ |
| $R_n^2(\sigma)$ | | | $-(5)!\rho^2 e^{-\rho/2}$ | $-(6)!(6 - \rho)\rho^2 e^{-\rho/2}$ |
| $R_n^3(\sigma)$ | | | | $-(7)!\rho^3 e^{-\rho/2}$ |

It follows that:

$$\ell < n \tag{4.10.19}$$

Combining all results shows that $R(\rho)$ depends upon both quantum numbers n and ℓ , and is equal to:

$$R_n^\ell(\rho) = \rho^\ell e^{-\rho/2} \sum_{j=0}^{n-\ell-1} (-1)^{j+1} \frac{(n + \ell)!^2 \rho^j}{(n - j - \ell - 1)! j! (2\ell + j + 1)!} \tag{4.10.20}$$

Functional values for $n = 1$ through 4 are listed in Table 4.10.1.

Wave function normalization follows from Eq. (4.10.20), and the integral result:

$$I_n^\ell = \int_0^\infty \rho^2 d\rho R_n^\ell(\rho) R_q^\ell(\rho) = \frac{2n(n + \ell)!^3}{(n - \ell - 1)!} \delta(n, q) \tag{4.10.21}$$

The first row of Table 4.10.1 shows that the largest value of the function occurs at the origin. Including the origin, there are a total of ℓ maxima as a function of radius. The remaining rows show that the radius raised to power ℓ multiplies each function. Therefore the value is equal to zero at the origin for all except $\ell = 0$ and the radius of the region with a negligibly small value of charge increases with increasing values of ℓ .

4.11. Hydrogen Atom Eigenfunctions

The full expression for an eigenfunction of a trapping spherical potential has the form:

$$U_{n\ell m}(r, \theta, \phi) = A_{n\ell m} R_n^\ell(\alpha_n r) P_\ell^m(\cos \theta) e^{-im\phi} \tag{4.11.1}$$

It is shown in Secs. 4.9 and 4.10 that both quantum numbers n and ℓ are integers. A separate requirement that ℓ and m be integers follows from

the requirement that the full range of solid angle be available for angular solutions. Also since the full range of angles are available the coefficients of Legendre functions of the second kind are all equal to zero. From the theory of Legendre polynomials:

$$\int_0^\pi \sin \theta \, d\theta [P_\ell^m(\cos \theta)]^2 = \frac{4\pi}{2\ell + 1} \frac{(\ell + m)!}{(\ell - m)!} \quad (4.11.2)$$

Using Eqs. (4.10.21) and (4.11.2) to solve for the total probability of each state, then normalizing that value to unity, permits solving for the constant coefficients of Eq. (4.11.1). The result is:

$$|A_{n\ell m}| = \left\{ \frac{\alpha_n^3}{4\pi n} \frac{(n - \ell - 1)! (2\ell + 1)(\ell - m)!}{(n + \ell)!^3 (\ell + m)!} \right\}^{0.5} \quad (4.11.3)$$

Each wave function has $(n - \ell)$ zeros, including infinity, and undergoes $(n - \ell)$ nodes (functional maxima) as a function of radius. Several complete eigenfunctions are listed in Table 4.11.1.

The energy levels of Eq. (4.10.12) show that the energy depends upon quantum number n but not upon quantum numbers ℓ and m . In common with other boundary value problems only eigenfunction solutions can exist. Parameter r_0 of Eq. (4.10.13) is a normalizing radial factor that shows atomic radii to be of the order of 0.1 nm.

Since wave functions with $m = 0$ have spherical symmetry the charge density associated with them produce monopole electrostatic fields. There is a charge density node at the origin and $(n - 1)$ others at increasing values of radius. Wave functions with $m = 1$ have bilateral symmetry. There is a null in the charge density at the origin and $(n - 1)$ nodes. Wave functions with $m = 2$ have quadrilateral symmetry. There is a charge density null at the origin and $(n - 2)$ nodes, etc.

For $n = 1$, both ℓ and m are equal to zero and there is but one eigenfunction. There is no degeneracy. For $n = 2$ there are two types of solutions: one is $\ell = 1$ with an accompanying triplet of state values of m : $m = -1, 0, +1$. The other is the singlet $\ell = 0$ with an accompanying singlet state value of m : $m = 0$. Since the energy depends only upon n , and since for each value of ℓ there are $(2\ell + 1)$ values of m , the result is a $(2\ell + 1)$ fold energy degeneracy. For each value of n there are $n - 1$ values of ℓ . Hence the total energy degeneracy is:

$$\sum_{\ell=1}^{n-1} (2\ell + 1) = n^2 \quad (4.11.4)$$

That is, there are n^2 possible solutions for each value of energy.

Table 4.11.1. Hydrogen atom eigenfunctions for $n = 1$ through 3, $(1/\langle r \rangle)$ depends upon quantum number n only.

| | |
|--|--|
| $U_{100} = \sqrt{\frac{1}{\pi}} \left(\frac{Z}{r_0}\right)^{3/2} e^{-Zr/r_0}$ | $\frac{1}{\langle 1/r \rangle} = \frac{r_0}{Z}$ |
| $U_{200} = \frac{1}{\sqrt{32\pi}} \left(\frac{Z}{r_0}\right)^{3/2} \left(2 - \frac{Zr}{r_0}\right) e^{-Zr/2r_0}$ | $\frac{1}{\langle 1/r \rangle} = \frac{4r_0}{Z}$ |
| $U_{210} = \frac{1}{\sqrt{32\pi}} \left(\frac{Z}{r_0}\right)^{3/2} \left(\frac{Zr}{r_0}\right) e^{-Zr/2r_0} \cos \theta$ | |
| $U_{21\pm 1} = \frac{1}{8\sqrt{\pi}} \left(\frac{Z}{r_0}\right)^{3/2} \left(\frac{Zr}{r_0}\right) e^{-Zr/2r_0} \sin \theta e^{\pm i\phi}$ | |
| $U_{300} = \frac{1}{81\sqrt{3\pi}} \left(\frac{Z}{r_0}\right)^{3/2} \left(27 - 18\frac{Zr}{r_0} + 2\frac{Z^2 r^2}{r_0^2}\right) e^{-Zr/3r_0}$ | $\frac{1}{\langle 1/r \rangle} = \frac{9r_0}{Z}$ |
| $U_{310} = \frac{\sqrt{2}}{81\sqrt{\pi}} \left(\frac{Z}{r_0}\right)^{3/2} \left(6 - \frac{Zr}{r_0}\right) \left(\frac{Zr}{r_0}\right) e^{-Zr/3r_0} \cos \theta$ | |
| $U_{31\pm 1} = \frac{1}{81\sqrt{\pi}} \left(\frac{Z}{r_0}\right)^{3/2} \left(6 - \frac{Zr}{r_0}\right) \left(\frac{Zr}{r_0}\right) e^{-Zr/3r_0} \sin \theta e^{\pm i\phi}$ | |
| $U_{320} = \frac{1}{81\sqrt{6\pi}} \left(\frac{Z}{r_0}\right)^{3/2} \left(\frac{Z^2 r^2}{r_0^2}\right) e^{-Zr/3r_0} (3\cos^2 \theta - 1)$ | |
| $U_{32\pm 1} = \frac{1}{81\sqrt{\pi}} \left(\frac{Z}{r_0}\right)^{3/2} \left(\frac{Z^2 r^2}{r_0^2}\right) e^{-Zr/3r_0} \sin \theta \cos \theta e^{\pm i\phi}$ | |
| $U_{32\pm 2} = \frac{1}{162\sqrt{\pi}} \left(\frac{Z}{r_0}\right)^{3/2} \left(\frac{Z^2 r^2}{r_0^2}\right) e^{-Zr/3r_0} \sin^2 \theta e^{\pm i2\phi}$ | |

The degeneracy is lifted if the electron system is immersed in a static electric or magnetic field. The $m = 0$ states are more closely tied to the nucleus than are the $m = \pm 1$ states, which extend further outward from the nucleus. Therefore a static electric field affects the different states differently and removes the degeneracy. This is the Stark effect. The $m = 0$ state supports no angular momentum and produce no net magnetic moment. The $m = \pm 1$ states do support angular momentum and do produce a magnetic moment. Hence, the states respond differently to an applied static magnetic field. The different response removes the energy degeneracy and the result is the Zeeman effect.

4.12. Perturbation Analysis

Consider an atom immersed in an external force field. So long as the applied field and its gradient are much less than those of the trapping potential the wave functions retain their original character and solutions entail a re-scrambling of the occupied states. As an example, consider the special case of an atom immersed in static, externally applied electric field with magnitude small compared with the Coulomb field. Modifications result in a change of occupational probability of the original eigenfunctions.

To show that this is true, let the Hamiltonian operator H_0 characterize the energy of an isolated electron system. The resulting total eigenfunction is a sum over wave functions that are solutions of the Schrödinger equation with operator H_0 . Let one possible eigenfunction be U_{n0} . The possible eigenfunctions and the corresponding energies W_{n0} are known and each satisfies the relationship:

$$\int (U_{n0}^* H_0 U_{n0}) dV = W_{n0} \int U_{n0}^* U_{n0} dV \quad (4.12.1)$$

A small external force field is applied that modifies the Hamiltonian to the operational form:

$$H = H_0 + H_1 \quad (4.12.2)$$

Since the external field is controllable by external means, for example the intensity of an applied laser beam, the actual operational form may be written as:

$$H = H_0 + \alpha H_1 \quad (4.12.3)$$

An experimenter may control the value of α from zero to one. The eigenfunctions and energies are functions of α . If the applied force is small enough a power series in powers of α will converge, with the result that:

$$\begin{aligned} U_n &= U_{n0} + \alpha U_{n1} + \alpha^2 U_{n2} + \cdots = \sum_r \alpha^r U_{nr} \\ W_n &= W_{n0} + \alpha W_{n1} + \alpha^2 W_{n2} + \cdots = \sum_s \alpha^s W_{ns} \end{aligned} \quad (4.12.4)$$

The “0” subscripts form the total solution in the absence of the external field, the “1” subscripts describe the first order correction, the “2” subscripts describe the second order correction, etc. For small fields, only the

correction terms that are first order in α are large enough to be of interest and terms proportional to α^2 may be ignored. The first order terms are:

$$\begin{aligned}
 & \int \{ (U_{n0}^* + \alpha U_{n1}^*) (H_0 + \alpha H_1) (U_{n0} + \alpha U_{n1}) \} dV \\
 &= \int \{ (U_{n0}^* + \alpha U_{n1}^*) (W_{n0} + \alpha W_{n1}) (U_{n0} + \alpha U_{n1}) \} dV \\
 &\cong \int \{ U_{n0}^* H_0 U_{n0} + \alpha [U_{n1}^* H_0 U_{n0} + U_{n0}^* H_1 U_{n0} + U_{n0}^* H_0 U_{n1}] \} dV \\
 &= \int \{ W_{n0} U_{n0}^* U_{n0} + \alpha [W_{n0} U_{n1}^* U_{n0} + W_{n1} U_{n0}^* U_{n0} + W_{n0} U_{n0}^* U_{n1}] \} dV
 \end{aligned} \tag{4.12.5}$$

Confining attention to the last equality of Eq. (4.12.5), the first terms of the first and last integrals are equal and may be subtracted out. The procedure may be repeated for the first terms within the square brackets. Applying the Hermitian property of quantum operators to the last terms within the square brackets shows that they too are equal and they, too, may be subtracted out of the equation. Eliminating these three terms leaves the center terms within the square brackets:

$$\int U_{n0}^* H_1 U_{n0} dV = W_{n1} \int U_{n0}^* U_{n0} dV = W_{n1} \tag{4.12.6}$$

This is the first order correction term. Equation (4.12.6) shows that it is not necessary to know the corrected wave function to calculate first order energy changes. It is only necessary to know how the first order Hamiltonian correction affects unperturbed eigenfunctions.

4.13. Non-Ionizing Transitions

If the Hamiltonian operator H_0 , eigenfunctions ψ_n , and energies W_n apply to an electron in an unperturbed atom, Schrödinger's equation is:

$$H_0 \psi_n(\mathbf{r}_1, t) = W_n \psi_n(\mathbf{r}_1, t) \tag{4.13.1}$$

The total wave function is a weighed sum over all possible wave functions:

$$\Psi(\mathbf{r}_1, t) = \sum_n a_n \psi_n(\mathbf{r}_1, t) \tag{4.13.2}$$

Next, let a second electron be attached to the same atom, affected by the same Hamiltonian operator, and have the same set of eigenfunctions and

energies but a different set of coefficients:

$$\Psi(\mathbf{r}_2, t) = \sum_n b_n \psi_n(\mathbf{r}_2, t) \quad (4.13.3)$$

Make the definitions:

$$\begin{aligned} \psi_{mn}(\mathbf{r}, t) &= \psi_m(\mathbf{r}_1, t) \psi_n(\mathbf{r}_2, t) \\ U_{mn}(\mathbf{r}) &= u_m(\mathbf{r}_1) u_n(\mathbf{r}_2) \\ W_{mn} &= W_m + W_n \end{aligned}$$

The equation that describes both electrons is:

$$\begin{aligned} \Psi(\mathbf{r}, t) &= \sum_m \sum_n c_{mn} \psi_{mn}(\mathbf{r}, t) \\ &= \sum_m \sum_n a_m b_n U_{mn}(\mathbf{r}_1, \mathbf{r}_2) \exp\left(\frac{iW_{mn}t}{\hbar}\right) \end{aligned} \quad (4.13.4)$$

If a perturbing field is applied that changes the Hamiltonian operator from H_0 to $H_0 + H_1$, the wave functions remain unaltered and the probability coefficients, c_{mn} , become time dependent. To show this, write Eq. (4.13.4) in the form:

$$(H_0 + H_1) \sum_m \sum_n c_{mn}(t) \psi_{mn}(\mathbf{r}, t) = \frac{\hbar}{i} \frac{\partial}{\partial t} \sum_m \sum_n c_{mn}(t) \psi_{mn}(\mathbf{r}, t) \quad (4.13.5)$$

Writing out the equation term by term gives:

$$\begin{aligned} &\sum_m \sum_n [c_{mn}(t) H_0 \psi_{mn} + c_{mn}(t) H_1 \psi_{mn}] \\ &= \sum_m \sum_n \left[\frac{\hbar}{i} c_{mn}(t) \frac{\partial \psi_{mn}(t)}{\partial t} + \frac{\hbar}{i} \frac{\partial c_{mn}(t)}{\partial t} \psi_{mn} \right] \end{aligned} \quad (4.13.6)$$

The first terms on either side are equal; subtracting them leaves the equality:

$$\sum_m \sum_n c_{mn}(t) H_1 \psi_{mn}(\mathbf{r}, t) = \frac{\hbar}{i} \sum_m \sum_n \frac{\partial c_{mn}(t)}{\partial t} \psi_{mn}(\mathbf{r}, t) \quad (4.13.7)$$

Multiplying through by $\psi_{pq}(\mathbf{r}, t)$ and integrating over all space gives:

$$\frac{d}{dt} c_{pq}(t) = \frac{i}{\hbar} \sum_m \sum_n c_{mn}(t) \int \psi_{pq}^* H_1 \psi_{mn} dV \quad (4.13.8)$$

The integral is over the volume occupied by both electrons. Make the definition:

$$\langle pq | H_1 | mn \rangle = \int U_{pq}^* H_1 U_{mn} dV \quad (4.13.9)$$

The terms of Eq. (4.13.9) are, by definition, the matrix elements of interaction potential H_1 . With the aid of Eq. (4.5.13), Eq. (4.13.8) may be written in the form:

$$\frac{dc_{pq}(t)}{dt} = \frac{i}{\hbar} \sum_m \sum_n c_{mn} \langle pq | H_1 | mn \rangle \exp \left[\frac{i(W_m + W_n - W_p - W_q)t}{\hbar} \right] \quad (4.13.10)$$

As a special case suppose that at time $t = 0$ the electrons are in states m and n and find the probability, as a function of time, that they will occupy states p and q . The initial condition is that

$$\frac{dc_{pq}(t)}{dt} = \frac{i}{\hbar} \langle pq | H_1 | mn \rangle \exp \left[\frac{i(W_p + W_q - W_m - W_n)t}{\hbar} \right] \quad (4.13.11)$$

Coefficient c_{mn} is equal to one at time $t = 0$, when all other coefficients are equal to zero. Make the definition that:

$$\Delta W = W_p + W_q - W_m - W_n$$

Restricting analyses to times short enough so that c_{mn} remains nearly equal to one, the integral over time shows the initial time dependence of the coefficient to be:

$$c_{pq}(t) = \langle pq | H_1 | mn \rangle \frac{\exp(i\Delta W t / \hbar) - 1}{\Delta W} \quad (4.13.12)$$

The probability of state (p, q) being occupied is:

$$c_{pq}^* c_{pq} = 4 \langle pq | H_1 | mn \rangle^2 \frac{\sin^2(\Delta W t / 2\hbar)}{(\Delta W)^2} \quad (4.13.13)$$

Equation (4.13.13) shows that the probability that a particular transition will occur is proportional to the square of the matrix element. The magnitude of the matrix element depends upon both sets of quantum numbers, pq and mn . Transitions are “forbidden” if the matrix element is equal to zero. Since the ratio $\sin^2(x)/x^2$ has maximum magnitude at $x = 0$, it follows that energy conservation requires that the most probable value of ΔW be zero.

4.14. Absorption and Emission of Radiation

The purpose of this section is to describe the absorption and emission, i.e. reception and transmission, of radiation by an atom with a full complement of electrons. The atom is immersed within an externally applied plane wave

of radian frequency ω where the wavelength is much greater than the initial size of an atom.

The calculation begins with the relationships between the Hamiltonian, H , the state energy written in operator form, and the time dependence of the applied field as described by the time-dependent Schrödinger equation. The relationships are, see Eq. (4.5.11):

$$\frac{\hbar}{i} \frac{\partial}{\partial t} \psi_n(\mathbf{r}, t) = H \psi_n(\mathbf{r}, t) = W_n \psi_n(\mathbf{r}, t) \quad (4.14.1)$$

It follows from Eqs. (4.5.13) and (4.5.14) that the time-dependent eigenfunctions are related to the time-independent ones as:

$$\psi_n(\mathbf{r}, t) = U_n(\mathbf{r}) e^{iW_n t / \hbar} \quad (4.14.2)$$

The complete wave function $\Psi(\mathbf{r}, t)$ is a weighted sum over all possible eigenfunctions:

$$\Psi(\mathbf{r}, t) = \sum_n c_n(t) U_n(\mathbf{r}) e^{i\omega_n t} \quad (4.14.3)$$

As in Sec. 4.13, it is possible that the probability coefficients are time dependent. Substituting the first order perturbation equation, Eq. (4.12.6), into Eqs. (4.14.1) and (4.14.3) gives the differential equation that describes the rate of change of the coefficients as a function of the coefficients themselves:

$$\frac{\hbar}{i} \sum_n \frac{\partial c_n(t)}{\partial t} U_n(\mathbf{r}) e^{i\omega_n t} = \sum_n c_n(t) H_1 U_n(\mathbf{r}) e^{i\omega_n t} \quad (4.14.4)$$

Symbol H_1 represents the operator form of the modification to the Hamiltonian due to the perturbation. This equation shows that the primary affect of the applied field is to make the state coefficients time dependent.

The electric field intensity in the perturbing plane wave is $\mathbf{E}(\mathbf{r}, t)$ and it varies with time as $\cos(\omega t)$. Although $\mathbf{E}(\mathbf{r}, t)$ is a real function, it is convenient to rewrite it in complex terms as the sum of complex conjugate functions:

$$\mathbf{E}(\mathbf{r}, t) = \mathbf{E}_0 e^{i(\omega t - \mathbf{k} \cdot \mathbf{r})} + \text{c.c.} \quad (4.14.5)$$

For atoms of diameter much less than a wavelength, the perturbing energy is approximately equal to:

$$H_1 = -e\mathbf{E}(t) \cdot \mathbf{r}(t) \quad (4.14.6)$$

Combining Eq. (4.14.6) with Eq. (4.14.4) gives:

$$\begin{aligned} & \sum_n \frac{\partial c_n(t)}{\partial t} e^{i\omega_n t} U_n(\mathbf{r}) \\ &= -\frac{ie}{\hbar} \sum_n \left\{ e^{i(\omega_n t + \omega t - \mathbf{k} \cdot \mathbf{r})} + e^{i(\omega_n t - \omega t + \mathbf{k} \cdot \mathbf{r})} \right\} c_n(t) \mathbf{E}_0 \cdot \mathbf{r} U_n(\mathbf{r}) \end{aligned} \quad (4.14.7)$$

To determine the effect of interaction between states n and k , multiply Eq. (4.14.7) through by $U_k(\mathbf{r})$ and integrate over all space. The result is:

$$\begin{aligned} \frac{\partial c_k(t)}{\partial t} &= -\frac{ie}{\hbar} \sum_n c_n(t) \left\{ e^{i\mathbf{k} \cdot \mathbf{r}^{i(\omega_n - \omega_k - \omega)t}} \right. \\ &\quad \left. + e^{-i\mathbf{k} \cdot \mathbf{r} e^{i(\omega_n - \omega_k + \omega)t}} \right\} \mathbf{E}_0 \cdot \langle U_k | \mathbf{r} | U_n \rangle \end{aligned} \quad (4.14.8)$$

Symbol $\langle U_k | \mathbf{r} | U_n \rangle$ is defined in Eq. (4.13.9). To simplify the problem consider as a boundary condition that at initial time $t = 0$ only the single state 'n' is occupied by an electron. Therefore only c_n is different from zero and it is equal to one. Doing the time integral of Eq. (4.14.8) under these circumstances gives the initial solution:

$$\begin{aligned} c_k(t) &= -\frac{ie}{\hbar} \left\{ e^{i\mathbf{k} \cdot \mathbf{r}} \left[\frac{e^{i(\omega_n - \omega_k - \omega)t} - 1}{(\omega_n - \omega_k - \omega)} \right] + e^{-i\mathbf{k} \cdot \mathbf{r}} \left[\frac{e^{i(\omega_n - \omega_k + \omega)t} - 1}{(\omega_n - \omega_k + \omega)} \right] \right\} \\ &\quad \times \mathbf{E}_0 \cdot \langle U_k | \mathbf{r} | U_n \rangle \end{aligned} \quad (4.14.9)$$

The exponential phase factor may be expanded as $[e^{-i\mathbf{k} \cdot \mathbf{r}} \approx 1 - i\mathbf{k} \cdot \mathbf{r} + \dots]$. The first order value, one, is sufficient since atomic sizes are much less than a wavelength. Making the replacement shows that the square of the magnitude of Eq. (4.14.9) may be written as:

$$|c_k(t)|^2 = (2eE_0)^2 \langle U_k | \mathbf{r} | U_n \rangle^2 \left\{ \frac{\sin^2 \left[\frac{1}{2\hbar} (W_n - W_k \pm \hbar\omega) t \right]}{(W_n - W_k \pm \hbar\omega)^2} \right\} \quad (4.14.10)$$

The term within the curly brackets of Eq. (4.14.10) is significantly different from zero only if the argument of the sine is equal to zero. This requires that:

$$\omega_k = \omega_n \pm \omega \quad (4.14.11)$$

Multiplying Eq. (4.14.11) through by \hbar shows that $(W_k - W_n) = \pm \hbar\omega$. If $(W_k > W_n)$ energy $\hbar\omega$ is added to the system and the transition is associated with energy absorption. If $(W_k < W_n)$ energy $\hbar\omega$ is removed from the system and the transition is associated with energy emission. Therefore, it seems reasonable to ascribe the upper or lower sign of Eq. (4.14.11) respectively to energy absorption or emission by the electron. Equation (4.14.11)

also shows that the transition probabilities for emission and absorption are the same. Equation (4.14.10) is valid only over times so small that $c_n(t)$ remains nearly equal to one and all other $c_k(t)$ remain much less than one. For simplicity, the development is carried out with this restriction.

If the radius of the atom is equal to the first Bohr orbit, see Eq. (4.10.14), and the wavelength is at the center of the optical band, 500 nm:

$$2kr = 6.65 \times 10^{-4} (n^2/Z) \quad (4.14.12)$$

If n is small enough so the magnitude of Eq. (4.14.12) is much less than one, the perturbation expansion of Eq. (4.12.4) converges rapidly and calculated results may be limited to the first correction term only.

4.15. Electric Dipole Selection Rules for One Electron Atoms

To obtain the probability of an energy exchange by absorption or emission of radiation it is necessary to evaluate the matrix element. For an atom with only one electron, the wave functions are given by Eq. (4.11.1) and in Table 4.11.1. The components of the matrix elements directed along the three rectangular coordinate axes are:

$$\begin{aligned} X &= \int_0^\infty r^2 dr \int_0^\pi \sin \theta d\theta \int_0^{2\pi} U_{n'\ell'm'}^* U_{n\ell m} r \sin \theta \cos \phi d\phi \\ Y &= \int_0^\infty r^2 dr \int_0^\pi \sin \theta d\theta \int_0^{2\pi} U_{n'\ell'm'}^* U_{n\ell m} r \sin \theta \sin \phi d\phi \\ Z &= \int_0^\infty r^2 dr \int_0^\pi \sin \theta d\theta \int_0^{2\pi} U_{n'\ell'm'}^* U_{n\ell m} r \cos \theta d\phi \end{aligned} \quad (4.15.1)$$

The total wave function is related to the individual functions as:

$$U_{n\ell m}(r, \theta, \phi) = A_{n\ell m} R_n^\ell(\alpha_n r) P_\ell^m(\cos \theta) e^{-im\phi} \quad (4.15.2)$$

Combining the first of Eq. (4.15.1) with Eq. (4.15.2) gives:

$$\begin{aligned} X &= A_{n'\ell'm'}^* A_{n\ell m} \int_0^\infty R_{n'}^{\ell'} R_n^\ell r^3 dr \int_0^\pi P_{\ell'}^{m'} P_\ell^m \sin^2 \theta d\theta \\ &\quad \times \int_0^{2\pi} e^{i(m'-m)\phi} \cos \phi d\phi \end{aligned} \quad (4.15.3)$$

Evaluation of the azimuth angle integral gives:

$$\int_0^{2\pi} d\phi \cos \phi [\cos(m'-m)\phi + i \sin(m'-m)\phi] = \pi \delta(m', m \pm 1) \quad (4.15.4)$$

Incorporating Eq. (4.15.4) then using the identity of Table A.21.1.7, gives:

$$\begin{aligned}\sin^2 \theta P_{\ell'}^{m+1} P_{\ell}^m &= \frac{1}{2\ell+1} \sin \theta (P_{\ell+1}^{m+1} - P_{\ell-1}^{m+1}) P_{\ell'}^{m+1} \\ \sin^2 \theta P_{\ell'}^{m-1} P_{\ell}^m &= \frac{1}{2\ell'+1} \sin \theta (P_{\ell'+1}^m - P_{\ell'-1}^m) P_{\ell}^m\end{aligned}\quad (4.15.5)$$

Combining Eqs. (4.15.3) and (4.15.5) shows that for both values of m the zenith angle integral of Eq. (4.15.3) has the form:

$$\frac{1}{2\ell+1} \int_0^{\pi} \sin \theta (P_{\ell+1}^{m+1} - P_{\ell-1}^{m+1}) P_{\ell'}^{m+1} d\theta$$

Consider the integral:

$$\begin{aligned}&\int_0^{\pi} P_{\ell'}^{m'} P_{\ell}^m \sin^2 \theta d\theta \int_0^{2\pi} \cos \phi e^{i(m'-m)\phi} d\phi \\ &= \frac{2\pi \delta(m', m \pm 1)}{(2\ell+1)} \left\{ \frac{1}{(2\ell+3)} \frac{(\ell+m+2)!}{(\ell-m)!} \delta(\ell', \ell+1) \right. \\ &\quad \left. - \frac{1}{(2\ell-1)} \frac{(\ell+m)!}{(\ell-m-2)!} \delta(\ell', \ell-1) \right\}\end{aligned}\quad (4.15.6)$$

The integral is different from zero only if:

$$\ell' = \ell \pm 1 \quad (4.15.7)$$

Combining the second of Eq. (4.15.1) with Eq. (4.15.2) gives similar results and combining the last of Eq. (4.15.1) with Eq. (4.15.2) gives:

$$Z = A_{n'\ell'm'}^* A_{n\ell m} \int_0^{\infty} R_{n'}^{\ell'} R_n^{\ell} r^3 dr \int_0^{\pi} P_{\ell'}^{m'} P_{\ell}^m \sin \theta \cos \theta d\theta \int_0^{2\pi} e^{i(m'-m)\phi} d\phi \quad (4.15.8)$$

Table A.21.1.4, shows that:

$$\sin \theta \cos \theta P_{\ell'}^m P_{\ell}^m = \frac{1}{2\ell+1} \sin \theta [(\ell-m+1)P_{\ell+1}^m - (\ell+m)P_{\ell-1}^m] P_{\ell'}^m \quad (4.15.9)$$

Combining with the zenith angle integral of Eq. (4.15.7) leaves the form:

$$\frac{1}{2\ell+1} \int_0^{\pi} \sin \theta [(\ell-m+1)P_{\ell+1}^m - (\ell+m)P_{\ell-1}^m] P_{\ell'}^m d\theta \quad (4.15.10)$$

Consider the integrals:

$$\begin{aligned} & \frac{1}{(2\ell+1)} \int_0^\pi \sin\theta [(\ell-m+1)P_{\ell+1}^m - (\ell+m)P_{\ell-1}^m] P_{\ell'}^m d\theta \int_0^{2\pi} d\phi e^{i(m'-m)\phi} \\ &= \frac{4\pi\delta(m',0)}{(2\ell+1)} \left\{ (\ell-m+1) \frac{(\ell+m+1)!}{(\ell-m+1)} \delta(\ell',\ell+1) \right. \\ & \quad \left. - (\ell+m) \frac{(\ell+m-1)!}{(\ell-m-1)} \delta(\ell',\ell-1) \right\} \end{aligned} \quad (4.15.11)$$

Like Eqs. (4.15.6), (4.15.11) is different from zero only if Eq. (4.15.7) is satisfied. Since the radial integrer provides no restrictions on n , electric dipole transitions occur only if:

$$\Delta\ell = \pm 1 \quad \text{and} \quad \Delta m = \pm 1 \quad \text{or} \quad 0 \quad (4.15.12)$$

The interpretation of Eqs. (4.9.10) and (4.15.12) is that the z -component of radiated angular momentum is equal to zero or to \hbar . Since the angular momentum of the source changes by that amount, it must be carried by the radiation.

4.16. Electron Spin

It was known before Schrödinger's equation was known that a complete description of electronic events requires four quantum numbers. An integral part of Dirac's equations is that electron characteristics include more than charge and mass: there is a permanent angular momentum and a permanent magnetic dipole moment.

The angular momentum of a particle in terms of its mass and velocity is:

$$\mathbf{l} = m \mathbf{r} \times \mathbf{v} \quad (4.16.1)$$

By definition \mathbf{l} is the angular momentum, \mathbf{r} the radius about a fixed point, and \mathbf{v} the velocity of the point mass. If the mass also supports charge q , the magnetic moment is:

$$\boldsymbol{\Omega} = q\mathbf{r} \times \mathbf{v}/2 \quad (4.16.2)$$

Comparison of Eqs. (4.16.1) and (4.16.2) shows that

$$\boldsymbol{\Omega} = q\mathbf{l}/2m \quad (4.16.3)$$

Thus the expected relationship between an electron's magnetic and mechanical moments, Eq. (4.16.3), is equal to:

$$\boldsymbol{\Omega} = -e\mathbf{l}/2m \quad (4.16.4)$$

However, the proportionality between spin magnetic moment and angular momentum is twice as large as the ratio of the intrinsic magnetic moment and angular momentum.

It is found that the intrinsic angular momentum obeys rules similar to those of orbital motion about a central force field, Eqs. (4.9.10) and (4.9.11), except that with spin the only allowed quantum numbers are plus and minus one half. That is, the total angular momentum is:

$$\mathbf{s} \cdot \mathbf{s} = s(s+1)\hbar^2 \quad (4.16.5)$$

The component along a particular axis is:

$$s_z = m_s \hbar \quad (4.16.6)$$

Quantum numbers m_s are equal to either $\pm 1/2$. Combining terms shows that the magnetic moment can have either of the two values:

$$\Omega_z = \pm e\hbar/2m \quad (4.16.7)$$

The absolute value of the moment is called the Bohr magneton, and of value:

$$\Omega_z = 9.274 \times 10^{-24} \text{ J/T} \quad (4.16.8)$$

These relationships may be put in appropriate quantum theory terms by considering S to be an eigenfunction, and writing in the form of an operator:

$$\hat{s}_z S = \pm \hbar S/2 \quad (4.16.9)$$

The total spin wave function combines the functions with coefficients as:

$$S(s_z) = c_+ S_+(s_z) + c_- S_-(s_z) \quad (4.16.10)$$

The wave functions are orthogonal and normalized.

4.17. Many-Electron Problems

To examine a multi-electron atom note that the Hamiltonian operator of a system of n electrons may depend in a complicated way on the internal structure of each electron. Regardless of what the complications may be, a property of critical importance is that electrons are physically indistinguishable: all results are invariant upon interchange of electrons. That is, all energies, including both electron-nucleus and electron-electron interactions, are symmetrical with respect to an interchange of electrons.

Since the energy of an electron is proportional to the square of its wave function, symmetric energies occur with both symmetric and antisymmetric

wave functions. To examine the symmetry of a wave function break it into the sum of symmetric and antisymmetric parts, respectively:

$$\psi^{\text{Sy}}(\mathbf{r}, t) = \psi^{\text{Sy}}(-\mathbf{r}, t) \quad \text{and} \quad \psi^{\text{As}}(\mathbf{r}, t) = -\psi^{\text{As}}(-\mathbf{r}, t) \quad (4.17.1)$$

Any physically real function of time can be expressed as the sum of symmetric and antisymmetric functions of time. For the case of wave functions:

$$\psi(\mathbf{r}, t) = \psi^{\text{Sy}}(\mathbf{r}, t) + \psi^{\text{As}}(\mathbf{r}, t) \quad (4.17.2)$$

The energy density is proportional to the probability density and it is equal to:

$$\begin{aligned} \psi(\mathbf{r}, t)^* \psi(\mathbf{r}, t) &= \left[\psi^{\text{Sy}*}(\mathbf{r}, t) \psi^{\text{Sy}}(\mathbf{r}, t) + \psi^{\text{As}*}(\mathbf{r}, t) \psi^{\text{As}}(\mathbf{r}, t) \right] \\ &+ \left[\psi^{\text{Sy}*}(\mathbf{r}, t) \psi^{\text{As}}(\mathbf{r}, t) + \psi^{\text{As}*}(\mathbf{r}, t) \psi^{\text{Sy}}(\mathbf{r}, t) \right] \end{aligned} \quad (4.17.3)$$

The first term of Eq. (4.17.3) is invariant with respect to the interchange of electrons and the second term is not. It follows that the second term is equal to zero. Therefore the wave function may be either symmetric or antisymmetric but it cannot be a mixture.

The simplest possible multi-electron system has two electrons, say electron “a” and electron “b”. Let P_{ab} be a permutation operator that interchanges the electrons. It follows that:

$$P_{ab}\psi(a, b) = \psi(b, a) \quad \text{and} \quad P_{ab}P_{ab}\psi(a, b) = \psi(a, b) \quad (4.17.4)$$

In turn, it follows from Eq. (4.17.4) that:

$$P_{ab}P_{ab} = 1 \quad \text{and} \quad P_{ab} = \pm 1 \quad (4.17.5)$$

It follows that

$$P_{ab}\psi^{\text{As}}(\mathbf{r}, t) = -\psi^{\text{As}}(\mathbf{r}, t) \quad P_{ab}\psi^{\text{Sy}}(\mathbf{r}, t) = \psi^{\text{Sy}}(\mathbf{r}, t) \quad (4.17.6)$$

Since taking operations with respect to time in quantum theory does not affect positional symmetry, time does not affect symmetry: A state that is initially symmetric or antisymmetric before a quantum mechanical operation has the same symmetry after the operation. Whatever symmetry the wave function has at time $t = 0$, it keeps that symmetry for all time. This argument generalizes to include an arbitrary number of electrons. The conclusion is that either there is but one type of symmetry in nature, with all wave functions of the other symmetry everywhere equal to zero, or there are two separate types of physical reality. If two types of reality exist, one type of reality would be constructed of electrons with symmetric wave functions and the other would be constructed of electrons with antisymmetric wave

functions. Consider a two-electron atom for which the total and individual wave functions satisfy the relationships:

$$\begin{aligned}\psi(\mathbf{r}', \mathbf{r}'') &= \psi_a(\mathbf{r}')\psi_b(\mathbf{r}'') \\ &= \frac{1}{2}[\psi_a(\mathbf{r}')\psi_b(\mathbf{r}'') + \psi_b(\mathbf{r}')\psi_a(\mathbf{r}'')] \\ &\quad + \frac{1}{2}[\psi_a(\mathbf{r}')\psi_b(\mathbf{r}'') - \psi_b(\mathbf{r}')\psi_a(\mathbf{r}'')] \end{aligned} \quad (4.17.7)$$

The first and second terms are, respectively, symmetric and antisymmetric. Introduce the notation that:

$$\begin{aligned}\Gamma_{ab}(\mathbf{r}', \mathbf{r}'') &= [\psi_a(\mathbf{r}')\psi_b(\mathbf{r}'') + \psi_b(\mathbf{r}')\psi_a(\mathbf{r}'')] \\ \Psi_{ab}(\mathbf{r}', \mathbf{r}'') &= [\psi_a(\mathbf{r}')\psi_b(\mathbf{r}'') - \psi_b(\mathbf{r}')\psi_a(\mathbf{r}'')] \end{aligned} \quad (4.17.8)$$

Since both electrons occupy all points, examine conditions for $r' = r''$:

$$\begin{aligned}\Gamma_{ab}(\mathbf{r}', \mathbf{r}') &= 2\psi_a(\mathbf{r}')\psi_b(\mathbf{r}') \\ \Psi_{ab}(\mathbf{r}', \mathbf{r}'') &= 0 \end{aligned} \quad (4.17.9)$$

The electrostatic interaction energy between the two electrons is:

$$W_{ab} = \frac{e^2}{4\pi\epsilon} \int \left(\frac{1}{|r' - r''|} \right) \psi_{ab}(\mathbf{r}', \mathbf{r}'')\psi_{ab}^*(\mathbf{r}', \mathbf{r}'')dV \quad (4.17.10)$$

If the electron charge density is a continuous function of position, Eq. (4.17.10) gives a physically acceptable result with either electron symmetry. As expected from Eq. (4.17.9), the energy with symmetric functions is larger than that with antisymmetric functions. However, the definite integral of Eq. (4.17.10) correctly represents the system energy if and only if the wave functions are continuous functions of position. If there is a dimensional scale below which the charge density is granular, on that scale of dimensions it is necessary to replace the integration by a sum over interaction energies. With symmetric wave functions, by Eq. (4.17.9) the granular charges are adjacent or overlapping and the sum is singular; there is no parallel with antisymmetric wave functions since the overlapping densities vanish. It follows that if there is a dimensional scale below which the charge density is granular only antisymmetric wave functions exist. The Exclusion Principle, first formulated by Pauli, states that only antisymmetric wave functions exist. On the basis of the above argument, it also suggests that, on an appropriate dimensional scale, electron charge distributions are granular.

4.18. Measurement Discussion

In Chapter 2 the field intensity versus scattering angle is calculated by applying Maxwell equations to scattering of a plane wave by a sphere or a biconical antenna. The calculated intensity represents, at each point, actual outgoing power. Quite differently, the scattered wave function versus scattering angle, as calculated by applying Schrödinger's equation to electron scattering from an object, does not describe a physical quantity. Instead it describes the probability that a physical event will occur; it is the probability that the scattered electron will exit at any particular angle. The actual exit angle for a particular electron is both unknown and incalculable from quantum theory. It can become known only by making a measurement. If enough electrons are scattered the fraction scattered in each direction is equal to the calculated wave function, but for an individual electron Schrödinger's equation gives only the probability of occurrence. The measurement produces a "collapse" of the wave function from a value over all angles to a specific exit angle.

Wave function collapse is the inverse of the spreading of a trapped electron over available eigenstates, see Eq. (4.7.5) for example. With the extended electron model the inability to predict a particular scattering angle for a particular electron is because established quantum theory contains no information about detailed intra-electron charge and current densities. Without detailed incoming information there can be no detailed outgoing information and the only recourse is a statistical analysis. On the other hand, if intra-electron charge and current densities were available, in principle at least detailed results would be calculable.

References

- D. Bohm, *Quantum Theory*, Prentice Hall, Princeton NJ (1951).
- K. Kim, E. Wolf, "Non-Radiating Monochromatic Sources and their Fields," *Opt. Commun.* **59** (1986) 1–6.
- P.A.M. Dirac, *The Principles of Quantum Mechanics*, 4th edition, Oxford (1958).
- G. Greenstein, A.G. Zajonc, *The Quantum Challenge: Modern Research on the Foundations of Quantum Mechanics*, Jones and Bartlett Publishers (1997).
- W.E. Lamb, M.O. Scully, "The Photoelectric Effect Without Photons," in *Polarization, Matter and Radiation*, Presses Universitaires de France (1969) pp. 363–369.
- L.D. Landau, E.M. Lifshitz, *Quantum Mechanics: Non-Relativistic Theory*, Addison-Wesley, Reading MA (1958).

- A. Messiah, *Quantum Mechanics*, Vol. 1, trans. by G.M. Temmer, John Wiley, New York (1966).
- R. Omnès, *Understanding Quantum Mechanics*, Princeton University Press (1999).
- L.I. Schiff, *Quantum Mechanics*, McGraw-Hill Book Co., New York (1949).
- F. Schwabl, *Quantum Mechanics*, 2nd edition, Springer, New York (1995).
- R.C. Tolman, *The Principles of Statistical Mechanics* (1938), reprinted by Dover Publications (1979).

CHAPTER 5

Radiative Energy Exchanges

The quantum theory of radiation incorporates Planck's radiation law. Both that law and Hertz' discovery of the photoelectric effect were explained by Einstein in a pragmatic way. His pragmatism, however, was simply an expedient to help understand the onrush of experimental data about atomic phenomena. It seems certain he expected the pragmatism would later yield to a more general theory consistent with existing thought. This type of pragmatism is quite different from the pragmatic development of quantum theory a few decades later. The later pragmatists considered their quantum theory explanations to be complete and that a deeper understanding of the relationship between classical and quantum theories was not possible.

This chapter begins with several sections about Planck's radiation law and its implications. The law is then used to derive the zero-point field, that is the minimum level of background electromagnetic radiation. The photoelectric effect is introduced and an explanation for it is obtained using continuous electromagnetic fields. The Manley Rowe power-frequency relationships in nonlinear fields are derived. A match is made between properties of the final field set of Chapter 3 and radiation properties that are otherwise believed to be inconsistent with classical field theory.

5.1. Blackbody Radiation, Rayleigh–Jeans Formula

All materials, including both humans and the walls of an evacuated cavity, consist of atoms and electrons undergoing thermal oscillations. The higher the temperature the more the oscillations. Associated with the oscillations are accelerations of the contained charges which, in turn and dependent upon the relative phases, result in absorption and emission of electromagnetic energy. In general the higher the temperature T the greater the amount of absorption and emission. We seek to use conservation laws to obtain a thermodynamically quantitative understanding of the general properties of such phenomena. That is, we seek to achieve maximum field

characterization with minimum reliance upon details of specific emission and absorption processes.

An isolated cavity in equilibrium contains an associated, trapped electromagnetic energy field. That field exchanges an equilibrated amount of electromagnetic energy and momentum with the containing walls. Let the energy density of this radiation field be represented by $w(\omega, T)$ and given by:

$$w(\omega, T) = \frac{1}{2}(\varepsilon E^2 + \mu H^2) \quad (5.1.1)$$

Since the energy density is a function of frequency ω , let $w_\omega(\omega, T)d\omega$ represent the energy density existent between frequencies ω and $\omega + d\omega$. It follows that:

$$w(\omega) = \int_0^\infty w_\omega(\omega) d\omega \quad (5.1.2)$$

Next consider two separate objects, A and B, composed of different materials. The objects wholly contain cavities in which the energy densities are $w_{\omega A}$ and $w_{\omega B}$. The objects are placed in thermal contact and achieve equilibrium at temperature T. Next thermally isolate the objects and construct an optical system that exchanges radiation between them; the system contains an optical filter that passes only radiation between frequencies ω and $\omega + d\omega$. If placing the optical system into position produces a net energy exchange, the cavities each will achieve a new equilibrium with the temperature of one cavity increased and the other decreased. That temperature difference can be used to run a heat engine. Since this violates the second law of thermodynamics, it follows that there is no net energy exchange between the chambers at any frequency and that the equilibrium energy density is independent of the material of which the cavities are formed. Since this is true for all materials, it is independent of the color of the walls, the fraction of the incident radiation the walls reflect or absorb, or any other wall or cavity parameter. Kirchhoff first pointed out this remarkable result in 1859; it is expressed by the equation:

$$w_{\omega A}(\omega, T) = w_{\omega B}(\omega, T) \quad (5.1.3)$$

The result is exact for a cavity with a negligibly small aperture. The cavity contained radiation field is, by definition, the isothermal cavity radiation field. Next suppose that one cavity wall is ideally black. Since ideally black objects absorb all incident radiation, this energy field is also that of an ideal black object. Hence the radiation field is also called the blackbody radiation field.

Since the equilibrium electromagnetic energy density is not a function of the bounding material, without loss of generality we can construct the enclosure of whatever material is most convenient to analyze and, on that basis, apply the result to all materials. The enclosure of choice has walls of harmonic oscillators. Radiation is reflected or absorbed and re-emitted by the walls, thereby maintaining temperature T . The number of available frequency states per unit volume available is given by Eq. (1.13.14) and repeated here:

$$\frac{1}{V} dN = \frac{\omega^2}{\pi^2 c^3} d\omega \quad (5.1.4)$$

By the equipartition theorem of statistical mechanics each oscillator supports energy $kT/2$ per degree of freedom, where k is the Boltzmann constant. Therefore, since the walls are two-dimensional, each oscillator supports energy kT per mode. Substituting this into Eq. (5.1.4) gives:

$$w_\omega(\omega, T) = \frac{\omega^2}{\pi^2 c^3} kT \quad (5.1.5)$$

This equation is the long wavelength limit for the contained radiation field. It is the Rayleigh–Jeans formula for blackbody radiation and is valid for low enough frequencies or high enough temperatures so $\hbar\omega \ll kT$.

5.2. Planck's Radiation Law, Energy

In 1917 Einstein issued a significant paper on the absorption and emission of radiation by eigenstate electrons. It is based upon the conservation laws of energy and linear momentum and relativistic transformations between moving systems, see Sec. 1.3.2. The paper was a major step in the understanding of the processes of absorption and emission by confined electrons. This and the following section are drawn from that paper.

Let a cavity in thermal equilibrium at temperature T contain N identical and large gas molecules, where N is a very large number. Each molecule supports two non-degenerate energy levels, states Z_n and Z_s . The eigenstate energies of the levels are, respectively, W_n and W_s with $W_n > W_s$. The molecular mass is large enough so that all molecular speeds are much less than the speed of light. Einstein postulated that Maxwell statistics apply for large molecules in equilibrium. Therefore the number of large

molecules in state Z_s is N_s where:

$$N_s = \frac{N \exp(-W_s/kT)}{\exp(-W_n/kT) + \exp(-W_s/kT)} \quad (5.2.1)$$

In conformance with the theory of photoelectricity and with ω_n^s equal to the frequency, he required that molecules emit and absorb radiation in energy units:

$$\hbar\omega_n^s = W_n - W_s \quad (5.2.2)$$

Since harmonic oscillators satisfy this condition, see Eq. (4.8.16), walls made of harmonic oscillators satisfy the requirement. He also required that the Rayleigh–Jeans formula, Eq. (5.1.5), apply in the limit of low frequencies. Although that equation is based upon classical electrodynamics with continuous energy changes, in the low frequency limit the energy differences are vanishingly small and the Rayleigh–Jeans limit is satisfied.

Let the transition rate $d\Gamma/dt$ from state Z_n to state Z_s , with an accompanying emission of energy $\hbar\omega$, be:

$$\frac{d\Gamma_n^s}{dt} = N_n [A_n^s + B_n^s w(\omega_n^s)] \quad (5.2.3)$$

This transition rate is the sum of two parts: Spontaneous emission A_n^s is due to internal processes within the molecules and independent of the radiation field. Induced emission B_n^s is due to the radiation field and directly proportional to its field intensity. In the absence of spontaneous absorption the complete transition rate from state Z_s to Z_n is:

$$\frac{d\Gamma_s^n}{dt} = N_s B_s^n w(\omega_n^s) \quad (5.2.4)$$

Equal rates of absorption and emission are required at equilibrium. Equating them and collecting terms gives:

$$w(\omega_n^s) = \frac{A_n^s}{B_n^s \exp(\hbar\omega/kT) - B_s^n} \quad (5.2.5)$$

In the limit of small values of the exponential, Eq. (5.2.5) goes to:

$$w(\omega_n^s) = \frac{A_n^s}{B_n^s - B_s^n - B_n^s(\hbar\omega/kT)} \quad (5.2.6)$$

Equating Eqs. (5.1.5) and (5.2.6) gives:

$$B_n^s = B_s^n \quad \text{and} \quad A_n^s = \frac{(\omega_n^s)^2}{\pi^2 c^3} (\hbar\omega_n^s) B_n^s \quad (5.2.7)$$

Combining Eqs. (5.2.5) and (5.2.7) yields Planck's blackbody radiation law:

$$w(\omega, T) = \frac{\omega^2}{\pi^2 c^3} \left(\frac{\hbar\omega}{\exp(\hbar\omega/kT) - 1} \right) \quad (5.2.8)$$

This law describes the energy density in an equilibrated electromagnetic radiation field as a function of frequency and the temperature of its surroundings. In the low frequency limit it satisfies the Rayleigh–Jeans formula and in the high frequency limit it obeys the Wien formula, a form of the Maxwell distribution law:

$$w(\omega) = \frac{\hbar\omega^3}{\pi^2 c^3} \exp(-\hbar\omega/kT) \quad (5.2.9)$$

Actual values of A_n^s and B_n^s can be calculated using Eq. (4.14.10) for molecules with known eigenstates.

5.3. Planck's Radiation Law, Momentum

In the second part of his 1917 paper Einstein explained that thermodynamic problems are typically analyzed using energy exchanges, with momentum exchanges, which are less by a factor of c , ignored. For theoretical considerations, however, energy and momentum are on a par. A theory is only correct if the momentum transferred during energy exchanges leads to the same statistical results as energy considerations.

He then presented a development of Planck's radiation equation using momentum exchanges. He found that Planck's equation results only if the radiation is highly directed. That is, as a molecule emits or absorbs energy $\hbar\omega$ the exchange is accompanied by an exchange of linear momentum $\hbar\omega/c$: the molecule undergoes a push at least very nearly equal to $\hbar\omega/c$. Although laser beams may meet this condition, in the case of atomic radiation the diameter of the emitter may be less than a hundredth of an optical wavelength. Einstein viewed absorption from a plane wave as containing the energy and momentum in the same ratio as the wave. A cursory examination of the analyses of scattering problems, see Chapter 2, shows that this can occur only if there is no scattering. He viewed emission as being carried by spherical Hertzian waves, i.e. a multimodal expansion, with rotational symmetry about the radiation axis. For such waves the source suffers compression but not a push. This argument led Einstein to intuitively conclude that a quantum theory of radiation is *almost* unavoidable. He also explained that his theory has two weaknesses: it does nothing to illuminate the connection between quantized energy exchanges and Maxwell's wave theory and it leaves the time and direction of elementary processes to chance.

Following Einstein, we imagine a cavity containing molecular gas in thermal equilibrium at temperature T , but no radiation. The mass M of the molecules is large enough so molecular speeds are much less than c and relativistic speed corrections are not needed. Next introduce electromagnetic radiation as an isotropic distribution of plane waves that interact with the molecules in a way that retains the original temperature, T . Also, as in Sec. 5.1, only eigenstates Z_s and Z_n undergo energy exchanges.

Since at equilibrium the average molecular speed is zero, on the average all radiation-molecule interactions occur on stationary molecules. During events both energy and impulse are exchanged and produce an acquired molecular speed v . Although on the average a pre-event molecule sits in a uniform radiation field, a post-event one does not: For moving molecules the radiation field is not isotropic. There is a net field unbalance in the direction of motion and a change of frequency. This unbalance produces an altered event rate that, in turn, damps the molecular motion. Let each event transfer momentum Δ between the field and the molecule. Molecular damping is denoted as Rv where R is a field-dependent constant to be determined and acts in the direction opposite to the motion. Equilibrium requires, on the average, the speed to return to zero before the next event. It follows that during the period between events the momentum of the molecule is:

$$Mv - Rv\tau + \Delta$$

τ is time since the last event and $M \gg R\tau$.

For a system to remain in equilibrium the average velocity v at the time of an event remains equal to zero. This may be stated as:

$$\langle (Mv - Rv\tau + \Delta)^2 \rangle = \langle (Mv)^2 \rangle \quad (5.3.1)$$

Combining all the above gives:

$$\langle \Delta^2 \rangle = 2R\tau M \langle v^2 \rangle \quad (5.3.2)$$

A system analysis using momentum exchanges can be correct only if Eq. (5.3.2) is satisfied.

The mean-square velocity may be expressed in terms of temperature using Boltzman's one-dimensional law:

$$\frac{1}{2}M \langle v^2 \rangle = \frac{1}{2}kT \quad (5.3.3)$$

Damping Product Rv : To examine if Eq. (5.3.2) is satisfied by Sec. 5.2 we calculate the rate of momentum transfer from a moving molecule to an otherwise uniform radiation field made unbalanced by the motion. Although in

principle the problem is simple enough it is rather lengthy. Let the molecule be moving along z -axis with speed v in stationary coordinate system K . To calculate radiation damping we analyze conditions in coordinate system K' in which the molecule is at rest. Since radiation in system K is isotropic the field intensity and the radiation energy within differential solid angle $d\kappa$ and frequency range $d\omega$ is:

$$w(\omega) d\omega \frac{d\kappa}{4\pi} \quad (5.3.4)$$

The frequencies in K and K' differ by the Doppler frequency; in K' the intensity is a function of angle with respect to the z -axis:

$$w(\omega', \theta') d\omega' \frac{d\kappa'}{4\pi} \quad (5.3.5)$$

The relationship between Eqs. (5.3.4) and (5.3.5) follows by substituting the fields of Eq. (5.3.4), arrayed in the form of Eq. (1.6.4), into Eq. (1.3.2). For v/c much less than one the energy density, frequency, and angle with the z -axis transform as:

$$w(\omega', \theta') = w(\omega) \frac{d\omega}{d\omega'} \frac{d\kappa}{d\kappa'} \left(1 - 2\frac{v}{c} \cos \theta\right) \quad (5.3.6)$$

$$\omega' = \omega \left(1 - \frac{v}{c} \cos \theta\right) \quad (5.3.7)$$

$$\cos \theta' = \cos \theta - \frac{v}{c} (1 - \cos^2 \theta) \quad (5.3.8)$$

Since $v \ll c$ it follows from Eqs. (5.3.7) and (5.3.8) that:

$$\omega = \omega' \left(1 + \frac{v}{c} \cos \theta'\right) \quad (5.3.9)$$

$$w(\omega) = w\left(\omega' + \frac{v}{c} \omega' \cos \theta'\right) \cong w(\omega') + \left(\frac{v}{c} \omega' \cos \theta'\right) \frac{\partial w(\omega)}{\partial \omega} \Big|_{\omega=\omega'} \quad (5.3.10)$$

From Eq. (5.3.9):

$$\frac{d\omega}{d\omega'} = \left(1 + \frac{v}{c} \cos \theta'\right) \quad (5.3.11)$$

Combining the definitions of $d\kappa$ and $d\kappa'$ with Eq. (5.3.8) gives:

$$\frac{d\kappa}{d\kappa'} = \frac{\sin \theta d\theta}{\sin \theta' d\theta'} = \frac{d(\cos \theta)}{d(\cos \theta')} = 1 - 2\frac{v}{c} \cos \theta' \quad (5.3.12)$$

The radiation intensity in system K' follows by combining all the above and gives, through first order:

$$w(\omega', \theta') = \left[w(\omega') + \frac{v}{c} \omega' \cos \theta' \frac{\partial w(\omega)}{\partial \omega} \Big|_{\omega=\omega'} \right] \left(1 - 3\frac{v}{c} \cos \theta'\right) \quad (5.3.13)$$

For systems in equilibrium the rate of absorption events is:

$$B_s^n w(\omega', \theta') d\omega' \frac{d\kappa'}{4\pi} \quad (5.3.14)$$

Since this transfer rate is correct for a system in equilibrium, for a moving molecule it is also the rate at which momentum transfers would occur if the subsequent decay was instantaneous. The moving molecule, however, is not in equilibrium. By the ergodic theorem of statistics, for a constraint-free system in equilibrium the spatial average population of states is equal to the fraction of the time an individual molecule spends in each state. For this case the average fraction of equilibrated molecules in state Z_s , see Eq. (5.2.1), is equal to the fraction of time a specific molecule spends in that state. Therefore multiplying Eq. (5.3.14) by the fraction of the time the molecule spends in that state, Eq. (5.2.1), gives the number of absorption transitions due to radiation within differential solid angle $d\kappa'$ per second:

$$\frac{e^{-W_s/kT}}{e^{-W_n/kT} + e^{-W_s/kT}} B_s^n w(\omega', \theta') \frac{d\kappa'}{4\pi} \quad (5.3.15)$$

Next make the basic postulate that all radiation events are fully directed in that for either absorption or emission each event transfers momentum Δ to the molecule where:

$$\Delta = \pm \frac{W_n - W_s}{c} \cos \theta' \quad (5.3.16)$$

Applying the above arguments to emission, combining the absorption and emission results, and incorporating the first part of Eq. (5.2.8) gives the net momentum transferred from the molecule to the radiation:

$$\left(\frac{\exp(-W_s/kT) - \exp(-W_n/kT)}{\exp(-W_s/kT) + \exp(-W_n/kT)} \right) \frac{\hbar\omega}{4\pi c} B_s^n \int w(\omega', \theta') \cos \theta' d\kappa' \quad (5.3.17)$$

Substituting Eq. (5.3.13) into Eq. (5.3.17) and integrating over solid angle gives the momentum transferred from the molecules to the radiation:

$$\begin{aligned} & -\frac{\hbar\omega}{c^2} B_s^n \left(\frac{\exp(-W_s/kT) - \exp(-W_n/kT)}{\exp(-W_s/kT) + \exp(-W_n/kT)} \right) \\ & \times \left(w(\omega') - \frac{1}{3} \omega' \frac{\partial w(\omega)}{\partial \omega} \Big|_{\omega=\omega'} \right) v \end{aligned} \quad (5.3.18)$$

For v much less than c the difference between frequencies ω and ω' is small. Putting them equal and equating the expression to R gives:

$$R = \frac{\hbar\omega}{c^2} B_s^n \left(\frac{\exp(-W_s/kT)}{\exp(-W_s/kT) + \exp(-W_n/kT)} \right) \times (1 - e^{-\hbar\omega/kT}) \left(w(\omega) - \frac{1}{3}\omega \frac{\partial w(\omega)}{\partial \omega} \right) \quad (5.3.19)$$

It follows from Planck's radiation law that:

$$\left(w(\omega) - \frac{1}{3}\omega \frac{\partial w(\omega)}{\partial \omega} \right) (1 - e^{-\hbar\omega/kT}) = \frac{\hbar\omega}{3kT} w(\omega) \quad (5.3.20)$$

Combining:

$$R = \frac{\hbar^2\omega^2}{c^2} \left(\frac{\exp(-W_s/kT)}{\exp(-W_s/kT) + \exp(-W_n/kT)} \right) N B_s^n \frac{w(\omega)}{3kT} \quad (5.3.21)$$

Since spontaneous emission is postulated to be both fully directed and randomly oriented it does not affect the exchanged momentum and therefore is not considered here.

Momentum Transfer $\langle \Delta^2 \rangle$ The effect of random processes on the mechanical behavior of molecules is much easier to derive. Let z -directed linear momentum λ be transferred to a molecule with each energy exchange and let it be of varying magnitude and direction. The average value, however, is along the z -axis and is equal to zero. If the mean value of the momentum changes is zero and if l is the number of such events, it follows that:

$$\langle \Delta^2 \rangle = \langle l\lambda^2 \rangle \quad (5.3.22)$$

With each energy exchange, and consistent with the radiation results, the momentum transferred to the molecule is:

$$\lambda = \pm \frac{\hbar\omega}{c} \cos \theta \quad (5.3.23)$$

With this notation the limits on angle θ are $-\pi/2$ to $\pi/2$, from which it follows that:

$$\langle \lambda^2 \rangle = \frac{1}{3} \left(\frac{\hbar\omega}{c} \right)^2 \quad (5.3.24)$$

The number of events that occur in time τ is just twice the number of absorption processes:

$$l = \left(\frac{2 \exp(-W_s/kT)}{\exp(-W_s/kT) + \exp(-W_n/kT)} \right) B_s^n w(\omega) \tau \quad (5.3.25)$$

Combining Eqs. (5.3.22), (5.3.24), and (5.3.25) gives:

$$\frac{\langle \Delta^2 \rangle}{\tau} = \frac{2}{3} \left(\frac{\hbar \omega}{c} \right)^2 \left(\frac{\exp(-W_s/kT)}{\exp(-W_s/kT) + \exp(-W_n/kT)} \right) B_s^n w(\omega) \quad (5.3.26)$$

Comparing Eqs. (5.3.26) and (5.3.20) after including Eq. (5.3.3) gives:

$$\frac{\langle \Delta^2 \rangle}{\tau} = 2RkT \quad (5.3.27)$$

This result confirms that Einstein's model of fully directed radiation exchanges is a sufficient base upon which to derive Planck's radiation law. If this equation is exact, it is only fully consistent with the results of classical electromagnetism, Eqs. (2.22.10) and (2.22.11), if the absorbed and emitted energy-to-momentum ratios are equal, that is if both ratios are equal to c . Since there were several approximations involved the proof is that the linear momentum exchanged during absorption and emission processes is nearly the same.

5.4. The Zero Point Field

According to the equipartition theorem of statistical mechanics the energy per degree of freedom in a statistical system of equilibrated particles is:

$$\frac{\text{Energy}}{\text{Degree of freedom}} = kT/2 \quad (5.4.1)$$

Within an equilibrated electromagnetic energy field and at high temperatures the energy density at frequency ω is given by Planck's equation, Eq. (5.2.9). In the limit as the temperature goes to absolute zero that expression is also expressed as Eq. (5.2.9). The limiting value at very large temperatures is also of interest. For that case Eq. (5.2.8) goes to:

$$\lim_{T \rightarrow \infty} w_\omega(\omega) = \frac{\omega^2}{\pi^2 c^3} \left(\frac{\hbar \omega}{\hbar \omega/kT + (\hbar \omega/kT)^2/2} \right) \approx \frac{\omega^2}{\pi^2 c^3} \left(kT - \frac{\hbar \omega}{2} \right) \quad (5.4.2)$$

It follows from Eq. (1.13.13) that the spatial density of available energy states is:

$$N = \frac{\omega^2}{\pi^2 c^3} \quad (5.4.3)$$

Combining Eqs. (5.4.2) and (5.4.3) shows that the energy per state is:

$$kT - \frac{\hbar \omega}{2} \quad (5.4.4)$$

Since Eqs. (5.4.1) and (5.4.4) are inconsistent, it follows that the Planck expression should be amended to:

$$w_\omega = \frac{\omega^2}{\pi^2 c^3} \left(\frac{\hbar\omega}{e^{\hbar\omega/kT} - 1} + \frac{\hbar\omega}{2} \right) \quad (5.4.5)$$

It follows that in the limit as T approaches zero Planck's original radiant energy distribution term vanishes leaving only the zero point energy. That energy, in turn is in equilibrium with the zero-point energy of which the enclosing cavity walls are composed, see Eq. (4.8.16). Therefore even at absolute zero temperature both the harmonic oscillators and the radiation field maintain an irreducible energy density.

5.5. The Photoelectric Effect

In 1887 Hertz discovered that a spark jumps a small gap between conductors more easily when the conductors are illuminated than when in the dark. He found that the effect becomes more pronounced as the light spectrum goes from blue to ultraviolet, is most pronounced with clean and smooth terminals, and cathodes are more active than anodes. The result is a photocurrent due to the forcible ejection of electrons from the cathode. This analysis shows that the photoelectric effect may result from an interaction between a classical radiation field and a quantized electron.

Experimentally determined characteristics of photocurrents include the existence of stopping potential V_0 , the voltage difference between the two plates that just causes the current to cease. The electron stream continues so long as the electrons have sufficient energy to make the transit. It must be, therefore, that the actual voltage V satisfies the condition:

$$V > V_0 \quad (5.5.1)$$

Each type of metal has a characteristic frequency, ω_0 . A photocurrent exists only with light of that or a higher frequency ω . That is if:

$$\omega > \omega_0 \quad (5.5.2)$$

The magnitude of the photocurrent is proportional to the light intensity. If the symbol E_0 indicates the electric field intensity of the light:

$$I = I(E_0^2) \quad (5.5.3)$$

Photocurrent magnitude is independent of frequency for frequencies greater than the characteristic frequency, and onset occurs without a measurable time delay after onset of illumination. Expressed in terms of the

above symbols, the maximum kinetic energy per electron is:

$$W = \hbar(\omega - \omega_0) \quad (5.5.4)$$

Einstein analyzed the photocurrent problem by treating light as if it consisted of particles. In 1905 he postulated that when light interacts with matter it behaves as though it consists of light quanta of energy $\hbar\omega$ which can only be emitted or absorbed in those units. Electrons would absorb this energy and many of them would recoil with maximum energy equal ($\hbar\omega$ less the work function of the metal). This pragmatic argument was sufficiently convincing for most readers to accept it as the correct explanation. The analysis earned Einstein the 1921 Nobel Prize in Physics.

Although the light-as-a-particle explanation is sufficient, it is not necessary. In 1969 Lamb and Scully analyzed the effect using the interaction between electrons in quantized energy states and an engulfing plane wave. Their argument begins by letting the source metal be sized much larger than atomic dimensions and inside the metal electrons are trapped in quantized energy states. Since the skin depth of a good conductor in the mid-optical range is on the order of 10 nm, light penetrates the metal deeply enough to interact with the conducting band electrons. Let an electron in eigenstate “n” with energy W_n interact with an applied plane wave of frequency ω . Define the work function of the metal, W_0 , to be the additional energy an electron must have to exit the metal:

$$W_0 = \hbar\omega \quad (5.5.5)$$

It follows from Sec. 1.13 that there are electromagnetic cavity solutions of energy W_k within the containing box. As the size of the box, L , becomes large, the possible energy levels form a quasi-continuum. The transition equations of Eq. (4.14.10) are repeated here:

$$|c_k(t)|^2 = (2eE_0)^2 \langle U_k | \mathbf{r} | U_n \rangle^2 \left\{ \frac{\sin^2 \left[\frac{1}{2\hbar} (W_n - W_k \pm \hbar\omega)t \right]}{(W_n - W_k \pm \hbar\omega)^2} \right\} \quad (5.5.6)$$

Let Φ be the energy of the first state of the quasi-continuous spectrum. Photoelectron emission occurs because of a transition from state n to state k. Let the kinetic energy of the ejected electron be T_k . The relationship between the energies follows and is equal to:

$$W_k - W_n = \Phi + T_k \quad (5.5.7)$$

Rearranging and rewriting in terms of frequencies:

$$T_k = \hbar(\omega - \omega_0) \quad (5.5.8)$$

The voltage required to stop all emission follows from the above and is equal to:

$$V_0 = \frac{\hbar}{e}(\omega - \omega_0) \quad (5.5.9)$$

Combining Eq. (5.5.6) with Eqs. (5.5.7) and (5.5.8) gives an expression for the coefficient magnitude as a function of the electron kinetic energy and the applied frequency:

$$|c_k(t)|^2 = (2eE_0)^2 \langle U_k | \mathbf{r} | U_n \rangle^2 \left\{ \frac{\sin^2 \left[\frac{1}{2\hbar} (T_k - \hbar\omega)t \right]}{(T_k - \hbar\omega)^2} \right\} \quad (5.5.10)$$

To determine the rate of electron ejection it is necessary to integrate Eq. (5.5.10) over the full range of kinetic energies which, in turn, requires summing over the quasi-continuum states. Since it is a quasi-continuum, replace the summation with the integral shown:

$$P(t) = \sum_k |c_k(t)|^2 \Rightarrow (2eE_0)^2 \langle U_k | \mathbf{r} | U_n \rangle^2 \int_0^\infty \left\{ \frac{\sin^2 \left[\frac{1}{2\hbar} (T - \hbar\omega)t \right]}{(T - \hbar\omega)^2} \right\} dT \quad (5.5.11)$$

$P(t)$ is the probability that emission has occurred. The integral may be rewritten as a Dirac delta function using the relationship:

$$\left\{ \frac{\sin^2 \left[\frac{1}{2\hbar} (T - \hbar\omega)t \right]}{\left(\frac{t}{2\hbar} \right)^2 (T - \hbar\omega)^2} d \left(\frac{tT}{2\hbar} \right) \right\} = \delta(x - x_0) dx \quad (5.5.12)$$

Combining Eq. (5.5.11) with Eq. (5.5.12) and integrating over all possible kinetic energies gives:

$$P(t) = \frac{2e^2 E_0^2}{\hbar} \langle U_k | \mathbf{r} | U_n \rangle^2 t \quad (5.5.13)$$

This probability of emission, Eq. (5.5.13), is directly proportional to time and, therefore, with a constant light intensity electrons are ejected at a constant rate. There is no time delay between onset of the light and the onset of electron emission and the rate of electron ejection is proportional to the intensity of the illuminating field atomic states. The analysis of Secs. 4.13 and 4.14 contained the approximation that $c_n(t)$ remained constant, a result that served as a preliminary to generalized cases with $c_n(t)$ a variable. In this case, since the active electrons lie initially near the Fermi level and the conduction band is part of a quasi-continuum, the constancy is a reality.

5.6. Power-Frequency Relationships

Before continuing the discussion of quantized radiation, it is necessary to address possible power-frequency relationships in closed systems. Consider an equilibrated, charged system that supports an internal electromagnetic oscillation at frequency ω_s . The system is immersed in and perturbed by a plane wave of frequency ω . If the system is linear, in the sense that doubling an applied force doubles the system response, only the two frequencies ω and ω_s will exist inside the system. If the system response is not linear, there are additional responses at difference and sum frequencies. The system response may be written as:

$$S(t) = [A \cos(\omega_s t) + B \cos(\omega t)]^p \quad (5.6.1)$$

A , B , and p are constant, system-specific parameters. The system response may be expanded as a polynomial of trigonometric functions. An especially important example of a nonlinear response is the case of $p = 2$, for which:

$$\begin{aligned} S(t) = & \frac{A^2 + B^2}{2} + AB\{\cos[(\omega_s - \omega)t] + \cos[(\omega_s + \omega)t]\} \\ & + \frac{1}{2}\{A^2 \cos(2\omega_s t) + B^2 \cos(2\omega t)\} \end{aligned} \quad (5.6.2)$$

The constant term is unimportant for present purposes. The generated frequencies, $[(\omega_s \pm \omega), 2\omega_s, 2\omega]$, remain within the system and, being part of it, also drive it and thereby produce additional frequencies. The ultimate series of generated frequencies continues and includes all frequencies of the form $(m\omega + n\omega_s)$, where m and n are integers. The result is true for all values of p greater than one.

Energy is conserved in lossless systems independently of the degree of nonlinearity. Let $P_{m,n}$ represent the time average power out of a system at frequency $(m\omega + n\omega_s)$. For lossless systems, energy conservation requires that:

$$\sum_{m=-\infty}^{\infty} \sum_{n=-\infty}^{\infty} P_{m,n} = 0 \quad (5.6.3)$$

It is helpful for what lies ahead to rewrite Eq. (5.6.3) as:

$$\omega \sum_{m=-\infty}^{\infty} \sum_{n=-\infty}^{\infty} \frac{mP_{m,n}}{m\omega + n\omega_s} + \omega_s \sum_{m=-\infty}^{\infty} \sum_{n=-\infty}^{\infty} \frac{nP_{m,n}}{m\omega + n\omega_s} = 0 \quad (5.6.4)$$

Equation (5.6.4) contains redundant information since with integer pair (m_0, n_0) the sums are identical to the sums obtained using $(-m_0, -n_0)$.

The redundancy is removed yet all information retained by writing the sums as:

$$\omega \sum_{m=0}^{\infty} \sum_{n=-\infty}^{\infty} \frac{mP_{m,n}}{m\omega + n\omega_s} + \omega_s \sum_{m=-\infty}^{\infty} \sum_{n=0}^{\infty} \frac{nP_{m,n}}{m\omega + n\omega_s} = 0 \quad (5.6.5)$$

For example, an ideal, nonlinear capacitor is an example of a lossless, reactive system; other reactive systems may be analyzed in a parallel way. The charge on the capacitor may be expressed as:

$$q(t) = \frac{1}{2} \sum_{m=-\infty}^{\infty} \sum_{n=-\infty}^{\infty} Q_{m,n} \exp[i(m\omega + n\omega_s)t] \quad (5.6.6)$$

The value of $Q_{m,n}$ depends upon such parameters as the capacitor size, shape, permittivity and the supported voltage but does not depend upon frequency of operation. Since $q(t)$ is real, the condition $Q_{-m,-n}^* = Q_{m,n}$ follows. Similarly the voltage, $v(t)$, across the capacitor is:

$$v(t) = \frac{1}{2} \sum_{m=-\infty}^{\infty} \sum_{n=-\infty}^{\infty} V_{m,n} \exp[i(m\omega + n\omega_s)t] \quad (5.6.7)$$

Like $Q_{m,n}$, $V_{m,n}$ depends upon the capacitor parameters of size, shape, permittivity, and the contained charge but not frequency. The capacitive current $i(t)$ is equal to the rate of change of charge, and may be written:

$$\begin{aligned} i(t) &= \frac{1}{2} \sum_{m=-\infty}^{\infty} \sum_{n=-\infty}^{\infty} I_{m,n} \exp[i(m\omega + n\omega_s)t] \\ &= \frac{i}{2} \sum_{m=-\infty}^{\infty} \sum_{n=-\infty}^{\infty} (m\omega + n\omega_s) Q_{m,n} \exp[i(m\omega + n\omega_s)t] \end{aligned} \quad (5.6.8)$$

The second equality follows by differentiation of Eq. (5.6.6) with respect to time and shows that, differently from either the charge or voltage, current $I_{m,n}$ does depend upon the frequency. The time average power into the capacitor is:

$$-P_{m,n} = -\frac{1}{2} \operatorname{Re}(V_{m,n} I_{m,n}^*) = \frac{1}{2} (m\omega + n\omega_s) \operatorname{Re}(i V_{m,n} Q_{m,n}^*) \quad (5.6.9)$$

Combining gives:

$$\frac{P_{m,n}}{(m\omega + n\omega_s)} = -\frac{1}{2} \operatorname{Re}(i V_{m,n} Q_{m,n}^*) \quad (5.6.10)$$

Since the right side of Eq. (5.6.10) depends upon the product of $Q_{m,n}$ and $V_{m,n}$, which are frequency independent, the right side is frequency

independent. It follows that the left side is also frequency independent. The parallel argument follows if the roles of m and n are reversed. Hence, Eq. (5.6.5) has the general algebraic form:

$$c_1\omega + c_2\omega_s = 0 \quad (5.6.11)$$

Coefficients c_1 and c_2 are independent of frequency. Therefore the two frequencies are independent variables and both c_1 and c_2 are equal to zero.

Applying this result to Eq. (5.6.5) shows that the sums are separately equal to zero:

$$\begin{aligned} \sum_{m=0}^{\infty} \sum_{n=-\infty}^{\infty} \frac{mP_{m,n}}{m\omega + n\omega_m} &= 0 \\ \sum_{m=-\infty}^{\infty} \sum_{n=0}^{\infty} \frac{nP_{m,n}}{m\omega + n\omega_s} &= 0 \end{aligned} \quad (5.6.12)$$

To illustrate the use of this equation, consider a system in which one of two possible atomic states is occupied by an electron. The state frequencies are ω_{initial} and ω_{final} , for initially occupied and initially empty states. The ensemble is then enmeshed in a plane wave of frequency ω where the frequency of the applied wave satisfies the relationship

$$\omega = |\omega_{\text{initial}} - \omega_{\text{final}}| \quad (5.6.13)$$

Only the driven frequency, ω , and the system frequency, ω_{initial} , are present in linear systems. With nonlinear systems, all frequencies ($m\omega_{\text{initial}} + n\omega$) are driven and are potentially present. If the system is restricted to support only ω_{initial} and ω_{final} only the three frequencies ω , ω_{initial} , and ω_{final} are present. Consider the case of a nonlinear system that supports only frequencies ω_{initial} and ω_{final} and is driven at frequency ω .

For that case, if $\omega_{\text{initial}} > \omega$ and $\omega_{\text{initial}} > \omega_{\text{final}}$, Eq. (5.6.12) is satisfied for integer pairs ($m = 1, n = 0$) and ($m = 1, n = -1$); if $\omega_{\text{initial}} > \omega$ and $\omega_{\text{initial}} < \omega_{\text{final}}$, Eq. (5.6.12) is satisfied for integer pairs ($m = 0, \pm n = 1$) and ($m = -1, \pm n = 1$). Changing the power subscripts to match the frequency ones, for these special cases Eq. (5.6.12) go to:

$$\frac{P_{\text{initial}}}{\omega_{\text{initial}}} + \frac{P_{\text{final}}}{\omega_{\text{final}}} = 0 \quad \text{and} \quad \frac{P_{\text{initial}}}{\omega_{\text{initial}}} \pm \frac{P}{\omega} = 0 \quad (5.6.14)$$

In the second equation, the sign is respectively positive or negative if ω_{initial} is greater or less than ω_{final} . The energy flows are illustrated in Fig. 5.6.1.

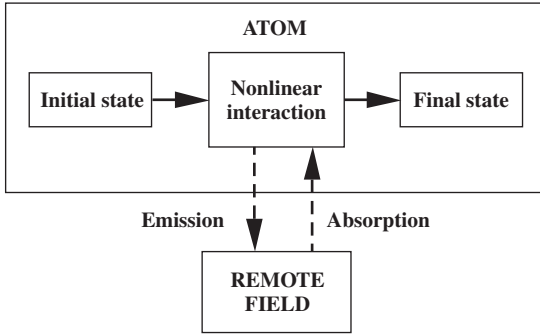


Fig. 5.6.1. Diagram illustrating power flows in a nonlinear source. Initial and remote field energies interact nonlinearly resulting in an energy flow from the initial state to the final state and either into or from the remote field.

By definition the energy that goes into the final state is:

$$W_{\text{final}} = \int P_{\text{final}} dt \quad (5.6.15)$$

Combining Eqs. (5.6.14) and (5.6.15) gives:

$$\left| \frac{W_{\text{initial}}}{\omega_{\text{initial}}} \right| = \left| \frac{W_{\text{final}}}{\omega_{\text{final}}} \right| = \left| \frac{W}{\omega} \right| \quad (5.6.16)$$

W_{final} is the energy that goes into the final state and W is the energy exchanged between the remote field and the electron as it undergoes a change of state. The energy-frequency ratio of Eq. (5.6.16) is independent of system parameters, therefore of system details and, consequently, the ratio is constant. For eigenstates that constant is Planck's constant, \hbar , and where the upper sign applies if $\omega_{\text{initial}} > \omega_{\text{final}}$, and vice versa:

$$W_{\text{final}} = -\hbar\omega_{\text{final}} \quad W_{\text{initial}} = \hbar\omega_{\text{initial}} \quad W = \pm\hbar\omega \quad (5.6.17)$$

The Manley Rowe results show that if the energy in the initial eigenstate is quantized into energy units proportional to frequency the energy exchanged among the radiation field and the initial and final energy eigenstates all have the same energy-to-frequency ratio.

Although Eqs. (5.6.1) through (5.6.14) apply both to linear and nonlinear systems, the magnitude of the energy flow at the sum or difference frequencies is zero for linear systems. Therefore Eqs. (5.6.15) through (5.6.17) are significant only for nonlinear systems. We conclude that the power-frequency relationships accompanying electron transitions are unique to nonlinear transitions, not to quantum effects.

5.7. Length of the Wave Train and Radiation Q

An important property of any radiation field is the length of the coherent wave train. The purpose of this section is to estimate that length for optical frequency photons. We begin by expressing the time varying electromagnetic power in a plane wave as a function of the magnitude and the frequency dependence of fields. For this purpose, let the electric and magnetic field intensities of a plane wave be expressed as integrals over all possible frequencies:

$$\mathbf{E}(t) = \int_{-\infty}^{\infty} \tilde{\mathbf{E}}(\omega) e^{i\omega t} d\omega \quad \text{and} \quad \mathbf{H}(t) = \int_{-\infty}^{\infty} \tilde{\mathbf{H}}(\omega) e^{i\omega t} d\omega \quad (5.7.1)$$

The rate at which energy passes through a unit area of surface follows from the Poynting theorem. With both fields perpendicular to the surface normal:

$$\begin{aligned} \int_{-\infty}^{\infty} N(t) dt &= \frac{1}{2} \text{Re} \int_{-\infty}^{\infty} \tilde{\mathbf{E}}(\omega) d\omega \int_{-\infty}^{\infty} \tilde{\mathbf{H}}(\omega')^* d\omega' \int_{-\infty}^{\infty} e^{i(\omega-\omega')t} dt \\ &= \pi \text{Re} \int_{-\infty}^{\infty} \tilde{\mathbf{E}}(\omega) d\omega \int_{-\infty}^{\infty} \tilde{\mathbf{H}}(\omega')^* d\omega' \delta(\omega, \omega') \\ &= 2\pi \text{Re} \int_0^{\infty} \tilde{\mathbf{E}}(\omega) \tilde{\mathbf{H}}^*(\omega) d\omega \end{aligned} \quad (5.7.2)$$

The electric and magnetic frequency dependencies are related by:

$$\eta |\mathbf{H}(\omega)| = |\mathbf{E}(\omega)| \quad (5.7.3)$$

Combining shows that the power through the surface is:

$$\int_{-\infty}^{\infty} N(t) dt = \frac{2\pi}{\eta} \int_0^{\infty} |\tilde{\mathbf{E}}(\omega)|^2 d\omega \quad (5.7.4)$$

If the plane wave is turned on at time $t = 0$ and terminated at time $t = \tau$, the result is a wave train of length $l = \tau c$. The relationship between the length of a wave train and the measured width of the frequency spectrum follows in a way similar to that used to demonstrate the uncertainty principle. Consider the special case where frequency ω' is turned on at time $-\tau/2$ and off at time $\tau/2$, and let $|\omega - \omega'| = \Delta\omega$. The resulting electric field

intensity is:

$$\begin{aligned} \mathbf{E}(t) &= \tilde{\mathbf{E}}_0 e^{i\omega't} & |t| \leq |\tau/2| \\ &= 0 & |t| \geq |\tau/2| \end{aligned} \quad (5.7.5)$$

$$\tilde{\mathbf{E}}(\omega) = \frac{\tilde{\mathbf{E}}_0}{2\pi} \int_{-\tau/2}^{\tau/2} e^{i(\omega' - \omega)t} dt = \frac{\tau \tilde{\mathbf{E}}_0}{2\pi} \left[\sin\left(\frac{\Delta\omega\tau}{2}\right) / \left(\frac{\Delta\omega\tau}{2}\right) \right] \quad (5.7.6)$$

The first zero of Eq. (5.7.6), half the width of the frequency pulse, occurs when the argument of the sine term is π . For that case:

$$\tau\Delta\omega = 2\pi \quad (5.7.7)$$

Substituting the length of the pulse train, $l = c\tau$, into Eq.(5.7.7) gives:

$$\frac{l}{\lambda} = n = \frac{\omega}{\Delta\omega} = Q \quad (5.7.8)$$

By definition n is the number of wavelengths in the wave train and the ratio $\Delta\omega/\omega$ is the fractional bandwidth. With λ equal to the wavelength and for a fixed value of Q the minimum duration of a pulse is:

$$\tau = \frac{2\pi Q}{\omega} = \frac{Q\lambda}{c} \quad (5.7.9)$$

Feynman's estimate of the Q of a photon begins with the definition of Eq. (3.5.11), and is repeated here:

$$Q = \frac{\omega W}{P_{\text{av}}} \quad (5.7.10)$$

Let a point electron oscillate between positions at $\pm z_0$, thereby producing electric dipole radiation. When oscillating at frequency ω the maximum energy of the electron is:

$$W = \frac{1}{2} m\omega^2 z_0^2 \quad (5.7.11)$$

The power output of an electric dipole radiator is listed in Table 3.12.1, with unit normalization. The normalization factor, $-k^3 e z_0 / 4\pi\epsilon$, follows by comparing the radial component of the electric field intensity with that listed in the table. Substituting in the actual values shows that:

$$P_{\text{av}} = \frac{e^2 \omega^4 z_0^2}{12\pi\epsilon c^3} \quad (5.7.12)$$

Combining shows the calculated Q , using Eq. (5.7.10), is approximately:

$$\frac{1}{Q} = \frac{e^2 \omega}{6\pi\epsilon m c^3} = \left(\frac{4\pi}{3\lambda}\right) \left(\frac{e^2}{4\pi\epsilon m c^2}\right) \quad (5.7.13)$$

The last bracket in Eq. (5.7.13) is the Lorentz radius of the electron, 2.82×10^{-15} m. At the center of the optical spectrum the wavelength is on

the order of $\lambda = 530$ nm, corresponding to a frequency of about 5.7×10^{14} Hz and a period of about 1.75 fs. Substituting these values into Eq. (5.7.13) gives:

$$Q \approx 4.5 \times 10^7 \quad (5.7.14)$$

Such an oscillator must radiate some 4.5×10^7 radians, or 7×10^6 oscillations, before dropping to $1/e$ of its original intensity. With a resulting decay time of about 10 ns, it follows that the wave train is about 3 m long. Certainly with wave trains of this length transient effects would not be significant.

It was shown earlier that the field energy also contributes to Q . For an electrically small dipole the calculated Q due to only the field energy is approximately:

$$Q \cong 1/(ka)^3 \quad (5.7.15)$$

At the radius of the first Bohr orbit 5.29×10^{-11} m, and at the frequency used in Eq. (5.7.14):

$$ka \cong 6.27 \times 10^{-4} \quad (5.7.16)$$

Combining Eq. (5.7.15) with Eq. (5.7.16):

$$Q \approx 4.0 \times 10^9 \quad (5.7.17)$$

The Q of the dipole field energy is approximately 100 times larger than Q calculated using the kinetic energy of a point electron generating a dipole mode. Since the calculated radiation Q of atomic radiation gives an unacceptably long estimated wave train length of nearly 300 m it follows that there is a fundamental error in the underlying assumptions upon which the argument is based. We will return to this result in Chapter 6.

5.8. The Extended Plane Wave Radiation Field

The phasor equation set that describes a circularly polarized, z -directed plane wave is given by extension of Eq. (2.1.2):

$$\begin{aligned} \tilde{\mathbf{E}} &= e^{-i\sigma \cos \theta} [\hat{r} \sin \theta + \hat{\theta} \cos \theta - j\hat{\phi}] e^{-j\phi} \\ \eta \mathbf{H} &= j\tilde{\mathbf{E}} \end{aligned} \quad (5.8.1)$$

The phasor equation set that describes the same plane wave follows by extension of Eqs. (2.1.8), (2.1.10), and (2.1.11):

$$\begin{aligned} \tilde{\mathbf{E}} = & \sum_{\ell=1}^{\infty} i^{-\ell} \frac{(2\ell+1)}{\ell(\ell+1)} \left\{ i\ell(\ell+1) \frac{j_{\ell}(\sigma)}{\sigma} P_{\ell}^1(\cos\theta) \hat{r} \right. \\ & + \left[j_{\ell}(\sigma) \frac{P_{\ell}^1(\cos\theta)}{\sin\theta} + ij_{\ell}^{\bullet}(\sigma) \frac{dP_{\ell}^1(\cos\theta)}{d\theta} \right] \hat{\theta} \\ & \left. - j \left[j_{\ell}(\sigma) \frac{dP_{\ell}^1(\cos\theta)}{d\theta} + ij_{\ell}^{\bullet}(\sigma) \frac{P_{\ell}^1(\cos\theta)}{\sin\theta} \right] \hat{\phi} \right\} \exp(-j\phi) \\ \eta\tilde{\mathbf{H}} = & j\tilde{\mathbf{E}} \end{aligned} \quad (5.8.2)$$

Equations (5.8.1) and (5.8.2) are identical.

Table 3.16.1 shows the radiation fields produced by four radiating, collocated electric and magnetic dipoles of degree one with one electric and one magnetic dipole oriented along the x -axis and an identical pair oriented along the y -axis. Although these dipole fields are proportional to spherical Hankel functions the relative phasing is the same as for the spherical Bessel functions in the plane wave of Eq. (5.8.1). These are the fields of Table 3.16.1, for which the radiating surface is resonant and for which the calculated source-associated standing energy is zero. Indeed, for all modal orders that meet the phase and orientation conditions the radiating surface is resonant and the source-associated standing energy is zero. The set of fields that meets the conditions of Table 3.16.2 is obtained by replacing the spherical Bessel functions of Eq. (5.8.2) with spherical Hankel functions and the modal coefficients by the real number F_{ℓ} :

$$\begin{aligned} \tilde{\mathbf{E}} = & \sum_{\ell=1}^{\infty} i^{-\ell} F_{\ell} \left\{ i\ell(\ell+1) \frac{h_{\ell}(\sigma)}{\sigma} P_{\ell}^1(\cos\theta) \hat{r} \right. \\ & + \left[h_{\ell}(\sigma) \frac{P_{\ell}^1(\cos\theta)}{\sin\theta} + ih_{\ell}^{\bullet}(\sigma) \frac{dP_{\ell}^1(\cos\theta)}{d\theta} \right] \hat{\theta} \\ & \left. - j \left[h_{\ell}(\sigma) \frac{dP_{\ell}^1(\cos\theta)}{d\theta} + ih_{\ell}^{\bullet}(\sigma) \frac{P_{\ell}^1(\cos\theta)}{\sin\theta} \right] \hat{\phi} \right\} \exp(-j\phi) \\ \eta\tilde{\mathbf{H}} = & j\tilde{\mathbf{E}} \end{aligned} \quad (5.8.3)$$

In accordance with the requirements of Table 3.16.2, but quite differently from Eq. (2.2.1), the magnitudes of the TM and TE modes are equal. The far field expressions for spherical Bessel and Neumann functions, Eq. (A.24.13), show they are identical except $\pi/2$ out of phase. Constructing a spherical Hankel function of the second kind by combining terms

makes the total field just twice the value of the spherical Bessel function acting alone.

The question we address here is how the fields of Eqs. (5.8.1) and (5.8.2) interact with a metastable source within a circumscribed sphere to produce the fields of Eq. (5.8.3). To find an answer, the first step is to examine the relative phases of the different field components. On the positive z -axis the angular functions, see Table A.18.1, are:

$$\begin{aligned} P_{\ell}^1(1) &= 0 \quad \frac{P_{\ell}^1(\cos \theta)}{\sin \theta} \Big|_{\theta=0} = \frac{dP_{\ell}^1(\cos \theta)}{d\theta} \Big|_{\theta=0} = \frac{\ell(\ell+1)}{2} \\ P_{\ell}^1(-1) &= 0 \quad \frac{P_{\ell}^1(\cos \theta)}{\sin \theta} \Big|_{\theta=0} = -\frac{dP_{\ell}^1(\cos \theta)}{d\theta} \Big|_{\theta=\pi} = (-1)^{\ell+1} \frac{\ell(\ell+1)}{2} \end{aligned} \quad (5.8.4)$$

From Eqs. (A.24.9) and (A.24.13) the expressions for the radial spherical and related functions are:

$$\begin{aligned} j_{\ell}(\sigma) &= \sum_{s=0}^{\infty} \frac{(-1)^s \sigma^{\ell+2s}}{(2s)!!(2\ell+2s+1)!!} \\ j_{\ell}^*(\sigma) &= \sum_{s=0}^{\infty} \frac{(-1)^s \sigma^{\ell+2s-1}}{(2s)!!(2\ell+2s-1)!!} \\ y_{\ell}(\sigma) &= -\sum_{s=0}^{\ell-1} \frac{(2\ell-2s-1)!!}{(2s)!!\sigma^{\ell+1-2s}} - \sum_{s=0}^{\infty} \frac{(-1)^s}{(2s-1)!!} \frac{\sigma^{\ell-1+2s}}{(2\ell+2s)!!} \\ y_{\ell}^*(\sigma) &= \sum_{s=0}^{\ell-1} \frac{(2\ell-2s-1)!!}{(2s)!!\sigma^{\ell+2-2s}} (\ell-2s) - \sum_{s=0}^{\infty} \frac{(-1)^s}{(2s-1)!!} \frac{\sigma^{\ell-2+2s}}{(2\ell+2s)!!} (\ell+2s) \end{aligned} \quad (5.8.5)$$

Combining Eqs. (5.8.3) through (5.8.5) shows the relative modal phases. With terms in square brackets indicating phase only and using the zenith angle electric field component as an example, on the positive z -axis:

$$\begin{aligned} E_{\theta} &\approx i^{-\ell} \{ [h_{\ell}(\sigma)] + i[h_{\ell}^*(\sigma)] \} \\ &= i^{-\ell} [j_{\ell}(\sigma) + y_{\ell}^*(\sigma)] - i^{1-\ell} [y_{\ell}(\sigma) - j_{\ell}^*(\sigma)] \end{aligned} \quad (5.8.6)$$

The first term in each of the square brackets of Eq. (5.8.6) is due to TM modes. The phase of the first term on the right side of Eq. (5.8.6) may be

written as:

$$\begin{aligned}
 i^{-\ell}[\mathbf{j}_\ell(\sigma) + \mathbf{y}_\ell^*(\sigma)] &= i^{-\ell}(-1)^s \sigma^{\ell+2s} - i^{-\ell}(-1)^s \sigma^{\ell+2s-2} + i^{-\ell} \sigma^{-\ell-2+2s} \\
 \ell \text{ odd} \\
 \ell = 1; &\approx \{-i[\sigma] + i[\sigma^3] - i[\sigma^5] + i[\sigma^7] \dots\} \\
 &\quad + \{i[\sigma^{-1}] - i[\sigma] + i[\sigma^3] - i[\sigma^5] + i[\sigma^7] \dots\} - i\sigma^{-3} \\
 \ell = 3; &\approx \{i[\sigma^3] - i[\sigma^5] + i[\sigma^7] \dots\} + \{-i[\sigma] + i[\sigma^3] - i[\sigma^5] + i[\sigma^7] \dots\} \\
 &\quad + i\{[\sigma^{-5}] + [\sigma^{-3}] + [\sigma^{-1}]\} \\
 \ell \text{ even} \\
 \ell = 2; &\approx \{-[\sigma^2] + [\sigma^4] - [\sigma^6] + [\sigma^8] \dots\} \\
 &\quad + \{[1] - [\sigma^2] + [\sigma^4] - [\sigma^6] + [\sigma^8] \dots\} - \{[\sigma^{-4}] + [\sigma^{-2}]\} \\
 \ell = 4; &\approx \{[\sigma^4] - [\sigma^6] + [\sigma^8] \dots\} + \{-[\sigma^2] + [\sigma^4] - [\sigma^6] + [\sigma^8] \dots\} \\
 &\quad + \{[\sigma^{-6}] + [\sigma^{-4}] + [\sigma^{-2}] + [1]\} \tag{5.8.7}
 \end{aligned}$$

The results contained in Eq. (5.8.7) show that for powers of σ greater than or equal to zero the phase of each power of the radius is the same for all moments. Therefore along the positive z -axis, and in the near field, driving one dipole moment drives the corresponding far-field radial components of all odd, higher order modes. Quite differently for powers of σ less than zero higher order terms have opposite signs and act to cancel the total near-field radial field component.

The second term on the right side of Eq. (5.8.6) is due to TE modes and may be written as:

$$\begin{aligned}
 i^{-\ell}[\mathbf{y}_\ell(\sigma) - \mathbf{j}_\ell^*(\sigma)] &= 2i^{1-\ell}(-1)^s \sigma^{\ell-1+2s} + i^{1-\ell} \sigma^{-\ell-1+2s} \\
 \ell \text{ odd} \\
 \ell = 1; &\approx 2\{[1] - [\sigma^2] + [\sigma^4] - [\sigma^6] \dots\} + [\sigma^{-2}] \\
 \ell = 3; &\approx 2\{-[\sigma^2] + [\sigma^4] - [\sigma^6] \dots\} - \{[\sigma^{-4}] + [\sigma^{-2}] + [1]\} \tag{5.8.8} \\
 \ell \text{ even} \\
 \ell = 2; &\approx 2i\{-[\sigma] + [\sigma^3] - [\sigma^5] + [\sigma^7] \dots\} - i\{[\sigma^{-3}] + [\sigma^{-1}]\} \\
 \ell = 4; &\approx 2i\{[\sigma^3] - [\sigma^5] + [\sigma^7] \dots\} + i\{[\sigma^{-5}] + [\sigma^{-3}] + [\sigma^{-1}] + [\sigma]\}
 \end{aligned}$$

Since the results of Eq. (5.8.8) are the same as those of Eq. (5.8.7), driving the magnetic dipole moments also drives the corresponding far-field radial components of all odd, higher order modes. For negative powers of σ the terms have opposite signs and act to cancel the total near-field radial field component. The relative phases of the two equations show that the dipole far-field terms of Eq. (5.8.7) produce the same phase, even order

terms as does Eq. (5.8.8), and the dipole far-field terms of Eq. (5.8.8) produce the same phase odd order terms as does Eq. (5.8.7). In this way, the system is phased so the dipole terms drive all higher order terms.

On the negative z -axis both TM and TE modes contain alternate signs of the expansion modes, with canceling phases and no field buildup.

We conclude that a buildup of a term proportional to σ^n , where $n \geq 0$, by any mode builds the magnitudes of the far-fields for all modes for $z > 0$ and, at the same time, reduces the magnitudes of the near-fields. This condition lends itself to a regenerative buildup of field magnitudes.

5.9. Gain and Radiation Pattern

Both Einstein and Planck referred to the “spherical symmetry” of radiation modes. It was surely his conception that the fields had spherical symmetry that was the basis for Einstein’s comment that the full directivity of quantized radiation made a quantum theory of radiation “almost unavoidable.” Even though modes of the type mentioned by Einstein have circular symmetry about the radiation axis, appropriate sets of such modes do carry a net linear momentum. In antenna theory this is referred to as antenna gain. Harrington, in 1960, published an expression for the maximum possible gain under such circumstances, about four decades after both Einstein’s 1917 paper on directivity and Planck’s 1920 Nobel prize paper addressed the same issue.

The gain of an antenna is a dimensionless power density ratio; it is the ratio of the maximum power density on the surface of a virtual, circumscribing sphere to the average surface power density. In mathematical terms:

$$G(\sigma) = \lim_{\sigma \rightarrow \infty} \frac{4\pi\sigma^2}{k^2} \frac{[N_r]_{\max}}{P_{\text{av}}} \quad (5.9.1)$$

Consider the gain of fields described by Eq. (5.8.3) after making the equality $i = j$. For this case the maximum value of $N_r(\sigma, \theta, \phi)$ occurs at angle $\theta = 0$. Making this substitution and using Table A.18.1 gives the fields:

$$\begin{aligned} \mathbf{E}(\sigma, 0) &= \frac{1}{2} \sum_{\ell=1}^{\infty} i^{-\ell} F_{\ell} \ell(\ell+1) [h_{\ell}(\sigma) + i h_{\ell}^*(\sigma)] \{\hat{\theta} - i \hat{\phi}\} e^{-i\phi} \\ \eta \mathbf{H}(\sigma, 0) &= \frac{1}{2} \sum_{\ell=1}^{\infty} i^{1-\ell} F_{\ell} \ell(\ell+1) [h_{\ell}(\sigma) + i h_{\ell}^*(\sigma)] \{\hat{\theta} - i \hat{\phi}\} e^{-i\phi} \end{aligned} \quad (5.9.2)$$

The radial component of the Poynting vector is:

$$\begin{aligned} \eta N_r(\sigma, 0) &= \frac{1}{2} \sum_{\ell=1}^{\infty} i^{-\ell} F_{\ell} \ell(\ell+1) [h_{\ell}(\sigma) + i h_{\ell}^{\bullet}(\sigma)] \\ &\quad \times \sum_{n=1}^{\infty} i^n F_n n(n+1) [h_n(\sigma) + i h_n^{\bullet}(\sigma)]^* \end{aligned} \quad (5.9.3)$$

Limiting forms of spherical Hankel functions are given in Eqs. (A.25.17) and (A.26.4). Substituting them into Eq. (5.9.3) gives the maximum value of the radial component of the Poynting vector:

$$N_r(\sigma, 0) = \frac{1}{\eta \sigma^2} \left[\sum_{\ell=1}^{\infty} F_{\ell} \ell(\ell+1) \right]^2 \quad (5.9.4)$$

Using the fields of Eq. (5.8.3), the output power on a virtual sphere of indefinitely large radius is:

$$\begin{aligned} P_{\text{av}} &= \frac{\sigma^2}{2\eta k^2} \sum_{\ell=1}^{\infty} \int_0^{2\pi} d\phi \int_0^{\pi} \sin \theta d\theta i^{-\ell} [F_{\ell}]^2 \left\{ \frac{e^{i(\ell+1)}}{\sigma} \left[\frac{P_{\ell}^1}{\sin \theta} + \frac{dP_{\ell}^1}{d\theta} \right] [\hat{\theta} - i \hat{\phi}] \right\} \\ &\quad \times i^{\ell} \left\{ \frac{e^{-i(\ell+1)}}{\sigma} \left[\frac{P_{\ell}^1}{\sin \theta} + \frac{dP_{\ell}^1}{d\theta} \right] [\hat{\theta} + i \hat{\phi}] \right\} \end{aligned} \quad (5.9.5)$$

Evaluation gives:

$$P_{\text{av}} = \frac{4\pi}{\eta k^2} \sum_{\ell=1}^{\infty} F_{\ell}^2 \left(\frac{\ell^2(\ell+1)^2}{2\ell+1} \right) \quad (5.9.6)$$

Substituting Eqs. (5.9.4) and (5.9.6) into Eq. (5.9.1) gives:

$$G(\sigma) = \left[\sum_{\ell=1}^{\infty} F_{\ell} \ell(\ell+1) \right]^2 \bigg/ \sum_{\ell=1}^{\infty} F_{\ell}^2 \frac{\ell^2(\ell+1)^2}{2\ell+1} \quad (5.9.7)$$

A particularly interesting special case occurs if the modal coefficients satisfy the relationship:

$$F_{\ell} = \frac{(2\ell+1)}{\ell(\ell+1)} \quad (5.9.8)$$

For this special case the gain is:

$$G = \sum_{\ell=1}^{\infty} (2\ell+1) \quad (5.9.9)$$

This expression for gain, first published by Harrington in 1960, vividly demonstrates that the radiation of spherical modes can be arranged to support power with a net gain: it does not possess circular symmetry. In many cases, including those of interest here, radiation with a gain other than unity produces a net transfer of linear momentum.

5.10. Kinematic Values of the Radiation

Radiation from electrically small sources is dominated, in the main, by the moment with the lowest power of ka . A primary reason is that the Qs of electrically small antennas producing single modes increase rapidly with increasing order, i.e. as $|\gamma(\sigma)|$ of Table 3.2.1. However it was shown in Sec. 3.16 that a multimodal source generating the fields of Eq. (5.8.3) does not necessarily extract a returnable standing energy from the source. By Eqs. (A.28.12) and (A.29.18) the magnitudes of electric and magnetic multipolar fields of order ℓ are respectively proportional to $(ka)^\ell$ and $(ka)^{\ell+1}$. The magnitude of fields scattered by a passive, electrically small object will, therefore, decrease rapidly with increasing modal order, see Eq. (2.3.10). For the case of interest here, however, the scatterer is not a passive object but an excited, eigenstate electron. The host atom is immersed within a z -directed, circularly polarized plane wave that somehow connects to a nonlinear, radiating transition to a lower energy eigenstate; the radiated fields are expected to be dramatically different from those of passive scatterers. We seek details.

With p_z and l_z representing respectively linear and angular momentum, the kinematic properties of atomic radiation are:

$$W/p_z = c \quad W/l_z = \omega \quad p_z/l_z = k \quad (5.10.1)$$

To examine results of the field set shown by Eq. (5.8.3) consider the rate at which energy, linear momentum, and angular momentum exit through the surface of a sphere of radius σ/k circumscribing the active region.

The rate at which energy is radiated follows by use of Eq. (1.9.11). The rate of energy loss through a spherical shell is:

$$\frac{dW}{dt} = \frac{\sigma^2}{k^2} \int_0^{2\pi} d\phi \int_0^\pi \text{Re}[N_r] \sin \theta d\theta \quad (5.10.2)$$

Since the momentum contained within a volume is equal to $1/c^2$ times the volume integral of the Poynting vector, see Eq. (1.9.7), the rate of

momentum loss through a spherical shell is

$$\mathbf{p} = \frac{1}{c^2 k^3} \int \sigma^2 d\sigma \int_0^{2\pi} d\phi \int_0^\pi \text{Re}[\mathbf{N}] \sin \theta d\theta \quad (5.10.3)$$

Since the equality holds for every volume in space the rate at which the z -component of momentum exits a closed volume is equal to c times the surface integral of the z -component of momentum:

$$\frac{dp_z}{dt} = \frac{\sigma^2}{ck^2} \int_0^{2\pi} d\phi \int_0^\pi \text{Re}[N_r \cos \theta - N_\theta \sin \theta] \sin \theta d\theta \quad (5.10.4)$$

Angular momentum is related to linear momentum by Eq. (4.9.1); it follows that the rate at which z -directed angular momentum exits a closed volume is:

$$\frac{dl_z}{dt} = \frac{\sigma^3}{ck^3} \int_0^{2\pi} d\phi \int_0^\pi \text{Re}[N_\phi] \sin^2 \theta d\theta \quad (5.10.5)$$

The Poynting vector components follow from the fields of Eq. (5.8.3) with coefficients F_ℓ as unknowns. Putting $j = i$ gives the Poynting vector:

$$\begin{aligned} N_r = & \frac{\text{Re}}{2\eta} \sum_{\ell=1}^{\infty} \sum_{n=1}^{\infty} F_\ell F_n^* i^{n-\ell} \left\{ (h_\ell h_n^* + h_\ell^* h_n) \left(\frac{P_\ell^1}{\sin \theta} \frac{dP_n^1}{d\theta} + \frac{P_n^1}{\sin \theta} \frac{dP_\ell^1}{d\theta} \right) \right. \\ & \left. - i(h_\ell h_n^* - h_n^* h_\ell) \left(\frac{P_\ell^1}{\sin \theta} \frac{P_n^1}{\sin \theta} + \frac{dP_\ell^1}{d\theta} \frac{dP_n^1}{d\theta} \right) \right\} \end{aligned} \quad (5.10.6)$$

$$N_\theta = -\frac{\text{Re}}{2\sigma\eta} \sum_{\ell=1}^{\infty} \sum_{n=1}^{\infty} F_\ell F_n^* i^{n-\ell} [n(n+1)h_n^* h_\ell^* + \ell(\ell+1)h_\ell h_n^*] \frac{P_\ell^1 P_n^1}{\sin \theta} \quad (5.10.7)$$

$$\begin{aligned} N_\phi = & \frac{\text{Re}}{2\sigma\eta} \sum_{\ell=1}^{\infty} \sum_{n=1}^{\infty} F_\ell F_n^* i^{n-\ell} \left\{ \left(n(n+1)h_n^* h_\ell^* P_n^1 \frac{dP_\ell^1}{d\theta} - \ell(\ell+1)h_\ell h_n^* P_\ell^1 \frac{dP_n^1}{d\theta} \right) \right. \\ & \left. - i \left([\ell(\ell+1) + n(n+1)] h_\ell h_n^* \frac{P_\ell^1 P_n^1}{\sin \theta} \right) \right\} \end{aligned} \quad (5.10.8)$$

Substituting these values into Eqs. (5.10.2), (5.10.4), and (5.10.5), evaluating the integrals using Table A.22.1, and replacing the spherical radial

functions by letter functions gives:

$$\frac{dW}{dt} = \frac{4\pi}{\eta k^2} \sum_{\ell=1}^{\infty} \frac{\ell^2(\ell+1)^2}{(2\ell+1)} F_{\ell} F_{\ell}^* \quad (5.10.9)$$

$$\begin{aligned} \frac{dp_z}{dt} = & \frac{2\pi}{\eta c k^2} \sum_{\ell=1}^{\infty} \operatorname{Re} \left\{ F_{\ell} F_{\ell}^* \frac{\ell(\ell+1)}{(2\ell+1)} (A_{\ell}^2 + B_{\ell}^2 + C_{\ell}^2 + D_{\ell}^2) \right. \\ & - F_{\ell} F_{\ell}^* \frac{2\ell^2(\ell+1)^2}{\sigma(2\ell+1)} (A_{\ell} C_{\ell} + B_{\ell} D_{\ell}) \\ & + F_{\ell} F_{\ell+1}^* \frac{\ell^2(\ell+1)(\ell+2)^2}{(2\ell+1)(2\ell+3)} (A_{\ell} C_{\ell+1} - A_{\ell+1} C_{\ell} + B_{\ell} D_{\ell+1} - B_{\ell+1} D_{\ell}) \\ & - 2F_{\ell} F_{\ell+1}^* \frac{2\ell^2(\ell+1)^2(\ell+2)^2}{(2\ell+1)(2\ell+3)\sigma} (A_{\ell} C_{\ell+1} + B_{\ell} D_{\ell+1}) \\ & + F_{\ell} F_{\ell-1}^* \frac{(\ell-1)^2\ell(\ell+1)^2}{(2\ell+1)(2\ell-1)} (A_{\ell-1} C_{\ell} - A_{\ell} C_{\ell-1} + B_{\ell-1} D_{\ell} - B_{\ell} D_{\ell-1}) \\ & \left. - 2F_{\ell} F_{\ell-1}^* \frac{2(\ell-1)^2\ell^2(\ell+1)^2}{(2\ell+1)(2\ell-1)\sigma} (A_{\ell} C_{\ell-1} + B_{\ell} D_{\ell-1}) \right\} \quad (5.10.10) \end{aligned}$$

$$\begin{aligned} \frac{dl_z}{dt} = & \frac{4\pi}{\eta \omega k^2} \sum_{\ell=1}^{\infty} \operatorname{Re} \left\{ F_{\ell} F_{\ell}^* \frac{\ell^2(\ell+1)^2}{(2\ell+1)} (A_{\ell}^2 + B_{\ell}^2) \right. \\ & - (F_{\ell} F_{\ell-1}^* - F_{\ell-1} F_{\ell}^*) \frac{(\ell-1)^2\ell^2(\ell+1)^2}{2(2\ell+1)(2\ell-1)} \\ & \times [(A_{\ell} C_{\ell-1} + B_{\ell} D_{\ell-1}) - i(A_{\ell} D_{\ell-1} - B_{\ell} C_{\ell-1})] \\ & - (F_{\ell+1} F_{\ell}^* - F_{\ell} F_{\ell+1}^*) \frac{\ell^2(\ell+1)^2(\ell+2)^2}{2(2\ell+1)(2\ell+3)} \\ & \left. \times [(A_{\ell} C_{\ell+1} + B_{\ell} D_{\ell+1}) - i(A_{\ell} D_{\ell+1} - B_{\ell} C_{\ell+1})] \right\} \quad (5.10.11) \end{aligned}$$

As the radius becomes limitlessly large these values go to:

$$\begin{aligned} \frac{dW}{dt} &= \frac{4\pi}{\eta k^2} \sum_{\ell=1}^{\infty} F_{\ell} F_{\ell}^* \frac{\ell^2(\ell+1)^2}{(2\ell+1)} \\ \frac{dp_z}{dt} &= \frac{4\pi}{\eta c k^2} \sum_{\ell=1}^{\infty} \frac{\ell(\ell+1)}{(2\ell+1)} \left\{ F_{\ell} F_{\ell}^* + F_{\ell} F_{\ell+1}^* \frac{\ell(\ell+2)^2}{(2\ell+3)} + F_{\ell} F_{\ell-1}^* \frac{(\ell-1)^2(\ell+1)}{(2\ell-1)} \right\} \\ \frac{dl_z}{dt} &= \frac{4\pi}{\eta \omega k^2} \sum_{\ell=1}^{\infty} F_{\ell} F_{\ell}^* \frac{\ell^2(\ell+1)^2}{(2\ell+1)} \quad (5.10.12) \end{aligned}$$

Equation (5.10.12) shows that both the energy-to-angular momentum ratio and the energy-to-linear momentum ratio depend upon the magnitude of recursion relation F_ℓ . Before solving for F_ℓ , it is necessary to consider some additional factors.

A field described by Eq. (5.8.3) can be put in closed form for only a very large or a very small radius. For a very large radius, from Eq. (A.24.13), the limiting values of the radial functions are:

$$\begin{aligned} \lim_{\sigma \rightarrow \infty} j_\ell(\sigma) &= \frac{1}{\sigma} \cos \left[\sigma - \frac{\pi}{2}(\ell + 1) \right] \\ \lim_{\sigma \rightarrow \infty} y_\ell(\sigma) &= \frac{1}{\sigma} \sin \left[\sigma - \frac{\pi}{2}(\ell + 1) \right] = \frac{1}{\sigma} \cos \left[\sigma - \frac{\pi}{2}(\ell + 2)\ell \right] \end{aligned} \quad (5.10.13)$$

The two functions differ in phase by $\pi/2$. Next, multiply the Neumann functions by $(\pm i)$, as is necessary to form spherical Hankel functions. This changes the phase by another $\pi/2$ and causes the Bessel and Neumann functions either to be in phase or π out of phase, depending upon whether the phase shift adds or subtracts. The result is that in the limit of infinite radius changing spherical Bessel functions to spherical Hankel functions results in the far field sum of Bessel and Neumann parts either to double or to sum to zero.

In the limit of small radius, the two functions are equal to:

$$\lim_{\sigma \rightarrow 0} j_\ell(\sigma) = \frac{\sigma^\ell}{(2\ell + 1)!!} \quad \text{and} \quad \lim_{\sigma \rightarrow 0} y_\ell(\sigma) = -\frac{(2\ell - 1)!!}{\sigma^{\ell+1}} \quad (5.10.14)$$

Spherical Bessel function solutions are continuous through all orders at the origin and spherical Neumann function solutions undergo an $(\ell + 1)$ -order singularity. Spherical Neumann functions therefore are essential for the description of generated or absorbed fields but not for scattered ones.

In a step which we support in Chapter 6 we assert that the correct recursion relationship of the field coefficients is:

$$F_\ell = \frac{(2\ell + 1)}{\ell(\ell + 1)} F \quad (5.10.15)$$

F is real and independent of ℓ . Substituting the relationship back into field Eq. (5.8.3) repeats Eq. (5.8.2) except for the radial functions and

the limiting values obtained using Eqs. (5.10.13) and (5.10.14) apply.

$$\begin{aligned} \tilde{\mathbf{E}} = & \sum_{\ell=1}^{\infty} i^{-\ell} \frac{(2\ell+1)}{\ell(\ell+1)} \left\{ i \ell(\ell+1) \frac{h_{\ell}(\sigma)}{\sigma} P_{\ell}^1(\cos\theta) \hat{r} \right. \\ & + \left[h_{\ell}(\sigma) \frac{P_{\ell}^1(\cos\theta)}{\sin\theta} + i h_{\ell}^{\bullet}(\sigma) \frac{dP_{\ell}^1(\cos\theta)}{d\theta} \right] \hat{\theta} \\ & \left. - i \left[h_{\ell}(\sigma) \frac{dP_{\ell}^1(\cos\theta)}{d\theta} + i h_{\ell}^{\bullet}(\sigma) \frac{P_{\ell}^1(\cos\theta)}{\sin\theta} \right] \hat{\phi} \right\} \exp(-i\phi) \\ \eta \tilde{\mathbf{H}} = & i \tilde{\mathbf{E}} \end{aligned} \quad (5.10.16)$$

The combined functional forms of Legendre functions that appear in Eq. (5.8.3), with axial values detailed in Eq. (5.8.4), add in phase along the positive z -axis and out of phase along the negative z -axis. Modifications of this axial result extend over the full range of solid angles and result in the gain calculated by Harrington, Eq. (5.9.8). Both Einstein and Planck missed this mechanism for circularly symmetric modal sources to transfer linear momentum.

The rate at which the kinematic parameters are carried away from a source producing the fields of Eq. (5.10.16) may be calculated by substituting Eq. (5.10.16) into Eq. (5.10.12). Values are:

$$\begin{aligned} \lim_{\sigma \rightarrow \infty} \frac{dW}{dt} &= \frac{4\pi F^2}{\eta k^2} \sum_{\ell=1}^{\infty} (2\ell+1) \\ \lim_{\sigma \rightarrow \infty} \frac{dp_z}{dt} &= \frac{4\pi F^2}{\eta c k^2} \sum_{\ell=1}^{\infty} (2\ell+1) \\ \lim_{\sigma \rightarrow \infty} \frac{dl_z}{dt} &= \frac{4\pi F^2}{\eta \omega k^2} \sum_{\ell=1}^{\infty} (2\ell+1) \end{aligned} \quad (5.10.17)$$

It follows from Eq. (5.10.17) that:

$$\begin{aligned} \lim_{\sigma \rightarrow \infty} \frac{dW}{dt} \bigg/ \frac{dp_z}{dt} &= c \\ \lim_{\sigma \rightarrow \infty} \frac{dW}{dt} \bigg/ \frac{dl_z}{dt} &= \omega \\ \lim_{\sigma \rightarrow \infty} \frac{dp_z}{dt} \bigg/ \frac{dl_z}{dt} &= k \end{aligned} \quad (5.10.18)$$

Since the time-variations of the three kinematic properties are identical, Eq. (5.10.18) leads directly to Eq. (5.10.1). The conclusions are: (1) the kinematic properties of this radiation are the same as the kinematic properties of photons, (2) there is no dichotomy between the kinematic properties of photons and classical field theory, and (3) all three parameters are proportional to the gain, see Eq. (5.9.9).

It is shown in Sec. 3.16 that any field set that satisfies Eq. (5.8.2) is resonant and no net energy returns to the source. Additionally, as discussed in Sec. 5.8, the phases of recursion relationship Eq. (5.10.15) uniquely define fields for which equal powers of σ have equal phases in all modal orders. This creates cross coupling amongst all orders and thereby a regenerative far field drive. To examine magnitude effects of Eq. (5.10.15) it is necessary to consider details of field set Eq. (5.10.16).

References

- R. Becker, *Electromagnetic Fields and Interactions*, trans. by F. Sauter, Dover Publications (1964).
- M. Born, "Obituary, Max Karl Ernst Ludwig Planck," *Obituary Notices of Fellows of the Royal Society* **6** (1948) 161–180, also in *The World of the Atom*, H. A. Boorse and L. Motz, eds., Basic Books (1966) pp. 462–484.
- M.D. Crisp, E.T. Jaynes, "Radiative Effects in Semiclassical Theory," *Phys. Rev.* **179** (1969) 1253–1261.
- J. Dodd, "The Compton Effect — A Classical Treatment," *Eur. J. Phys.* **4** (1983) 205–211.
- A. Einstein, "The Quantum Theory of Radiation," *Phys. Z.* **18**, (1917) 121–128; also in *The World of the Atom*, H.A. Boorse and L. Motz, eds., Basic Books (1966) pp. 888–901.
- K. Huang, *Statistical Mechanics*, John Wiley & Sons, New York (1967).
- W.E. Lamb, Jr., M.O. Scully, "The Photoelectric Effect without Photons," in *Polarization, Matter and Radiation, Jubilee volume in honor of Alfred Kasper*, Presses Universitaires de France, Paris (1969) pp. 363–369.
- M. Planck, "The Origin and Development of the Quantum Theory," Nobel Prize in Physics Address, 1919, in *The World of the Atom*, H.A. Boorse and L. Motz, eds., Basic Books (1966) pp. 491–501.
- M. Planck, *The Theory of Heat Radiation*, trans. By M. Masius, Dover Publications (1959).
- R.C. Tolman, *The Principles of Statistical Mechanics* (1938), reprinted by Dover Publications (1979).

CHAPTER 6

Photons

This chapter calculates details of the fields produced by an electron as it transitions between eigenstates. Chapter 4 shows that Schrödinger's equation applies during periods of electron equilibrium and near-equilibrium, but not during transitions. A derivation of Schrödinger's equation is a necessary but insufficient condition for explaining quantum theory. It is insufficient because it is an energy conservation law and, as such, quite disparate atomic-level models can lead to it as a macroscopic result. Different models differ in that they support quite different physical interpretations of electronic reality. Surely the model that best satisfies the Law of Parsimony is desired; we believe the model presented in this book, extendable electrons and classical physics, meets the conditions of that law. Chapter 5 shows that the model and classical electromagnetic theory predict radiation exchanges where the radiation supports the kinematic properties of photons. A primary purpose of this chapter is to show that the model is sufficiently general to explain characteristics of electrically small regions during periods of energy exchanges, including all electromagnetic fields, near and far.

Quite differently from the kinematic conservation laws, electromagnetic fields are the unique result of specific charge and current distributions. The inverse is also true: a specific set of fields determines a unique set of charge and current distributions (with the exception of replacing sources by a circumscribing boundary). For these reasons the principal argument supporting this model of physical reality is the development of the photon solution, not Schrödinger's equation.

Consider the following question: if there are time hiatuses during which the Schrödinger equation does not apply, what does describe a transitioning electron? We show a uniquely arrayed and properly phased resonant set of dipolar TE and TM modal electromagnetic fields that are necessary for transition onset. Once begun the dipole modes drive the source in a way

that generates all higher-order modes of the same degree. The higher order modes, in turn, contribute to the driving force. The new driving force is nonlinear and the combination is regenerative; it drives the active region until all eigenstate energy is fully emitted or absorbed. Since the regeneration is at a particular frequency and phase, neither multiple frequencies nor combined absorption and emission are possible from a single-frequency regenerative drive.

An analysis of photon radiation fields is similar to an analysis of any other problem in electromagnetics. Chapter 2 contains several examples: The radiation kinematics of photons acts as boundary conditions on the multimodal field expansion of Eq. (1.12.9) and determine the full coefficient set. From that field set we learn that the near field radiation reaction pressure during transition processes dominates all other local forces, it is many orders of magnitude larger than the Coulomb trapping pressure, and it is directed and phased to regeneratively drive energy exchanges.

6.1. Telefields and Far Fields

The field intensities of a circularly polarized, z -directed plane wave are expressed in spherical coordinates by Eq. (5.8.1) and in terms of a multipolar expansion by Eq. (5.8.2.) The uniqueness theorem requires them to be identical. If a source or sink for the wave is included the applicable field set is expressed by the multipolar field expansion of Eq. (5.10.16). This field set is in the category of fields described in Sec. 3.16: it is resonant in the sense that a circumscribing sphere supports only exchanged energy and there is no source-associated standing energy at any point on the surface. A computational difficulty with such waves is that large modal orders are physically significant but difficult to mathematically evaluate. We therefore seek a spherical coordinate expression as similar as possible to that of Eq. (5.8.1) describing the fields of Eq. (5.10.16).

Since the magnitudes of the field terms of Eq. (5.8.1) are independent of distance, we define them to be telefield terms. For comparison, far field terms are proportional to $1/\sigma$, inverse square terms are proportional to $1/\sigma^2$, and near field terms are proportional to $1/\sigma^n$ where $n > 2$. After putting $j = i$, the electric and magnetic field intensities are related as

$$\eta \tilde{\mathbf{H}} = i \tilde{\mathbf{E}} \quad (6.1.1)$$

It is, therefore, sufficient to solve for the electric field only.

We begin by defining the following sums over the spherical functions:

$$\begin{aligned}
 S_1(\sigma, \theta) &= \sum_{\ell=1}^{\infty} i^{1-\ell} (2\ell + 1) h_{\ell}(\sigma) P_{\ell}^1(\cos \theta) = S_{11}(\sigma, \theta) - iS_{12}(\sigma, \theta) \\
 S_2(\sigma, \theta) &= \sum_{\ell=1}^{\infty} i^{-\ell} \frac{(2\ell + 1)}{\ell(\ell + 1)} h_{\ell}(\sigma) \frac{dP_{\ell}^1(\cos \theta)}{d\theta} = S_{21}(\sigma, \theta) - iS_{22}(\sigma, \theta) \quad (6.1.2) \\
 S_3(\sigma, \theta) &= \sum_{\ell=1}^{\infty} i^{-\ell} \frac{(2\ell + 1)}{\ell(\ell + 1)} h_{\ell}(\sigma) \frac{P_{\ell}^1(\cos \theta)}{\sin \theta} = S_{31}(\sigma, \theta) - iS_{32}(\sigma, \theta)
 \end{aligned}$$

The radial dependent portions of S_{n1} and S_{n2} are respectively spherical Bessel and Neumann functions. To complete the field sums, it is also necessary to evaluate the modified sums:

$$\mathbb{S}_2(\sigma, \theta) = \frac{i}{\sigma} \frac{\partial}{\partial \sigma} [\sigma S_2(\sigma, \theta)] \quad \text{and} \quad \mathbb{S}_3(\sigma, \theta) = \frac{i}{\sigma} \frac{\partial}{\partial \sigma} [\sigma S_3(\sigma, \theta)] \quad (6.1.3)$$

Combining Eqs. (6.1.2), (6.1.3) and (5.10.16) gives:

$$\begin{aligned}
 \sigma E_r &= S_1(\sigma, \theta) e^{-i\phi} \\
 E_{\theta} &= [S_3(\sigma, \theta) + \mathbb{S}_2(\sigma, \theta)] e^{-i\phi} \\
 E_{\phi} &= -i[S_2(\sigma, \theta) + \mathbb{S}_3(\sigma, \theta)] e^{-i\phi}
 \end{aligned} \quad (6.1.4)$$

It follows from Eqs. (6.1.2) and (6.1.3) that:

$$S_2(\sigma, \theta) = \frac{\partial}{\partial \theta} [\sin \theta S_3(\sigma, \theta)] \quad \text{and} \quad \mathbb{S}_2(\sigma, \theta) = \frac{\partial}{\partial \theta} [\sin \theta \mathbb{S}_3(\sigma, \theta)] \quad (6.1.5)$$

Equating the radial field components of Eqs. (5.8.1) and (5.8.2) gives:

$$S_{11} = \sigma \sin \theta e^{-i\sigma \cos \theta} \quad (6.1.6)$$

Equating the angular field components of Eqs. (5.8.1) and (5.8.2) gives:

$$\begin{aligned}
 \cos \theta e^{-i\sigma \cos \theta} &= \sum_{\ell=1}^{\infty} i^{-\ell} \frac{(2\ell + 1)}{\ell(\ell + 1)} \left[j_{\ell}(\sigma) \frac{P_{\ell}^1(\cos \theta)}{\sin \theta} + i j_{\ell}^{\bullet}(\sigma) \frac{dP_{\ell}^1(\cos \theta)}{d\theta} \right] \\
 e^{-i\sigma \cos \theta} &= \sum_{\ell=1}^{\infty} i^{-\ell} \frac{(2\ell + 1)}{\ell(\ell + 1)} \left[j_{\ell}(\sigma) \frac{dP_{\ell}^1(\cos \theta)}{d\theta} + i j_{\ell}^{\bullet}(\sigma) \frac{P_{\ell}^1(\cos \theta)}{\sin \theta} \right]
 \end{aligned} \quad (6.1.7)$$

To obtain an explicit functional form for the angular field, begin with the identities of Tables (A.21.1.1) and (A.21.1.5):

$$\begin{aligned}\frac{d}{d\theta}P_\ell^1(\cos\theta) &= \frac{1}{2}[\ell(\ell+1)P_\ell - P_\ell^2] \\ \frac{P_\ell^1(\cos\theta)}{\sin\theta} &= \frac{1}{2\cos\theta}[\ell(\ell+1)P_\ell + P_\ell^2]\end{aligned}\quad (6.1.8)$$

Substituting these identities into Eq. (6.1.7) gives:

$$\begin{aligned}\cos\theta e^{-i\sigma\cos\theta} &= \frac{1}{2}\left\{\sum_{\ell=1}^{\infty}i^{-\ell}(2\ell+1)\left[\mathbf{j}_\ell(\sigma)\frac{P_\ell(\cos\theta)}{\cos\theta} + i\mathbf{j}_\ell^\bullet(\sigma)P_\ell(\cos\theta)\right]\right. \\ &\quad \left. + \sum_{\ell=1}^{\infty}i^{-\ell}\frac{(2\ell+1)}{\ell(\ell+1)}\left[\mathbf{j}_\ell(\sigma)\frac{P_\ell^2(\cos\theta)}{\cos\theta} - i\mathbf{j}_\ell^\bullet(\sigma)P_\ell^2(\cos\theta)\right]\right\}\end{aligned}\quad (6.1.9)$$

$$\begin{aligned}e^{-i\sigma\cos\theta} &= \frac{1}{2}\left\{\sum_{\ell=1}^{\infty}i^{-\ell}(2\ell+1)\left[\mathbf{j}_\ell(\sigma)P_\ell(\cos\theta) + i\mathbf{j}_\ell^\bullet(\sigma)\frac{P_\ell(\cos\theta)}{\cos\theta}\right]\right. \\ &\quad \left. - \sum_{\ell=1}^{\infty}i^{-\ell}\frac{(2\ell+1)}{\ell(\ell+1)}\left[\mathbf{j}_\ell(\sigma)P_\ell^2(\cos\theta) + i\mathbf{j}_\ell^\bullet(\sigma)\frac{P_\ell^2(\cos\theta)}{\cos\theta}\right]\right\}\end{aligned}\quad (6.1.10)$$

The sums on the upper lines of Eqs. (6.1.9) and (6.1.10), derivable from Eq. (A.27.6), are in the form of linear, algebraic equations with the sums on the bottom lines as unknowns. Writing “x” and “y” for unknowns the equations have the general form:

$$f_1(\sigma, \cos\theta) = \frac{1}{2}\left(\frac{x}{\cos\theta} - iy\right) \quad f_2(\sigma, \cos\theta) = -\frac{1}{2}\left(x + \frac{iy}{\cos\theta}\right) \quad (6.1.11)$$

Solving Eq. (6.1.11) gives the equality:

$$\begin{aligned}\sum_{\ell=1}^{\infty}i^{-\ell}\frac{(2\ell+1)}{\ell(\ell+1)}\mathbf{j}_\ell P_\ell^2(\cos\theta) &= -\left(e^{-i\sigma\cos\theta} + \frac{\sin\sigma}{\sigma}\right) - \frac{2i}{\sigma\sin^2\theta} \\ &\quad \times [e^{-i\sigma\cos\theta}\cos\theta - (\cos\sigma\cos\theta - i\sin\sigma)]\end{aligned}\quad (6.1.12)$$

Multiply each part of Eq. (6.1.8) on the left by the operator:

$$O \Rightarrow \sum_{\ell=1}^{\infty}i^{-\ell}\frac{(2\ell+1)}{\ell(\ell+1)}\mathbf{j}_\ell(\sigma) \quad (6.1.13)$$

This gives the equality set:

$$\begin{aligned}
 & \sum_{\ell=1}^{\infty} i^{-\ell} \frac{(2\ell+1)}{\ell(\ell+1)} \frac{d}{d\theta} P_{\ell}^1(\cos\theta) \\
 &= \frac{1}{2} \left[\sum_{\ell=1}^{\infty} i^{-\ell} (2\ell+1) P_{\ell}(\cos\theta) - \sum_{\ell=1}^{\infty} i^{-\ell} \frac{(2\ell+1)}{\ell(\ell+1)} P_{\ell}^2(\cos\theta) \right] \\
 & \sum_{\ell=1}^{\infty} i^{-\ell} \frac{(2\ell+1)}{\ell(\ell+1)} \frac{P_{\ell}^1(\cos\theta)}{\sin\theta} \\
 &= \frac{1}{2\cos\theta} \left[\sum_{\ell=1}^{\infty} i^{-\ell} (2\ell+1) P_{\ell}(\cos\theta) + \sum_{\ell=1}^{\infty} i^{-\ell} \frac{(2\ell+1)}{\ell(\ell+1)} P_{\ell}^2(\cos\theta) \right]
 \end{aligned} \tag{6.1.14}$$

The sums on the right follow from Eqs. (A.27.6) and (6.1.12) and give exact values for angular sums:

$$\begin{aligned}
 S_{31} &= -\frac{i}{\sigma \sin^2 \theta} [e^{-i\sigma \cos \theta} - (\cos \sigma - i \sin \sigma \cos \theta)] \\
 S_{21} &= e^{-i\sigma \cos \theta} + \frac{i}{\sigma \sin^2 \theta} [e^{-i\sigma \cos \theta} \cos \theta - (\cos \sigma \cos \theta - i \sin \sigma)]
 \end{aligned} \tag{6.1.15}$$

Since these equation forms recur often in the ensuing discussion it is helpful to define the optical source functions $U(\sigma, \theta)$ and $V(\sigma, \theta)$:

$$\begin{aligned}
 U(\sigma, \theta) &= \frac{1}{\sigma \sin^2 \theta} [e^{-i\sigma \cos \theta} - (\cos \sigma - i \sin \sigma \cos \theta)] \\
 V(\sigma, \theta) &= \frac{1}{\sigma \sin^2 \theta} [e^{-i\sigma \cos \theta} \cos \theta - (\cos \sigma \cos \theta - i \sin \sigma)]
 \end{aligned} \tag{6.1.16}$$

In terms of $U(\sigma, \theta)$ and $V(\sigma, \theta)$, S_{21} and S_{31} are:

$$S_{31} = -iU(\sigma, \theta) \quad S_{21} = e^{-i\sigma \cos \theta} + iV(\sigma, \theta) \tag{6.1.17}$$

It follows from Eqs. (6.1.17) and (6.1.3) that:

$$\mathcal{S}_{31} = -iV(\sigma, \theta) \quad \mathcal{S}_{21} = e^{-i\sigma \cos \theta} \cos \theta + iU(\sigma, \theta) \tag{6.1.18}$$

For what follows it is necessary to separate Eq. (5.10.16) into TM and TE parts; after doing so the TM and TE portions are:

$$\begin{aligned}\tilde{\mathbf{E}}_{\text{TM}} &= \sum_{\ell=1}^{\infty} i^{-\ell} \frac{(2\ell+1)}{\ell(\ell+1)} \left\{ i\ell(\ell+1) \frac{h_{\ell}(\sigma)}{\sigma} P_{\ell}^1(\cos\theta) \hat{r} \right. \\ &\quad \left. + ih_{\ell}^{\bullet}(\sigma) \frac{dP_{\ell}^1(\cos\theta)}{d\theta} \hat{\theta} - h_{\ell}^{\bullet}(\sigma) \frac{P_{\ell}^1(\cos\theta)}{\sin\theta} \hat{\phi} \right\} e^{-i\phi} \\ \eta\tilde{\mathbf{H}}_{\text{TM}} &= \sum_{\ell=1}^{\infty} i^{-\ell} \frac{(2\ell+1)}{\ell(\ell+1)} \left\{ h_{\ell}(\sigma) \frac{P_{\ell}^1(\cos\theta)}{\sin\theta} \hat{\theta} - ih_{\ell}(\sigma) \frac{dP_{\ell}^1(\cos\theta)}{d\theta} \hat{\phi} \right\} e^{-i\phi}\end{aligned}\tag{6.1.19}$$

$$\begin{aligned}\eta\tilde{\mathbf{H}}_{\text{TE}} &= \sum_{\ell=1}^{\infty} i^{-\ell} \frac{(2\ell+1)}{\ell(\ell+1)} \left\{ \ell(\ell+1) \frac{h_{\ell}(\sigma)}{\sigma} P_{\ell}^1(\cos\theta) \hat{r} \right. \\ &\quad \left. - h_{\ell}^{\bullet}(\sigma) \frac{dP_{\ell}^1(\cos\theta)}{d\theta} \hat{\theta} - ih_{\ell}^{\bullet}(\sigma) \frac{P_{\ell}^1(\cos\theta)}{\sin\theta} \hat{\phi} \right\} e^{-i\phi} \\ \tilde{\mathbf{E}}_{\text{TE}} &= \sum_{\ell=1}^{\infty} i^{-\ell} \frac{(2\ell+1)}{\ell(\ell+1)} \left\{ ih_{\ell}(\sigma) \frac{P_{\ell}^1(\cos\theta)}{\sin\theta} \hat{\theta} + h_{\ell}(\sigma) \frac{dP_{\ell}^1(\cos\theta)}{d\theta} \hat{\phi} \right\} e^{-i\phi}\end{aligned}\tag{6.1.20}$$

Similarly the fields as expressed by Eq. (6.1.4) break into TM and TE parts as:

$$\begin{aligned}\tilde{\mathbf{E}}_{\text{TM}} &= [S_1 \hat{r} / \sigma + S_2 \hat{\theta} - iS_3 \hat{\phi}] e^{-i\phi} & \eta\tilde{\mathbf{H}}_{\text{TM}} &= [iS_3 \hat{\theta} + S_2 \hat{\phi}] e^{-i\phi} \\ \tilde{\mathbf{E}}_{\text{TE}} &= [S_3 \hat{\theta} - iS_2 \hat{\phi}] e^{-i\phi} & \eta\tilde{\mathbf{H}}_{\text{TE}} &= [iS_1 \hat{r} / \sigma + iS_2 \hat{\theta} + S_3 \hat{\phi}] e^{-i\phi}\end{aligned}\tag{6.1.21}$$

Substituting Eqs. (6.1.6), (6.1.17), and (6.1.18) into Eq. (6.1.21) gives the exact expression for the spherical Bessel functions portion of the TM fields:

$$\begin{aligned}\tilde{\mathbf{E}}_{\text{TM}} &= \{ \sin\theta e^{-i\sigma \cos\theta} \hat{r} + (\cos\theta e^{-i\sigma \cos\theta} + iU(\sigma, \theta)) \hat{\theta} - V(\sigma, \theta) \hat{\phi} \} e^{-i\phi} \\ \eta\tilde{\mathbf{H}}_{\text{TM}} &= \{ U(\sigma, \theta) \hat{\theta} + (e^{-i\sigma \cos\theta} + iV(\sigma, \theta)) \hat{\phi} \} e^{-i\phi}\end{aligned}\tag{6.1.22}$$

Exact values of the sums over spherical Bessel functions are listed in Table 6.1.1. Values on the positive and negative z -axes and in the equatorial plane are listed in Table 6.1.2.

Table 6.1.1. Closed form solutions for the field sums defined in Eqs. (6.1.2) and (6.1.3), over spherical Bessel functions.

| |
|--|
| $S_{11}(\sigma, \theta) = \sigma \sin \theta e^{-i\sigma \cos \theta}$ |
| $S_{21}(\sigma, \theta) = e^{-i\sigma \cos \theta} + \frac{i}{\sigma \sin^2 \theta} [e^{-i\sigma \cos \theta} \cos \theta - (\cos \sigma \cos \theta - i \sin \sigma)]$ |
| $S_{31}(\sigma, \theta) = -\frac{i}{\sigma \sin^2 \theta} [e^{-i\sigma \cos \theta} - (\cos \sigma - i \sin \sigma \cos \theta)]$ |
| $\$_{21}(\sigma, \theta) = \cos \theta e^{-i\sigma \cos \theta} + \frac{i}{\sigma \sin^2 \theta} [e^{-i\sigma \cos \theta} - (\cos \sigma - i \sin \sigma \cos \theta)]$ |
| $\$_{31}(\sigma, \theta) = -\frac{i}{\sigma \sin^2 \theta} [e^{-i\sigma \cos \theta} \cos \theta - (\cos \sigma \cos \theta - i \sin \sigma)]$ |

Table 6.1.2. Sums of Table 6.1.1 on the coordinate axes.

| | |
|--|---|
| 1. $S_{11}(\sigma, 0) = S_{11}(\sigma, \pi) = 0$ | $S_{11}(\sigma, \pi/2) = \sigma$ |
| 2. $S_{21}(\sigma, 0) = \frac{1}{2} \left[e^{-i\sigma} - \frac{\sin \sigma}{\sigma} \right]$ | $S_{21}(\sigma, \pi) = \frac{1}{2} \left[e^{i\sigma} - \frac{\sin \sigma}{\sigma} \right]$ |
| $S_{21}(\sigma, \pi/2) = \left[1 - \frac{\sin \sigma}{\sigma} \right]$ | |
| 3. $S_{31}(\sigma, 0) = \frac{1}{2} \left[e^{-i\sigma} - \frac{\sin \sigma}{\sigma} \right]$ | $S_{31}(\sigma, \pi) = -\frac{1}{2} \left[e^{i\sigma} - \frac{\sin \sigma}{\sigma} \right]$ |
| $S_{31}(\sigma, \pi/2) = -\frac{i}{\sigma} [1 - \cos \sigma]$ | |
| 4. $\$_{21}(\sigma, 0) = \frac{1}{2} \left[e^{-i\sigma} + \frac{\sin \sigma}{\sigma} \right]$ | $\$_{21}(\sigma, \pi) = -\frac{1}{2} \left[e^{i\sigma} + \frac{\sin \sigma}{\sigma} \right]$ |
| $\$_{21}(\sigma, \pi/2) = \frac{i}{\sigma} [1 - \cos \sigma]$ | |
| 5. $\$_{31}(\sigma, 0) = \frac{1}{2} \left[e^{-i\sigma} + \frac{\sin \sigma}{\sigma} \right]$ | $\$_{31}(\sigma, \pi) = \frac{1}{2} \left[e^{i\sigma} + \frac{\sin \sigma}{\sigma} \right]$ |
| $\$_{31}(\sigma, \pi/2) = \frac{\sin \sigma}{\sigma}$ | |

6.2. Evaluation of Sum S_{12} on the Axes

Evaluation of the desired sums over spherical Neumann functions is possible only on the coordinate axes. That portion of sum S_{12} , see Eq. (6.1.2), is:

$$S_{12}(\sigma, \theta) = \sum_{\ell=1}^{\infty} i^{1-\ell} (2\ell + 1) y_{\ell}(\sigma) P_{\ell}^1(\cos \theta) \quad (6.2.1)$$

Since the associated Legendre polynomial is proportional to $\sin \theta$ the sum is equal to zero on both the positive and negative z -axes:

$$S_{12}(\sigma, 0) = S_{12}(\sigma, \pi) = 0 \quad (6.2.2)$$

It remains to evaluate the sum in the equatorial plane, $\theta = \pi/2$. The series form of the associated Legendre polynomial at $\theta = \pi/2$ is given in Table A.18.1 and repeated here:

$$P_\ell^1(0) = (-1)^{(\ell-1)} \frac{(\ell)!!}{(\ell-1)!!} \delta(\ell, 2q+1) \quad (6.2.3)$$

The Kronecker delta function, with q representing an integer equal to or greater than zero, shows that the function vanishes for even numbered modes. The series forms of the spherical Neumann functions are given by Eq. (A.24.10) and repeated here:

$$y_\ell(\sigma) = - \sum_{s=0}^{\ell-1} \frac{(2\ell-2s-1)!!}{(2s)!!} \sigma^{-\ell-1+2s} - \sum_{s=0}^{\infty} \frac{(-1)^s}{(2s-1)!!} \frac{\sigma^{\ell-1+2s}}{(2\ell+2s)!!} \quad (6.2.4)$$

Substituting Eqs. (6.2.3) and (6.2.4) into Eq. (6.2.1) gives:

$$S_{12} \left(\sigma, \frac{\pi}{2} \right) = - \sum_{\ell_0;1}^{\infty} (2\ell+1) \frac{(\ell)!!}{(\ell-1)!!} \left\{ \sum_{s=0}^{\ell-1} \frac{(2\ell-2s-1)!!}{(2s)!!} \sigma^{-\ell-1+2s} + \sum_{s=0}^{\infty} \frac{(-1)^s}{(2s-1)!!} \frac{\sigma^{\ell-1+2s}}{(2\ell+2s)!!} \right\} \quad (6.2.5)$$

Lower limit ' $\ell_0; 1$ ' indicates the sum is over only odd values of ℓ and the series begins with $\ell = 1$. Since only odd modal orders contribute to the sum, it follows from Eq. (6.2.5) that only even powers of σ are present. It is of the form:

$$S_{12}(\sigma, \pi/2) = \sum_{n;-(\ell+1)}^{\infty} A_n \sigma^n \quad (6.2.6)$$

Lower limit ' $n; -(\ell+1)$ ' indicates the series contains only even values of n and begins with $n = -(\ell+1)$.

Combining Eqs. (6.2.5) and (6.2.6) to obtain coefficient A_n gives:

$$A_n = \left\{ -(-1)^{n/2} \sum_{\ell_0;1}^{n+1} \frac{(2\ell+1)(\ell)!(-1)^{(\ell-1)/2}}{(\ell-1)!(\ell+n+1)!(n-\ell)!} - \left(\text{Lim}_{L \rightarrow \infty} \right) \sum_{\ell_0;n+3}^L \frac{(2\ell+1)(\ell)!(\ell-n-2)!}{(\ell-1)!(\ell+n+1)!} \right\} \quad (6.2.7)$$

L is the largest modal number present. Consider the special case of n greater than zero and, in particular, $n = 2$. For this case the sum for A_2 obtained from Eq. (6.2.7) is:

$$\left\{ \frac{3}{8} - \frac{7}{32} - \frac{55}{1024} - \frac{105}{4096} - \frac{1995}{131078} - \frac{5313}{524288} - \frac{243243}{33554452} - \dots \right\} = 0 \quad (6.2.8)$$

The first two terms come from the first sum of Eq. (6.2.7) and the rest from the second sum. Although the equality is correct only in the limit of infinitely large L , the series converges rapidly. With L large but finite the limiting value is zero.

The coefficients of all other positive powers of σ follow in a similar way, and all of them are equal to zero. Although no individual term is equal to zero each modal order contributes the proper magnitude and phase for the sum to equal zero. Since the total field is equal to zero so is the field energy on the axis. Note that if the magnitude or the phase of coefficients for all values of ℓ is changed in a way that preserves recursion relationship Eq. (5.10.15) the field remains equal to zero. On the other hand, if the coefficient of any single mode differs from the value of Eq. (5.10.15) the field of that mode would support an additional energy field. When such variations occur the generalized gradient of the added energy describes a forcing function that drives the mode to restore Eq. (5.10.15); this is a unique characteristic of recursion relationship Eq. (5.10.15).

For negative powers of σ , the series diverges and, therefore, must terminate. With the coefficients of all modes of order greater than L equal to zero, the series is equal to:

$$S_{12}(\sigma, \pi/2) = - \sum_{\ell_0;n-1}^L (2\ell+1) \frac{(\ell)!}{(\ell-1)!} \frac{(\ell+n-2)!}{(\ell-n+1)! \sigma^n} \quad (6.2.9)$$

For the special case $n = 0$ the series of Eq. (6.2.9) is:

$$\begin{aligned} & - \left(\frac{3}{2} + \frac{21}{16} + \frac{165}{128} + \frac{2625}{2048} + \dots \right) \\ & = -(1.5 + 1.3125 + 1.2891 + 1.2817 + \dots) = -A_0 \end{aligned} \quad (6.2.10)$$

The terms approach unity as the modal number increases and A_0 is proportional to L . For L much larger than one this gives the approximate value:

$$A_0 \cong 5L/8 \quad (6.2.11)$$

For the special case $n = -2$, the series is equal to:

$$- \left(3 + \frac{63}{4} + \frac{2475}{64} + \frac{165,375}{2304} + \frac{16,967,475}{147,456} + \dots \right) = -A_2 \quad (6.2.12)$$

A_2 is proportional to L^3 . Since a term-by-term expansion shows that $A_n \approx L^{n+1}$, the sum, evaluated at the equator, is equal to:

$$\begin{aligned} S_{12}(\sigma, \pi/2) &= - \sum_{n=0;e}^{\infty} \frac{A_n}{\sigma^n} \\ A_n &= - \sum_{\ell_0; n-1}^L \frac{(2\ell+1)\ell!! (\ell+n-2)!!}{(\ell-1)!! (\ell-n+1)!!} \approx L^{n+1} \end{aligned} \quad (6.2.13)$$

Each coefficient A_n contains contributions from all modal orders. It follows from Eqs. (6.1.4), (6.1.6), and (6.2.13) that the radial component of the electric field intensity in the equatorial plane is:

$$E_r = \left\{ 1 + i \sum_{n;e;0}^{\infty} \frac{A_n}{\sigma^{n+1}} \right\} e^{-i\phi} \quad (6.2.14)$$

In summary, only negative powers of σ are present in the field expression and energy of the radial field component is localized to the source region.

6.3. Evaluation of Sums S_{22} and S_{32} on the Polar Axes

The spherical Neumann portion of sum S_{22} as defined by Eq. (6.1.2) is:

$$S_{22}(\sigma, \theta) = \sum_{\ell=1}^{\infty} i^{-\ell} \frac{(2\ell+1)}{\ell(\ell+1)} y_{\ell}(\sigma) \frac{dP_{\ell}^1(\cos\theta)}{d\theta} \quad (6.3.1)$$

The series forms of the associated Legendre polynomial at $\theta = 0$ and π are shown in Table A.18.1 and repeated here, see also Eq. (5.8.4):

$$\left. \frac{dP_{\ell}^1(\cos\theta)}{d\theta} \right|_{\theta=0} = \frac{\ell(\ell+1)}{2}, \quad \left. \frac{dP_{\ell}^1(\cos\theta)}{d\theta} \right|_{\theta=\pi} = (-1)^{\ell} \frac{\ell(\ell+1)}{2} \quad (6.3.2)$$

The spherical Neumann portion of sum S_{32} as defined by Eq. (6.1.2) is:

$$S_{32}(\sigma, \theta) = \sum_{\ell=1}^{\infty} i^{-\ell} \frac{(2\ell+1)}{\ell(\ell+1)} y_{\ell}(\sigma) \frac{P_{\ell}^1(\cos\theta)}{\sin\theta} \quad (6.3.3)$$

The series forms of the associated Legendre polynomial at $\theta = 0$ and π are shown in Table A.18.1 and repeated here:

$$\left. \frac{P_{\ell}^1(\cos\theta)}{\sin\theta} \right|_{\theta=0} = \frac{\ell(\ell+1)}{2}, \quad \left. \frac{P_{\ell}^1(\cos\theta)}{\sin\theta} \right|_{\theta=\pi} = (-1)^{\ell+1} \frac{\ell(\ell+1)}{2} \quad (6.3.4)$$

Comparing axial values of the two sums shows that:

$$S_{22}(\sigma, 0) = S_{32}(\sigma, 0), \quad S_{22}(\sigma, \pi) = -S_{32}(\sigma, \pi) \quad (6.3.5)$$

Because of these equalities, it is only necessary to evaluate one sum on the z -axes. Substituting Eq. (6.3.4) and the expansion for the spherical Neumann function, Eq. (6.2.4), into Eq. (6.3.3) gives the series expansion:

$$S_{32}(\sigma, 0) = \frac{1}{2} \sum_{\ell=1}^{\infty} i^{-\ell} (2\ell+1) y_{\ell}(\sigma) = \frac{1}{2} \sum_{\ell=0}^{\infty} i^{-\ell} (2\ell+1) y_{\ell}(\sigma) - \frac{1}{2} y_0(\sigma)$$

Inserting the expression for spherical Neumann functions gives:

$$S_{32}(\sigma, 0) = -\frac{1}{2} \sum_{\ell=0}^{\infty} i^{-\ell} (2\ell+1) \left\{ \sum_{s=0}^{\infty} \frac{(-1)^s}{(2s-1)!!} \frac{\sigma^{\ell-1+2s}}{(2\ell+2s)!!} + \sum_{s=0}^{\ell-1} \frac{(2\ell-2s-1)!!}{(2s)!!} \sigma^{-\ell-1+2s} \right\} + \frac{\cos\sigma}{2\sigma} \quad (6.3.6)$$

Although the desired sum is over values of ℓ ranging from one to infinity, it is convenient to retain the $\ell = 0$ term in the expansion and subtract it in a separate operation. Both even and odd numbered modes are present; even values of ℓ produce odd powers of σ and vice versa. Within the curly brackets of Eq. (6.3.6) the first term contains only positive powers of σ , $(\ell - 1)$ to ∞ , and the second term contains both positive and negative powers, $(-\ell + 1)$ to $(\ell - 3)$.

Next, let n be a positive integer and determine the coefficient of σ^n . It is convenient to separate Eq. (6.3.6) into sets of different parity:

$$\begin{aligned}
 S_{32} = & \left\{ i \frac{(-1)^{n/2}}{2} \sum_{\ell o; 1}^{n+1} \frac{(2\ell + 1)\sigma^n}{(n - \ell)!(n + \ell + 1)!!} \right. \\
 & \left. + \frac{i}{2} \sum_{\ell o; n+3}^{\infty} \frac{(-1)^{(\ell-1)/2} (2\ell + 1)(\ell - n - 2)!! \sigma^n}{(\ell + n + 1)!!} \right\} \\
 & \pm \left\{ \frac{(-1)^{(n-1)/2}}{2} \sum_{\ell e; 0}^{n+1} \frac{(2\ell + 1)\sigma^n}{(n - \ell)!(n + \ell + 1)!!} \right. \\
 & \left. - \frac{1}{2} \sum_{\ell e; n+3}^{\infty} \frac{(-1)^{\ell/2} (2\ell + 1)(\ell - n - 2)!! \sigma^n}{(\ell + n + 1)!!} + \frac{\cos \sigma}{2\sigma} \right\} \quad (6.3.7)
 \end{aligned}$$

The upper \pm sign is to be used at $\theta = 0$ and the lower at $\theta = \pi$. Defining S'_{32} to equal the top row of Eq. (6.3.7) and expanding the series gives:

n even, ℓ odd.

$$\begin{aligned}
 S'_{32} = & \frac{i(-1)^{n/2}}{2} \left\{ \left\{ \frac{3}{(n-1)!(n+2)!!} + \frac{7}{(n-3)!(n+4)!!} + \dots + \frac{(2n+3)}{(2n+2)!!} \right\} \right. \\
 & \left. - \left\{ \frac{(2n+7)(1)!!}{(2n+4)!!} - \frac{(2n+11)(3)!!}{(2n+6)!!} + \frac{(2n+15)(5)!!}{(2n+8)!!} - \dots \right\} \right\} \quad (6.3.8)
 \end{aligned}$$

The bottom row of Eq. (6.3.8) may be evaluated by writing $(2\ell + 1) = (\ell + n + 1) + (\ell - n)$ and regrouping the terms as:

$$\begin{aligned}
 & \left\{ (2n+4) \frac{(1)!!}{(2n+4)!!} + \frac{(1)!!}{(2n+4)!!} \left(3 - (2n+6) \frac{3}{(2n+6)} \right) \right. \\
 & \left. - \frac{(3)!!}{(2n+6)!!} \left(5 - (2n+8) \frac{5}{(2n+8)} \right) + \dots \right\} = \frac{1}{(2n+2)!!} \quad (6.3.9)
 \end{aligned}$$

Inserting Eq. (6.3.9) back into Eq. (6.3.8) gives:

n even, ℓ odd.

$$S'_{32} = \frac{i(-1)^{n/2}}{2} \left\{ \frac{3}{(n-1)!!(n+2)!!} + \frac{7}{(n-3)!!(n+4)!!} + \dots + \frac{(2n+3)}{(2n+2)!!} - \frac{1}{(2n+2)!!} \right\} \quad (6.3.10)$$

Evaluating Eq. (6.3.10) for the special case of $n = 0$ gives:

$$\frac{i}{2} \left(\frac{3}{2} - \frac{1}{2} \right) = \frac{i}{2}$$

Repeating the process for the special case of $n = 2$ results in:

$$-\frac{i}{2} \left(\frac{3}{8} + \frac{7}{48} - \frac{1}{48} \right) = -\frac{i}{4}$$

Repeating the process for all even, positive values of n equal zero or more then summing results in:

n even, ℓ odd.

$$S_{32} = \frac{i}{2} \cos \sigma \quad (6.3.11)$$

Repeating the process for the opposite parity results in:

n odd, ℓ even.

$$S_{32} = \pm \frac{1}{2} \sin \sigma \quad (6.3.12)$$

Combining results for non-negative values of n gives:

Positive powers of σ .

$$S_{32}(\sigma, 0) = \frac{1}{2} \left(ie^{-i\sigma} + \frac{\cos \sigma}{\sigma} \right), \quad S_{32}(\sigma, \pi) = \frac{1}{2} \left(ie^{i\sigma} - \frac{\cos \sigma}{\sigma} \right) \quad (6.3.13)$$

$$S_{22}(\sigma, 0) = \frac{1}{2} \left(ie^{-i\sigma} + \frac{\cos \sigma}{\sigma} \right), \quad S_{22}(\sigma, \pi) = -\frac{1}{2} \left(ie^{i\sigma} - \frac{\cos \sigma}{\sigma} \right)$$

The related sums are obtained by operating on Eq. (6.3.13) using Eq. (6.1.3):

Positive powers of σ .

$$\mathcal{S}_{32}(\sigma, 0) = \frac{1}{2} \left(ie^{-i\sigma} - \frac{\cos \sigma}{\sigma} \right), \quad \mathcal{S}_{32}(\sigma, \pi) = -\frac{1}{2} \left(ie^{i\sigma} + \frac{\cos \sigma}{\sigma} \right) \quad (6.3.14)$$

$$\mathcal{S}_{22}(\sigma, 0) = \frac{1}{2} \left(ie^{-i\sigma} - \frac{\cos \sigma}{\sigma} \right), \quad \mathcal{S}_{22}(\sigma, \pi) = \frac{1}{2} \left(ie^{i\sigma} + \frac{\cos \sigma}{\sigma} \right)$$

The magnitude and phase of each mode is the exact value needed for the sum to equal the transcendental functions of Eqs. (6.3.11) and (6.3.12); this

is a new type of wave that supports energy and momentum propagating away from the source. Although it is necessary to terminate the series at some highest modal number, L , it converges rapidly with increasing modal number and results are quite accurate for relatively small values of L . As with the spherical Bessel function terms, the magnitude of the first term in each sum is independent of σ . These characteristics are unique properties of recursion relationship Eq. (5.10.15).

The coefficients of negative powers of σ appear only in the second sum of Eq. (6.3.6). Writing negative powers of σ as positive values of n gives the sum:

$$-\frac{1}{2} \sum_{\ell=n-1}^{L+1} i^{-\ell} \frac{(2\ell+1)(\ell+n-2)!!}{(\ell-n+1)!!\sigma^n} \delta(\ell+n, 2q+1)$$

The sum is most easily evaluated by grouping the terms as $(2\ell+1) = (\ell-n+1) + (\ell+n)$ then expanding and regrouping. The result is:

$$\begin{aligned} & -\frac{i^{1-n}}{2\sigma^n} \left\{ \frac{(2n-3)!!}{(0)!!} \left((2n-1) - (2) \frac{(2n-1)}{(2)} \right) \right. \\ & - \frac{(2n-1)!!}{(2)!!} \left((2n+1) - (4) \frac{(2n+1)}{(4)} \right) \\ & \left. + \frac{(2n+1)!!}{(4)!!} \left((2n+3) - (6) \frac{(2n+3)}{(6)} \right) + \dots + \frac{i^{-L+n-2}(L+n)!!}{(L-n-1)!!} \right\} \end{aligned}$$

All except the last term are equal to zero. This leaves the series remainder:

$$-\frac{i^{-L-1}}{2\sigma^n} \frac{(L+n)!!}{(L-n+1)!!}$$

The full set of solutions for negative powers of σ are the remainders:

$$\begin{aligned} S_{32}(\sigma, 0) &= -\frac{i^{-L-1}}{2} \sum_{n=1}^{L+1} \frac{(L+n)!!}{(L-n+1)!!\sigma^n} \\ S_{32}(\sigma, \pi) &= -\frac{i^{L-1}}{2} \sum_{n=1}^{L+1} \frac{(L+n)!!}{(L-n+1)!!\sigma^n} \\ \mathcal{S}_{32}(\sigma, 0) &= \frac{i^{-L}}{2} \sum_{n=2}^{L+1} \frac{(n-1)(L+n)!!}{(L-n+1)!!\sigma^{n+1}} \\ \mathcal{S}_{32}(\sigma, \pi) &= \frac{i^L}{2} \sum_{n=2}^{L+1} \frac{(n-1)(L+n)!!}{(L-n+1)!!\sigma^{n+1}} \end{aligned} \tag{6.3.15}$$

Table 6.3.1. Field sums over spherical Neumann functions on both the positive and negative z -axes.

$$S_{22}(\sigma, 0) = S_{32}(\sigma, 0) = \frac{1}{2} \left(ie^{-i\sigma} + \frac{\cos \sigma}{\sigma} \right) - \frac{i^{-L-1}}{2} \sum_{n=1}^{L+1} \frac{(L+n)!!}{(L-n+1)!!\sigma^n}$$

$$\mathcal{S}_{22}(\sigma, 0) = \mathcal{S}_{32}(\sigma, 0) = \frac{1}{2} \left(ie^{-i\sigma} - \frac{\cos \sigma}{\sigma} \right) + \frac{i^{-L}}{2} \sum_{n=2}^{L+1} \frac{(n-1)(L+n)!!}{(L-n+1)!!\sigma^{n+1}}$$

$$S_{22}(\sigma, \pi) = -S_{32}(\sigma, \pi) = -\frac{1}{2} \left(ie^{i\sigma} - \frac{\cos \sigma}{\sigma} \right) + \frac{i^{L-1}}{2} \sum_{n=1}^{L+1} \frac{(L+n)!!}{(L-n+1)!!\sigma^n}$$

$$\mathcal{S}_{22}(\sigma, \pi) = -\mathcal{S}_{32}(\sigma, \pi) = \frac{1}{2} \left(ie^{i\sigma} + \frac{\cos \sigma}{\sigma} \right) + \frac{i^L}{2} \sum_{n=2}^{L+1} \frac{(n-1)(L+n)!!}{(L-n+1)!!\sigma^{n+1}}$$

Although the magnitude of the modal terms increases with increasing modal number, only the remainder is left and it is part of the highest order mode only. Therefore individual modes contribute nothing to the field and are not affected by them, so long as the relationship of Eq. (5.10.15) is maintained. If the relationship is disturbed the disturbed mode will create a radiation reaction force in a direction that reduces the field, thereby minimizing the field energy and maintaining Eq. (5.10.15).

Tabulated results are shown in Table 6.3.1.

6.4. Evaluation of Sum S_{32} in the Equatorial Plane

The spherical Neumann portion of sum S_{32} as defined by Eq. (6.1.2) is:

$$S_{32}(\sigma, \theta) = \sum_{\ell=1}^{\infty} i^{-\ell} \frac{(2\ell+1)}{\ell(\ell+1)} y_{\ell}(\sigma) \frac{P_{\ell}^1(\cos \theta)}{\sin \theta} \quad (6.4.1)$$

We seek simpler expressions on the coordinate axes. At $\theta = \pi/2$, the value of the Legendre function is, see Table A.18.1:

$$P_{\ell}^1(0) = i^{1-\ell} \frac{(\ell)!!}{(\ell-1)!!} \delta(\ell, 2q+1) \quad (6.4.2)$$

Substituting Eq. (6.4.2) and the spherical Neumann function, Eq. (6.2.4), into Eq. (6.4.1) gives the expression for the sum at the equator:

$$S_{32}(\sigma, \pi/2) = i \sum_{\ell \geq 1}^{\infty} \frac{(2\ell + 1)(\ell - 2)!!}{(\ell + 1)!!} \left\{ \sum_{s=0}^{\ell-1} \frac{(2\ell - 2s - 1)!!}{(2s)!!} \sigma^{-\ell-1+2s} + \sum_{s=0}^{\infty} \frac{(-1)^s}{(2s - 1)!!} \frac{\sigma^{\ell-1+2s}}{(2\ell + 2s)!!} \right\} \quad (6.4.3)$$

Since there are only odd values of ℓ , only even powers of σ are present and the sum over the positive powers of σ has the form:

$$S_{32} \left(\sigma, \frac{\pi}{2} \right) = i \sum_{n \in \text{ne}}^{\infty} B_n'' \sigma^n \quad (6.4.4)$$

Combining Eqs. (6.4.3) and (6.4.4) gives:

$$B_n'' = \left\{ (-1)^{n/2} \sum_{\ell \geq 1}^{n+1} \frac{(2\ell + 1)(\ell - 2)!! (-1)^{(\ell-1)/2}}{(\ell + 1)!! (n - \ell)!! (\ell + n + 1)!!} + i \sum_{\ell \geq n+3}^{\infty} \frac{(2\ell + 1)(\ell - 2)!! (\ell - n - 2)!!}{(\ell + 1)!! (\ell + n + 1)!!} \right\} \quad (6.4.5)$$

Consider coefficients B_0'' and B_2'' as special cases. Writing out Eq. (6.4.5) term by term for these cases gives:

$$B_0'' = \left(\frac{3}{2 \times 2} + \frac{7}{4!! \times 4!!} + \frac{11 \times 3^2}{6!! \times 6!!} + \dots \right) = 1 \quad (6.4.6)$$

$$B_2'' = \left(-\frac{3}{2 \times 4!!} + \frac{7}{4!! \times 6!!} + \frac{11 \times 3^2}{6!! \times 8!!} + \dots \right) = -\frac{1}{6}$$

Extending the evaluation to all positive values of n , then summing gives:

$$S_{32}(\sigma, \pi/2)_{n \geq 0} = i \frac{\sin \sigma}{\sigma} \quad (6.4.7)$$

To evaluate the coefficients of negative powers of σ , define a new set of coefficients B_n and write the expansion as:

$$S_{32}(\sigma, \pi/2)_{n < 0} = i \frac{B_n}{\sigma^n} \quad (6.4.8)$$

Combining Eqs. (6.4.5) and (6.4.8) gives:

$$B_n = \sum_{\ell \geq n+1}^L \frac{(2\ell + 1)(\ell - 2)!! (\ell + n - 2)!!}{(\ell + 1)!! (\ell - n + 1)!!} \quad (6.4.9)$$

The coefficients of the first two terms are:

$$\begin{aligned} B_2 &= i(1.3125 + 1.28906 + 1.28174 + 1.27853 + \dots) \approx L/2. \\ B_4 &= i(36.09375 + 69.21387 + 106.58936 + 165.99072 + \dots) \approx L^3 \end{aligned} \quad (6.4.10)$$

With each succeeding increase in n the power of L increases by two.

Combining equatorial values for both positive and negative powers of σ gives:

$$S_{32}(\sigma, \pi/2) = \frac{i}{\sigma} \sin \sigma + i \sum_{n=2}^L \frac{B_n}{\sigma^n} \quad (6.4.11)$$

The related sum follows by operating on Eq. (6.4.11) using Eq. (6.1.5):

$$\mathcal{S}_{32}(\sigma, \pi/2) = -\frac{1}{\sigma} \cos \sigma + \sum_{n=2}^L \frac{(n-1)B_n}{\sigma^{n+1}} \quad (6.4.12)$$

Each mode contributes the exact amount required for the positive powers of σ to equal the transcendental functions of Eqs. (6.4.11) and (6.4.12); this is a unique property of recursion relationship Eq. (5.10.15).

6.5. Evaluation of Sum S_{22} in the Equatorial Plane

The spherical Neumann portion of sum S_{22} as defined by Eq. (6.1.2) is:

$$S_{22}(\sigma, \theta) = \sum_{\ell=1}^{\infty} i^{-\ell} \frac{(2\ell+1)}{\ell(\ell+1)} y_{\ell}(\sigma) \frac{dP_{\ell}^1(\cos \theta)}{d\theta} \quad (6.5.1)$$

We seek to find a simpler expression for the sum. At $\theta = \pi/2$, the value of the Legendre function is, see Table A.18.1:

$$\frac{dP_{\ell}^1(0)}{d\theta} = i^{\ell} \frac{(\ell+1)!!}{(\ell-2)!!} \delta(\ell, 2q) \quad (6.5.2)$$

Since the derivatives of odd order Legendre functions with respect to θ vanish at the equator, only even values of ℓ appear in the summation. Substituting the spherical Neumann function, in the form of Eqs. (6.2.4), and (6.5.2) into Eq. (6.5.1) gives the expression for the sum at the equator:

$$\begin{aligned} S_{22}\left(\sigma, \frac{\pi}{2}\right) &= -\sum_{\ell e; 0}^{\infty} \frac{(2\ell+1)(\ell-1)!!}{(\ell)!!} \left\{ \sum_{s=0}^{\ell-1} \frac{(2\ell-2s-1)!!}{(2s)!!} \sigma^{-\ell-1+2s} \right. \\ &\quad \left. + \sum_{s=0}^{\infty} \frac{(-1)^s}{(2s-1)!!} \frac{\sigma^{\ell-1+2s}}{(2\ell+2s)!!} \right\} + \frac{\cos \sigma}{\sigma} \end{aligned} \quad (6.5.3)$$

For convenience in evaluating the sum, the $\ell = 0$ term is added and subtracted. Since only even orders of ℓ are present only odd powers of σ appear in the sum. The result is:

$$S_{22} \left(\sigma, \frac{\pi}{2} \right) = \sum_{\text{no};1}^{\infty} C_n'' \sigma^n + \frac{\cos \sigma}{\sigma} \quad (6.5.4)$$

Comparing Eqs. (6.5.4) and (6.5.3) gives:

$$C_n'' = \left\{ (-1)^{(n-1)/2} \sum_{\ell e;0}^{n+1} \frac{(2\ell+1)(\ell-1)!!}{(\ell)!!} \frac{(-1)^{\ell/2}}{(n-\ell)!!(\ell+n+1)!!} - \sum_{\ell e;n+3}^{\infty} \frac{(2\ell+1)(\ell-1)!!}{(\ell)!!} \frac{(\ell-n-2)!!}{(\ell+n+1)!!} \right\} \quad (6.5.5)$$

Evaluation of the special cases $n = 1$ and $n = 3$ gives:

$$C_1'' = - \left\{ -\frac{1}{2} + \frac{5}{2!! \times 4!!} + \frac{9 \times 3!! \times 1!!}{4!! \times 6!!} + \dots \right\} = 0$$

$$C_3'' = - \left\{ \frac{1}{3!! \times 4!!} - \frac{5 \times 1!!}{2!! \times 6!!} + \frac{9 \times 3!!}{4!! \times 8!!} + \frac{13 \times 5!! \times 1!!}{6!! \times 10!!} + \dots \right\} = 0 \quad (6.5.6)$$

Extending the evaluation to all positive values of 'n' followed by summing gives, for ℓ equal to or greater than zero and positive powers of σ

$$S_{22} \left(\sigma, \frac{\pi}{2} \right) = \frac{\cos \sigma}{\sigma} \quad (6.5.7)$$

The reduction of Eq. (6.5.3) to this simple form is a unique property of Eq. (5.10.15).

To examine the coefficients for negative powers of σ , define the new coefficients:

$$S_{22}(\sigma, \pi/2)_{n<0} = \sum_{\text{no};1}^L \frac{C_n}{\sigma^n} \quad (6.5.8)$$

Combining Eq. (6.5.8) with Eq. (6.5.3) shows that:

$$C_n = - \sum_{\ell e;n-1}^L \frac{(2\ell+1)(\ell-1)!!}{(\ell)!!} \frac{(\ell+n-2)!!}{(\ell-n+1)!!} \quad (6.5.9)$$

Evaluation of the $n = 1$ term gives:

$$C_1 = 1 + 1.25 + 1.256 + \dots \cong 5L/8 \quad (6.5.10)$$

The lower limit on ℓ is zero since that term is included in Eq. (6.5.7) and is subtracted out in Eq. (6.5.10). With each succeeding increase in n the power of L in the approximate equality increases by two.

The total value of the sum is equal to the sum of Eqs. (6.5.8) and (6.5.9)

$$\begin{aligned} S_{22} \left(\sigma, \frac{\pi}{2} \right) &= \frac{\cos \sigma}{\sigma} - \sum_{n \geq 1}^{\infty} \frac{C_n}{\sigma^n} \quad \text{and} \\ \mathcal{S}_{22} \left(\sigma, \frac{\pi}{2} \right) &= -i \frac{\sin \sigma}{\sigma} + i \sum_{n \geq 1}^{\infty} \frac{(n-1)C_n}{\sigma^{n+1}} \end{aligned} \quad (6.5.11)$$

6.6. Summary of the Axial Fields

Sums of spherical Hankel functions on the $+z$ -axis follow from the values for spherical Bessel functions of Table 6.1.2 and the spherical Neumann functions from Secs. 6.2 through 6.5. The associated sums follow from the regular sums and Eq. (6.1.5):

$$\begin{aligned} S_1(\sigma, 0) &= 0 \\ S_2(\sigma, 0) &= e^{-i\sigma} \left(1 - \frac{i}{2\sigma} \right) - \frac{i^{-L-1}}{2} \sum_{n=1}^{L+1} \frac{(L+n)!!}{(L-n+1)!! \sigma^n} \\ S_3(\sigma, 0) &= S_2(\sigma, 0) \\ \mathcal{S}_2(\sigma, 0) &= e^{-i\sigma} \left(1 + \frac{i}{2\sigma} \right) + \frac{i^{-L}}{2} \sum_{n=2}^{L+1} \frac{(n-1)(L+n)!!}{(L-n+1)!! \sigma^{n+1}} \\ \mathcal{S}_3(\sigma, 0) &= S_2(\sigma, 0) \end{aligned} \quad (6.6.1)$$

The remainders arise from the highest order mode only, and are valid if the recursion relationship of Eq. (5.10.15) holds through order L and all higher order have zero magnitude. Putting these sums into the field forms of Eq. (6.1.4) and ignoring the remainder gives the electric field intensity on the positive z -axis:

$$\begin{aligned} E_r &= 0 \\ E_\theta &= 2e^{-i\sigma} e^{-i\phi} \\ E_\phi &= -i2e^{-i\sigma} e^{-i\phi} \end{aligned} \quad (6.6.2)$$

The field is circularly polarized and the magnitude is independent of distance from the source. The time average Poynting vector is:

$$\begin{aligned} \mathbf{N} &= \frac{1}{2} \text{Re}(\tilde{\mathbf{E}} \times \tilde{\mathbf{H}}^*) = -\frac{1}{2\eta} \text{Re}(i\tilde{\mathbf{E}} \times \tilde{\mathbf{E}}^*) \\ \mathbf{N} &= \hat{z} N_z = \frac{4}{\eta} \hat{z} \end{aligned} \quad (6.6.3)$$

The axial power density is independent of distance from the source and totally directed in the positive z -direction.

The remainders in the equatorial plane are quite different from those on the z -axes; each mode contributes a proportionate share to the whole and fields exist throughout the region. The sums are:

$$\begin{aligned}
 S_1(\sigma, \pi/2) &= \sigma + i \sum_{ne;0}^L \frac{A_n}{\sigma^n} \\
 S_2(\sigma, \pi/2) &= \left[1 - \frac{i}{\sigma} e^{-i\sigma} \right] + i \sum_{no;1}^L \frac{C_n}{\sigma^n} \\
 S_3(\sigma, \pi/2) &= -\frac{i}{\sigma} [1 - e^{-i\sigma}] + \sum_{ne;2}^L \frac{B_n}{\sigma^n} \\
 S_2(\sigma, \pi/2) &= \frac{i}{\sigma} [1 - e^{-i\sigma}] + \sum_{no;3}^L \frac{(n-1)C_n}{\sigma^{n+1}} \\
 S_3(\sigma, \pi/2) &= \frac{i}{\sigma} e^{-i\sigma} - i \sum_{ne;2}^L \frac{(n-1)B_n}{\sigma^{n+1}}
 \end{aligned} \tag{6.6.4}$$

The letter functions representing the remainders are:

$$\begin{aligned}
 A_n &= \sum_{\ell o; n-1}^L \frac{(2\ell+1)\ell!! (\ell+n-2)!!}{(\ell-1)!! (\ell-n+1)!!} \\
 B_n &= \sum_{\ell o; n+1}^L \frac{(2\ell+1)(\ell-2)!! (\ell+n-2)!!}{(\ell+1)!! (\ell-n+1)!!} \\
 C_n &= \sum_{\ell e; n-1}^L \frac{(2\ell+1)(\ell-1)!! (\ell+n-2)!!}{(\ell)!! (\ell-n+1)!!}
 \end{aligned} \tag{6.6.5}$$

Substituting these results into the field forms gives the field:

$$\begin{aligned}
 \tilde{\mathbf{E}}(\sigma, \pi/2) &= \left[1 - i \sum_{ne;0}^{\infty} \frac{A_n}{\sigma^{n+1}} \right] e^{-i\phi} \hat{r} + \left\{ \sum_{ne;2}^{\infty} \frac{B_n}{\sigma^n} + \sum_{no;3}^{\infty} \frac{(n-1)C_n}{\sigma^{n+1}} \right\} e^{-i\phi} \hat{\theta} \\
 &\quad - i \left\{ 1 + i \sum_{no;1}^{\infty} \frac{C_n}{\sigma^n} - i \sum_{ne;2}^{\infty} \frac{(n-1)B_n}{\sigma^{n+1}} \right\} e^{-i\phi} \hat{\phi}
 \end{aligned} \tag{6.6.6}$$

With O representing order, these fields produce the Poynting vector:

$$\mathbf{N}(\sigma, \pi/2) = \frac{1}{\eta} \left\{ O\left(\frac{1}{\sigma^2}\right) \hat{r} + \left[-1 + O\left(\frac{1}{\sigma^2}\right) \right] \hat{\theta} + O\left(\frac{1}{\sigma^2}\right) \hat{\phi} \right\} \tag{6.6.7}$$

The radial term is an outbound power density proportional to B^2/σ^2 . The zenith angle term is a power density of magnitude independent of distance and directed in the positive z -direction. It describes an energy flow from the lower to the upper hemisphere.

On the negative z -axis, as it was on the positive one, the remainder is from the highest order mode only and it does not contain contributions from each mode. The other terms are equal to:

$$\begin{aligned} S_2(\sigma, \pi) &= -\frac{i}{2\sigma} e^{-i\sigma} & S_3(\sigma, \pi) &= \frac{i}{2\sigma} e^{-i\sigma} \\ S_2(\sigma, \pi) &= -\frac{i}{2\sigma} e^{-i\sigma} & S_3(\sigma, \pi) &= \frac{i}{2\sigma} e^{-i\sigma} \end{aligned} \quad (6.6.8)$$

Putting these sums into the field forms of Eq. (6.1.4) shows that the electric field intensity and the Poynting vector on the negative z -axis are equal to zero:

$$\tilde{\mathbf{E}}(\sigma, \pi) = 0 \quad (6.6.9)$$

So long as the recursion relationship of Eq. (5.10.15) holds, any field that exists on the negative z -axis arises from the remainder of the highest order moment.

These results show that positive powers of the radial terms result in a normalized power density of $4/\eta$ along the positive z -axis, z -directed uniform power density of $1/\eta$ in the equator, and no power at all along the negative z -axis. The first order, negative power terms show radially outbound power in the equatorial plane. This result combines with energy conservation to require energy that exits the generating source in the lower hemisphere to pass upward through the equator. By Eq. (6.6.3), all energy ultimately becomes positive z -directed.

6.7. Radiation Pattern at Infinite Radius

To go from axial field expressions to expressions over the full range of coordinates begin by noting in the limit of very large radius the spherical Bessel, Neumann, and Hankel functions satisfy the equalities, see Eq. (A.24.13):

$$\begin{aligned} \lim_{\sigma \rightarrow \infty} y_\ell(\sigma) &= -dj_\ell(\sigma)/d\sigma \\ \lim_{\sigma \rightarrow \infty} h_\ell(\sigma) &= \left[1 + i \frac{d}{d\sigma} \right] j_\ell(\sigma) \end{aligned} \quad (6.7.1)$$

Equation (6.7.1) gives the complete expression for spherical Hankel functions at all coordinate angles but only at infinite radius. The field solutions

with Hankel functions follow from the Bessel function field solutions of Eqs. (6.1.21) and (6.7.1):

$$\begin{aligned} \lim_{\sigma \rightarrow \infty} \tilde{\mathbf{E}}(\sigma, \theta, \phi) = & \left(1 + i \frac{\partial}{\partial \sigma}\right) \{ [S_{11} \hat{r} / \sigma + (S_{21} + S_{31}) \hat{\theta} \\ & - i(S_{21} + S_{31}) \hat{\phi}] e^{-i\phi} \} \end{aligned} \quad (6.7.2)$$

Carrying out the indicated operations on sums S_{11} and S_{31} gives:

$$\begin{aligned} \lim_{\sigma \rightarrow \infty} S_1 = & \sigma \sin \theta \left(1 + \cos \theta + \frac{i}{\sigma}\right) e^{-i\sigma \cos \theta} \\ \lim_{\sigma \rightarrow \infty} S_3 = & -i \left(U + V - \frac{i}{\sigma} U\right) \end{aligned} \quad (6.7.3)$$

Using Eqs. (6.1.3) and (6.1.5) to operate on Eq. (6.7.3) gives:

$$\begin{aligned} \lim_{\sigma \rightarrow \infty} S_2 = & i \left(U + V - \frac{i}{\sigma} V\right) + \left(1 + \cos \theta - \frac{i}{\sigma}\right) e^{-i\sigma \cos \theta} \\ \lim_{\sigma \rightarrow \infty} S_3 = & -i \left(U + V - \frac{i}{\sigma} V - \frac{1}{\sigma^2} U\right) + \frac{i}{\sigma} e^{-i\sigma \cos \theta} \\ \lim_{\sigma \rightarrow \infty} S_2 = & i \left(U + V - \frac{i}{\sigma} U - \frac{1}{\sigma^2} V\right) + \left(\cos \theta (1 + \cos \theta) - \frac{1}{\sigma^2}\right) e^{-i\sigma \cos \theta} \end{aligned} \quad (6.7.4)$$

Values of the infinite radius sums are listed in Table 6.7.1.

Table 6.7.1. Large-radius solutions of sums over spherical Hankel functions.

| |
|---|
| $S_1^0(\sigma, \theta) = \sigma \sin \theta \left(1 + \cos \theta + \frac{i}{\sigma}\right) e^{-i\sigma \cos \theta}$ |
| $S_2^0(\sigma, \theta) = \left(1 + \cos \theta - \frac{i}{\sigma}\right) e^{-i\sigma \cos \theta} + i [U(\sigma, \theta) + V(\sigma, \theta)] + \frac{V(\sigma, \theta)}{\sigma}$ |
| $S_3^0(\sigma, \theta) = -i [U(\sigma, \theta) + V(\sigma, \theta)] - \frac{U(\sigma, \theta)}{\sigma}$ |
| $\$2^0(\sigma, \theta) = \left[\cos \theta (1 + \cos \theta) - \frac{1}{\sigma^2}\right] e^{-i\sigma \cos \theta} + i [U(\sigma, \theta) + V(\sigma, \theta)] + \frac{U(\sigma, \theta)}{\sigma} - \frac{iV(\sigma, \theta)}{\sigma^2}$ |
| $\$3^0(\sigma, \theta) = \frac{i}{\sigma} e^{-i\sigma \cos \theta} - i [U(\sigma, \theta) + V(\sigma, \theta)] - \frac{V(\sigma, \theta)}{\sigma} + \frac{iU(\sigma, \theta)}{\sigma^2}$ |

Combining the fields of Eq. (6.1.4) with Eqs. (6.7.3) and (6.7.4) gives:

$$\begin{aligned} \lim_{\sigma \rightarrow \infty} \tilde{\mathbf{E}} = & \left\{ \hat{r} \sin \theta \left(1 + \cos \theta + \frac{i}{\sigma} \right) e^{-i\sigma \cos \theta} \right. \\ & + \hat{\theta} \left[\left(\cos \theta (1 + \cos \theta) - \frac{1}{\sigma^2} \right) e^{-i\sigma \cos \theta} - \frac{i}{\sigma^2} \mathbf{V} \right] \\ & \left. - i\hat{\phi} \left[(1 + \cos \theta) e^{-i\sigma \cos \theta} + \frac{i}{\sigma^2} \mathbf{U} \right] \right\} e^{-i\phi} \quad (6.7.5) \\ \eta \tilde{\mathbf{H}} = & i \tilde{\mathbf{E}} \end{aligned}$$

These fields may also be used to construct the phasor fields that apply for energy absorption, since the complex conjugate of any electromagnetic phasor field is another electromagnetic phasor field. Keeping only the teledistant fields gives:

Energy emission

$$\hat{\mathbf{E}}(\sigma, \theta, \phi) = e^{-i\sigma \cos \theta} \left\{ \begin{array}{l} \hat{r} \sin \theta (1 + \cos \theta) \\ + (\hat{\theta} \cos \theta - i\hat{\phi})(1 + \cos \theta) \end{array} \right\} e^{-i\phi} \quad (6.7.6)$$

Energy absorption

$$\hat{\mathbf{E}}(\sigma, \theta, \phi) = e^{i\sigma \cos \theta} \left\{ \begin{array}{l} \hat{r} \sin \theta (1 + \cos \theta) \\ + (\hat{\theta} \cos \theta + i\hat{\phi})(1 + \cos \theta) \end{array} \right\} e^{i\phi}$$

The fields are circularly polarized. The emission equations describe a wave that exits its source at $z = 0$ and forms a fully z -directed plane wave that travels to $z = +\infty$. The absorption equations describe an oppositely directed plane wave at $z = \infty$ that travels to a sink at $z = 0$. The Poynting vectors are equal to:

$$\mathbf{N}_c = \pm \frac{1}{\eta} (1 + \cos \theta)^2 \hat{z} \quad (6.7.7)$$

The upper and lower signs of Eq. (6.7.7) apply respectively to emission and absorption. A type of radiation pattern is shown in Fig. 6.7.2. The figure is similar to conventional radiation patterns in that the magnitude of the power density at each angle is proportional to the distance from the origin. Unlike other patterns, all energy flows in the direction of the pattern maximum. The result is fully directed, z -oriented power of magnitude independent of distance from the source. It remains to be determined how such a condition is consistent with energy conservation.

The absorption and emission discussions of Chapter 2 involve structures with ideally conducting surfaces and for which, except for a biconical

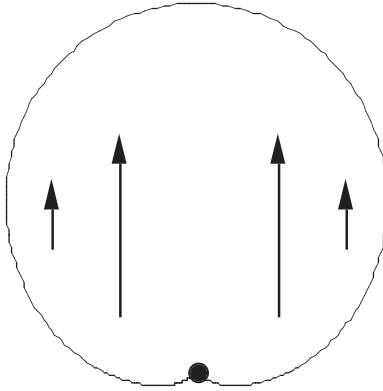


Fig. 6.7.2. Radiation pattern for fully directed radiation. Source is located at the midpoint on the bottom of the curve. Similar to other radiation patterns field values at a particular angle are proportional to indicated distance from the origin. Unlike other field patterns, all power flows in the direction of the pattern maximum and, at a specific angle, power density is independent of radius.

receiving antenna, the absorbed power is zero. They respond linearly to the incoming plane wave fields of Eq. (2.1.11), and the powers are given by Eqs. (2.2.7) and (2.14.11). The extinction power is proportional to the first power of the scattering coefficients, α_ℓ and β_ℓ , and the scattered power is proportional to the square of the coefficients. The response of a nonlinear sink is quite different. An active region somehow generates the near fields that extract energy from the perturbing field, in just the inverse of an emission process. After the absorption process has begun, the exterior fields at the source are those of Eq. (5.10.16), not Eq. (2.1.11). Changing from emission fields to absorption fields is the equivalent of changing the sign of the time independent parts.

6.8. Multipolar Moments

The purpose of this section is to discuss the symmetry and anticipated magnitudes of high-order modes generated within a charged cloud. The magnitudes of the high-order field components of a plane wave are far too small to produce the coefficients needed to produce the fields of Eq. (5.10.16). They do possess charge arrays with the needed symmetry. Once formed, other forces with the necessary magnitudes drive such arrays.

When a passive, perfectly conducting sphere is immersed in a plane wave, at the surface of the scatterer the magnitudes of the scattered and incident waves are the same, see Eq. (2.3.1). The equality requires the ratio

of field coefficients to be:

$$\frac{\text{Incident field magnitude}}{\text{Scattered field magnitude}} = \frac{(ka)^{2\ell+1}}{(2\ell+1)!!(2\ell-1)!!} \quad (6.8.1)$$

With $(ka) \ll 1$ the ratio of Eq. (6.8.1) is so small and decreases so rapidly with increasing modal number ℓ that the lowest order terms dominate all others during the scattering process.

When an atom in a high-energy state is immersed in a plane wave, at the surface of the emitter the magnitude of the emitted wave is much larger than that of the incident wave. For the incident wave coefficients of Eq. (5.8.2) to produce the emitted wave coefficients of Eq. (5.10.16) requires the ratio of field coefficients to be:

$$\frac{\text{Incident field magnitude}}{\text{Scattered field magnitude}} = \frac{(2\ell+1)!!(2\ell-1)!!}{(ka)^{2\ell+1}} \quad (6.8.2)$$

With $(ka) \ll 1$ the ratio of Eq. (6.8.2) is so large and increases so rapidly with increasing ℓ that the highest order terms dominate all others during emission process.

Modifying the coefficients Eq. (5.8.2) to those of Eq. (5.10.16) is possible only because electron-generated radiation does not involve scattering. The process involves equilibrated metastable atomic states. An instability produces radiation onset that, in turn, produces radiation reaction forces of the appropriate symmetry whose magnitude far exceeds those of a perturbing wave. To examine a possible source of the driving fields consider an occupied metastable state with time-average current and charge densities at all points within the region. By Eqs. (4.5.2) and (4.5.4), the time-average values of charge and current densities are respectively

$$e\psi^*(\mathbf{r}, t)\psi(\mathbf{r}, t) \quad \text{and} \quad \frac{\hbar e}{2im}[\psi^*(\mathbf{r}, t)\nabla\psi(\mathbf{r}, t) - \psi(\mathbf{r})\nabla\psi^*(\mathbf{r})]$$

By Lenz's law, see Sec. 2.16, with biconical receiving antennas the time changing magnetic field induces currents that generate an opposing field. Quite differently, an intrinsic magnetic moment interacts with the applied magnetic field to generate a field in the direction of the incoming magnetic field.

Consider a spherical cloud of charge to which the continuity equation applies. In Fig. 6.8.1, an applied field drives a dipole mode, as illustrated by the center arrow. The smaller arrows illustrate two electric current options. Some terminate on the edge of the source, leaving a net charge density that generates an electric octupole field. The interior charge structure drives

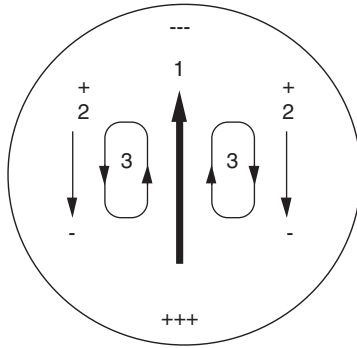


Fig. 6.8.1. Source modes resulting from an electric dipole formed within an electric charge distribution. Arrows indicate current densities. Current {1} creates a dipole source, Currents {1} and {2} together create an electric octupole source, and Currents {3} create a magnetic quadrupole source. By continuation, this creates all odd numbered TM field sources and all even number TE field sources. With a dual source of a magnetic charge distribution, the result is creation of all even numbered TM field sources and all odd numbered TE field sources.

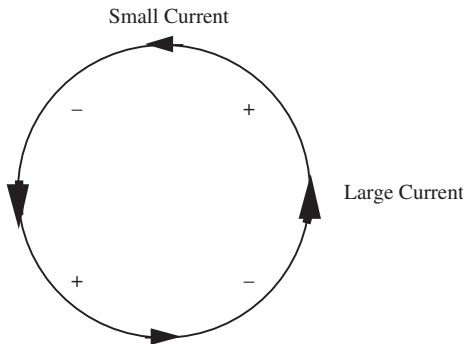


Fig. 6.8.2. Magnetic dipole source with accompanying electric quadrupole. Arrows indicate current direction and magnitude. Currents at the sides are larger than on the top and bottom. Result is charge buildups as indicated. These, in turn, generate an electric quadrupole field.

continuous current loops that generate a magnetic quadrupole field. So long as source constraints permit the charge density to be further subdivided in this way, each current path produces a similar set of higher order modes. The result is that an oscillating electric dipole moment drives all odd-order electric multipolar moments, TM fields, of the same degree and all even-order magnetic multipolar moments, TE fields, of the same degree.

Similarly using magnetic circuit techniques and an effective magnetic current density, an analysis shows the dual effect of an oscillating magnetic dipole moment that drives all even-order TM fields, and all odd-order TE fields of the same degree.

Appendices 28 and 29 contain respectively analyses of electric and magnetic multipolar sources. For the special case of electrically small systems for which $ka \ll 1$ the field coefficients are the multipolar coefficients listed in Tables A.28 and A.29. As shown by the multipolar field coefficients for quantized radiation, the field coefficients of the expansion terms needed for a plane wave expansion are proportional to the generating charge times ka raised to an integer power. The electric and magnetic multipolar moments of order ℓ are respectively proportional to

$$(ka)^\ell \quad \text{and} \quad (ka)^{\ell+1}$$

Electric moments therefore dominate over magnetic moments of the same order.

Each multipole is constructed from an array of charges distributed in a way that contributes to the primary multipolar moment and to higher order moments of the same parity, but not either to lower order moments or higher order ones of the opposite parity. Column 1 of Table 6.8.1 shows the order. Column 2 shows the charge distribution needed on the surface of a sphere of radius a to produce primary z -directed electric moments with primary orders one through seven. Column 3 shows the electric multipolar moment needed to produce the same primary field in the limit as the ratio of sphere size to wave length becomes vanishingly small, and Column 4 shows the number of separate charges necessary to produce each static multimoment.

In Column 3, the even order moments are equal to:

$$p_\ell = \frac{(\ell)!}{(2\ell + 1)!!} q a^\ell \cong q(a/2)^\ell \quad (6.8.3)$$

ℓ even

The odd orders are similar in magnitude, and both decrease rapidly with increasing order.

Column 4 shows that 2^ℓ charges are necessary to support a linear source. If a continuous charge distribution exists, changing from individual charges to charge density permits changing calculation techniques from sums over individual charges to volume integrals over charge distributions. So long as

Table 6.8.1. Surface charge distributions on a sphere of radius a that produce the electric moments of column three. Column 4 lists the least possible number of static charges necessary to produce each moment.

| | Charge Density | Electric Moment | # |
|---|--|--|-----|
| 1 | $a \cos \theta (\cos \theta)$ | $p_1 = \frac{1}{3} qa^2$ | 2 |
| 2 | $a^2 \cos^2 \theta \left(-\frac{3}{2} \sin^2 \theta + 1 \right)$ | $p_2 = \frac{2}{15} qa^2$ | 4 |
| 3 | $a^3 \cos^3 \theta \left(-\frac{5}{3} \cos^3 \theta + \cos \theta \right)$ | $p_3 = -\frac{4}{105} qa^3$ | 8 |
| 4 | $a^4 \cos^4 \theta \left(\frac{35}{8} \sin^4 \theta - 5 \sin^2 \theta + 1 \right)$ | $p_4 = \frac{8}{315} qa^4$ | 16 |
| 5 | $a^5 \cos^5 \theta \left(\frac{21}{5} \cos^5 \theta - \frac{14}{3} \cos^3 \theta + \cos \theta \right)$ | $p_5 = \frac{64}{10,395} qa^5$ | 32 |
| 6 | $a^6 \cos^6 \theta \left(-\frac{231}{16} \sin^6 \theta + \frac{189}{8} \sin^4 \theta - \frac{21}{2} \sin^2 \theta + 1 \right)$ | $p_6 = \frac{16}{3003} qa^6$ | 64 |
| 7 | $a^7 \cos^7 \theta \left(-\frac{429}{35} \cos^7 \theta + \frac{99}{5} \cos^5 \theta - \frac{315}{35} \cos^3 \theta + \cos \theta \right)$ | $p_7 = -\left(\frac{256}{225,225} \right) qa^7$ | 128 |

the charge density is continuous ever-larger orders will be driven. It ceases only when the dimensional scale is so small that granules of charge appear as a three-dimensional mosaic. That is, electric charge density is a valid concept if and only if the charge density is continuous in the neighborhood of a source point, see Sec. 1.5. Maximum modal number, L , is determined by the lower limit on the granularity of the electron charge distribution and for example a fixed array with $L = 200$ requires 2^L units, i.e. 1.6×10^{60} . Arguments in support of a classical photon require a source capable of such a distribution. There is every reason to believe this lies within the scope of nonlocal electrons.

If the radiating sphere is not electrically small results are quite different. This is most easily seen by reference to Appendix 14. By Eq. (A.14.7) the external electric field intensity is proportional to the inverse of the Hankel function at the surface of the sphere; if the radius is electrically small it is proportional to $(ka)^{-\ell+2}$ but if the radius is not electrically small the number is much smaller. Therefore the estimated electric multipolar moment is a strong function of radius and the atomic radius during emission is unknown. It is only known that a large expansive force is present that dominates other local forces.

6.9. Multipolar Photon-Field Stress and Shear

Dipoles: Consider as an example the dipolar portion of the fields of Eq. (5.10.16), two electric and two magnetic dipoles oriented along the x - and y -axes. The fields are detailed in Eq. (6.9.1). The pressure follows similarly to the example of Sec. 4.2 and the radial field component of the stress tensor follows from the expression for $w_T(t_R)$ of Table 3.16.1. Since all fields are continuous across virtual boundaries the pressure gradient is equal to the spatial directional derivative of the pressure. The surface shears follow from Eq. (4.2.17) and the field expressions of Eq. (5.10.16). Values are listed in Eq. (6.9.2). Although the total surface pressure is independent of time, the shears are not and act to produce continuous eddies within the charged region. Field values are:

$$\begin{aligned} E_r &= 3 \left[-\frac{1}{\sigma^2} + \frac{i}{\sigma^3} \right] \sin \theta e^{-i\sigma} e^{-i\phi} \\ E_\theta &= \frac{3}{2} \left[\frac{i}{\sigma} (1 + \cos \theta) + \frac{1}{\sigma^2} (1 + \cos \theta) - \frac{i}{\sigma^3} \cos \theta \right] e^{-i\sigma} e^{-i\phi} \\ E_\phi &= \frac{3}{2} \left[\frac{1}{\sigma} (1 + \cos \theta) - \frac{i}{\sigma^2} (1 + \cos \theta) - \frac{1}{\sigma^3} \right] e^{-i\sigma} e^{-i\phi} \end{aligned} \quad (6.9.1)$$

The shears are time dependent with both static and dynamic parts. Values are listed in Eq. (6.9.2).

$$\begin{aligned} S_{r\theta} &= -\frac{9\varepsilon}{4} \left\{ \left[\frac{1}{\sigma^6} + \left(\frac{2}{\sigma^4} - \frac{1}{\sigma^6} \right) \cos(2\omega t_R) - \left(\frac{1}{\sigma^3} - \frac{2}{\sigma^5} \right) \sin(2\omega t_R) \right] \cos \theta \right. \\ &\quad \left. + \left[-\frac{2}{\sigma^4} \cos(2\omega t_R) + \left(\frac{1}{\sigma^3} - \frac{1}{\sigma^5} \right) \sin(2\omega t_R) \right] \right\} \sin \theta \\ S_{r\phi} &= -\frac{9\varepsilon}{4} \left\{ \left[\left(\frac{1}{\sigma^3} + \frac{1}{\sigma^5} \right) + \left(\frac{1}{\sigma^3} - \frac{1}{\sigma^5} \right) \cos(2\omega t_R) + \frac{2}{\sigma^4} \sin(2\omega t_R) \right] \cos \theta \right. \\ &\quad \left. + \left[\frac{1}{\sigma^3} + \left(\frac{1}{\sigma^3} - \frac{2}{\sigma^5} \right) \cos(2\omega t_R) - \frac{1}{\sigma^6} \sin(2\omega t_R) \right] \right\} \sin \theta \end{aligned} \quad (6.9.2)$$

The energy density and T_{rr} are both time-independent. T_{rr} and the static portions of the shears are listed in Eq. (6.9.3):

$$\begin{aligned} T_{rr} &= \frac{9\varepsilon}{16} \left\{ \left(\frac{4}{\sigma^4} + \frac{4}{\sigma^6} \right) \sin^2 \theta - \left(\frac{2}{\sigma^2} + \frac{1}{\sigma^6} \right) (1 + \cos^2 \theta) - \frac{4}{\sigma^2} \cos \theta \right\} \\ \langle S_{r\theta} \rangle &= -\frac{9\varepsilon}{4\sigma^6} \sin \theta \cos \theta \\ \langle S_{r\phi} \rangle &= -\frac{9\varepsilon}{4} \left\{ \left(\frac{1}{\sigma^3} + \frac{1}{\sigma^5} \right) \cos \theta + \frac{1}{\sigma^3} \right\} \sin \theta \end{aligned} \quad (6.9.3)$$

Values of Eq. (6.9.3) are plotted in Figs. 6.9.1 and show the radiation reaction pressure and the time-average shears on radiating spheres of radius $ka = 5, 1, \text{ and } 0.1$, if all fields at smaller radii are zero.

The far field, $ka = 5$, pressure and shears of Figs. 6.9.1 show the pressure magnitude is small, maximum value -0.18 , compressive, and occurs at $\theta = 0$. It decreases monotonically with increasing angle to approximately zero at $\theta = \pi$. This far field pressure is compressive and produces a net momentum transfer between the field and the source, pushing them in

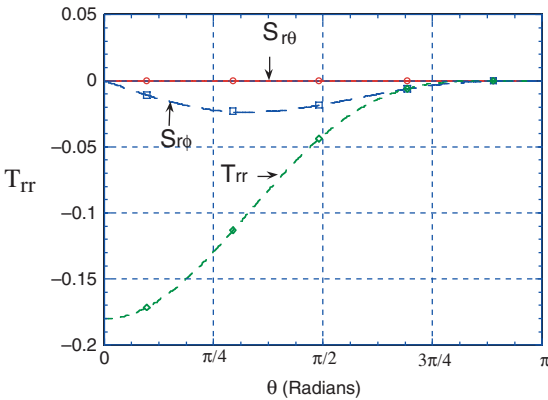


Fig. 6.9.1(a). Four dipole radiation reaction pressure T_{rr} and shears $S_{r\theta}$ and $S_{r\phi}$ on a virtual sphere of electrical radius $ka = 5.0$ if all interior fields are zero, see Eq. (6.9.3), and $L = 1$.

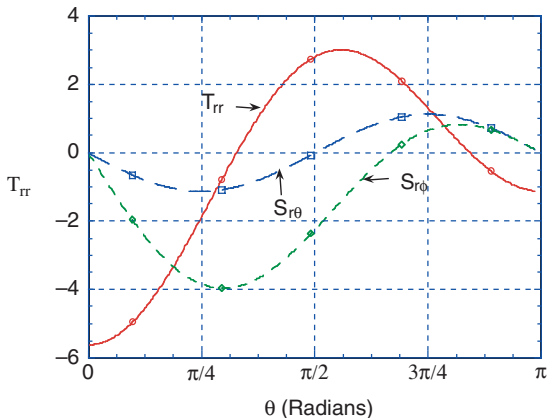


Fig. 6.9.1(b). Four dipole radiation reaction pressure T_{rr} and shears $S_{r\theta}$ and $S_{r\phi}$ on a virtual sphere of electrical radius $ka = 1.0$ if all interior fields are zero, see Eq. (6.9.3) and $L = 1$.

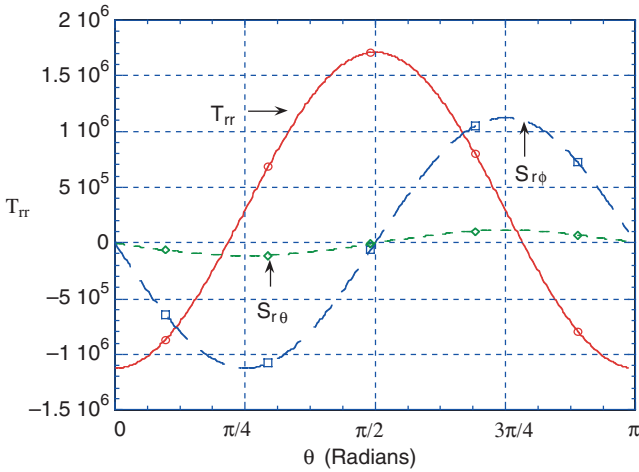


Fig. 6.9.1(c). Four dipole radiation reaction pressure T_{rr} and shears $S_{r\theta}$ and $S_{r\phi}$ on a virtual sphere of electrical radius $ka = 0.1$ if all interior fields are zero, see Eq. (6.9.3), and $L = 1$.

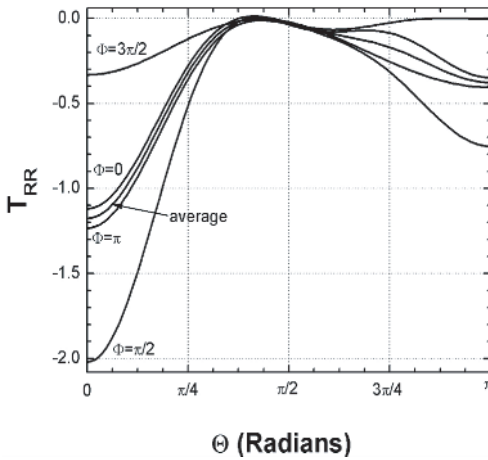


Fig. 6.9.2(a). Plot for $L = 2$, electric field radiation pressure T_{rr} versus zenith angle θ at phases $\Phi = 0, \pi/2, \pi, 3\pi/2$ and the time average value, all at normalized radius $ka = 5.0$. Figs. 6.9.1–6.9.4 have the same normalization; $\Phi = 2(\omega t - \phi)$.

opposite directions. This is part of the mechanism for the transfer of linear momentum, the rest coming from the zenith-directed shear.

Near field pressure at range $ka = 0.1$ is shown in Fig. 6.9.1(c); it is compressive on the z -axis, about -10^6 , and expansive in the xy -plane, about $+1.6 \times 10^6$. The positive force acts to expand an originally spherical radiator

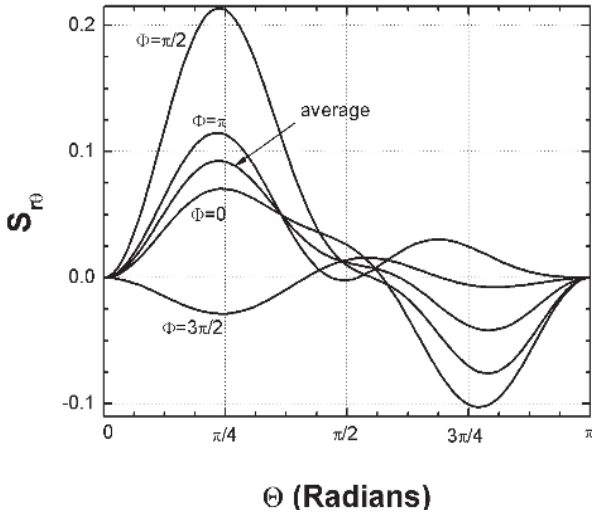


Fig. 6.9.2(b). Plot for $L = 2$, electric field radiation shear $S_{r\theta}$ versus zenith angle θ at phases $\Phi = 0, \pi/2, \pi, 3\pi/2$ and the time average value, all at normalized radius $ka = 5.0$. Figures 6.9.1–6.9.4 have the same normalization; $\Phi = 2(\omega t - \phi)$.

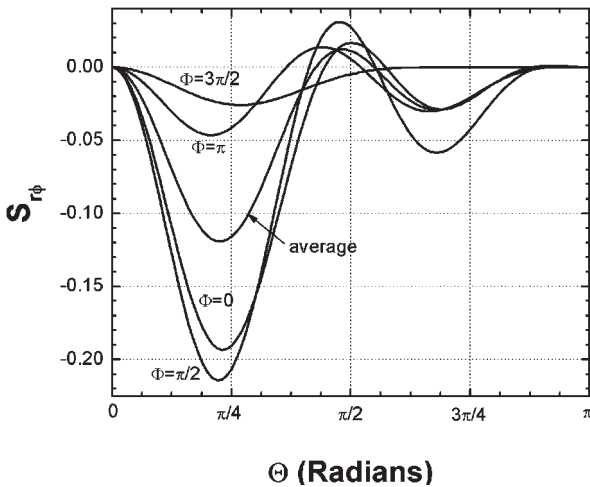


Fig. 6.9.2(c). Plot for $L = 2$, electric field shear $S_{r\phi}$ versus zenith angle θ at phases $\Phi = 0, \pi/2, \pi, 3\pi/2$ and the time average value, all at normalized radius $ka = 5.0$. Figures 6.9.1–6.9.4 have the same normalization; $\Phi = 2(\omega t - \phi)$.

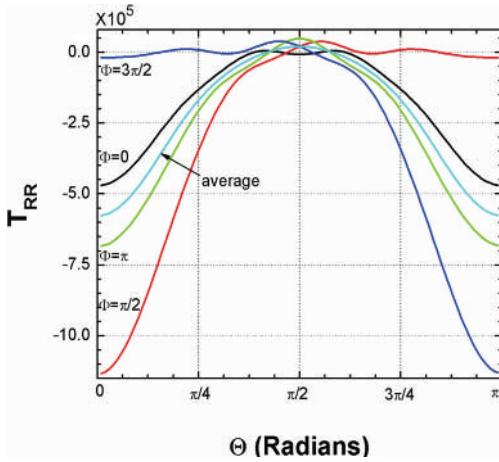


Fig. 6.9.3(a). Plot for $L = 2$, electric field radiation pressure T_{RR} versus zenith angle θ at phases $\Phi = 0, \pi/2, \pi, 3\pi/2$ and the time average value, all at normalized radius $ka = 1.0$. Figures 6.9.1–6.9.4 have the same normalization; $\Phi = 2(\omega t - \phi)$.

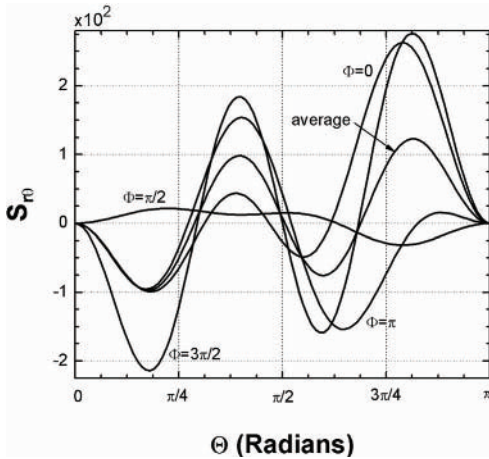


Fig. 6.9.3(b). Plot for $L = 2$, electric field radiation shear $S_{r,\theta}$ versus zenith angle θ at phases $\Phi = 0, \pi/2, \pi, 3\pi/2$ and the time average value, all at normalized radius $ka = 1.0$. Figures 6.9.1–6.9.4 have the same normalization; $\Phi = 2(\omega t - \phi)$.

to a disc whose normal is in the direction of the outbound radiation. The maximum azimuth-directed surface shear is about 10^6 , it is time dependent, see Eq. (6.9.1), and acts to produce azimuth-directed eddy currents. Zenith-directed shear is about a factor of ten smaller than the azimuth value.

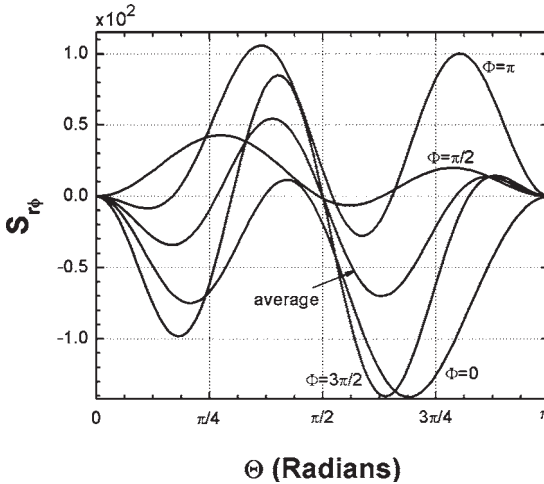


Fig. 6.9.3(c). Plot for $L = 2$, electric field shear $S_{r\phi}$ versus zenith angle θ at phases $\Phi = 0, \pi/2, \pi, 3\pi/2$ and the time average value, all at normalized radius $ka = 1.0$. Figures 6.9.1–6.9.4 have the same normalization; $\Phi = 2(\omega t - \phi)$.

Intermediate range, $ka = 1$, field pressure is shown in Fig. 6.9.1(b). The magnitude is on the order of five; it is expansive in the xy -plane and compressive on the z -axis but by a lesser amount on the negative axis than the positive axis. Both zenith and azimuth shears are significantly large. The forces act to extend an originally spherical radiator to an oblate ellipsoid with maximum radius of approximately $ka = 2$, independently of the original size of the system. That is, with this model, independently of the size of the original radiator, dipole forces act to alter a radiating source from a sphere to an oblate ellipsoid with approximate radius $ka = 2$.

Although the sum of the electric and magnetic field terms, i.e. the total pressure, is constant individual field pressures are not. The radial tensor components due to the electric and magnetic fields are:

$$\begin{aligned} \frac{\varepsilon}{2} E_r^2 &= \frac{\varepsilon}{(ka)^4} \left\{ \left(1 + \frac{1}{(ka)^2} \right) + \left(1 + \frac{1}{(ka)^2} \right) \cos(2\omega t_R) + \frac{2}{(ka)} \sin(2\omega t_R) \right\} \\ \frac{\mu}{2} H_r^2 &= \frac{\varepsilon}{(ka)^4} \left\{ \left(1 + \frac{1}{(ka)^2} \right) - \left(1 + \frac{1}{(ka)^2} \right) \cos(2\omega t_R) - \frac{2}{(ka)} \sin(2\omega t_R) \right\} \end{aligned} \quad (6.9.4)$$

The electric field acts only on electric charge densities and the magnetic field acts only on the current densities. Although the difference is not significant on a rigid surface it is on a surface sufficiently flexible to respond separately

to the different pressures; such differences are expected to produce source turbulence.

Dipoles plus Quadrupoles: Consider as a second example superimposed dipoles and quadrupoles with the relative magnitudes and phases of Eq. (5.10.16). The pressure and shears follow in the same manner as for dipoles alone. Electric field values are listed in Eq. (6.9.5). Again, although the total surface pressure is independent of time, the shears are not; they are time dependent and act to produce continuous eddies within the charged region.

$$\begin{aligned}
 E_r &= \left\{ -\frac{1}{\sigma^2}(3 + 15 \cos \theta) + \frac{i}{\sigma^3}(3 + 45 \cos \theta) + \frac{1}{\sigma^4}45 \cos \theta \right\} \sin \theta e^{-i\sigma} e^{-i\phi} \\
 E_\theta &= \left\{ -\frac{i}{\sigma}(1 - 4 \cos \theta - 5 \cos^2 \theta) - \frac{1}{\sigma^2}(6 - 9 \cos \theta + 15 \cos^2 \theta) \right. \\
 &\quad \left. + \frac{i}{\sigma^3}(15 - 9 \cos \theta - 30 \cos^2 \theta) + \frac{1}{\sigma^4}(15 - 30 \cos^2 \theta) \right\} e^{-i\sigma} e^{-i\phi} \\
 E_\phi &= \left\{ +\frac{1}{\sigma}(-1 + 4 \cos \theta + 5 \cos^2 \theta) + \frac{i}{\sigma^2}(6 - 9 \cos \theta - 15 \cos^2 \theta) \right. \\
 &\quad \left. + \frac{1}{\sigma^3} \left(\frac{15}{2} - \frac{33}{2} \cos \theta - 15 \cos^2 \theta \right) + \frac{15i}{\sigma^4} \cos \theta \right\} e^{-i\sigma} e^{-i\phi}
 \end{aligned} \tag{6.9.5}$$

Figures 6.9.2(a)–6.9.2(c) show normalized values of pressure and shear at $ka = 5.0, 1.0,$ and 0.1 at phases $2(\omega t - \phi) =: 0, \pi/2, \pi,$ and $3\pi/2$ and the time-average value.

Figure 6.9.2(a) shows that the time-average radiation pressure is compressive except in the vicinity of $\theta = 7\pi/16$, where it is always positive and nearly constant. On the positive and negative z -axes the surface pressure varies respectively between -0.3 and -2.0 and between 0 and -0.8 . Although the structure of atomic electrons may not permit significant compression, it is much more likely to permit extension of the original radiating sphere to a radiating plate, bent slightly into the direction of the output radiation beam. The dominantly negative pressure results in a transfer of linear momentum between the field and the source.

Figure 6.9.2(b) shows that the zenith angle shear, though time varying, is dominantly positive and negative respectively in the upper and lower half planes. The time-average value contributes to linear momentum transfer between the radiator and the field and the time-varying part acts to drive zenith-directed eddy currents on the radiating surface.

Figure 6.9.2(c) shows that the azimuth angle shear is time varying and dominantly negative. The average value results in angular momentum transfer between the radiator and the field and the time-varying part acts to drive azimuth-directed eddy currents on the radiating surface.

Figure 6.9.3(a) shows the time-average radiation pressure is compressive except in the vicinity of $\theta = \pi/2$, where it is always positive. On the z -axis the surface pressure varies between about zero and -10^6 . Presumably the structure of atomic electrons does not permit extensive electron compression but does permit extension of the original radiating sphere in the equatorial region.

Figure 6.9.3(c) shows that the azimuth angle shear is time varying, and acts to drive azimuth-directed eddy currents on the radiating surface.

Figure 6.9.4(a) shows that the radiation pressure is extensive between $\pi/8$ and $3\pi/8$ and between $5\pi/8$ and $7\pi/8$ and compressive elsewhere. The maximum time-average extensive pressure is about 10^{10} and acts to extend a radiating sphere in two separate parts. The time variation acts to produce radial oscillations of the radiating surface.

Figure 6.9.4(b) shows that the zenith angle shear is time varying with maximum value of about 10^{10} ; the time variation acts to drive zenith-directed eddy currents on the radiating surface.

Figure 6.9.4(c) shows a negative, time-average azimuth shear, with maximum value of about 5×10^9 at $\theta = 3\pi/8$. The average value transfers

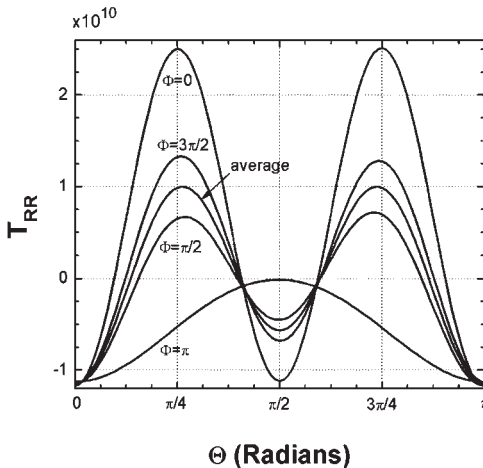


Fig. 6.9.4(a). Plot for $L = 2$, electric field radiation pressure T_{rr} versus zenith angle θ at phases $\Phi = 0, \pi/2, \pi, 3\pi/2$ and the time average value, all at normalized radius $ka = 0.1$. Figures 6.9.1–6.9.4 have the same normalization; $\Phi = 2(\omega t - \phi)$.

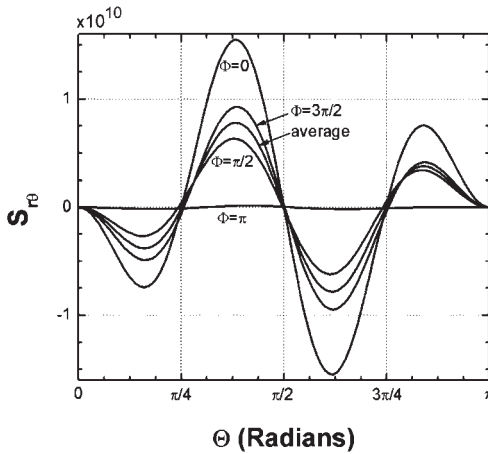


Fig. 6.9.4(b). Plot for $L = 2$, electric field radiation shear $S_{r\theta}$ versus zenith angle θ at phases $\Phi = 0, \pi/2, \pi, 3\pi/2$ and the time average value, all at normalized radius $ka = 0.1$. Figures 6.9.1–6.9.4 have the same normalization; $\Phi = 2(\omega t - \phi)$.

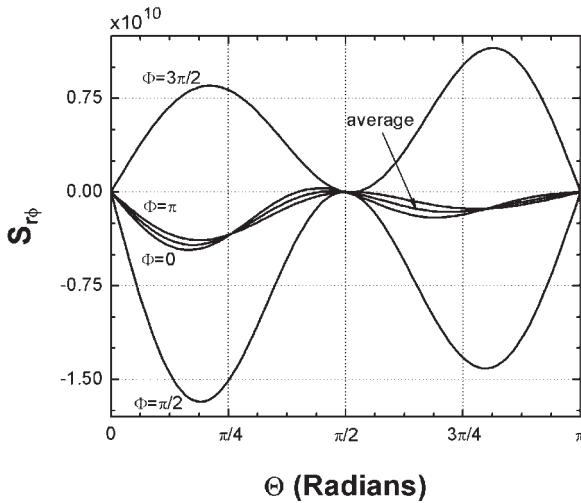


Fig. 6.9.4(c). Plot for $L = 2$, electric field shear $S_{r\phi}$ versus zenith angle θ at phases $\Phi = 0, \pi/2, \pi, 3\pi/2$ and the time average value, all at normalized radius $ka = 0.1$. Figures 6.9.1–6.9.4 have the same normalization; $\Phi = 2(\omega t - \phi)$.

angular momentum between the source and the field and the time varying value acts to drive azimuth-directed eddy currents on the radiating surface.

*L*th-order Modal Sources: The equatorial values of the electric field components were summed exactly and are given by the axial fields summarized

in Eq. (6.6.5):

$$\begin{aligned} \tilde{\mathbf{E}}\left(\sigma, \frac{\pi}{2}, \phi\right) = & \left[1 + i \sum_{\text{ne};0}^{\infty} \frac{A_n}{\sigma^{n+1}}\right] e^{-i\phi \hat{r}} + \left[\sum_{\text{ne};2}^{\infty} \frac{B_n}{\sigma^n} + \sum_{\text{no};3}^{\infty} \frac{(n-1)C_n}{\sigma^{n+1}}\right] e^{-i\phi \hat{\theta}} \\ & - i \left[1 + i \sum_{\text{no};1}^{\infty} \frac{C_n}{\sigma^n} - i \sum_{\text{ne};2}^{\infty} \frac{(n-1)B_n}{\sigma^{n+1}}\right] e^{-i\phi \hat{\phi}} \end{aligned} \quad (6.9.8)$$

The radial component contains a constant term and odd-modal-order terms with odd, negative powers of sigma; the angular components contain odd-modal-order terms with even, negative powers of σ and even-modal-order terms with odd, negative powers of σ . The relative magnitudes of A_0 and C_1 , by Eqs. (6.2.13) and (6.5.9), are:

$$A_0 = \sum_{\ell_0;1}^L \frac{(2\ell+1)\ell!! (\ell-2)!!}{(\ell-1)!! (\ell+1)!!} \cong 0.65 L \quad (6.9.9)$$

$$C_1 = \sum_{\ell e;0}^L \frac{(2\ell+1)(\ell-1)!!^2}{(\ell)!!^2} \cong 0.64 L \quad (6.9.10)$$

For the special cases $L = 59$ and 99 , A_0 is equal to 39.746 and 65.179. For the special cases $L = 60$ and 100 , C_1 is equal to 39.153 and 64.618. It follows that the two magnitudes are approximately related as:

$$A_0 \cong C_1 + 1 \quad (6.9.11)$$

Combining Eqs. (6.9.8) and (6.9.11) shows the far field portion of the electric field intensity is:

$$\tilde{\mathbf{E}}\left(\sigma, \frac{\pi}{2}, \phi\right) = \left\{ \hat{r} \left[1 + \frac{i}{\sigma}(1 + C_1)\right] - i\hat{\phi} \left[1 + \frac{i}{\sigma}C_1\right] \right\} e^{-i\phi} \quad (6.9.12)$$

The Poynting vector is:

$$\mathbf{N}_c = -\hat{\theta} \left[1 + \frac{C_1}{\sigma^2}(1 + C_1)\right] \quad (6.9.13)$$

This equation shows that energy flows up through the equator. The first term is independent of the radius and the second term decreases as the inverse square of the distance. The stress tensor components due to

Eq. (6.12.12) are:

$$\begin{aligned}
 T_{rr} \left(\sigma, \frac{\pi}{2}, \phi \right) &= \frac{\varepsilon}{4} \left\{ \frac{1}{\sigma^2} (1 + 2C_1) + \left(2 - \frac{1}{\sigma^2} (2C_1^2 + 2C_1 + 1) \right) \right. \\
 &\quad \left. \times \cos 2(\omega t - \sigma - \phi) - 2 \left(\frac{1}{\sigma} (2C_1 + 1) \right) \sin 2(\omega t - \sigma - \phi) \right\} \\
 S_{r\phi} \left(\sigma, \frac{\pi}{2}, \phi \right) &= \frac{\varepsilon}{2} \left\{ -\frac{1}{\sigma} + \frac{(1 + 2C_1)}{\sigma} \cos 2(\omega t - \sigma - \phi) \right. \\
 &\quad \left. + \left[1 - \frac{1}{\sigma^2} C_1 (1 + C_1) \right] \sin 2(\omega t - \sigma - \phi) \right\} \quad (6.9.14)
 \end{aligned}$$

In the far field limit a small, positive force is present on the equatorial zone of the radiating surface. This expansive, inverse square radial pressure affects the outer reaches of a radiating electron. The odd numbered modes are expansive and the even numbered modes are compressive. That is not to say, however, that the even modes are everywhere compressive. For the special case $L = 2$, as shown in Fig. 6.9.4(a) the pressure is compressive at $\theta = \pi/2$ but expansive at $\theta = \pi/4$ and $3\pi/4$. Such pressures act to change an originally spherical radiating region to a greatly expanded region in the general shape of a biconical antenna rotated about an axis at the conical points and perpendicular to the antenna axis.

The constant portion of the azimuth-directed shear contributes to the exchange of angular momentum between the source and the field. There are also time-varying parts with different radius dependencies that act to force the source charge into oscillations.

6.10. Self-Consistent Fields

The sums of Table 6.1.1 are over products of spherical Bessel functions and associated Legendre polynomials of degree one. Since energy transfer within localized regions is described by sums over spherical Hankel functions, see Eq. (3.4.11), a description of photons can only exist if sums over spherical Neumann functions are included. Although the sums of Eq. (6.1.4) are complete, and as such contain all needed information, evaluation of the sums is realistic only for modal orders less than about 30, as discussed in Chapter 2. We therefore seek more tractable field expressions. For this purpose we begin with spherical Bessel function solutions, known at all coordinates, and use that result to construct the full Neumann function solutions, otherwise known only on the coordinate axes. The first step towards expanding the solution is to use the relationship between teledistant spherical Bessel

and Neumann functions to obtain the full field set valid at all angles and limitlessly large radii.

The next step is to apply the Maxwell curl equations iteratively; this is the method of self-consistent fields. It is a powerful analytical tool that bears the same relationship to electromagnetic fields Taylor series do to other mathematical functions. If the fields are continuous through all orders and if the solution is known exactly at any point, self-consistent fields may be used to construct the fields at any other point. The result is a field expression valid at all angles and radii $r > 0$.

The starting sums over spherical Bessel function sums were obtained in Sec. 6.1:

$$\begin{aligned} S_{31} &= -iU(\sigma, \theta) & S_{21} &= e^{-i\sigma \cos \theta} + iV(\sigma, \theta) \\ S_{11} &= \sigma \sin \theta e^{-i\sigma \cos \theta} \\ \mathcal{S}_{31} &= -iV(\sigma, \theta) & \mathcal{S}_{21} &= e^{-i\sigma \cos \theta} \cos \theta + iU(\sigma, \theta) \end{aligned} \quad (6.10.1)$$

When the sums are combined to form the field vectors, see Eq. (5.8.1), only teledistant terms remain.

It is shown in Sec. 6.1 that the TM portion of the field is:

$$\tilde{\mathbf{E}}_{\text{TM}} = [S_1 \hat{r} / \sigma + \mathcal{S}_2 \hat{\theta} - i\mathcal{S}_3 \hat{\phi}] e^{-i\phi}, \quad \eta \tilde{\mathbf{H}}_{\text{TM}} = [iS_3 \hat{\theta} + S_2 \hat{\phi}] e^{-i\phi} \quad (6.10.2)$$

The starting fields are those of Table 6.7.1. Superscripts indicate the order of the iteration. Italicized or non-italicized terms indicate the term arises respectively from spherical Bessel or spherical Neumann functions. The sum $U + V$ contains both radial and unidirectional exponential functions, and presumably describes both z -directed and radially outbound power.

$$(U + V) = \frac{1}{\sigma(1 - \cos \theta)} [e^{-i\sigma \cos \theta} - e^{-i\sigma}] \quad (6.10.3)$$

The method of self-consistent fields uses iterative applications of the Maxwell curl equations:

$$\eta \tilde{\mathbf{H}} = \frac{i}{k} \nabla \times \tilde{\mathbf{E}} \quad \tilde{\mathbf{E}} = \frac{i\eta}{k} \nabla \times \tilde{\mathbf{H}} \quad (6.10.4)$$

If the full starting field expression is available, the solution extends to a smaller radius with each iteration. Although labor intensive, the process may be continued as many times as desired to obtain a satisfactory solution. There are inherent difficulties with the technique if the starting fields are

inexact: only those symmetries present in the starting function are present in the ultimate result and iterative errors quickly accumulate.

Combining the electric field portion of Eq. (6.10.2) with Eq. (6.10.4) gives the relationship:

$$\eta\tilde{\mathbf{H}} = \left\{ \frac{\hat{r}}{\sigma \sin \theta} \left[\frac{\partial(\sin \theta \mathcal{S}_3)}{\partial \theta} - \mathcal{S}_2 \right] + \hat{\theta} \left[\frac{S_1}{\sigma^2 \sin \theta} - \frac{1}{\sigma} \frac{\partial(\sigma \mathcal{S}_3)}{\partial \sigma} \right] + \hat{\phi} \left[\frac{i}{\sigma} \frac{\partial(\sigma \mathcal{S}_2)}{\partial \sigma} - \frac{i}{\sigma^2} \frac{\partial S_1}{\partial \theta} \right] \right\} e^{-i\phi} \quad (6.10.5)$$

Equating the magnetic field portion of Eq. (6.10.2) with Eq. (6.10.5) and combining gives:

$$0 = \left[\frac{\partial(\sin \theta \mathcal{S}_3)}{\partial \theta} - \mathcal{S}_2 \right] \quad S_3 = \left[\frac{i}{\sigma} \frac{\partial(\sigma \mathcal{S}_3)}{\partial \sigma} - i \frac{S_1}{\sigma^2 \sin \theta} \right]$$

$$S_2 = \left[\frac{i}{\sigma} \frac{\partial(\sigma \mathcal{S}_2)}{\partial \sigma} - \frac{i}{\sigma^2} \frac{\partial S_1}{\partial \theta} \right] \quad (6.10.6)$$

Combining the magnetic field portion of Eq. (6.10.2) with Eq. (6.10.4) gives the relationship:

$$\tilde{\mathbf{E}} = \left\{ \frac{i\hat{r}}{\sigma \sin \theta} \left[S_3 - \frac{\partial(\sin \theta S_2)}{\partial \theta} \right] + i \frac{\hat{\theta}}{\sigma} \frac{\partial(\sigma S_2)}{\partial \sigma} - i \frac{\hat{\phi}}{\sigma} \frac{\partial(\sigma S_3)}{\partial \sigma} \right\} e^{-i\phi} \quad (6.10.7)$$

Equating Eq. (6.10.7) and the electric field portion of Eq. (6.10.2) gives:

$$S_1 = \frac{i}{\sin \theta} \left[S_3 - \frac{\partial(\sin \theta S_2)}{\partial \theta} \right], \quad \mathcal{S}_2 = \frac{i}{\sigma} \frac{\partial(\sigma S_2)}{\partial \sigma}, \quad \mathcal{S}_3 = \frac{i}{\sigma} \frac{\partial(\sigma S_3)}{\partial \sigma} \quad (6.10.8)$$

The procedure for obtaining the full field set begins with the expressions of Table 6.7.1. Iterations are obtained by substitution into Steps 5 and 6 of Table 6.10.1 then following the chart. The circular process is repeated as many times as desired. All sums follow from S_3 ; its values through six iterations are listed in Table A.30.1.

Table 6.10.1. Flow chart for evaluating field sums.

-
1. Use S_3^ℓ to find $\mathfrak{S}_3^\ell = \frac{i}{\sigma} \frac{\partial}{\partial \sigma} [\sigma S_3^\ell]$
 2. Use S_2^ℓ to find $\mathfrak{S}_2^\ell = \frac{i}{\sigma} \frac{\partial}{\partial \sigma} [\sigma S_2^\ell]$
 3. Check $\mathfrak{S}_2^\ell = \frac{\partial}{\partial \theta} (\sin \theta S_2^\ell)$
 4. Use S_3^ℓ and S_2^ℓ to find $S_1^\ell = \frac{i}{\sin \theta} [S_3^\ell - \partial(\sin \theta S_2^\ell)/\partial \theta]$
 5. Use \mathfrak{S}_3^ℓ and S_1^ℓ to find $S_3^{\ell+1} = \frac{i}{\sigma} \left[\partial(\sigma \mathfrak{S}_3^\ell)/\partial \sigma - \frac{S_1^\ell}{\sigma \sin \theta} \right]$
 6. Use \mathfrak{S}_2^ℓ and S_1^ℓ to find $S_2^{\ell+1} = \frac{i}{\sigma} \left[\partial(\sigma \mathfrak{S}_2^\ell)/\partial \sigma - \frac{\partial S_1^\ell}{\sigma \partial \theta} \right]$
 7. Check $S_2^{\ell+1} = \frac{\partial}{\partial \theta} (\sin \theta S_3^{\ell+1})$
 8. Redefine $\ell + 1 \rightarrow \ell$
 9. Return to Step 1 and follow the chart steps
-

6.11. Energy Exchanges

To obtain the power and energy supported by self-consistent fields, begin with the complex Poynting vector. With the fields of Eq. (5.10.16), it may be written:

$$\mathbf{N}_c = \frac{1}{2} \text{Re}(\tilde{\mathbf{E}} \times \tilde{\mathbf{H}}^*) = \frac{1}{2\eta} \text{Re}[\tilde{\mathbf{E}} \times (i\tilde{\mathbf{E}})^*] \quad (6.11.1)$$

The surface power on a circumscribing sphere surrounding the source follows from the angular field components, shown in Tables A.30.3 and A.30.4.

Quite differently from individual multipolar fields, the energy transferred by the fields of Eq. (5.10.16) changes its direction of travel as distance from the source increases. This may be seen by writing Eq. (6.1.16), which appears in both angular field terms, in the form:

$$\begin{aligned} U(\sigma, \theta) &= \frac{1}{\sigma \sin^2 \theta} \left[e^{-i\sigma \cos \theta} - \frac{1}{2}(e^{-i\sigma}(1 + \cos \theta) + e^{i\sigma}(1 - \cos \theta)) \right] \\ V(\sigma, \theta) &= \frac{1}{\sigma \sin^2 \theta} \left[e^{-i\sigma \cos \theta} \cos \theta - \frac{1}{2}(e^{-i\sigma}(1 + \cos \theta) + e^{i\sigma}(1 - \cos \theta)) \right] \end{aligned} \quad (6.11.2)$$

Tables A.30.2–A.30.4 show all field terms that do not include $U(\sigma, \theta)$ and $V(\sigma, \theta)$ travel in the $+z$ direction and vary with radius at powers ranging from zero to $-(2N + 1)$, where N is the number of iterations. Terms involving $U(\sigma, \theta)$ and $V(\sigma, \theta)$ vary with radius at powers ranging from -3 to $-(2N + 3)$. It follows that energy flow at very large radii is $+z$ directed and at very small radii is both axially and radially directed.

In common with the output powers analyzed in Chapters 2 and 3, only products of one spherical Bessel and one spherical Neumann function integrate to a real power over an enclosing surface. In this case since all pertinent sums over spherical Bessel function terms are teledistant, each surface power term is the product of at least one teledistant field term. The fields of Eq. (5.10.16) *without* the spherical Bessel terms describe standing energy. A plane wave impressed on such a field that supplies the leading terms produces an energy exchange. The power on a spherical surface of radius ka circumscribing the radiator follows by applying Eq. (6.11.1) to the fields of Tables A.30.3 and A.30.4 and taking the surface integral.

As an example consider the third iteration fields; the electric components are listed in Eqs. (6.11.3)–(6.11.5).

$$\begin{aligned}
 {}^3E_r = \sin \theta \left\{ (1 + \cos \theta) + \frac{i}{\sigma}(1 + 6 \sin^2 \theta) + \frac{1}{\sigma^2}(54 - 36 \cos^2 \theta) \cos \theta \right. \\
 - \frac{i}{\sigma^3}(114 - 84 \sin^2 \theta - 120 \sin^4 \theta) - \frac{1}{\sigma^4}(192 - 840 \sin^2 \theta) \cos \theta \\
 \left. - \frac{i}{\sigma^5}(864 - 1080 \sin^2 \theta) \right\} e^{-i\sigma \cos \theta} e^{-i\phi} \quad (6.11.3)
 \end{aligned}$$

$$\begin{aligned}
 {}^3E_\theta = \left[\cos \theta(1 + \cos \theta) + \frac{i}{\sigma}6 \sin^2 \theta \cos \theta + \frac{1}{\sigma^2}(5 + 36 \cos^2 \theta - 36 \cos^4 \theta) \right. \\
 - \frac{i}{\sigma^3}(18 + 144 \cos^2 \theta - 120 \cos^4 \theta) \cos \theta + \frac{1}{\sigma^4}(124 - 252 \cos^2 \theta) \\
 - \frac{i}{\sigma^5}(684 - 600 \cos^2 \theta) \cos \theta - \frac{1}{\sigma^6}(480 + 840 \cos^2 \theta) \\
 \left. + \frac{(7)!i}{2\sigma^7} \cos \theta + \frac{(7)!}{\sigma^8} \right] e^{-i\sigma \cos \theta} e^{-i\phi} \\
 - (6)! \left[i \left(\frac{1}{(6)!\sigma^2} - \frac{3}{(4)!\sigma^4} + \frac{5}{(2)!\sigma^6} - \frac{7}{\sigma^8} \right) V \right. \\
 \left. + \left(\frac{2}{(5)!\sigma^3} - \frac{4}{(3)!\sigma^5} + \frac{6}{\sigma^7} \right) U \right] e^{-i\phi} \quad (6.11.4)
 \end{aligned}$$

$$\begin{aligned}
{}^3E_\phi = & -i \left\{ (1 + \cos \theta) + \frac{i}{\sigma} 6 \sin^2 \theta + \frac{1}{\sigma^2} (6 + 36 \cos^2 \theta) \cos \theta \right. \\
& + \frac{i}{\sigma^3} (42 - 216 \cos^2 \theta + 120 \cos^4 \theta) + \frac{1}{\sigma^4} (144 - 360 \cos^2 \theta) \cos \theta \\
& + \left. \frac{i}{\sigma^5} (36 + 360 \cos^2 \theta) + \frac{480}{\sigma^6} \cos \theta - \frac{i}{\sigma^7} 1800 \right\} e^{-i\sigma \cos \theta} e^{-i\phi} \\
& - i(6)! \left[i \left(\frac{1}{(6)! \sigma^2} - \frac{3}{(4)! \sigma^4} + \frac{5}{(2)! \sigma^6} - \frac{7}{\sigma^8} \right) U \right. \\
& + \left. \left(\frac{2}{(5)! \sigma^3} - \frac{4}{(3)! \sigma^5} + \frac{6}{\sigma^7} \right) V \right] e^{-i\phi} \tag{6.11.5}
\end{aligned}$$

Values of output power as functions of radius calculated using the fields of Tables A.30.3 and A.30.4 are listed in Table 6.11.1.

In Chapters 2 and 3, the time-average surface power is supported by the product of field terms, each of which is proportional to $1/\sigma$, for example Eqs. (3.3.1) and (3.3.2). Since the area increases as σ^2 , the product of far field power density and area is independent of distance. The radiation

Table 6.11.1. Calculated output power by number of iterations, N.

$$\begin{aligned}
{}^0P_r &= \frac{2\pi\sigma^2}{\eta k^2} \left\{ \frac{4}{3} - \frac{2}{\sigma^2} + \frac{1}{\sigma^4} - \frac{1}{\sigma^4} \cos(2\sigma) \right\} \\
{}^1P_r &= \frac{2\pi\sigma^2}{\eta k^2} \left\{ \left[\frac{4}{3} + \frac{10}{3\sigma^2} + \frac{5}{\sigma^4} - \frac{6}{\sigma^6} \right] - \frac{1}{\sigma^4} \left[\left(1 - \frac{6}{\sigma^2} \right) \cos(2\sigma) - \frac{4}{\sigma} \sin(2\sigma) \right] \right\} \\
{}^2P_r &= \frac{2\pi\sigma^2}{\eta k^2} \left\{ \left[\frac{4}{3} + \frac{102}{5\sigma^2} + \frac{9}{\sigma^4} - \frac{84}{\sigma^6} + \frac{120}{\sigma^8} \right] - \frac{1}{\sigma^4} \left[\left(1 - \frac{36}{\sigma^2} + \frac{120}{\sigma^4} \right) \cos(2\sigma) \right. \right. \\
&\quad \left. \left. - \left(\frac{8}{\sigma} - \frac{96}{\sigma^3} \right) \sin(2\sigma) \right] \right\} \\
{}^3P_r &= \frac{2\pi\sigma^2}{\eta k^2} \left\{ \left[\frac{4}{3} + \frac{38}{\sigma^2} + \frac{9}{\sigma^4} - \frac{330}{\sigma^6} + \frac{3240}{\sigma^8} - \frac{5040}{\sigma^{10}} \right] - \frac{1}{\sigma^4} \left[\left(1 - \frac{90}{\sigma^2} + \frac{1800}{\sigma^4} - \frac{5040}{\sigma^6} \right) \right. \right. \\
&\quad \left. \left. \times \cos(2\sigma) - \left(\frac{12}{\sigma} - \frac{480}{\sigma^3} + \frac{4320}{\sigma^5} \right) \sin(2\sigma) \right] \right\} \\
{}^4P_r &= \frac{2\pi\sigma^2}{\eta k^2} \left\{ \frac{4}{3} + \frac{866}{5\sigma^2} + \frac{1}{\sigma^4} - \frac{1320}{\sigma^6} + \frac{21,840}{\sigma^8} - \frac{221,760}{\sigma^{10}} + \frac{362,880}{\sigma^{12}} \right. \\
&\quad - \frac{1}{\sigma^4} \left[\left(1 - \frac{168}{\sigma^2} + \frac{8400}{\sigma^4} - \frac{141,120}{\sigma^6} + \frac{362,880}{\sigma^8} \right) \cos(2\sigma) \right. \\
&\quad \left. \left. - \left(\frac{16}{\sigma} - \frac{1344}{\sigma^3} + \frac{40,320}{\sigma^5} - \frac{322,560}{\sigma^7} \right) \sin(2\sigma) \right] \right\}
\end{aligned}$$

analyzed here is dramatically different. The power from the first terms listed in Table 6.11.1 increase with distance as σ^2 , the second terms are independent of σ , the third terms decreases as $1/\sigma^2$, etc. through higher powers. Yet, energy conservation requires the total value to be independent of distance. This, in turn, requires the energies carried by the higher order terms to transfer to lower order terms as the energy travels outward from the source. The calculated output power remains finite only because of the finite length of the wave train.

6.12. Self-Consistent Photon-Field Stress and Shear

We seek to evaluate the pressure and shear on a radiating sphere as it generates the self-consistent fields calculated in Sec. 6.10. First note from Tables A.30.2–A.30.4 that the far field and telefield electric field terms after N iterations are:

$$\begin{aligned} \tilde{\mathbf{E}}(\sigma, \theta, \phi) = & \left\{ \hat{\mathbf{r}} \sin \theta \left[(1 + \cos \theta) + \frac{i}{\sigma} (1 + 2N \sin^2 \theta) \right] \right. \\ & + \hat{\theta} \cos \theta \left[(1 + \cos \theta) + \frac{i}{\sigma} 2N \sin^2 \theta \right] \\ & \left. - i \hat{\phi} \left[(1 + \cos \theta) + \frac{i}{\sigma} 2N \sin^2 \theta \right] \right\} e^{-i\sigma \cos \theta} e^{-i\phi} \end{aligned} \quad (6.12.1)$$

For the special case $\theta = \pi/2$, the field is:

$$\tilde{\mathbf{E}}\left(\sigma, \frac{\pi}{2}, \phi\right) = \left\{ \hat{\mathbf{r}} \left[1 + \frac{i}{\sigma} (1 + 2N) \right] - i \hat{\phi} \left[1 + \frac{i}{\sigma} 2N \right] \right\} e^{-i\phi} \quad (6.12.2)$$

Comparison with Eq. (6.9.12) shows that the results are the same as those obtained by direct summation of axial values if:

$$C_1 \cong 0.64 L = 2N \quad \text{or} \quad N \cong L/3 \quad (6.12.3)$$

If both N and L are large N is equivalent to about $L/3$. The surface pressure follows by noting from Eq. (5.10.16) that the magnitudes of the electric and magnetic fields are the same, from Eq. (4.2.17) the proper form for the pressure, then combining with Eqs. (6.12.1) and (6.12.3) to obtain:

$$T_{rr} = \frac{\varepsilon L}{3(ka)^2} \quad (6.12.4)$$

Therefore, regardless of the radius of the radiating region, a positive pressure exists that acts to extend it to ever-larger values.

For the general case, pressure and shears on the radiating surface follow from the fields. The field set of Eqs. (6.11.3)–(6.11.5), i.e. $N = 3$, has the structure of Eq. (3.16.3), where the electric and magnetic fields are equal magnitude and out of the phase. The field pressure, therefore, is constant. However since the electric and magnetic fields affect different entities, charge and current densities, we track only the electric values. Figures 6.12.1–6.12.3 show such normalized values of pressure and shear at $ka = 5.0, 1.0, \text{ and } 0.1$ and at time phases $2(\omega t - \phi)$ equal: $0, \pi/2, \pi,$ and $3\pi/2$.

The time average value of Fig. 6.12.1(a) shows that the average value is extensive from about $\theta = 3\pi/8$ to $5\pi/8$, reaching a maximum value of about 0.5 in the upper half plane. Extreme values of about -4 and -0.5 occur respectively on the positive and negative z -axes. Tracing the time dependent curves shows alternately compressive and extensive traveling waves start at the negative z -axis and travel to the positive one, reaching a maximum magnitude in the upper equatorial region. These travelling, peristaltic, pressure waves travel along the spherical surface. They act to produce radial oscillations of the surface, alternately expanding and contracting the equatorial zone of the radiating sphere, and compress the z -axis region of the surface.

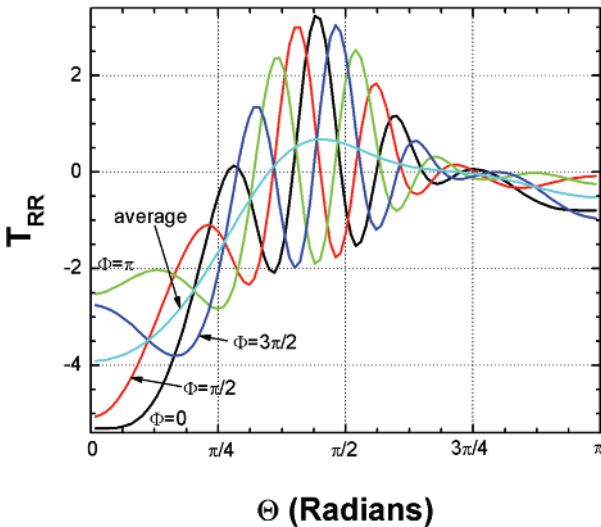


Fig. 6.12.1(a). Self-consistent field, $N=3$, electric field radiation pressure T_{RR} versus zenith angle θ at phases $\Phi = 0, \pi/2, \pi, 3\pi/2$ and the time average value, all at normalized radius $ka = 5.0$. Figures 6.9.1–6.9.4, 6.12.1–6.12.3 all have the same normalization; $\Phi = 2(\omega t - \phi)$.

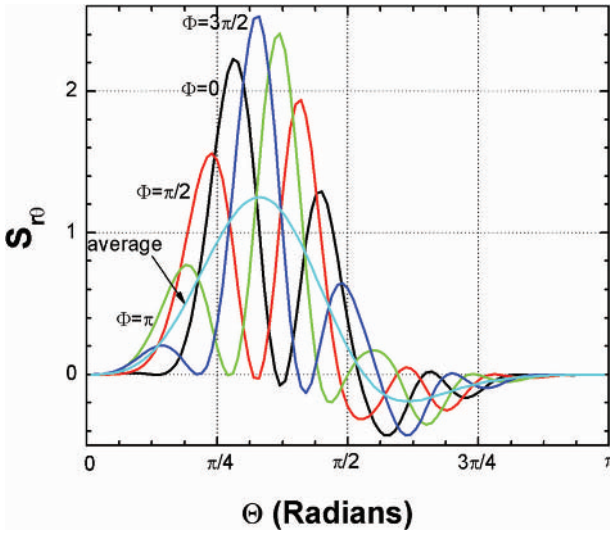


Fig. 6.12.1(b). Self-consistent field, $N = 3$, electric field radiation shear $S_{r\theta}$ versus zenith angle θ at phases $\Phi = 0, \pi/2, \pi, 3\pi/2$ and the time average value, all at normalized radius $ka = 5.0$. Figures 6.9.1–6.9.4, 6.12.1–6.12.3 all have the same normalization; $\Phi = 2(\omega t - \phi)$.

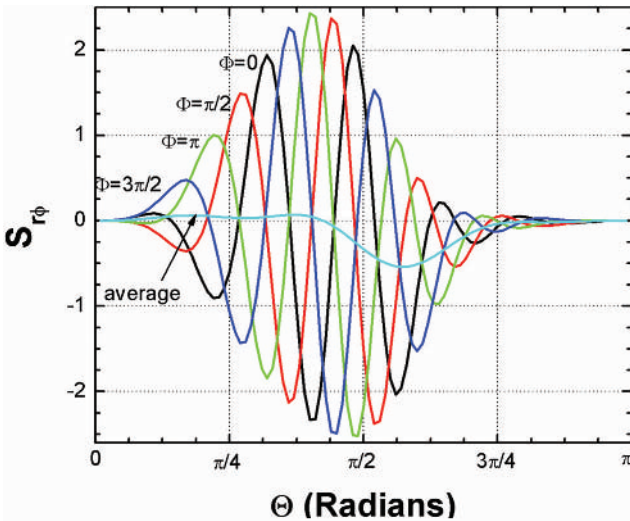


Fig. 6.12.1(c). Self-consistent field, $N = 3$, electric field radiation shear $S_{r\phi}$ versus zenith angle θ at phases $\Phi = 0, \pi/2, \pi, 3\pi/2$ and the time average value, all at normalized radius $ka = 5.0$. Figures 6.9.1–6.9.4, 6.12.1–6.12.3 all have the same normalization; $\Phi = 2(\omega t - \phi)$.

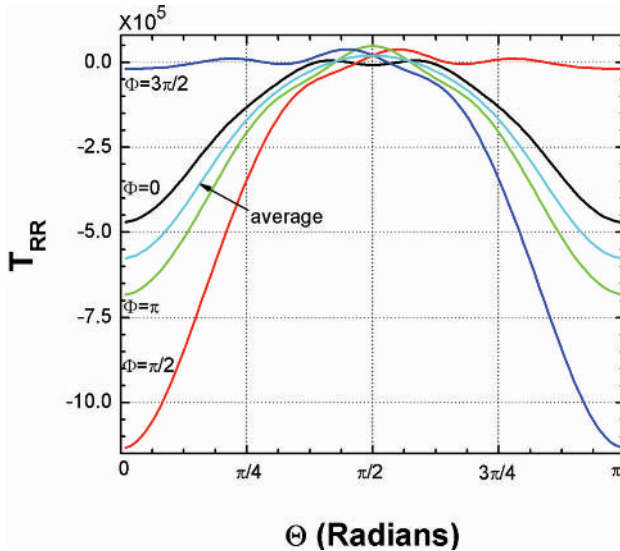


Fig. 6.12.2(a). Self-consistent field, $N = 3$, electric field radiation pressure T_{RR} versus zenith angle θ at phases $\Phi = 0, \pi/2, \pi, 3\pi/2$ and the time average value, all at normalized radius $ka = 1.0$. Figures 6.9.1–6.9.4, 6.12.1–6.12.3 all have the same normalization; $\Phi = 2(\omega t - \phi)$.

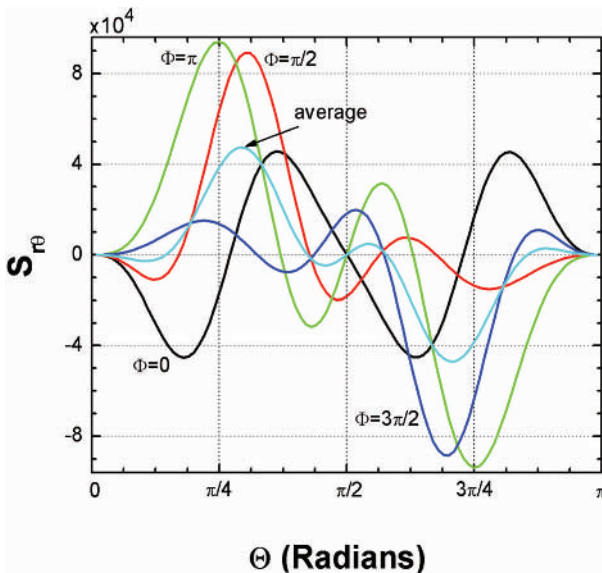


Fig. 6.12.2(b). Self-consistent field, $N = 3$, electric field shear $S_{r\theta}$ versus zenith angle θ at phases $\Phi = 0, \pi/2, \pi, 3\pi/2$ and the time average value, all at normalized radius $ka = 1.0$. Figures 6.9.1–6.9.4, 6.12.1–6.12.3 all have the same normalization; $\Phi = 2(\omega t - \phi)$.

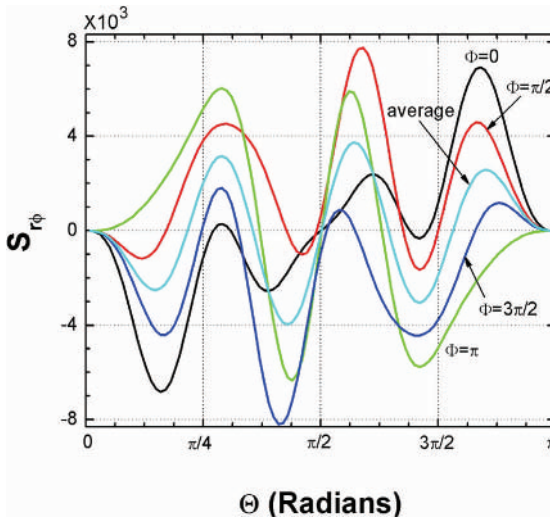


Fig. 6.12.2(c). Self-consistent field, $N = 3$, electric field sheara $S_{r\phi}$ versus zenith angle θ at phases $\Phi = 0, \pi/2, \pi, 3\pi/2$ and the time average value, all at normalized radius $ka = 1.0$. Figures 6.9.1–6.9.4, 6.12.1–6.12.3 all have the same normalization; $\Phi = 2(\omega t - \phi)$.

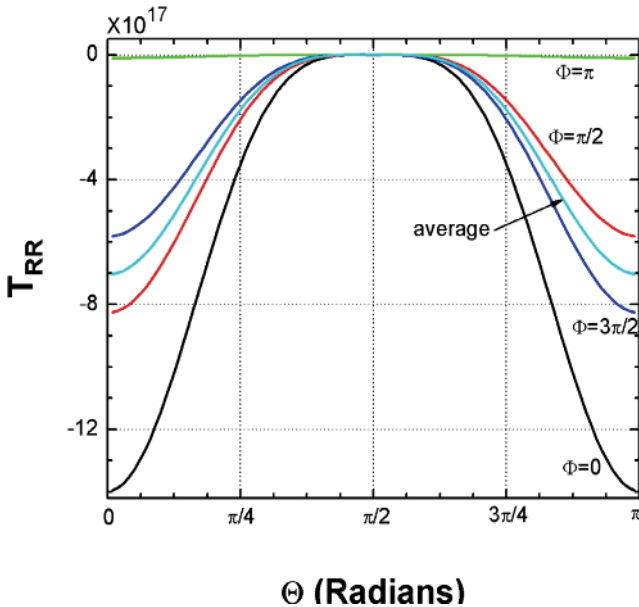


Fig. 6.12.3(a). Self-consistent field, $N = 3$, electric field radiation pressure T_{RR} versus zenith angle θ at phases $\Phi = 0, \pi/2, \pi, 3\pi/2$ and the time average value, all at normalized radius $ka = 0.1$. Figures 6.9.1–6.9.4, 6.12.1–6.12.3 all have the same normalization; $\Phi = 2(\omega t - \phi)$.

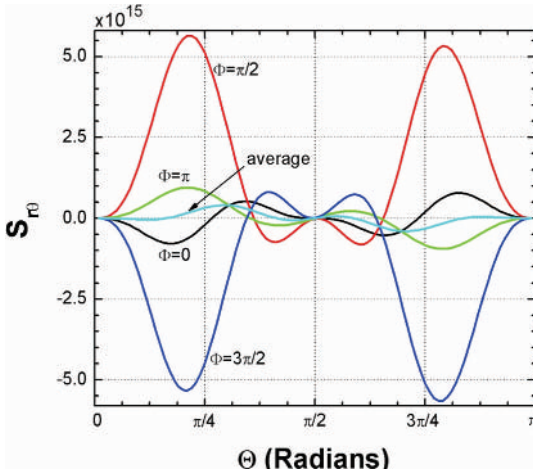


Fig. 6.12.3(b). Self-consistent field, $N = 3$, electric field shear $S_{r\theta}$ versus zenith angle θ at phases $\Phi = 0, \pi/2, \pi, 3\pi/2$ and the time average value, all at normalized radius $ka = 1.0$. Figures 6.9.1–6.9.4, 6.12.1–6.12.3 all have the same normalization; $\Phi = 2(\omega t - \phi)$.

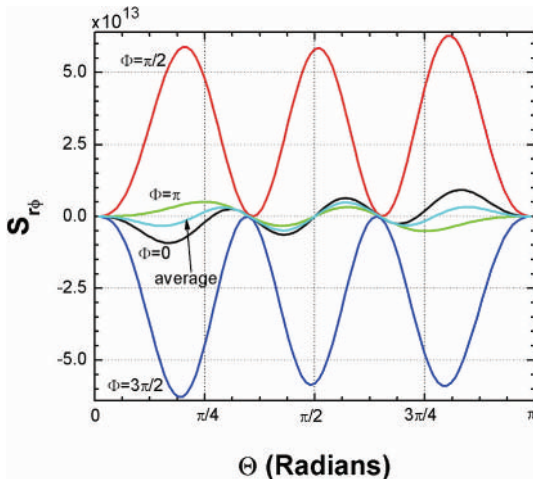


Fig. 6.12.3(c). Self-consistent field, $N = 3$, electric field shear $S_{r\phi}$ versus zenith angle θ at phases $\Phi = 0, \pi/2, \pi, 3\pi/2$ and the time average value, all at normalized radius $ka = 1.0$. Figures 6.9.1–6.9.4, 6.12.1–6.12.3 all have the same normalization; $\Phi = 2(\omega t - \phi)$.

Shear $S_{r\theta}$ is dominantly positive with a maximum value of 2.5 in the upper half plane and negative maximum value of -0.5 in the lower half plane. Like the compressional waves, the shear waves travel from the negative to positive z -axes. These waves play the dual role of (1) driving zenith-directed current eddies that, in turn, act as field sources and (2) combine with the compressional waves to change the radial thrust of the pressure wave to a downward one. The downward thrust is responsible for the linear momentum exchange between the source and field. The combined motion is, perhaps, analogous to the propulsion system used by squids to propel themselves through the sea.

The time-average shear $S_{r\phi}$ is nearly constant in the upper half plane and negative with a maximum value of -0.5 in the lower half plane. Like the θ -directed counterpart, these ϕ -directed waves go from the negative to positive z -axes, act to drive azimuth-directed current eddies that, in turn, act as field sources, and the average value acts to spin the source electron.

The forces acting on a radiator with $ka = 1$ are much larger than those acting on a radiator with $ka = 5$. Comparing Figs. 6.12.1(a) and 6.12.2(a) shows the $ka = 1$ surface area is less by a factor of 25 and the pressure is more by a factor of about 10^5 . The pressure waves that typified the surface at larger radii are essentially nonexistent here. Figure 6.12.2(a) shows that the pressure is small and positive near $\theta = \pi/2$ and negative elsewhere. At $\Phi = \pi/2$ the pressure on the positive z -axis is about -10^6 and on the negative axis about -10^4 ; magnitudes are reversed at $\Phi = 3\pi/2$.

At radius $ka = 1.0$ the upper and lower half planes of $S_{r\theta}$ are respectively dominantly positive and negative. The value averaged over both time and zenith angle is nearly zero. Like the pressure counterpart, the traveling wave aspect is essentially gone, leaving oscillating values of shear at each angle. Maximum values are about 90,000, as contrasted with 2.5 for the larger radius. The oscillations act to drive zenith-directed current eddies that, in turn, act as field sources.

The average shear $S_{r\phi}$ at $ka = 1.0$, taken over both time and zenith angle, is nearly zero, and, like the compression and zenith shear counterparts, the traveling wave aspect is essentially gone. Maximum oscillatory values are about 8000, as contrasted with 2.5 at the larger radius, and act to drive azimuth-directed current eddies that, in turn, act as field sources.

The forces acting on a radiator with $ka = 0.1$ are much larger than those acting on a radiator with $ka = 1.0$. Comparison of Figs. 6.12.2(a) and 6.12.3(a) shows that the pressure is larger by a factor of about 10^{12} . It is

small and positive near $\theta = \pi/2$ and negative elsewhere. At $\Phi = 0$ pressure values on both the positive and negative z -axes are about -1.4×10^{18} and average values are about half that amount.

At radius $ka = 0.1$ the time average value of $S_{r\theta}$ is much less than the time varying part. The maximum time average values of about 10^{14} are at about $\theta = 5\pi/16$ and $11\pi/16$; the former is positive and the latter negative. Maximum oscillatory difference of about 10^{16} occurs at about $\theta = 3\pi/16$ and $13\pi/16\pi$, and are in phase. The oscillations act to drive zenith-directed current eddies that act as field sources.

At $ka = 0.1$ the average shear $S_{r\phi}$ magnitude varies between about $\pm 10^{12}$. Maximum oscillatory values are $\pm 10^{14}$, and act to drive azimuth-directed current eddies that, in turn, act as field sources.

Taken together, this set of figures, Figs. 6.12.1–6.12.3, shows that dominating electromagnetic forces exist on the surface of a radiating sphere at three radii where values were determined. In each case the forces act to expand the equatorial region, to compress the poles, and support shear forces that act to drive current eddies. They also exchange linear and angular momentum between the field and its source or sink. These forces are the origin of the regenerative drive mechanism that produces the nonlinear response to a driving field.

To illustrate the magnitude, phasing, and orientation of these radiation reaction forces it was necessary to pick specific sources as examples. The principles, however, are not radius-specific. The large radiation reaction pressure-to-Coulomb pressure ratios are robust, and similar results are obtained for any reasonable choice of examples.

6.13. Thermodynamic Reciprocity

The self-consistent field expansion of Sec. 6.12 shows that only the Neumann portion of the radial functions is affected by the regenerative field buildup. Although Neumann functions have an $\ell + 1$ order singularity at the origin, it appears only because there is a size below which the descriptive equations cease to apply and we have not entered an appropriate description of the source charges and currents. However, since exterior fields may be calculated from the surface fields, see Appendix A.7, conclusions about exterior field properties may be drawn without knowledge of the source. Conversely, detailed internal structure cannot be deduced from the external fields. In

what follows we examine external field characteristics applicable to multi-modes of the orders and degree that appear in Eqs. (5.8.3) and (5.10.16).

General differences between Hankel and Neumann field descriptions may be illustrated by electric dipole radiation. Two possible radial dipole functions, $y_1(\sigma)$ and $h_1(\sigma)$, are:

$$y_1(\sigma) = -\frac{1}{\sigma} \left(\frac{1}{\sigma} \cos \sigma + \sin \sigma \right) \quad h_1(\sigma) = \frac{1}{\sigma} \left(-1 + \frac{i}{\sigma} \right) e^{-i\sigma} \quad (6.13.1)$$

To analyze differences between z -directed electric dipoles creating, respectively, Hankel and Neumann functions consider a unit magnitude field coefficient for dipolar fields:

$$\begin{aligned} \sigma \tilde{\mathbf{E}}_r &= 2z_1(\sigma) \cos \theta \\ \tilde{\mathbf{E}}_\theta &= -z_1'(\sigma) \sin \theta \\ \eta \tilde{\mathbf{H}}_\phi &= iz_1(\sigma) \sin \theta \end{aligned} \quad (6.13.2)$$

Spherical Hankel function: Replacing $z_1(\sigma)$ with $h_1(\sigma)$ reproduces the radiation values listed in Table 3.12.1. Since the outgoing wave separates from the source the standing energy is that which remains after subtracting the outgoing energy from the total. The time average Poynting vector, N_r , the standing energy density, $w_T - w_N$, and the total standing energy W are:

$$\begin{aligned} N_r &= \frac{1}{2\eta} \left\{ j_1(\sigma) \frac{dy_1(\sigma)}{d\sigma} - y_1(\sigma) \frac{dj_1(\sigma)}{d\sigma} \right\} \sin^2 \theta = \frac{2}{2\eta\sigma^2} \sin^2 \theta \\ w_T - w_N &= \frac{\varepsilon}{4} \left\{ \frac{4}{\sigma^4} \left(1 + \frac{1}{\sigma^2} \right) \cos^2 \theta + \frac{1}{\sigma^6} \sin^2 \theta \right\} \\ W &= \frac{2\pi\varepsilon}{3k^3} \left\{ \frac{1}{(ka)^3} + \frac{2}{(ka)} \right\} \end{aligned} \quad (6.13.3)$$

The real part of N_r is proportional to the product of spherical Bessel and Neumann functions. That is, a net output power requires the presence of both radial functions, equally weighted and $\pi/2$ out of phase, i.e. a Hankel function.

Spherical Neumann function: Replacing $z_1(\sigma)$ with $y_1(\sigma)$ leads to a different set of parameters: time average Poynting vector, N_r , total energy density,

w_T , and total field energy, W :

$$\begin{aligned}
 N_r &= \frac{1}{2\eta} \operatorname{Re} \tilde{\mathbf{E}}_\theta \tilde{\mathbf{H}}_\phi^* = 0 \\
 w_T &= \frac{\varepsilon^2}{4} \left[4 \left(\frac{1}{\sigma^4} \sin^2 \sigma + \frac{2}{\sigma^5} \sin \sigma \cos \sigma + \frac{1}{\sigma^6} \cos^2 \sigma \right) \cos^2 \theta \right. \\
 &\quad \left. + \left(\frac{1}{\sigma^2} + \frac{1}{\sigma^4} \sin^2 \sigma + \frac{2}{\sigma^5} \sin \sigma \cos \sigma \right. \right. \\
 &\quad \left. \left. - \left(\frac{1}{\sigma^4} - \frac{1}{\sigma^6} \right) \cos^2 \sigma \right) \sin^2 \theta \right] \\
 \lim_{R \rightarrow \infty} W &\cong \left(\frac{2\pi\varepsilon}{3k^3} \right) \left[\frac{1}{2(ka)^3} + \frac{1}{(ka)} + kR \right]
 \end{aligned} \tag{6.13.4}$$

The absence of a real part of N_r shows that no energy permanently leaves the system; all radiated energy remains attached to the source. The last term in the energy expression is proportional to the radius, R , of the outer limit of the radiation; it increases without limit as the source continues to radiate. This effect has not been considered in the theory of radiation exchanges by atoms.

At the smallest possible circumscribing surface about an electrically small radiating source the difference between the Neumann- and Hankel-described fields is quite small. The leading real and imaginary Hankel function terms are:

$$\lim_{ka \rightarrow 0} h_1(ka) = \frac{ka}{3} + \frac{i}{(ka)^2} \tag{6.13.5}$$

With a Neumann source the real part is equal to zero. With a Hankel function source the Bessel-to-Neumann ratio is $(ka)^3/3$, a very small number if ka itself is much less than one. Hence, although its effect on standing energy is enormous the difference between Neumann and Hankel function descriptions at the source is vanishingly small. Since, in this way, a slight source perturbation greatly reduces the standing energy a Neumann source is in unstable equilibrium. Thermal noise within a conducting wire is sufficient to assure a Hankel function description. With the eigenstate source of Sec. 6.12, however, thermal noise is not a factor; it applies to each atom *en toto*, not to electronic effects internal to atoms. There is no feedback path from the field to the source and, therefore, fields described by Neumann functions remain in metastable equilibrium. Although this discussion is confined to electric dipole radiation, it applies to all modes that form part of the positive feedback described in Sec. 6.12.

Reciprocity: Thermodynamics requires reciprocity between absorption and emission. Although the condition can be met mathematically by a simple time reversal in Eq. (5.10.16), the physics of the situation is more difficult. How can an electrically small region extract enough energy from a low intensity field to initiate the regenerative process? We next describe a scenario that appears to satisfy all constraints.

As a Lorentz-like electron enters an eigenstate it accelerates and, by virtue of the acceleration, produces a radiation field. That field, in turn, produces both pressure and shears on the source of the same order of magnitude as the trapping Coulomb force, see Secs. 4.2 and 4.3. The primary postulatory base of Chapter 4 is that the radiation pressure and shears combine to transfigure the electron from an entity much smaller than an atom to an ensemble of charge and current densities that occupies the volume of the eigenstate. An acceptable model is the intra-eigenstate electron ensemble that constitutes a nonlocal electron. Whatever the model, the physical significance of $eU^*(r)U(r)$ within an equilibrated eigenstate more closely resembles a time-average charge density than a probability. Intrinsic and local forces assure that the electron structure continuously evolves.

Let a single electron be trapped by a potential well with at least two non-degenerate eigenstates of the same parity. Eventually the electron structure evolves to produce the sources of Sec. 3.16, after which the state is regeneratively driven. Terms in the field equations proportional to spherical Bessel and Neumann functions have opposite parity. Since the radiation source is low- Q , resonantly generated energy would dissociate itself from the source except, as shown in Sec. 6.12 and Appendix 30, the parity of the regenerative process drives *only* the spherical Neumann functions. The regenerative buildup described in Sec. 6.12 produces the radiation field:

$$\begin{aligned} \tilde{\mathbf{E}} = \sum_{\ell=1}^{\infty} i^{-\ell} \frac{(2\ell+1)}{\ell(\ell+1)} \left\{ \ell(\ell+1) \frac{y_{\ell}(\sigma)}{\sigma} P_{\ell}^1(\cos\theta) \hat{r} \right. \\ \left. - i \left[y_{\ell}(\sigma) \frac{P_{\ell}^1(\cos\theta)}{\sin\theta} + iy_{\ell}^{\bullet}(\sigma) \frac{dP_{\ell}^1(\cos\theta)}{d\theta} \right] \hat{\theta} \right. \\ \left. - \left[y_{\ell}(\sigma) \frac{dP_{\ell}^1(\cos\theta)}{d\theta} + iy_{\ell}^{\bullet}(\sigma) \frac{P_{\ell}^1(\cos\theta)}{\sin\theta} \right] \hat{\phi} \right\} \exp(-j\phi) \end{aligned} \quad (6.13.6)$$

$$\eta \tilde{\mathbf{H}} = i \tilde{\mathbf{E}}$$

Spontaneous emission: A regeneratively driven electron is configured as an antenna for radiation described by Neumann functions, but not by Bessel

functions. There is no exterior outbound traveling wave and the field energy remains attached to the source. Source attachment is broken by the addition of Bessel function terms supplied by one of two ways: continued evolution of the electron picostructure or the Planck thermal radiation field. Depending upon the phase with which it develops the result is either re-absorption of the standing energy to the state from which it came or the spontaneous emission of eigenstate energy $\hbar\omega$. Since eigenstate configurational evolution is not instantaneous a time delay is expected between the application of an external field and before an initially nascent atom becomes an active one. The duration of the delay depends upon the initial ensemble picostructure and, hence, the evolutionary changes required before the transition process begins. In this way the occurrence of energy exchanges is statistical in nature. This meets Einstein's objection that a system should be either stable or unstable and, in one case, begins the decay process without delay and, in the other, remain stable.

Induced emission: The regenerative field buildup is triggered from the outside by an applied field. An incoming plane wave field contains all necessary triggering field phases. Whether it produces absorption or emission depends upon whether the triggered electron is in a high or low energy state. Absorption and emission regenerative processes are alike and equality fulfills the reciprocity requirement. Although electromagnetic field theory is capable of describing the full event, it is not capable of determining the immediate energy source for absorption from a weak field; that lies beyond the reach of electromagnetic field theory. Suggestions based upon the electron models are (1) that an energy absorbing, nonlocal electron could, with no time delay, capture energy from a broad region, or (2) that the energy could come temporarily from a vacuum state.

Miscellaneous: Full directivity follows from appropriately combined field modes; the relationships between the output energy and momenta may be seen from Eq. (5.10.12). Both the output energy and the far field angular momentum are described by sums over products of modes of equal order. Quite differently, the linear momentum consists of three separate sums, two of which are products of a modal order with modal orders that differ by one. That is, although modal interactions affect neither the amount of energy radiated nor its far field rotation, they do affect the direction in which the energy travels.

Plots of radiation reaction pressure and shears that affect electric charge densities on a radiating sphere of radius a are shown in Sec. 6.12. Since

the regenerative drive is nonlinear the Manley Rowe equations apply and Eqs. (5.6.14) and (5.6.17) correctly predict the observed power-frequency relationships. The nonlinearity voids any possibility of describing the process using equilibrium equations, such as the Schrödinger time-independent equation, Eq. (4.3.14), or the Dirac equations; no linear equation can describe such nonlinear events. The time-dependent Schrödinger equation, Eq. (4.5.10), describes near-equilibrium characteristics applicable over times long compared with changes in the electron ensemble. It describes events leading up to the transition and it describes events after the transition but it does not describe transitions.

With appropriate energy and stability constraints, each electron may be statistically distributed over the full array of available eigenstates. Since the proposed radiation description shows that, in the main, the regenerative buildup supports only one frequency, phase, and polarization. It is, therefore, the radiation properties of the regenerative system that results in but one transition observed per measurement; imposition of currently accepted special quantum mechanical postulates about the behavior of eigenstate electrons are not needed.

An experimental indication that all absorbed energy does not come from the same emitted energy packet comes from photons passing through optical fibers. For example, as a photon enters an optical fiber it may be separated from the outer reaches of its fields. Since the energy in a coherent beam is decreased by incomplete internal reflection in sharply bent fibers, a purely wave-like phenomenon, an exiting photon will carry less energy than it did when it entered. The probability of photon-induced transitions seems to depend only upon the intensity and frequency of the fields at the active region, not on the history of the photons of which it is composed. Neither is there an entry in the quantum theory of transition probability accounting for the history of transition-inducing photons. This combination of observations implies that, under certain circumstances, an incoming photon need only trigger radiation onset, with the remaining energy supplied by other sources. The emitted energy can, in turn, drive absorption or emission by other atoms.

6.14. Atomic Radiation

As noted in Chapter 2, although an externally applied plane wave supports the space and time symmetries required for photon radiation, the magnitudes of the high-order modes are far too small to produce the

required multipolar coefficients. The physical origin of the pressure and the shears discussed in Sec. 6.12 is the local standing energy fields. The radiation reaction pressure and shears of such fields also support the space and time symmetries required for photon radiation, and are of the needed order of magnitude.

Although the resonant array of charge and current densities driven in this way permits energy to exit (enter) the source (sink), only steady state fields operating since time $t = -\infty$ were analyzed. The wave train, therefore, was infinitely long. Since sources start and stop actual wave trains, of course, have a finite length and calculated kinematic results are meaningful only within a circumscribing sphere of radius equal to the length of the wave train. For a wave train of length $c\tau$, let W be the total radiated energy and $F_0(t)$ be the normalizing field constant. It follows from the powers listed in Table 6.11.1 that W is approximately equal to:

$$W \cong \frac{8\pi(kc\tau)^2}{3\eta k^2} \int_0^\tau [F_0(t)]^2 dt \quad (6.14.1)$$

A separate expression for the total output energy follows from Eq. (5.10.17):

$$W = \frac{4\pi}{\eta k^2} \sum_{\ell=1}^L (2\ell + 1) \int_0^\tau [F_0(t)]^2 dt \cong \frac{4\pi L^2}{\eta k^2} \int_0^\tau [F_0(t)]^2 dt \quad (6.14.2)$$

To estimate $F_0(t)$, note the exchanged energy is also equal to $\hbar\omega$. Making the equality and, to form a definite model, letting $F_0(t)$ be a constant during the time period between 0 and τ and zero at all other times:

$$F_0 = \sqrt{3\mu\hbar/(4\lambda\tau^3)} \quad (6.14.3)$$

Energy passing through the equator between the limit of the active region, a , and the extent of the radiation, $c\tau$, may be obtained by integrating the Poynting vector of Eq. (6.9.13) over that equatorial surface. Keeping only the dominant term shows the energy that moves upward through the equatorial plane is approximately equal to:

$$W_z \cong \frac{2\pi}{\eta k^2} F_0^2 \int_0^\tau (k^2 c^2 t^2 dt) = \hbar\omega/4 \quad (6.14.4)$$

Approximately one-fourth of the emitted energy exits the source in the lower hemisphere then passes upward through the equator. Linear momentum Eq. (5.10.10) confirms that as the radius increases the energy veers towards the z -direction.

If the exiting energy went directly from the source to infinity, equating Eqs. (6.14.1) and (6.14.2) would establish a link between the length of the wave train and the maximum modal number:

$$L^2 \cong \frac{2}{3}(kc\tau)^2 \quad (6.14.5)$$

For example, if L were equal to 20 or 200 the wave train would respectively be equal to about:

$$c\tau \cong 3.9\lambda \text{ or } 39\lambda \quad (6.14.6)$$

Combining Eqs. (5.7.8) and (6.14.5) gives a radiation bandwidth respectively of about $1/3.9$ or $1/39$: both numbers are much larger than observed from the bandwidth of certain optical absorption and emission lines. We suggest that although the electrical size of the radiator during energy exchange is unknown, it is surely many times larger than the nascent value, see Eq. (6.12.4). Therefore, the electrical size of the radiator, due to its ability to respond (deform) in response to applied forces, is relatively large and a much lower value of Q is expected.

References

- R. Becker, *Electromagnetic Fields and Interactions*, Trans. by F. Sauter, Dover Publications (1964).
- D.M. Grimes, C.A. Grimes, "A Classical Field Theory Explanation of Photons," in T.W. Barrett, D.M. Grimes, eds., *Advanced Electromagnetism: Foundations, Theory and Applications*, World Scientific (1995) pp. 250–277.
- R.F. Harrington, "Effect of Antenna Size on Gain, Bandwidth, and Efficiency," *J. Res. National Bureau of Standards* **64D** (1960) 1–12.
- J.D. Jackson, *Classical Electrodynamics*, 2nd edition, John Wiley (1975).
- L.D. Landau, E.M. Lifshitz, *The Classical Theory of Fields*, Addison-Wesley (1951), trans. By M. Hamermesh.
- J.M. Manley, H.E. Rowe, "Some general properties of nonlinear elements, Part I: General energy relations," *Proc. IRE* **44** (1956) 904–913, and "General energy relations," *Proc. IRE* **47** (1959) 2115–2116.
- W.K.H. Panofsky, M. Phillips, *Classical Electricity and Magnetism*, 2nd edition, Addison-Wesley (1962).
- W.R. Smythe, *Static and Dynamic Electricity*, 3rd edition, McGraw-Hill (1968).
- J.A. Stratton, *Electromagnetic Theory*, McGraw-Hill (1941).

CHAPTER 7

Epilogue

7.1. Historical Background

Particles have played a critical role in the analysis of physical events at least since Newton examined them in the latter part of the seventeenth century. For the next several centuries, studies involving combinations of elastic spheres dominated physics. Perhaps as a result, electrical problems were first interpreted by analyzing the behavior of charged particles; Maxwell used the force between “two very small bodies” to discuss implications of Coulomb’s law. Although Maxwell’s equations showed that fields are essential to explain occurrences that particles alone cannot, still the lore of particles permeated physics at the end of the nineteenth century. Therefore, after Thompson discovered and measured particle-like free electrons, the idea of electrons as particles was widely accepted, along with the Lorentz particle-electron and, later, the Bohr atomic model. The finely honed and widespread skills of classical mechanics were carried over to quantum effects; even the name “quantum mechanics” is indicative of such an origin.

Thirty years later Bell proved a theorem about two entangled electrons, and another twenty years later the idea was subject to a definitive test by Aspect *et al.* The conclusion was and is that entangled electrons are nonlocal entities over arbitrarily large distances.

Building upon his earlier work with particles, Newton compared the propagation of light with that of projectiles. According to him, luminous bodies eject light-making projectiles that continue in flight until acted upon by other objects. Quite differently, Huygens compared the propagation of light with the propagation of sound through air and waves on water. According to him, light was not a thing but a disturbance that propagated through space. Light is emitted over a spread of angles by a luminous object. It bounces off objects and the total of all bounces off all objects that is intercepted by an observer forms his field of view. After Huygens, more than a century passed before Young in England and, in an arguably unparalleled

technical outpouring, Fresnel in France confirmed that light is propagated as a wave with transverse vibrations and, therefore, two polarizations.

The modern theoretical basis for the wave theory of light began with Maxwell. Hertz, who had earlier discovered the photoelectric effect by showing that ultraviolet light increases current emission from a cathode, was the first to construct a transmitting-receiving pair of electric dipoles. With them, he confirmed that electromagnetic waves transport energy through space. His dipole radiation has rotational symmetry about its axis, a symmetry that Einstein later referred to as “spherical” symmetry.

In 1900 Planck showed that quantizing electromagnetic energy in units of $W = \hbar\omega$ accounts for otherwise significant discrepancies between observations and calculated laws that describe equilibrium conditions between radiation and matter. He wrote that a most suitable body for energy exchange seemed to be Hertz’s dipole with its “spherical” waves. A few years later, 1916, Planck showed that his 1900 expression for radiation density was consistent with thermodynamic reciprocity only if he added a zero-point energy term. That term is temperature independent and exists throughout all space.

Einstein used field energy quantization to explain the photoelectric effect. He later extended and simplified Planck’s derivation of the radiation law, and he showed that the laws of statistical mechanics require quantized radiant energy exchanges to be accompanied by quantized momentum exchanges of equal value upon emission or absorption. This, in turn, is satisfied if all of each unit of radiated energy travels in the same direction. Einstein wrote: “. . . (Atomic) emission in spherical waves does not occur, the molecule suffers a recoil of magnitude $\hbar\omega/c$. This seems to make a quantum theory of radiation almost unavoidable.”

These events seemed to rather conclusively show that electromagnetic energy is exchanged between atoms and radiation fields in quantized units, and this result, in turn, led to a fundamental difficulty. Einstein wrote that quite differently from results of the Maxwell wave equation “monochromatic radiation . . . behaves in thermodynamic theoretical relationships *as though it consists* of distinct independent energy quanta of magnitude $W = \hbar\omega$.”

Planck wrote, “There is one particular question the answer to which will, in my opinion, lead to an extensive elucidation of the entire problem. What happens to the energy of a light-quantum after its emission? Does it pass outwards in all directions, according to Huygens’ wave theory, continually increasing in volume and tending towards infinite dilution? Alternatively, does it, as in Newton’s emanation theory fly like a projectile in one direction

only? In the former case the quantum would never again be in a position to concentrate its energy at a spot strongly enough to detach an electron from its atom.”

These were the first and still are the primary reasons why it is commonly accepted that light propagates as if it consists solely of waves and exchanges energy as if it consists solely of particles.

Only a few years after Einstein's “quantized momentum” paper, electrons were shown to support an intrinsic magnetic moment. There was an immediate problem with the result: If the moment arises because the electron charge spins about an axis at a distance equal to the Lorentz electron radius, the necessary circumferential speed is many times the speed of light. Then Schrödinger published the equation that bears his name, followed a few years later by Dirac's equations. Both the Schrödinger and the Dirac equations correctly describe the behavior of electrons in equilibrium. The Schrödinger equation is correct at non-relativistic electron speeds and the Dirac equations at all speeds; electron spin is inherent to the Dirac equations but must be added in an *ad hoc* way to the Schrödinger equation. Both equations yield the probability that an electron will enter a transition. When it does, the input and output energies and the correct power-frequency relationships result. Both equations treat electrons as waves. Therefore, like light, an electron has historically been thought to have both wave and particle natures.

Schrödinger developed his equation by combining the de Broglie wavelength and an analogy with a known relationship between classical mechanics and geometric optics. According to Mehra, Dirac in the search for his equations, “started playing with equations rather than trying to introduce the right physical idea. A great deal of (the) work is just playing with the equations and seeing what they give.” Physically, it is the model used to derive an equation that determines the interpretation ascribed to it. Since both Schrödinger's and Dirac's equations came without a model neither came with an inherent or obvious physical interpretation of the results. Therefore, although both equations give correct time-average values of measurable quantities, the question of how to interpret them remains.

One difficulty with combining quantum and classical theories is that by classical theory accelerating charged particles produce far field radiation and far field radiation supports an output power. Eliminating such radiation requires the source to assume the form of closed current loops, a spherically symmetric region of charge that pulsates radially, or some combination thereof. Yet the Bohr orbit is some 20,000 larger than Lorentz's estimated

electron size, point electrons must accelerate to maintain an orbital position, and atoms are stable. Neither Schrödinger's nor Dirac's equation addresses this issue.

Schrödinger had severe reservations about the interpretation accorded his equation; he preferred to explain electron stability by ascribing physical significance to electron waves. For this reason he rejected the idea that wave functions represent a probability of occupation by a point electron and preferred a mass density created by standing electron waves. He was deeply interested in how electrons transition between eigenstates. The electromagnetic equations require a transient solution, transient solutions support a continuous spectrum of emitted radiation, and yet a continuous spectrum is not observed. His linear equations do not describe energy jumps, and yet such jumps occur. Schrödinger commented to Bohr "If we have to put up with these damned jumps I'm sorry I got involved." Bohr answered that although Schrödinger's arguments were correct, since quantum jumps occur it must be that the pictorial concepts of classical physics used to describe such events are insufficient. Schrödinger's reaction is evidenced by later comments about the "quaint basic assumption" of a discontinuity between states.

Both Dirac and Schrödinger were concerned about the frequencies of eigenstate radiation. Dirac wrote, "One would expect to be able to include the various frequencies in a scheme comprising certain fundamental frequencies and their harmonics. This is not observed to be the case. Instead, there is observed a new and unexpected connexion between the frequencies." He went on to say that this result is "quite unintelligible from the classical standpoint."

In stark contrast with quantum theory, electromagnetic field theory rests on only a few, very general axioms. Quantum theory requires that classical electromagnetic laws apply partially but not fully apply within atoms. To some, it seems incongruous that nature should require such disparate and seemingly conflicting bases for such strongly overlapping sciences. To this end, Einstein wrote that: "I am, in fact, firmly convinced that the essentially statistical character of contemporary quantum theory is solely to be ascribed to the fact that this theory operates with an incomplete description of physical systems." He also said he had devoted more time to thinking about this subject than any other. Although he believed that the mathematics of quantum theory is uniquely correct, he was bothered by the statistical nature of radiation onset from an atom that is initially in a high-energy state. He argued that either an atom is stable or it is unstable.

If it is stable it will not spontaneously decay, and if it is unstable it will begin the decay process without a time delay. Yet an atom is stable until it spontaneously undergoes a discontinuous energy drop and emits a pulse of radiation. He concluded that the wave function description of this event is incomplete. In a 1935 thought experiment that the pragmatic school was never able to fully counter, Einstein, Podolsky, and Rosen began with two paired electrons described by a single wave function, separated them an arbitrary distance, then measured one of them. A measurement permits exact knowledge of the other without measuring it, in violation of the constraints of conventional quantum theory. They concluded that either the quantum equations are incomplete as they stand or information passes between the two electrons with no time delay; that is, electrons are nonlocal entities. Einstein wrote: "Assuming the success of efforts to accomplish a complete physics description, the statistical quantum theory would, within the framework of future physics, take an approximately analogous position to statistical mechanics within the framework of classical mechanics. I am rather firmly convinced that the development of theoretical physics will be of this type; but the path will be lengthy and difficult."

Currently many theoretical physicists believe the linear differential equations of Schrödinger and Dirac are complete and describe all that can be known about quantum mechanical events. This viewpoint is not consistent with our Chapters 4 through 6, where we show the Schrödinger equation is based upon applying the conservation laws for energy and charge to an eigenstate electron in the form of a statistical ensemble of charge and current density elements. Measurement results are unpredictable only because of the lack of detailed knowledge of the ensemble.

While attention was focused on discussions of quantum theory, advances in electromagnetism of ultimate consequence to quantum theory were being made. Mie used the classical wave theory of light and spherical functions to analyze scattering of light by electrically small metallic particles. Forty years later Chu showed that emission of electromagnetic energy is necessarily accompanied by a source-associated standing energy. As the size-to-wavelength ratio decreases the standing energy of radiated mode ℓ increases as the inverse size-to-wavelength ratio raised to the $\ell(\ell + 1)$ power. Harrington showed that the maximum possible gain of a single radiated mode is $(2\ell + 1)$; the value increases without limit as the modal order increases. For atoms of diameter 0.1 nm immersed in light of 500 nm wavelength, the standing energy, by Chu's calculations, necessary to support a maximum modal number that, by Harrington's calculations, is necessary

to obtain an apparently infinite gain is so large that, when compared with current antenna technology, the idea of fully directed energy emission seems untenable.

During the next decade, Manley and Rowe derived the power-frequency relationships in nonlinear systems. Their result would satisfactorily explain atomic power-frequency relationships if the atomic response was a nonlinear function of the driving force, but the quantum theory equations are linear.

7.2. Overview

Because standing energy about an antenna was first analyzed in 1948, the interpreters of modern quantum theory could not have understood its overriding importance to radiation properties. That the pragmatic school of theoretical physicists constructed a logically coherent and complete interpretation of quantum mechanics without it is moot testimony to the ingenuity of the individuals. The conceptual framework, however, comes at a significant cost: It requires rejection of causality in the sense that the dynamical structure of the universe at a given instant does not uniquely determine the dynamical structure at the next instant. We suggest that at least some of the non-causal interpretation of quantum theory was required because standing energy and its effects are ignored in their analysis of atomic processes.

The axioms upon which electromagnetic theory is based show no dependence upon the velocity of an observer. A conclusion is that the speed of light in free space is the same in all inertial frames of reference. In free space, the same axioms show no dependence upon the size of an observer; the conclusion appears to be that the equations apply equally well to all sizes. Experimental evidence shows that the axioms upon which electromagnetic theory are based apply equally well from the nanometer scale of electronic devices at least through the scale of galaxies. Yet it is widely believed that selected parts of electromagnetic field theory partially break down on the picometer scale of atoms. We suggest that the equations apply through the picometer scale of dimensions, without restrictions. Belief to the contrary is caused, in large part, by an insufficient accounting of the affects of standing electromagnetic energy.

It has been recognized for more than eighty years that, in some circumstances, electrons act as a wave and, in other circumstances, as a particle. Although a detailed characterization of an eigenstate electron is unknown, surely understanding eigenstate electrons requires a detailed

analysis of its internal dynamics. Before addressing the problem, note that there is a tendency to think that upon going from the macroscopic to the atomic scale of dimensions things will simplify. The notion has no logical or experimental basis. There is no theoretical or experimental reason to believe an electron is a simple object but there are many reasons to believe it is not. Certainly all of chemistry is based on entangled pairs and entangled pairs were shown to demonstrate nonlocality. But does nonlocality require multiple electrons, or is it a fundamental electron characteristic the demonstration of which requires a pair? Single nonlocal electrons that occupy the full range of eigenstates satisfy our stability and source requirements.

Consider the following scenario. As a point-electron enters an eigenstate it accelerates and radiates by bremsstrahlung. While being trapped it starts to generate an electric dipole radiation field, the power and energy of which are shown in Fig. 7.2.1. The figure is an extension of Fig. 3.12.1 and shows the relative magnitudes and phases of the surface power and energy densities, values of which are time dependent and out of phase. Time variations

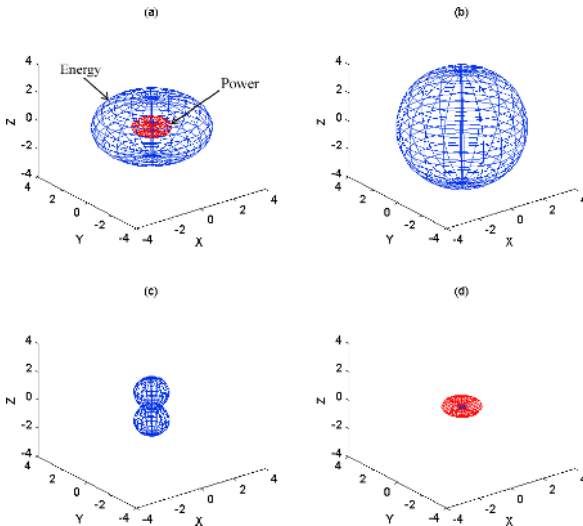


Fig. 7.2.1. Normalized power and energy density on a spherical surface circumscribing a generator of z -directed electric dipole radiation. Plots are at radius $ka = 1$. To aid direct comparison all powers were divided by c and all plots made to the same scale. Frames a,b,c,d are respectively at phases $0, \pi/2, \pi, 3\pi/2$. Only in frame (a) are both energy and power noticeable. Frames (b) and (c) contain only energy and frame (d) only power. Both energy and power densities are strongly time dependent.

are due to the large surface reactance and require a strongly time varying source. The time dependence keeps the interior charge and current density distributions in continual motion.

Pressure and shear on a dipole source are shown in Fig. 4.2.1. Over a spread of angles centered on the z -axis the dipole extensive pressure is larger than the compressive pressure of the trapping Coulomb field. That is, as an electron begins to generate dipole radiation, that radiation produces a dominating, reactive radiation reaction force that leads to our basic postulate: Source mutations of the string-cloud comprising the electron continue to occur until all radiation is squelched. That is, the radiation pressure and shear transform the trapped electron from a single entity much smaller than an atom to a stable ensemble of charge and current densities distributed throughout the eigenstate. Intrinsic and local forces assure that the structures continuously evolve. For example, interactions between the electron and orbital magnetic moments result in a continuous torque on what might otherwise be a fixed orbit. Analyses based upon classical electromagnetism show that there are possible arrays of stable, dynamic charge and current density combinations that generate no far fields. Based upon this model and using the classical thermodynamics approach of combining energy conservation with a dynamic ensemble yields the Schrödinger wave equation as a statistical descriptor of events. A requirement is for the ensemble to be in or near equilibrium. That is, the linear Schrödinger equation applies to eigenstate electrons *if and only if* the electron is in or near a state of equilibrium.

Although the laws of electrodynamics, see Eq. (1.7.2), assure that an accelerating charge radiates, they are mute about the fate of the radiation. The radiation must obey the electromagnetic laws, and hence are described by a multipolar expansion, but the critical unanswered question is whether spherical Neumann or Hankel functions describe the radial portion. Bessel functions cannot be complete since they vanish at the origin, but both Neumann and Hankel functions are singular and, therefore, form acceptable sources. With Neumann sources all radiated energy remains attached to the source, with Hankel functions all but the source-associated energy of Sec. 3.16 exits the system. This difference in stored energy causes Hankel function radiation to be in steady state equilibrium and Neumann function radiation to be in metastable steady state equilibrium. Sources subject to random fluctuation, such as thermal agitation, generate Hankel function radiation.

Multipolar radiation by a point charge is limited to low-order radiation fields. Generally speaking a dynamic, steady state, multipolar field of order

L requires 2^{L-1} separate units of charge. Therefore high order, multipolar radiation requires an extended ensemble as a source. A distributed electron, for example an electron composed of strings, is adequate for the purpose. If such an ensemble generates electric dipole radiation, that radiation produces a force that drives higher order radiation of the parity $\mathbf{E}(\theta) = \mathbf{E}(-\theta)$: electric dipole radiation leads to magnetic quadrupole radiation that leads to electric octupole radiation, *etc.* Similarly, if an ensemble structure generates magnetic dipole radiation, that radiation produces a force driving higher order radiation of parity $\mathbf{E}(\theta) = -\mathbf{E}(-\theta)$: magnetic dipole radiation leads to electric quadrupole radiation which leads to magnetic octupole radiation, *etc.* Neither set of parities, acting alone, is resonant.

Quite differently, if the structure drives both parities, properly phased and oriented, the system is resonant in the sense that there is no reactive power on the radiating surface. In that case, instead of squelching the radiation it *regeneratively increases it*. The reaction force due to this radiation becomes many orders of magnitude larger than the Coulomb binding force and dominates all other local forces. One result is a rapid energy transition between eigenstates: that is, an energy jump. Another is that the Manley Rowe power-frequency relationships apply during the steady state portion of the nonlinear process and correctly predict the observed Ritz power-frequency relationships.

The basis set of elements used to produce photon radiation consists of four radiating elements that produce equal output powers. The four elements consist of two sets of elements, one each TM source and TE source. Each ℓ -order element set has one displacement in the z -direction and $\ell - 1$ displacements in the orthogonal direction. The sets are spatially orthogonal and phased in time-quadrature. With such an embodiment capacitive and inductive effects cancel and a circumscribing surface is resonant in the sense that the reactive powers sum to zero at all surface points at all times. For the dipole case surface power and energy densities are shown in Fig. 7.2.2. Dramatically differently from the single dipole case of Fig. 7.2.1 values are time independent. Stability results in a stable source that produces an inter-modal regenerative driving force on all higher order modes. Gain of the radiation pattern increases with modal number as $(2\ell + 1)$.

With this model full photon directivity is achieved with spherical radiation field modes that originate within the electron ensemble. Since the regenerative extensive pressure is many times larger than the Coulomb pressure it is expected to dominate actions. The nonlinearity voids any possibility of describing the process using equilibrium equations, that is,

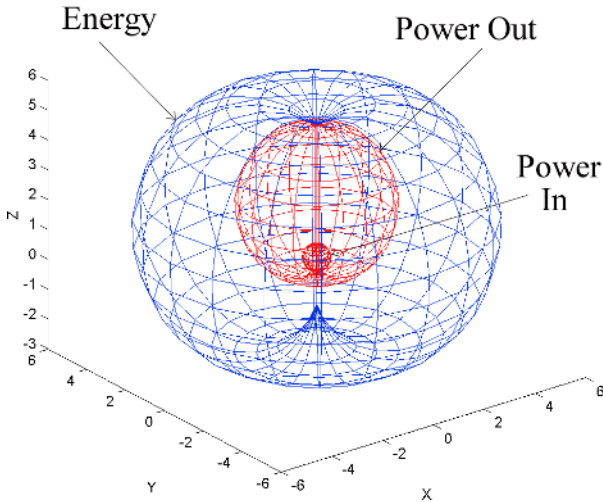


Fig. 7.2.2. Normalized power and energy densities on the spherical surface $ka = 1$ circumscribing the generating source of Sec. 3.16. The energy and power densities have circular symmetry about the z -axis and, although full time dependence is included in the plot, do not vary with time! The net power is outbound; power density is outbound in the upper and part of the lower hemispheres, but inbound, as indicated, near the negative z -axis. To aid magnitude comparisons the power density is divided by c .

Schrödinger's or Dirac's equations; as emphasized by Schrödinger a linear equation cannot describe such nonlinear events. Schrödinger's time-dependent equation describes near-equilibrium characteristics that lead to the transition and events after the transition, but it does not describe events during the transition. In other words transitions occur during a hiatus between equilibrium periods.

Let an atom in thermal equilibrium at temperature T contain a single electron and three non-degenerate energy levels, states Z_n , Z_r , and Z_s . The eigenstate energy levels are, respectively, W_n , W_r , and W_s where $W_n > W_r > W_s$ and $W_r - W_s > W_n - W_r$. An electron, within its stability constraints, is thermally distributed among available eigenstates. When the system is disturbed possible outcomes are photon exchanges at frequency $\omega_{rs} = W_r - W_s$ or $\omega_{nr} = W_n - W_r$. The radiation reaction forces support whichever frequency and phase starts and quenches all others, including possible transient frequencies. Regenerative drives can occur at a single frequency and phase and do not support simultaneous radiation at other frequencies.

We suggest the following sequence of events during electromagnetic energy exchanges: A single electron exists in the presence of two available eigenstates with matching symmetry, and is in dynamic equilibrium between the two states. As part of its continuing evolution through all possible stable distributions, eventually the dipolar structure occurs that is necessary to begin the regenerative buildup of the field structure described in Sec. 3.16, see Table 3.16.1, and Sec. 6.9. The modes consist entirely of terms for which the radial part is a spherical Neumann function. This construction is independent of whether the electron is initially in the upper or lower eigenstate. There is therefore no exterior, outbound traveling wave and the field energy remains attached to its source until one of two things happens. First, continued eigenstate evolution supplies the electron picostructure that produces the Bessel function portion of the field. Depending upon the phase of that field the result is either re-absorption of the Neumann energy field or its spontaneous emission. Second, an external, incoming field supplies the required Bessel field terms. Depending upon the relative phases the field interactions produce either absorption or emission. Since the phases of the standing and incoming fields are independently determined, there is equal probability of the two events.

7.3. The Radiation Scenario

Classical statistical mechanics analyzes an ensemble of identical particles. The particles are modeled as realistically as possible and there is little or no difficulty interpreting ensemble-averaged results. The positions and velocities of the component parts specify the state of the ensemble and are sufficient to determine the system energy. With statistical mechanics, studies of complicated systems are accomplished with no knowledge of the precise state of individual particles. The actual state is assumed the most probable state, and if there is full knowledge of an ensemble at a particular instant its value at the next instant is predictable.

A question fundamental to quantum theory is why an individual eigenstate electron acts as a statistical ensemble. The radiation reaction forces, see Eq. (4.2.13), provides at least a partial answer; it is an extensive force of magnitude greater than the attractive Coulomb force. With an eigenstate ensemble as the physical entity to be described, the Fourier integral transforms of Eq. (4.3.7) provide a general mathematical description of the unknown physical realities. To match known results, it is necessary for the eigenstate electrons to contain a definite, though unknown,

distribution of charge and current densities; the smallest unit is determined by the discreteness of the charge distribution and occupies a volume much smaller than physical extent of the state. The uncertainty of calculated results, Eq. (4.4.7), arises because of the absence of information about detailed charge and current distributions, not because of inherent properties of the distributions. Causality applies in the sense that the detailed structures and kinematics of all charge and current densities at one instant uniquely determine the values at the next instant. Although this difference does not affect expectation values, it has a profound effect upon the interpretational philosophy and the characterization of measurable quantities. Causality also retains Einstein's deterministic view of atoms.

A set of resonant, regeneratively driven electromagnetic field modes is shown in Sec. 3.16; this modal set and certain of its properties are listed in Table 3.16.1. Section 5.10 shows that using this modal set as the basis set and imposing the kinematic properties of photons as a boundary condition yields a unique field set. The fields are resonant and they are not subject to Chu's proof of limitations on electrically small radiators. Therefore large magnitudes of large order radiation modes are expected.

The solution includes a complete expression for all fields, near and far, during the transition process. In this sense, the analysis is as complete as the fields of biconical antennas, see Chapter 2. The electromagnetic background necessary to understand this aspect of the physics was simply not available when the phenomena was originally studied. No linear source can both generate this electromagnetic radiation field and satisfy thermodynamic reversibility. The linear equations of quantum theory describe only the equilibrated states before and after transitions, Secs. 4.3 and 4.5, and the dipole moment of interaction between states that, in turn, determines the probability of a transition. There is no way Einstein could have been aware of these results or of the properties of Eq. (5.10.16) when he wrote that full directivity makes "a quantum theory of radiation almost unavoidable."

Equilibrium periods during which the linear quantum theory equations apply are separated by time hiatuses during which energy exchanges occur. As shown in Chapter 5, the initial radiation produces a radiation reaction force on the source that drives it regeneratively and produces more radiation. The process continues until all available energy is gone and the electron has entered a new energy state. Because the process is nonlinear the Manley Rowe equations apply to the radiation. As with statistical mechanics, the ensemble is expected to cycle through all possible states.

There is no way Dirac could know of time hiatuses during which linear equations do not apply when he wrote: “there is observed a new and unexpected connexion between the frequencies.” There is no way Schrödinger could have known of the Manley Rowe equations when he tried to understand the same unexpected connection between frequencies. Since Schrödinger could not have known his equations were applicable only during quasiequilibrium conditions, he was unaware of time hiatuses when his equation does not apply. This was the reason for his problem with quantum jumps. Bohr explained that new physical phenomena were required to explain them; we concur and believe those phenomena to be the combination of extended eigenstate electrons and the electromagnetic radiation processes described herein.

An ensemble of charge and current densities has many degrees of freedom. Interactions between separate charge and current densities produce a continuous torque on the ensemble, and thereby a dynamic configuration. The turbulence of its constituent parts is subject only to the constraints imposed by the symmetry, energy, momentum, and angular momentum of the state. As in statistical mechanics we presume an evolving system sequentially occupies all possible configurations within the limitations of the conservation laws, eventually and in turn occupying each of them. When a radiating configuration occurs with charge and current density arrays that support the Neumann portion of four dipoles, two electric and two magnetic ones, with equal output power, the proper phase differences and alignment, see Table 3.16.1, there is an exodus of the energy from the eigenstate. That energy forms a standing energy field centered on the emitter. The standing energy remains in existence until a companion Bessel function field is somehow superimposed. If the Bessel field comes from the continued evolution of the eigenstate, depending upon its phase the energy is either re-absorbed, with no exchange of either energy or momentum, or there is spontaneous emission. If the Bessel field is applied from outside the system depending upon its phase either induced absorption or emission results.

Generally speaking, the radiation, including transients, emitted by an electron transitioning between different pairs of states is expected to produce a spread of frequencies. However, since regenerative forces are monochromatic even though a transient followed by steady state fields might characterize radiation onset, all except the single frequency are squelched.

An electron simultaneously and statistically occupies the full array of states available to it until a measurement is made. Since only one frequency

achieves regeneration, it is radiation limitations that force the wave function to collapse to a single transition between a single pair of states. This “measurement problem”, the collapse of the wave function, is therefore a property of the regenerative radiation field not of the electron itself.

Were the length of the emitted wave train and the upper modal limit of the source fields both infinite, the field would be fully directed and it would retain its original shape and size over arbitrarily large values of time and distance. However, since both are finite the size of the calculated steady state wave packet presumably increases with increasing distance from the source. Although flux closures must occur, it is unknown if closures produce a fully directed wave packet; that is, it is unknown if the energy packet arriving from a distant star has the same physical extent it had when emitted or is extended over a larger volume. We know only that the total energy in the coherent wave packet remains constant as it travels through lossless space.

The descriptive transcendental terms in the field equations of Secs. 6.2 through 6.5 come, bit-by-bit, from each mode and are approached only if the maximum modal number L is large. An important question is why the recursion formula of Eq. (5.9.8), the recursion relationship of spherical Bessel function terms in a plane wave, is uniquely correct for quantized radiation. The reasons appear to be that only this particular recursion formula produces a set of z -axis transcendental fields that support energy flow to or from the source, and only it produces a null in the source-associated standing energy. As may be seen from Secs. 6.1 through 6.5, a greater or lesser dependence of modal coefficients upon modal number would result in fields that depended upon all modes, not just the highest numbered ones. For such a case, reactive energy that does not contribute to the regenerative drive would be present and the radiation reaction force of Eq. (4.2.8) would apply, braking power emission. The recursion relationship of Eq. (5.9.8) uniquely accomplishes two things: it avoids the radiation reaction of Eq. (4.2.8) and it meets the requirements of Sec. 3.16. Only with Eq. (5.9.8) do the radiation reaction forces on an electron reduce to that caused by energy escaping from the system, Eq. (4.2.7).

Spherical Bessel functions give rise only to half the teledistant terms of Eqs. (6.11.3) through (6.11.5), the other half and all other terms come from spherical Neumann functions. Yet, all Poynting vector terms that describe unidirectional energy flow are products of a spherical Bessel term and a spherical Neumann function term. A possible radiation scenario is that the picostructure of an eigenstate evolves to produce the Neumann function

terms of Tables A.30.2 through A.30.4; the parity is wrong for a regenerative drive to also produce the spherical Bessel function term. With this field the source is immersed in its own standing energy field without an energy loss from the atom. An incoming wave, be it part of the equilibrium thermal radiation field or an externally applied one, is described using only spherical Bessel function terms. When the two fields are superimposed and are of the appropriate frequency, phase, and orientation, all field forms are present that are needed for radiation to occur and the external field needs supply only a minor part of the energy output. Absorption occurs when an emitted photon encounters a like atom in the lower energy eigenstate; the photon has the necessary array of phases and magnitudes to drive absorption. Planck could not have been aware of this when he wrote of extended photons “a quantum would never again be in a position to concentrate its energy at a spot strongly enough to detach an electron from its atom.”

As described herein, the primary historical obstacle to understanding atomic-level phenomena was that the persons involved lacked the tools necessary to account for the radiation reaction force of the generated fields, and they modeled an electron as a point charge. Reasoning on this basis they were forced to conclude that electromagnetic field theory is not totally applicable within atoms. We show that consistent application of electromagnetic field theory within atoms, without restrictions, leads to self-consistent results and to quantum theory itself.

A question fundamental to all of quantum theory is why an individual eigenstate electron acts as a statistical ensemble. We note with interest that one of several possible satisfactory models is an electron composed of string-sized objects which, when free, form into a droplet sized on the order of the Lorentz electron but, when under the influence of radiation reaction forces, expand to fill the full eigenstate. A primary supporting argument for this model is the development of Schrödinger’s equation, a necessary but insufficient result. The principal argument is the hitherto unavailable full field solution of the full photon problem.

The authors suggest that within this book the parsimonious use of separate postulates and the totality of the results, taken together, are strong circumstantial evidence for extended, nonlocal electrons and the full applicability of electromagnetic theory within atoms.

References

- N. Bohr, “On the Constitution of Atoms and Molecules,” *Phil. Mag.* **26** (1913) 1–19, Also in *The World of the Atom*, eds. H.A. Boorse and L. Motz, Basic Books (1966) pp. 751–765.

- M. Born, "Max Karl Ludwig Planck" *Obituary Notice of Fellows of the Royal Society*, **6** (1948) pp. 161–180 also in *The World of the Atom*, eds. H.A. Boorse and L. Motz, Basic Books (1966) p. 475.
- M. Born, E. Wolf, *Principles of Optics Electromagnetic Theory of Propagation, Interference and Diffraction of Light*, 3rd edition, Pergamon Press (1965).
- L.J. Chu, "Physical Limitations of Omni-Directional Antennas," *J. Appl. Phys.* **19** (1948) 1163–1175.
- P.A.M. Dirac, *The Principles of Quantum Mechanics*, 4th edition, Oxford Press (1958) pp. 1–2.
- A. Einstein, "Concerning a Heuristic Point of View About the Creation and Transformation of Light," *Ann. Phys.* **17** (1905) 132–148; also in *The World of the Atom*, eds. H.A. Boorse and L. Motz, Basic Books (1966) pp. 544–557.
- A. Einstein, "The Quantum Theory of Radiation," *Phys. Z.* **18** (1917) 121–128; also in *The World of the Atom*, eds. H.A. Boorse and L. Motz, Basic Books (1966) pp. 888–901.
- A. Einstein, "Reply to Criticisms" in *Albert Einstein, Philosopher and Scientist*, (ed., P.A. Schilpp) Harper Torchbooks Science Library (1959) pp. 665–688.
- A. Einstein, B. Podolsky, N. Rosen, "Can Quantum-Mechanical Description of Physical Reality be Considered Complete?" *Phys. Rev.* **47** (1935) 777–780.
- R.F. Harrington, "Effect of Antenna Size on Gain, Bandwidth, and Efficiency," *J. Res. Nat. Bureau of Standards* **64D** (1960) 1–12.
- H. Hertz, *Electric Waves: Researches on the Propagation of Electric Action with Finite Velocity Through Space* (1893) translated by D.E. Jones, Dover Publications (1962).
- C. Huygens, "Treatise on Light," (1678) trans. by S.P. Thompson, Dover Publication (1912); also *The World of the Atom*, eds. H.A. Boorse and L. Motz, Basic Books (1966) pp. 69–85.
- H.A. Lorentz, *The Theory of Electrons*, (1909) also Dover Publications 2nd edition (1952); also Pais, A., "The Early History of the theory of the Electron: 1897–1947," in *Aspects of Quantum Theory*, eds. A. Salam and P. Wigner, Cambridge Press (1972) pp. 79–93.
- J.M. Manley, H.E. Rowe, "Some general properties of nonlinear elements, Part I: General energy relations," *Proc. IRE* **44** (1956) 904–913, and "General energy relations," *Proc. IRE* **47** (1959) 2115–2116.
- J.C. Maxwell, *A Treatise on Electricity and Magnetism*, 3rd edition (1891) reprint Dover Publications (1954).
- J. Mehra, "'The Golden Age of Theoretical Physics': P.A.M. Dirac's Scientific Work from 1924–1933," in *Aspects of Quantum Theory*, Cambridge Press (1972) p. 45.
- G. Mie, "A Contribution to Optical Extinction by Metallic Colloidal Suspensions," *Ann. Physik.* **25** (1908) p. 377.
- W.J. Moore, *Schrödinger, Life and Thought*, Cambridge Press, (1989), pp. 227–228.
- I. Newton, *Mathematical Principles of Natural Philosophy*, (1687); translated by I.B. Cohen, A. Whitman, Univ. of California Press (1999).
- I. Newton, *Optiks*, (1704); Dover Publications (1952).

- R. Penrose, *The Emperor's New Mind Concerning Computers, Minds, and the Laws of Physics*, Penguin Books (1991).
- M. Planck, "The Origin and Development of the Quantum Theory," Nobel Prize in Physics Address, 1919, in *The World of the Atom*, eds. H.A. Boorse and L. Motz, Basic Books (1966) pp. 491–501.
- E. Schrödinger, *Ann. Phys.* **79** (1926) p. 489; also "Wave Mechanics," in *The World of the Atom*, eds. H.A. Boorse and L. Motz, Basic Books (1966) pp. 1060–1076.
- E. Schrödinger, "Are There Quantum Jumps?" *Brit. J. Phil. Sci.* **3** (1952) 109–123 and 233–247.
- J.J. Thompson, "Cathode Rays," *Phil. Mag.* **44** (1897) 293–311, also *The World of the Atom*, eds. H.A. Boorse and L. Motz, Basic Books (1966) pp. 416–426.

Appendices

1. Introduction to Tensors

The application of field concepts to classical physics is made easier by the use of tensors. Tensor notation simplifies what would otherwise be tedious notational bookkeeping. The simplest and lowest rank tensor is a scalar, the next higher ranking tensor is a vector, and higher order tensors are referred to simply as tensors:

Table A.1.1. Properties of Tensors.

| Rank | |
|---------|--------|
| $r = 0$ | Scalar |
| $r = 1$ | Vector |
| $r = 2$ | Tensor |

The number of numbers that it takes to construct a tensor, N_0 , depends upon the rank of the tensor and the number of dimensions. If N and r are, respectively, the number of dimensions and the rank, the number of numbers is:

$$N_0 = N^r \tag{A.1.1}$$

Independently of the number of dimensions, a scalar is fully described by a single number. Examples are the speed of light, c , and electron charge, q . Scalars have the same value in all inertial frames.

It takes as many numbers as there are dimensions to describe a vector. Examples of vectors are electric field intensity, velocity, and position. Let vector, \mathbf{A} , be known in three dimensions. The three numbers represent components along each of the three orthogonal coordinate axes, (x_1, x_2, x_3) . If the same vector is determined using a set of axes rotated to new coordinate positions (x'_1, x'_2, x'_3) the result is the new vector

components:

$$\begin{aligned} A'_1 &= A_1 \cos(x'_1, x_1) + A_2 \cos(x'_2, x_1) + A_3 \cos(x'_3, x_1) \\ A'_2 &= A_1 \cos(x'_1, x_2) + A_2 \cos(x'_2, x_2) + A_3 \cos(x'_3, x_2) \\ A'_3 &= A_1 \cos(x'_1, x_3) + A_2 \cos(x'_2, x_3) + A_3 \cos(x'_3, x_3) \end{aligned} \quad (\text{A.1.2})$$

The directional cosine of the angle between axis “i” in the prime coordinates and axis “j” in the unprimed coordinates is signified by $\cos(x'_i, x_j)$. With the definition that the direction cosine $c_{ik} = \cos(x'_i, x_k)$, Eq. (A.1.2) may take the more compact form:

$$A'_j = \sum_{k=1}^3 c_{ik} A_k \quad (\text{A.1.3})$$

It follows that:

$$A_r = \sum_{k=1}^3 c_{kr} A'_k \quad (\text{A.1.4})$$

An example of a second rank tensor is the stress tensor in crystals. Such a tensor transforms between coordinate systems as:

$$T'_{rs} = \sum_{i=1}^3 \sum_{j=1}^3 c_{ri} c_{sj} T_{ij} \quad (\text{A.1.5})$$

The number of direction cosines for a transformation between coordinates systems is the same as the rank of the tensor.

Like all other vectors, a position vector transforms between coordinate frames as:

$$\begin{aligned} x'_1 &= c_{11}x_1 + c_{12}x_2 + c_{13}x_3 \\ x'_2 &= c_{21}x_1 + c_{22}x_2 + c_{23}x_3 \\ x'_3 &= c_{31}x_1 + c_{32}x_2 + c_{33}x_3 \end{aligned} \quad (\text{A.1.6})$$

By definition the rotation matrix is:

$$(c_{ij}) = \begin{pmatrix} c_{11} & c_{12} & c_{13} \\ c_{21} & c_{22} & c_{23} \\ c_{31} & c_{32} & c_{33} \end{pmatrix} \quad (\text{A.1.7})$$

The length of a differential vector in three dimensions is:

$$(\Delta \mathbf{r})^2 \equiv (\Delta x'_1)^2 + (\Delta x'_2)^2 + (\Delta x'_3)^2 \equiv (\Delta x_1)^2 + (\Delta x_2)^2 + (\Delta x_3)^2 \quad (\text{A.1.8})$$

The transformation equalities derived from Eq. (A.1.8) are:

$$c_{11}^2 + c_{21}^2 + c_{31}^2 = 1 = c_{12}^2 + c_{22}^2 + c_{32}^2 = c_{13}^2 + c_{23}^2 + c_{33}^2 \quad (\text{A.1.9})$$

This may be written as

$$\sum_{i=1}^3 c_{ij}c_{ij} = 1 \quad \text{and} \quad \sum_{i=1}^3 c_{ij}c_{ik} = 0; \quad j \neq k$$

The Kronecker delta function is defined by the relationship:

$$\delta_{jk} = 1 \quad \text{if } j = k; \quad \delta_{jk} = 0 \quad \text{if } j \neq k \quad (\text{A.1.10})$$

Using this definition, the condition on directional cosines may be written more compactly as:

$$\sum_{i=1}^3 c_{ij}c_{ik} = \delta_{jk} \quad (\text{A.1.11})$$

A useful exercise is to show the determinant is normalized:

$$\det|c_{ij}| = 1 \quad (\text{A.1.12})$$

Solution: Let the volume of cube $x_1x_2x_3$ equal one. The volume in the transformed coordinates is unchanged by describing it in another frame, so it too is equal to one. The volume is given by:

$$V = \mathbf{x}'_1 \cdot (\mathbf{x}'_2 \times \mathbf{x}'_3) = 1$$

Writing out cross products in terms of directional cosines gives:

$$\mathbf{x}'_2 \times \mathbf{x}'_3 = \mathbf{x}_1(c_{22}c_{33} - c_{23}c_{32}) + \mathbf{x}_2(c_{33}c_{11} - c_{31}c_{13}) + \mathbf{x}_3(c_{11}c_{22} - c_{12}c_{21})$$

From which it follows that:

$$\begin{aligned} \mathbf{x}'_1 \cdot (\mathbf{x}'_2 \times \mathbf{x}'_3) &= [c_{11}(c_{22}c_{33} - c_{23}c_{32}) + c_{12}(c_{23}c_{31} - c_{21}c_{33}) \\ &\quad + c_{13}(c_{21}c_{32} - c_{22}c_{31})] \end{aligned}$$

The determinant of c_{ij} is:

$$|c_{ij}| = c_{11}(c_{22}c_{33} - c_{23}c_{32}) + c_{12}(c_{23}c_{31} - c_{21}c_{33}) + c_{13}(c_{21}c_{32} - c_{22}c_{31})$$

Comparing the above equations gives:

$$|c_{ij}| = 1$$

2. Tensor Operations

A common summation convention that reduces the number of symbols that would otherwise be required is that if an index occurs twice a summation over all possible values is required. That is:

$$c_{ij}c_{ik} = \delta_{jk} \quad (\text{A.2.1})$$

Consider some arithmetic operations on tensor fields. Tensor addition is defined only for tensors of equal rank; for example, addition of a scalar and a vector is not defined. Addition of tensors of equal rank is by:

$$C_{ij} = A_{ij} + B_{ij} \quad (\text{A.2.2})$$

Proof consists of showing that the sum obeys the coordinate rotation properties of a second rank tensor. In Eq. (A.2.2) indices “i” and “j” appear only once in each term and, therefore, are running indices. Equation (A.2.2) consists of nine separate summations.

Subtraction is accomplished by multiplying B_{ij} by minus one and adding; multiplication is defined between tensors of arbitrary rank. By definition,

$$C_{i..jr..s} = A_{i..j}B_{r..s} \quad (\text{A.2.3})$$

The rank of C is the sum of the ranks of A and B. For example the product of vector A_i and scalar a is aA_i , another vector. The product between two vectors is a second rank tensor, for example the product of A_i and B_j is $C_{ij} = A_iB_j$, where indices “i” and “j” are both running indices; C_{ij} represents nine numbers.

Division by tensors other than rank zero is not defined.

In addition to these scalar-like arithmetic operations there are operations confined to tensors. Tensor contraction is accomplished by equating two indices. Equal indices signify a summation and summation results in a tensor reduced in rank by two from the initial one. The process is, therefore, restricted to tensors of rank $r \geq 2$. As an example:

$$A'_{rstu} = c_{ri}c_{sj}c_{tk}c_{ul}A_{ijkl} \quad (\text{A.2.4})$$

After equating “s” and “t” and summing:

$$A'_{rssu} = c_{ri}c_{sj}c_{sk}c_{ul}A_{ijkl} \quad (\text{A.2.5})$$

Since:

$$c_{sj}c_{sk} = \delta_{jk} \quad \text{and} \quad A'_{rssu} = c_{ri}c_{ul}A_{ijj\ell} \quad (\text{A.2.6})$$

This is a tensor of rank two less than the starting one.

A common example is the scalar product between two vectors, A_i and B_i . To evaluate, begin with the product:

$$C_{ij} = A_i B_j \tag{A.2.7}$$

Equating indices “i” and “j” and summing over the indices gives:

$$C_{ii} = A_i B_i = D \tag{A.2.8}$$

The product forms scalar D .

3. Tensor Symmetry

Physically real tensors are either symmetric or antisymmetric. Terms of different symmetry are defined as:

$$\begin{aligned} \text{Symmetric tensor} \quad A_{rstu} &= A_{rtsu} \\ \text{Antisymmetric tensor} \quad A_{rstu} &= -A_{rtsu} \end{aligned} \tag{A.3.1}$$

Symmetric and antisymmetric tensors have, respectively, $N(N + 1)/2$ and $N(N - 1)/2$ terms.

An important special case is a three dimensional tensor of rank two, say T_{ij} . Such tensors transform as:

$$T'_{ij} = c_{ir} c_{js} T_{rs} \tag{A.3.2}$$

Equation (A.3.2) is short hand notation for the nine terms of T'_{ij} , each of which contains nine separate numbers. For example:

$$\begin{aligned} T'_{12} = c_{1r} c_{2s} T_{rs} &= [c_{11} c_{21} T_{11} + c_{11} c_{22} T_{12} + c_{11} c_{23} T_{13} \\ &+ c_{12} c_{21} T_{21} + c_{12} c_{22} T_{22} + c_{12} c_{23} T_{23} \\ &+ c_{13} c_{21} T_{31} + c_{13} c_{22} T_{32} + c_{13} c_{23} T_{33}] \end{aligned} \tag{A.3.3}$$

If T_{ij} is antisymmetric, $T_{ij} = -T_{ji}$ and the transformation simplifies to:

$$\begin{aligned} T'_{23} &= c_{11} T_{23} + c_{12} T_{31} + c_{13} T_{12} \\ T'_{31} &= c_{21} T_{23} + c_{22} T_{31} + c_{23} T_{12} \\ T'_{12} &= c_{31} T_{23} + c_{32} T_{31} + c_{33} T_{12} \end{aligned} \tag{A.3.4}$$

The proof of Eq. (A.3.4) follows by writing out the terms in the form:

$$\begin{aligned} T'_{12} &= [0 + c_{11} c_{22} T_{12} - c_{11} c_{23} T_{31} - c_{12} c_{21} T_{12} + 0 + c_{12} c_{23} T_{23} \\ &+ c_{13} c_{21} T_{31} - c_{13} c_{22} T_{23} + 0] \\ &= (c_{11} c_{22} - c_{12} c_{21}) T_{12} + (c_{12} c_{23} - c_{13} c_{22}) T_{23} + (c_{13} c_{21} - c_{11} c_{23}) T_{31} \end{aligned}$$

Similarly:

$$T'_{23} = (c_{21}c_{32} - c_{22}c_{31})T_{12} + (c_{22}c_{33} - c_{23}c_{32})T_{23} + (c_{23}c_{31} - c_{21}c_{33})T_{31}$$

From the determinant:

$$c_{11}(c_{22}c_{33} - c_{23}c_{32}) + c_{12}(c_{23}c_{31} - c_{21}c_{33}) + c_{13}(c_{21}c_{32} - c_{22}c_{31}) = 1$$

Combining this result with $c_{ij}c_{ik} = \delta_{jk}$ results in:

$$c_{11}c_{11} + c_{12}c_{12} + c_{13}c_{13} = 1$$

The latter two equations combine to show that:

$$c_{11} = (c_{22}c_{33} - c_{23}c_{32}); \quad c_{12} = (c_{23}c_{31} - c_{21}c_{33}); \quad c_{13} = (c_{21}c_{32} - c_{22}c_{31})$$

Substitution of this result back into the expansion results in Eq. (A.3.4.)

This result shows that an antisymmetric second rank tensor, T_{ij} , transforms like a vector. It is tempting to call it a vector, but if the coordinate system is switched from a right hand system to a left-hand system the components change sign. It is therefore a pseudovector.

4. Differential Operations on Tensor Fields

The gradient operation increases the rank of a tensor by one. As an example, let $\sigma(\mathbf{r})$ represent a scalar field. Taking the partial derivative:

$$\frac{\partial \sigma(\mathbf{r})}{\partial x_i} = V_i \tag{A.4.1}$$

Make the equality:

$$\frac{\partial \sigma(\mathbf{r})}{\partial x_i} = \frac{\partial x'_j}{\partial x_i} \frac{\partial \sigma(\mathbf{r})}{\partial x'_j} = c'_{ij} V_j$$

Combining gives:

$$V_i = c'_{ij} V'_j \tag{A.4.2}$$

Since V_i transforms as a vector, it is a vector, and the divergence operation decreases the rank of a tensor by one. The gradient and divergence

operations may be conducted on tensors of any rank. For example:

$$T_{ij..kl} = \frac{\partial R_{ij..k}}{\partial x_\ell} \tag{A.4.3}$$

$$\sigma(\mathbf{r}) = \frac{\partial V_i}{\partial x_\ell} \tag{A.4.4}$$

To show that $\sigma(\mathbf{r})$ is a scalar, write it as:

$$\sigma(\mathbf{r}) = \frac{\partial x'_k}{\partial x_i} \frac{\partial(c'_{ij} V'_j)}{\partial x'_k} = c'_{ij} c'_{ik} \frac{\partial V'_j}{\partial x'_k} = \frac{\partial V'_j}{\partial x'_j} = \sigma'(\mathbf{r}) \tag{A.4.5}$$

The divergence operation may be conducted on tensors of any rank:

$$T_{i..j} = \frac{\partial R_{i..jk}}{\partial x_k} \tag{A.4.6}$$

Proof follows in the same way as for Eq. (A.4.4.)

The curl operation begins with the vector differential operation:

$$T_{i..j..kn} = \frac{\partial R_{i..j..k}}{\partial x_n} - \frac{\partial R_{i..n..k}}{\partial x_j} \tag{A.4.7}$$

This increases the rank by one. A particularly useful special case is for vectors. Let:

$$T_{in} = \frac{\partial R_i}{\partial x_n} - \frac{\partial R_n}{\partial x_i} \tag{A.4.8}$$

Note that since T_{ij} is antisymmetric it has $N(N - 1)/2$ independent numbers. In three dimensions, it has three, the same as a vector and we already saw that antisymmetric second rank tensors transform like vectors.

Table A.4.1. Table of vector properties.

| | |
|---|---|
| 1 | $\mathbf{A} \times (\mathbf{B} \times \mathbf{C}) = \mathbf{B}(\mathbf{A} \cdot \mathbf{C}) - \mathbf{C}(\mathbf{A} \cdot \mathbf{B})$ |
| 2 | $\text{grad}(\phi\psi) = \nabla(\phi\psi) = \phi\nabla\psi + \psi\nabla\phi$ |
| 3 | $\text{div}(\phi\mathbf{A}) = \nabla \cdot (\phi\mathbf{A}) = \phi\nabla \cdot \mathbf{A} + \nabla\phi \cdot \mathbf{A}$ |
| 4 | $\text{curl}(\phi\mathbf{A}) = \nabla \times (\phi\mathbf{A}) = \phi\nabla \times \mathbf{A} + \nabla\phi \times \mathbf{A}$ |
| 5 | $\nabla \cdot (\mathbf{A} \times \mathbf{B}) = \mathbf{B} \cdot (\nabla \times \mathbf{A}) - \mathbf{A} \cdot (\nabla \times \mathbf{B})$ |
| 6 | $\nabla \times (\mathbf{A} \times \mathbf{B}) = \mathbf{A}(\nabla \cdot \mathbf{B}) - \mathbf{B}(\nabla \cdot \mathbf{A}) + (\mathbf{B} \cdot \nabla)\mathbf{A} - (\mathbf{A} \cdot \nabla)\mathbf{B}$ |
| 7 | $\nabla(\mathbf{A} \cdot \mathbf{B}) = \mathbf{A} \times (\nabla \times \mathbf{B}) + \mathbf{B} \times (\nabla \times \mathbf{A}) + (\mathbf{B} \cdot \nabla)\mathbf{A} + (\mathbf{A} \cdot \nabla)\mathbf{B}$ |
| 8 | $\nabla^2(1/r) = 0, \text{ if } r > 0$ |
| 9 | $\nabla^2\mathbf{A} = \nabla(\nabla \cdot \mathbf{A}) - \nabla \times (\nabla \times \mathbf{A})$ |

Table A.4.2. Integrals over closed surfaces.

$$10 \oint \mathbf{A} \cdot d\mathbf{S} = \int (\nabla \cdot \mathbf{A}) dV$$

$$11 \oint \phi d\mathbf{S} = \int (\nabla \phi) dV$$

$$12 \oint \mathbf{A} \times d\mathbf{S} = - \int (\nabla \times \mathbf{A}) dV$$

Table A.4.3. Integrals over open surfaces.

$$13 \oint \phi d\ell = \int d\mathbf{S} \times \nabla \phi$$

$$14 \oint \mathbf{A} \cdot d\ell = \int (\nabla \times \mathbf{A}) \cdot d\mathbf{S}$$

Therefore, the curl of a vector changes the vector to an antisymmetric second rank tensor that is pseudovector. The pseudovector acts like a vector in any given coordinate system but changes sign if the systems are changed from a left to right hand system.

5. Green's Function

The 4-Laplacian of the electromagnetic potential is defined by Eq. (1.5.4), and repeated here:

$$\frac{\partial^2 A_\nu}{\partial X_\beta \partial X_\beta} = -\mu J_\nu \quad (\text{A.5.1})$$

We seek to integrate that differential equation in order to obtain a general expression for the electromagnetic potential itself. For this purpose, it is helpful to define a similar but simpler function, to integrate that function, then to use the integral to obtain an expression for the electromagnetic potential. The function is Green's function $G(X_\alpha, X'_\alpha)$. By definition it is:

$$\frac{\partial^2 G(X_\alpha, X'_\alpha)}{\partial X_\beta \partial X_\beta} = -[\delta(X_\alpha - X'_\alpha)]^4 \quad (\text{A.5.2})$$

In Eq. (A.5.2), the four-dimensional delta function indicates the Dirac delta. By definition the one dimensional Dirac delta function satisfies the integral

relationship:

$$\int f(x)d(x - x')dx = \begin{cases} f(x') \\ 0 \end{cases} \tag{A.5.3}$$

The upper or lower solution applies if the range of integration respectively does or does not include x' . The integrand magnitude of a Dirac delta function increases without limit and the width Δx decreases without limit in a way that retains a product value of one.

Construct the equation:

$$\int d[g(x) - g(x')]dx = \int \left(\frac{d[g(x) - g(x')]}{dg(x)/dx} \right) dg(x)$$

It follows from the definition of the delta function that:

$$\int f(x)d[g(x) - g(x')]dx = \frac{f(x)}{dg(x)/dx} \Big|_{x=x'} \tag{A.5.4}$$

The method used to integrate Eq. (A.5.1) is a four-dimensional extension of a common three-dimensional technique. The procedure begins with the quadruple integral:

$$\iiint\iiint \left\{ A_\alpha \frac{\partial^2 G}{\partial X_\beta \partial X_\beta} - G \frac{\partial^2 A}{\partial X_\beta \partial X_\beta} \right\} dX_1 dX_2 dX_3 dX_4 = 0 \tag{A.5.5}$$

The equality results since all integrals are evaluated at $\pm\infty$ and the integrand decreases with distance rapidly enough so the integral is zero at the infinite limits. Substituting Eq. (A.5.2) into the first term in the integrand and substituting Eq. (A.5.1) into the second gives:

$$A_\alpha(X_\beta) = \mu \iiint\iiint J_\alpha(X'_\gamma)G(X'_\gamma, X_\gamma)dX_1 dX_2 dX_3 dX_4 \tag{A.5.6}$$

Since $J_\alpha(X'_\gamma)$ is known but $G(X'_\gamma, X_\gamma)$ is not, it is necessary to solve for $G(X'_\gamma, X_\gamma)$ using Eq. (A.5.6) before, in turn, solving for $A_\alpha(X_\beta)$. For this purpose, consider an aside on the four dimensional Fourier transform pair:

$$\begin{aligned} F(X_\gamma) &= \left(\frac{1}{2\pi} \right)^2 \iiint\iiint H(K_\gamma)e^{-iX_\gamma K_\gamma} dK_1 dK_2 dK_3 dK_4 \\ H(K_\gamma) &= \left(\frac{1}{2\pi} \right)^2 \iiint\iiint F(X_\gamma)e^{iX_\gamma K_\gamma} dX_1 dX_2 dX_3 dX_4 \end{aligned} \tag{A.5.7}$$

K_γ and X_γ are unknown conjugate variables that are to be determined. Making the definition that:

$$F(X_\gamma) = [\delta(X_\gamma - X'_\gamma)]^4 \tag{A.5.8}$$

Combining Eqs. (A.5.7) and (A.5.8) results in:

$$[\delta(X_\gamma - X'_\gamma)]^4 = \left(\frac{1}{2\pi}\right)^2 \iiint\!\!\!\int e^{-iK_\gamma(X_\gamma - X'_\gamma)} dK_1 dK_2 dK_3 dK_4$$

$$H(K_\gamma) = \left(\frac{1}{2\pi}\right)^2 e^{iK_\gamma K'_\gamma} \quad (\text{A.5.9})$$

It is convenient to introduce an additional function, $g(K_\gamma)$, defined by the equation:

$$G(X_\gamma, X'_\gamma) = \iiint\!\!\!\int g(K_\alpha) e^{-iK_\gamma(X_\gamma - X'_\gamma)} dK_1 dK_2 dK_3 dK_4 \quad (\text{A.5.10})$$

To solve for the function $g(K_\gamma)$ consider, as an example, the conjugate pair x and k_x to be a single dimension of Eqs. (A.5.2) and (A.5.9) with the equalities:

$$\frac{\partial^2 G(x - x')}{\partial x^2} = -\delta(x - x')$$

$$\delta(x - x') = \left(\frac{1}{2\pi}\right)$$

$$G(x, x') = \int g(k_x) e^{-ik_x(x-x')} dk_x \quad (\text{A.5.11})$$

Differentiating $G(x, x')$ twice with respect to x gives:

$$\delta(x - x') = k_x^2 \int g(k_x) e^{-ik_x(x-x')} dk_x \quad (\text{A.5.12})$$

Combining gives:

$$k_x^2 g(k_x) = \frac{1}{2\pi} \quad (\text{A.5.13})$$

Extension to four dimensions gives:

$$g(K_\gamma) = \left(\frac{1}{2\pi}\right)^2 \frac{1}{K_\alpha K'_\alpha} \quad (\text{A.5.14})$$

Substituting Eq. (A.5.14) back into Eq. (A.5.10) results in:

$$G(X_\gamma, X'_\gamma) = \left(\frac{1}{2\pi}\right)^4 \iiint\!\!\!\int \frac{e^{-iK_\gamma(X_\gamma - X'_\gamma)}}{K_\alpha K'_\alpha} dK_1 dK_2 dK_3 dK_4 \quad (\text{A.5.15})$$

It is convenient to use three-dimensional notation to evaluate Eq. (A.5.15). For this purpose note that the four variable set (x, y, z, ict) is complex and, if the exponentials are to remain oscillating functions, it is

necessary that the conjugate variable set K_α also be complex. Writing it as $(k_x, k_y, k_z, i\omega/c)$ and substituting into Eq. (A.5.15) gives:

$$G(X_\gamma, X'_\gamma) = \frac{i}{c} \left(\frac{1}{2\pi} \right)^4 \iiint \frac{e^{-iK_\gamma(X_\gamma - X'_\gamma)}}{k^2 - \omega^2} d\mathbf{k} d\omega \quad (\text{A.5.16})$$

where

$$k^2 = k_x^2 + k_y^2 + k_z^2; \quad d\mathbf{k} = dk_x dk_y dk_z \quad (\text{A.5.17})$$

Equation (A.5.16) is the sum of two Cauchy integrals, integrals that may be evaluated by use of the Cauchy integral identity:

$$2\pi i f(z') = \oint \frac{f(z)}{z - z'} dz \quad (\text{A.5.18})$$

Introducing p as a small, real, positive number used as a construction tool whose value is eventually put equal to zero, Eq. (A.5.16) may be written as:

$$G(X_\gamma, X'_\gamma) = \frac{ic}{(2\pi)^4} \iiint d\mathbf{k} \oint \frac{d\omega e^{-iK_\gamma(X_\gamma - X'_\gamma)}}{(\omega - ck - ip)(\omega + ck + ip)}$$

Moving the space portion of the exponential out from under the time-dependent integral results in:

$$G(X_\gamma, X'_\gamma) = \frac{ic}{(2\pi)^4} \iiint d\mathbf{k} e^{-i\mathbf{k} \cdot \mathbf{r}} \oint \frac{d\omega e^{-i\omega(t-t')}}{(\omega - ck - ip)(\omega + ck + ip)} \quad (\text{A.5.19})$$

Restated, the problem is that given an electric charge at (\mathbf{r}', t') to find the function $G(X_\gamma, X'_\gamma)$. The field is zero before the charge is introduced. That is, with $t'' = t - t'$ all fields are zero for $t'' < 0$. The last integral of Eq. (A.5.19) may be evaluated first along the real axis and then back around an infinite, complex ω path. For $t'' < 0$ the return path encompasses the lower half-plane, where no poles are enclosed. For $t'' > 0$ the return path is around the upper half of the complex plane, where two poles are enclosed.

Evaluation of the integral gives:

$$\oint \frac{d\omega e^{-i\omega t''}}{(\omega - ck - ip)(\omega + ck + ip)} = 2\pi i \left[\frac{e^{-it''(ck+ip)}}{2ck} - \frac{e^{-it''(-ck+ip)}}{2ck} \right] \\ = \frac{2\pi}{ck} \sin(ckt'') \quad (\text{A.5.20})$$

Combining Eqs. (A.5.20) and (A.5.21) gives:

$$G(X_\gamma, X'_\gamma) = \frac{i}{(2\pi)^3} \iiint \frac{1}{k} d\mathbf{k} e^{-i\mathbf{k}\cdot\mathbf{r}} \sin(ckt'') \quad (\text{A.5.21})$$

Next let \mathbf{R} be the space vector from source point \mathbf{r}' to field point \mathbf{r} , and choose it to be in the z -direction. Then $\mathbf{k} \cdot \mathbf{r} = kR \cos \theta$ where θ is the polar angle. Also, replace $d\mathbf{k}$ with $k^2 dk \sin \theta d\theta d\phi$:

$$G(X_\gamma, X'_\gamma) = \frac{i}{(2\pi)^3} \iiint k dk \sin \theta d\theta d\phi e^{-ikR \cos \theta} \sin(ckt'') \quad (\text{A.5.22})$$

Evaluating the angular integrals over an enclosing sphere gives:

$$G(X_\gamma, X'_\gamma) = \frac{2i}{(2\pi)^2} \int_0^\infty \frac{dk}{R} \sin(kR) \sin(ckt'') \quad (\text{A.5.23})$$

Since the integral of Eq. (A.5.23) is an even function of k , it may, without changing the value of the integral, be replaced by the equation:

$$G(X_\gamma, X'_\gamma) = \frac{i}{8\pi^2 R} \int_{-\infty}^\infty dk [e^{-i(\omega t'' - kR)} - e^{i(\omega t'' + kR)}] \quad (\text{A.5.24})$$

Equation (A.5.10) shows that Eq. (A.5.24) is the sum of two Dirac delta functions. The second one is evaluated at advanced time $t'' < 0$ when there are no charges, and if causality applies all results from it are equal to zero. Working with the retarded time $t'' > 0$ when there are charges, using Eq. (A.5.3) it follows that:

$$\delta(R - ct'') = -\frac{1}{c} \delta(t'' - R/c) \quad (\text{A.5.25})$$

Combining with the first term in the integrand of Eq. (A.5.24) gives:

$$G(X_\gamma, X'_\gamma) = \frac{1}{4i\pi R c} \delta(t'' - R/c) \quad (\text{A.5.26})$$

This completes the derivation of $G(X_\gamma, X'_\gamma)$.

6. The Potentials

To obtain potential A_ν of a moving charge density, substitute Eq. (A.5.26) into Eq. (A.5.5). The result is:

$$A_\nu(X_\gamma) = \frac{\mu}{4\pi} \iiint dV' \int dt \frac{J_\nu(X'_\alpha)}{R(X_\gamma, X'_\gamma)} \delta(t'' - R/c) \quad (\text{A.6.1})$$

Distance $R(X_\gamma, X'_\gamma)$ is the distance between the source and field points. Using Eq. (A.5.3) to evaluate Eq. (A.6.1) gives:

$$\begin{aligned} A(\mathbf{r}, t) &= \frac{\mu}{4\pi} \iiint \frac{J(\mathbf{r}', t)}{(R - \mathbf{R} \cdot \mathbf{v}/c)} dV' \\ \Phi(\mathbf{r}, t) &= \frac{\mu}{4\pi} \iiint \frac{\rho(\mathbf{r}', t)}{(R - \mathbf{R} \cdot \mathbf{v}/c)} dV' \end{aligned} \quad (\text{A.6.2})$$

Equation (A.6.2) is the final form for the electromagnetic 4-potential of a moving charge. Distance from the point of field emission to the field point when the radiation is received. These are the Liénard–Wiechert potentials.

To obtain the potential A_ν of an oscillating charge density, note that Eq. (A.6.2) remains applicable except, for this case, the average velocity of the oscillating charge is zero. The resulting equation is:

$$A_{0\nu}(\mathbf{r}) e^{i\omega t} = \frac{\mu}{4\pi} \int dV' \int dt' \frac{J_{0\nu}(\mathbf{r}', t')}{R(\mathbf{r}, \mathbf{r}')} \delta(t', t - R/c) \quad (\text{A.6.3})$$

Subscripts “0” indicate the value is independent of time. Applying Eq. (A.6.3) to a differential volume in space gives shows that in three dimensions the potentials at position \mathbf{r} due to a current density are given by:

$$\begin{aligned} A(\mathbf{r}) e^{i\omega t} &= \frac{\mu}{4\pi} \int \frac{J(\mathbf{r}') e^{i\omega(t-R/c)}}{R(\mathbf{r}, \mathbf{r}')} dV' \\ \Phi(\mathbf{r}) e^{i\omega t} &= \frac{1}{4\pi\epsilon} \int \frac{\rho(\mathbf{r}') e^{i\omega(t-R/c)}}{R(\mathbf{r}, \mathbf{r}')} dV' \end{aligned} \quad (\text{A.6.4})$$

These are the retarded potentials.

7. Equivalent Sources

It is shown in Sec. 1.10 that the force fields satisfy the partial differential equations:

$$\nabla \times (\nabla \times \mathbf{E}) + \epsilon\mu \frac{\partial^2 \mathbf{E}}{\partial t^2} = 0 \quad \text{and} \quad \nabla \times (\nabla \times \mathbf{B}) + \epsilon\mu \frac{\partial^2 \mathbf{B}}{\partial t^2} = 0 \quad (\text{A.7.1})$$

Other helpful relationships are:

$$\nabla \times (\nabla \times \mathbf{E}) = \nabla(\nabla \cdot \mathbf{E}) - \nabla^2 \mathbf{E} \quad \text{and} \quad \varepsilon\mu \frac{\partial^2 \mathbf{E}}{\partial t^2} = -k^2 \mathbf{E} \quad (\text{A.7.2})$$

Combining the two equations shows that:

$$\nabla^2 \mathbf{E} + k^2 \mathbf{E} = 0 \quad \text{and} \quad \nabla^2 \mathbf{B} + k^2 \mathbf{B} = 0 \quad (\text{A.7.3})$$

These are the Helmholtz equations for the field intensities. In rectangular coordinates the form of the vector and scalar Laplacian operators are identical.

The objective is to obtain expressions for the field vectors at any field point, $\mathbf{r}(x, y, z)$, external to a field-generating volume as a function of field values on the surface of the volume. The development requires three vector integral equations, the divergence theorem and two related ones. Let dS represent a scalar differential area on the surface of the volume and n be a unit vector directed normal to the surface at the same point. At the surface, fields \mathbf{F} and ϕ have the continuity properties of electromagnetic fields: they are continuous with continuous first derivatives.

$$\oint d\mathbf{S} \cdot \mathbf{F} = \int \nabla \cdot \mathbf{F} dV; \quad \oint d\mathbf{S} \times \mathbf{F} = \int \nabla \times \mathbf{F} dV; \quad \oint \phi d\mathbf{S} = \int \nabla \phi dV \quad (\text{A.7.4})$$

Next let ϕ and ψ each represent scalar fields and construct the function $\phi \nabla \psi$. Substituting the new function into the divergence equation gives:

$$\oint \phi \nabla \psi \cdot d\mathbf{S} \equiv \int \nabla \cdot (\phi \nabla \psi) dV = \int [\nabla \phi \cdot \nabla \psi + \phi \nabla^2 \psi] dV \quad (\text{A.7.5})$$

Reversing the roles of ϕ and ψ and subtracting the result from Eq. (A.7.5) gives

$$\oint [\phi \nabla \psi - \psi \nabla \phi] \cdot d\mathbf{S} = \int [\phi \nabla^2 \psi - \psi \nabla^2 \phi] dV \quad (\text{A.7.6})$$

For the special case of an oscillating charge, the defining equation for Green's function, Eq. (A.5.1), in three-dimensional form satisfies an equation similar to that of the Helmholtz wave equation. With point $\mathbf{r}'(x', y', z')$ representing the source position:

$$\nabla^2 G(\mathbf{r}, \mathbf{r}') + k^2 G(\mathbf{r}, \mathbf{r}') = -\delta(\mathbf{r}, \mathbf{r}') \quad (\text{A.7.7})$$

In free space, the solution is:

$$G(\mathbf{r}, \mathbf{r}') = -\frac{e^{-ik \cdot (\mathbf{r} - \mathbf{r}')}}{R(\mathbf{r}, \mathbf{r}')} \quad (\text{A.7.8})$$

The objective is to construct a virtual sphere about a source then to calculate the fields at an arbitrary field point, $\mathbf{r}(x, y, z)$, in terms of the fields

that exist on the surface of the virtual sphere. In this way, the fields can be obtained without knowledge of the source itself. For this purpose, begin by substituting into Eq. (A.7.6) that $\phi = G$ and ψ is equal to one component of the electric field intensity. Then repeat twice with ψ representing the other electric field components and sum over the three equations. The result is the vector form of Eq. (A.7.6):

$$\oint \{ \mathbf{E}(\mathbf{r}') [n' \cdot \nabla' G(\mathbf{r}, \mathbf{r}')] - G(\mathbf{r}, \mathbf{r}') [n' \cdot \nabla'] \mathbf{E}(\mathbf{r}') \} dS' \\ = \int [\mathbf{E}(\mathbf{r}') \nabla'^2 G(\mathbf{r}, \mathbf{r}') - G(\mathbf{r}, \mathbf{r}') \nabla'^2 \mathbf{E}(\mathbf{r}')] dV' \quad (\text{A.7.9})$$

Next, let the field point be in the vicinity of the source and construct a virtual sphere with a radius just large enough to contain both source and field points. Substituting Eqs. (A.7.3) and (A.7.7) into the volume integrals of Eq. (A.7.9) results in:

$$\int \mathbf{E}(\mathbf{r}') \delta(\mathbf{r}, \mathbf{r}') dV' = \mathbf{E}(\mathbf{r}) \quad (\text{A.7.10})$$

The second term in the surface integral of Eq. (A.7.9) may be written:

$$G(n' \cdot \nabla') \mathbf{E} = n' \cdot \nabla' (G \mathbf{E}) - \mathbf{E} (n' \cdot \nabla' G) \quad (\text{A.7.11})$$

Combining shows that:

$$\mathbf{E}(\mathbf{r}) = \oint \{ 2\mathbf{E}(\mathbf{r}') [n' \cdot \nabla' G(\mathbf{r}, \mathbf{r}')] - [n' \cdot \nabla'] [G(\mathbf{r}, \mathbf{r}') \mathbf{E}(\mathbf{r}')] \} dS' \quad (\text{A.7.12})$$

This equation expresses the field intensity at the field point in terms of field values on the surface of a virtual sphere surrounding both the source and the field. Although Eq. (A.7.12) expresses the electric field intensity at the field point in terms of values on the surface of an external virtual sphere, it is not satisfactory since the divergence operation contains derivatives of the electric field intensity.

Next, consider the field point to be outside the virtual sphere and, for completeness construct a second virtual sphere. It is concentric with the first one and of radius large enough to contain both source and field positions, and it contains no other sources. With no sources, the volume integral of Eq. (A.7.9) is equal to zero. The integral similar to Eq. (A.7.12), for this case, is equal to zero:

$$\oint \{ 2\mathbf{E}(\mathbf{r}') [n' \cdot \nabla' G(\mathbf{r}, \mathbf{r}')] - [n' \cdot \nabla'] [G(\mathbf{r}, \mathbf{r}') \mathbf{E}(\mathbf{r}')] \} dS' = 0 \quad (\text{A.7.13})$$

The integral is taken over both the inner and outer spherical surfaces, with the normal direction always extending outward from the field containing volume. Next, let the radius of the outer surface increase without limit, in which case, as discussed below, the integral over the exterior surface is equal to zero. Comparing Eqs. (A.7.12) and (A.7.13) then shows that the surface integral over the inner surface is equal to $-\mathbf{E}(\mathbf{r})$.

To restate Eq. (A.7.12) in a way that involves field vectors only note that the last term of Eq. (A.7.13) may be written as a volume integral:

$$\oint n' \cdot \nabla'(\mathbf{GE}) dS = \int \nabla'^2(\mathbf{GE}) dV$$

Substitute vector (\mathbf{GE}) into the vector identity:

$$\nabla^2(\mathbf{GE}) = \nabla[\nabla \cdot (\mathbf{GE})] - \nabla \times [\nabla \times (\mathbf{GE})]$$

After combining and using the second and third integrals of Eq. (A.7.4) to return to surface integrals, Eq. (A.7.13) goes to:

$$\oint \{2\mathbf{E}(n' \cdot \nabla'G) - n'[\nabla' \cdot (\mathbf{GE})] + n' \times [\nabla' \times (\mathbf{GE})]\} dS = 0 \quad (\text{A.7.14})$$

Completing both the divergence and curl operations and using the Maxwell equations to substitute for vector operations results in:

$$\oint \{2\mathbf{E}(n' \cdot \nabla G) - n'(\mathbf{E} \cdot \nabla G) - i\omega n' \times \mathbf{B} + n' \times (\nabla'G \times \mathbf{E})\} dS = 0 \quad (\text{A.7.15})$$

Substituting for the triple product and simplifying results in:

$$\oint \{-i\omega(n' \times \mathbf{B})G + (n' \cdot \mathbf{E})\nabla'G + (n' \times \mathbf{E}) \times \nabla'G\} dS = 0 \quad (\text{A.7.16})$$

By Eq. (A.7.13), the value of the surface integral is equal to $-\mathbf{E}(\mathbf{r})$. However, as defined above the normal is from the field-containing region to the source-containing region. Reversing the direction so the normal extends outward gives:

$$\begin{aligned} \mathbf{E}(\mathbf{r}) = \oint \{ & -i\omega[n' \times \mathbf{B}(\mathbf{r}')]G(\mathbf{r}, \mathbf{r}') + [n' \cdot \mathbf{E}(\mathbf{r}')] \nabla'G(\mathbf{r}, \mathbf{r}') \\ & + [n' \times \mathbf{E}(\mathbf{r}')] \times \nabla'G(\mathbf{r}, \mathbf{r}') \} dS \end{aligned} \quad (\text{A.7.17})$$

The requirements are that the field point is external to the contained region and the source is fully contained by it.

This equation, when combined with Eq. (A.7.8), is the exact expression for the exterior electric field intensity in terms of the surface fields

on a source-containing region. It is not necessary to know anything about the source other than that it created the surface fields. Although both the external electric field intensity and the fields on the surface are unique, the inverse is not true: the source necessary to produce $\mathbf{E}(\mathbf{r})$ is not unique.

The corresponding expression for the magnetic flux density follows in a similar way. Carrying out the calculation gives:

$$\mathbf{B}(\mathbf{r}) = \oint \{i\omega\mu\epsilon[n' \times \mathbf{E}(\mathbf{r}')]G(\mathbf{r}, \mathbf{r}') + [n' \cdot \mathbf{B}(\mathbf{r}')] \nabla' G(\mathbf{r}, \mathbf{r}') - [n' \times \mathbf{B}(\mathbf{r}')] \times \nabla' G(\mathbf{r}, \mathbf{r}')\} dS \quad (\text{A.7.18})$$

With static sources Green's function decreases as the inverse of the radius, the electric field intensity decreases as the inverse square of the radius, and the surface area increases as the square of the radius. Therefore in the limit as the radius becomes infinite the contribution to field intensities $\mathbf{E}(\mathbf{r})$ and $\mathbf{B}(\mathbf{r})$ due to the outer surface goes to zero. On the other hand, for dynamic sources, Green's function and the electric field intensity both decrease as the inverse of the radius and the surface area increases as the square of the radius. From this point of view, contributions of the outer surface integral to $\mathbf{E}(\mathbf{r})$ and $\mathbf{B}(\mathbf{r})$ remain constant in the limit of infinite radius. That the null result remains, however, may be seen by application of a dynamic boundary condition: The radius of the outer sphere is greater than the speed of light, c , times whatever time is of interest in the problem. Even with dynamic sources, the outer surface integral has no influence on fields $\mathbf{E}(\mathbf{r})$ or $\mathbf{B}(\mathbf{r})$.

8. A Series Resonant Circuit

An important special case is a series arrangement of inductor L , resistor R , and capacitor C . The differential equation relating the current and voltage is:

$$v(t) = L \frac{di(t)}{dt} + Ri(t) + \frac{1}{C} \int i(t) dt \quad (\text{A.8.1})$$

To obtain the steady state solution define the current in the circuit to be:

$$i(t) = I_0 \cos(\omega t) \quad (\text{A.8.2})$$

Combining Eqs. (A.8.1) and (A.8.2) shows that the voltage across the circuit is:

$$v(t) = I_0 R \cos(\omega t) - I_0 \left(\omega L - \frac{1}{\omega C} \right) \sin(\omega t) \quad (\text{A.8.3})$$

The power into each element is:

$$p(t) = v_S(t)i(t) \quad (\text{A.8.4})$$

The voltage across the element in question is $v_S(t)$. The power into each element is:

$$\begin{aligned} p_L(t) &= -\frac{\omega L I_0^2}{2} \sin(2\omega t) & p_C(t) &= \frac{I_0^2}{2\omega C} \sin(2\omega t) \\ p_R(t) &= \frac{R I_0^2}{2} [1 + \cos(2\omega t)] \end{aligned} \quad (\text{A.8.5})$$

The energy stored in each reactive element is:

$$\begin{aligned} W_L(t) &= \frac{L I_0^2}{4} [1 + \cos(2\omega t)] \\ W_C(t) &= \frac{I_0^2}{4\omega^2 C} [1 - \cos(2\omega t)] \end{aligned} \quad (\text{A.8.6})$$

It would be convenient to relate the voltage and current by a multiplicative constant. Comparing Eqs. (A.8.2) and (A.8.3) shows that this cannot be done with trigonometric functions. However, adding an imaginary term to Eq. (A.8.2) gives the exponential function:

$$i(t) = I_0 [\cos(\omega t) + i \sin(\omega t)] = I_0 e^{i\omega t} \quad (\text{A.8.7})$$

Equation (A.8.7) is the phasor form of the current. The phasor form of the circuit voltage is:

$$v(t) = \left[R + i \left(\omega L - \frac{1}{\omega C} \right) \right] I_0 e^{i\omega t} \quad (\text{A.8.8})$$

By definition, the input impedance, Z , of the circuit is equal to the complex voltage-to-complex current ratio at the circuit terminals. For this case:

$$Z = R + i \left(\omega L - \frac{1}{\omega C} \right) \quad (\text{A.8.9})$$

Using phasor notation the exponential is suppressed and the reader is supposed to know it should be there. Using phasor notation in this case the current and voltage are:

$$I = I_0 \quad \text{and} \quad V = I_0 \left[R + i \left(\omega L - \frac{1}{\omega C} \right) \right] \quad (\text{A.8.10})$$

Although phasors provide a constant multiplicative relationship between the current and voltage, other problems arise. Each variable, i.e. phasor current and phasor voltage, consists of terms that do and terms that do not

represent physical reality, the actual and virtual terms. Separating actual from virtual values in the voltage and current expressions can easily be done since the actual values appear as real numbers and the virtual values appear as imaginary ones. However, when products are taken things are not so simple. Using power as an example, the product of the phasor current and voltage consists of four types of terms: actual current times actual voltage, actual current times virtual voltage, virtual current times actual voltage, and virtual current times virtual voltage. Of these four products, only the first type represents actuality and only it is desired. The second and third types are multiplied by “ i ” and thus may be discarded. The fourth type, however, is a real, unwanted number. Special multiplication rules are necessary to eliminate the fourth type of product.

Consider circuit power as an example. From Eq. (A.8.5) the time varying input power is:

$$p(t) = \frac{I_0^2}{2} \left\{ R[1 + \cos(2\omega t)] - \left[\omega L - \frac{1}{\omega C} \right] \sin(2\omega t) \right\} \quad (\text{A.8.11})$$

By way of contrast consider the product phasor $P_c = VI^*/2$:

$$P_c = \frac{I_0^2}{2} \left\{ R + i \left[\omega L - \frac{1}{\omega C} \right] \right\} \quad (\text{A.8.12})$$

The real and reactive powers shown in Eq. (A.8.11) are phased in time quadrature. The real part of P_c is equal to the time-average power. The imaginary part of P_c is equal to the magnitude of the reactive power. Since the instantaneous value of the power is, in many cases, of no interest, the remaining quantities of interest are both contained in Eq. (A.8.12): the time-average real power, P_{av} , and the magnitude of the reactive power, P_{re} . Because of these relationships, it is common when dealing with power in electrical circuits, to work with the complex power:

$$P_c = P_{av} + i P_{re} \quad (\text{A.8.13})$$

Although the power is complex, it is not a phasor: both real and imaginary parts represent physical reality and there is no virtual part.

9. Q of Time Varying Systems

Q is a dimensionless ratio that describes the quality of anything that oscillates. Although developed for application to a closed system, such as an electrical circuit, a bouncing ball, or a swaying bridge, Q is also useful for dealing with the open system of a radiating antenna. For example,

antenna Q is important in communication antennas since modulation is essential, modulation requires a minimum bandwidth, and there is a direct relationship between Q and bandwidth. For high power antennas, Q is a measure of how much energy must be stored about an antenna to obtain the minimum acceptable power output. This is significant in such diverse applications as the decay of atomic states and electrically small, high power antennas used to communicate around the surface of the earth. In nearly all radiation problems, Q is a critical measure of antenna worthiness.

Since only energy within a half wavelength of an antenna can return to it during steady state operation, only this near field energy affects an antenna's input impedance. To the driving terminals of an antenna, energy radiated permanently away from the system is indistinguishable from energy absorbed by a resistor; the power loss is therefore measured as an effective antenna resistance. Since the energy that oscillates to and from an antenna is indistinguishable from reactive energy, the oscillation results in an effective radiation reactance. To the driving circuit, this input impedance is indistinguishable from the input impedance of a properly synthesized closed circuit. Hence, from the point of view of the driving source, an antenna may be replaced by and analyzed as if it were an electric circuit.

Anything that oscillates can be assigned a value of Q . Defining $W(t)$ as the energy stored in the system, the magnitude of the Q of any system is defined to be the dimensionless ratio:

$$Q = \frac{\omega W(t)}{dW(t)/dt} \quad (\text{A.9.1})$$

Q is a measure of how rapidly a system grows or decays. Rewriting Eq. (A.9.1) for a lossy system gives:

$$\frac{dW(t)}{dt} = -\frac{\omega}{Q}W(t) \quad (\text{A.9.2})$$

The solution of Eq. (A.9.2) is:

$$W(t) = W_0 e^{-\omega t/Q} \quad (\text{A.9.3})$$

W_0 is the initial value of energy. As an example, consider a ball bouncing on a smooth, horizontal, surface. In a uniform gravitational field, the energy is proportional to the height and, at maximum height the energy is entirely due to gravity. The maximum height reached by the ball follows the exponential decay of Eq. (A.9.3), and the ratio of heights on successive bounces is $e^{-\omega/Q}$.

Inductors require a current path and current paths, generally speaking, are also resistive. The ratio of inductance, L , to resistance, R , depends upon the nature of the path (the wire) and its geometrical arrangement. Since the peak energy per cycle is equal to the total oscillating energy, a definition derived from Eq. (A.9.1) is the peak cyclic value of stored energy-to-average energy loss per radian ratio:

$$Q = \frac{\omega W(t)_{\text{pk}}}{P(t)_{\text{av}}} \quad (\text{A.9.4})$$

The current and voltage in an RL circuit may be written:

$$\begin{aligned} i(t) &= I_0 \cos(\omega t) \\ v(t) &= I_0 [R \cos(\omega t) - \omega L \sin(\omega t)] \end{aligned} \quad (\text{A.9.5})$$

The power dissipated in the resistor is:

$$P_R(t) = \frac{RI_0^2}{2} [1 + \cos(2\omega t)] \quad (\text{A.9.6})$$

The energy stored in the inductor is:

$$W_L(t) = \frac{LI_0^2}{4} [1 + \cos(2\omega t)] \quad (\text{A.9.7})$$

Combining Eqs. (A.9.4), (A.9.6), and (A.9.7) shows that:

$$Q = \frac{\omega L}{R} \quad (\text{A.9.8})$$

For an RLC circuit, the instantaneous energy-to-time average power ratio is equal to:

$$\frac{\frac{LI_0^2}{4} [1 + \cos(2\omega t)] + \frac{I_0^2}{4C} [1 - \cos(2\omega t)]}{\frac{RI_0^2}{2} [1 + \cos(2\omega t)]} \quad (\text{A.9.9})$$

From Eq. (A.9.9) it follows that, if the inductive energy exceeds the capacitive energy, Eq. (A.9.8) gives Q . If the capacitive energy exceeds the inductive energy, Q is:

$$Q = \frac{1}{\omega RC} \quad (\text{A.9.10})$$

At the resonant frequency, where subscript “av” denotes time-average values, a commonly used formula is:

$$Q = \frac{2\omega W_{L\text{av}}}{P_{\text{av}}} \quad (\text{A.9.11})$$

For these simple circuits, values calculated using Eqs. (A.9.9)–(A.9.11) are equal at resonance. In more complicated circuits where the reactive elements are driven with different phases, Eq. (A.9.11) is not exact.

A slightly modified definition that is sometimes used with simple systems is to equate Q with the tangent of the impedance phase angle. So long as the system frequency is low enough for capacitive effects to be negligible the definition reproduces Eq. (A.9.8) for the simple case of an RL circuit. Using all three definitions, results with lossy capacitors are similar to those with lossy inductors. By all three definitions, a capacitor C in series with resistor R simply replaces ωL by $1/\omega C$.

$$Q = 1/(\omega CR) \quad (\text{A.9.12})$$

With an antenna radiating in the steady state since time $t = -\infty$ there is an infinite amount of energy in the field. The difficulty with calculating Q is separate the finite field that returns to the source upon shutdown from that which does not. During steady state operation, the magnitudes of the field intensities decrease with increasing radius. The Maxwell stress tensor shows that radiation fields exert an expansive self-pressure equal to the gradient in field energy density. In this way, the tensor describes forces acting to drive the field energy ever outward. However, upon source turnoff, shutdown, the inverse is true. If the fields vanish near the source the tensor describes compressive forces that act to drive the field energy back to the source; it is the returned energy that forms the numerator of the expression for Q , see Eq. (A.9.1).

10. Bandwidth

The normalized bandwidth is defined as the ratio of the frequency difference between the two points at which a resonant circuit drops to half the resonant power (half power points) divided by the resonant frequency.

By definition, the resonance frequency of a series circuit is that frequency at which the reactive power vanishes. From Eq. (A.8.3) the input voltage is:

$$v(t) = I_0 R \cos(\omega t) - I_0 \left[\omega L - \frac{1}{\omega C} \right] \sin(\omega t) \quad (\text{A.10.1})$$

From Eq. (A.8.11) the input power is:

$$p(t) = \frac{I_0^2}{2} \left\{ R[1 + \cos(2\omega t)] - \left[\omega L - \frac{1}{\omega C} \right] \sin(2\omega t) \right\} \quad (\text{A.10.2})$$

The resonance frequency, ω_0 , is the frequency at which the reactive power vanishes. It is equal to:

$$\omega_0^2 = \frac{1}{LC} \quad (\text{A.10.3})$$

To begin a dimensionless analysis of bandwidth introduce the expressions:

$$\omega_1 = \omega_0(1 + \delta) \quad \text{and} \quad \omega_2 = \omega_0(1 - \delta) \quad (\text{A.10.4})$$

Frequencies ω_1 and ω_2 are the half power frequencies. With no loss of rigor, it is convenient to have the circuit be subject to a constant current input. For that case, the dissipated power drops by half when the real and reactive voltage magnitudes are equal. This occurs for:

$$\frac{\omega_0 L}{R} = \frac{\delta(2 + \delta)}{(1 + \delta)} \cong 2\delta \quad (\text{A.10.5})$$

The bandwidth is $2\delta\omega_0$. A result of combining Eqs. (A.10.4) and (A.10.5) is:

$$Q \cong \frac{1}{2\delta} = \frac{\omega_0}{\omega_1 - \omega_2} \quad (\text{A.10.6})$$

For more complicated circuits, the actual circuit may be replaced by its equivalent Thévenin or Norton circuit and analyzed in a similar way. For structured circuits in which different passive elements have differently phased driving currents the inductive and capacitive energies are not in phase quadrature. The peak value of stored energy contains contributions from both inductors and capacitors.

11. Instantaneous and Complex Power in Radiation Fields

To compare methods of describing power, for steady-state radiation fields return to the Maxwell equations using \mathbf{H} notation, Eqs. (1.6.8) and (1.6.11):

$$\begin{aligned} \nabla \times \mathbf{E} + \mu \frac{\partial \mathbf{H}}{\partial t} &= 0 & \nabla \cdot \mu \mathbf{H} &= 0 \\ \nabla \times \mathbf{H} - \varepsilon \frac{\partial \mathbf{E}}{\partial t} &= \mathbf{J} & \nabla \cdot \varepsilon \mathbf{E} &= \rho \end{aligned} \quad (\text{A.11.1})$$

Integrating over any closed volume and using Gauss's law gives:

$$\oint \mathbf{N} \cdot d\mathbf{S} + \int \left(\mu \mathbf{H} \cdot \frac{\partial \mathbf{H}}{\partial t} + \varepsilon \mathbf{E} \cdot \frac{\partial \mathbf{E}}{\partial t} \right) dV = - \int \mathbf{E} \cdot \mathbf{J} dV \quad (\text{A.11.2})$$

This is the Poynting theorem, a restatement of Eq. (1.9.9). Vector \mathbf{N} is defined by Eq. (1.8.5). The term on the right side of Eq. (A.11.2), complete with the sign, is the rate at which energy enters the volume. The volume integral on the left is the rate at which energy enters the field. Conservation of energy requires the first term on the left to be the rate at which energy leaves through the surface. This interpretation is independent of any particular wave shape.

When dealing with sinusoidal, steady state radiation it is often convenient to use phasor notation. With $\exp(i\omega t)$ time dependence the phasor version of Maxwell's equations is:

$$\begin{aligned}\nabla \times \tilde{\mathbf{E}} + i\omega\mu\tilde{\mathbf{H}} &= 0 & \nabla \cdot \mu\tilde{\mathbf{H}} &= 0 \\ \nabla \times \tilde{\mathbf{H}} - i\omega\varepsilon\tilde{\mathbf{E}} &= \tilde{\mathbf{J}} & \nabla \cdot \varepsilon\tilde{\mathbf{E}} &= \rho\end{aligned}\quad (\text{A.11.3})$$

By definition the complex Poynting vector is:

$$\mathbf{N}_c = N_{cr} - iN_{ci} = \tilde{\mathbf{E}} \times \tilde{\mathbf{H}}^*/2 \quad (\text{A.11.4})$$

Taking the divergence gives

$$\nabla \cdot \mathbf{N}_c = \frac{1}{2}[\tilde{\mathbf{H}}^* \cdot (\nabla \times \tilde{\mathbf{E}}) - \tilde{\mathbf{E}} \cdot (\nabla \times \tilde{\mathbf{H}}^*)] \quad (\text{A.11.5})$$

Integrating Eq. (A.11.5) over the same closed volume as used with Eq. (3.11.2), substituting from Eq. (A.11.3), and using Gauss's law gives:

$$\oint \mathbf{N}_c \cdot d\mathbf{S} = 2i\omega \int \frac{1}{4}(\mu\tilde{\mathbf{H}} \cdot \tilde{\mathbf{H}}^* - \varepsilon\tilde{\mathbf{E}} \cdot \tilde{\mathbf{E}}^*)dV - \frac{1}{2} \int \tilde{\mathbf{E}} \cdot \tilde{\mathbf{J}}^* dV \quad (\text{A.11.6})$$

The last term of Eq. (A.11.6), complete with sign, is the average rate at which energy enters the volume. Since the first term on the right has no real part, the real part of the left side must be the rate at which energy leaves the volume. The imaginary part of the left side is equal to 2ω times the difference between the mean values of electric and magnetic field energy in the volume plus the imaginary part of the second term and, in most instances, that term is real. It follows that:

$$(W_M - W_E) = \frac{1}{2\omega} \text{Im} \oint \mathbf{N}_c \cdot d\mathbf{S} \quad (\text{A.11.7})$$

As a side remark, note that although the complex Poynting vector is a complex quantity, it is not a phasor, since both real and imaginary parts represent actual quantities.

Consider the volume of integration to be spherical, let δ be a vanishingly small distance, and place the source currents on the sphere. Consider three volumes: (i) A virtual sphere contains all radii less than $a - \delta$; there are no sources and all fields are ignored. (ii) Concentric spheres of radii within the range $a \pm \delta$; this region contains all sources. (iii) Exterior region contains all radii larger than $a + \delta$; there are fields but no sources.

Since the exterior region contains no currents, within that region the current-containing integral of Eq. (A.11.6) is equal to zero. Since the volume integral on the left has no real part the sum of the real part of the surface integral taken at infinity and at $a + \delta$ is equal to zero. For finite fields,

in the limit of infinite radius the imaginary portion of \mathbf{N}_c decreases more rapidly than $1/r^2$. Therefore, as the radius becomes infinite the imaginary part of the surface integral is equal to zero and the imaginary part at radius $a + \delta$ is equal to $(\omega/2) \times$ {the difference between the time-average magnetic and electric field energies}:

$$\text{Im} \left[\oint_{a+\delta} \mathbf{N}_c \cdot d\mathbf{S} \right] = \frac{\omega}{2} \int \{ \mu \tilde{\mathbf{H}} \cdot \tilde{\mathbf{H}}^* - \epsilon \tilde{\mathbf{E}} \cdot \tilde{\mathbf{E}}^* \} dV \quad (\text{A.11.8})$$

Within the source region, $a \pm \delta$, the volume is proportional to 2δ . There are no singularities in the fields and the first volume integral goes to zero with δ . This leaves:

$$\text{Im} \left[\oint \mathbf{N}_c \cdot d\mathbf{S} \right] + \frac{1}{2} \text{Im} \left[\int \tilde{\mathbf{E}} \cdot \tilde{\mathbf{J}}^* dV \right] = 0 \quad (\text{A.11.9})$$

For simplicity consider the special case where radius $a \ll \lambda$, an electrically small antenna. Sources may then be considered as circuit elements and the current containing integral of Eq. (A.11.6) may be written as:

$$\frac{1}{2} \int \tilde{\mathbf{E}} \cdot \tilde{\mathbf{J}}^* dV = \frac{1}{2} \sum_{j=1}^k V_j I_j^* \quad (\text{A.11.10})$$

With more than one current source, unless the sources meet one of the phase conditions of Eq. (3.1.13) powers do not combine by simple addition. Therefore, unless that condition is met Eq. (A.11.10) does not correctly describe the complex power. If not, the right side of Eq. (A.11.6) is not the complex power and, if it is not, neither is the surface integral.

12. Conducting Boundary Conditions

Let an electric field intensity exist in the vicinity of a smooth boundary about a closed volume that is immersed in the field. The volume is arbitrary in size and shape. Requirements on the volume are that its size be much less than a wavelength, in all three dimensions, and that it includes regions on both sides of the boundary. Apply the condition of Eq. (1.6.8), that:

$$\nabla \cdot \mathbf{E} = \rho/\epsilon \quad (\text{A.12.1})$$

Evaluate the integral of Eq. (A.12.1) over the volume in question, with the result:

$$\int \nabla \cdot \mathbf{E} dV = \oint \mathbf{E} \cdot d\mathbf{S} = q/\epsilon \quad (\text{A.12.2})$$

Symbol “q” indicates all charge within the volume. Next, let the dimension normal to the boundary become vanishingly small on both sides of the

boundary so the shape approaches that of a disc. The contribution to the surface integral due to electric field intensity normal to the disc is thereby vanishingly small. Thus, only the normal components of the field intensity are of interest, and Eq. (A.12.2) goes to:

$$\oint \mathbf{E} \cdot d\mathbf{S} = \rho/\varepsilon \quad (\text{A.12.3})$$

Symbol ρ indicates the charge per unit area at the interface. From Eq. (A.12.3), since charge density in free space is equal to zero the normal component of the electric field intensity on any virtual boundary is continuous.

If an electric field intensity existed inside a nearly ideal conductor, it would drive a nearly infinite current density that would, in turn, absorb a nearly infinite amount of power. Therefore an electric field intensity inside an ideal conductor is zero. In turn, if an electric field intensity is applied normal to the surface of an ideal conductor, by Eq. (A.12.3) it is equal to the charge density on the surface normalized by the permittivity of free space.

For a magnetic field intensity, by Eq. (1.6.11):

$$\nabla \times \mathbf{E} = -\frac{\partial \mathbf{B}}{\partial t} \quad (\text{A.12.4})$$

Consider the surface integral of Eq. (A.12.4) over an open area that, like the volume of Eq. (A.12.1), extends on either side of a smooth boundary. The integral is:

$$\oint \mathbf{E} \cdot d\ell = -\int \frac{\partial \mathbf{B}}{\partial t} \cdot d\mathbf{S} \quad (\text{A.12.5})$$

The symbol $d\ell$ indicates differential distance along the periphery of the open area. Next, let the dimension normal to the boundary become vanishingly small. In this limit, the open area becomes vanishingly small and since \mathbf{B} is finite, the entire right side of the equation is vanishingly small. Therefore, the line integral of the electric field intensity around the loop is equal to zero. Since the length of the loop is the same on either side of the boundary, and since $d\ell$ is oppositely directed on either side, the tangential component of the electric field intensity is continuous through virtual boundaries. At a boundary between free space and a conductor since the electric field component inside the conductor is equal to zero it is also equal to zero just off the conducting surface.

Let n be a unit vector normal to a smooth surface. For a virtual surface, the boundary separates regions one and two. For a conducting surface, the field is in the free space region only:

Virtual Surface

$$n \times (\mathbf{E}_1 - \mathbf{E}_2) = 0; \quad n \cdot (\mathbf{E}_1 - \mathbf{E}_2) = 0 \quad (\text{A.12.6})$$

Conducting Surface

$$n \times \mathbf{E} = 0; \quad n \cdot \mathbf{E} = \rho_S / \varepsilon$$

Consider a closed volume that is immersed in a magnetic field. Like the volume considered for the normal component of the electric field intensity, it may be arbitrary in size and shape. The requirements are that its size be much less than a wavelength, in all three dimensions, and that it includes regions on both sides of the boundary. Apply the condition of Eq. (1.6.11):

$$\nabla \cdot \mathbf{B} = 0 \quad (\text{A.12.7})$$

Take the volume integral of Eq. (A.12.7) over the volume in question, with the result:

$$\oint \mathbf{B} \cdot d\mathbf{S} = 0 \quad (\text{A.12.8})$$

Since Eq. (A.12.8) applies to a closed volume, let the dimension normal to the boundary become vanishingly small so the shape approaches that of a disc. It follows that the normal component of \mathbf{B} is continuous through the boundary. Inside a conductor, \mathbf{B} is constant since otherwise Eq. (A.12.5) shows that it would produce an electric field intensity there. For time varying radiation fields, the normal component of the magnetic field intensity is equal to zero.

By Eq. (1.6.8):

$$\nabla \times \mathbf{B} = \mu\varepsilon \frac{\partial \mathbf{E}}{\partial t} + \mu \mathbf{J} \quad (\text{A.12.9})$$

Consider the surface integral of Eq. (A.12.9) over an open area that includes a smooth boundary. The integral is:

$$\oint \mathbf{B} \cdot d\ell = \mu\varepsilon \int \frac{\partial \mathbf{E}}{\partial t} \cdot d\mathbf{S} + \mu \int \mathbf{J} \cdot d\mathbf{S} \quad (\text{A.12.10})$$

Let the dimension normal to the boundary become vanishingly small. In this limit, the open area becomes vanishingly small and, since \mathbf{E} is finite, the first term on the right side is vanishingly small, leaving:

$$\oint \mathbf{B} \cdot d\ell = \mu \int \mathbf{J} \cdot d\mathbf{S} = \mu I_S \quad (\text{A.12.11})$$

Symbol I_S represents the total electric current I that flows through the open area. In free space, there is no current and the line integral of the magnetic field intensity around the loop is equal to zero. Since surface currents may exist on conductors, the tangential component of a time varying magnetic field just off the surface of a conductor is equal in magnitude and perpendicular in direction to the current per unit length on the surface:

$$n \times \mathbf{B} = \mu I_S \quad (\text{A.12.12})$$

Summarizing boundary conditions:

Virtual Surface

$$n \times (\mathbf{B}_1 - \mathbf{B}_2) = 0; \quad n \cdot (\mathbf{B}_1 - \mathbf{B}_2) = 0 \quad (\text{A.12.13})$$

Conducting Surface

$$n \times \mathbf{B} = \mu I_S; \quad n \cdot \mathbf{B} = 0$$

Both field vectors are continuous through a virtual surface. On conducting surfaces the tangential component of the electric field intensity and the normal component of a time varying magnetic field intensity are both equal to zero. Just off the conducting surface, the normal component of the electric field intensity is equal to the surface charge density and the tangential component of the magnetic field is equal to the surface current density in amperes per meter.

13. Uniqueness

If, within a given boundary, a potential reduces to the correct value on the boundary, or to the correct normal derivative of the potential on that boundary, then that potential is unique. This theorem justifies the use of arbitrary solution methods so long as the resulting solution obeys Laplace's equation in the charge-free regions. No matter how the solution is obtained, if it satisfies these conditions the solution is unique.

Taking $\phi \nabla \phi$ to be a vector field and substituting into the divergence theorem gives:

$$\int \phi \nabla \phi \cdot d\mathbf{S} = \int \nabla \cdot (\phi \nabla \phi) dV = \int [(\nabla \phi)^2 + \phi \nabla^2 \phi] dV \quad (\text{A.13.1})$$

Since Laplace's equation is satisfied, the last term is equal to zero. Suppose ϕ_1 and ϕ_2 are different potentials that have either equal values of potential or normal derivatives thereof on every conductor in the field:

$$\int (\phi_1 - \phi_2) \nabla(\phi_1 - \phi_2) \cdot d\mathbf{S} = \int [\nabla(\phi_1 - \phi_2)]^2 dV = 0 \quad (\text{A.13.2})$$

Either equality at the conductors requires the surface integral to equal zero. Since the volume integral is equal to zero it follows that the integrand is equal to zero everywhere. Therefore the potential and/or the electric field intensity are equal everywhere in the field and, therefore, the functions are the same.

For time-dependent solutions, it is only necessary to substitute functions ψ_1 and ψ_2 of Sec. 1.12 into the divergence theorem and repeat the above procedure.

14. Spherical Shell Dipole

Calculations of electromagnetic effects about virtual shells commonly consider exterior effects but ignore interior ones. To establish the approximate magnitude of possible error, consider the interior-to-standing exterior energy ratio for an electric dipole. For this purpose, begin with a spherical shell of radius a that supports a surface electric charge density:

$$\rho(\theta, t) = \frac{q}{2\pi a^2} \cos \theta e^{i(\omega t - ka)} \tag{A.14.1}$$

This is the static and time varying charge combination that occurs by driving an originally uniformly charged sphere to its maximum extent as a dipole. The resulting electric dipole moment, (see Eq. (A.28.7)), is:

$$p_z = \frac{2qa}{3} e^{i(\omega t - ka)} \tag{A.14.2}$$

The time dependence of the change is associated with the surface current density:

$$I_s = -i \frac{qkc}{2\pi a} \sin \theta e^{i(\omega t - ka)} \hat{\theta} \tag{A.14.3}$$

The time varying charge and current densities create, respectively, electric and magnetic fields in both interior and exterior regions about the shell. The field forms follow from Eq. (1.12.9); all coefficients are equal to zero except those of order one and degree zero. The field components are:

$$\begin{aligned} E_{re} &= F \frac{2}{\sigma} h_1(\sigma) \cos \theta e^{i(\omega t - \sigma)} & E_{ri} &= G \frac{2}{\sigma} j_1(\sigma) \cos \theta e^{i(\omega t - \sigma)} \\ E_{\theta e} &= -F h_1^*(\sigma) \sin \theta e^{i(\omega t - \sigma)} & E_{\theta i} &= -G j_1^*(\sigma) \sin \theta e^{i(\omega t - \sigma)} \\ \eta H_{\phi e} &= i F h_1(\sigma) \sin \theta e^{i(\omega t - \sigma)} & \eta H_{\phi i} &= i G j_1(\sigma) \sin \theta e^{i(\omega t - \sigma)} \end{aligned} \tag{A.14.4}$$

F and G are complex field coefficients to be determined. Phase factor $\exp(-i ka)$ is added as a notational convenience.

Applying the field boundary conditions of Eqs. (A.12.6) and (A.12.13) gives:

$$\begin{aligned}\frac{\mathfrak{q}k}{4\pi\epsilon a} e^{i(\omega t - ka)} &= Fh_1(ka) - Gj_1(ka) \\ \frac{\mathfrak{q}k}{2\pi\epsilon a} e^{i(\omega t - ka)} &= Fh_1(ka) + Gj_1(ka)\end{aligned}\tag{A.14.5}$$

Solving for the coefficients gives:

$$F = \frac{3\mathfrak{q}}{8\pi\epsilon a^2} \frac{(ka)}{h_1(ka)} e^{i(\omega t - ka)} \quad G = \frac{\mathfrak{q}}{8\pi\epsilon a^2} \frac{(ka)}{j_1(ka)} e^{i(\omega t - ka)}\tag{A.14.6}$$

Inserting the coefficients into the fields gives:

Exterior:

$$\begin{aligned}\mathbf{E}_e &= \frac{3}{2} \left(\frac{\mathfrak{q}}{4\pi\epsilon a^2} \right) \left(\frac{ka}{h_1(ka)} \right) \left\{ \hat{\mathbf{r}} \frac{2}{\sigma} h_1(\sigma) \cos \theta - \hat{\theta} h_1(\sigma) \sin \theta \right\} e^{i(\omega t - \sigma)} \\ \eta \mathbf{H}_e &= \frac{3i}{2} \left(\frac{\mathfrak{q}}{4\pi\epsilon a^2} \right) \left(\frac{ka}{h_1(ka)} \right) \hat{\phi} h_1(\sigma) \sin \theta e^{i(\omega t - \sigma)}\end{aligned}\tag{A.14.7}$$

Interior:

$$\begin{aligned}\mathbf{E}_i &= \frac{1}{2} \left(\frac{\mathfrak{q}}{4\pi\epsilon a^2} \right) \left(\frac{ka}{j_1(ka)} \right) \left\{ \hat{\mathbf{r}} \frac{2}{\sigma} j_1(\sigma) \cos \theta - \hat{\theta} j_1(\sigma) \sin \theta \right\} e^{i(\omega t - \sigma)} \\ \eta \mathbf{H}_i &= \frac{i}{2} \left(\frac{\mathfrak{q}}{4\pi\epsilon a^2} \right) \left(\frac{ka}{j_1(ka)} \right) \hat{\phi} j_1(\sigma) \sin \theta e^{i(\omega t - \sigma)}\end{aligned}\tag{A.14.8}$$

The fields just off the surface of an emitter with ka much less than one are:

Exterior:

$$\begin{aligned}\mathbf{E}_e &= \frac{3}{2} \left(\frac{\mathfrak{q}}{4\pi\epsilon a^2} \right) \{ 2\hat{\mathbf{r}} \cos \theta + \hat{\theta} \sin \theta \} e^{i(\omega t - ka)} \\ \eta \mathbf{H}_e &= \frac{3}{2} \left(\frac{\mathfrak{q}}{4\pi\epsilon a^2} \right) (ka) \hat{\phi} \sin \theta e^{i(\omega t - ka)}\end{aligned}\tag{A.14.9}$$

Interior:

$$\begin{aligned}\mathbf{E} &= \left(\frac{\mathfrak{q}}{4\pi\epsilon a^2} \right) \{ \hat{\mathbf{r}} \cos \theta - \hat{\theta} \sin \theta \} e^{i(\omega t - ka)} \\ &= \left(\frac{\mathfrak{q}}{4\pi\epsilon a^2} \right) \hat{\mathbf{z}} e^{i(\omega t - ka)} \\ \eta \mathbf{H} &= \frac{i}{2} \left(\frac{\mathfrak{q}}{4\pi\epsilon a^2} \right) \sigma \hat{\phi} \sin \theta e^{i(\omega t - ka)}\end{aligned}\tag{A.14.10}$$

The time-average, outbound power density follows from Eq. (A.14.8):

$$\begin{aligned} N_r &= \frac{9}{8\eta} \left(\frac{q}{4\pi\epsilon a^2} \right)^2 \left| \frac{ka}{h_1(ka)} \right|^2 \operatorname{Re}(i h_1^*(\sigma) h_1^*(\sigma)) \sin^2 \theta \\ &\cong \frac{9}{8\eta} \left(\frac{q}{4\pi\epsilon a^2} \right)^2 \frac{(ka)^6}{\sigma^2} \sin^2 \theta \end{aligned} \quad (\text{A.14.11})$$

The approximate equality is after incorporating $ka \ll 1$.

The time-average energy density at each exterior point is:

$$\begin{aligned} w_T &= \frac{9}{16\epsilon} \left(\frac{q}{4\pi a^2} \right)^2 \left| \frac{ka}{h_1(ka)} \right|^2 \left\{ \frac{4}{\sigma^2} |h_1(\sigma)|^2 \cos^2 \theta \right. \\ &\quad \left. + [|h_1^*(\sigma)|^2 + |h_1(\sigma)|^2] \sin^2 \theta \right\} \\ w_T &\cong \frac{9}{16\epsilon} \left(\frac{q}{4\pi a^2} \right)^2 (ka)^6 \left\{ \left[\frac{4}{\sigma^6} + \frac{4}{\sigma^4} \right] \cos^2 \theta \right. \\ &\quad \left. + \left[\frac{2}{\sigma^2} + \frac{1}{\sigma^6} \right] \sin^2 \theta \right\} \end{aligned} \quad (\text{A.14.12})$$

By Sec. 3.11, in this case the source-associated energy density is equal to the energy density minus the energy density of the Poynting vector at each point. Combining Eqs. (A.14.11) and (A.14.12) gives the source-associated energy density:

$$w_S \cong \frac{9}{16\epsilon} \left(\frac{q}{4\pi a^2} \right)^2 (ka)^6 \left\{ \left(\frac{4}{\sigma^6} + \frac{4}{\sigma^4} \right) \cos^2 \theta + \frac{1}{\sigma^6} \sin^2 \theta \right\} \quad (\text{A.14.13})$$

Integrating over exterior space gives the total source associated standing energy:

$$W_S = \frac{3q^2}{32\pi\epsilon a} (1 + 2ka) \quad (\text{A.14.14})$$

The time-average interior energy density follows from Eq. (A.14.8):

$$w_I = \frac{1}{4\epsilon} \left[\frac{q}{8\pi a^2} \right]^2 \left\{ \left(4 - \frac{2\sigma^2}{5} \right) \cos^2 \theta + \left(4 + \frac{\sigma^2}{5} \right) \sin^2 \theta \right\} \quad (\text{A.14.15})$$

Integrating over interior space gives:

$$W_I = \left(\frac{q^2}{48\pi\epsilon a} \right) \left[1 + \frac{(ka)^2}{10} \right] \quad (\text{A.14.16})$$

Taking the ratio of Eq. (A.14.16) to Eq. (A.14.14) shows the ratio of the source-associated energies is:

$$W_I/W_S \cong 2/9 \quad (\text{A.14.17})$$

For the important case of a radiating dipole shell the often-ignored time-average interior stored energy is about 22% of the exterior source associated energy. So long as the region remains small the ratio is independent both of size and wavelength.

15. Gamma Functions

Products in which successive factors differ by one occur frequently in the formation of power series. If ℓ is an integer, such products may be expressed as special products of a certain number of integers, beginning with one. The factorial of integer ℓ is, by definition:

$$\ell! = 1 \cdot 2 \cdot 3 \cdots \ell \quad (\text{A.15.1})$$

This may be written in the compact form:

$$\ell! = \ell(\ell - 1)! \quad (\text{A.15.2})$$

The same symbolism is useful for noninteger numbers, ν . A similar equation is defined:

$$\nu! = \nu(\nu - 1)! \quad (\text{A.15.3})$$

Similarly:

$$\nu(\nu - 1)(\nu - 2) \cdots (\nu - m + 1) = \frac{\nu!}{(\nu - m)!} \quad (\text{A.15.4})$$

Let $f(\nu)$ be any function that satisfies the condition:

$$f(\nu) = \nu f(\nu - 1) \quad (\text{A.15.5})$$

Taking the ratio of Eqs. (A.15.5) to (A.15.3) shows that:

$$\phi(\nu) = \frac{f(\nu)}{\nu!} = \frac{f(\nu - 1)}{(\nu - 1)!} = \phi(\nu - 1) \quad (\text{A.15.6})$$

It follows that $\phi(\nu)$ is a periodic function of period ν .

Euler proposed that the definition of a noninteger factorial be:

$$\nu! = \int_0^{\infty} t^{\nu} e^{-t} dt \quad (\text{A.15.7})$$

Euler's definition is valid over the range:

$$-1 < \nu \leq 0 \quad (\text{A.15.8})$$

Factorial $\nu!$ can be evaluated for any value of ν using Eq. (A.15.3). For example, if $-2 < \nu < -1$ then $\nu!$ can be written

$$\nu! = \frac{(\nu + 1)!}{\nu + 1} = \frac{(\nu + 1)!(\nu + 2)!}{(\nu + 1)(\nu + 2)} = \frac{(\nu + 1)!(\nu + 2)! \cdots (\nu + n)!}{(\nu + 1)(\nu + 2) \cdots (\nu + n)} \quad (\text{A.15.9})$$

Equation (A.15.9) shows a simple pole exists for ν equal to a negative integer. Other results of Eq. (A.15.7) are that:

$$0! = 1 = 1! \quad (\text{A.15.10})$$

$$(-1/2)! = \sqrt{\pi} \quad (\text{A.15.11})$$

$$(-\nu)!(\nu - 1)! = \frac{\pi}{\sin(\pi\nu)} \quad (\text{A.15.12})$$

The Stirling formula for the approximate value of $\nu!$, in the limit of large values of ν , is:

$$\nu! = \left(\frac{\nu}{e}\right)^\nu \sqrt{2\pi\nu} \quad (\text{A.15.13})$$

A related and frequently recurring product form is with succeeding numbers that differ by two:

$$\nu(\nu - 2)(\nu - 4)(\nu - 6) \cdots$$

The series is denoted by the double factorial:

$$\nu!! = \nu(\nu - 2)(\nu - 4)(\nu - 6) \cdots \quad (\text{A.15.14})$$

It follows that for even and odd integers, respectively:

$$(2\ell)!! = 2^\ell(\ell)! \quad \text{and} \quad (2\ell + 1)!! = \frac{(2\ell + 1)!}{(2\ell)!!} \quad (\text{A.15.15})$$

The left and right equations of Eq. (A.15.15) for $\ell = 0$ show that:

$$(0)!! = 1 \quad \text{and} \quad (1)!! = 1 \quad (\text{A.15.16})$$

Although Eq. (A.15.15) is in indeterminate form for $\ell = -1$, evaluating the identity:

$$\frac{(\ell)!}{(\ell)!!} = (\ell - 1)!! \quad (\text{A.15.17})$$

For the special case of $\ell = 0$, Eq. (A.15.17) gives:

$$(-1)!! = 1 \quad (\text{A.15.18})$$

Table A.15.1 contains a listing of useful and selected sums involving factorials.

Table A.15.1. A table of sums over factorials.

$$\begin{aligned}
2 \sum_{m \in 0}^{\ell} \frac{(\ell+m-1)!(\ell-m-1)!!}{(\ell+m)!(\ell-m)!!} U(m) \delta(\ell+m, 2q) &= 1 \\
\sum_{m \in 1}^{\ell} \frac{(-1)^{(\ell-m)/2} m(\ell+m-1)!(\ell-m-1)!!}{(\ell+m)!(\ell-m)!!} \delta(\ell+m, 2q) &= \frac{\ell!!}{(\ell-1)!!} \\
2 \sum_{m \in 2}^{\ell} \frac{(-1)^{(\ell-m)/2} m^2(\ell+m-1)!(\ell-m-1)!!}{\ell(\ell+1)(\ell+m)!(\ell-m)!!} \delta(\ell+m, 2q) &= \frac{(\ell-1)!!}{\ell!!} \\
4 \sum_{m=0}^{\ell-1} \frac{(\ell+m)!(\ell-m)!!}{\ell(\ell+1)(\ell+m-1)!(\ell-m-1)!!} U(m) \delta(\ell+m, 2q+1) &= 1 \\
4 \sum_{m=0}^{\ell} \frac{m^2(\ell+m-1)!(\ell-m-1)!!}{\ell(\ell+1)(\ell+m)!(\ell-m)!!} \delta(\ell+m, 2q) &= 1 \\
8 \sum_{m \in 0}^{\ell} \frac{(-1)^{(\ell-m-1)/2} (\ell+m)!(\ell-m)!!}{\ell(\ell+1)(\ell+m-1)!(\ell-m-1)!!} \delta(\ell+m, 2q+1) U(m) &= \frac{\ell!!}{(\ell-1)!!} \\
2 \sum_{m \in 1}^{\ell} \frac{(-1)^{(\ell-m-1)/2} m(\ell+m)!(\ell-m)!!}{\ell(\ell+1)(\ell+m-1)!(\ell-m-1)!!} \delta(\ell+m, 2q+1) &= \frac{(\ell-1)!!}{\ell!!} \\
2 \sum_{s=0}^{(\ell-m-1)/2} \frac{\ell(-1)^s \delta(\ell+m, 2q+1)}{(\ell+m+2s+1)!(\ell-m-2s-1)!!} &= \frac{1}{(\ell+m-1)!(\ell-m-1)!!}
\end{aligned}$$

16. Azimuth Angle Trigonometric Functions

Solutions of Eq. (1.11.11) are trigonometric functions:

$$\Phi(\phi) = \sum_m [C_m \cos(m\phi) + D_m \sin(m\phi)] \quad (\text{A.16.1})$$

An equally satisfactory solution is:

$$\Phi(\phi) = \sum_m [\hat{C}_m e^{jm\phi} + \hat{D}_m e^{-jm\phi}] \quad (\text{A.16.2})$$

By definition $j^2 = (-1)$. For cases of interest here, the azimuth angle occupies the full range of angle from 0 through 2π . This condition requires the solution to satisfy the relationship:

$$\Phi(\phi) = \Phi(\phi + 2\pi) \quad (\text{A.16.3})$$

Equations (A.16.1) through (A.16.3) are jointly satisfied only if m represents the full range of positive integers, including zero.

The trigonometric functions form an orthogonal set. Trigonometric identities show that:

$$\int_0^{2\pi} \cos(m\phi) \cos(n\phi) d\phi = \frac{1}{2} \int_0^{2\pi} d\phi [\cos[(m-n)\phi] + \cos[(m+n)\phi]] \quad (\text{A.16.4})$$

Evaluating the integral on the right gives:

$$\int_0^{2\pi} \cos(m\phi) \cos(n\phi) d\phi = \left(\frac{\sin[(m-n)\phi]}{2(m-n)} + \frac{\sin[(m+n)\phi]}{2(m+n)} \right) \Big|_0^{2\pi} \quad (\text{A.16.5})$$

Since both m and n are positive integers, the second term on the right of Eq. (A.16.5) is always zero; the first term is also positive unless $m = n$, for which case the result is indeterminate. Evaluation may be accomplished by either evaluating the indeterminate or by substituting into the integrand the identity:

$$\cos^2(m\phi) \equiv \frac{1}{2} [1 + \cos(2m\phi)] \quad (\text{A.16.6})$$

Integrating Eq. (A.16.6) gives:

$$\int_0^{2\pi} d\phi \cos^2(m\phi) = \frac{1}{2} \int_0^{2\pi} d\phi [1 + \cos(2m\phi)] = \pi \quad (\text{A.16.7})$$

Combining Eqs. (A.16.5) through (A.16.7):

$$\int_0^{2\pi} \cos(m\phi) \cos(n\phi) d\phi = \pi \delta(m, n) \quad (\text{A.16.8})$$

The Kronecker delta function is indicated by $\delta(m, n)$. By definition:

$$\delta(m, n) = \begin{cases} 1 & \text{if } m = n \\ 0 & \text{if } m \neq n \end{cases} \quad (\text{A.16.9})$$

It follows in a similar way that:

$$\int_0^{2\pi} \sin(m\phi) \sin(n\phi) d\phi = \pi \delta(m, n) \quad (\text{A.16.10})$$

$$\int_0^{2\pi} \sin(m\phi) \cos(n\phi) d\phi = 0 \quad (\text{A.16.11})$$

Combining Eqs. (A.16.8) through (A.16.11) gives:

$$\int_0^{2\pi} e^{j(m-n)\phi} d\phi = 2\pi \delta(m, n) \quad (\text{A.16.12})$$

For example, Eq. (A.16.12) may be used to evaluate the product function:

$$\begin{aligned} \int_0^{2\pi} e^{j(m-m')\phi} \sin \phi \, d\phi &= \frac{1}{2j} \int_0^{2\pi} (e^{j(m'-m+1)\phi} - e^{j(m'-m-1)\phi}) \, d\phi \\ &= \pi j [\delta(m', m+1) - \delta(m', m-1)] \end{aligned} \quad (\text{A.16.13})$$

It is often convenient to express functions in terms of the order of trigonometric functions. The formulas for going from power to order follow directly from the geometry; all possible combinations are given by the four sums:

$$\cos^{2\ell} \phi \equiv \frac{1}{2^{2\ell}} \left\{ \sum_{k=0}^{\ell-1} \frac{2(2\ell)!}{(2\ell-k)!k!} \cos[2(\ell-k)\phi] + \frac{(2\ell)!}{(\ell!)^2} \right\} \quad (\text{A.16.14})$$

$$\sin^{2\ell} \phi \equiv \frac{1}{2^{2\ell}} \left\{ \sum_{k=0}^{\ell-1} (-1)^{\ell-k} \frac{2(2\ell)!}{(2\ell-k)!k!} \cos[2(\ell-k)\phi] + \frac{(2\ell)!}{(\ell!)^2} \right\} \quad (\text{A.16.15})$$

$$\cos^{2\ell-1} \phi \equiv \frac{4}{2^{2\ell}} \left\{ \sum_{k=0}^{\ell-1} \frac{(2\ell-1)!}{(2\ell-k-1)!k!} \cos[(2\ell-2k-1)\phi] \right\} \quad (\text{A.16.16})$$

$$\sin^{2\ell-1} \phi \equiv \frac{4}{2^{2\ell}} \left\{ \sum_{k=0}^{\ell-1} (-1)^{\ell-k-1} \frac{(2\ell-1)!}{(2\ell-k-1)!k!} \sin[(2\ell-k-1)\phi] \right\} \quad (\text{A.16.17})$$

An expansion for $1/(\sin \phi)$ is necessary to accomplish needed calculations. To form the expansion, note that since $1/(\sin \phi)$ is an odd function of ϕ it is expressible as:

$$\frac{1}{\sin \phi} = \sum_{s=1}^{\infty} A_s \sin(2s-1)\phi \quad (\text{A.16.18})$$

To evaluate coefficients A_s , multiply Eq. (A.16.18) by $\sin(2p-1)\phi$ and integrate over the full range of the variable. The result is:

$$\begin{aligned} \int_0^{2\pi} d\phi \frac{\sin(2p-1)\phi}{\sin \phi} &= \sum_{s=1}^{\infty} A_s \int_0^{2\pi} d\phi \sin[(2s-1)\phi] \sin[(2p-1)\phi] \\ &= \pi A_p \delta(p, s) \end{aligned} \quad (\text{A.16.19})$$

The left side of Eq. (A.16.19) is a periodic trigonometric function for all terms except $p = 1$ and all periodic terms integrate to zero. This leaves:

$$\int_0^{2\pi} d\phi \frac{\sin(2p-1)\phi}{\sin \phi} = 2\pi \quad (\text{A.16.20})$$

Substituting back into Eq. (A.16.18):

$$\frac{1}{\sin \phi} = 2 \sum_{s=1}^{\infty} \sin(2s-1)\phi \quad (\text{A.16.21})$$

The corresponding sum with cosines replacing sines is equal to zero:

$$\sum_{s=0}^{\infty} \cos[(2s-1)\phi] = 0 \quad (\text{A.16.22})$$

It follows that:

$$\frac{1}{\sin \phi} = 2j \sum_{s=0}^{\infty} e^{-j(2s+1)\phi} \quad (\text{A.16.23})$$

17. Zenith Angle Legendre Functions

The easiest way to obtain the general solution of Eq. (1.11.10) is to first solve the special case $m = 0$, for which case the equation is:

$$\frac{d^2\Theta}{d\theta^2} + \cot \theta \frac{d\Theta}{d\theta} + \nu(\nu+1)\Theta = 0 \quad (\text{A.17.1})$$

The character of separation constant ν depends upon the boundary conditions applicable to the region in which the equation is applied. In the case of spherical waves in free space, for example, ν is an integer, and denoted by $\nu = \ell$. For lossless waves in conical structures ν is real and noninteger. If there is loss, ν is imaginary. In this book since only lossless problems are considered ν is real in all cases.

Since Eq. (A.17.1) contains a singularity on the polar axes, the character of the functions $\Theta(\theta)$ in the region away from the axes are of special interest. Rather than go directly to a solution, consider first the solution form in the region of interest. A useful substitution is:

$$\Theta = \frac{1}{(\sin \theta)^{1/2}} \tilde{\Theta} \quad (\text{A.17.2})$$

Differentiating gives:

$$\begin{aligned} \frac{d\Theta}{d\theta} &= \frac{1}{(\sin \theta)^{1/2}} \frac{d\tilde{\Theta}}{d\theta} - \frac{\cos \theta}{2(\sin \theta)^{3/2}} \tilde{\Theta} \\ \frac{d^2\Theta}{d\theta^2} &= \frac{1}{(\sin \theta)^{1/2}} \frac{d^2\tilde{\Theta}}{d\theta^2} - \frac{\cos \theta}{(\sin \theta)^{3/2}} \frac{d\tilde{\Theta}}{d\theta} + \left[\frac{3 \cos^2 \theta}{4(\sin \theta)^{5/2}} + \frac{1}{2(\sin \theta)^{1/2}} \right] \tilde{\Theta} \end{aligned} \quad (\text{A.17.3})$$

Combining Eqs. (A.17.1) through (A.17.3) gives:

$$\frac{d^2\tilde{\Theta}}{d\theta^2} + \left\{ \left(\nu + \frac{1}{2} \right)^2 + \frac{1}{4}(1 + \cot^2\theta) \right\} \tilde{\Theta} = 0 \quad (\text{A.17.4})$$

For θ near $\pi/2$, $\cot^2\theta$ is much less than one and Eq. (A.17.4) is nearly equal to:

$$\frac{d^2\tilde{\Theta}}{d\theta^2} + \left\{ \left(\nu + \frac{1}{2} \right)^2 + \frac{1}{4} \right\} \tilde{\Theta} = 0 \quad (\text{A.17.5})$$

Solutions of Eq. (A.17.5) are:

$$\Theta(\theta) = \frac{1}{(\sin\theta)^{1/2}} [A_\nu \cos(\kappa_\nu\theta) + B_\nu \sin(\kappa_\nu\theta)] \quad (\text{A.17.6})$$

By definition:

$$\kappa_\nu = \left[\left(\nu + \frac{1}{2} \right)^2 + \frac{1}{4} \right]^{1/2} \quad (\text{A.17.7})$$

Near the equator the zenith angle functions are trigonometric functions of $(\kappa_\nu\theta)$ normalized by the square root of $\sin\theta$. The interval over which Eq. (A.17.6) is valid increases with increasing values of ν .

To examine the solution near its singularity, begin near the positive z -axis, where

$$\cot\theta \cong \frac{1}{\theta} \quad (\text{A.17.8})$$

Equation (A.17.1) has the form:

$$\frac{d^2\Theta}{d\theta^2} + \frac{1}{\theta} \frac{d\Theta}{d\theta} + \nu(\nu+1)\Theta = 0 \quad (\text{A.17.9})$$

Equation (A.17.9) is the cylindrical Bessel equation. To begin the solution process, make the definition:

$$\beta = [\nu(\nu+1)]^{1/2} \quad (\text{A.17.10})$$

The two independent solutions of Eq. (A.17.9) may be written as:

$$\Theta(\theta) = A_\nu J_0(\beta\theta) + B_\nu Y_0(\beta\theta) \quad (\text{A.17.11})$$

$J_0(\beta\theta)$ and $Y_0(\beta\theta)$ represent, respectively, cylindrical Bessel and Neumann functions of zero order. In the limit as θ goes to zero, $J_0(\beta\theta)$ goes to unity

and $Y_0(\beta\theta)$ becomes logarithmically singular:

$$\Theta(0) = \hat{C}_\nu Y_0(0) \quad (\text{A.17.12})$$

By symmetry, near the negative z -axis the function takes the same form. The local solution is:

$$\Theta(\pi - \theta) = \hat{A}_\nu Y_0(\beta(\pi - \theta)) + \hat{B}_\nu J_0(\beta(\pi - \theta)) \quad (\text{A.17.13})$$

Combining gives:

$$\Theta(\pi) = \hat{D}_\nu J_0(0) + \hat{C}_\nu Y_0(0) \quad (\text{A.17.14})$$

It follows that if one solution of Eq. (A.17.1) is $P_\nu(\cos\theta)$, the other is $P_\nu(-\cos\theta)$. The first solution is regular on the positive z -axis and singular on the negative z -axis and the second solution is singular on the positive z -axis and regular on the negative z -axis. Both functions are periodic, (see Eq. (A.17.6)), in the center region. The full solution is:

$$\Theta(\theta) = A_\nu P_\nu(\cos\theta) + B_\nu P_\nu(-\cos\theta) \quad (\text{A.17.15})$$

For values of m different from zero it is convenient to rewrite Eq. (A.17.1) by introducing the variable χ where:

$$\chi = \frac{1}{2}(1 - \cos\theta) = \sin^2(\theta/2) \quad (\text{A.17.16})$$

Derivatives are:

$$\begin{aligned} \frac{d\Theta}{d\chi} &= \frac{d\Theta}{d(\cos\theta)} \frac{d(\cos\theta)}{d\chi} = -2 \frac{d\Theta}{d(\cos\theta)} \\ \frac{d^2\Theta}{d\chi^2} &= \frac{d^2\Theta}{d(\cos\theta)^2} \left[\frac{d(\cos\theta)}{d\chi} \right]^2 + \frac{d\Theta}{d(\cos\theta)} \frac{d^2(\cos\theta)}{d\chi^2} \end{aligned} \quad (\text{A.17.17})$$

Combining Eqs. (A.17.16) and (A.17.17) with Eq. (A.17.1) gives:

$$\chi(1 - \chi) \frac{d^2\Theta}{d\chi^2} + (1 - 2\chi) \frac{d\Theta}{d\chi} + \nu(\nu + 1)\Theta = 0 \quad (\text{A.17.18})$$

A power series expansion results in:

$$\begin{aligned} \Theta(\chi) &= \sum_{j=0}^{\infty} a_j \chi^j \\ \frac{d}{d\chi} \Theta(\chi) &= \sum_{j=0}^{\infty} a_j j \chi^{j-1} \\ \frac{d^2}{d\chi^2} \Theta(\chi) &= \sum_{j=0}^{\infty} a_j j(j-1) \chi^{j-2} \end{aligned} \quad (\text{A.17.19})$$

Combining Eqs. (A.17.18) and (A.17.19) gives:

$$\sum_{j=0}^{\infty} [(j+1)^2 a_{j+1} - j(j+1)a_j + \nu(\nu+1)a_j] \chi^j = 0 \quad (\text{A.17.20})$$

Since Eq. (A.17.20) is an identity in χ , the coefficient of each power of χ is separately equal to zero. It results in the recursion relationship:

$$\frac{a_{j+1}}{a_j} = \frac{j(j+1) - \nu(\nu+1)}{(j+1)^2} \quad (\text{A.17.21})$$

If ν is an integer, the numerator of Eq. (A.17.21) is equal to zero at $\nu = j$ and the series terminates. Substituting Eq. (A.17.21) in the first series of Eq. (A.17.19) results in the solution:

$$P_\nu(\cos \theta) = \sum_{j=0}^{\infty} \frac{(-1)^j (\nu+j)!}{(j)!^2 (\nu-j)!} \sin^{2j} \left(\frac{\theta}{2} \right) \quad (\text{A.17.22})$$

$P_\nu(-\cos \theta)$ is also a solution; changing the sign in Eq. (A.17.17) gives:

$$\chi = \frac{1}{2}(1 + \cos \theta) = \cos^2 \left(\frac{\theta}{2} \right) \quad (\text{A.17.23})$$

Combining Eqs. (A.17.22) and (A.17.23) gives the second solution:

$$P_\nu(-\cos \theta) = \sum_{j=0}^{\infty} \frac{(-1)^j (\nu+j)!}{(j)!^2 (\nu-j)!} \cos^{2j} \left(\frac{\theta}{2} \right) \quad (\text{A.17.24})$$

Neither Eq. (A.17.22) nor (A.17.24) is fully an even or odd function of θ . Since it is convenient to work with equations of definite parity, it is convenient to define the new functions:

$$\begin{aligned} L_\nu(\cos \theta) &= \frac{1}{2} \{P_\nu(\cos \theta) + P_\nu(-\cos \theta)\} \\ M_\nu(\cos \theta) &= \frac{1}{2} \{P_\nu(\cos \theta) - P_\nu(-\cos \theta)\} \end{aligned} \quad (\text{A.17.25})$$

The functional symmetry is:

$$L_\nu(\cos \theta) = L_\nu(-\cos \theta); \quad M_\nu(\cos \theta) = -M_\nu(-\cos \theta) \quad (\text{A.17.26})$$

Since the regions of convergence for $P_\nu(\cos \theta)$ are $-1 < \cos \theta \leq 1$ or $0 \leq \theta < \pi$, the region of convergence for L_ν and M_ν are $0 < \theta < \pi$.

18. Legendre Polynomials

To solve problems with the z -axis included in the region where a solution is necessary, all functions must remain bounded at the endpoints: $0 \leq \theta \leq \pi$. This happens only if separation constant n is an integer and the series solution of Eq. (A.17.21) terminates. For that case both Eqs. (A.17.22) and (A.17.24) remain bounded on both the $\pm z$ -axes, but are not independent. Since the product $\ell(\ell+1)$ is the same for $\ell = n$ as it is for $\ell = -(n+1)$, solutions are the same for the range of integers respectively from 0 to $+\infty$ and from -1 to $-\infty$. Therefore, only positive values of ℓ need be considered.

To characterize Legendre polynomials, it is more convenient to redo the expansion than to work with the existing solutions. For this purpose, rewrite Eq. (A.17.1) by replacing noninteger ν by integer ℓ and defining $\chi = \cos \theta$, to obtain:

$$(1 - \chi^2) \frac{d^2\Theta}{d\chi^2} - 2\chi \frac{d\Theta}{d\chi} + \ell(\ell + 1)\Theta = 0 \quad (\text{A.18.1})$$

The power series expansion is:

$$\begin{aligned} \Theta(\chi) &= \sum_{j=0}^{\infty} a_j \chi^j \\ \frac{d\Theta(\chi)}{d\chi} &= \sum_{j=0}^{\infty} a_j j \chi^{j-1} \\ \frac{d^2\Theta(\chi)}{d\chi^2} &= \sum_{j=0}^{\infty} a_j j(j-1) \chi^{j-2} \end{aligned} \quad (\text{A.18.2})$$

Combining Eqs. (A.18.1) and (A.18.2) gives:

$$\sum_{j=0}^{\infty} [(j+1)(j+2)a_{j-2} - j(j+1)a_j + \ell(\ell+1)a_j] \chi^j = 0 \quad (\text{A.18.3})$$

Since Eq. (A.18.1) is an identity in χ it follows that:

$$\frac{a_{j+2}}{a_j} = \frac{j(j+1) - \ell(\ell+1)}{(j+1)(j+2)} \quad (\text{A.18.4})$$

Substituting Eq. (A.18.4) the expansion into the first part of Eq. (A.18.2) gives:

$$\Theta_{\ell}(\chi) = a_0 \sum_{j=0}^{\infty} \frac{(-1)^j \chi^{2j} (\ell)!! (\ell + 2j - 1)!!}{(2j)! (\ell - 1)!! (\ell - 2j)!!} \quad (\text{A.18.5})$$

Values are:

$$\Theta_0(\chi) = a_0; \quad \Theta_1(\chi) = a_0(1 - 3\chi^2); \quad \Theta_2(\chi) = a_0 \left(1 - 10\chi^2 + \frac{35}{3}\chi^4 \right) \tag{A.18.6}$$

a_0 is an arbitrary constant and is redefined for each value of ℓ to make $\Theta_\ell(0) = 1$. With that definition, functions $\Theta_\ell(\chi)$ are defined to be Legendre polynomials of the first kind, and indicated by $P_\ell(\cos \theta)$. Therefore $P_\ell(\chi)$ is given by the series:

$$P_\ell(\chi) = \frac{1}{2^\ell} \sum_{s=0}^{[\ell/2]} \frac{(-1)^s}{s!} \frac{(2\ell - 2s)!}{(\ell - s)!(\ell - 2s)!} \chi^{\ell - 2s} \tag{A.18.7}$$

The symbol $[\ell/2]$ indicates the largest integer contained in $\ell/2$. From Eq. (A.18.7), it follows that:

$$P_\ell(1) = 1; \quad P_{2\ell+1}(0) = 0; \quad P_{2\ell}(0) = (-1)^\ell \frac{(2\ell-1)!!}{(2\ell)!!};$$

$$P_\ell(-\chi) = (-1)^\ell P_\ell(\chi)$$

Values of the important functional combinations on the axes are shown in Table A.18.1.

For even values of ℓ , the expansion may be written:

$$P_\ell(\chi) = \frac{1}{2^\ell (\ell)!} \frac{d^\ell}{d\chi^\ell} \sum_{s=0}^{\ell} \frac{(-1)^s (\ell)!}{(s)!(\ell - s)!} \chi^{2\ell - 2s} \tag{A.18.8}$$

The binomial expansion is:

$$(\chi^2 - 1)^\ell = \sum_{s=0}^{\ell} \frac{(-1)^s (\ell)!}{(s)!(\ell - s)!} \chi^{2\ell - 2s} \tag{A.18.9}$$

Table A.18.1. Values of selected functions on the axes.

| | $P_\ell(\cos \theta)$ | $\frac{dP_\ell^1(\cos \theta)}{d\theta}$ | $\frac{P_\ell^1(\cos \theta)}{\sin \theta}$ |
|--------------------------|---|---|---|
| $\theta = 0$ | 1 | $\frac{1}{2}\ell(\ell + 1)$ | $\frac{1}{2}\ell(\ell + 1)$ |
| $\theta = \pi$ | $(-1)^\ell$ | $\frac{1}{2}\ell(\ell + 1)(-1)^{(\ell+1)/2}$ | $\frac{1}{2}\ell(\ell + 1)(-1)^{(\ell-1)/2}$ |
| $\theta = \frac{\pi}{2}$ | $i^\ell \frac{(\ell - 1)!!}{\ell!!} \delta(2q, \ell)$ | $i^\ell \frac{(\ell + 1)!!}{(\ell - 2)!!} \delta(2q, \ell)$ | $i^{\ell-1} \frac{(\ell)!!}{(\ell - 1)!!} \delta(2q + 1, \ell)$ |

Combining results gives another expression for Legendre polynomials:

$$P_\ell(\chi) = \frac{1}{2^\ell(\ell)!} \frac{d^\ell}{d\chi^\ell} (\chi^2 - 1)^\ell \quad (\text{A.18.10})$$

Equation (A.18.10) is the Rodrigues formula for Legendre polynomials.

Comparison using Eqs. (A.17.27) and (A.18.9) shows, for integer orders:

$$L_{2\ell}(\chi) = P_{2\ell}(\chi); \quad M_{2\ell+1}(\chi) = P_{2\ell+1}(\chi) \quad (\text{A.18.11})$$

The second integer-order solution to Eq. (A.18.1) is commonly defined as:

$$Q_\nu(\chi) = \frac{\pi}{2 \sin(\nu\pi)} [P_\nu(\chi) \cos(\nu\pi) - P_\nu(-\chi)] \quad (\text{A.18.12})$$

$Q_\nu(\chi)$ is obviously a solution of the Legendre differential equation and, when ν is equal to integer ℓ ; it is in indeterminate form. Differentiating numerator and denominator then letting ν become an integer:

$$\begin{aligned} Q_\ell(\chi) &= \lim_{\nu \rightarrow \ell} \frac{1}{2 \cos(\nu\pi)} \left[-\pi \sin(\nu\pi) P_\nu(\chi) + \cos(\nu\pi) \frac{dP_\nu(\chi)}{d\nu} - \frac{dP_\nu(-\chi)}{d\nu} \right] \\ &= \frac{1}{2} \left\{ \frac{dP_\nu(\chi)}{d\nu} - \frac{dP_\nu(-\chi)}{d\nu} \right\}_{\nu=\ell} \end{aligned} \quad (\text{A.18.13})$$

Using Eq. (A.18.13), the functions at the lowest three orders are:

$$\begin{aligned} Q_0(\chi) &= \ln[\cot(\theta/2)] \\ Q_1(\chi) &= (\cos \theta) \ln\left(\cot \frac{\theta}{2}\right) - 1 \\ Q_2(\chi) &= \frac{1}{2}(3 \cos^2 \theta - 1) \ln\left(\cot \frac{\theta}{2}\right) - \frac{3}{2} \cos \theta \end{aligned} \quad (\text{A.18.14})$$

Comparison with the noninteger functions, Eq. (A.18.12), shows that:

$$\begin{aligned} Q_{2\ell}(\chi) &= \left. \frac{\partial M_\nu(\chi)}{\partial \nu} \right|_{\nu \Rightarrow 2\ell} \\ Q_{2\ell+1}(\chi) &= \left. \frac{\partial L_\nu(\chi)}{\partial \nu} \right|_{\nu \Rightarrow 2\ell+1} \end{aligned} \quad (\text{A.18.15})$$

In the remainder of this book we are concerned only with the zero-order function, $Q_0(\chi)$.

19. Associated Legendre Functions

Associated Legendre functions are solutions for the extended case $m > 0$. The Legendre differential equation, Eq. (1.11.10), may be rewritten as:

$$(1 - \chi^2) \frac{d^2\Theta}{d\chi^2} - 2\chi \frac{d\Theta}{d\chi} + \left[\nu(\nu + 1) - \frac{m^2}{(1 - \chi^2)} \right] \Theta = 0 \quad (\text{A.19.1})$$

Solutions are most easily obtained by starting with the $m = 0$ equation and differentiating m times to obtain:

$$(1 - \chi^2) \frac{d^{m+2}\Theta}{d\chi^{m+2}} - 2(m+1)\chi \frac{d^{m+1}\Theta}{d\chi^{m+1}} + [\nu(\nu + 1) - m(m+1)] \frac{d^m\Theta}{d\chi^m} = 0 \quad (\text{A.19.2})$$

Introducing construction function $W(\theta)$ and solving for the first two derivatives:

$$\begin{aligned} \Theta(\theta) &= W(\theta) \sin^m \theta \\ \frac{d\Theta}{d\chi} &= \frac{dW}{d\chi} \sin^m \theta - mW \sin^{m-2} \theta \cos \theta \\ \frac{d^2\Theta}{d\chi^2} &= \frac{d^2W}{d\chi^2} \sin^m \theta - 2m \frac{dW}{d\chi} \sin^{m-2} \theta \cos \theta \\ &\quad + m(m-2)W \sin^{m-4} \theta \cos^2 \theta - mW \sin^{m-2} \theta \end{aligned} \quad (\text{A.19.3})$$

Substituting Eq. (A.19.3) into Eq. (A.19.1) for the special case $m = 0$ results in:

$$\frac{d^2W}{d\chi^2} \sin^2 \theta - 2(m+1) \frac{dW}{d\chi} \cos \theta + [\nu(\nu + 1) - m(m+1)]W = 0 \quad (\text{A.19.4})$$

For the special case where $\nu = \ell$, an integer, comparison of Eqs. (A.19.2) and (A.19.4) shows that W is given by:

$$W_\ell(\theta) = \frac{d^m P_\ell(\cos \theta)}{d\chi^m} \quad (\text{A.19.5})$$

Since Eq. (A.19.5) satisfies the associated Legendre differential equation, the solution of that equation is:

$$\Theta(\theta) = P_\ell^m(\cos \theta) = \sin^m \theta \frac{d^m P_\ell(\cos \theta)}{d\chi^m} \quad (\text{A.19.6})$$

The equality holds for all integer orders, ℓ , and degrees, m . Combining Eq. (A.19.6) with the Rodrigues formula shows that the corresponding expression for associated Legendre functions is:

$$P_\ell^m(\chi) = \frac{1}{(2\ell)!!} (1 - \chi^2)^{m/2} \frac{d^{\ell+m}}{d\chi^{\ell+m}} (\chi^2 - 1)^\ell \quad (\text{A.19.7})$$

20. Orthogonality

Integral relationships for products of Legendre polynomials follow directly from the differential equation, Eq. (A.19.1), for integer orders. Multiplying the differential equation by another Legendre polynomial of the same degree but unspecified order gives:

$$\int_{-1}^1 P_n^m(\chi) \left\{ \frac{d}{d\chi} \left[(1 - \chi^2) \frac{d^2 P_\ell^m}{d\chi^2} \right] + \left[\ell(\ell + 1) - \frac{m^2}{(1 - \chi^2)} \right] P_\ell^m \right\} d\chi = 0 \quad (\text{A.20.1})$$

To evaluate the left side, integrate the first term once by parts. The result is:

$$\int_{-1}^1 \left\{ (1 - \chi^2) \frac{dP_\ell^m}{d\chi} \frac{dP_n^m}{d\chi} + \left[\ell(\ell + 1) - \frac{m^2}{(1 - \chi^2)} \right] P_\ell^m P_n^m \right\} d\chi = 0 \quad (\text{A.20.2})$$

Next exchange positions of ℓ and n , repeat the process, and subtract the second integral from the first. The result is:

$$[\ell(\ell + 1) - n(n + 1)] \int_{-1}^1 P_\ell^m(\chi) P_n^m(\chi) d\chi = 0 \quad (\text{A.20.3})$$

The result shows that the associated Legendre polynomials form an orthogonal set.

To evaluate the integral with $\ell = n$, put I_1 equal to the integral:

$$I_1 = \int_{-1}^1 [P_\ell^m(\chi)]^2 d\chi \quad (\text{A.20.4})$$

Combining Eqs. (A.19.7) and (A.20.4):

$$I_1 = \frac{(-1)^m}{[(2\ell)!!!]^2} \int_{-1}^1 d\chi \frac{d^{\ell+m}}{d\chi^{\ell+m}} (\chi^2 - 1)^\ell \left[(\chi^2 - 1)^m \frac{d^{\ell+m}}{d\chi^{\ell+m}} (\chi^2 - 1)^\ell \right] \quad (\text{A.20.5})$$

Integrating by parts $\ell + m$ times leaves:

$$I_1 = \frac{1}{[(2\ell)!!!]^2} \int_{-1}^1 d\chi \left\{ (1 - \chi^2)^\ell \frac{d^{\ell+m}}{d\chi^{\ell+m}} \left[(\chi^2 - 1)^m \frac{d^{\ell+m}}{d\chi^{\ell+m}} (\chi^2 - 1)^\ell \right] \right\} \quad (\text{A.20.6})$$

Only the highest power of χ survives the indicated differentiation operations:

$$\begin{aligned} \frac{d^{\ell+m}}{d\chi^{\ell+m}} \left[(\chi^2 - 1)^m \frac{d^{\ell+m}}{d\chi^{\ell+m}} (\chi^2 - 1)^\ell \right] &= \frac{d^{\ell+m}}{d\chi^{\ell+m}} \left[\chi^{2m} \frac{d^{\ell+m}}{d\chi^{\ell+m}} \chi^{2\ell} \right] \\ &= \frac{(2\ell)!}{(\ell - m)!} \frac{d^{\ell+m}}{d\chi^{\ell+m}} \chi^{\ell+m} = \frac{(2\ell)!(\ell + m)!}{(\ell - m)!} \end{aligned} \quad (\text{A.20.7})$$

Combining Eqs. (A.20.6) and (A.20.7) leaves:

$$I_1 = \frac{(2\ell)!(\ell+m)!}{[(2\ell)!!]^2(\ell-m)!} \int_{-1}^1 d\chi (1-\chi^2)^\ell \quad (\text{A.20.8})$$

Using the binomial expansion, Eq. (A.18.9), and integrating:

$$I_1 = \frac{2(-1)^\ell(2\ell-1)!!(\ell+m)!}{(2\ell)!!(\ell-m)!} \sum_{s=0}^{\ell} \frac{(-1)^s \ell!}{s!(\ell-s)!(2\ell-2s+1)} \quad (\text{A.20.9})$$

The sum may be written in closed form as:

$$I_1 = \frac{2}{(2\ell+1)} \frac{(\ell+m)!}{(\ell-m)!} \quad (\text{A.20.10})$$

Combining Eqs. (A.20.3) and (A.20.10) gives the orthogonality relationship for associated Legendre polynomials:

$$I_1 = \int_{-1}^1 P_\ell^m(\chi) P_n^m(\chi) d\chi = \frac{2}{(2\ell+1)} \frac{(\ell+m)!}{(\ell-m)!} \delta(\ell, n) \quad (\text{A.20.11})$$

A similar integral, the value of which follows after a slight extension of the above, is:

$$I_2 = \int_{-1}^1 P_\ell^m(\chi) P_\ell^{m+2s}(\chi) d\chi = (-1)^s \frac{2}{(2\ell+1)} \frac{(\ell+m)!}{(\ell-m-2s)!} \quad (\text{A.20.12})$$

21. Recursion Relationships

It is helpful to compile a table of identities involving associated Legendre polynomials. A convenient starting point for determining the recursion relationships is Eq. (A.18.7). For the case that ℓ is odd the upper limit is $(\ell-1)/2$. Substituting $p = (\ell-1-2s)/2$ into the equation yields:

$$P_\ell(\chi) = \frac{\chi(-1)^{(\ell-1)/2}}{2^\ell} \sum_{p=0}^{(\ell-1)/2} \frac{(-1)^p (\ell+1+2p)!}{(2p+1)! \left(\frac{\ell-1-2p}{2}\right)! \left(\frac{\ell+1+2p}{2}\right)!} \chi^{\ell-2s} \quad (\text{A.21.1})$$

Rewrite the equation as:

$$P_\ell(\chi) = (-1)^{(\ell-1)/2} \frac{(\ell)!!}{(\ell-1)!!} \sum_{s=0}^{(\ell-1)/2} \frac{(-1)^s \chi^{2s+1} (\ell+2s)!! (\ell-1)!!}{(2s+1)! (\ell)!! (\ell-1-2s)!!} \quad (\text{A.21.2})$$

For the case of ℓ even, the upper limit is $\ell/2$. In a similar way the equation goes to:

$$P_\ell(\chi) = (-1)^{\ell/2} \frac{(\ell - 1)!!}{(\ell)!!} \sum_{s=0}^{\ell/2} \frac{(-1)^s \chi^{2s} (\ell - 1 + 2s)!! (\ell)!!}{(2s)!(\ell - 1)!!(\ell - 2s)!!} \tag{A.21.3}$$

With Eq. (A.21.3), replace ℓ by $(\ell + 1)$ and write out the first few terms, then repeat with ℓ replaced by $(\ell - 1)$. The resulting series are:

$$\begin{aligned} P_{\ell+1}(\chi) &= (-1)^{(\ell+1)/2} \frac{(\ell)!!}{(\ell + 1)!!} \\ &\times \left\{ 1 - \frac{\chi^2}{2!} \frac{(\ell + 2)!! (\ell + 1)!!}{(\ell)!! (\ell - 1)!!} + \frac{\chi^4}{4!} \frac{(\ell + 4)!! (\ell + 1)!!}{(\ell)!! (\ell - 3)!!} - \dots \right\} \\ P_{\ell-1}(\chi) &= (-1)^{(\ell-1)/2} \frac{(\ell - 2)!!}{(\ell - 1)!!} \\ &\times \left\{ 1 - \frac{\chi^2}{2!} \frac{(\ell)!! (\ell - 1)!!}{(\ell - 2)!! (\ell - 3)!!} + \frac{\chi^4}{4!} \frac{(\ell + 2)!! (\ell - 1)!!}{(\ell - 2)!! (\ell - 5)!!} - \dots \right\} \end{aligned}$$

These expressions combine to form the indicated sum:

$$\begin{aligned} &\ell P_{\ell-1}(\chi) + (\ell + 1) P_{\ell+1}(\chi) \\ &= (-1)^{(\ell-1)/2} \frac{(2\ell + 1)(\ell)!!}{(\ell - 1)!!} \left\{ \frac{\chi^2}{1!} - \frac{\chi^4}{3!} (\ell + 2)(\ell - 1) + \dots \right\} \\ &= (-1)^{(\ell-1)/2} \frac{(2\ell + 1)(\ell)!!}{(\ell - 1)!!} \sum_{s=0}^{(\ell-1)/2} \frac{(-1)^s \chi^{2s+2} (\ell + 2s)!! (\ell - 1)!!}{(2s + 1)(\ell)!! (\ell - 1 - 2s)!!} \end{aligned} \tag{A.21.4}$$

Combining Eqs. (A.21.3) and (A.21.5) results in:

$$(2\ell + 1)\chi P_\ell(\chi) = \ell P_{\ell-1}(\chi) + (\ell + 1) P_{\ell+1}(\chi) \tag{A.21.5}$$

Proofs for even values of ℓ follow in a parallel way and give the same result. Equation (A.21.5) is the first recursion relationship.

The same technique with the indicated operations results in the second recursion relationship:

$$(2\ell + 1)P_\ell(\chi) = \frac{dP_{\ell+1}(\chi)}{d\chi} - \frac{dP_{\ell-1}(\chi)}{d\chi} \tag{A.21.6}$$

The integral expression of Eq. (A.21.7) follows from Eq. (A.21.6):

$$\int P_\ell(\chi) d\chi = \left[\frac{P_{\ell+1}(\chi) - P_{\ell-1}(\chi)}{(2\ell + 1)} \right] \tag{A.21.7}$$

Differentiating Eq. (A.21.5) by χ and adding $\ell \times$ Eq. (A.21.6) gives:

$$(\ell + 1)P_\ell(\chi) = \frac{dP_{\ell+1}(\chi)}{d\chi} - \chi \frac{dP_\ell(\chi)}{d\chi} \quad (\text{A.21.8})$$

Differentiating Eq. (A.21.8) m times, multiplying through by $\sin^{m+1} \theta$, and using Eq. (A.19.7) gives:

$$P_{\ell+1}^{m+1}(\chi) = \chi P_\ell^{m+1}(\chi) + (\ell + m + 1) \sin \theta P_\ell^m(\chi) \quad (\text{A.21.9})$$

A series of identities follows by mixing and matching. Selected ones are listed in Table A.21.1.

Associated Legendre functions have even or odd parity, respectively, if the sum $(\ell + m)$ is even or odd:

$$P_\ell^m(\chi) = (-1)^{\ell+m} P_\ell^m(-\chi) \quad (\text{A.21.10})$$

Table A.21.1. A table of identities for legendre functions.

| | |
|----|--|
| 1 | $\frac{dP_\ell^m}{d\theta} = \frac{1}{2}[(\ell + m)(\ell - m + 1)P_\ell^{m-1} - P_\ell^{m+1}]$ |
| 2 | $\frac{mP_\ell^m}{\sin \theta} = \frac{1}{2}[(\ell + m)(\ell - m + 1)P_{\ell-1}^{m-1} + P_{\ell-1}^{m+1}]$ |
| 3 | $\sin \theta \frac{dP_\ell^m}{d\theta} = \frac{1}{2\ell + 1}[\ell(\ell - m + 1)P_{\ell+1}^m - (\ell + m)(\ell + 1)P_{\ell-1}^m]$ |
| 4 | $\cos \theta P_\ell^m = \frac{1}{2\ell + 1}[(\ell - m + 1)P_{\ell+1}^m + (\ell + m)P_{\ell-1}^m]$ |
| 5 | $P_\ell^{m+1} = 2m \cot \theta P_\ell^m - (\ell + m)(\ell - m + 1)P_\ell^{m-1}$ |
| 6 | $(\ell - m + 1)P_{\ell+1}^m = (2\ell + 1) \cos \theta P_\ell^m - (\ell + m)P_{\ell-1}^m$ |
| 7 | $(2\ell + 1) \sin \theta P_\ell^m = P_{\ell+1}^{m+1} - P_{\ell-1}^{m+1}$ |
| 8 | $P_{\ell+1}^{m+1} = \cos \theta P_\ell^{m+1} + (\ell + m + 1) \sin \theta P_\ell^m$ |
| 9 | $P_{\ell-1}^{m+1} = \cos \theta P_{\ell-1}^{m+1} - (\ell - m) \sin \theta P_\ell^m$ |
| 10 | $\frac{dP_\ell^m}{d\theta} = m \cot \theta P_\ell^m - P_\ell^{m+1}$ |
| 11 | $\frac{dP_\ell^m}{d\theta} = -m \cot \theta P_\ell^m + (\ell + m)(\ell - m + 1)P_\ell^{m-1}$ |

Let delta be a Kronecker delta and let q equal any of the field of positive integers, including zero. At $\theta = \pi/2$, the equator, functional values are:

$$P_\ell^m(0) = (-1)^{(\ell-m)/2} \frac{(\ell+m+1)!}{(\ell-m)!} \delta(2q, \ell+m) \tag{A.21.11}$$

$$\left. \frac{d^r}{d\theta^r} P_\ell^m(\cos \theta) \right|_{\frac{\pi}{2}} = P_\ell^{m+r}(0) \tag{A.21.12}$$

In the tables to follow, order is ℓ , degree is m , and $\chi = \cos \theta$. Polynomials are even or odd functions of χ as $(\ell+m)$ is even or odd, respectively; absence of a superscript indicates degree 0. Normalization is chosen to make $P_\ell(1) = 1$.

Table A.21.2 contains values of associated Legendre polynomials. Useful recursion relationships for constructing the table are:

$$P_\ell^m(\chi) = \frac{1}{\ell-m} [(2\ell-1)\chi P_{\ell-1}^m(\chi) - (\ell-1+m)P_{\ell-2}^m(\chi)]$$

$$P_\ell^m(\chi) = [2(m-1) \cot \theta P_\ell^{m-1}(\chi) - (\ell-1+m)(\ell+2-m)P_\ell^{m-2}(\chi)]$$

$$P_\ell^1(\chi) = -\frac{dP_\ell}{d\theta}$$

Table A.21.2(a). Table of associated Legendre polynomials, $P_\ell^m(\chi)$.

| ℓ $m = 0$, Values for $P_\ell(1)$ | $m = 1$, Values for $P_\ell^1(\chi)$ |
|---|--|
| 0 1 | |
| 1 χ | $\sin \theta$ |
| 2 $\frac{1}{2}(3\chi^2 - 1)$ | $3\chi \sin \theta$ |
| 3 $\frac{\chi}{2}(5\chi^2 - 3)$ | $\frac{3}{2}(5\chi^2 - 1) \sin \theta$ |
| 4 $\frac{1}{8}(35\chi^4 - 30\chi^2 + 3)$ | $\frac{5\chi}{2}(7\chi^2 - 3) \sin \theta$ |
| 5 $\frac{\chi}{8}(63\chi^4 - 70\chi^2 + 15)$ | $\frac{15}{8}(21\chi^4 - 14\chi^2 + 1) \sin \theta$ |
| 6 $\frac{1}{16}(231\chi^6 - 315\chi^4 + 105\chi^2 - 5)$ | $\frac{21\chi}{8}(33\chi^4 - 30\chi^2 + 5) \sin \theta$ |
| 7 $\frac{\chi}{16}(429\chi^6 - 693\chi^4 + 315\chi^2 - 35)$ | $\frac{7}{16}(429\chi^6 - 495\chi^4 + 135\chi^2 - 5) \sin \theta$ |
| 8 $\frac{1}{16}(6435\chi^8 - 12012\chi^6 + 6930\chi^4 - 1260\chi^2 + 35)$ | $\frac{9\chi}{128}(715\chi^6 - 1001\chi^4 + 385\chi^2 - 35) \sin \theta$ |
| 9 $\frac{\chi}{16}(12155\chi^8 - 25740\chi^6 + 18018\chi^4 - 4620\chi^2 + 315)$ | $\frac{45}{128}(2431\chi^8 - 4004\chi^6 + 2002\chi^4 - 308\chi^2 + 7) \sin \theta$ |

Table A.21.2(b). Table of associated Legendre polynomials, $P_\ell^m(\chi)$.

| ℓ | $m = 2$, Values for $P_\ell^2(\chi)$ | $m = 3$, Values for $P_\ell^3(\chi)$ |
|--------|--|---|
| 2 | $3 \sin^2 \theta$ | |
| 3 | $15\chi \sin^2 \theta$ | $15 \sin^3 \theta$ |
| 4 | $\frac{15}{2}(7\chi^2 - 1) \sin^2 \theta$ | $105\chi \sin^3 \theta$ |
| 5 | $\frac{105\chi}{2}(3\chi^2 - 1) \sin^2 \theta$ | $\frac{105}{2}(9\chi^2 - 1) \sin^3 \theta$ |
| 6 | $\frac{105}{8}(33\chi^4 - 18\chi^2 + 1) \sin^2 \theta$ | $\frac{315\chi}{2}(11\chi^2 - 3) \sin^3 \theta$ |
| 7 | $\frac{63\chi}{8}(143\chi^4 - 110\chi^2 + 15) \sin^2 \theta$ | $\frac{315}{8}(143\chi^4 - 66\chi^2 + 3) \sin^3 \theta$ |
| 8 | $\frac{315}{16}(143\chi^6 - 143\chi^4 + 33\chi^2 - 1) \sin^2 \theta$ | $\frac{3465\chi}{8}(39\chi^4 - 26\chi^2 + 3) \sin^3 \theta$ |
| 9 | $\frac{495\chi}{16}(221\chi^6 - 273\chi^4 + 91\chi^2 - 7) \sin^2 \theta$ | $\frac{3465}{16}(221\chi^6 - 195\chi^4 + 39\chi^2 - 1) \sin^3 \theta$ |

Table A.21.2(c). Table of associated Legendre polynomials, $P_\ell^m(\chi)$.

| ℓ | $m = 4$, Values for $P_\ell^4(\chi)$ | $m = 5$, Values for $P_\ell^5(\chi)$ |
|--------|---|---|
| 4 | $105 \sin^4 \theta$ | |
| 5 | $945\chi \sin^4 \theta$ | $945 \sin^5 \theta$ |
| 6 | $945(11\chi^2 - 1) \sin^4 \theta/2$ | $10395\chi \sin^5 \theta$ |
| 7 | $3465\chi(13\chi^2 - 3) \sin^4 \theta/2$ | $10395(13\chi^2 - 1) \sin^5 \theta/2$ |
| 8 | $10395(65\chi^4 - 26\chi^2 + 1) \sin^4 \theta/8$ | $135135\chi(5\chi^2 - 1) \sin^5 \theta/2$ |
| 9 | $135135\chi(17\chi^4 - 10\chi^2 + 1) \sin^4 \theta/8$ | $135135(85\chi^4 - 30\chi^2 + 1) \sin^5 \theta/8$ |

Table A.21.2(d). Table of associated Legendre polynomials, $P_\ell^m(\chi)$.

| ℓ | $m = 6$, Values for $P_\ell^6(\chi)$ | $m = 7$, Values for $P_\ell^7(\chi)$ |
|--------|--|---|
| 6 | $10395 \sin^6 \theta$ | |
| 7 | $135135\chi \sin^6 \theta$ | $135135 \sin^7 \theta$ |
| 8 | $135135(15\chi^2 - 1) \sin^6 \theta/2$ | $2027025\chi \sin^7 \theta$ |
| 9 | $675675\chi(17\chi^2 - 3) \sin^6 \theta/2$ | $2027025(17\chi^2 - 1) \sin^7 \theta/2$ |

Table A.21.2(e). Table of associated Legendre polynomials, $P_\ell^m(\chi)$.

| ℓ | $m = 8$, Values for $P_\ell^8(\chi)$ | $m = 9$, Values for $P_\ell^9(\chi)$ |
|--------|---------------------------------------|---------------------------------------|
| 8 | $2027025 \sin^8 \theta$ | |
| 9 | $34459425 \chi \sin^8 \theta$ | $34459425 \sin^9 \theta$ |

Table A.21.3(a). Table of spherical angular function $dP_\ell^m/d\theta$.

| ℓ | $m = 1$, $dP_\ell^1/d\theta = -\cot \theta P_\ell^1 + \ell(\ell + 1)P_\ell$ | $m = 2$, $dP_\ell^2/d\theta = -2 \cot \theta dP_\ell^2 + (\ell - 1)(\ell + 2)dP_\ell^1$ |
|--------|---|---|
| 1 | χ | |
| 2 | $3(2\chi^2 - 1)$ | $6\chi \sin \theta$ |
| 3 | $\frac{3}{2}\chi(15\chi^2 - 11)$ | $15(3\chi^2 - 1) \sin \theta$ |
| 4 | $\frac{5}{2}(28\chi^4 - 27\chi^2 + 3)$ | $30\chi(7\chi^2 - 4) \sin \theta$ |
| 5 | $\frac{15\chi}{8}(105\chi^4 - 126\chi^2 + 29)$ | $\frac{105}{2}(15\chi^4 - 12\chi^2 + 1) \sin \theta$ |
| 6 | $\frac{21}{8}(198\chi^6 - 285\chi^4 + 100\chi^2 - 5)$ | $\frac{105\chi}{4}(99\chi^4 - 102\chi^2 + 19) \sin \theta$ |
| 7 | $\frac{7\chi}{16}(3003\chi^6 - 5049\chi^4 + 2385\chi^2 - 275)$ | $\frac{63}{8}(1001\chi^6 - 1265\chi^4 + 375\chi^2 - 15) \sin \theta$ |
| 8 | $\frac{9}{16}(5720\chi^8 - 11011\chi^6 + 6545\chi^4 - 1225\chi^2 + 35)$ | $\frac{315\chi}{8}(286\chi^6 - 429\chi^4 + 176\chi^2 - 17) \sin \theta$ |
| 9 | $\frac{45\chi}{16}(21879\chi^8 - 47464\chi^6 + 34034\chi^4 - 8932\chi^2 + 623)$ | $\frac{495}{16}(1989\chi^8 - 3458\chi^6 + 1820\chi^4 - 294\chi^2 + 7) \sin \theta$ |

The sum of all coefficients in the expansion for $P_\ell^m(\chi)$ is $\frac{(\ell+m)!}{2^m(m)!(\ell-m)!}$. To normalize, multiply each associated Legendre function by

$$\sqrt{(2\ell + 1)(\ell - m)!/2(\ell + m)!}.$$

Table A.21.3 contains values of spherical angular function $dP_\ell^m/d\theta$, based upon the relationship:

$$dP_\ell^m/d\theta = -m \cot \theta P_\ell^m + (\ell + m)(\ell - m + 1)P_\ell^{m-1} = m \cot \theta P_\ell^m - P_\ell^{m+1}$$

Table A.21.3(b). Table of spherical angular function $dP_\ell^m/d\theta$.

| ℓ | $m = 3,$ $dP_\ell^3/d\theta = -3 \cot \theta P_\ell^3 + (\ell - 2)(\ell + 3)P_\ell^2$ | $m = 4,$ $dP_\ell^4/d\theta = -4 \cot \theta P_\ell^4 + (\ell - 3)(\ell + 4)P_\ell^3$ |
|--------|--|--|
| 3 | $45\chi \sin^2 \theta$ | |
| 4 | $105(4\chi^2 - 1) \sin^2 \theta$ | $420\chi \sin^3 \theta$ |
| 5 | $\frac{315}{2}\chi(15\chi^2 - 7) \sin^2 \theta$ | $945(5\chi^2 - 1) \sin^3 \theta$ |
| 6 | $\frac{945}{2}(22\chi^4 - 15\chi^2 + 1) \sin^2 \theta$ | $945\chi(33\chi^2 - 13) \sin^3 \theta$ |
| 7 | $\frac{315}{8}(1001\chi^4 - 902\chi^2 + 141) \sin^2 \theta$ | $\frac{3465}{2}(91\chi^4 - 54\chi^2 + 3) \sin^3 \theta$ |
| 8 | $\frac{10395}{8}(104\chi^6 - 117\chi^4 + 30\chi^2 - 1) \sin^2 \theta$ | $\frac{10395}{2}(130\chi^4 - 104\chi^2 + 14) \sin^3 \theta$ |
| 9 | $\frac{10395}{16}(663\chi^6 - 897\chi^4 + 325\chi^2 - 27) \sin^2 \theta$ | $\frac{135135}{8}(153\chi^6 - 155\chi^4 + 35\chi^2 - 1) \sin^3 \theta$ |

Table A.21.3(c). Table of spherical angular function $dP_\ell^m/d\theta$.

| ℓ | $m = 5,$ $dP_\ell^5/d\theta = -5 \cot \theta P_\ell^5 + (\ell - 4)(\ell + 5)P_\ell^4$ | $m = 6,$ $dP_\ell^6/d\theta = -6 \cot \theta P_\ell^6 + (\ell - 5)(\ell + 6)P_\ell^5$ |
|--------|--|--|
| 5 | $4725\chi \sin^4 \theta$ | |
| 6 | $4725(6\chi^2 - 1) \sin^4 \theta$ | $62370\chi \sin^5 \theta$ |
| 7 | $10395\chi(91\chi^2 - 31) \sin^4 \theta$ | $135135(7\chi^2 - 1) \sin^5 \theta$ |
| 8 | $135135(40\chi^2 - 21\chi^2 + 1) \sin^4 \theta$ | $810810\chi(10\chi^2 - 3) \sin^5 \theta$ |
| 9 | $675675\chi(153\chi^2 - 110\chi^2 + 13) \sin^4 \theta/8$ | $2027025(51\chi^2 - 24\chi^2 + 1) \sin^5 \theta$ |

Table A.21.3(d). Table of spherical angular function $dP_\ell^m/d\theta$.

| ℓ | $m = 7,$ $dP_\ell^7/d\theta = -7 \cot \theta P_\ell^7 + (\ell - 6)(\ell + 7)P_\ell^6$ | $m = 8,$ $dP_\ell^8/d\theta = -8 \cot \theta P_\ell^8 + (\ell - 7)(\ell + 8)P_\ell^7$ | $m = 9,$ $dP_\ell^9/d\theta = -9 \cot \theta P_\ell^9 + (\ell - 8)(\ell + 9)P_\ell^8$ |
|--------|--|--|--|
| 7 | $945945\chi \sin^6 \theta$ | | |
| 8 | $2027025(8\chi^2 - 1) \sin^6 \theta$ | $16216200\chi \sin^7 \theta$ | |
| 9 | $2027025(153\chi^2 - 41) \sin^6 \theta$ | $34459425(9\chi^2 - 1) \sin^7 \theta$ | $310134825\chi \sin^8 \theta$ |

22. Integrals of Legendre Functions

Solutions of the problems considered in the text require integrals of several functional combinations of Legendre polynomials. One is the integral:

$$I_3 = m \int_0^\pi \frac{d}{d\theta} (P_\ell^m P_n^m) d\theta = 0 \quad (\text{A.22.1})$$

The equality follows since the integrand is a perfect differential and $P_\ell^m(\pm 1) = 0$ for $m > 0$.

Consider the integral:

$$I_4 = \int_0^\pi \left\{ \frac{dP_\ell^m}{d\theta} \frac{dP_n^m}{d\theta} + \frac{m^2 P_\ell^m P_n^m}{\sin^2 \theta} \right\} \sin \theta d\theta \quad (\text{A.22.2})$$

The first term in the integrand may be written:

$$\frac{dP_\ell^m}{d\theta} \frac{dP_n^m}{d\theta} = \frac{1}{\sin \theta} \frac{d}{d\theta} \left[\sin \theta P_\ell^m \frac{dP_n^m}{d\theta} \right] - \frac{P_\ell^m}{\sin \theta} \frac{d}{d\theta} \left[\sin \theta \frac{dP_n^m}{d\theta} \right]$$

The second term in the integrand, after using the differential equation, may be written:

$$\frac{m^2 P_\ell^m P_n^m}{\sin^2 \theta} = \frac{P_\ell^m}{\sin \theta} \frac{d}{d\theta} \left[\sin \theta \frac{dP_n^m}{d\theta} \right] + n(n+1) P_n^m P_\ell^m$$

Combining results in:

$$I_4 = \int_0^\pi \sin \theta d\theta \left\{ \frac{1}{\sin \theta} \frac{d}{d\theta} \left[\sin \theta P_\ell^m \frac{dP_n^m}{d\theta} \right] + n(n+1) P_\ell^m P_n^m \right\} \quad (\text{A.22.3})$$

The first term is an exact differential that integrates to zero, leaving:

$$I_4 = n(n+1) \int_0^\pi \sin \theta d\theta P_\ell^m P_n^m = \frac{2\ell(\ell+1)(\ell+m)!}{(2\ell+1)(\ell-m)!} \delta(\ell, n) \quad (\text{A.22.4})$$

Consider the integral

$$I_5 = \int_0^\pi \cos \theta \sin \theta d\theta \left\{ \frac{dP_\ell^m}{d\theta} \frac{dP_n^m}{d\theta} + \frac{m^2 P_\ell^m P_n^m}{\sin^2 \theta} \right\} \quad (\text{A.22.5})$$

The procedure is similar to that for I_4 . Replace the first term using the differential equation, sum, and partially integrate once to obtain:

$$I_5 = \int_0^\pi \sin \theta d\theta \left\{ \left[\sin \theta P_\ell^m \frac{dP_n^m}{d\theta} \right] + n(n+1) \cos \theta P_\ell^m P_n^m \right\}$$

Combining with recursion relationships, Tables A.21.1.3 and A.21.1.4, shows that:

$$I_5 = \int_0^\pi \sin \theta d\theta P_\ell^m \left[\frac{n(n-m+1)(n+2)}{(2n+1)} P_{n+1}^m + \frac{(n+m)(n^2-1)}{(2n+1)} P_{n-1}^m \right]$$

Evaluation using Eq. (A.20.11) gives:

$$I_5 = \left[\frac{2n(n+2)(n+m+1)!}{(2n+1)(2n+3)(n-m)!} \delta(\ell, n+1) + \frac{(n^2-1)(n+m)!}{(2n-1)(2n+1)(n-m-1)!} \delta(\ell, n-1) \right] \quad (\text{A.22.6})$$

The next integral of interest is:

$$I_6 = \int_0^\pi \sin^2 \theta \, d\theta \frac{d}{d\theta} (\mathbf{P}_\ell^m \mathbf{P}_n^m) \quad (\text{A.22.7})$$

Expanding the differential and using recursion relationship Table A.21.1.3 results in:

$$I_6 = \int_0^\pi \sin \theta \, d\theta \left\{ \mathbf{P}_\ell^m \left[\frac{n(n-m+1)}{(2n+1)} \mathbf{P}_{n+1}^m - \frac{(n+m)(n-1)}{(2n+1)} \mathbf{P}_{n-1}^m \right] + \mathbf{P}_n^m \left[\frac{(\ell-m+1)}{(2\ell+1)} \mathbf{P}_{\ell+1}^m - \frac{(\ell+m)(\ell-1)}{(2\ell+1)} \mathbf{P}_{\ell-1}^m \right] \right\}$$

Term-by-term evaluation shows that:

$$I_6 = 0 \quad (\text{A.22.8})$$

The next integral of interest is:

$$I_7 = \int_0^\pi \sin^2 \theta \, d\theta \left[\frac{d\mathbf{P}_\ell^m}{d\theta} \frac{d\mathbf{P}_n^{m+1}}{d\theta} + \frac{m(m+1)}{\sin^2 \theta} \mathbf{P}_\ell^m \mathbf{P}_n^{m+1} \right] \quad (\text{A.22.9})$$

Substituting the differential equation into the first term, summing, and taking one partial integration results in:

$$\int_0^\pi \sin \theta \, d\theta \mathbf{P}_n^{m+1} \left\{ -\cos \theta \frac{d\mathbf{P}_\ell^m}{d\theta} + \left[\ell(\ell+1) \sin \theta + \frac{m}{\sin \theta} \right] \mathbf{P}_\ell^m \right\}$$

After using the recursion relationship of Table A.21.1.10 on the first term then summing the curly bracket becomes:

$$\{[\ell(\ell+1) + m] \sin \theta \mathbf{P}_\ell^m + \cos \theta \mathbf{P}_\ell^{m+1}\}$$

With the use of the recursion relationships of Tables A.21.1.4 and A.21.1.7 the bracket becomes:

$$\left\{ \mathbf{P}_{\ell+1}^{m+1} \left[\frac{\ell(\ell+2)}{(2\ell+1)} \right] - \mathbf{P}_{\ell-1}^{m+1} \left[\frac{(\ell-1)(\ell+1)}{(2\ell+1)} \right] \right\}$$

Putting the bracket back under the integral sign and integrating gives:

$$\begin{aligned}
 I_7 &= \frac{2\ell(\ell+2)(\ell+m+2)!}{(2\ell+1)(2\ell+3)(\ell-m)!} \delta(n, \ell+1) \\
 &\quad - \frac{2(\ell-1)(\ell+1)(\ell+m)!}{(2\ell-1)(2\ell+1)(\ell-m-2)!} \delta(n, \ell-1)
 \end{aligned} \tag{A.22.10}$$

The next integral of interest is:

$$I_8 = \int_0^\pi \sin \theta \, d\theta \left((m+1)P_\ell^{m+1} \frac{dP_n^m}{d\theta} + mP_n^m \frac{dP_\ell^{m+1}}{d\theta} \right) \tag{A.22.11}$$

This may be rewritten as:

$$\int_0^\pi d\theta \left(\sin \theta P_\ell^{m+1} \frac{dP_n^m}{d\theta} + m \sin \theta \frac{d}{d\theta} [P_n^m P_\ell^{m+1}] \right)$$

Integrating the perfect differential by parts gives:

$$\int_0^\pi \sin \theta \, d\theta P_\ell^{m+1} \left(\frac{dP_n^m}{d\theta} - m \cot \theta P_n^m \right) = - \int_0^\pi \sin \theta \, d\theta P_\ell^{m+1} P_n^{m+1}$$

The second equality is in the proper form to use Table A.21.1.10. The result is:

$$I_8 = - \frac{2}{(2\ell+1)} \frac{(\ell+m+1)!}{(\ell-m-1)!} \delta(\ell, n) \tag{A.22.12}$$

Similarly, using Table A.21.1.11, integrals with $(m-1)$ replacing $(m+1)$ may be evaluated, and are listed in Table A.22.1.

23. Integrals of Fractional Order Legendre Functions

The Legendre differential equation of fractional order is:

$$\frac{1}{\sin \theta} \frac{d}{d\theta} \left(\sin \theta \frac{d\Theta_\nu^m(\cos \theta)}{d\theta} \right) + \left(\nu(\nu+1) - \frac{m^2}{\sin^2 \theta} \right) \Theta_\nu^m = 0 \tag{A.23.1}$$

Functions $\Theta_\nu^m(\cos \theta)$ represent $L_\nu^m(\cos \theta)$, $M_\nu^m(\cos \theta)$, or any linear combination thereof. Useful boundary conditions are:

$$M_\nu^m(\cos \theta)|_{\theta=\psi} = 0 \quad \text{and} \quad \left. \frac{dL_\nu^m(\cos \theta)}{d\theta} \right|_{\theta=\psi} = 0 \tag{A.23.2}$$

This evaluation of integrals over noninteger order Legendre functions includes the boundary conditions of Eq. (A.23.2).

Table A.22.1. Table of integrals of Legendre polynomials.

| | |
|----|---|
| 1 | $I_{\ell\ell} = \int_0^\pi P_\ell^m P_n^m \sin \theta \, d\theta = \frac{2(\ell+m)!}{(2\ell+1)(\ell-m)!} \delta(\ell, n)$ |
| 2 | $\int_0^\pi P_\ell^m P_\ell^{m+2s} \sin \theta \, d\theta = \frac{2(-1)^s (\ell+m)!}{(2\ell+1)(\ell-m-2s)!}$ |
| 3 | $m \int_0^\pi \frac{d}{d\theta} (P_\ell^m P_n^m) \, d\theta = 0$ |
| 4 | $m \int_0^\pi \frac{d}{d\theta} (P_\ell^m P_n^m) \cos \theta \, d\theta = \frac{2m(\ell+m)!}{(2\ell+1)(\ell-m)!} \delta(\ell, n)$ |
| 5 | $\int_0^\pi \frac{d}{d\theta} (P_\ell^m P_n^m) \sin^2 \theta \, d\theta = 0$ |
| 6 | $\int_0^\pi \left[\frac{dP_\ell^m}{d\theta} \frac{dP_n^m}{d\theta} + \frac{m^2 P_\ell^m P_n^m}{\sin^2 \theta} \right] \sin \theta \, d\theta = \frac{2\ell(\ell+1)(\ell+m)!}{(2\ell+1)(\ell-m)!} \delta(\ell, n)$ |
| 7 | $\int_0^\pi \left[\frac{dP_\ell^m}{d\theta} \frac{dP_n^m}{d\theta} + \frac{m^2 P_\ell^m P_n^m}{\sin^2 \theta} \right] \cos \theta \sin \theta \, d\theta$ $= \left\{ \frac{2\ell(\ell+2)(\ell+m+1)!}{(2\ell+1)(2\ell+3)(\ell-m)!} \delta(n, \ell+1) + \frac{2(\ell-1)(\ell+1)(\ell+m)!}{(2\ell-1)(2\ell+1)(\ell-m-1)!} \delta(n, \ell-1) \right\}$ |
| 8 | $\int_0^\pi \left[\frac{dP_\ell^m}{d\theta} \frac{dP_n^{m+1}}{d\theta} + \frac{m(m+1)P_\ell^m P_n^{m+1}}{\sin^2 \theta} \right] \sin^2 \theta \, d\theta$ $= \left\{ \frac{2\ell(\ell+2)(\ell+m+2)!}{(2\ell+1)(2\ell+3)(\ell-m)!} \delta(n, \ell+1) - \frac{2(\ell-1)(\ell+1)(\ell+m)!}{(2\ell-1)(2\ell+1)(\ell-m-2)!} \delta(n, \ell-1) \right\}$ |
| 9 | $\int_0^\pi \left[\frac{dP_\ell^m}{d\theta} \frac{dP_n^{m-1}}{d\theta} + \frac{m(m-1)P_\ell^m P_n^{m-1}}{\sin^2 \theta} \right] \sin^2 \theta \, d\theta$ $= \left\{ -\frac{2\ell(\ell+2)(\ell+m)!}{(2\ell+1)(2\ell+3)(\ell-m)!} \delta(\ell, n+1) + \frac{2(\ell-1)(\ell+1)(\ell+m)!}{(2\ell-1)(2\ell+1)(\ell-m)!} \delta(\ell, n-1) \right\}$ |
| 10 | $\int_0^\pi P_\ell^m (\cos \theta) \sin^{\ell+1} \theta \, d\theta = (-1)^{(\ell-m)/2} \frac{2^{\ell+1}(\ell)!(\ell+m)!}{(2\ell+1)!} \delta(\ell+m, 2q)$ |
| 11 | $\int_0^\pi \left((m+1)P_\ell^{m+1} \frac{dP_n^m}{d\theta} + mP_n^m \frac{dP_\ell^{m+1}}{d\theta} \right) \sin \theta \, d\theta = -\frac{2}{(2\ell+1)} \frac{(\ell+m+1)!}{(\ell-m-1)!} \delta(\ell, n)$ |
| 12 | $\int_0^\pi \left((m-1)P_\ell^{m-1} \frac{dP_n^m}{d\theta} + mP_n^m \frac{dP_\ell^{m-1}}{d\theta} \right) \sin \theta \, d\theta = -\frac{2}{(2\ell+1)} \frac{(\ell+m)!}{(\ell-m)!} \delta(\ell, n)$ |

Consider the integral

$$I_9 = \int_{\psi}^{\pi-\psi} \sin \theta \, d\theta \left(\frac{dM_{\nu}^m}{d\theta} \frac{dP_n^m}{d\theta} + \frac{m^2 M_{\nu}^m P_n^m}{\sin^2 \theta} \right) \quad (\text{A.23.3})$$

The evaluation procedure is to use the differential equation and rewrite the first term as:

$$\frac{dM_{\nu}^m}{d\theta} \frac{dP_n^m}{d\theta} = \frac{1}{\sin \theta} \frac{d}{d\theta} \left(\sin \theta M_{\nu}^m \frac{dP_n^m}{d\theta} \right) - \frac{M_{\nu}^m}{\sin \theta} \frac{d}{d\theta} \left(\sin \theta \frac{dP_n^m}{d\theta} \right) \quad (\text{A.23.4})$$

The first term on the right side of Eq. (A.23.4) forms a perfect differential and, after imposing Eq. (A.23.2), the integral of that differential is equal to zero. With the differential equation substituted into the remaining term, the result is:

$$I_9 = n(n+1) \int_{\psi}^{\pi-\psi} M_{\nu}^m P_n^m \sin \theta \, d\theta \quad (\text{A.23.5})$$

To evaluate Eq. (A.23.5), since $M_{\nu}^m(\cos \theta)$ has odd parity and $P_n^m(\cos \theta)$ is even or odd as $(n+m)$ is even or odd, the integral vanishes if $(n+m)$ is even. If $(n+m)$ is odd, repeat the procedure used in Eqs. (A.20.1) through (A.20.3). The result is:

$$I_9 = \int_{\psi}^{\pi-\psi} M_{\nu}^m P_n^m \sin \theta \, d\theta = \left\{ \frac{\sin \theta \left[P_n^m \frac{dM_{\nu}^m}{d\theta} - M_{\nu}^m \frac{dP_n^m}{d\theta} \right]}{n(n+1) - \nu(\nu+1)} \right\}_{\psi}^{\pi-\psi}$$

After imposing the boundary condition of Eq. (A.23.2):

$$\int_{\psi}^{\pi-\psi} M_{\nu}^m P_n^m \sin \theta \, d\theta = -2 \sin \psi \left\{ \frac{P_n^m(\cos \psi) \frac{dM_{\nu}^m(\cos \psi)}{d\theta}}{n(n+1) - \nu(\nu+1)} \right\} \delta(n, 2q+1) \quad (\text{A.23.6})$$

The integer “q” represents any positive integer, including zero.

The next integral to be evaluated is:

$$I_{10} = \int_{\psi}^{\pi-\psi} \sin \theta \, d\theta \left(\frac{dL_{\mu}^m}{d\theta} \frac{dP_n^m}{d\theta} + \frac{m^2 L_{\mu}^m P_n^m}{\sin^2 \theta} \right) \quad (\text{A.23.7})$$

The same technique that was applied to Eq. (A.23.2) applied to Eq. (A.23.7) results in:

$$I_{10} = \mu(\mu+1) \int_{\psi}^{\pi-\psi} L_{\mu}^m P_n^m \sin \theta \, d\theta \quad (\text{A.23.8})$$

The same technique applied to Eq. (A.23.4) results in:

$$I_{10} = \int_{\psi}^{\pi-\psi} L_{\mu}^m P_n^m \sin \theta d\theta = 2 \sin \psi \left\{ \frac{L_{\mu}^m(\cos \psi) \frac{dP_n^m(\cos \psi)}{d\theta}}{n(n+1) - \mu(\mu+1)} \right\} \delta(n, 2q) \quad (\text{A.23.9})$$

It follows from the parity of the functions that the integral:

$$I_{11} = \int_{\psi}^{\pi-\psi} \sin \theta d\theta \left(\frac{dM_{\nu}^m}{d\theta} \frac{dL_{\mu}^m}{d\theta} + \frac{m^2 M_{\nu}^m L_{\mu}^m}{\sin^2 \theta} \right) = 0 \quad (\text{A.23.10})$$

The next integral of interest is:

$$I_{12} = \int_{\psi}^{\pi-\psi} \sin \theta d\theta \left(\frac{dM_{\nu}^m}{d\theta} \frac{dM_{\mu}^m}{d\theta} + \frac{m^2 M_{\nu}^m M_{\mu}^m}{\sin^2 \theta} \right) \quad (\text{A.23.11})$$

The technique used to evaluate the previous integrals when applied to Eq. (A.23.2) gives:

$$I_{12} = \nu(\nu+1) \int_{\psi}^{\pi-\psi} \sin \theta d\theta M_{\nu}^m M_{\mu}^m \quad (\text{A.23.12})$$

Applying the technique to Eq. (A.23.4) gives:

$$\int_{\psi}^{\pi-\psi} M_{\nu}^m M_{\mu}^m \sin \theta d\theta = \left\{ \frac{\sin \theta \left[M_{\mu}^m \frac{dM_{\nu}^m}{d\theta} - M_{\nu}^m \frac{dM_{\mu}^m}{d\theta} \right]}{\mu(\mu+1) - \nu(\nu+1)} \right\}_{\psi}^{\pi-\psi}$$

The boundary condition shows that the result is zero unless $\mu(\mu+1) - \nu(\nu+1)$. For that case, evaluating the indeterminate form gives:

$$I_{12} = \int_{\psi}^{\pi-\psi} M_{\nu}^m M_{\mu}^m \sin \theta d\theta = \frac{2 \sin \psi}{2\nu+1} \left[\frac{\partial M_{\nu}^m(\cos \psi)}{\partial \nu} \frac{\partial M_{\nu}^m(\cos \psi)}{\partial \theta} \right] \delta(\nu, \mu) \quad (\text{A.23.13})$$

The delta function indicates a Kronecker delta function with a noninteger argument.

Consider the integral

$$I_{13} = \int_{\psi}^{\pi-\psi} \sin \theta \, d\theta \left(\frac{dL_{\nu}^m}{d\theta} \frac{dL_{\mu}^m}{d\theta} + \frac{m^2 dL_{\nu}^m dL_{\mu}^m}{\sin^2 \theta} \right) \quad (\text{A.23.14})$$

In a way similar to the earlier integrals:

$$I_{13} = \mu(\mu + 1) \int_{\psi}^{\pi-\psi} \sin \theta \, d\theta L_{\nu}^m L_{\mu}^m \quad (\text{A.23.15})$$

$$I_{13} = \int_{\psi}^{\pi-\psi} L_{\nu}^m L_{\mu}^m \sin \theta \, d\theta = -\frac{2 \sin \psi}{2\mu + 1} \left[L_{\mu}^m(\cos \psi) \frac{\partial^2 L_{\mu}^m(\cos \psi)}{\partial \nu \partial \theta} \right] \delta(\nu, \mu) \quad (\text{A.23.16})$$

Values are calculated and tabulated in Table A.23.1.

Table A.23.1. Table of integrals, noninteger order Legendre functions.

| | | |
|---|---|--|
| 1 | $I_{\nu n} = \int_{-\psi}^{\psi} M_{\nu}^m P_n^m \sin \theta \, d\theta = -2 \sin \psi \left\{ \frac{P_n^m(\cos \psi) \frac{\partial M_{\nu}^m(\cos \psi)}{\partial \theta}}{n(n+1) - \nu(\nu+1)} \right\} \delta(m+n, 2q+1)$ | |
| 2 | $\int_{-\psi}^{\psi} \left(\frac{dM_{\nu}^m}{d\theta} \frac{dP_n^m}{d\theta} + \frac{m^2 M_{\nu}^m P_n^m}{\sin^2 \theta} \right) \sin \theta \, d\theta = n(n+1) I_{\nu n}$ | |
| 3 | $K_{\mu n} = \int_{\psi}^{\pi-\psi} L_{\mu}^m P_n^m \sin \theta \, d\theta = 2 \sin \psi \left\{ \frac{L_{\mu}^m(\cos \psi) \frac{\partial P_n^m(\cos \psi)}{\partial \theta}}{n(n+1) - \mu(\mu+1)} \right\} \delta(n, 2q)$ | |
| 4 | $\int_{\psi}^{\pi-\psi} \left(\frac{dL_{\mu}^m}{d\theta} \frac{dP_n^m}{d\theta} + \frac{m^2 L_{\mu}^m P_n^m}{\sin^2 \theta} \right) \sin \theta \, d\theta = \mu(\mu+1) I_{\mu n}$ | |
| 5 | $\int_{\psi}^{\pi-\psi} \left(\frac{dM_{\nu}^m}{d\theta} \frac{dL_{\mu}^m}{d\theta} + \frac{m^2 M_{\nu}^m L_{\mu}^m}{\sin^2 \theta} \right) \sin \theta \, d\theta = 0$ | |
| 6 | $I_{\nu \nu} = \int_{\psi}^{\pi-\psi} M_{\nu}^m M_{\mu}^m \sin \theta \, d\theta = \frac{2 \sin \psi}{2\nu+1} \left[\frac{\partial M_{\nu}^m(\cos \psi)}{\partial \nu} \frac{\partial M_{\nu}^m(\cos \psi)}{\partial \theta} \right] \delta(\nu, \mu)$ | |
| 7 | $\int_{\psi}^{\pi-\psi} \left(\frac{dM_{\nu}^m}{d\theta} \frac{dM_{\mu}^m}{d\theta} + \frac{m^2 M_{\nu}^m M_{\mu}^m}{\sin^2 \theta} \right) \sin \theta \, d\theta = \nu(\nu+1) I_{\nu \nu}$ | |
| 8 | $K_{\mu \mu} = \int_{\psi}^{\pi-\psi} L_{\nu}^m L_{\mu}^m \sin \theta \, d\theta = -\frac{2 \sin \psi}{2\mu+1} \left[L_{\mu}^m(\cos \psi) \frac{\partial^2 L_{\mu}^m(\cos \psi)}{\partial \nu \partial \theta} \right] \delta(\nu, \mu)$ | |
| 9 | $\int_{\psi}^{\pi-\psi} \left(\frac{dL_{\nu}^m}{d\theta} \frac{dL_{\mu}^m}{d\theta} + \frac{m^2 L_{\nu}^m L_{\mu}^m}{\sin^2 \theta} \right) \sin \theta \, d\theta = \mu(\mu+1) K_{\mu \mu}$ | |

24. The First Solution Form

Since the radial differential equation, Eq. (1.11.7), is independent of separation parameter m , so are the solutions. The spherical Bessel differential equation with separation parameter ν is:

$$\frac{1}{\sigma^2} \frac{d}{d\sigma} \left(\sigma^2 \frac{dR}{d\sigma} \right) + \left(1 - \frac{\nu(\nu+1)}{\sigma^2} \right) R = 0 \quad (\text{A.24.1})$$

Solutions valid for all points $r > 0$ are obtained by using a power series expansion. The series and its first two derivatives are:

$$\begin{aligned} R_\nu(\sigma) &= \sum_{s=0}^{\infty} a_s \sigma^{s+p} \\ \frac{dR_\nu(\sigma)}{d\sigma} &= \sum_{s=0}^{\infty} (s+p) a_s \sigma^{s+p-1} \\ \frac{d^2 R_\nu(\sigma)}{d\sigma^2} &= \sum_{s=0}^{\infty} (s+p)(s+p-1) a_s \sigma^{s+p-2} \end{aligned} \quad (\text{A.24.2})$$

Substituting Eq. (A.24.2) into Eq. (A.24.1) and solving leads to:

$$\left\{ [p(p+1) - \nu(\nu+1)] a_0 \sigma^{p-2} + [(p+1)(p+2) - \nu(\nu+1)] a_1 \sigma^{p-1} + \sum_{s=0}^{\infty} \{ [(s+p+2)(s+p+3) - \nu(\nu+1)] a_{s+2} + a_s \} \sigma^{s+p} \right\} = 0 \quad (\text{A.24.3})$$

Since the series of Eq. (A.24.3) is an identity in σ , the coefficient of each power of ν is separately equal to zero. There are but two nontrivial ways that the coefficients of σ^{p-2} and σ^{p-1} can both be equal to zero. One is if a_0 is equal to zero and $(p+1)(p+2) = \nu(\nu+1)$; the other is if a_1 is equal to zero and $p(p+1) = \nu(\nu+1)$. Arbitrarily making the second choice, the condition that $p(p+1) = \nu(\nu+1)$ is met either of two ways: $p = \nu$ or $p = -(\nu+1)$; the choice determines the two independent solutions.

For the case $p = \nu$ the portion of Eq. (A.24.3) in the curly brackets is zero, and gives the recursion relationship:

$$\frac{a_{s+2}}{a_s} = - \frac{1}{(s+2)(2\nu+s+3)} \quad (\text{A.24.4})$$

This relationship, after redefining the dummy index, leads to the functional form of the radial function $R_\nu(\sigma)$:

$$R_\nu(\sigma) = a_0 \sum_{s=0}^{\infty} \frac{(-1)^s (2\nu + 1)!!}{2^s s! (2\nu + 2s + 1)!!} \sigma^{\nu+2s} \tag{A.24.5}$$

Making the definition that $a_0 = 1/(2\nu + 1)!!$ the result is the function:

$$j_\nu(\sigma) = \sum_{s=0}^{\infty} \frac{(-1)^s}{2^s s! (2\nu + 2s + 1)!!} \sigma^{\nu+2s} \tag{A.24.6}$$

Functions $j_\nu(\sigma)$ are the spherical Bessel functions of order ν . The functional limit at small values of σ follows from Eq. (A.24.6), and is equal to:

$$\lim_{\sigma \rightarrow 0} [j_\nu(\sigma)] = \frac{\sigma^\nu}{(2\nu + 1)!!} \tag{A.24.7}$$

For the case $p = -(\nu + 1)$, the last term of Eq. (A.24.5) results in the recursion relationship:

$$\frac{a_{s+2}}{a_s} = \frac{1}{(s + 2)(2\nu - s - 1)} \tag{A.24.8}$$

This relationship leads directly to the series solution:

$$y_\nu(\sigma) = \frac{a_0}{\sigma^{\nu+1}} \left\{ 1 + \frac{\sigma^2}{2(2\nu - 1)} + \frac{\sigma^4}{2 \cdot 4(2\nu - 1)(2\nu - 3)} + \dots \right. \\ \left. + \frac{\sigma^{2p}}{(2p)!!(2\nu - 1) \dots (2\nu - 2p - 1)} + \dots + \frac{\sigma^{2(\nu-1)}}{(2\nu - 2)!!(2\nu - 1)!!} \right. \\ \left. - \frac{\sigma^{2\nu}}{1 \cdot (2\nu)!!(2\nu - 1)!!} + \frac{\sigma^2}{3 \cdot (2\nu + 2)!!(2\nu - 1)!!} - \dots \right\} \tag{A.24.9}$$

The series is monotone for s less than ν and oscillatory for s greater than ν . The combination is readily described by separate sums over the monotone and oscillatory portions. After using the definition $a_0 = 1/(2\nu + 1)!!$ and again redefining the dummy index:

$$y_\nu(\sigma) = - \sum_{s=0}^{[\nu]} \frac{(2\nu - 2s - 1)!!}{(2s)!! \sigma^{\nu+1-2s}} - \sum_{s=0}^{\infty} \frac{(-1)^s}{(2s - 1)!!} \frac{\sigma^{\nu-1+2s}}{(2\nu + 2s)!!} \tag{A.24.10}$$

The symbol $[\nu]$ indicates the largest integer less than ν . The first sum of Eq. (A.24.10) describes a monotone power series with inverse powers of ν , powers that range upward from $-(\nu + 1)$ to $(\nu + 1)$ and a second sum that represents an alternating series with positive powers of ν . The sums are

the spherical Neumann functions; Eq. (A.4.10) shows the functional small argument limit of $j_\nu(\sigma)$ to be:

$$\text{Lim}_{\sigma \rightarrow 0} [y_\nu(\sigma)] = -\frac{(2\nu - 1)!!}{\sigma^{\nu+1}} \quad (\text{A.24.11})$$

For integer orders, ν equal integer ℓ and $\sigma \gg 1$, the functions are determined by Eq. (A.24.6) and the second part of Eq. (A.24.10):

$$\begin{aligned} j_\ell(\sigma) &= \sum_{s=0}^{\infty} \frac{(-1)^s}{(2s)!!(2\ell + 2s + 1)!!} \sigma^{\ell+2s} \\ y_\ell(\sigma) &\cong -\sum_{s=0}^{\infty} \frac{(-1)^s}{(2s-1)!!(2\ell + 2s)!!} \sigma^{\ell-1+2s} \end{aligned} \quad (\text{A.24.12})$$

Term-by-term comparison of the series representation of expansions for the trigonometric functions and Eq. (A.24.12) shows that:

$$\begin{aligned} \text{Lim}_{\sigma \rightarrow \infty} j_\ell(\sigma) &= \frac{1}{\sigma} \cos \left[\sigma - \frac{\pi}{2}(\ell + 1) \right] \\ \text{Lim}_{\sigma \rightarrow \infty} y_\ell(\sigma) &= \frac{1}{\sigma} \sin \left[\sigma - \frac{\pi}{2}(\ell + 1) \right] \end{aligned} \quad (\text{A.24.13})$$

Using Eq. (A.24.15), it follows that the Bessel and Neumann functions are related as:

$$\begin{aligned} \text{Lim}_{\sigma \rightarrow \infty} \left\{ j_\ell(\sigma) = \frac{d}{d\sigma} y_\ell(\sigma) \right\} \\ \text{Lim}_{\sigma \rightarrow \infty} \left\{ y_\ell(\sigma) = -\frac{d}{d\sigma} j_\ell(\sigma) \right\} \end{aligned} \quad (\text{A.24.14})$$

25. The Second Solution Form

If the separation constant is an integer, the spherical Bessel differential equation, Eq. (1.11.7), is given by:

$$\frac{1}{\sigma^2} \frac{d}{d\sigma} \left(\sigma^2 \frac{dR}{d\sigma} \right) + \left(1 - \frac{\ell(\ell + 1)}{\sigma^2} \right) R = 0 \quad (\text{A.25.1})$$

Equation (A.25.1) is a second order equation with two independent solutions. Because of a singularity at the origin, solutions are satisfied over the region $0 < \sigma \leq \infty$. For the range of solutions in which $\sigma^2 \gg \ell(\ell + 1)$, the differential equation goes to:

$$\frac{1}{\sigma^2} \frac{d}{d\sigma} \left(\sigma^2 \frac{dR(\sigma)}{d\sigma} \right) + R(\sigma) = 0 \quad (\text{A.25.2})$$

If Eq. (A.25.2) were an exact solution the result would be exponential with constant coefficients. Although Eq. (A.25.2) is not exact, it is helpful to

write Eq. (A.24.3) in the form:

$$R_\ell(\sigma) = F_\ell(\sigma)e^{-i\sigma} + G_\ell(\sigma)e^{i\sigma} \tag{A.25.3}$$

A requirement is that at large radii $F_\ell(\sigma)$ and $G_\ell(\sigma)$ vary much less rapidly with increasing radius than do the exponentials. Also since $F_\ell(\sigma)$ and $G_\ell(\sigma)$ are complex conjugates it is only necessary to solve for one of them.

A convenient method of finding $F_\ell(\sigma)$ is a power series expansion. The series and the first two derivatives are:

$$\begin{aligned} R_\ell(\sigma) &= F_\ell(\sigma)e^{-i\sigma}; \quad \frac{dR_\ell(\sigma)}{d\sigma} = \left[\frac{dF_\ell(\sigma)}{d\sigma} - iF_\ell(\sigma) \right] e^{-i\sigma} \\ \frac{d^2R_\ell(\sigma)}{d\sigma^2} &= \left[\frac{d^2F_\ell(\sigma)}{d\sigma^2} - 2i\frac{dF_\ell(\sigma)}{d\sigma} - F_\ell(\sigma) \right] e^{-i\sigma} \end{aligned} \tag{A.25.4}$$

Substituting Eq. (A.25.4) into Eq. (A.25.1) results in the differential equation:

$$\frac{d^2F_\ell(\sigma)}{d\sigma^2} + 2\left(\frac{1}{\sigma} - i\right)\frac{dF_\ell(\sigma)}{d\sigma} - \left(\frac{2i}{\sigma} + \frac{\ell(\ell+1)}{\sigma^2}\right)F_\ell(\sigma) = 0 \tag{A.25.5}$$

The most convenient method of solving Eq. (A.25.5) is with a power series expansion. The series and the first two derivatives are:

$$\begin{aligned} F_\ell(\sigma) &= \sum_{s=0}^{\infty} a_s \sigma^{s+p} \\ \frac{dF_\ell(\sigma)}{d\sigma} &= \sum_{s=0}^{\infty} (s+p)a_s \sigma^{s+p-1} \\ \frac{d^2F_\ell(\sigma)}{d\sigma^2} &= \sum_{s=0}^{\infty} (s+p)(s+p-1)a_s \sigma^{s+p-2} \end{aligned} \tag{A.25.6}$$

Inserting Eq. (A.25.6) into Eq. (A.25.5) and gathering similar powers of σ results in:

$$\left\{ \frac{p(p+1) - \ell(\ell+1)}{\sigma^{p-2}} + \sum_{s=0}^{\infty} \sigma^{s+p+1} \{ a_{s+1} [(s+p+1)(s+p+2) - \ell(\ell+1)] - 2ia_s(s+p+1) \} \right\} = 0 \tag{A.25.7}$$

Since the series is an identity, the coefficient of each power of σ is equal to zero. It follows from the σ^{p-2} term that either $p = \ell$ or $p = -(\ell+1)$

and it follows from the square brackets that:

$$\frac{a_{s+1}}{a_s} = \frac{2i(s+p+1)}{(s+p+1)(s+p+2) - \ell(\ell+1)} \quad (\text{A.25.8})$$

With the option $p = \ell$, in the limit as σ becomes infinite Eq. (A.25.8) goes to:

$$\text{Lim}_{s \rightarrow \infty} \left(\frac{a_{s+1}}{a_s} \right) = \frac{2i}{s} \quad (\text{A.25.9})$$

Equation (A.25.9) is also the limiting form for a series expansion of $\exp(2i\sigma)$. Therefore, since $F_\ell(\sigma)$ varies more slowly with σ than $\exp(-i\sigma)$ the recursion relationship of Eq. (A.25.8) is not an acceptable solution. Returning to the option that $p = -(\ell+1)$, Eq. (A.25.7) goes to:

$$\frac{a_{s+1}}{a_s} = \frac{2i(\ell-s)}{(s+1)(2\ell-s)} \quad (\text{A.25.10})$$

Since the progression of Eq. (A.25.10) terminates at $s = \ell$ the power series truncates to a polynomial of highest order ℓ . The general term is:

$$\frac{a_{s+1}}{a_s} = \frac{(2i)^s \ell! (2\ell-s)!}{s! (2\ell)! (\ell-s)!} \quad (\text{A.25.11})$$

The series results in solution $R_\ell(\sigma)$ where:

$$R_\ell(\sigma) = \frac{e^{-i\sigma}}{\sigma} \sum_{s=0}^{\ell} \frac{(2i)^s \ell! (2\ell-s)!}{s! (2\ell)! (\ell-s)!} a_0 \quad (\text{A.25.12})$$

To characterize the solution substitute $p = \ell - s$, rewrite Eq. (A.25.12) as a sum over p , then change the dummy index back to s . The result is:

$$R_\ell(\sigma) = a_0 \frac{e^{-i\sigma}}{\sigma} \frac{\ell! (2i)^\ell}{(2\ell)!} \sum_{s=0}^{\ell} \frac{(\ell+s)!}{s! (\ell-s)!} \left(\frac{1}{2i\sigma} \right)^s \quad (\text{A.25.13})$$

With the definition that $a_0 = i(2\ell-1)!!$, the full solution is the function $h_\ell(\sigma)$ where:

$$h_\ell(\sigma) = \frac{i^{\ell+1} e^{-i\sigma}}{\sigma} \sum_{s=0}^{\ell} \frac{(\ell+s)!}{s! (\ell-s)!} \left(\frac{1}{2i\sigma} \right)^s \quad (\text{A.25.14})$$

Function $h_\ell(\sigma)$ is a spherical Hankel function of the second kind. The real part is a spherical Bessel function and the negative of the imaginary part

is a spherical Neumann function. By definition:

$$h_\ell(\sigma) = j_\ell(\sigma) - iy_\ell(\sigma) \tag{A.25.15}$$

The complex conjugate of Eq. (A.25.14) is the second independent solution of the equation. It is a spherical Hankel function of the first kind. In this work, we shall be concerned primarily with Hankel functions of the second kind.

For vanishingly small values of σ the dominant term in Eq. (A.25.14) is:

$$\lim_{\sigma \rightarrow 0} [h_\ell(\sigma)] = \frac{i(2\ell + 1)!!}{\sigma^{\ell+1}} \tag{A.25.16}$$

As the radius increases without limit, the dominant term is:

$$\lim_{\sigma \rightarrow \infty} [h_\ell(\sigma)] = \frac{i^{\ell+1}}{\sigma} e^{-i\sigma} \tag{A.25.17}$$

Equation (A.25.17) shows that as the radius increases without limit the function $[\sigma h_\ell(\sigma)]$ does not approach a limit. For those cases where it is necessary to impose a limit condition, it is necessary to use the solutions of Sec. A.24. For all other cases, the above form is convenient and applicable.

26. Tables of Spherical Bessel, Neumann, and Hankel Functions

To evaluate spherical Bessel, Neumann, and Hankel functions, it is helpful to factor each function into rational and transcendental parts. We introduce rational functions $A_\ell(\sigma)$ and $B_\ell(\sigma)$. In these terms the functions of Eqs. (A.25.14) and (A.25.15) are:

$$\begin{aligned} j_\ell(\sigma) &= \frac{1}{\sigma} \{B_\ell(\sigma) \cos \sigma + A_\ell(\sigma) \sin \sigma\} \\ y_\ell(\sigma) &= \frac{1}{\sigma} \{-A_\ell(\sigma) \cos \sigma + B_\ell(\sigma) \sin \sigma\} \\ h_\ell(\sigma) &= \frac{1}{\sigma} \{B_\ell(\sigma) + iA_\ell(\sigma)\} e^{-i\sigma} \end{aligned} \tag{A.26.1}$$

Comparison of the equations shows, with q equal to any integer, that:

$$\begin{aligned} A_\ell(\sigma) &= \sum_{s=0}^{\ell} \frac{(\ell + s)!}{s!(\ell - s)!} \left(\frac{1}{2\sigma}\right)^s (-1)^{(\ell-s)/2} \delta(\ell + s, 2q) \\ B_\ell(\sigma) &= \sum_{s=0}^{\ell} \frac{(\ell + s)!}{s!(\ell - s)!} \left(\frac{1}{2\sigma}\right)^s (-1)^{(\ell-s+1)/2} \delta(\ell + s, 2q + 1) \end{aligned} \tag{A.26.2}$$

Comparison of the equations shows values of the letter functions. The primary recursion relationship used to develop the table follows from

Eq. (A.24.6):

$$j_{\ell+2}(\sigma) = \frac{2\ell + 3}{\sigma} j_{\ell+1}(\sigma) - j_{\ell}(\sigma) \tag{A.26.3}$$

Important related functions are obtained by operating on the radial function to obtain the special function:

$$h_{\ell}^*(\sigma) = \frac{1}{\sigma} \frac{d}{d\sigma} [\sigma h_{\ell}(\sigma)] \tag{A.26.4}$$

Similarly to Eq. (A.26.1), the related functions factor into rational and transcendental parts:

$$\begin{aligned} j_{\ell}^*(\sigma) &= \frac{1}{\sigma} \{D_{\ell}(\sigma) \cos \sigma + C_{\ell}(\sigma) \sin \sigma\} \\ y_{\ell}^*(\sigma) &= \frac{1}{\sigma} \{-C_{\ell}(\sigma) \cos \sigma + D_{\ell}(\sigma) \sin \sigma\} \\ h_{\ell}^*(\sigma) &= \frac{1}{\sigma} \{D_{\ell}(\sigma) + iC_{\ell}(\sigma)\} e^{-i\sigma} \end{aligned} \tag{A.26.5}$$

Term-by-term comparison shows that:

$$\frac{dA_{\ell}(\sigma)}{d\sigma} = B_{\ell}(\sigma) + C_{\ell}(\sigma) \quad \frac{dB_{\ell}(\sigma)}{d\sigma} = D_{\ell}(\sigma) - A_{\ell}(\sigma) \tag{A.26.6}$$

It follows upon combining Eq. (A.26.4) with Eqs. (A.24.9) and (A.24.13) that in the limit of a vanishingly small radius:

$$\lim_{\sigma \rightarrow 0} j_{\ell}^*(\sigma) = \frac{(\ell + 1)\sigma^{\ell-1}}{(2\ell + 1)!!} \quad \lim_{\sigma \rightarrow 0} y_{\ell}^*(\sigma) = \frac{\ell(2\ell - 1)!!}{\sigma^{\ell+2}} \tag{A.26.7}$$

It follows similarly upon combining Eq. (A.26.4) with Eq. (A.24.15) that in the limit of an infinitely large radius:

$$\begin{aligned} \lim_{\sigma \rightarrow \infty} j_{\ell}^*(\sigma) &= -\frac{1}{\sigma} \sin \left[\sigma - \frac{\pi}{2}(\ell + 1) \right] \\ \lim_{\sigma \rightarrow \infty} y_{\ell}^*(\sigma) &= -\frac{1}{\sigma} \cos \left[\sigma - \frac{\pi}{2}(\ell + 1) \right] \end{aligned} \tag{A.26.8}$$

Table A.26.1. Table of values of the radial letter functions.

| ℓ | $A_{\ell}(\sigma)$ | $B_{\ell}(\sigma)$ | $C_{\ell}(\sigma)$ | $D_{\ell}(\sigma)$ |
|--------|----------------------------------|-----------------------------|--|----------------------------------|
| 0 | 1 | 0 | 0 | 1 |
| 1 | $1/\sigma$ | -1 | $-1/\sigma^2 + 1$ | $1/\sigma$ |
| 2 | $3/\sigma^2 - 1$ | $-3/\sigma$ | $-6/\sigma^3 + 3/\sigma$ | $6/\sigma^2 - 1$ |
| 3 | $15/\sigma^3 - 6/\sigma$ | $-15/\sigma^2 + 1$ | $-45/\sigma^4 + 21/\sigma^2 - 1$ | $45/\sigma^3 - 6/\sigma$ |
| 4 | $105/\sigma^4 - 45/\sigma^2 + 1$ | $-105/\sigma^3 + 10/\sigma$ | $-420/\sigma^5 + 195/\sigma^3 - 10/\sigma$ | $420/\sigma^4 - 55/\sigma^2 + 1$ |

Table A.26.1. (Continued)

| |
|---|
| $A_5 = 945/\sigma^5 - 420/\sigma^3 + 15/\sigma$ |
| $B_5 = -945/\sigma^4 + 105/\sigma^2 - 1$ |
| $C_5 = -5(9!!)/\sigma^6 + 2205/\sigma^4 - 120/\sigma^2 + 1$ |
| $D_5 = 5(9!!)/\sigma^5 - 630/\sigma^3 + 15/\sigma$ |
| $A_6 = (11!!)/\sigma^6 - 5(9!!)/\sigma^4 + 210\sigma^2 - 1$ |
| $B_6 = -(11!!)/\sigma^5 + 1260/\sigma^3 - 21/\sigma$ |
| $C_6 = -6(11!!)/\sigma^7 + 31(9!!)/\sigma^5 - 1680/\sigma^3 + 21/\sigma$ |
| $D_6 = 6(11!!)/\sigma^6 - 8505/\sigma^4 + 231/\sigma^2 - 1$ |
| $A_7 = (13!!)/\sigma^7 - 6(11!!)/\sigma^5 + 3150/\sigma^3 - 28/\sigma$ |
| $B_7 = -(13!!)/\sigma^6 + 17,325/\sigma^4 - 378/\sigma^2 + 1$ |
| $C_7 = -7(13!!)/\sigma^8 + 43(11!!)/\sigma^6 - 26,775/\sigma^4 + 406/\sigma^2 - 1$ |
| $D_7 = 7(13!!)/\sigma^7 - 131,670/\sigma^5 + 4662/\sigma^3 - 28/\sigma$ |
| $A_8 = (15!!)/\sigma^8 - 7(13!!)/\sigma^6 + 5(11!!)/\sigma^4 - 630/\sigma^2 + 1$ |
| $B_8 = -(15!!)/\sigma^7 + 2(13!!)/\sigma^5 - 6930/\sigma^3 + 36/\sigma$ |
| $C_8 = -8(15!!)/\sigma^9 + 57(13!!)/\sigma^7 - 46(11!!)/\sigma^5 + 8190/\sigma^3 - 36/\sigma$ |
| $D_8 = 8(15!!)/\sigma^8 - 17(13!!)/\sigma^6 + 7(11!!)/\sigma^4 - 666/\sigma^2 + 1$ |
| $A_9 = (17!!)/\sigma^9 - 8(15!!)/\sigma^7 + 7(13!!)/\sigma^5 - 13,860/\sigma^3 + 45/\sigma$ |
| $B_9 = -(17!!)/\sigma^8 + 35(13!!)/\sigma^6 - (13!!)/\sigma^4 + 990/\sigma^2 - 1$ |
| $C_9 = -9(17!!)/\sigma^{10} + 9(17!!)/\sigma^8 - 70(13!!)/\sigma^6 + 17(11!!)/\sigma^4 - 1035/\sigma^2 + 1$ |
| $D_9 = 9(17!!)/\sigma^9 - 22(15!!)/\sigma^7 + 11(13!!)/\sigma^5 - 15,840/\sigma^3 + 45/\sigma$ |

Table A.26.2. Radial function identities.

| | |
|--|--|
| 1 $dA_\ell/d\sigma = C_\ell + B_\ell$ | $dB_\ell/d\sigma = D_\ell - A_\ell$ |
| 2 $A_{\ell-1} + A_{\ell+1} = \frac{2\ell+1}{\sigma}A_\ell$ | $B_{\ell-1} + B_{\ell+1} = \frac{2\ell+1}{\sigma}B_\ell$ |
| 3 $\ell A_{\ell-1} - (\ell+1)A_{\ell+1} = (2\ell+1) \left[\frac{dA_\ell}{d\sigma} - \frac{A_\ell}{\sigma} - B_\ell \right]$ | |
| | $\ell B_{\ell-1} - (\ell+1)B_{\ell+1} = (2\ell+1) \left[\frac{dB_\ell}{d\sigma} - \frac{B_\ell}{\sigma} + A_\ell \right]$ |
| 4 $dA_\ell/d\sigma = -\frac{\ell}{\sigma}A_\ell + A_{\ell-1} + B_\ell$ | $dB_\ell/d\sigma = -\frac{\ell}{\sigma}B_\ell + B_{\ell-1} - A_\ell$ |
| 5 $dA_\ell/d\sigma = \frac{\ell+1}{\sigma}A_\ell - A_{\ell+1} + B_\ell$ | $dB_\ell/d\sigma = \frac{\ell+1}{\sigma}B_\ell - B_{\ell+1} - A_\ell$ |
| 6 $C_\ell = -\frac{\ell}{\sigma}A_\ell + A_{\ell-1} = \frac{\ell+1}{\sigma}A_\ell - A_{\ell+1}$ | $D_\ell = -\frac{\ell}{\sigma}B_\ell + B_{\ell-1} = \frac{\ell+1}{\sigma}B_\ell - B_{\ell+1}$ |
| 7 $dC_\ell/d\sigma = -\left[1 - \frac{\ell(\ell+1)}{\sigma^2} \right] A_\ell + D_\ell$; | $dD_\ell/d\sigma = -\left[1 - \frac{\ell(\ell+1)}{\sigma^2} \right] B_\ell - C_\ell$ |
| 8 $A_\ell D_\ell - B_\ell C_\ell = 1$ | |

Table A.26.2. (Continued)

| | | |
|----|---|--|
| 9 | $A_\ell B_{\ell-1} - A_{\ell-1} B_\ell = 1$ | $C_\ell D_{\ell-1} - C_{\ell-1} D_\ell = -\left(1 + \frac{\ell^2}{\sigma^2}\right)$ |
| | $A_{\ell+1} D_\ell - B_{\ell+1} C_\ell = \frac{\ell+1}{\sigma}$ | $A_\ell D_{\ell+1} - B_\ell C_{\ell+1} = \frac{\ell+1}{\sigma}$ |
| 10 | $A_{\ell+2} B_\ell - A_\ell B_{\ell+2} = \frac{2\ell+3}{\sigma}$ | $C_{\ell+2} D_\ell - C_\ell D_{\ell+2} = \frac{\ell+3}{\sigma} \left(1 - \frac{(\ell+1)(\ell+2)}{\sigma^2}\right)$ |
| 11 | $(A_\ell^2 - B_\ell^2 - C_\ell^2 + D_\ell^2) = \int d\sigma \left\{ 4(A_\ell - D_\ell)(B_\ell + C_\ell) - 2(A_\ell C_\ell - B_\ell D_\ell) \frac{\ell(\ell+1)}{\sigma^2} \right\}$ | |
| | $(A_\ell^2 + B_\ell^2 + C_\ell^2 + D_\ell^2) = \int d\sigma \left\{ 2(A_\ell C_\ell + B_\ell D_\ell) \frac{\ell(\ell+1)}{\sigma^2} \right\}$ | |
| 12 | $(A_\ell B_\ell - C_\ell D_\ell) = -\int d\sigma \left\{ [(A_\ell - D_\ell)^2 + (B_\ell + C_\ell)^2] + (A_\ell D_\ell + B_\ell C_\ell) \frac{\ell(\ell+1)}{\sigma^2} \right\}$ | |
| | $(A_\ell B_\ell + C_\ell D_\ell) = \int d\sigma \left\{ -(A_\ell^2 + B_\ell^2 - C_\ell^2 + D_\ell^2) + (A_\ell D_\ell + B_\ell C_\ell) \frac{\ell(\ell+1)}{\sigma^2} \right\}$ | |
| 13 | $(A_\ell C_\ell - B_\ell D_\ell) = \int d\sigma \left\{ [-(A_\ell - D_\ell)^2 + (B_\ell + C_\ell)^2] + (A_\ell^2 - B_\ell^2) \left(\frac{\ell(\ell+1)}{\sigma^2} \right) \right\}$ | |
| | $(A_\ell C_\ell + B_\ell D_\ell) = \int d\sigma \left\{ (-A_\ell^2 - B_\ell^2 + C_\ell^2 + D_\ell^2) + (A_\ell^2 + B_\ell^2) \left(\frac{\ell(\ell+1)}{\sigma^2} \right) \right\}$ | |
| 14 | $[A_\ell D_\ell + B_\ell C_\ell - (-1)^\ell] = \int d\sigma \left\{ -2(A_\ell - D_\ell)(B_\ell + C_\ell) + 2A_\ell B_\ell \left(\frac{\ell(\ell+1)}{\sigma^2} \right) \right\}$ | |
| 15 | $\frac{d}{d\sigma} (A_\ell A_n + B_\ell B_n + C_\ell C_n + D_\ell D_n)$ | |
| | $= \frac{1}{\sigma^2} [\ell(\ell+1)(A_\ell C_n + B_\ell D_n) + n(n+1)(A_n C_\ell + B_n D_\ell)]$ | |
| 16 | $\frac{d}{d\sigma} (A_\ell B_n - B_\ell A_n + C_\ell D_n - D_\ell C_n)$ | |
| | $= \frac{1}{\sigma^2} [\ell(\ell+1)(A_\ell D_n - B_\ell C_n) - n(n+1)(A_n D_\ell - B_n C_\ell)]$ | |
| 17 | $\frac{d}{d\sigma} (A_\ell C_n - C_\ell A_n + B_\ell D_n - D_\ell B_n)$ | |
| | $= \frac{1}{\sigma^2} [n(n+1) - \ell(\ell+1)](A_\ell A_n + B_\ell B_n)$ | |
| 18 | $\frac{d}{d\sigma} (A_\ell C_n + C_\ell A_n - B_\ell D_n - D_\ell B_n) = \left\{ \frac{1}{\sigma^2} [n(n+1) - \ell(\ell+1)](A_\ell A_n + B_\ell B_n) \right.$ | |
| | $\left. + 2(A_\ell D_n + A_n D_\ell + B_\ell C_n + B_n C_\ell) - 2(A_\ell A_n - B_\ell B_n - C_\ell C_n + D_\ell D_n) \right\}$ | |
| 19 | $\frac{d}{d\sigma} (A_\ell B_n + B_\ell A_n - C_\ell D_n - D_\ell C_n) = \left\{ \frac{1}{\sigma^2} [\ell(\ell+1)(A_\ell D_n + B_\ell C_n) \right.$ | |
| | $\left. + n(n+1)(A_n D_\ell + B_n C_\ell) + 2(A_\ell D_n + A_n D_\ell + B_\ell C_n + B_n C_\ell) \right.$ | |
| | $\left. - 2(A_\ell A_n - B_\ell B_n - C_\ell C_n + D_\ell D_n) \right\}$ | |
| 20 | $\frac{d}{d\sigma} \left(\frac{A_\ell B_\ell}{A_\ell^2 - B_\ell^2} \right) = \frac{(A_\ell^2 + B_\ell^2)}{(A_\ell^2 - B_\ell^2)^2} [1 - (A_\ell^2 + B_\ell^2)]$ | |

Table A.26.3. Radial dependence of $[A_\ell D_\ell + B_\ell C_\ell - (-1)^\ell]$.

| ℓ | $[A_\ell D_\ell + B_\ell C_\ell - (-1)^\ell]$ |
|--------|---|
| 1 | $2/\sigma^2$ |
| 2 | $36/\sigma^4 - 18/\sigma^2$ |
| 3 | $1350/\sigma^6 - 720/\sigma^4 + 72/\sigma^2$ |
| 4 | $88200/\sigma^8 - 49350/\sigma^6 + 6000/\sigma^4 + 200/\sigma^2$ |
| 5 | $8930250/\sigma^{10} - 5159700/\sigma^8 + 699300/\sigma^6 - 31500/\sigma^4 + 450/\sigma^2$ |
| 6 | $1296672300/\sigma^{12} - 766215450/\sigma^{10} + 111370140/\sigma^8 - 5900580/\sigma^6 + 123480/\sigma^4 - 882/\sigma^2$ |

Table A.26.4. Radial dependence of $[A_\ell C_\ell - B_\ell D_\ell]$.

| ℓ | $[A_\ell C_\ell - B_\ell D_\ell]$ |
|--------|--|
| 1 | $-1/\sigma^3 + 2/\sigma$ |
| 2 | $-18/\sigma^5 + 33/\sigma^3 - 6/\sigma$ |
| 3 | $-675/\sigma^7 + 1250/\sigma^5 - 276/\sigma^3 + 12/\sigma$ |
| 4 | $-44100/\sigma^9 + 83475/\sigma^7 - 20220/\sigma^5 + 1300/\sigma^3 - 20/\sigma$ |
| 5 | $-4465125/\sigma^{11} + 8533350/\sigma^9 - 2201850/\sigma^7 + 169470/\sigma^5 - 4425/\sigma^3 + 30/\sigma$ |
| 6 | $-648,336,150/\sigma^{13} + 1,247,555,935/\sigma^{11} - 335,975,850/\sigma^9 + 28,797,930/\sigma^7 - 961,380/\sigma^5 + 12,201/\sigma^3 - 42/\sigma$ |

Table A.26.5. Radial dependence of $[A_\ell C_\ell + B_\ell D_\ell]$.

| ℓ | $[A_\ell C_\ell + B_\ell D_\ell]$ |
|--------|---|
| 1 | $-1/\sigma^3$ |
| 2 | $-18/\sigma^5 - 3/\sigma^3$ |
| 3 | $-675/\sigma^7 - 90/\sigma^5 - 6/\sigma$ |
| 4 | $-44100/\sigma^9 - 4725/\sigma^7 - 270/\sigma^5 - 10/\sigma^3$ |
| 5 | $-4465125/\sigma^{11} - 396900/\sigma^9 - 18900/\sigma^7 - 630/\sigma^5 - 15/\sigma^3$ |
| 6 | $-648336150/\sigma^{13} - 49116375/\sigma^{11} - 1984500/\sigma^9 - 56700/\sigma^7 - 1260/\sigma^5 - 21/\sigma^3$ |

Table A.26.6. Radial dependence of $2(A_\ell - D_\ell)(B_\ell + C_\ell)$.

| ℓ | $2(A_\ell - D_\ell)(B_\ell + C_\ell)$ |
|--------|--|
| 1 | 0 |
| 2 | $36/\sigma^5$ |
| 3 | $2700/\sigma^7 - 360/\sigma^5$ |
| 4 | $264000/\sigma^9 - 65100/\sigma^7 + 1800/\sigma^5$ |
| 5 | $352711500/\sigma^{11} - 11510100/\sigma^9 + 642600/\sigma^7 - 6300/\sigma^5$ |
| 6 | $6,483,361,500/\sigma^{13} - 2,436,172,200/\sigma^{11} + 189,162,540/\sigma^9 - 3,969,000/\sigma^7 + 17,640\sigma^5$ |

Table A.26.7. Radial dependence of $(A_\ell - D_\ell)^2 - (B_\ell + C_\ell)^2$.

| ℓ | $(A_\ell - D_\ell)^2 - (B_\ell + C_\ell)^2$ |
|--------|---|
| 1 | $-1/\sigma^4$ |
| 2 | $-36/\sigma^6 - 9/\sigma^4$ |
| 3 | $-2025/\sigma^8 + 1440/\sigma^6 - 36/\sigma^4$ |
| 4 | $-176400/\sigma^{10} + 174825/\sigma^8 - 14400/\sigma^6 + 100/\sigma^4$ |
| 5 | $-22325625/\sigma^{12} + 26195400/\sigma^{10} - 3316950/\sigma^8 + 81900/\sigma^6 - 225/\sigma^4$ |
| 6 | $-3890016900/\sigma^{14} + 5058986625/\sigma^{12} - 802531800/\sigma^{10}$ $+ 32345224/\sigma^8 - 335160/\sigma^6 + 44/\sigma^4$ |

Table A.26.8. Radial dependence of $(A_\ell - D_\ell)^2 + (B_\ell + C_\ell)^2$.

| ℓ | $(A_\ell - D_\ell)^2 + (B_\ell + C_\ell)^2$ |
|--------|--|
| 1 | $1/\sigma^4$ |
| 2 | $36/\sigma^6 + 9/\sigma^4$ |
| 3 | $2025/\sigma^8 + 360/\sigma^6 + 36/\sigma^4$ |
| 4 | $176400/\sigma^{10} + 23625/\sigma^8 + 1800/\sigma^6 + 100/\sigma^4$ |
| 5 | $22325625/\sigma^{12} + 2381400/\sigma^{10} + 141750/\sigma^8 + 6300/\sigma^6 + 225/\sigma^4$ |
| 6 | $3890016900/\sigma^{14} + 343814625/\sigma^{12} + 16669800/\sigma^{10}$ $+ 593224/\sigma^8 + 17640/\sigma^6 + 441/\sigma^4$ |

27. Spherical Bessel Function Sums

Any electromagnetic field may be expressed as the product of spherical Bessel, Neumann, Hankel functions of σ , or linear combinations thereof, times linear combinations of Legendre functions of θ , times linear combinations of trigonometric functions of azimuth angle ϕ .

A particularly useful function is a z -directed plane wave: $e^{-ikz} = e^{-i\sigma \cos \theta}$. It follows that functions with $m = 0$ are present, and there is no dependence upon ϕ . Since the function is regular on the z -axis, only spherical Bessel functions are present. The result, expressed using spherical coordinates, is the general solution form expressed as a sum over the single product:

$$e^{-i\sigma \cos \theta} = \sum_{\ell=0}^{\infty} a_\ell j_\ell(\sigma) P_\ell(\cos \theta) \quad (\text{A.27.1})$$

The objective is to evaluate each of the infinite number of constants a_ℓ . To do so, multiply both sides by $P_n(\cos \theta)$ and integrate over the full range

of zenith angle. The result is:

$$\frac{2j_\ell(\sigma)}{(2\ell + 1)} a_\ell = \int_0^\pi \sin \theta \, d\theta P_\ell(\cos \theta) e^{-i\sigma \cos \theta} \quad (\text{A.27.2})$$

Differentiating both sides ℓ times with respect to σ then going to the limit of vanishing small radius, see Eq. (A.24.7), gives:

$$\frac{2a_\ell i^\ell}{(2\ell + 1)} \frac{\ell!}{(2\ell + 1)!!} = \int_0^\pi \sin \theta \, d\theta P_\ell(\cos \theta) \cos^\ell \theta \quad (\text{A.27.3})$$

The integral is listed in Table A.22.1.10. Doing the integration and solving for a_ℓ gives:

$$a_\ell = i^{-\ell} (2\ell + 1) \quad (\text{A.27.4})$$

Combining Eq. (A.27.1) with Eq. (A.27.4) gives:

$$e^{-i\sigma \cos \theta} = \sum_{\ell=0}^{\infty} i^{-\ell} (2\ell + 1) j_\ell(\sigma) P_\ell(\cos \theta) \quad (\text{A.27.5})$$

Other related sums follow from Eq. (A.27.5). Differentiating both sides of Eq. (A.27.5) with respect to θ and using Table A.21.1.10 gives:

$$\sigma e^{-i\sigma \cos \theta} = \sum_{\ell=1}^{\infty} i^{1-\ell} (2\ell + 1) j_\ell(\sigma) \frac{P'_\ell(\cos \theta)}{\sin \theta} \quad (\text{A.27.6})$$

Evaluating Eq. (A.27.1) on the positive z -axis gives the three series:

$$\begin{aligned} e^{-i\sigma} &= \sum_{\ell=0}^{\infty} i^{-\ell} (2\ell + 1) j_\ell(\sigma) \\ \sin \sigma &= \sum_{\ell=0;1}^{\infty} (-1)^{(\ell-1)/2} (2\ell + 1) j_\ell(\sigma) \\ \cos \sigma &= \sum_{\ell=0}^{\infty} (-1)^{\ell/2} (2\ell + 1) j_\ell(\sigma) \end{aligned} \quad (\text{A.27.7})$$

Subscripts “o;1” and “e;0” indicate respectively odd integers beginning with one and even integer beginning with zero.

Evaluation of Eqs. (A.27.5) and (A.27.6) at $\theta = \pi/2$, see Table A.18.1, gives:

$$1 = \sum_{\ell e; 0}^{\infty} (2\ell + 1) \frac{(\ell - 1)!!}{(\ell!!)^2} j_{\ell}(\sigma) \quad (\text{A.27.8})$$

$$\sigma = \sum_{\ell o; 1}^{\infty} (2\ell + 1) \frac{(\ell)!!}{(\ell - 1)!!^2} j_{\ell}(\sigma)$$

Application of Eq. (A.26.4) to Eq. (A.27.8) gives:

$$\frac{1}{\sigma} = \sum_{\ell e; 0}^{\infty} (2\ell + 1) \frac{\ell!!}{(\ell!!)^2} j_{\ell}^*(\sigma) \quad (\text{A.27.9})$$

$$1 = \sum_{\ell o; 1}^{\infty} \frac{(2\ell + 1)}{2} \frac{\ell!!}{(\ell - 1)!!^2} j_{\ell}^*(\sigma)$$

Use of Eq. (A.7.6) to integrate Eq. (A.27.5) over θ gives:

$$\left[\frac{e^{-i\sigma \cos \theta}}{\sigma} \right]_{\theta_1}^{\theta_2} = \sum_{\ell=0}^{\infty} i^{-\ell-1} j_{\ell}(\sigma) [P_{\ell+1}(\cos \theta) - P_{\ell-1}(\cos \theta)]_{\theta_1}^{\theta_2} \quad (\text{A.27.10})$$

Evaluation of Eq. (A.27.10) between limits $\theta = \pi$ and $\pi/2$ gives:

$$\left(\frac{1 - e^{i\sigma}}{\sigma} \right) = \sum_{\ell=0}^{\infty} i^{-\ell-1} j_{\ell}(\sigma) [P_{\ell+1}(0) - P_{\ell-1}(0)] - ij_0(\sigma) \quad (\text{A.27.11})$$

Evaluation of Eq. (A.27.11) between limits $\theta = \pi/2$ and 0 gives:

$$\left(\frac{e^{-i\sigma} - 1}{\sigma} \right) = -ij_0(\sigma) - \sum_{\ell=0}^{\infty} i^{-\ell-1} j_{\ell}(\sigma) [P_{\ell+1}(0) - P_{\ell-1}(0)] \quad (\text{A.27.12})$$

Subtracting Eq. (A.27.11) from Eq. (A.27.12) gives:

$$\frac{\cos \sigma - 1}{\sigma} = \sum_{\ell=0}^{\infty} (2\ell + 1) \frac{(\ell - 1)!}{(\ell - 1)!!(\ell + 1)!!} j_{\ell}(\sigma) \quad (\text{A.27.13})$$

The operation of Eq. (A.26.4) results in:

$$\frac{\sin \sigma}{\sigma} = \sum_{\ell=0}^{\infty} (2\ell + 1) \frac{(\ell - 1)!}{(\ell - 1)!!(\ell + 1)!!} j_{\ell}^*(\sigma) \quad (\text{A.27.14})$$

When evaluated on the positive z -axis this gives

$$\sigma e^{-i\sigma} = \frac{1}{2} \sum_{\ell=1}^{\infty} i^{1-\ell} (2\ell + 1) \ell(\ell + 1) j_{\ell}(\sigma) \quad (\text{A.27.15})$$

Table A.27.1. Table of sums over spherical Bessel functions.

| | |
|----|--|
| 1 | $e^{-i\sigma \cos \theta} = \sum_{\ell=0}^{\infty} i^{-\ell} (2\ell + 1) j_{\ell}(\sigma) P_{\ell}(\cos \theta)$ |
| 2 | $\sigma \sin \theta e^{-i\sigma \cos \theta} = \sum_{\ell=1}^{\infty} i^{1-\ell} (2\ell + 1) j_{\ell}(\sigma) P_{\ell}^1(\cos \theta)$ |
| 3 | $\frac{1 - \cos \sigma}{\sigma} = \sum_{\ell=0;1}^{\infty} (2\ell + 1) \frac{(\ell - 2)!!}{(\ell + 1)!!} j_{\ell}(\sigma)$ |
| 4 | $\frac{\sin \sigma}{\sigma} = \sum_{\ell=0;1}^{\infty} (2\ell + 1) \frac{(\ell - 2)!!}{(\ell + 1)!!} j_{\ell}^{\bullet}(\sigma)$ |
| 5 | $1 = \sum_{\ell e;0}^{\infty} (2\ell + 1) \frac{(\ell - 1)!!}{\ell!!} j_{\ell}(\sigma)$ |
| 6 | $\frac{1}{\sigma} = \sum_{\ell e;0}^{\infty} (2\ell + 1) \frac{(\ell - 1)!!}{(\ell)!!} j_{\ell}^{\bullet}(\sigma)$ |
| 7 | $\sigma = \sum_{\ell o;1}^{\infty} (2\ell + 1) \frac{(\ell)!!}{(\ell - 1)!!} j_{\ell}(\sigma)$ |
| 8 | $1 = \sum_{\ell o;1}^{\infty} \frac{(2\ell + 1)}{2} \frac{(\ell)!!}{(\ell - 1)!!} j_{\ell}^{\bullet}(\sigma)$ |
| 9 | $\sigma e^{-i\sigma} = \frac{1}{2} \sum_{\ell=1}^{\infty} i^{1-\ell} (2\ell + 1) \ell(\ell + 1) j_{\ell}(\sigma)$ |
| 10 | $(2 - i\sigma)e^{-i\sigma} = \frac{1}{2} \sum_{\ell=1}^{\infty} i^{1-\ell} (2\ell + 1) (\ell + 1) j_{\ell}^{\bullet}(\sigma)$ |

The exponential contains the two equations:

$$\begin{aligned} \sigma \cos \sigma &= \frac{1}{2} \sum_{\ell o;1}^{\infty} (-1)^{(\ell-1)/2} (2\ell + 1) \ell(\ell + 1) j_{\ell}(\sigma) \\ \sigma \sin \sigma &= \frac{1}{2} \sum_{\ell e;2}^{\infty} (-1)^{\ell/2} (2\ell + 1) \ell(\ell + 1) j_{\ell}(\sigma) \end{aligned} \tag{A.27.16}$$

Table A.27.1 contains a listing of sums over different functions of spherical Bessel functions.

28. Static Scalar Potentials

To examine physical sources of TM modal coefficients $F(\ell, m)$, it is convenient to start with the static scalar potential field, $\Phi(\mathbf{r})$. By Eq. (1.5.4) the

differential equation that governs the scalar potential is:

$$\nabla^2\Phi = \rho/\varepsilon \quad (\text{A.28.1})$$

By this equation the scalar potential has a spatial curvature only where electric charges exist and a field function exists only if the curvature is other than zero. It follows that static scalar potentials arise only from electric charges.

To characterize such potentials we establish an origin near or in a region that contains static electric charges. Based upon that origin, the coordinates within the charged region are $\mathbf{r}(x, y, z)$. The field points at which the potential is to be evaluated are $\mathbf{r}(x, y, z)$. The field point may be either interior or exterior to the charge-containing region. The distance from the source to the field point is R where, by definition:

$$R(\mathbf{r}, \mathbf{r}) = [(x - x)^2 + (y - y)^2 + (z - z)^2]^{1/2} \quad (\text{A.28.2})$$

The potential at an arbitrary field point was previously calculated, Eq. (1.5.9), and is given by:

$$\Phi(\mathbf{r}) = \frac{1}{4\pi\varepsilon} \int \frac{\rho(\mathbf{r})}{R} dV \quad (\text{A.28.3})$$

It is convenient to work with distance from the origin to field point \mathbf{r} , but the function in the denominator of Eq. (A.28.3) is the distance from the differential source point to field point R . To replace $1/R$ by a function of $1/r$, use the Taylor series expansion:

$$\frac{1}{R} = \left\{ \frac{1}{r} + x_i \frac{\partial}{\partial x_i} \left(\frac{1}{R} \right)_r + \frac{1}{2} x_i x_j \frac{\partial}{\partial x_i} \frac{\partial}{\partial x_j} \left(\frac{1}{R} \right)_r + \frac{1}{6} x_i x_j x_k \frac{\partial}{\partial x_i} \frac{\partial}{\partial x_j} \frac{\partial}{\partial x_k} \left(\frac{1}{R} \right)_r + \frac{1}{24} x_i x_j x_k x_m \frac{\partial}{\partial x_i} \frac{\partial}{\partial x_j} \frac{\partial}{\partial x_k} \frac{\partial}{\partial x_m} \left(\frac{1}{R} \right)_r + \dots \right\} \quad (\text{A.28.4})$$

Placing the expansion of Eq. (A.28.4) into Eq. (A.28.3) results in the desired form:

$$\begin{aligned} \Phi(\mathbf{r}) = & \frac{1}{4\pi\varepsilon} \left\{ \left(\frac{1}{r} \right) \int \rho(\mathbf{r}) dV + \frac{\partial}{\partial x_i} \left(\frac{1}{R} \right)_r \int x_i \rho(\mathbf{r}) dV \right. \\ & + \frac{1}{2} \frac{\partial}{\partial x_i} \frac{\partial}{\partial x_j} \left(\frac{1}{R} \right)_r \int x_i x_j \rho(\mathbf{r}) dV \\ & \left. + \frac{1}{6} \frac{\partial}{\partial x_i} \frac{\partial}{\partial x_j} \frac{\partial}{\partial x_k} \left(\frac{1}{R} \right)_r \int x_i x_j x_k \rho(\mathbf{r}) dV + \dots \right\} \quad (\text{A.28.5}) \end{aligned}$$

The first term of Eq. (A.28.5) has a first order singularity at the origin:

$$\Phi_0(r, \theta, \phi) = \frac{1}{4\pi\epsilon} \frac{q}{r} \quad \text{where } q = \int \rho(\mathbf{r})dV \quad (\text{A.28.6})$$

Succeeding terms have successively higher order singularities. Fields associated with succeeding singularities are generated by equal values of positive and negative charge, spaced incremental distances apart. The total potential is the sum of that from each charge and, in the limit as the inter-charge spacing goes to zero, the mathematical affect on the potential is the same as obtained by differentiating with respect to x_i . For example, for the special case of charge separation z_0 all differentials in Eq. (A.28.5) are z -directed.

Consider the multipolar electric moment of a charge distribution with ℓ displacements. The moment is of order ℓ and degree m :

$$p_\ell^m = \int \rho(\mathbf{r})x_i x_j \cdots x_k dV \quad (\text{A.28.7})$$

Moments are designated by the number of charges involved; moment p_ℓ^m , where ℓ is the order, is formed by 2^ℓ charges. Charges are arrayed according to the coefficients of a binomial expansion of the same order. Let a total of $(\ell - m)$ displacements be z -directed, let s of them be x -directed, and of them $(m - s)$ be y -directed.

Easily verified equalities satisfied by the Legendre polynomials are:

$$P_\ell(\cos \theta) = \frac{1}{\ell!} \frac{\partial^\ell}{\partial z^\ell} \left(\frac{1}{R} \right)_r \quad (\text{A.28.8})$$

$$P_\ell^1(\cos \theta) \sin \phi = \frac{1}{(\ell - 1)!} \frac{\partial^\ell}{\partial y \partial z^{\ell-1}} \left(\frac{1}{R} \right)_r$$

Consider, as examples, structures that generate the lowest order multipolar moments. A dipole consists of two discrete charges: charge q at $z_0/2$ and charge $-q$ at $-z_0/2$; the volume integral, Eq. (A.28.7), over order one is qz_0 and over any even order is zero. A linear quadrupole consists of four discrete charges: charges q at $+z_0$ and $-z_0$ and charge $-2q$ at the origin; the volume integral over order two is $2qz_0^2$ and over any odd order is zero. A linear octupole consists of eight discrete charges: charge q at $3z_0/2$, $-3q$ at $z_0/2$, $3q$ at $-z_0/2$, $-q$ at $-3z_0/2$. For a source of order three, the volume integral is $qz_0^3/4$. The same integral over any even order is zero. The volume integral over order one is zero but the volume integral for odd orders greater than three is not zero.

In all cases, the volume integral of Eq. (A.28.7) is zero if the charge distribution and the displacements have opposite parity. It is also equal to

zero if there are fewer charges than the number of displacements. In all other cases, the integral is non-zero. Tables A.28.1 and A.28.2 show some basic features of common multipolar electric moments. In each table column one shows the order of the source. Column two shows the discrete charge distribution that generates that order of singularity. Column three shows the volume integral of Eq. (A.28.7). Column four shows the lowest non-vanishing order of the potential. With the aid of the static portion of Eq. (A.28.6), column five shows the radial components of the generated electric field intensity. Table A.28.1 is for only z -directed displacements and Table A.28.2 is for one y - and $(\ell - 1)$ z -directed displacements. Table A.28.1 uses scalar charge q as the unit cell and Table A.28.2 uses a y -directed dipole as the unit cell. For the two cases the multipolar moments are:

$$p_\ell = \ell!qz_0^\ell \quad \text{and} \quad p_\ell^1 = (\ell - 1)!qy_0z_0^{\ell-1}$$

The scalar potential of an arbitrary charge distribution is the simple sum of values obtained from each moment:

$$\Phi(r, \theta, \phi) = \frac{1}{4\pi\epsilon} \sum_{\ell=0}^{\infty} \sum_{m=-\ell}^{\ell} \frac{P_\ell^m}{r^{\ell+1}} P_\ell^m(\cos\theta) e^{-jm\phi} \tag{A.28.9}$$

Table A.28.1. Electrostatic potentials of a linear array of sources, ℓ charges spaced distance z_0 apart.

| ℓ | Charge Sites | p_ℓ | $4\pi\epsilon\Phi_\ell(r, \theta)$ | $4\pi\epsilon E_{r\ell}(r, \theta)$ |
|--------|--|----------------------------|------------------------------------|-------------------------------------|
| 0 | +q at 0 | q | $\frac{q}{r}$ | $\frac{q}{r^2}$ |
| 1 | -q at $-z_0/2$ +q at $z_0/2$ | $p_1 = qz_0$ | $\frac{p_1}{r^2} P_1(\cos\theta)$ | $\frac{2p_1}{r^3} P_1(\cos\theta)$ |
| 2 | +q at $-z_0$ -2q at 0 +q at z_0 | $p_2 = 2p_1z_0 = 2qz_0^2$ | $\frac{p_2}{r^3} P_2(\cos\theta)$ | $\frac{3p_2}{r^4} P_2(\cos\theta)$ |
| 3 | -q at $-3z_0/2$; +3q at $-z_0/2$; -3q at $z_0/2$ +q at $3z_0/2$ | $p_3 = 3p_2z_0 = 6qz_0^3$ | $\frac{p_3}{r^4} P_3(\cos\theta)$ | $\frac{4p_3}{r^5} P_3(\cos\theta)$ |
| 4 | +q at $-2z_0$ -4q at $-z_0$ +6q at 0 -4q at z_0 ; +q at $2z_0$ | $p_4 = 4p_3z_0 = 24qz_0^4$ | $\frac{p_4}{r^5} P_4(\cos\theta)$ | $\frac{5p_4}{r^6} P_4(\cos\theta)$ |

Table A.28.2. Electrostatic source potentials, one y_0 and $(\ell - 1)z_0$ charge spacings.

| ℓ | Charge and Sites | p_ℓ^1 | $\frac{4\pi\epsilon\Phi_\ell^1(r, \theta, \phi)}{\sin \phi}$ | $\frac{4\pi\epsilon E_{r\ell}(r, \theta, \phi)}{\sin \phi}$ |
|--------|---|----------------------|--|---|
| 1 | +q at $y_0/2$ -q at $-y_0/2$ | $p_1^1 = qy_0$ | $\frac{p_1^1}{r^2} P_1^1(\cos \theta)$ | $\frac{2p_1^1}{r^3} P_1^1(\cos \theta)$ |
| 2 | +q at $(y_0 + z_0)/2$ -q at $(-y_0 + z_0)/2$ +q at $-(y_0 + z_0)/2$ -q at $(y_0 - z_0)/2$ | $p_2^1 = p_1^1 z_0$ | $\frac{p_2^1}{r^3} P_2^1(\cos \theta)$ | $\frac{3p_2^1}{r^4} P_2^1(\cos \theta)$ |
| 3 | +q at $(y_0 \pm 2z_0)/2$ -2q at $y_0/2$ +2q at $-y_0/2$ -q at $(-y_0 \pm 2z_0)/2$ | $p_3^1 = 2p_2^1 z_0$ | $\frac{p_3^1}{r^4} P_3^1(\cos \theta)$ | $\frac{4p_3^1}{r^5} P_3^1(\cos \theta)$ |
| 4 | +q at $\pm(y_0 + 3z_0)/2$ -3q at $\pm(y_0 + z_0)/2$ -q at $\pm(y_0 - 3z_0)/2$ 3q at $\pm(y_0 - z_0)/2$ | $p_4^1 = 3p_3^1 z_0$ | $\frac{p_4^1}{r^5} P_4^1(\cos \theta)$ | $\frac{5p_4^1}{r^6} P_4^1(\cos \theta)$ |

This is the static scalar potential at an arbitrary, exterior field point due to the charge distribution. The radial component of the electric field intensity follows from Eq. (A.28.9) with the aid of the static portion of Eq. (1.6.3), and is equal to:

$$E_r(r, \theta, \phi) = \frac{1}{4\pi\epsilon} \sum_{\ell=0}^{\infty} \sum_{m=-\ell}^{\ell} \frac{(\ell + 1)P_\ell^m}{r^{\ell+2}} P_\ell^m(\cos \theta) e^{-jm\phi} \quad (\text{A.28.10})$$

This is the radial field on a circumscribing sphere if the radius of that sphere is vanishingly small. Direct comparison of the coefficients of Eqs. (1.12.9) and (A.28.10) in the limit as the frequency goes to zero, after combining with Eq. (A.25.16), gives:

$$E_r(r, \theta, \phi) = - \sum_{\ell=0}^{\infty} \sum_{m=0}^{\ell} i^{-\ell} F(\ell, m) \ell(\ell + 1) \frac{(2\ell - 1)!!}{\sigma^{\ell+2}} P_\ell^m(\cos \theta) e^{-jm\phi} \quad (\text{A.28.11})$$

Comparison of Eqs. (A.28.10) and (A.28.11) gives:

$$F(\ell, m) = - \frac{1}{4\pi\epsilon} \frac{i^\ell k^{\ell+2} p_\ell^m}{\ell(2\ell - 1)!!} \quad (\text{A.28.12})$$

For the special case of a z -directed electric dipole of moment p_1 , it follows from the third row of Table A.28.1 that:

$$\Phi_1 = \frac{p_1 \cos \theta}{4\pi\epsilon r^2} \quad \text{and} \quad E_r = \frac{2p_1 \cos \theta}{4\pi\epsilon r^3} \quad (\text{A.28.13})$$

29. Static Vector Potentials

To examine physical sources of TE modal coefficients $G(\ell, m)$, it is convenient to start with the vector scalar potential field, $\mathbf{A}(\mathbf{r})$. By Eq. (1.5.4) the differential equation that governs the vector potential is:

$$\nabla^2 \mathbf{A}(\mathbf{r}) = \mu \mathbf{J}(\mathbf{r}) \quad (\text{A.29.1})$$

By this equation the vector potential has a non-zero spatial curvature only where electric currents exist. Since a field function cannot exist unless, somewhere, the curvature is not zero, it follows that static vector potentials arise only from electric currents.

Although the formal descriptions of the scalar and vector potential are similar, the sources are not. Static scalar potentials arise from stationary electric charges and vector potentials arise from moving ones. The integrated form of Eq. (A.29.1) follows from Eq. (1.5.8). With $\mathbf{J}(\mathbf{r})$ representing a continuum charge distribution it is:

$$\mathbf{A}(\mathbf{r}) = \frac{\mu}{4\pi} \oint \frac{\mathbf{J}(\mathbf{r}')}{R(\mathbf{r}, \mathbf{r}')} dV' \quad (\text{A.29.2})$$

Combining the Taylor distance expansion of Eq. (A.28.4) with Eq. (A.29.2) gives:

$$\begin{aligned} \mathbf{A}(\mathbf{r}) = \frac{\mu}{4\pi} \left\{ \left(\frac{1}{R} \right)_r \int \mathbf{J}(\mathbf{r}') dV' + \left(\frac{\partial}{\partial x_i} \frac{1}{R} \right)_r \int x_i \mathbf{J}(\mathbf{r}') dV' \right. \\ \left. + \frac{1}{2} \left(\frac{\partial}{\partial x_i} \frac{\partial}{\partial x_j} \frac{1}{R} \right)_r \int x_i x_j \mathbf{J}(\mathbf{r}') dV' \right. \\ \left. + \frac{1}{6} \left(\frac{\partial}{\partial x_i} \frac{\partial}{\partial x_j} \frac{\partial}{\partial x_k} \frac{1}{R} \right)_r \int x_i x_j x_k \mathbf{J}(\mathbf{r}') dV' \right\} \quad (\text{A.29.3}) \end{aligned}$$

Consider a filamentary current of magnitude I that is located in the xy plane at $z = 0$. The current at radius a flows in the $\hat{\phi}$ direction. By Eq. (A.29.1), the potential component in a particular direction is proportional to the current in that direction and there is no z -component of the current. Therefore, there is no z -component of the potential. Since the current has rotational symmetry about the z -axis there is no loss of generality in placing the field

point in the xz -plane, say $(x_0, 0, z_0)$. With the differential source at position $a(\hat{x} \cos \phi + \hat{y} \sin \phi) = x\hat{x} + y\hat{y}$ the source to field distance is

$$R = [(x_0 - x)^2 + y^2 + z_0^2]^{1/2}$$

By Eq. (A.29.2) the zero order vector potential is:

$$\mathbf{A}_0(\mathbf{r}) = \frac{\mu I}{4\pi r} \int_0^{2\pi} a(-\hat{x} \sin \phi + \hat{y} \cos \phi) d\phi = 0 \quad (\text{A.29.4})$$

To evaluate the first order vector potential of the current loop, note the partial derivatives:

$$\frac{\partial}{\partial x} \left(\frac{1}{R} \right)_r = \frac{1}{r^2} \sin \theta; \quad \frac{\partial}{\partial y} \left(\frac{1}{R} \right)_r = 0;$$

The first order vector potential is:

$$\mathbf{A}_1(\mathbf{r}) = \frac{\mu}{4\pi} \frac{\sin \theta}{r^2} \int_0^{2\pi} a \cos \phi \cdot \mathbf{I}(-\hat{x} \sin \phi + \hat{y} \cos \phi) \cdot a d\phi = \frac{\mu I \pi a^2 \sin \theta}{4\pi} \frac{\hat{\phi}}{r^2} \quad (\text{A.29.5})$$

Since the field point is in the xz -plane, the y -direction of Eq. (A.29.5) generalizes to the ϕ direction.

To evaluate the second order vector potential, note the partial derivatives:

$$\frac{\partial^2}{\partial x^2} \left(\frac{1}{R} \right)_r = \frac{1}{r^3} (3 \sin^2 \theta - 1); \quad \frac{\partial^2}{\partial x \partial y} \left(\frac{1}{R} \right)_r = 0 \quad \frac{\partial^2}{\partial y^2} \left(\frac{1}{R} \right)_r = -\frac{3}{r^3}$$

The second order vector potential is:

$$\mathbf{A}_2(\mathbf{r}) = \frac{\mu}{4\pi} \left\{ \frac{1}{r^3} (3 \sin^2 \theta - 1) \int_0^{2\pi} a^2 \cos^2 \phi \cdot \mathbf{I}(-\hat{x} \sin \phi + \hat{y} \cos \phi) \cdot a d\phi - \frac{3}{r^3} \int_0^{2\pi} a^2 \sin^2 \phi \cdot \mathbf{I}(-\hat{x} \sin \phi + \hat{y} \cos \phi) \cdot a d\phi \right\} = 0 \quad (\text{A.29.6})$$

Since all integrals vanish, so does the potential of this and all other even orders.

To evaluate the third order vector potential, note the partial derivatives:

$$\begin{aligned} \frac{\partial^3}{\partial x^3} \left(\frac{1}{R} \right)_r &= \frac{3}{r^4} \sin \theta (5 \sin^2 \theta - 3); & \frac{\partial^3}{\partial x^2 \partial y} \left(\frac{1}{R} \right)_r &= 0; \\ \frac{\partial^3}{\partial x \partial y^2} \left(\frac{1}{R} \right)_r &= -3 \frac{\sin \theta}{r^4}; & \frac{\partial^3}{\partial y^3} \left(\frac{1}{R} \right)_r &= 0 \end{aligned}$$

The third order vector potential is:

$$\begin{aligned} \mathbf{A}_3(\mathbf{r}) &= \frac{\mu I}{24\pi} \left\{ 3 \frac{a^4}{r^4} \sin \theta (5 \sin^2 \theta - 3) \int_0^{2\pi} (-\sin \phi \hat{x} + \cos \phi \hat{y}) \cos^3 \phi \, d\phi \right. \\ &\quad \left. - 9 \frac{a^4}{r^4} \sin \theta \int_0^{2\pi} (-\sin \phi \hat{x} + \cos \phi \hat{y}) \cos \phi \sin^2 \phi \, d\phi \right\} \quad (\text{A.29.7}) \end{aligned}$$

Evaluation of the integrals gives:

$$\mathbf{A}_3(\mathbf{r}) = \frac{3\mu I \pi a^4 \hat{\phi}}{32\pi r^4} \sin \theta (5 \sin^2 \theta - 4) \quad (\text{A.29.8})$$

The radial component of the magnetic field follows by adding Eqs. (1.2.17), (A.29.5), and (A.29.8):

$$B_{r1} = \frac{2\mu I \pi a^2 \cos \theta}{4\pi r^3} = \frac{2\mu I \pi a^2}{4\pi r^3} P_1(\cos \theta) \quad (\text{A.29.9})$$

$$B_{r3} = \frac{3\mu I \pi a^4}{8\pi r^5} \cos \theta (5 \cos^2 \theta - 3) = \frac{3\mu I \pi a^4}{4\pi r^5} P_3(\cos \theta) \quad (\text{A.29.10})$$

The magnetic dipole moment of the loop is, by definition:

$$\mathbf{m}_1 = m_1 \hat{z} = \pi a^2 I \hat{z} \quad (\text{A.29.11})$$

For non-circular loops, with S representing the planar area of the closed current, the definition generalizes to:

$$m_1 = IS \quad (\text{A.29.12})$$

It follows from Eqs. (A.29.5) and (A.29.11) that the dipole potential is expressible as:

$$\mathbf{A}_1(\mathbf{r}) = \frac{\mu}{4\pi} \mathbf{m}_1 \times \left(\frac{\hat{\mathbf{r}}}{r^2} \right) \quad (\text{A.29.13})$$

For the special case of a z -directed magnetic dipole of moment m_1 , combining Eqs. (A.29.9), (A.29.12) and (A.29.13) gives:

$$\mathbf{A}_1 = \frac{\mu m_1 \sin \theta}{4\pi r^2} \hat{\phi} \quad \text{and} \quad B_r = \frac{2\mu m_1 \cos \theta}{4\pi r^3} \quad (\text{A.29.14})$$

The electric field of Eq. (A.28.13) and the magnetic field of Eq. (A.29.9) are identical in form. Therefore, field form cannot be used to determine whether

a magnetic source consists of separated magnetic monopoles or a current loop. In other words, the role played by a current loop in determining the vector potential is the same as that played by separated charges in determining scalar potential.

Extension to higher order moments follows similarly to the dipole case. An electric quadrupole consists of two superimposed sets of separated electric charges and a magnetic quadrupole consists of two superimposed sets of separated current loops. With linear displacements, current loops follow the same rule as electric moments with one lateral and $(\ell - 1)$ linear displacements. Results for several orders are compiled in Tables A.29.1 and A.29.2.

Tables A.29.1 and A.29.2 display features of multipolar magnetic moments. In each case, column one shows the order of the source. Column two shows the discrete current distributions that generate that order of singularity. Column three shows the value of the volume integrals that appear in Eq. (A.29.3). Column four shows the lowest order derived potentials. Column five shows the radial components of the generated electric field intensity. Table A.29.1 is based upon a z -directed loop and Table A.28.2 is based upon a y -directed loop. In both cases, all displacements are z -directed.

Equating the field value of Eq. (A.29.10) with the octupole moment of Table A.29.1 shows that the octupole moment of a circular current loop is:

$$m_3 = \frac{3I\pi a^4}{4} \tag{A.29.15}$$

The value of odd, higher order moments follow similarly.

Table A.29.1. Magnetostatic vector potentials and radial fields of sources, z -directed current loops of area S_0 with $(\ell - 1)z_0$ separations.

| ℓ Loop Direction, Sites | m_ℓ | $4\pi A_{\phi\ell}(r, \theta)/\mu$ | $4\pi B_{r\ell}(r, \theta)/\mu$ |
|--|-----------------|---|-------------------------------------|
| 1 \uparrow at 0 | $m_1 = IS_0$ | $\frac{m_1}{r^2} \sin \theta$ | $\frac{2m_1}{r^3} P_1(\cos \theta)$ |
| 2 \downarrow at $-z_0/2$ \uparrow at $+z_0/2$ | $m_2 = 2m_1z_0$ | $\frac{m_2}{2r^3} 3 \sin \theta \cos \theta$ | $\frac{3m_2}{r^4} P_2(\cos \theta)$ |
| 3 \uparrow at $-z_0$ $2\downarrow$ at 0 \uparrow at $-z_0$ | $m_3 = 3m_2z_0$ | $\frac{m_3}{2r^4} \sin \theta(5 \cos^2 \theta - 1)$ | $\frac{4m_3}{r^5} P_3(\cos \theta)$ |
| 4 \downarrow at $-3z_0/2$ $3\uparrow$ at $-z_0/2$ $3\downarrow$ at $z_0/2$ \uparrow at $3z_0/2$ | $m_4 = 4m_3z_0$ | $\frac{5m_4}{32r^5} \sin \theta(7 \cos^3 \theta - 3 \cos \theta)$ | $\frac{5m_4}{r^6} P_4(\cos \theta)$ |

Note: Arrows indicate direction of magnetic dipoles forming the multipole.

Table A.29.2. Magnetostatic vector potentials and radial fields of sources, y -directed current loops of area S_0 , $(\ell - 1)z_0$ separations.

| ℓ | Loop Direction, Sites | m_ℓ^1 | $4\pi\mathbf{A}_\ell(r, \theta, \phi)/\mu$ | $\frac{4\pi B_{r\ell}(r, \theta, \phi)}{\mu \sin \phi}$ |
|--------|--|----------------------|---|---|
| 1 | \rightarrow at 0 | $m_1^1 = IS_0$ | $\frac{\mu m_1^1}{4\pi r^2}(\hat{\theta} \cos \phi - \hat{\phi} \cos \theta \sin \phi)$ | $\frac{2m_1^1}{r^3} P_1^1(\cos \theta)$ |
| 2 | \leftarrow at $-z_0/2$ \rightarrow at $+z_0/2$ | $m_2^1 = m_1^1 z_0$ | $\frac{m_2^1}{r^3} [(-\hat{r} \sin \theta + 2\hat{\theta} \cos \theta) \cos \phi - \hat{\phi}(3 \cos^2 \theta - 1) \sin \phi]$ | $\frac{3m_2^1}{r^4} P_2^1(\cos \theta)$ |
| 3 | \rightarrow at $z_0/2$ 2 \leftarrow at 0 \rightarrow at $z_0/2$ | $m_3^1 = 2m_2^1 z_0$ | $\frac{3m_3^1}{8r^4} (-2\hat{r} \sin \theta \cos \theta \cos \phi + \hat{\theta}(3 \cos^2 \theta - 1) \cos \phi - \hat{\phi}(5 \cos^2 \theta - 3) \cos \theta \sin \phi)$ | $\frac{4m_3^1}{r^5} P_3^1(\cos \theta)$ |
| 4 | \leftarrow at $-3z_0/2$ 3 \rightarrow at $-z_0/2$ 3 \leftarrow at $+z_0/2$ \rightarrow at $+3z_0/2$ | $m_4^1 = 3m_3^1 z_0$ | $\frac{m_4^1}{2r^5} (3\hat{r}(1 - 5 \cos^2 \theta) \sin \theta \cos \phi + 4\hat{\theta}(5 \cos^2 \theta - 3) \cos \theta \cos \phi - \hat{\phi}(35 \cos^4 \theta - 30 \cos^2 \theta + 3) \sin \phi)$ | $\frac{5m_4^1}{r^6} P_4^1(\cos \theta)$ |

Note: Arrows indicate direction of magnetic dipoles forming the multipole.

Contrasting Tables A.28.1, A.28.2, A.29.1 and A.29.2 shows that Tables A.28.1 and A.29.1 have identical structures, quite different potentials, and identical force fields; the same is true of Tables A.28.2 and A.29.2. Since there are electric monopoles but not magnetic monopoles, the $\ell = 0$ case occurs only in Table A.28.1. For all higher order modes, Tables A.28.1 and A.29.1 have z -directed dipoles as the unit cell. Tables A.28.2 and A.29.2 have y -directed dipoles as the unit cell, with identical structures except the source structure of Table A.28.1, order ℓ , is the same as that of Table A.29.1, order $(\ell + 1)$.

All orders and degrees of any source may be described similarly to those of the tables. The result is the radial component of the static magnetic field component of arbitrary order:

$$B_r(r, \theta) = \frac{\mu}{4\pi} \sum_{\ell=0}^{\infty} \sum_{m=-\ell}^{\ell} \frac{(\ell + 1)m_\ell^m}{r^{\ell+2}} P_\ell^m(\cos \theta) e^{-jm\phi} \quad (\text{A.29.16})$$

Similarly to the case of the electric field, in the limit as the frequency goes to zero, the radial component of the magnetic field of Eq. (1.12.7) goes to:

$$B_r = \frac{j}{c} \sum_{\ell=0}^{\infty} \sum_{m=0}^{\ell} i^{-\ell} G(\ell, m) \ell(\ell + 1) \frac{(2\ell - 1)!!}{\sigma^{\ell+2}} P_\ell^m(\cos \theta) e^{-jm\phi} \quad (\text{A.29.17})$$

Combining Eqs. (A.29.15) and (A.29.17) gives:

$$G(\ell, m) = -\frac{\eta}{4\pi} \frac{i^\ell k^{\ell+2} \mathbf{m}_\ell^m}{\ell(2\ell-1)!!} \quad (\text{A.29.18})$$

30. Full Field Expansion

The Fields: The photon fields follow from Eqs. (5.8.1) and (5.8.2) for plane waves and, with the inclusion of a source, becomes Eq. (5.10.16). Computer methods of evaluation are insufficient. We, therefore, seek other methods of evaluating the series. Exact values on the coordinate axes, and of sums over spherical Bessel functions at all angles, are obtained, see Sec. 6.6. The full solution at limitlessly large radius follows from Eq. (A.30.1):

Plane wave

$$\begin{aligned} \tilde{\mathbf{E}} &= [\sin \theta \hat{r} + \cos \theta \hat{\theta} - i \hat{\phi}] e^{-i\phi} \\ &= [S_{11} \hat{r} / \sigma + (S_{31} + \mathcal{S}_{21}) \hat{\theta} - i(S_{21} + \mathcal{S}_{31}) \hat{\phi}] e^{-i\phi} \\ \lim_{\sigma \rightarrow \infty} \{\text{photon wave}\} &= \left(1 + i \frac{d}{d\sigma}\right) \{\text{plane wave}\} \end{aligned} \quad (\text{A.30.1})$$

Solutions are formed by optical source functions $U(\sigma, \theta)$ and $V(\sigma, \theta)$, see Eq. (6.1.16), where:

$$\begin{aligned} U(\sigma, \theta) &= \frac{1}{\sigma \sin^2 \theta} [e^{-i\sigma \cos \theta} - (\cos \sigma - i \sin \sigma \cos \theta)] \\ V(\sigma, \theta) &= \frac{1}{\sigma \sin^2 \theta} [e^{-i\sigma \cos \theta} \cos \theta - (\cos \sigma \cos \theta - i \sin \sigma)] \end{aligned} \quad (\text{A.30.2})$$

These functions are indeterminate on the z -axes where, at $\theta = 0$ and π :

$$\begin{aligned} \lim_{\theta \rightarrow 0, \pi} U(\sigma, \theta) &= \frac{i}{2} \cos \theta \left[e^{-i\sigma \cos \theta} - \frac{\sin \sigma}{\sigma} \right] \\ \lim_{\theta \rightarrow 0, \pi} V(\sigma, \theta) &= \frac{i}{2} \left[e^{-i\sigma \cos \theta} + \frac{\sin \sigma}{\sigma} \right] \end{aligned} \quad (\text{A.30.3})$$

With the values of Table 6.7.1 as the starting point and using flow chart Table 6.8.1 sums are obtained after any desired number of iterations. S_3 is the source of the other sums, and it is tabulated as a function of iteration numbers one through four in Table A.30.1. Using the values of Table A.30.1 to obtain all other sums then combining to obtain the field components gives the field values of Tables A.30.2–A.30.4.

Table A.30.1. Sums S_3 for iterations zero through four. Sums S_2 , S_1 , S_0 , and S_{-1} are calculable from S_3 .

$$\begin{aligned}
{}^0S_3 &= -i[U + V] - \frac{U}{\sigma} \\
{}^1S_3 &= \frac{2}{\sigma^2} e^{-i\sigma \cos \theta} - i[U + V] - \left[\left(\frac{1}{\sigma} - \frac{2}{\sigma^3} \right) U + i \frac{2}{\sigma^2} V \right] \\
{}^2S_3 &= \left[\frac{4}{\sigma^2} - \frac{12i}{\sigma^3} \cos \theta - \frac{12}{\sigma^4} \right] e^{-i\sigma \cos \theta} - i[U + V] \\
&\quad - \left[\left(\frac{1}{\sigma} - \frac{12}{\sigma^3} + \frac{224}{\sigma^5} \right) U - i \left(\frac{4}{\sigma^2} - \frac{24}{\sigma^4} \right) V \right] \\
{}^3S_3 &= \left[\frac{6}{\sigma^2} - \frac{i36}{\sigma^3} \cos \theta - \frac{(6)!}{(3)!\sigma^4} \left(\frac{11}{10} - \sin^2 \theta \right) + \frac{(6)!i}{(3)!\sigma^5} \cos \theta + \frac{(6)!}{2\sigma^6} \right] e^{-i\sigma \cos \theta} \\
&\quad - i[U + V] - (6)! \left[\left(\frac{1}{(6)!\sigma} - \frac{1}{(4)!\sigma^3} + \frac{1}{(2)!\sigma^5} - \frac{1}{\sigma^7} \right) U \right. \\
&\quad \left. - i \left(\frac{1}{(5)!\sigma^2} - \frac{1}{(3)!\sigma^4} + \frac{1}{\sigma^6} \right) V \right] \\
{}^4S_3 &= \left[\frac{8}{\sigma^2} - \frac{i}{\sigma^3} 72 \cos \theta - \frac{480}{\sigma^4} \left(\frac{57}{60} - \sin^2 \theta \right) + \frac{i(8)!}{(4)!\sigma^5} \left(\frac{6}{7} - \sin^2 \theta \right) \cos \theta \right. \\
&\quad \left. + \frac{(8)!}{(4)!\sigma^6} (2 - \sin^2 \theta) - \frac{i(8)!}{(3)!\sigma^7} \cos \theta - \frac{(8)!}{2\sigma^8} \right] e^{-i\sigma \cos \theta} - i[U + V] \\
&\quad - (8)! \left[\left(\frac{1}{(8)!\sigma} - \frac{1}{(6)!\sigma^3} + \frac{1}{(4)!\sigma^5} - \frac{1}{(2)!\sigma^7} + \frac{1}{\sigma^9} \right) U \right. \\
&\quad \left. - i \left(\frac{1}{(7)!\sigma^2} - \frac{1}{(5)!\sigma^4} + \frac{1}{(3)!\sigma^6} - \frac{1}{\sigma^8} \right) V \right] \\
{}^5S_3 &= \left[\frac{10}{\sigma^2} - \frac{i}{\sigma^3} (192 - 72 \sin^2 \theta) \cos \theta - \frac{1}{\sigma^4} (1080 - 1200 \sin^2 \theta) \right. \\
&\quad \left. + \frac{i}{\sigma^5} (6000 - 10,080 \sin^2 \theta + 1680 \sin^4 \theta) \cos \theta \right. \\
&\quad \left. + \frac{1}{\sigma^6} (24,720 - 48,720 \sin^2 \theta + 30,240 \sin^4 \theta) - \frac{i(10)!}{(5)!\sigma^7} (2 + 2 \cos^2 \theta) \cos \theta \right. \\
&\quad \left. - \frac{(10)!}{(4)!\sigma^8} (1 + \cos^2 \theta) + \frac{i(10)!}{(3)!\sigma^9} \cos \theta + \frac{(10)!}{(2)!\sigma^{10}} \right] e^{-i\sigma \cos \theta} - i[U + V] \\
&\quad - \left[(10)! \left(\frac{1}{(10)!\sigma} - \frac{1}{(8)!\sigma^3} + \frac{1}{(6)!\sigma^5} - \frac{1}{(4)!\sigma^7} + \frac{1}{(2)!\sigma^9} - \frac{1}{\sigma^{11}} \right) U \right. \\
&\quad \left. - i(10)! \left(\frac{1}{(9)!\sigma^2} - \frac{1}{(7)!\sigma^4} + \frac{1}{(5)!\sigma^6} - \frac{1}{(3)!\sigma^8} + \frac{1}{\sigma^{10}} \right) V \right]
\end{aligned}$$

Table A.30.1. (Continued)

$$\begin{aligned}
 {}^6S_3 = & \left\{ \frac{1}{\sigma^2} 12 - \frac{i}{\sigma^3} (222 - 42 \sin^2 \theta) \cos \theta - \frac{1}{\sigma^4} (2676 - 3984 \sin^2 \theta + 1008 \sin^4 \theta) \right. \\
 & \frac{i}{\sigma^5} (16,224 - 25,872 \sin^2 \theta + 1680 \sin^4 \theta) \cos \theta \\
 & + \frac{1}{\sigma^6} (105,120 - 294,000 \sin^2 \theta + 245,280 \sin^4 \theta - 36,960 \sin^6 \theta) \\
 & - \frac{i}{\sigma^7} (409,920 - 866,880 \sin^2 \theta + 628,320 \sin^4 \theta) \cos \theta \\
 & - \frac{(12)!}{(6)! \sigma^8} (3 - 3 \sin^2 \theta + \sin^4 \theta) + \frac{(12)! i}{(5)! \sigma^9} (1 + \cos^2 \theta) \cos \theta + \frac{(12)!}{(4)! \sigma^{10}} (1 + \cos^2 \theta) \\
 & \left. - \frac{i(12)!}{(3)! \sigma^{11}} \cos \theta - \frac{(12)!}{\sigma^{12}} \right\} e^{-i\sigma \cos \theta} - i[U + V] \\
 & - (12)! \left\{ \left[\frac{1}{\sigma} - \frac{1}{(10)! \sigma^3} + \frac{1}{8! \sigma^2} - \frac{1}{6! \sigma^7} + \frac{1}{4! \sigma^9} - \frac{1}{2! \sigma^{11}} + \frac{1}{\sigma^{13}} \right] U \right. \\
 & \left. + i \left[1 - \frac{1}{(11)! \sigma^2} + \frac{1}{9! \sigma^4} - \frac{1}{7! \sigma^6} + \frac{1}{5! \sigma^8} - \frac{1}{3! \sigma^{10}} + \frac{1}{\sigma^{12}} \right] V \right\}
 \end{aligned}$$

Note: Only the term $-iU(\sigma, \theta)$ arises from spherical Bessel functions. Since the parities of the spherical Bessel and Neumann are different, buildup of the Neumann terms cannot include the Bessel term; it must be supplied separately.

A characteristic of optical source functions $U(\sigma, \theta)$ and $V(\sigma, \theta)$ may be seen by writing them in the form:

$$\begin{aligned}
 U(\sigma, \theta) &= \frac{1}{\sigma \sin^2 \theta} \left[e^{-i\sigma \cos \theta} - \frac{1}{2} (e^{-i\sigma} (1 + \cos \theta) + e^{i\sigma} (1 - \cos \theta)) \right] \\
 V(\sigma, \theta) &= \frac{1}{\sigma \sin^2 \theta} \left[e^{-i\sigma \cos \theta} \cos \theta - \frac{1}{2} (e^{-i\sigma} (1 + \cos \theta) + e^{i\sigma} (1 - \cos \theta)) \right]
 \end{aligned}
 \tag{A.30.4}$$

The three exponentials represent waves traveling in the $+z$ -direction and the $\pm r$ -direction. The radially outbound and inbound waves dominate respectively in the upper and lower hemispheres. Tables A.30.2–A.30.4 show that fields vary with radius at powers ranging from zero to $(2N + 1)$, where N is the number of iterations. Terms involving $U(\sigma, \theta)$ and $V(\sigma, \theta)$ vary at powers ranging from three to $(2N + 3)$. It follows that energy flow at very large radii is dominated by the former and at very small radii by the latter; the direction of power flow depends upon the distance from the source.

Table A.30.2. Radial phasor electric field intensities for iterations one through four. Only the italicized 'one' arises from spherical Bessel functions.

$$\begin{aligned}
 {}^0E_r &= \sin \theta \left(1 + \cos \theta + \frac{i}{\sigma} \right) e^{-i\sigma \cos \theta} e^{-i\phi} \\
 {}^1E_r &= \sin \theta \left\{ (1 + \cos \theta) + \frac{i}{\sigma} (1 + 2 \sin^2 \theta) + \frac{6}{\sigma^2} \cos \theta + \frac{2i}{\sigma^3} \right\} e^{-i\sigma \cos \theta} e^{-i\phi} \\
 {}^2E_r &= \sin \theta \left\{ (1 + \cos \theta) + \frac{i}{\sigma} (1 + 4 \sin^2 \theta) + \frac{1}{\sigma^2} (24 - 12 \cos^2 \theta) \cos \theta \right. \\
 &\quad \left. - \frac{i}{\sigma^3} (36 - 60 \sin^2 \theta) + \frac{48}{\sigma^4} \cos \theta \right\} e^{-i\sigma \cos \theta} e^{-i\phi} \\
 {}^3E_r &= \sin \theta \left\{ (1 + \cos \theta) + \frac{i}{\sigma} (1 + 6 \sin^2 \theta) + \frac{1}{\sigma^2} (54 - 36 \cos^2 \theta) \cos \theta \right. \\
 &\quad \left. - \frac{i}{\sigma^3} (114 - 84 \sin^2 \theta - 120 \sin^4 \theta) \right. \\
 &\quad \left. - \frac{1}{\sigma^4} (192 - 840 \sin^2 \theta) \cos \theta - \frac{i}{\sigma^5} (864 - 1080 \sin^2 \theta) \right\} e^{-i\sigma \cos \theta} e^{-i\phi} \\
 {}^4E_r &= \sin \theta \left\{ (1 + \cos \theta) + \frac{i}{\sigma} (1 + 8 \sin^2 \theta) + \frac{1}{\sigma^2} 96 \cos \theta \right. \\
 &\quad \left. - \frac{i}{\sigma^3} (232 + 24 \sin^2 \theta - 480 \sin^4 \theta) - \frac{1}{\sigma^4} (1056 - 4080 \sin^2 \theta) \cos \theta \right. \\
 &\quad \left. - \frac{i}{\sigma^5} (12,960 \sin^2 \theta - 15,120 \sin^4 \theta) \right. \\
 &\quad \left. - \frac{1}{\sigma^6} (15,360 - 26,880 \sin^2 \theta) \cos \theta \right\} e^{-i\sigma \cos \theta} e^{-i\phi}
 \end{aligned}$$

Power and energy: The real part of the radial component of the Poynting vector may be written:

$$N_r = \frac{1}{2} \operatorname{Re}(\tilde{\mathbf{E}} \times \tilde{\mathbf{H}}^*)_r = -\frac{1}{2} \operatorname{Im}(\tilde{\mathbf{E}} \times \tilde{\mathbf{E}}^*)_r = \frac{\operatorname{Re}}{\eta} (iE_\phi E_\theta^*) \quad (\text{A.30.5})$$

The fields of Tables A.30.3 and A.30.4 have the form:

$$\begin{aligned}
 {}^1E_\theta &= [\cos \theta (1 + \cos \theta) + \chi + i\delta \cos \theta] e^{-i\sigma \cos \theta} e^{-i\phi} - [iAV + BU] e^{-i\phi} \\
 {}^1E_\phi &= -i\{(1 + \cos \theta) + \gamma \cos \theta + i\kappa\} e^{-i\sigma \cos \theta} e^{-i\phi} - [iAU + BV] e^{-i\phi}
 \end{aligned} \quad (\text{A.30.6})$$

Net power is described only by product of functions that are sums over spherical Bessel with those that are sums over spherical Neumann functions. The product of Bessel times Neumann functions giving the portion of the radial component of the Poynting vector that does not integrate to zero

Table A.30.3. Zenith angle phasor electric field intensities for iterations zero through four. Only the italicized “one” arises from spherical Bessel functions.

$$\begin{aligned}
 {}^0E_\theta &= \left[\cos \theta (1 + \cos \theta) - \frac{i}{\sigma} - \frac{1}{\sigma^2} \right] e^{-i\sigma \cos \theta} e^{-i\phi} - i \frac{V(\sigma, \theta)}{\sigma^2} \\
 {}^1E_\theta &= \left[\cos \theta (1 + \cos \theta) + \frac{2i}{\sigma} \sin^2 \theta \cos \theta + \frac{1}{\sigma^2} + \frac{3i}{\sigma^3} \cos \theta + \frac{6}{\sigma^4} \right] e^{-i\sigma \cos \theta} e^{-i\phi} \\
 &\quad - \left[i \left(\frac{1}{\sigma^2} - \frac{6}{\sigma^4} \right) V + \frac{4}{\sigma^3} U \right] e^{-i\phi} \\
 {}^2E_\theta &= \left[\cos \theta (1 + \cos \theta) + \frac{i}{\sigma} 4 \sin^2 \theta \cos \theta + \frac{1}{\sigma^2} (3 + 12 \cos^2 \theta - 12 \cos^4 \theta) \right. \\
 &\quad \left. - \frac{i}{\sigma^3} 12 \cos \theta + \frac{1}{\sigma^4} (24 - 12 \cos^2 \theta) - \frac{(5)!i}{2\sigma^5} \cos \theta - \frac{(5)!}{\sigma^6} \right] e^{-i\sigma \cos \theta} e^{-i\phi} \\
 &\quad - (4)! \left[i \left(\frac{1}{(4)!\sigma^2} - \frac{3}{(2)!\sigma^4} + \frac{5}{\sigma^6} \right) V + \left(\frac{2}{(3)!\sigma^3} - \frac{4}{\sigma^5} \right) U \right] e^{-i\phi} \\
 {}^3E_\theta &= \left[\cos \theta (1 + \cos \theta) + \frac{i}{\sigma} 6 \sin^2 \theta \cos \theta + \frac{1}{\sigma^2} (5 + 36 \cos^2 \theta - 36 \cos^4 \theta) \right. \\
 &\quad \left. - \frac{i}{\sigma^3} (18 + 144 \cos^2 \theta - 120 \cos^4 \theta) \cos \theta + \frac{1}{\sigma^4} (124 - 252 \cos^2 \theta) \right. \\
 &\quad \left. - \frac{i}{\sigma^5} (684 - 600 \cos^2 \theta) \cos \theta - \frac{1}{\sigma^6} (480 + 840 \cos^2 \theta) \right. \\
 &\quad \left. + \frac{(7)!i}{2\sigma^7} \cos \theta + \frac{(7)!}{\sigma^8} \right] e^{-i\sigma \cos \theta} e^{-i\phi} - (6)! \left[i \left(\frac{1}{(6)!\sigma^2} - \frac{3}{(4)!\sigma^4} + \frac{5}{(2)!\sigma^6} - \frac{7}{\sigma^8} \right) V \right. \\
 &\quad \left. + \left(\frac{2}{(5)!\sigma^3} - \frac{4}{(3)!\sigma^5} + \frac{6}{\sigma^7} \right) U \right] e^{-i\phi} \\
 {}^4E_\theta &= \left[\cos \theta (1 + \cos \theta) + \frac{i}{\sigma} 8 \sin^2 \theta \cos \theta + \frac{1}{\sigma^2} (7 + 72 \cos^2 \theta - 72 \cos^4 \theta) \right. \\
 &\quad \left. + \frac{i}{\sigma^3} (8 - 576 \cos^2 \theta + 480 \cos^4 \theta) \cos \theta \right. \\
 &\quad \left. + \frac{1}{\sigma^4} (384 - 216 \cos^2 \theta - 2440 \cos^4 \theta + 1680 \cos^6 \theta) \right. \\
 &\quad \left. - \frac{i}{\sigma^5} (4680 - 6240 \cos^2 \theta) \cos \theta + \frac{1}{\sigma^6} (960 - 22,800 \cos^2 \theta + 18,480 \cos^4 \theta) \right. \\
 &\quad \left. + \frac{i}{\sigma^7} (8400 + 15,120 \cos^2 \theta) \cos \theta + \frac{1}{\sigma^8} (40,320 + 60,480 \cos^2 \theta) \right. \\
 &\quad \left. - \frac{i}{\sigma^9} 181,440 \cos \theta - \frac{1}{\sigma^{10}} 362,880 \right] e^{-i\sigma \cos \theta} e^{-i\phi} \\
 &\quad - (8)! \left[i \left(\frac{1}{(8)!\sigma^2} - \frac{3}{(6)!\sigma^4} + \frac{5}{(4)!\sigma^6} - \frac{7}{(2)!\sigma^8} + \frac{9}{\sigma^{10}} \right) V \right. \\
 &\quad \left. + \left(\frac{2}{(7)!\sigma^3} - \frac{4}{(5)!\sigma^5} + \frac{6}{(3)!\sigma^7} - \frac{8}{\sigma^9} \right) U \right] e^{-i\phi}
 \end{aligned}$$

Table A.30.4. Azimuth angle phasor electric field intensities for iterations zero through four. Only the italicized "one" arises from spherical Bessel functions.

$$\begin{aligned}
 {}^0E_\phi &= -i \left(1 + \cos \theta + \frac{i}{\sigma} \right) e^{-i\sigma \cos \theta} e^{-i\phi} + \frac{U(\sigma, \theta)}{\sigma^2} \\
 {}^1E_\phi &= -i \left\{ (1 + \cos \theta) + \frac{i}{\sigma} 2 \sin^2 \theta + \frac{2}{\sigma^2} \cos \theta - \frac{2i}{\sigma^3} \right\} e^{-i\sigma \cos \theta} e^{-i\phi} \\
 &\quad - i(2)! \left[i \left(\frac{1}{(2)!\sigma^2} - \frac{3}{\sigma^4} \right) U + \frac{2}{\sigma^3} V \right] e^{-i\phi} \\
 {}^2E_\phi &= -i \left\{ (1 + \cos \theta) + \frac{i}{\sigma} 4 \sin^2 \theta + \frac{1}{\sigma^2} (16 - 12 \cos^2 \theta) \cos \theta \right. \\
 &\quad \left. + \frac{i}{\sigma^3} (4 - 12 \cos^2 \theta) - \frac{24}{\sigma^4} \cos \theta + \frac{36i}{\sigma^5} \right\} e^{-i\sigma \cos \theta} e^{-i\phi} \\
 &\quad - i(4)! \left[i \left(\frac{1}{(4)!\sigma^2} - \frac{3}{(2)!\sigma^4} + \frac{5}{\sigma^6} \right) U + \left(\frac{2}{(3)!\sigma^3} - \frac{4}{\sigma^5} \right) V \right] e^{-i\phi} \\
 {}^3E_\phi &= -i \left\{ (1 + \cos \theta) + \frac{i}{\sigma} 6 \sin^2 \theta + \frac{1}{\sigma^2} (6 + 36 \cos^2 \theta) \cos \theta \right. \\
 &\quad \left. + \frac{i}{\sigma^3} (42 - 216 \cos^2 \theta + 120 \cos^4 \theta) + \frac{1}{\sigma^4} (144 - 360 \cos^2 \theta) \cos \theta \right. \\
 &\quad \left. + \frac{i}{\sigma^5} (36 + 360 \cos^2 \theta) + \frac{480}{\sigma^6} \cos \theta - \frac{i}{\sigma^7} 1800 \right\} e^{-i\sigma \cos \theta} e^{-i\phi} \\
 &\quad - i(6)! \left[i \left(\frac{1}{(6)!\sigma^2} - \frac{3}{(4)!\sigma^4} + \frac{5}{(2)!\sigma^6} - \frac{7}{\sigma^8} \right) U \right. \\
 &\quad \left. + \left(\frac{2}{(5)!\sigma^3} - \frac{4}{(3)!\sigma^5} + \frac{6}{\sigma^7} \right) V \right] e^{-i\phi} \\
 {}^4E_\phi &= -i \left\{ (1 + \cos \theta) + \frac{i}{\sigma} 8 \sin^2 \theta + \frac{1}{\sigma^2} (80 - 72 \cos^2 \theta) \cos \theta \right. \\
 &\quad \left. + \frac{i}{\sigma^3} (136 - 720 \cos^2 \theta + 480 \cos^4 \theta) \right. \\
 &\quad \left. + \frac{1}{\sigma^4} (1440 - 3840 \cos^2 \theta + 1680 \cos^4 \theta) \cos \theta \right. \\
 &\quad \left. + \frac{i}{\sigma^5} (504 - 4320 \cos^2 \theta + 6720 \cos^4 \theta) \right. \\
 &\quad \left. - \frac{1}{\sigma^6} (960 - 6720 \cos^2 \theta) \cos \theta + \frac{i}{\sigma^7} (5040 - 21,840 \cos^2 \theta) \right. \\
 &\quad \left. - \frac{1}{\sigma^8} 40,320 \cos \theta + \frac{i}{\sigma^9} 141,120 \right\} e^{-i\sigma \cos \theta} e^{-i\phi} \\
 &\quad - i(8)! \left[i \left(\frac{1}{(8)!\sigma^2} - \frac{3}{(6)!\sigma^4} + \frac{5}{(4)!\sigma^6} - \frac{7}{(2)!\sigma^8} + \frac{9}{\sigma^{10}} \right) U(\sigma, \theta) \right. \\
 &\quad \left. + \left(\frac{2}{(7)!\sigma^3} - \frac{4}{(5)!\sigma^5} + \frac{6}{(3)!\sigma^7} - \frac{8}{\sigma^9} \right) V(\sigma, \theta) \right] e^{-i\phi}
 \end{aligned}$$

Table A.30.5. The radial component of the complex Poynting vector that provides an integrated value.

| | |
|---|---|
| 0 | $\eta^0 N_r = 2 \cos^2 \theta$ |
| 1 | $\eta^1 N_r = 2 \cos^2 \theta + \frac{1}{\sigma^2} (1 + 3 \cos^2 \theta)$ |
| 2 | $\eta^2 N_r = 2 \cos^2 \theta + \frac{1}{\sigma^2} (3 + 28 \cos^2 \theta - 23 \cos^4 \theta) + \frac{1}{\sigma^4} (36 - 48 \cos^2 \theta)$ |
| 3 | $\eta^3 N_r = 2 \cos^2 \theta + \frac{1}{\sigma^2} (15 + 111 \cos^2 \theta + 55 \cos^4 \theta) + \frac{1}{\sigma^4} (412 - 108 \cos^2 \theta + 30 \cos^4 \theta)$ |
| 4 | $\eta^4 N_r = 2 \cos^2 \theta + \frac{1}{\sigma^2} [42 + 592 \cos^2 \theta + 150 \cos^4 \theta]$ $- \frac{1}{\sigma^4} [8 - 3984 \cos^2 \theta + 10,480 \cos^4 \theta - 3360 \cos^6 \theta]$ $+ \frac{1}{\sigma^6} [69,504 + 177,840 \cos^2 \theta + 53,760 \cos^4 \theta]$ |

over the surface of a circumscribing sphere has the form:

$$\eta N_r = 2 \cos^2 \theta + \gamma \cos^2 \theta + \chi - \frac{B}{\sigma} + \frac{1}{\sigma} [A \sin \sigma + B \cos \sigma] \cos(\sigma \cos \theta) \quad (\text{A.30.7})$$

The power on the surface of a circumscribing shell follows:

$$\begin{aligned}
 P_r &= \frac{2\pi\sigma^2}{k^2} \int_0^\pi N_r \sin \theta \, d\theta \\
 P_r &= \frac{2\pi\sigma^2}{\eta k^2} \left\{ \int_0^\pi [2 \cos^2 \theta + \gamma \cos^2 \theta + \chi] \sin \theta \, d\theta \right. \\
 &\quad \left. + \left[\left(\frac{A}{\sigma^2} - \frac{2B}{\sigma} \right) - \frac{1}{\sigma^2} [A \cos(2\sigma) - B \sin(2\sigma)] \right] \right\} \quad (\text{A.30.8})
 \end{aligned}$$

The integral forms used includes:

$$\int_0^\pi \cos(\sigma \cos \theta) \sin \theta \, d\theta = \frac{2}{\sigma} \sin \sigma \quad (\text{A.30.9})$$

Using the field parameters listed in Tables A.30.3 and A.30.4 gives the complex Poynting vector listed in Table A.30.5. The integrated output power obtained from Table A.30.5 is listed in Table 6.11.6.

References

- W. Kaplan, *Advanced Calculus*, Addison-Wesley (1952).
- J.D. Jackson, *Classical Electrodynamics*, 2nd edition, John Wiley (1975).
- T.W. Körner, *Fourier Analysis*, Cambridge University Press (1988).
- R.B. Leighton, *Principles of Modern Physics*, McGraw-Hill (1959).
- P.M. Morse, H. Feshbach, *Methods of Theoretical Physics*, McGraw-Hill (1953).
- W.K.H. Panofsky, M. Phillips, *Classical Electricity and Magnetism*, 2nd edition, Addison-Wesley (1962).
- S.A. Schelkunoff, *Advanced Antenna Theory*, John Wiley (1952).
- S.A. Schelkunoff, *Applied Mathematics for Engineers and Scientists*, 2nd edition, Van Nostrand (1965).
- R. Scott, *Linear Circuits*, 2nd edition, Addison-Wesley (1962).
- W.R. Smythe, *Static and Dynamic Electricity*, 3rd edition, McGraw-Hill (1968).
- M.E. VanValkenburg, *Network Analysis*, 3rd edition, Prentice Hall (1974).
- J.R. Wait, *Electromagnetic Wave Theory*, Harper & Row (1985).

Index

- absorbed power, 36, 81, 84, 91, 270
- accelerating charge, 13
- Aharonov–Bohm effect, 1
- anechoic chamber, 160, 165
- angular momentum, 143, 241, 242, 283, 285, 298
- antenna Q, 99, 115, 120, 158, 166, 342
- antisymmetric, 327–330
 - tensor, 10, 12, 327
- associated Legendre polynomial, 254, 257, 285, 367, 368, 371–373
- atomic stability, 173

- Bessel function, 23, 24, 26, 32, 34, 42, 49, 69, 75, 85, 88, 112, 118, 236, 237, 244, 249, 252, 253, 260, 265, 267, 268, 285, 286, 289, 319, 320, 360, 382–384, 386, 387, 392, 395, 407–410
- biconical antenna, 31, 45, 58, 60, 61, 136, 154, 157, 158, 285, 317
- blackbody, 216–218, 220
- Bohr, 235
 - magneton, 211
- boundary condition, 22, 24, 27, 46, 47, 52–56, 84, 88, 89, 248, 317, 347, 350, 352, 377
- bremsstrahlung, 312

- cavity, 26–28, 216–218, 221, 226, 227
- Chu, 115, 116, 118–120, 122–126, 134, 140, 151, 152, 166, 168, 169, 310, 321
- circumscribing sphere, 82, 136, 154, 239, 248, 288, 399, 411

- classical
 - electrodynamics, 247, 305
 - electromagnetism, 313
- Collin, 149, 151, 152, 169
- complete, 216, 219, 249, 267, 285, 310, 317, 334, 345, 346
- completeness, 46, 48, 69, 79, 84, 86, 92, 99
- complex power, 66, 67, 102, 103, 108–112, 116, 123, 133, 142, 148, 149, 341, 345, 347
- cone
 - angles, 46, 62, 66
 - length, 46, 84, 105, 136
- cosmological principle, 2
- Coulomb’s law, 1, 306

- de Broglie, 308
- degenerate, 190
- degree of degeneracy, 190
- Dirac, 308–310, 321, 330
 - delta function, 228, 330
- directivity, 31, 141, 239, 314, 317
- dynamic equilibrium, 172, 316

- eddy currents, 279, 281–283
- effective mass, 7
- eigenfunction, 188–190, 199–203, 206, 211
- eigenstate, 218, 220, 221, 227, 232, 241, 247, 248, 309–316, 319, 320
- Einstein, 216, 218, 220, 221, 227, 239, 246, 307, 309, 310, 317, 321
- electrodynamics, 7

- electromagnetic
 - mass, 17
 - stress tensor, 14, 15
- electron spin, 308
- equipartition theorem, 218, 225
- equivalent
 - circuit, 117, 118, 120, 122, 124, 134, 141, 142, 146, 151
 - sources, 136, 335
- ergodic theorem, 130, 223
- exclusion principle, 172, 213
- expectation values, 317
- exterior region, 47, 75, 88, 346
- extinction power, 36, 39, 81, 83, 85, 96, 270
- Fante, 152, 169
- field
 - coefficients, 28, 32, 48, 51, 69–71, 74, 86, 92, 94, 271, 273
 - momentum, 18
- fields in a box, 26
- fluid, 172
- force, 38, 39
 - density, 12, 14, 18
- four-acceleration, 12
- four-current density, 8, 10, 12
- four-divergence, 8
- four-momentum, 6, 7
- four-potential, 8, 9
- four-scalar, 12
- four-tensors, 7, 10
- four-vector, 5–8, 12, 14
- four-velocity, 5, 6, 8, 12
- Fourier integral, 30, 316
 - expansions, 21
- gamma power, 108
- Gaussian wave function, 184, 185
- geometric cross section, 37, 39, 43, 80
- group velocity, 109
- Hamiltonian operator, 188, 202, 203
- Hankel functions, 23, 26, 34, 48, 65, 75, 88, 126, 137, 236, 240, 244, 265, 267, 268, 285, 386, 387, 392
- Hansen, 23, 24
- harmonic
 - functions, 56
 - oscillator, 113, 191, 218, 219
- Harrington, 169, 239, 241, 305, 310, 321
- Helmholtz equation, 21, 22, 24, 336
- Hermite polynomials, 193
- Hertz, 216, 226, 307, 321
- Hertzian waves, 220
- input
 - impedance, 31, 60–62, 64, 91, 102, 114, 117, 119, 122, 129, 133, 142, 147, 153, 160, 340, 342
 - power, 36, 45, 65, 80, 101, 111, 154, 165, 166, 344
- interior region, 48, 63–65, 88, 95
- kinematic properties, 17, 241, 246, 247, 317
- Kirchhoff, 217
 - circuit laws, 103
- Kronecker delta function, 78, 254
- Laplacian, 8, 10, 21, 336
- Law of Parsimony, 247
- Legendre function, 23, 24, 26, 32, 47, 48, 55, 57, 58, 69, 88, 94, 261, 263, 359, 366, 370, 375, 377, 381, 392
- Lenz's law, 86, 94, 95, 271
- letter functions, 103, 118, 126, 127, 130, 132, 133, 137, 243, 266, 387, 388
- Lorentz
 - contraction, 3, 7
 - frames, 7
 - radius, 234
 - transformation, 3
- magnetic moment, 86, 95, 163, 164, 271, 273, 308, 313, 403
- Manley Rowe equations, 317
- Maxwell equations, 1, 11, 12, 17, 27, 46, 345

- Mie region, 44
- Minkowski force, 6
- Neumann, 257, 261, 263, 267, 285, 387, 392, 407
 function, 23, 24, 26, 32, 48, 49, 69, 112, 118, 236, 244, 249, 253, 254, 257, 261–263, 265, 285, 286, 289, 319, 360, 384, 387, 408
- Newton's law, 17
- non-ionizing transitions, 203
- nonlinear systems, 232, 311
- nonlocal electron, 310
- nonradiating motion, 172
- optical
 region, 44
 source, 251
- orthogonality, 57, 58, 152, 367, 368
- oscilloscope, 159, 160, 162
- Pauli, 213
- permeability, 8
- permittivity, 9, 230, 348
- perturbation, 206, 208
 analysis, 202
- photoelectric effect, 226, 306
- photoelectricity, 219
- Planck, 216, 218, 220, 224–226, 232, 239, 307, 320, 322
 constant, 180, 184, 232
 radiation law, 216, 218, 220, 224, 225
 radiation field, 302
- plane wave, 31, 32, 34, 36–38, 40, 43, 67, 69, 71, 72, 74, 75, 80, 84, 85, 94, 96, 98, 151, 220, 227, 229, 233, 235, 236, 241, 248, 269–271, 273, 289, 319, 392
- potential field, 7, 8
- power frequency, 303, 308, 311, 314
- Poynting
 theorem, 35
 vector, 15, 35, 38, 64, 66, 76, 104, 106, 127, 129, 132, 139, 140, 149, 240–242, 265, 267, 284, 288, 319, 346, 353, 408, 411
- pragmatism, 216
- pressure, 130, 248, 275–277, 279–282, 285, 291, 292, 294, 295, 297, 298, 313, 314
- proper time, 5
- radar cross section, 37, 38, 44
- radiating shell, 116
- radiation Q, 112, 115, 141, 153, 157–159, 161–166, 168, 169, 233, 235
- radiation reaction, 248, 261, 271, 276, 277, 298, 315, 317, 319, 320
- Rayleigh region, 44
- Rayleigh–Jeans Formula, 216, 218–220
- reaction force, 313, 314, 316, 319
- reactive energy, 121, 155, 319
- real power, 64, 66, 67, 101, 107, 109, 111, 151, 159, 160, 168, 289, 341
- receiving antenna, 31, 67, 80, 84, 86, 94, 270, 271
- recursion relationship, 244, 255, 260, 263, 265, 267, 362, 368, 369, 371, 375, 376, 382, 383, 387
- rest mass, 6
- scalar potential, 9, 395, 396, 400, 403
- scatterer, 34–38, 40–43, 75, 80, 81, 84, 96, 241, 270
- scattering, 31, 34, 37, 38, 40, 43–45, 67, 80, 83–87, 96, 97, 160, 161, 220, 270, 271, 310
 coefficients, 34, 40–42
 cross section, 37, 80, 97
- Schrödinger, 247, 308–310, 313, 315, 321, 322
- selection rules, 208
- shear, 275–283, 285, 291–298, 313
- skin depth, 227

- spherical
 - potential, 199
 - waves, 31, 359
- spontaneous emission, 219, 224
- standing energy, 46, 64, 115, 123–125, 128–130, 133, 139, 143, 146–148, 151–154, 156, 158, 159, 162, 166, 169, 236, 241, 248, 289, 310, 311, 320, 353
- statistical mechanics, 218, 225, 307, 316, 317
- step function, 38
- string theory, 173, 312
- surface
 - currents, 31, 38, 84, 95, 115
 - tension, 312
- symmetric, 95, 308, 327
 - tensor, 14, 15, 327
- TE modes, 25, 33, 34, 71, 75, 86, 87, 104, 108, 122, 124, 125, 137, 151, 239
- telefield terms, 248
- TEM mode, 46, 49–53, 65, 87
- Thévenin, 345
 - circuit, 102, 151
- time
 - dilatation, 4
 - domain, 153, 154
- time-independent wave equation, 180, 184, 186, 188
- TM modes, 25, 34, 46, 52, 71, 75, 94, 104, 108, 116, 122–126, 142, 152, 237
- transmitting antenna, 45, 46
- traveling waves, 32
- turnstile antenna, 154, 157–159, 161–163
- uncertainty principle, 233
- uniqueness theorem, 248
- wave
 - admittance, 46
 - function, 309, 310
 - expansion, 273
 - waveform generator, 160
- Wien formula, 220